

Punctuality of Railway Operations and Timetable Stability Analysis

Rob M.P. Goverde

Punctuality of Railway Operations and Timetable Stability Analysis

Proefschrift

ter verkrijging van de graad van doctor
aan de Technische Universiteit Delft,
op gezag van de Rector Magnificus prof.dr.ir. J.T. Fokkema,
voorzitter van het College voor Promoties,

in het openbaar te verdedigen op maandag 3 oktober 2005 om 10:30 uur

door

Robert Michaël Petrus GOVERDE

doctorandus in de wiskunde
geboren te Arnhem

Dit proefschrift is goedgekeurd door de promotor:

Prof.Dr.-Ing. I.A. Hansen

Samenstelling Promotiecommissie:

Rector Magnificus	voorzitter
Prof.Dr.-Ing. I.A. Hansen	Technische Universiteit Delft, promotor
Prof.dr. G.J. Olsder	Technische Universiteit Delft
Prof.dr. M. Carey	Queen's University Belfast
Prof.Dr.-Ing. E. Hohnacker	Universität Karlsruhe
Prof.dr. L.G. Kroon	Erasmus Universiteit Rotterdam
Dr. J.W. van der Woude	Technische Universiteit Delft
Prof.dr. H.J. van Zuylen	Technische Universiteit Delft, reservelid

This publication is a result of the research programme *Seamless Multimodal Mobility*, carried out within the Netherlands TRAIL Research School for Transport, Infrastructure and Logistics, and financed by Delft University of Technology.

TRAIL Thesis Series no. T2005/10, The Netherlands TRAIL Research School

TRAIL

P.O. Box 5017

2600 GA Delft

The Netherlands

Phone: +31 (0) 15 27 86046

Fax: +31 (0) 15 27 84333

E-mail: info@rsTRAIL.nl

ISBN 90-5584-068-8

Keywords: railway timetable, max-plus algebra, railway operations

Copyright © 2005 by Rob M.P. Goverde

All rights reserved. No part of the material protected by this copyright notice may be reproduced or utilized in any form or by any means, electronic or mechanical, including photocopying, recording or by any information storage and retrieval system, without written permission from the author.

Printed in The Netherlands

PREFACE

This PhD thesis is the result of research work carried out at the Transport & Planning Department of Delft University of Technology. I started working at this department in 1996 on several R&D projects of Railned Innovation on “Capacity Utilization and Synchronization Management,” including a project on the applicability of max-plus algebra to railway capacity management based on the PhD thesis of Hans Braker. The follow-up of these projects was embedded in the DIOC research programme *Seamless Multimodal Mobility* (SMM) financed by Delft University of Technology and supported by Railned, Railinfrabeheer, Railverkeersleiding, and Holland Railconsult. This enabled a more fundamental research approach finally resulting in this thesis.

I hereby want to thank the members in the user committee of the SMM rail research projects for their enthusiasm, feedback, and provision of data: Alfons Schaafsma, Laurens Berger & Jurjen Hooghiemstra (Railned), Dick Tersteeg (Railverkeersleiding), F. Koster & J. Lodder (Railinfrabeheer), and Ello Weits & Lieuwe Zigterman (Holland Railconsult). Over the last few years I am indebted to Dick Middelkoop (ProRail/Railned) for his support and provision of data. In addition, I thank anyone from the railway organizations who in any way helped me in my understanding of the railway field.

I also like to thank the other PhD researchers in the SMM rail research projects for their collaboration: Antoine de Kort, Robert-Jan van Egmond, Gerardo Soto y Koelemeijer, and Subiono. I regret that the first two decided to quit their PhD research before the end. I also wish to express my gratitude to the post-docs and senior researchers who participated in these SMM projects: Gerard Hooghiemstra, Rik Lopuhaä, and Bernd Heidergott, as well as my colleagues from the TRAIL research school and the Transport & Planning Department, and in particular: Paul Wiggendaad, Theo Muller, and prof. Piet Bovy.

My sincere gratitude goes to Remco Johanns (BIN Bedrijfsadviezen) for his work on TNV-Prepare, and Michiel Odijk and Paul Goldman (ORTEC) for their work on PETER. Their cooperation and programming skills made these software tools as they are now.

Special thanks go to Jurjen Hooghiemstra for giving me the opportunity to work at ProRail/Railned in the project PRRING (*Planning en Realizatie van RailInfraGebruik*). I learned a lot from his experience and our discussions. I hope that his valuable idea(s) for improving the railways will find their way into the railway practice. I wish him all the best in his new career as an independent consultant under the name *Kwaliteit in Verbinding*.

I am very grateful to my promotor prof. Ingo Hansen for trusting my mathematical opinions whilst guiding me to the world of transport, traffic and railways over all these years. His door was always open to me and I highly appreciate our cooperation. I also thank prof. Geert Jan Olsder for his everlasting support. I owed my PhD-position to his contacts with the Transport & Planning Department for which I am enormously thankful.

I sincerely thank my promotion committee for reading the entire manuscript and especially prof. Leo Kroon for his detailed comments.

Finally, I thank my parents for their support and all my friends who never stopped believing, and in particular: Patrick Timmers, Joke van den Bogert, and Wies Hendriks.

Rob Goverde
September 2005

CONTENTS

1	INTRODUCTION	1
1.1	Background	1
1.1.1	The Railways in the Netherlands at the Start of the 21st Century	1
1.1.2	Railway Operations and Timetable Stability	2
1.2	Setting the Scene	4
1.2.1	The Railway Timetable	4
1.2.2	Infrastructure Capacity Utilization and Timetable Performance	5
1.2.3	Social Relevance	7
1.3	Research Objectives	8
1.3.1	Ex-Post Traffic Analysis: Punctuality of Railway Operations	8
1.3.2	Ex-Ante Traffic Analysis: Railway Timetable Stability	9
1.4	Contributions	10
1.5	Thesis Outline	12
2	FUNDAMENTALS OF RAILWAY OPERATIONS	15
2.1	Introduction	15
2.2	The Hierarchical Railway Planning Process	16
2.2.1	Transport Demand	17
2.2.2	Railway Network Design	17
2.2.3	Line Systems	18
2.2.4	Railway Timetabling	20
2.2.5	Rolling Stock Circulations	22
2.2.6	Crew Schedules and Rosters	23
2.3	Safety and Signalling Systems	24
2.3.1	Train Detection	24
2.3.2	Fixed Block Signalling	25
2.3.3	Automatic Train Protection	27
2.3.4	Train Descriptor Systems (TNV)	28
2.3.5	Interlocking	29
2.3.6	Dispatching	31
2.3.7	Traffic Control	32
2.4	Train Delays	33
2.4.1	Primary Delays	33
2.4.2	Secondary Delays	34
2.5	Conclusions	35
3	RAILWAY TIMETABLES	37
3.1	Introduction	37
3.2	Running Time	38
3.2.1	Running Time Calculations	38
3.2.2	Running Time Margin	39
3.3	Blocking times and Minimum Headway	41

3.4	Dwell Time	45
3.5	Transfer Time	46
3.6	Layover Time	47
3.7	Synchronization Time	47
3.8	Buffer Time versus Scheduled Waiting Time	48
3.8.1	Buffer Time	48
3.8.2	Scheduled Waiting Time	49
3.9	Literature Review of Railway Timetabling	50
3.9.1	Timetable Feasibility	50
3.9.2	Timetable Optimization	53
3.9.3	Deterministic Timetable Performance Evaluation Models	56
3.9.4	Stochastic Models of Railway Operations	58
3.9.5	Network Simulation	62
3.10	Conclusions	64
4	TRAIN DETECTION DATA AND TNV-PREPARE	67
4.1	Introduction	67
4.2	TNV-Logfiles	68
4.2.1	Train Number Events	69
4.2.2	Infrastructure Events	70
4.3	TNV-Prepare	71
4.3.1	The Internal Database	71
4.3.2	Generation of TNV-Tables	73
4.3.3	TNV-Tables	78
4.3.4	Accuracy and Reliability of TNV-Tables	80
4.4	TNV-Filter	81
4.4.1	Filtering of Train Paths through Stations	81
4.4.2	Speed Profile Estimation	82
4.4.3	Train Length Estimation	87
4.4.4	Running Time on Platform Tracks	88
4.4.5	Arrival and Departure Delays	94
4.5	Conclusions and Recommendations	95
5	STATISTICAL ANALYSIS: THE EINDHOVEN CASE	97
5.1	Introduction	97
5.2	Railway station Eindhoven	98
5.3	Punctuality Analysis	100
5.3.1	Arrival Delay	100
5.3.2	Departure Delay	102
5.3.3	Dwell Time	104
5.3.4	Transfer Time	105
5.4	Regression Analysis	107
5.4.1	Introduction	107
5.4.2	Robust LTS Regression	108
5.4.3	Transfers between IC800 Hlm-Mt and IR1900 Rtd-VI	110
5.4.4	Transfers between IC800 Mt-Hlm and IR1900 VI-Rtd	111
5.4.5	Transfer IC900 Hlm-Ehv to IC1500 Gvc-Hrl	112

5.4.6	Transfer IC1500 Hrl-Gvc to IC900 EHV-Hlm	113
5.4.7	Stability	114
5.5	Probability Distributions	115
5.5.1	Arrival Delay	115
5.5.2	Departure Delay	117
5.5.3	Dwell Time	118
5.5.4	Transfer Time	120
5.6	Conclusions	120
6	TIMED EVENT GRAPHS	123
6.1	Introduction	123
6.2	Petri Nets and Timed Event Graphs	124
6.2.1	Basic Definitions	124
6.2.2	Building Blocks of Timed Event Graphs	126
6.3	Basic Modelling Approach of Railway Systems	128
6.3.1	Train Circulations	128
6.3.2	Train Synchronizations	129
6.3.3	Headway Constraints	130
6.4	Behavioural Properties	132
6.4.1	Liveness	132
6.4.2	Reachability	134
6.4.3	Periodicity	138
6.4.4	Boundedness	139
6.5	Synthesis of Scheduled Railway Systems	140
6.5.1	Input Data	140
6.5.2	Timed Event Graph Construction	143
6.5.3	Event Domain Description	148
6.6	Conclusions	150
7	MAX-PLUS ALGEBRA	153
7.1	Introduction	153
7.2	Max-Plus Semirings	154
7.2.1	Basic Definitions: Semirings, Semifields, Dioids	154
7.2.2	The $(\max, +)$ -Semifield	156
7.2.3	Max-Plus Polynomials	157
7.2.4	Max-Plus Matrices	159
7.2.5	Precedence Graphs and Path Matrices	163
7.2.6	Polynomial Matrices and Timed Event Graphs	167
7.2.7	Partially Ordered Semirings	171
7.3	Max-Plus Semimodules	173
7.3.1	Semimodules over the $(\max, +)$ -Semiring	173
7.3.2	Linear and Weak Independence	174
7.3.3	Linear Mappings	178
7.4	Max-Plus (Generalized) Eigenproblems	179
7.4.1	Introduction	179
7.4.2	Eigenstructure of Irreducible Matrices	180
7.4.3	State Classification and the Reduced Graph	185

7.4.4	Eigenstructure of Reducible Matrices	188
7.4.5	The Cycle Time Vector	194
7.4.6	The Policy Iteration Algorithm	196
7.4.7	Alternative Eigenproblem Algorithms	205
7.5	Longest Path Algorithms	208
7.5.1	All-Pair Longest Paths	208
7.5.2	Single-Origin Longest Paths	209
7.5.3	All Critical Circuits	212
7.6	Conclusions	215
8	RAILWAY TIMETABLE STABILITY ANALYSIS	217
8.1	Introduction	217
8.2	Max-Plus Linear Systems	218
8.2.1	First-Order State-Space Equations	218
8.2.2	Higher-Order State-Space Equations	220
8.2.3	Polynomial Matrix Representation	221
8.2.4	Autonomous Max-Plus Linear Systems	222
8.2.5	First-Order Representations	223
8.3	Max-Plus Spectral Analysis	226
8.3.1	Timetable Stability and Critical Circuits	226
8.3.2	Network Throughput	228
8.3.3	Stability Margin	228
8.4	Timetable Realizability	229
8.5	Timetable Robustness	231
8.5.1	The Recovery Matrix	231
8.5.2	Delay Impact Vectors	234
8.5.3	Delay Sensitivity Vectors	234
8.5.4	Circulation Recovery Times	235
8.6	Delay Propagation	236
8.6.1	Introduction	236
8.6.2	The Delay Propagation Model	236
8.6.3	A Bucket-Based Delay Propagation Algorithm	239
8.7	PETER	244
8.7.1	Introduction	244
8.7.2	Input Data	245
8.7.3	Functionalities	246
8.8	Case Study: The Dutch National Railway Timetable	251
8.8.1	Model Variants	251
8.8.2	Critical Circuit Analysis	252
8.8.3	Delay Propagation and Recovery Time Analysis	254
8.9	Conclusions	256
9	CONCLUSIONS	257
9.1	Main Conclusions	257
9.1.1	Analysis of Train Detection Data	257
9.1.2	Timetable Stability Analysis	259
9.2	Recommendations and Future Research	260

9.2.1	Train Detection Data and Railway Operations Quality Management . .	260
9.2.2	Max-Plus Algebra	262
BIBLIOGRAPHY		265
A GLOSSARY		279
A.1	General Abbreviations	279
A.2	Station Abbreviations	279
A.3	Mathematical Symbols and Variables	280
SUMMARY		283
NEDERLANDSE SAMENVATTING (DUTCH SUMMARY)		287
ABOUT THE AUTHOR		293

Chapter 1

INTRODUCTION

1.1 Background

1.1.1 The Railways in the Netherlands at the Start of the 21st Century

Punctuality and reliability of public (rail) transport are vital components of quality of service and passenger satisfaction. In the Netherlands, an increasing number of disruptive incidents in conjunction with an increasingly saturated railway capacity has led to a decline of reliability and punctuality over the last decade. In contrast to the growing national mobility and increasing congestion on the Dutch motorways, the railways in the Netherlands hardly attract new passengers. Nevertheless, the railways have a responsibility to significantly contribute to the mobility of persons to keep the heavily populated and industrialized *Randstad* — the conurbation in the western Netherlands — reachable. Reliability and capacity utilization must therefore be improved considerably to accommodate this increase in train traffic volume. The Dutch railway infrastructure is already one of the most intensely utilized national railway networks in the world with 50,000 train kilometres per track kilometre per year [163, 179]. On an average working day 5,000 passenger trains carry 1 million passengers, and additional freight trains carry about 100,000 ton of goods. Freight trains have currently only a small share of 7% of total railway traffic, but at least a doubling of freight traffic is expected after opening the international railway market for freight transport in 2008 [149].

Punctuality of railway services depends heavily on reliability of resources (railway infrastructure, safety and signalling systems, rolling stock, and personnel). Since 1995, the number of infrastructure malfunctions increased considerably in the Netherlands [78], mainly due to insufficient maintenance. Moreover, rolling stock breakdown and scarcity, as well as distress amongst train personnel further contributed to a considerable decrease in punctuality. The disastrous leaves on the railway tracks in the autumn of 2001 accumulated to a decline of annual punctuality (percentage of trains less than 3 minutes late) to below 80%. The annual passenger kilometres also began to show a negative trend since 2001, after years of growth during the second half of the 1990s [148]. Many of these problems can be traced back to the Dutch railway reform in 1995 [120, 179, 203] conform to the European Directive 91/440/EEC on the development of the Community's railways. In this directive and the subsequent rail infrastructure package — directives 2001/12/EC, 2001/13/EC and 2001/14/EC — the European Union commissioned the decoupling of railway infrastructure ownership from train operators and opening the national railway markets for competition between train operators [61]. This led to radical changes in the European railway markets, where national railways used to be organized in state monopolies.

In the Netherlands, the railway reform suffered from political uncertainty. On January 1, 1995, the Dutch monopolist NS (*Nederlandse Spoorwegen*) was separated into several organizations.

Management of the Dutch railway infrastructure was transferred to three newly founded task organizations which were responsible on behalf of the government for maintenance (*Railinfrabeheer*), traffic control (*Railverkeersleiding*), and capacity management (*Railned*). NS was furthermore split into several divisions, including the passenger train operator *NS Reizigers* (NSR), the freight train operator *NS Cargo*, and the rolling stock maintenance division *Ned-Train*. The freight division was discharged in 1999, after a fusion of NS Cargo and the German DB Cargo under the name *Railion*. Furthermore, new train operators were introduced in the regional passenger markets (NoordNed, Syntus) and especially in the rail freight market (e.g. ACTS, ShortLines, ERS Railways). During 1996–1999 the Ministry of Transport allowed competition between NSR and the new passenger train operator Lovers Rail for running concurrent train services on shared tracks. The experiment drastically failed and was discontinued in 1999 [203]. The new policy of the Ministry of Transport was a concession of all main passenger lines — the core network — to one operator under a performance regime, and tendering of regional lines by regional transport authorities. In the mean time NS hesitated to invest in new rolling stock due to the uncertainty of future operation rights. In 2001, NS finally ordered new passenger coaches which however became only gradually available in 2002 and 2003. As a result, NSR suffered from a rolling stock shortage for several years, also because of an increasing passenger volume in 1999–2000. On January 1, 2003, the three task organizations were again united into the single rail infrastructure manager *ProRail*. The Ministry of Transport finally granted NSR a concession for 2003–2015 to operate all passenger train lines on the core Dutch railway network [203].

In 2003, the Dutch railway sector presented their vision in the report *Benutten en Bouwen* [149], including the ambition to achieve a punctuality level of 95% in 2015, with punctuality measured as the percentage of trains less than 3 minutes late at 32 major stations. However, the highest measured punctuality up to date was 86.5% in 1999, and a significant increase of traffic intensity is expected for 2015. Hence, such a high performance can only be achieved if the timetable is robust to regular process time variations and stable to propagation of delays. Obviously, reliability of resources is a strict requirement for punctual railway operations. The Dutch railway sector therefore gives high priority to the improvement of the current infrastructure condition and an incentive to preventive maintenance [149]. Still, even on a perfectly reliable infrastructure and with ditto rolling stock railway traffic will experience variations from hour-to-hour and day-to-day that prevents the theoretical capacity from being fully used. For example, fluctuating numbers of passengers boarding and alighting at stations cause variations in station dwell times or seasonal variations in wheel-rail adhesion due to weather conditions cause variations in running times.

1.1.2 Railway Operations and Timetable Stability

Train operations are typically exposed to disruptions in train running times and dwell times which result in primary delays. Moreover, once a train is delayed this may produce severe delay propagation over the network when trains are highly interconnected. The Netherlands have a dense railway network that is heavily operated based on an integrated periodic timetable with highly synchronized train services at transfer stations all over the network. Interdependencies between train services are generated from passenger connections, headway separation through the safety and signalling systems, rolling stock connections and circulations, and train crew transfers. Moreover, an increasing saturation of railway infrastructure capacity increases the

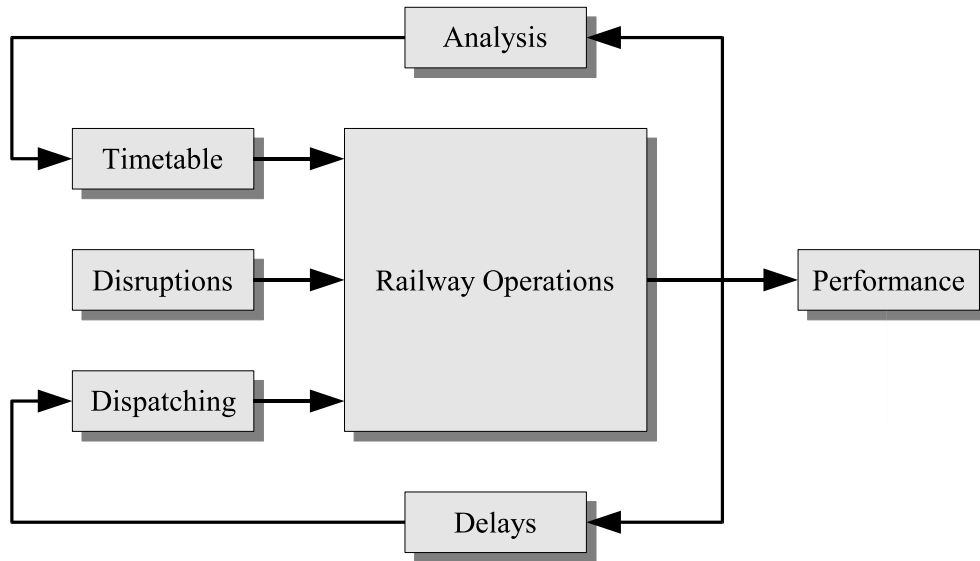


Figure 1.1 Feedback loops in railway operations

probability of conflicting train paths. A railway timetable must therefore contain sufficient time supplements and buffer times to be self-regulating with respect to minor daily disruptions and to grant control space that dispatchers can utilize for managing larger delays, see Figure 1.1. Feedback of operational data is essential for quantifying the necessary timetable slack and buffer that guarantees a desired quality of service, see the upper feedback loop in Figure 1.1. The lower feedback loop concerns larger delays that require intervention by dispatchers, who must find effective control actions in short-time. Since the timetable must accommodate such (local) disruptions it must have been tested a priori for recovery times and delay reduction capabilities to avoid a collapse of the entire timetable structure.

A robust timetable must be able to deal with a certain amount of delay without traffic control intervention. Timetable robustness therefore determines the effectiveness of schedule adherence after disruptions. Analysis of real-world operations data and train performance enables structural feedback between operations and timetabling. Evaluating a train network timetable on stability and robustness is an important part of the timetable design process and typically requires a computer-aided approach since it is hard to foresee how the system responds to disruptions due to the many cyclic train interdependencies over the (layered) network structure.

Stability of public transport chains and rail traffic networks is indispensable for managing service disruptions and propagation of delays. Nevertheless, sound criteria for rail transport and traffic network stability are practically nonexistent. The design of a *robust timetable* for dense train traffic requires a careful analysis of railway operations to put just enough slack at critical locations without being excessive. Because of the saturated railway capacity and train interconnections any slightly delayed train may cause a *domino effect* of secondary delays across the entire timetable, unless enough buffer time is incorporated to prevent or reduce delay propagation. On the other hand, excessive use of timetable slack increases travel times and infrastructure capacity. Moreover, excessive spare time raises the operating costs due to increased train circulation times and additional train crews and rolling stock.

In this thesis we will exploit the usage of existing empirical data of the railway signalling and safety system to bridge the gap between planning and realization of the railway timetable. More-

over we will develop a mathematical model that effectively describes the network structure and system behaviour, derive transparent stability criteria, and present an implementation of the approach in a computer application. The proposed methodology quantifies network performance and identifies the critical services in the railway transport and traffic network, and thus gives insight in the dynamic system behaviour, which can be utilized for improving timetable designs and supporting disruption management.

1.2 Setting the Scene

1.2.1 The Railway Timetable

A master timetable is the backbone of scheduled railway systems and determines directly or indirectly effective railway capacity, traffic performance, quality of transport service, passenger satisfaction, train circulations, and schedules for railway personnel. As such the timetable concerns many actors including (potential) passengers, (passenger and freight) train operators, train personnel, dispatchers, traffic controllers, infrastructure maintenance planners, and connecting public transport providers.

European passenger railways are typically based on a periodic railway timetable, where train lines are operated with regular intervals throughout a day and consistent transfers are provided at transfer stations between train lines of different type or directions. The basic *cycle time* is typically one hour, which means that the same pattern of train services repeats each hour. Train lines may have a higher service frequency and still fit the overall timetable cycle time. The *line cycle time* is then simply the overall cycle time divided by the line frequency, e.g., a train line with 4 trains per hour has a regular interval of 15 minutes. A periodic timetable is popular and effective to transport networks with diffused origin-destination demand matrices, where train lines are synchronized at transfer stations to offer seamless connections between many different origins and destinations.

The annual *published timetable* made available to travellers gives an overview of the planned arrival and departure times of all trains on the railway network for a year ahead and thus presents the transport service supply to (potential) travellers. Apart from the scheduled departure and arrival times, this timetable also implicitly provides information on service frequency and thus flexibility of departure time choice, (planned) travel times, and availability of direct trips or alternatively the number of transfers and associated transfer time. A main advantage of periodic timetables is that transport chains are fixed throughout the day and travellers only have to remember the departure time of their (first) train in a basic hour, e.g. ‘departure at 05 and 35 minutes of each hour’. Depending on transport demand the periodic timetable may be made more (or less) dense by adding (removing) train services in peak (off-peak) periods.

The published timetable is based on a much more detailed *working timetable* for railway personnel and traffic management systems. The working timetable specifies for each active train number on each day:

- Origin and destination station;
- Running tracks and stops, including station routes and platform tracks;
- Scheduled arrival and departure time at each stop;

- Passage times at certain locations (through stations);
- Timetable speed and sometimes overtaking speed (maximum speed in case of punctual and delayed running, respectively);
- Passenger connections at transfer stations;
- Rolling stock connections at main stations and terminals.

The working timetable may be adjusted up to the day of operation to include short-term train path requests, such as freight trains and trains for special events (football match, pop concert). Moreover, during operation the timetable may be adjusted in real-time by dispatchers and traffic controllers to react on operational conditions and disruptive incidents in the train traffic system. Because the annual passenger timetable is published a year in advance it may differ from the actual daily working timetable.

Conventional railway timetables are in general conflict-free and allocate trains to the available railway infrastructure in so-called *train paths* or time-distance graphs. If all trains adhere to their schedule then the timetable guarantees a safe and smooth train traffic without mutual hindrance on conflicting routes. Hence, the timetable represents a *green wave* of signal aspects to all trains running according to schedule. On conventional railway lines equipped with block signals the train driver relies completely on the trackside signals and the timetable, and has no information nor visual clues about the progress of the preceding train due to the large headway distances imposed by long braking distances and fixed block lengths. If a train is forced to stop at the open track before a red signal aspect this results in a large time loss as the acceleration time of a train from standstill to full speed is a matter of one to several minutes depending on train and track characteristics. In particular freight trains may suffer a time loss of more than 5 minutes when forced to an unscheduled stop.

The timetable is also the basis for dispatchers or automatic route setting (ARS) systems to set the routes for each approaching and ready-to-depart train according to the scheduled route and arrival/departure/through time. Also duty rosters of train crews (drivers, conductors) depend on the timetable, and so do rolling stock circulations, including shunting at stations, deadheading (empty running), cleaning at terminals, and periodic maintenance at depots. Hence, in case of disruptions timetable perturbations may cause wide-spread logistic problems. Train units, locomotives, coaches, and train crews may be in the wrong place at the wrong time resulting in altered train compositions and an increasingly distorted rolling stock and crew allocation.

1.2.2 Infrastructure Capacity Utilization and Timetable Performance

The *theoretical capacity* of railway lines and station layouts is defined as the maximum number of trains per unit of time that can be run, i.e., the reciprocal of the average minimum headway. Theoretical capacity is determined by both infrastructure and rolling stock characteristics. Infrastructure is characterized by the railway layout (single-track, double-track, sidings, junctions, number of platform tracks), track speed limits (depending on e.g. curves, grades, switches), and the signalling system (block lengths, number of signalling aspects, train protection). Rolling stock characteristics of interest are e.g. braking and acceleration capacity, maximum speed, train composition, and door widths.

Capacity also depends on how the traffic is organized in e.g. a timetable. The *effective capacity* of railway infrastructure is therefore defined as the maximal number of trains per unit of time

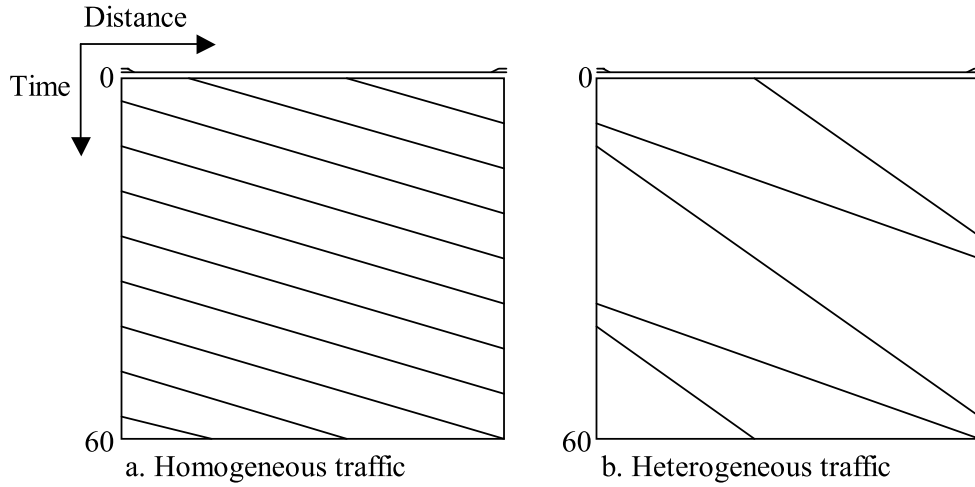


Figure 1.2 Time-distance diagrams showing the effect of traffic heterogeneity on effective capacity

that can be operated given the traffic pattern, operational characteristics or timetable structure. Effective capacity thus depends on the mix of train services with different characteristics (speed, stopping pattern, frequency), train sequences and orders, and connections at stations [192, 191]. Effective *route* capacity is mainly determined by the mix and order of train services — the traffic *heterogeneity* — and conflicting train routes at junctions. From a purely operational perspective the most efficient use of capacity occurs when trains have similar (homogeneous) performance characteristics, such as metro systems, see Figure 1.2. Effective *station* capacity is mainly determined by conflicting train routes and platform dwell times which also depend on scheduled train connections (transfers, rolling stock connections).

In practice part of the infrastructure capacity must also be reserved for traffic control to manage disruptions. The percentage of (effective) capacity per time unit is called the *capacity utilization*. In periodic schedules capacity utilization is measured as the ratio of cumulative blocking time and timetable cycle time (usually one hour).

There is an important distinction between primary and secondary delays. A *primary delay* is a schedule deviation caused by some disruption at any location due to variations within a process, such as restricted acceleration and speed due to low electricity supply, an unusual high number of boarding passengers, or behaviour of train driver, conductor and dispatcher. Primary delays are managed by computing reliable process times including margins in running and dwell times. On the other hand, a *secondary delay* is a process time extension caused by another train, e.g. catching up a delayed slow train on an open track or waiting for a delayed feeder train at a transfer station. Secondary delays are managed by buffer times between pairs of subsequent train paths to prevent or reduce hindrance and delay propagation.

In the Netherlands, timetable slack is incorporated by increasing a theoretical train running time by a given percentage — usually 7% — and adding a few minutes of recovery time at key points on a train route, usually at transfer stations, terminals, or at meeting stations on single-track routes. The function of these process time margins is twofold: preventing primary delays and absorbing existing delay. Often also “pathing time” or scheduled waiting time is included in a train schedule to avoid timing conflicts with other services in the timetable. Although slack is

important for reliable train operations, and should be retained in some form, it should be limited to avoid a significant reduction of capacity and speed. A satisfactory level of capacity utilization depends on the desired level of service quality, defined as a maximum total or average amount of primary and secondary delay over a given time period.

When the infrastructure manager and train operators together achieve a high standard of operational performance, timetable slack can be reduced and capacity utilization may be increased by scheduling additional train paths, increasing operating speed, or providing an improved market oriented timetable. High capacity utilization thus requires process times with small variance and scheduled values that are highly reliable corresponding to a high percentile of the realized process time distributions. However, there must still be sufficient spare capacity in the form of timetable slack to accommodate a certain lateness of trains and to recover from traffic disruptions.

Persistent poor performance reduces the effective capacity and thus prevents increasing the quality of service or performing engineering work within tightly designated slots. Punctuality and reliability are necessary prerequisites for increasing capacity utilization. Operating more trains on a given infrastructure network reduces the amount of “white space” (eventually unused train slots) in the timetable, which means less ability to recover from service irregularities and smaller time windows for engineering work and infrastructure inspection between trains.

1.2.3 Social Relevance

Dispunctuality and unreliability in public (rail) transport has a disastrous effect on passenger satisfaction. Delayed trains, missed connections and train cancellations are particularly annoying because they cause unexpected waiting time and introduce travel time uncertainty. Absence of reliable passenger information magnifies impatience and distress even more. Most vulnerable are transport chains where travellers have to change trains or transfer between different modes of transport (e.g. train–bus). A *small train delay* of a few minutes may cause a missed connection and thus lead to a *large passenger delay* of 30 or 60 minutes, depending on the frequency of the connecting service [173]. When repeatedly confronted with delays, travellers even anticipate on larger travel times than published and adjust their departure time choice accordingly, especially when the arrival time at the destination is important, e.g. to attend a business meeting. Thus, short but unrealistic scheduled running or transfer times lead to large travel time expectations of travellers, after a transient period of annoying travel experiences [178]. Moreover, unreliability generates negative word-of-mouth publicity, a deteriorating image of public transport and loss of public transport travellers.

Reducing passenger waiting time is an effective means to increase the quality of service. Unacceptable waiting times lead to a low perception of service and in addition generates negative word-of-mouth publicity. Whether a waiting time is judged as excessive depends on the discrepancy between *perceived* waiting time and *expected* waiting time [146]. Expectation may be distinguished in a desired/anticipated level and a tolerable level. The *desired/anticipated* level of expected waiting time is based on the published timetable and past experience. The timetable should therefore be a close reflection of the realized services. Nevertheless, passengers are willing to accept a larger *tolerable* waiting time expectation in recognition of the uncertainties involved in railway transport and traffic operations. Waiting may not be a critical issue as long as the discrepancy between perception and expectation is within an acceptable region. When

expectations are confirmed, cognitive assimilation occurs and the difference in perception and expectation is reduced. For moderate levels of discrepancy in either direction, passengers adjust their perception of waiting time to be more consistent with their expectation. However, when the discrepancy is beyond the region of acceptance, the contrast between perception and expectation magnifies passenger dissatisfaction.

Reliable *passenger information* helps passengers to set realistic expectations of waiting time and thus reduces the discrepancy between expected and perceived waiting time. Hence, if actual waiting time can not be avoided train operators can still reduce passenger dissatisfaction by providing passenger information on waiting time in case of delays. Although this has little effect on perceived waiting time it affects judgment on the quality of service indirectly through acceptability of waiting time [146]. Informed passengers are mentally prepared for the wait and have control over how to spend the waiting time. This way, passengers are likely to be more understanding and tolerant to waiting. However, if the information turns out to be unreliable passenger satisfaction is worsened even more.

1.3 Research Objectives

1.3.1 Ex-Post Traffic Analysis: Punctuality of Railway Operations

The first research objective of this PhD Thesis concerns the *ex-post analysis* of railway operations to obtain reliable process times and close the feedback-loop between planning and operations, see Figure 1.3. Ex-post analysis is retrospective and tries to decide what (design and control) decisions would have been optimal given the information on what actually happened. The results can then be utilized to improve the consistency of plan and realization.

A crucial aspect in achieving and maintaining reliable timetables is the availability of accurate empirical data to compare the timetable design and its realization. In the construction of a new (annual) timetable historical data may be used, but also during operation of a timetable regular empirical evaluation should be applied to detect and manage discrepancies between plan and realization. However, the data collection and registration method via the traffic control systems used by (ProRail) Railverkeersleiding for punctuality analysis reports does not meet scientific requirements on precision and accuracy. The registered arrival and departure delays are only indicative with an absolute error up to several minutes, and moreover delays below 3 minutes are not registered at all¹ [46, 80]. A detailed punctuality analysis of train traffic requires data with an accuracy of several seconds in order to determine small delays and even early arrivals at a precision of at least a tenth of a minute. This leads to the first research objective of this thesis.

Research Objective 1 *Developing a data mining tool to retrieve accurate and reliable realizations of train movements from data records of the signalling and safety system.*

A potential source of traffic data is given by train detection devices, which act as sensors of the safety and signalling systems. This train detection data is utilized by train describers — in

¹Situation in 1997

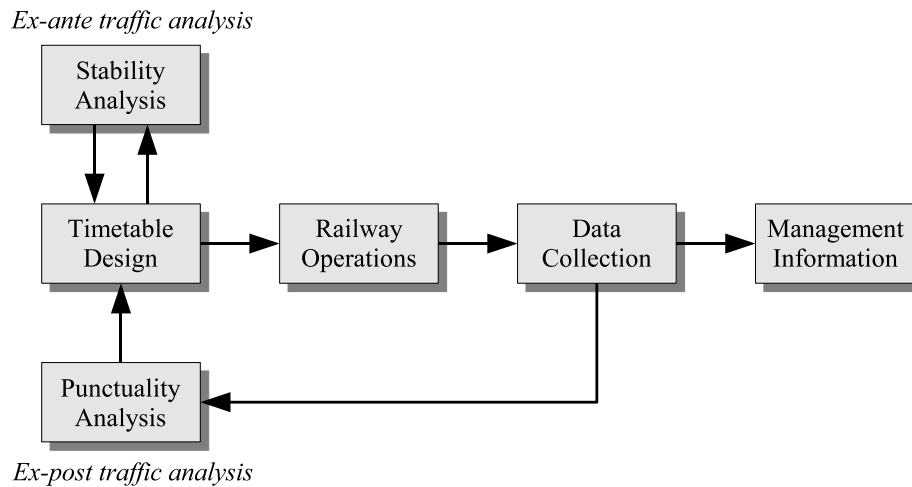


Figure 1.3 Feedback loops in robust timetable design

the Netherlands known as TNV-systems — to monitor the progress of trains over the railway network, and one of the functionalities of TNV-systems is to automatically keep a record of all data traffic with communicating control systems. These *TNV-logfiles* therefore contain infrastructure and train number messages with a precision of one second. However, the infrastructure messages only give a change in status of a certain infrastructure element, such as a track section that gets occupied or has just been released. The message does not contain any information on the train that triggered the state change. Hence, the challenge remained to convert TNV-logfiles to accurate train data where infrastructure messages are coupled to train numbers.

Main railway stations are served by various train lines of different directions which are synchronized to offer seamless transfer opportunities according to the ‘timed transfer’ philosophy of periodic network timetables. These stations are therefore a potential source of disruptions and delay propagations and thus qualify for a detailed statistical analysis of punctuality and identification of critical train interactions. When accurate train arrival and departure data becomes available (Research Objective 1) such an analysis can be performed at a high level of reliability for the first time. This is the second research objective of this thesis.

Research Objective 2 *Performing a detailed punctuality analysis with the emphasis on fitting probability distributions of characteristic operations performance indicators and quantifying disruptive train dependencies.*

1.3.2 Ex-Ante Traffic Analysis: Railway Timetable Stability

The third research objective is concerned with an *ex-ante analysis* of candidate railway timetables. Ex-ante analysis is based on a model of the expected system behaviour, which is used to improve design decisions before they become operational. The relation between the three research objectives is visualized in Figure 1.3.

A new timetable or a major (annual) update of an existing timetable should be carefully tested on stability and delay sensitivity prior to operation to assure good performance in managing

secondary delays. In fact, a timetable should only be authorized if the planners or inframangers are confident about its robust performance. However, an objective means of performance evaluation is not yet available other than simulation, which is typically very involved and time consuming for large networks. Hence, there is a need for an efficient and effective analytical approach to evaluate network timetables on stability and network performance, which gives the third research objective of this thesis:

Research Objective 3 *Developing an analytical approach to evaluate and quantify critical network dependencies on capacity utilization and timetable stability.*

In this thesis we propose an analytical method based on *max-plus algebra*. Braker [21] and Subiono [196] showed how the essential network timetable structure can be modelled as a discrete-event dynamic system that is linear in the max-plus algebra. However, the efficiency of a railway timetable is typically limited by the railway infrastructure (including signalling system), which has a major effect on the train traffic dynamics. We therefore extend the modelling approach by incorporating infrastructure constraints. Using this model we may then identify and efficiently compute the most critical circuits — the closed paths in a periodic network with the least average slack — and the (not necessarily cyclic) paths without any buffer time whatsoever, with respect to the scheduled process times, the timetable structure, and the infrastructure constraints. The underlying idea being that in a highly-synchronized periodic railway timetable delays initiated at some point in the network are likely to spread throughout the entire network unless enough time reserves are built in at strategic places. We thus want to find the most sensitive links in the network, i.e., the train paths containing the least slack to recover from delays. The max-plus algebra framework enables us to use available and develop new highly efficient algorithms that compute the critical circuits/paths for large-scale networks within some seconds.

1.4 Contributions

This thesis contributes to the understanding of railway operations and timetable design aspects that are important to construct robust timetables for reliable railway operations.

The first research objective led to the development of the software application *TNV-Prepare* based on train description messages and messages from the safety and signalling systems as recorded in TNV-logfiles. TNV-Prepare is able to match the infrastructure messages to train numbers by which train paths through stations can be traced offline on track-circuit (or section) level to and from the platform tracks. As a result, station arrival and departure times can be derived with a precision and accuracy in the order of a second.

- This thesis shows that standard train describer records can be utilized to obtain accurate data of infrastructure utilization and train punctuality by means of the developed software TNV-Prepare.

The developed software TNV-Prepare enabled detailed analyses of train traffic and infrastructure utilization in railway stations. A punctuality analysis of the railway traffic at station Eindhoven has been realized conform the second research objective.

- The tool TNV-Prepare has been applied to train detection data of station Eindhoven. This allowed an extensive statistical analysis of punctuality revealing a structural increase of delays due to tight train interdependencies despite long scheduled dwell times.
- Probability distributions of train events and station process times have been derived and statistically confirmed based on the empirical train detection data.

The third research objective has been realized by extending the modelling and analysis of railway timetables in max-plus algebra. Moreover, the algorithms described in this thesis have led to the development of the software application PETER (Performance Evaluation of Timed Events in Railways). PETER facilitates the accessibility of the max-plus system analysis method to the railway community.

- The modelling of railway timetables in max-plus algebra is generalized and extended with infrastructure constraints.
- Key performance indicators are defined to assess railway timetables on stability and robustness.
- Efficient algorithms have been developed that enable fast evaluation of large-scale railway timetables on stability and effective capacity utilization.
- The understanding of the max-plus modelling and analysis approach is enhanced by modelling a railway traffic system as a timed event graph in conjunction with its max-plus state-space representation.

Significant theoretical contributions have also been accomplished in the field of max-plus algebra in the following directions.

- Max-plus polynomial matrices are shown to be a key element in the performance analysis of timed event graphs and higher-order max-plus linear systems.
- The generalized eigenstructure of any irreducible and reducible max-plus polynomial matrix has been completely described.

The findings of this thesis led to the development of several software products, which facilitate understanding and direct usage in the rail traffic management practice:

- TNV-Prepare[©]: this software application enables accurate analysis of infrastructure utilization by matching information from safety & signalling systems to train numbers. TNV-Prepare may encourage feedback of realization data into the planning practice and enables an empirical foundation to performance evaluation of railway timetables and capacity assessment of railway infrastructure.
- TNV-Filter: this MATLAB program computes accurate estimates of arrival and departure delays at platform tracks in complex railway stations based on tables generated by TNV-Prepare and additional information on infrastructure section lengths.
- PETER[©]: this software application implements the max-plus stability analysis approach with graphical views of computational results, which includes critical circuit analysis, recovery time analysis, and delay propagation. A special import functionality makes PETER compatible with DONS, the timetable design system used at NSR and ProRail.

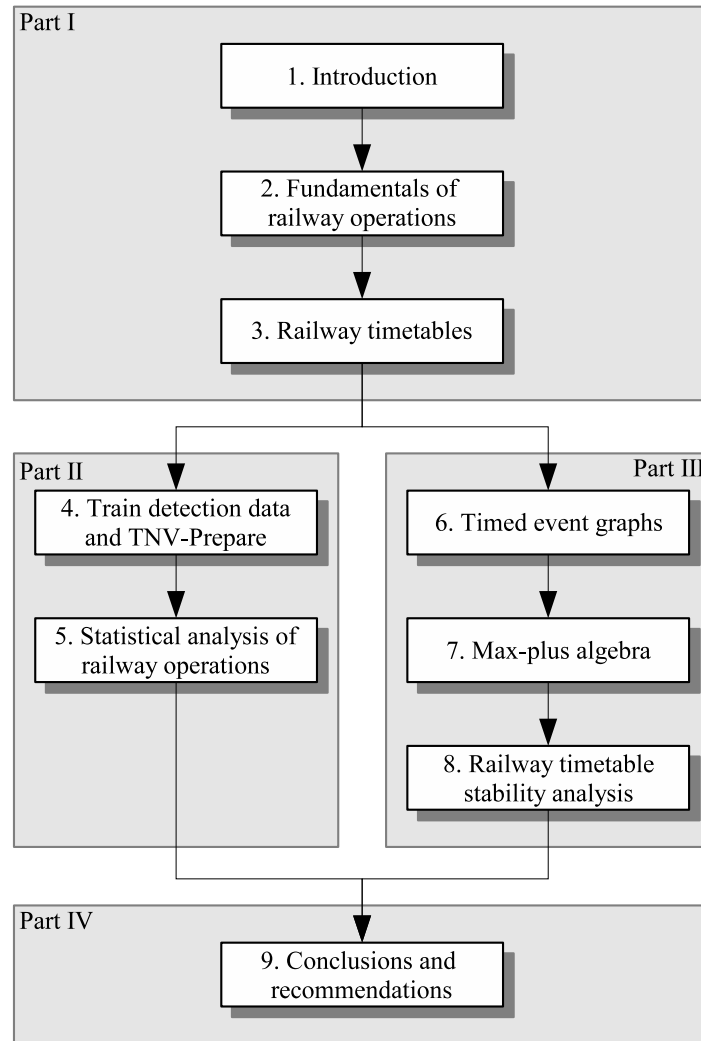


Figure 1.4 Thesis outline

The software applications TNV-Prepare and PETER have both been extensively evaluated at ProRail (Railned) during their development. TNV-Prepare is fully licensed to ProRail since 2001. ProRail also has a license to PETER since the beginning of 2005.

1.5 Thesis Outline

This thesis contains four main parts, see Figure 1.4. Part I is an introduction to the problem field including the present chapter with a general introduction (Chapter 1). Chapter 2 presents a concise overview of the hierarchical railway planning process, the railway safety and control systems in the Netherlands, and a classification of primary and secondary delays. Chapter 3 reviews the calculation methods for the various timetable components (process times) and presents a literature review of railway timetabling and timetable evaluation.

Part II is concerned with the first main research stream corresponding to research objectives 1 and 2 on the comparison of scheduled process times with their realizations during railway op-

erations. Chapter 4 shows that the information contained in the logfiles of TNV-systems can be used to match infrastructure utilization to train numbers, and describes the developed tools TNV-Prepare and TNV-Filter. In Chapter 5 the application of these tools are demonstrated in a case study of the railway station Eindhoven. This chapter gives a detailed punctuality analysis and shows by means of simple linear regression analysis the strong dependencies between train services with a transfer connection and the impact of the bottleneck Eindhoven-Boxtel before its upgrade to four tracks.

Part III deals with stability analysis on a network level conform research objective 3. Chapter 6 considers *timed event graphs*, a special class of Petri nets that provides a graphical modelling approach for max-plus linear systems. A timed event graph models the interconnection structure of events (nodes) and processes between events (arcs), and moreover denotes active processes (e.g. train runs, transferring passengers) by assigning a token to the active processes. The tokens move over the graph governed by the occurrence of events, which describes the dynamic behaviour of the modelled system. Basic building blocks and behavioural properties are presented that can be used for the synthesis of complex timed event graphs. Chapter 7 introduces the theory of max-plus algebra and explains the relations to other mathematical disciplines such as graph theory, Petri nets (timed event graphs), dynamic programming, Markov decision processes, and the theory of nonnegative matrices, from which efficient algorithms have been derived to compute characteristics of max-plus matrices and the associated graphs. Chapter 8 explains the principles of max-plus linear system theory and describes the system analysis approach to large-scale timetabled train traffic systems, as implemented in the developed software application PETER. The software PETER is briefly described and the analysis capabilities are demonstrated by a case study of an (hourly) periodic timetable based on the Dutch national railway timetable of 2000/2001.

Finally, Part IV (Chapter 9) summarizes the main conclusions based on the own research contributions and the recommendations for future practice and research.

Chapter 2

FUNDAMENTALS OF RAILWAY OPERATIONS

2.1 Introduction

This chapter gives an overview of passenger railway planning and railway safety and signalling systems. In particular, we introduce trains lines and connections between train lines which together with the railway network is important input to the timetabling process. The safety and signalling systems are also of main importance to derive minimum headway constraints that must be incorporated in the timetable design to compute a feasible timetable that coordinates the train traffic with respect to train route conflicts and safe train distances. Rolling stock circulations are another important aspect that must be taken into account in the timetable design because the various rolling stock types have different characteristics (maximum speed, acceleration/deceleration rate) that influence the realizability of the running times. Moreover, (de-)coupling of rolling stock and turns at terminals are also important parameters that influence minimum layover times and dwell times.

This chapter gives a review of the Dutch railway systems architecture including train detection, train description, interlocking and traffic control. We emphasize the data flows between the various safety and control systems and show that all information on infrastructure elements is collected by the train describer systems (TNV-systems in Dutch) which is used to monitor the movements of all trains on the network using their train descriptions (train numbers). A crucial observation is that all infrastructure and train description events are recorded by the Dutch train describer systems into TNV-logfiles, which will be used in the sequel of this thesis as an essential data collection device.

We furthermore consider the capacity allocation process in the Netherlands in which the train path requests of various train operators are coordinated by the infrastructure manager. This capacity allocation has been initiated in Europe to grant competition between different (freight and passenger) train operators according to directive 2001/14/EC on railway capacity allocation of the European Union [60]. These European regulations have led to a drastic change from the traditional monopolistic state railway companies to privatized train operators.

The outline of this chapter is as follows. Section 2.2 considers the various stages of (passenger) railway planning, including line system planning (§2.2.3) and railway timetabling (§2.2.4). Section 2.3 is concerned with the railway safety, signalling and control systems with an emphasis on the architecture in the Netherlands. Section 2.4 classifies delays and considers a wide range of sources of delays.

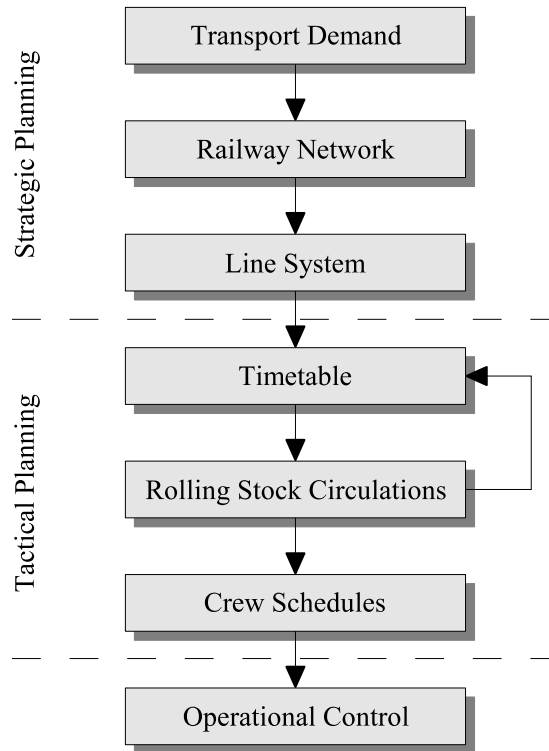


Figure 2.1 The hierarchical railway planning process

2.2 The Hierarchical Railway Planning Process

Railway planning involves a number of steps from the estimation of transport demand to the operational control of actual railway operations, see Figure 2.1. Each individual decision problem is already that complicated that a hierarchical approach must be pursued where in each step decisions are made that influence the subsequent planning stages [26, 38]. In this process iterations between several stages may be necessary to resolve capacity problems at some stage by reconsidering decisions made at an earlier stage. In passenger railways this is typically an ongoing process where the annual timetable is updated each year with respect to changes in passenger flows, exploitation of new infrastructure, and allocation of new or refurbished rolling stock.

The railway planning process typically distinguishes between three levels of different planning horizons [179]. *Strategic planning* is concerned with the strategic design of the scheduled transport network and the long-term capacity management of resources or traffic means to meet future traffic demand. The resources include sufficient infrastructure capacity, rolling stock and train personnel to accommodate the expected traffic flows. Typically, strategic decision-making involves large investments and long planning horizons, such as for instance building new infrastructure, manufacturing new rolling stock, or hiring and training new personnel. The strategic planning phase translates travel demand into transport supply (train lines) and provides (constraints on) the traffic means for allocation to the transport services. *Tactical planning* is concerned with capacity allocation of resources (traffic means) to transport services for the intermediate planning horizon. Typical tactical planning problems are the allocation of infrastructure time-distance slots, rolling stock, and crews to trains. *Operational planning* is concerned with

rescheduling during operations in face of unforeseen events, disruptive incidents or accidents.

In this thesis we are mainly concerned with the analysis of timetables, which is part of the tactical planning phase. We therefore assume strategic decisions as given, that is, infrastructure and train lines are fixed. Furthermore, rolling stock circulations and crew schedules must be consistent with the timetable and may define additional interdependencies. In the next subsections we briefly consider the successive railway planning stages with the focus on their impact to the timetable. For alternative reviews, see e.g. Bussieck *et al.* [26], Cordeau *et al.* [38] and Kroon [124].

2.2.1 Transport Demand

The first step of *strategic planning* is *demand estimation*. Forecasting future travel demand is an econometric problem directed towards the determination of *origin-destination* (OD) matrices partitioned by transport mode according to travel choice behaviour [157]. In particular the *modal split* between individual car and public transport is of strategic demographical importance and depends on the available infrastructure and quality of service of public (rail) transport, which can be influenced by strategic political decisions. Each entry in a (rail transport) OD-matrix gives (an estimate of) the number of passengers travelling from one station in the railway network to another. The passenger transport demand in the form of an OD-matrix is the basis of each following stage in the railway planning process and in particular to the design of network structure and the train lines.

2.2.2 Railway Network Design

The railway *network design* problem aims at the determination of railway tracks and stations given the railway transport and traffic demand. Building new railway infrastructure is very costly and has a severe environmental, economical, and social impact for many decades. Long-term infrastructure investments are therefore subject to political debate and based on strategic studies that estimate future demand for and utilization of railway infrastructure. Railway infrastructure issues can also be considered as part of the railway network design, such as electrification of railway lines and the choice of safety and signalling systems.

The existing railway infrastructure is a product of historically made strategic decisions. In the Netherlands the main part of the railway lines originate from the large railway construction projects at the end of the 19th century [62]. In the late 21st century a number of suburban railway lines were built, such as the Zoetermeerlijn and the Flevolijn from Weesp to Almere and Lelystad, and a large number of new suburban stations were opened at existing lines. Also a number of rural railway lines were closed in the 21st century as they were superseded by road traffic. Nowadays, railway engineering projects mainly focus on capacity expansions of saturated infrastructure such as upgrading single-track to double-track or double-track to four-track lines, eliminating crossings by fly-overs and extending station layouts. International developments have also led to two major recent railway infrastructure projects of the *Betuweroute*, a dedicated freight route from the Rotterdam harbour to Germany, and the *HSL-Zuid*, the high-speed line from Amsterdam to Belgium [102]. Current network design issues also involve extending or replacing conventional (heavy) railway lines by light-rail lines.

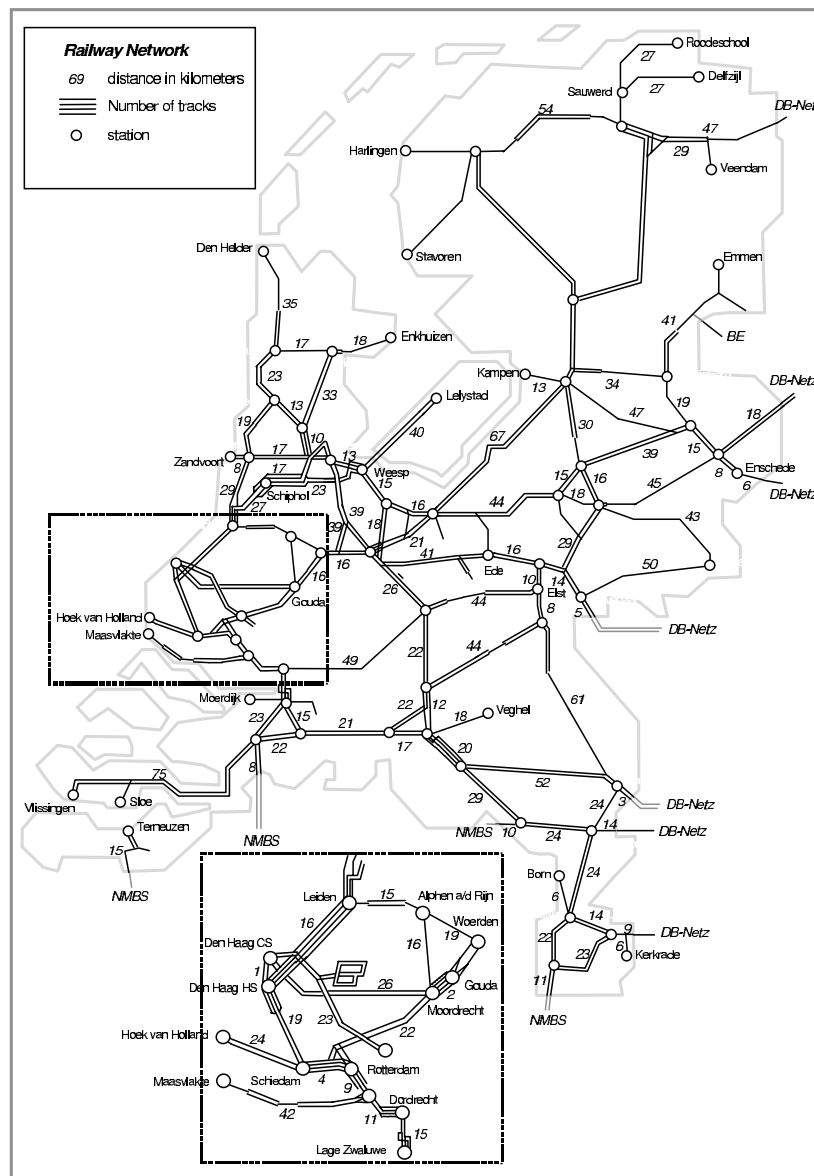


Figure 2.2 The Dutch railway network [Source: Network Statement 2003]

Figure 2.2 gives an overview of the national Dutch railway network. Most railway lines are double-track with occasional four-track lines in the Randstad and recently between Boxtel and Eindhoven. Single-track lines can be found in rural areas.

2.2.3 Line Systems

A *train line* is a train service characterized by a route from an origin station to a destination station, the served intermediate stations along the route, and the service frequency. A train line is operated by a fleet of trains running typically at a regular interval. A *line schedule* contains the running times between the successive stations and the dwell times at the stations. The *line system* or line network is an integrated set of lines defined by their characteristics and a set of connections at transfer stations where lines meet and passengers may change lines.

A railway network is usually operated by heterogeneous train types serving different transport markets, such as long-distance trains and regional trains. This leads to a natural decomposition of the line system into subsystems or supply networks according to train type. Generally, the subsystems concurrently use the same tracks although some decisive train type features may rule out certain parts of the railway network, e.g. electric multiple units (EMUs) require electrified tracks and high-speed lines have restrictions on track curvature. Common passenger train services in Europe are

- (i) High-speed trains (HST): international passenger train services connecting major cities at top speeds over 200 km/h.
- (ii) Intercity (IC) trains: long-distance passenger trains connecting the major national stations only.
- (iii) Interregional (IR) trains: intermediate-distance passenger trains connecting major and large stations,
- (iv) Agglo/regional (AR) trains: local passenger trains serving all stations on their route.

The agglo/regional train lines are also called regional (R) train lines.

Passenger demand is usually specified in an origin-destination matrix for the complete train service network. However, the passenger flows are distributed over the different subsystems. Oltrogge [20] proposed a procedure for splitting the OD-matrix into separate OD-matrices for the subsystems, the so-called *system split*. The method assumes a hierarchy of the subsystems where the lowest level network has the finest grid of stops served by slow trains (as a result of the stopping pattern), and the highest level subsystem connects only main stations with high speed. For example, the three national passenger train subsystems in the Netherlands are arranged as $IC \subset IR \subset AR$, i.e., the IC stations are a subset of the IR stations and the IR stations are a subset of the AR stations. An admissible journey is then a transport chain with transfers to a higher level network near the origin and transfers to a lower level network near the destination. The problem then reduces to finding the shortest path over a *supernetwork* consisting of the supply networks with additional transfer arcs at the stations where passengers may change to another subsystem. Oltrogge [20] proposed a sophisticated valuation of the travel paths based on travel time, price, level of comfort, and the number of system changes. Note that at this stage the transfer waiting times are still unknown since a timetable is not yet available. The valuation differs with trip purpose (e.g. business, leisure) and accordingly provides an assignment of traffic volume to the different travel routes. The distribution of passengers over the supernetwork gives the number of passengers or *traffic load* for each link in the supply networks. Aggregating over all assigned routes and all OD-pairs gives the OD-matrix estimates for each subsystem.

Given passenger demand and railway network, the *line optimization problem* aims at finding feasible lines (routes and frequencies) satisfying a set of constraints and optimizing some objective function. Constraints specify e.g. that all travellers are transported, passenger loads do not exceed train capacities, and track capacities are not exceeded. Typical objectives are maximization of the number of direct trips (or minimization of transfers)[20] and minimization of operating costs [25, 76, 77, 230]. The optimization problem is a mixed-integer programming (MIP) problem, which is NP-complete. Branch-and-bound and heuristic algorithms have been developed for solving practical instances of this problem [20, 24, 25, 76, 77, 230].

Based on the approach of Oltrogge [20] the program PROLOP (PROgram for Line OPTimization) was developed for the analysis of passenger flows over a line system, which was used in the

Netherlands by NSR and Railned [45]. PROLOP contains three modules: the line optimization model, an assignment model, and a comparison model. NSR and Railned used mainly the last two models to evaluate passenger flows. Input to the assignment model is the railway network, the train lines, an OD-matrix, and optionally a timetable. The assignment model assigns travellers to train lines based on a generalized travel time utility function, as described above. The output includes passenger loads, track load, and passenger flows at stations. The comparison model evaluates the differences between two line systems. In 2000, NSR and Railned decided to develop a new program with an improved interface, called TRANS (*Toedelen Reizigers Aan Network Systemen*). Nevertheless, the assignment method developed in PROLOP has been preserved in TRANS.

2.2.4 Railway Timetabling

Timetabling is the problem of matching the train line system to the available infrastructure, i.e., finding for each train line a feasible schedule of arrival and departure times at the consecutive served stations taking into account constraints with respect to e.g. the safety and signalling system, transfer connections, and regularity requirements. In this section we consider the main timetable aspects and the timetabling process within the railway planning process. Section 3.9 gives a review of mathematical approaches of railway timetabling.

The basis of the Dutch railway timetable is a *basic hour pattern* (BHP)¹ over the corridors and a basic platform occupation (BPO)² in stations. All train lines operate with a cycle time of one hour or at regular intervals within a cycle of one hour (e.g. 30 or 15 minutes). Hence, the arrival and departure times at all stations are essentially the same for each hour over a day, and moreover the connections and transfer times between train lines at transfer stations are equal over the day. This periodic timetable implies that travellers can take the same trains and connections with equal (scheduled) travel times for each period of the day and day of the week without consulting the timetable, which offers a great quality of service for regular train travellers. A BHP thus consists of all arrival, departure and through times scheduled in a basic hour. BHPs are visualized by time-distance diagrams or train path diagrams. In addition, a BPO shows the dwell times (and arrival and departure times) and through times at the station platform tracks during a basic hour. BPOs are visualized by platform occupation diagrams.

From a timetabling point-of-view this periodicity imposes additional restrictions to the train schedules and their synchronization at transfer stations, since the round-trip time of each train must be a multiple of an hour which bounds the amount of slack and buffer time that can be built into the line schedule. Moreover, this generally holds for each closed sequence of train runs (circuits) in the timetable (modulo the cycle time), see e.g. Odijk [154], Goverde [81] and Peeters [159]. In the Netherlands, the system DONS is used to interactively determine a set of feasible constraints for which then a network timetable is computed, see e.g. Hooghiemstra [101].

A strictly periodic daily timetable can be obtained by concatenating 24 BHPs. However, in practice traffic demand fluctuates over a day and over the week. In a strictly periodic timetable this would lead to crowded trains in peak periods and almost empty trains in the off-peak.

¹In Dutch: basisuurpatroon (BUP)

²In Dutch: basisspooropstelling (BSO)

Hence, a BHP is adapted to different periods, such as extra commuter trains in peak hours and cutting down some train lines in off-peak hours (e.g. from 60 to 30 minutes). The annual timetable is thus obtained by connecting variants of a BHP with particular concern for train circulations. In the short term additional perturbations of the annual timetable may be necessary due to e.g. maintenance or additional trains for special events (e.g., popular football matches or concerts). This results in the *daily timetable* for each day of the year.

The BHP is also used in the capacity allocation of railway infrastructure to various train operators. For each annual timetable all train operators must submit a formal request for train paths to the infrastructure manager conform directive 2001/14/EC on railway capacity allocation of the European Union [60]. In the Netherlands these requests are submitted as a BHP according to the Dutch annual Network Statements [165]. The BHPs are evaluated by ProRail using pre-established planning norms [166, Appendix 25] and conflicting train path requests are resolved with the relevant operators. After approval of the BHP the train operators may design their daily timetables in accordance to the BHP.

In the Netherlands, the tactical timetabling and capacity allocation process is supported by the *VPT-Planning* system. VPT-Planning contains a database of the railway infrastructure and the characteristics of all used rolling stock, and consists of several subsystems for supporting the design of BHPs, annual and daily timetables, rolling stock circulations, and crew schedules [164]. During the development of VPT-Planning the Dutch Railways were still the only train operator in the Netherlands. Nowadays, the VPT-Planning system is available to all train operators and ProRail but it is still maintained by NSR. ProRail is currently developing a new application (PTI) which will replace VPT-Planning. Below we briefly describe the railway capacity allocation process in the Netherlands.

Railway Capacity Allocation

Train operators must submit their requests for infrastructure capacity to the infrastructure manager ProRail Capacity Allocation nine months in advance of a new operational annual timetable. The requests must be submitted as a draft timetable in the form of a BHP using the Dutch *VPT-Planning* system. Applicants who do not have access to the VPT-Planning system and are not affiliated to operators having such access can also submit their request via a specification for a timetable to be designed by the infrastructure manager. Freight train operators may also request specific freight paths instead of hour patterns, and may even request freight paths in the short-term, i.e., a few days in advance. For this, freight train paths are reserved in the BHP (and its elaboration) by the infrastructure manager. Furthermore, the infrastructure manager also reserves capacity for maintenance work.

ProRail Capacity Allocation takes two months for evaluating the BHPs using pre-established planning norms [166, Appendix 25], see also Chapter 3. During this evaluation period ProRail also requests cross-border (passenger and freight) train paths for the international annual timetable at the meetings of the *Forum Train Europe* (FTE), the pan-European organisation for international timetable coordination and harmonization of train paths allocation. After a month an FTE meeting decides on the international harmonization of requests and thereby establishes the international timetables. Around seven months before the start of the new timetable ProRail sends a formal approval to the various train operators with possible alterations to the requested BHPs conform the international timetable and the resolution of conflicting train paths.

After submission of the capacity request to ProRail — nine months before the start of the new timetable — the train operators expand the BHP to standard daily timetables supported by the subsystem *VPT-Jaarplan Dienstregeling* (VPT-Year Plan Timetable). In VPT-Jaarplan Dienstregeling the BHPs are put together to a complete 24 hour timetable with schedules for all train numbers. The basic structure is adjusted by removing (overlapping) train paths to come up with basic timetables for each day of the week taking into account e.g. deviating structures at weekends and restrictions such as bridge openings at special hours. Also standard holiday timetables are prepared. Special consideration is given to rolling stock circulations which must be in balance at all stations during the day, i.e., at each station sufficient units are available for the next period (early morning hours, morning peak, off-peak, evening peak, late evening hours), see Section 2.2.5.

Seven months before the new annual timetable the train operators receive the formal approval by ProRail including possible adjustments. This may lead to modifications of the standard daily timetables and thus also to the assignment of rolling stock. In the next step standard week timetables can be designed with a rolling stock assignment that is also in balance from day to day, i.e., at each station the number of starting units at the beginning of the day must be equal to the number of terminating units of the day before plus the amount already available at the station, see Section 2.2.5.

Two months before operation of the new annual timetable a standard week timetable must be available in VPT-Jaarplan Dienstregeling which is in accordance to the approved BHP. This timetable is then published to the customers (*het Spoorboekje*).

During the year that a timetable is operational the daily plans may still be modified up to the day before using the subsystem VPT-Dagplan. During the entire timetable year the successive daily plans are kept up-to-date conform special circumstances, such as infrastructure unavailability due to scheduled maintenance and running extra trains to accommodate large passenger volumes at special events (e.g. Queen's Day, pop concerts, football matches). This is the most complex part of the timetabling process which requires ad-hoc adjustments of timetable, rolling stock circulations, and crew schedules. Local shunting movements and duty rosters of train crews are also subject to last-minute changes in the day plan depending on availability of personnel, rolling stock, and local infrastructure. The final day plan is sent to VPT-VKL as the *electronic process plan*, which then contains the timetable including rolling stock schedules. The entire railway timetabling and infrastructure coordination process takes about a year from the design of the BHP to the daily timetables before a new annual timetable becomes operational.

2.2.5 Rolling Stock Circulations

The *rolling stock planning* problem assigns rolling stock units to train lines. A train line is generally operated by one type of rolling stock. However, the train length — measured in number of carriages — may vary over the line and over a day according to passenger demand. Passenger rolling stock consists of locomotive hauled carriages, electrical multiple units (EMUs) and diesel multiple units (DMUs). A multiple unit is a train unit of several carriages with a driving cabin at both ends, see Figure 2.3. A specific type of multiple unit may have different subtypes with a different number of carriages, which can again be coupled into larger train compositions to generate trains of various seating capacity. Multiple unit trains are popular in

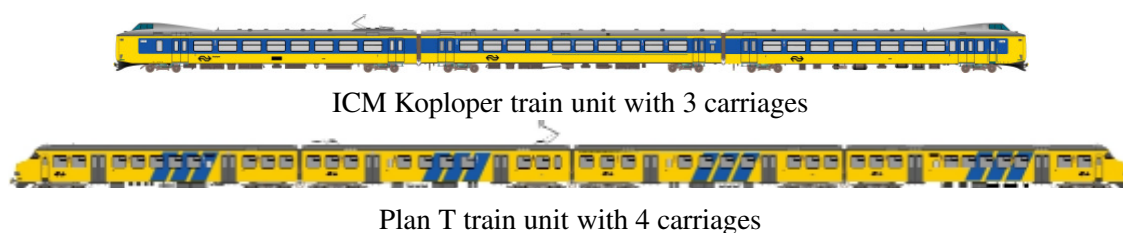


Figure 2.3 Train units for intercity trains (top) and regional trains (bottom)

European passenger railways because of their efficiency in coupling, decoupling, shunting and turning as compared to locomotive hauled carriages. In the Netherlands, passenger train lines are nowadays mainly operated by multiple unit trains.

Rolling stock planning takes several stages. The first step is a basic assignment of rolling stock type to each train line and a feasible allocation of train units to all trains running during a basic (peak) hour. Abbink *et al.* [1] describe a binary linear programming problem to compute the most effective allocation of rolling stock units to trains during a basic hour, where the train capacities match the passenger demand as well as possible. In particular, the *eight o'clock cross-section* is the rolling stock assignment to all trains running between 8:00 and 9:00 in the morning, which is considered the busiest period of the day and thus requires the maximal amount of rolling stock [1]. The constraints guarantee e.g. that the number of allocated train units does not exceed the total available number of units and that the total length of allocated train units to a train does not exceed the shortest platform along the route.

The next step is to expand the eight o'clock cross-section to all hours of the day and each day of the week, where train units may be coupled or decoupled at intermediate main stations in agreement to varying passenger demand on long train lines. The rolling stock assignment must be in balance on each day, i.e., at each station the number of incoming units, outgoing units and shunted units are conserved. Next, the rolling stock assignment must also be in balance *across* the days for all days in a standard week: on each shunting yard the number of overnight train units must meet the number of starting units on the next morning. Schrijver [182] showed that in the special case of one rolling stock type (and subtype) this allocation problem can be formulated as a min-cost circulation problem, which can be solved efficiently by standard min-cost circulation algorithms or linear programming. Multiple rolling stock types and/or subtypes however result in a multi-commodity flow problem, which is an integer programming problem and takes more effort to solve [4, 65, 160, 182].

2.2.6 Crew Schedules and Rosters

The final stage in planning railway operations is crew planning of both drivers and guards, which is again an NP-hard problem. The problem is generally decomposed in two stages: crew scheduling and crew rostering [27]. The *crew scheduling* problem combines train runs into duties. Typically, there are multiple depots and each driver and guard belongs to one depot. A typical constraint in the railway crew scheduling problem is that all crew members start and end in their home depot. The *crew rostering* problem combines sequences of duties into rosters and assigns crew members (drivers and guards) to the rosters. Crew rostering is usually a local planning problem for each depot. NS Reizigers use the crew planning systems CREWS and TURNI to compute crew schedules and rosters [125].

Crew schedules obviously generate dependencies between trains because a crew must be available before a train can depart. Rosters contain at least two duties (because of a lunch break in between) and so drivers and guards must transfer from one train unit to another in their duty roster. To prevent delay propagation, crew transfer times must contain buffer time. It may also be effective to combine driver/guard pairs into rosters to prevent dependencies from multiple ‘feeder’ trains. For a wide range of practical considerations of railway crew planning in the Netherlands, see Kroon & Fischetti [125].

2.3 Safety and Signalling Systems

Railways have unique characteristics that result in potential risks: heavy vehicles run at considerable speed over fixed rails while braking capacity is small due to minimal friction between metal wheels and rails. These characteristics generally prevent that trains can be brought to a standstill within the distance that can safely be observed by the driver and neither is a driver able to steer away to avoid conflicts. Therefore, railway networks are equipped with safety systems for excluding risks of derailments (by e.g. a broken rail, open movable bridge, unlocked switch), collisions between trains, collisions between trains and road vehicles on level-crossings, and accidents with maintenance workers.

The main interface between the safety system and the trains are the trackside signals which can be partitioned into automatic and controlled signals. Train separation on open tracks is guarded by automatic block systems in conjunction with automatic train protection (in the Netherlands). Block signals protect block sections and operate completely automatically based on train detection and interlinked signals. Block systems are complemented by train protection systems to further avoid human errors or failure (of the train driver). Signals also protect routes through station layouts to avoid head-on, end-on, and flank collisions. These signals are controlled by dispatchers and the interlocking system. Safety and signalling systems rely on train detection systems for track occupancy and track-free detection.

The next subsections give a concise overview of the various railway safety and signalling systems with an emphasis on the current situation in the Netherlands. More background on railway systems can be found in e.g. Bailey [12], Fenner *et al.* [63], Hall [92] and Pachl [158]. Van der Werff *et al.* [206] give a historical survey of the signalling systems in the Netherlands.

This section subsequently considers the following topics: train detection (§2.3.1), fixed block systems (§2.3.2), automatic train protection (§2.3.3), train describer systems (§2.3.4), interlocking systems (§2.3.5), dispatching systems (§2.3.6) and traffic control systems (§2.3.7).

2.3.1 Train Detection

In modern railways the presence of a train on a track section is automatically detected by train detection systems, which act as the sensors to the railway safety and signalling systems. The most common train detection devices are track circuits and axle counters. More precisely, track circuits and axle counters are *track-free detection* systems. This means that they either detect that

- the track section is free, or
- the track is occupied or there is a failure in the detection system.

This design of train detection is based on the fail-safe principle which prevents that a track section is faulty detected clear.

Safety systems rely on track-free detection systems to prove that a track section is clear before trains are given permission to enter a route, a switch can be operated, a level-crossing is released, et cetera. Additionally, these detection devices are used as train *passage detection* to trigger e.g. automatic level crossings. Passage detection is also used for non-vital functions such as train monitoring (train description) and feeding passenger information panels.

The most used train detection device is the *track circuit*. A track circuit is a track section where a weak electric current circulates over both rails and a connecting electric wire at the section ends, which are electrically insulated from its adjacent track circuit. The current is fed into the track circuit by a power supply at one end while at the other end the current passes through a relay, which remains energized as long as the track is free. When a railway vehicle enters the track section the low axle resistance causes a short circuit and diverts the current away from the track relay which then drops indicating an occupied track. In addition, power breakdown, a break of the rails or any bridging of the rails by an obstacle also causes loss or diversion of current and thereby a drop of the track relay. Also track circuits using a single rail exist. Track circuits have varying lengths ranging in the Netherlands from 25 m to 1200 m (600m for single rail). The minimum length must exceed the longest distance between two axles to avoid loss-of-shunt. Track circuits are usually of short length in junction and station areas, and long on open tracks.

An *axle counter* is a train detection device that consists of (two) wheel detectors and a counter. At both ends of a track section a wheel detector is attached to the rail. When a train passes over a wheel detector each wheel is detected and stored in the counter. At the other end of the track section the number of passing wheels are also counted and if the two counts agree the section is assumed to be clear. Axle counters are used on non-electrified railway lines operated by (light) diesel trainsets. Note that axle counters can not detect track obstructions.

A part of a track that is equipped with a track-free detection system is also called a (track) *section* based on the track circuit terminology. A track is hence divided into sections that represent the smallest units of train detection. This should not be confused with block sections nor train number positions which may contain multiple track sections on a train route, see Section 2.3.4.

2.3.2 Fixed Block Signalling

Trains have to be protected against head-tail collisions on railway lines between stations (open tracks). In modern railways this is mainly realized by *Automatic Block Signalling* (ABS). The open track is here partitioned in *fixed block* sections, which may be occupied by only one train at a time. Each block section is protected by a signal that gives permission to the driver to enter the block (proceed aspect), or if the block is occupied by another train then the driver must stop the train in front of the signal (stop aspect). The name *open track* refers to the proceed aspect (green light) shown by all block signals in the absence of running trains, i.e., if a train enters an open track and no other train is present then the train can run over the open track

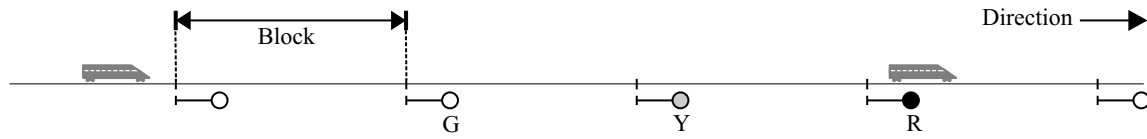


Figure 2.4 Three-aspect fixed block system

unhindered. Block signals are *automatic signals* operating automatically based on the train detection devices. In contrast, the *starting signal* at the entry of an open track and the *home signal* at the end of the open track are *controlled signals*, which are operated by the interlocking system of the associated stations, see Section 2.3.5.

In the Netherlands, essentially a *three-aspect* fixed block system is used, see Figure 2.4. This means that a signal shows one of three aspects: red, yellow or green³. If no trains are present on an open track, all block signals show a proceed aspect (green light). If a train enters a block this is detected by track circuits (or axle counters at non-electrified tracks) and the associated block signal automatically changes to a stop aspect (red light), which instructs a (next) train driver to stop in front of the signal. Moreover, a warning aspect (yellow light) is shown at the entry of the preceding block to notify a train driver that the signal ahead is red and s/he must slow down and prepare to stop. As soon as a block section is detected free and the next signal protects the train, the block signal displays a proceed aspect again, which is yellow as long as the signal ahead is at danger (red). This three-aspect signalling system implies that the distance between any two trains running at unrestricted speed is at least two blocks. If the following train reaches the leading train at a distance of two blocks it must slow down as indicated by a yellow signal. Such a system is therefore also called a three-aspect two-block signalling system.

Table 2.1 Speed signalling aspects in the Netherlands (source: IVW [107])

Signal aspect	Implication
Green	Proceed at the speed indicated by trackside speed signs
Flashing green + speed indicator	Proceed at the indicated speed
Flashing green	Proceed at 40 km/h
Yellow + flashing speed indicator	Reduce speed to the indicated speed and do not interrupt braking when the next signal indicates a further speed restriction (used at blocks shorter than regular)
Yellow + speed indicator	Reduce speed to the indicated speed before the next signal
Yellow	Reduce speed to 40 km/h and drive on sight while preparing to stop before a red signal
Flashing yellow	Drive on sight at a maximum speed of 40 km/h and prepare to stop before any obstruction
Red	Stop before signal

In the Netherlands, block signals are also employed as a *speed signalling* system, see Table 2.1. In speed signalling supplementary speed indicator below the signal shows the permitted speed in a tenth of km/h, e.g., the numeral 13 means a speed of 130 km/h. A yellow aspect and a speed indicator 8 implies for instance that the driver must slow down to 80 km/h before the next signal. Reductions in speed are required to e.g. stop in time for a red signal at short

³In the Netherlands there are no separate distant signals

blocks, for permanent speed restrictions of line sections (by e.g. track curvature, switch speed limits at station areas), or for temporary speed restrictions (e.g. maintenance sites). We refer to Bailey [12] for an overview of the different signalling aspects used throughout Europe.

2.3.3 Automatic Train Protection

Automatic train protection (ATP) systems have been developed to support train drivers and avoid human errors or failure. ATP shows signal information in the cabin (cab signalling), checks whether the driver respects the signalling commands, and intervenes when necessary. In the Netherlands, ATP is used as an additional safety layer above the automatic block system with trackside (block) signals.

In the Netherlands, the ATB (*Automatische Trein Beïnvloeding*) system is used on all electrified railway lines [12, 212]. ATB invokes an emergency braking up to standstill when overspeed is detected without braking activity from the driver within two seconds. ATB supervises five speed limits (40, 60, 80, 130, and 140 km/h) based on track-to-train transmission through a (pulse) code in the track circuits generated by the trackside speed signalling system. The on-board ATB system includes a *cab signalling* display that shows the allowed speed. However, because of the limitation in available speed levels, the cab signal may display a higher speed than the local maximum speed as shown by fixed trackside speed signs and signals. Therefore, the trackside signalling is still decisive while the cab signalling is only supportive. Audible information is given when the speed level changes (gong) and when overspeed is detected without braking activation from the driver (continuous bell). If the brakes are activated the bell signal stops, and when the speed is sufficiently reduced this is indicated by an intermittent bell signal. ATB does not work for speeds below 40 km/h; in this case the driver must follow the instructions of the trackside signals. The 40 km/h speed limit applies when no ATB-code is received. So in the event of signalling failure and absence of ATB-code, the train driver has to rely on driving on sight with a 40 km/h speed limit. ATB is a *continuous* ATP system because of the coded track circuits, implying that a change in aspect of the next signal is immediately transmitted to the train. A driver may therefore increase speed as soon as the cab signalling indicates a less restrictive speed limit. Note that ATB can only be used on electrified tracks with (coded) track circuits.

ATB-NG (*ATB-New Generation*) [212] is used in the Netherlands on non-electrified railway lines and for light trainsets that are not detected well by track circuits. ATB-NG relies on axle counters for train detection and separate beacons between the rails for data transmission. ATB-NG applies a speed supervision in steps of 10 km/h and in particular also supervises speeds below 40 km/h. The information received from a beacon contains the distance to the next signal (beacon) and the maximum speed allowed at this point. Using additional static information on the train characteristics the onboard equipment computes a braking curve that must be respected by the driver. Hence, a train operating with ATB-NG does not have to slow down immediately when passing a (yellow) warning signal — as in ATB — but according to a train-specific braking curve. However, ATB-NG is an *intermittent* ATP system, implying that track-to-train data transmission only occurs at discrete points on the track. Intermediate aspect changes of the next signal are therefore only received at the next beacon.

Most Dutch railway lines are equipped with conventional ATB which is nowadays also known as ATB-EG (ATB-first generation) to distinguish from ATB-NG. ATB-NG is implemented on

several railway lines in (mostly) the east and north-east of the Netherlands. A few local Dutch railway lines still have no ATP-system installed [165].

2.3.4 Train Describer Systems (TNV)

Each running train is assigned a unique number by which it is recognized by the control systems and railway personnel. The *train number* or train description describes the train line and starting time: the first part denotes the train line number (characterizing the train type, terminal stations, route, and served stations) and the last two digits represent a counter for the successive trains over the day. As an example, consider the regional train line 5600 Utrecht-Zwolle. The first train departs from Utrecht at 6:02 with train number 5615, the next train departs at 6:32 with number 5617, et cetera, until the last train of 0:02 with number 5687. The even numbers are used for the trains in the opposite direction. These numbers are also shown in the published timetable [152] and the online train travel planner.

A *train describer* is a system that identifies a train at a particular position and keeps track of its progress at discrete steps over its route. In the Netherlands, train describers are known as TNV-systems (*Treinumervolgsystemen*). The position of a train number is based on TNV-windows. A TNV-window is a route between two (not necessarily adjacent) signals. At the start of a train journey the assigned train number is inserted into the TNV-system at the TNV-window of the departure platform. This insertion is either done manually by a dispatcher or automatically (e.g. at line ends). The TNV-window in which a train number is located is called its train number position or *TNV-position*. The movement and direction of a train is deduced from received safety and signalling information of signal controls, switch detection, and track circuits. The next TNV-position is determined by the set route after the destination signal of the current TNV-position. A TNV-step of the train number to the next TNV-position is triggered when the train enters the first associated track section. Hence, the TNV-position of a train corresponds with the track circuit occupancy but moves in larger steps. See Bailey [12] for more background on train describers.

The Dutch railway network has been partitioned into 13 TNV traffic control areas, each having a separate TNV-system. If a train approaches an adjacent traffic control area, its number is transmitted to the associated TNV-system. When the train enters the next traffic control area the train number is cleared from the current TNV-system and inserted into the next.

A TNV-system must be continuously aware of the state of all relevant signalling controls and monitoring information, including track, signal, switch, and route relays. It therefore scans and records messages received from signalling control systems (EBP and EBS, see §2.3.5), other TNV-systems, and manual instructions from operators. Based on this information it keeps track of the TNV-positions of all train numbers in the system, determines TNV-steps, and inserts and deletes train numbers. Finally, the TNV-system communicates TNV-steps to the corresponding train traffic control system (VPT-VKL) and passenger information systems (BEPAC). Figure 2.5 shows the data flows between a TNV-system and its control environment.

A TNV-system keeps a real-time record of received inputs and TNV-events. These *TNV-logfiles* contain chronological information about all signalling and interlocking events in a traffic control area. TNV-logfiles thus contain invaluable realization data of railway operations, although quite inaccessible by their size (about 25 MB ASCII-format per day per TNV-system). Therefore, the

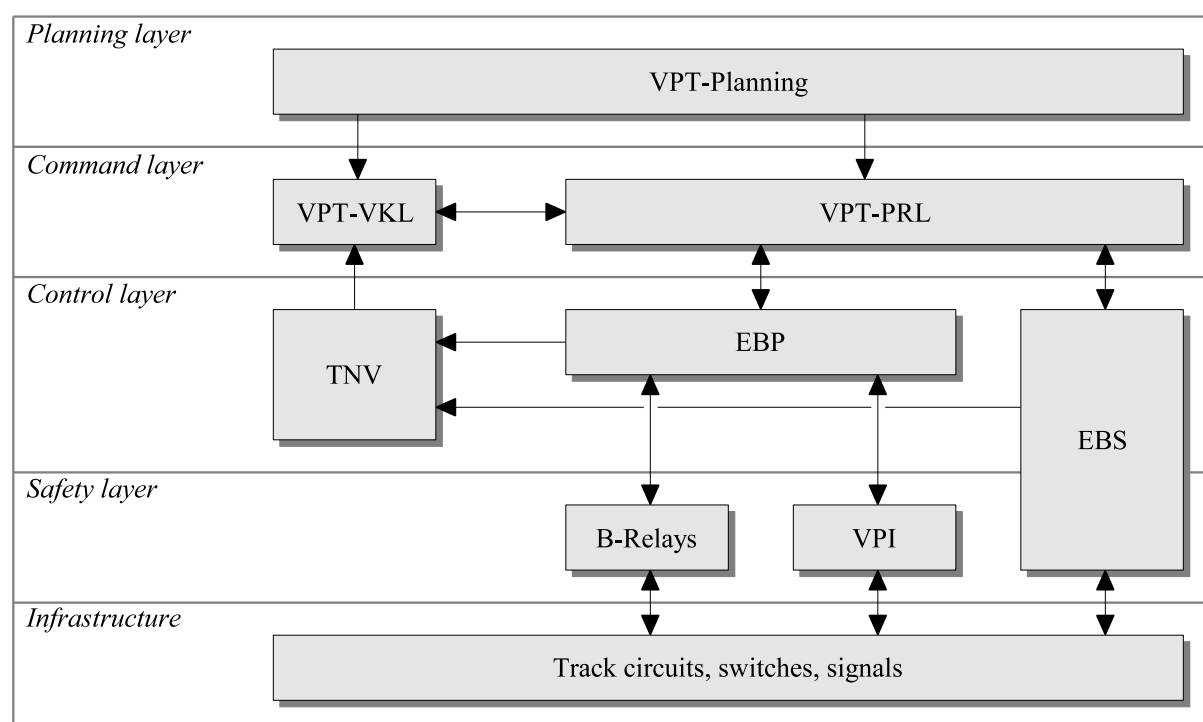


Figure 2.5 Architecture of the Dutch signalling system

TNV-Prepare application has been developed to recover appropriate events along a train route from TNV-logfiles, see Chapter 4.

2.3.5 Interlocking

Interlocking systems ensure safe train movements at junctions or station layouts by interlocking switches and signals to prevent conflicting or not properly set routes. Interlocking systems essentially consist of vital and non-vital functions, which may either be integrated or separated. Vital functions must guarantee safety of operations and are based on the fail-safe principle. These functions include control of switches and prevent simultaneously authorizing conflicting routes. This part of the interlocking is also called the *safety system*. Non-vital functions include the user interface with dispatchers and communication with the safety systems. This part of the interlocking is also called the *control system*.

In the Netherlands, the interlocking areas are remotely controlled from one of four centralized traffic control (CTC) centres. The classic operator interface consists of a control desk or monitor showing the track layout with push buttons for manual route setting in the appropriate places. Indication lamps (LEDS) on the control desk or on a separate indication panel are provided to confirm the various steps in the route setting and locking, and to indicate the passing of a train through a set route. Routine operations are addressed by a timetable-based automatic route setting (ARS) program. Manual route setting consists of pushing a sequence of three buttons (either physical or via a keyboard): first one of several common buttons for respectively a normal, automatic, or drive-on-sight route, followed by a button at entrance, and third a button at exit. A route is manually cancelled by pushing a common button followed by pushing the

entrance button. During the late 1990s the operator interface has been integrated in the VPT-system, see Section 2.3.6.

After request of a route the interlocking system applies the following three steps:

- (i) *Route calling*: the interlocking system checks the availability of the chosen route. The availability check typically requires switches on the route in correct position or free to move, no opposing route called, local control (for shunting) not selected, staff protection system not in use, and no route already selected from the entrance signal.
- (ii) *Route setting*: when a route is proved available, it is automatically set, that is, switches move to their required position and are locked.
- (iii) *Route locking*: immediately after the route has been set it is locked. After a proved route locking the entrance signal is allowed to show a proceed aspect.

If a train does not traverse a set route and a conflicting route is required to be set, the original route has to be cancelled. To ensure that a route is not released in the face of an approaching train it is *approach locked*. In the Netherlands a time delay of two minutes is used during which a set and locked route can not be cancelled. The approach locking starts immediately after the entrance signal is cleared. As long as this signal has not yet been cleared the route can be cancelled without delay. Normally, a route is released by a passing train according to the *sectional-release route-locking* principle, which releases the route section by section after clearance by the rear of the train. A train running over an interlocked route thus generates a number of signalling steps:

- (i) *Entrance signal to danger*: when the train occupies the first track circuit on the set route.
- (ii) *Release of approach locking*: when the train occupies the first and second track circuit of the set route.
- (iii) *Sectional release*: the sections of a set route are successively released by track-free detection.

During the passage of a train *route holding* makes sure that the sections not yet released remain locked. Switches are released together with the associated section(s).

Three types of modern interlockings are currently operable in the Netherlands. The most applied configuration is *EBP (Elektronische Bedienpost)* in combination with NX interlocking based on B-relays for the vital functions [202]. In EBP the non-vital relay logic is executed by computers. The second configuration is *EBS (Elektronische Beveiliging SIMIS)* based on SIMIS (Sicheres Mikrocomputer Siemens) [202]. EBS is an integrated electronic interlocking system in which all vital and non-vital functions are executed by computer programs. EBS is considered fail-safe through a dual hardware structure. Each program is synchronously run on two independent computers, after which both outputs are compared before further processing. Different output shuts down the process output and disconnects energy supply to the elements. EBS is able to control large areas. The third configuration is EBP in combination with *VPI* [202]. *Vital Processor Interlocking (VPI)* is an electronic safety system in which the vital interlocking circuits are represented by boolean expressions and logical rules. VPI runs on only one processor. The fail-safe principle is obtained by running all functions twice in a main cycle and a recheck cycle, and using code words including control numbers. VPIs are particularly applied in smaller station areas.

In the late 1990s, the dispatching system *VPT-PRL* (*VPT-Procesleiding*⁴) [171, 211] was developed containing an integrated interface over the existing interlocking systems so that each workplace is equivalent regardless the underlying interlocking configuration. Indeed, the essential interlocking features are equivalent amongst the different configurations EBP/B-Relays, EBP/VPI, or EBS. In addition, the electronic interlocking systems VPI and EBS include a procedure to check the correct working of track circuits, taking care of occasional loss-of-shunt. The sectional route release is here implemented by *proved sequential* occupation and subsequent clearing of tracks [12, 202].

2.3.6 Dispatching

Vervoer Per Trein (*VPT*) is the information, communication, and command systems architecture of the Dutch train traffic planning and control tasks [54, 171]. The development and implementation of VPT is still an ongoing process that started in 1994. VPT is an integrated interface over the various train control systems that enables a unified and synchronized planning and control working environment. It consists of three subsystems: VPT-Planning, VPT-VKL (Traffic Control), and VPT-PRL (Dispatching). Figure 2.5 gives an overview of the VPT systems architecture.

VPT-Procesleiding (VPT-PRL) is the system concerned with monitoring, dispatching and passenger information used by dispatchers at railway stations. The introduction of VPT-PRL established a uniform workplace consisting of a keyboard, mouse and several monitors, which are used to operate all underlying train control systems, see Figure 2.6. This uniform user-interface replaced the various screens and display panels of EBS and EBP. VPT-PRL also provides a uniform interface to the different interlocking systems (EBP/B-Relays, EBP/VPI, EBS). Each interlocking system communicates with VPT-PRL in the same way (through the interface), by which each location is capable of running the same software on any possible different configuration [171, 211].

Various functionalities were developed and implemented in VPT-PRL to support dispatchers in their route setting task. The *route process plan* contains a database of all possible routes that can be set over the station layout between an entrance track and an exit track including the scheduled times that train movements are to take place. A link with the traffic control system VPT-VKL ensures that the route process plan is kept up-to-date with actual delays and cancelled trains. The automatic route setting system *ARI* (*Automatische RijwegInstelling*) automatically sets all routes specified in the route process plan. ARI is activated (route calling) at the specified time in the route process plan for each arriving, departing, through, or shunting train. Routes are accepted only if several conditions are met: the difference between the actual time and planned time is less than a number of minutes specified by the dispatcher, the starting track contains the correct train number, and the sequence indicated by the process plan is maintained on the destination track (the train sequence on the open track must be respected) [171, 211].

Another feature of VPT-PRL is the Conflict Detection and Decision Support (CD/DS) utility. *Conflict Detection* supports the dispatcher by highlighting inconsistencies and conflicts in the route process plan. Conflicts include broken passenger connections, route conflicts, occupied

⁴VPT (*Vervoer Per Tein*) is the Dutch railway systems architecture developed since 1994. In the international literature the VPT systems are also known as TRACE



Figure 2.6 Dispatcher workplace in a centralized traffic control centre (VPT-PRL)

platform tracks (a platform can only be used simultaneously if trains are coupled), unavailable routes (when part of infrastructure is out of service), and broken rolling stock connections. *Decision Support* helps a dispatcher to resolve detected conflicts. It computes and proposes several sets of actions to obtain a feasible route process plan. If the dispatcher selects one of the recommendations the route process plan is changed accordingly [194].

2.3.7 Traffic Control

VPT-Verkeersleiding (VPT-VKL) is the traffic control system concerned with the daily control of train traffic within a certain traffic control area. The VKL-systems receive daily the actual timetable (day plan) of the day after tomorrow from VPT-Planning (VPT-Dagplan). VPT-VKL supports the traffic controller by maintaining and displaying for any selected corridor time-distance diagrams of the planned (day) timetable, automatically calculating and displaying train delays based on information received by TNV-systems, and showing relevant textual messages that are to be acknowledged [54].

Each TNV-system is linked to a VKL system to which it communicates any change in train number positions (TNV-positions). Based on the train number and its actual TNV-position the VKL-system searches the associated event in the actual timetable. VKL then calculates the deviation from schedule by comparing the receiving time of the train number position message to the scheduled event time using a correction term for the difference in the TNV-measurement point (usually at entry or exit signals) and the associated timetable point (platform centre). The resulting delay message (if any) is shown on the VPT-VKL message display (if it exceeds a predefined threshold) and transmitted to the relevant local VPT-PRL systems. The traffic controller must acknowledge any presented delay message. The calculated realization time (time stamp of train number message and correction time) is also stored in the VKL-database and sent to other VKL-systems if certain conditions are satisfied, as well as to the VGB database (*Vervoersgegevensbank*). The VGB contains the planned and realized arrival, departure and through times of all trains over the last two years for management information and punctuality reports.

A monitor displays a table of current train positions with train numbers and delays (if present in the VKL-database) for any selected corridor, which is updated each minute. Furthermore, a traf-

fic controller can switch between (scheduled) time-distance diagrams for any route, check the timetable of any individual train, and modify the timetable. Mutations in the timetable are automatically transmitted to all involved traffic controllers and dispatchers. The traffic controllers are responsible for controlling the traffic at incidents (e.g. signal malfunctioning, accidents with road vehicles at level crossings, and catenary breakdown), which results in mutations to the timetable. The changes in the actual timetable may also necessitate modifications in train and crew circulations. Since the split of train operators and traffic control this is the responsibility of separate transport controllers from the relevant train operators. These transport controllers are located separately in the traffic control centre and also have access to the VPT-VKL system.

2.4 Train Delays

2.4.1 Primary Delays

Modern railways consist of many interacting processes on a railway network that depend on a wide range of technical devices such as rolling stock, electrification, and safety installations. This leads to potential risks of disruptions to the traffic processes by technical malfunctions and deterioration, e.g. failing moving parts of the infrastructure (switches), damaged door locks, temporary speed limits due to maintenance work, problematic coupling or decoupling, failing braking-test, ATP-application, and engine breakdown.

Train running time between stations and dwell time at stations (slightly) varies for each trip depending on a wide range of factors from within the railway system and from exogenous sources. Internal sources of process time variation are technical malfunctions but also human-related factors such as nonpaying passengers, delay by catering, and large passenger flows (alighting and boarding times). In addition the environment presents exogenous sources of randomness like weather conditions. These sources of random variations are difficult to forecast and form a fundamental part of the practice of railway operations. Therefore there will always be a certain amount of trips that exceed a scheduled process time leading to *primary delays*, although scheduled running times and dwell times usually contain some margin or slack time to compensate for small variations.

Definition 2.4.1 (Primary delay) *A primary delay is the deviation from a scheduled process time caused by disruption within the process.*

Table 2.2 gives an overview of disruptions resulting in primary delays.

Other sources of delay are major *incidents* such as train engine breakdown and damage to the overhead catenary system, which result in large delays. However, these delays are not structural and (should) occur only seldom. Trains affected by an uncommon event experience delays that are clearly not representative to the usual stochastic behaviour. These situations are the subject of incidence management rather than daily operations practice. From a statistical analysis point of view these delays are usually identified as outliers.

The fluctuations in technical and environmental conditions, and behaviour of personnel and travellers make the process times random variables. The main objective of railway traffic management is to keep variations in the process times as small as possible. Therefore, the planned

Table 2.2 Sources of primary delays

<i>Infrastructure: Technical Malfunctioning, Maintenance & Construction</i>	
Rail network	Tracks; Switches; Structures (tunnels, bridges)
Electrification	Supply; Catenary
Signalling	Signals; Interlocking; Train detection (track circuits, axle counters); Automatic level crossings
<i>Train Operators</i>	
Rolling stock	ATB-application; Malfunctioning traction, engine, brakes, running gear, doors;
Personnel	Driver and conductor behaviour (experience, routine, discipline, stress, illness)
Logistics	Loading/unloading; Catering
Train circulations	Shunting; Cleaning; Braking test
Passengers	Volume alighting and boarding; Supporting disabled; Aggression; Nonpaying passengers
<i>Railway Traffic Management</i>	
Systems	Disposition; Traffic control; Communication; Automatic Route Setting
Personnel	Dispatcher behaviour (experience, routine, discipline, stress, illness)
Plan	Timetable bottlenecks; Rolling stock scarcity; Crew scarcity
<i>External</i>	
Weather	Frost; Heat; Wind; Sight; Lightning; Slipperiness (leaves on track)
Vandalism	Track obstruction
Environment	Incidents at level crossings; Animals on tracks; Trespassers on tracks; Suicides

process times contain margins that allow a high probability of process time adherence. Additionally, buffer times between train paths prevent or reduce hinder between trains paths.

2.4.2 Secondary Delays

Train running times are also influenced by hinder of other trains via the signalling system such as a slow train upstream a single track section or a conflicting train movement at a junction or crossing. This results in so-called *secondary delays*. Another source of secondary delays is a scheduled transfer at a station when a connecting train waits for a delayed feeder train.

Definition 2.4.2 (Secondary delay) *A secondary delay is the deviation of a scheduled process time caused by conflicting train paths or waiting for delayed trains.*

A conflicting train path may result from a deviation of another train from its scheduled train path, which occurs both for late and early train. But also a conflict with a scheduled train path due to a primary delay may cause a further increase of the delay. Table 2.3 gives an overview of secondary delays.

The distinction between primary and secondary delays is fundamental. Primary delays cannot always be avoided. On the other hand, secondary delays depend on the interactions on the railway network and synchronization in the train service network. Secondary delays are a major problem if the train service network is highly interconnected and served close to its capacity like in The Netherlands. The occurrence of secondary delays can be reduced by incorporating buffer times in the railway timetable.

Table 2.3 Secondary delays

Type	Example
Hinder	Slow leading train
	Conflicting train route
	Occupied platform track
Synchronization	Transfer connection (waiting for delayed feeder train)
	Rolling stock connection (coupling/decoupling, turn)
	Crew transfer

Two main classes of secondary delays can be distinguished. First, secondary delay results from mutual *hindering* of trains at conflict points. This is a direct consequence of the mutual usage of track infrastructure by different vehicles and the safety and signalling systems in railway systems. The mutual hindering of trains can be influenced by headway buffer times in the timetable. Other solutions are highly expensive and long-term projects: extensions of railway infrastructure like crossovers, overtaking sections, or doubling of rail tracks at certain routes. Substitution of the fixed-block safety system for a moving-block safety system also has a large impact. The minimum headway between trains is then smaller, which decreases restrictions due to crossings.

The second class of secondary delays arise due to *synchronization* of trains at (transfer) stations for logistic or passenger connections. An arrival delay of a feeder train then causes a departure delay to a connecting train that has to wait to secure the connection. Apart from the timetable, these delays depend on the line system, crew schedule, and rolling stock circulation. A transfer connection may be cancelled if an arrival delay is too large. Therefore, a transfer is a flexible or *soft* connection. A connecting train may wait for delayed feeder trains to secure the connection. However, if the delay is too large then the connection is cancelled and the train may depart as scheduled. The maximum train waiting times are regulated by guidelines (the WRT).

On the other hand there are also *hard* connections that cannot be cancelled, for instance train pairs that have to be (de-)coupled at an intermediate or terminal station when coaches change lines. A hard connection thus means that a train can not depart before the connection is completed. Another hard connection arises when (part of) the crew of the feeder train has to transfer to the connecting train. In this case the connecting train can not depart either before (some time after) the feeder train has arrived. The difference between hard and soft constraints should be incorporated in the timetable design process by incorporating enough buffer time in the connection times. Hard constraints are a major cause for delay propagation and can be controlled only by expensive measures like allocating reserve crew and/or rolling stock at stations.

2.5 Conclusions

This chapter gave an overview of the complicated planning process of passenger railways, the railway signalling systems which must guarantee safe train traffic, and the inevitable train delays caused by the complex interaction of human behaviour and technical systems.

Due to the complexity and size of the various subproblems the railway planning process cannot be solved all at once but is decomposed into a number of hierarchical decision problems that are

solved sequentially where each stage is based on the decisions made earlier. The hierarchical approach enables an iterative solution procedure where previous decisions must be adjusted to find a feasible or optimal solution in a later stage, although each stage typically takes several months to complete. The railway planning process is however repeated annually by which solutions of the previous year can be evaluated and reused or improved in the current designs.

The characteristics of railway transport are well-known: the rail-wheel contact allows a minimal friction between vehicle and track which implies an energy-efficient way of transport. However, at the same time the braking distances of heavy vehicles running at high speed require a sophisticated safety and signalling system that protects trains from collisions. We have seen examples of such systems as used in the Netherlands, and in particular saw how trains are automatically detected and monitored. The train description or TNV-system is an important element in the railway systems architecture: TNV-systems inform the dispatcher and traffic control systems on the progress of trains as they run over the network using detailed information received from safety and signalling systems. Both received and generated information is recorded in real-time by the TNV-systems into so-called TNV-logfiles. In Chapter 4 we will see how we can exploit the TNV-logfiles as a reliable and accurate source for analysing the railway traffic and infrastructure utilization.

Railway traffic relies on both human behaviour and a large amount of technical equipment such as the infrastructure, rolling stock and control systems, which are all sources of highly unpredictable fluctuations in performance and more severe disruptions causing primary delays. In addition, because of the interdependencies in the timetable and shared use of infrastructure, existing delays may propagate and thus generate secondary delays. In the next chapter we will see how railway timetables are designed to compensate for delays and reduce or prevent delay propagation.

Chapter 3

RAILWAY TIMETABLES

3.1 Introduction

The quality of a timetable is in first instance determined by realistic scheduled process times for the separate processes. In practice, the individual process times will hardly be exactly the same from hour-to-hour or day-to-day because of variations in internal and environmental conditions. This is accounted for by the inclusion of some time supplement so that the process time can be realized with high probability. A scheduled process time typically consists of the following components:

- a *nominal* process time for ideal or average traffic conditions;
- a *margin* to compensate for less favourable traffic conditions; and
- *scheduled waiting time* to fit the process conflict-free in the timetable.

An example of scheduled waiting time is when the time-distance trajectory of a train run is slightly bended to fit in between other reserved train paths. Another typical occurrence of scheduled waiting time is at a station stop when a train is overtaken by a faster train. The process time margin is usually specified as a fixed percentage of the nominal process time, e.g., 7%. Obviously, the variation in process time realizations should be reflected in the amount of applied margin. A timetable contains various traffic processes: running time refers to a train run from one station to the next, dwell time relates to alighting and boarding passengers, transfer time corresponds to transferring passengers, etc. The expression *minimum* process time is generally used for the sum of the nominal process time and a margin that must be maintained to guarantee a reliable process time. For instance, a minimum transfer time relates to the amount of time that is necessary for a large group of passengers to transfer from the feeder train to the connecting train including e.g. crowding effects at stairways and in pedestrian tunnels on the route from the arrival to the departure platform, and *not* to the time needed by a single fast traveller. The terminology related to running time slightly differs from all other process times: in this case the minimum running time usually equals the nominal running time whilst the running time margin can be used to reduce delays.

To reduce delay propagation an additional amount of slack may be provided between two processes. This *buffer time* is not part of the process time but can be used to even out minor delays. In the case of station dwell time some buffer time may be added before the next train run to compensate for possible arrival delays. In this case the distinction between dwell time margin and buffer time is not that clear. Often a scheduled process time is rounded up to minutes so that the associated events are given in whole minutes. This time supplement may also be interpreted as either margin or buffer time.

In contrast to scheduled waiting time, buffer time can be used to reduce or avoid propagation of train delays. The term buffer time is mainly reserved for time gaps between two events, e.g., between the arrival of transferring passengers at the connecting train and the departure of this train, or between the release of a crossing by one train and blocking the crossing by the next train. Thus, buffer time can be seen as idle time between two train paths that prevents direct hindrance if one of the trains deviates slightly from schedule. In this sense, buffer time is not an integrated part of a process time but increases the interval time between two events corresponding to the end and start of two subsequent processes.

This chapter gives a review of the various timetable components and railway timetabling. Section 3.2 considers train running time. Section 3.3 deals with blocking times and minimum headway between train runs. The next sections consider process times at stations including dwell time (§3.4), transfer time (§3.5), layover time (§3.6) and synchronization time (§3.7). Buffer times and scheduled waiting times are explained in Section 3.8. Section 3.9 gives a literature review of the construction and analysis of railway timetables.

3.2 Running Time

Traditionally, train running times are calculated as the sum of a nominal running time and a running time margin [115, 180], rounded up to whole minutes [179], see Figure 3.1. The nominal running time is calculated using a theoretical running time calculation model using train and track characteristics, see Section 3.2.1. The running time margin is usually given as a percentage of the nominal running time, see Section 3.2.2.

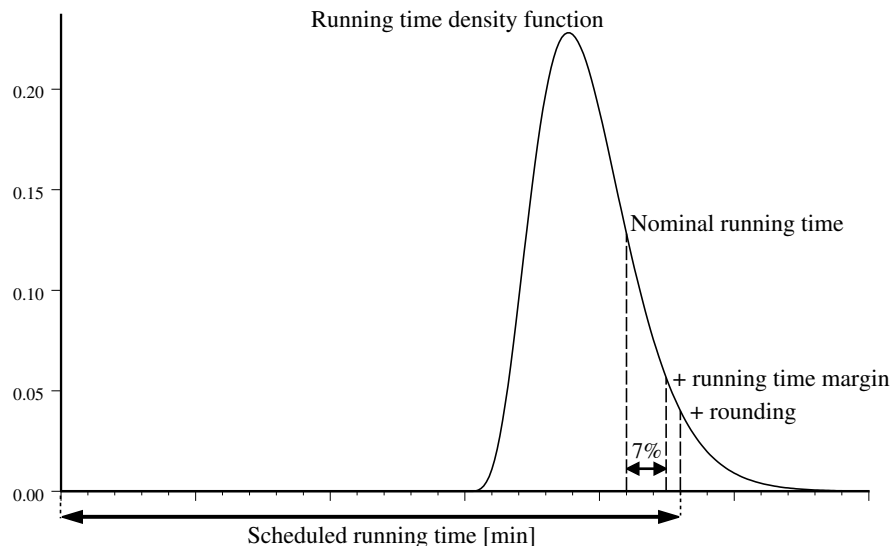


Figure 3.1 Scheduled running time

3.2.1 Running Time Calculations

The *nominal running time* of a train run is calculated from the principles of train dynamics. The change of train speed is determined from the force equilibrium equations of the tractive force

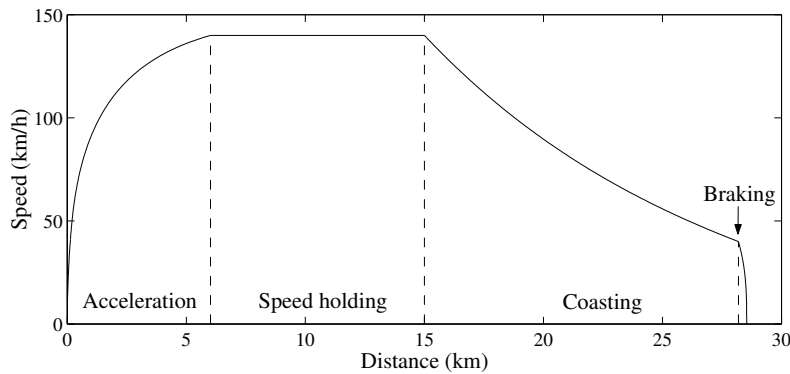


Figure 3.2 Speed profile with coasting regime

and various resistive forces acting on the train during motion [9, 214, 223]. The total resistance to motion is the sum of several resistance components: the running resistance (rolling resistance and bearing resistance), air resistance, alignment resistance (curvature resistance and gradient resistance), and acceleration resistance, and is a function of speed. Tractive effort is the sum of tractive forces at the driving wheels — the wheels providing traction — and is also a function of speed (for fixed control settings).

Depending on speed limit and station spacing a train run has generally five regimes: acceleration, speed holding, coasting, braking, and standing, see Figure 3.2. In the *acceleration* regime tractive effort exceeds total resistance. This phase starts with maximum tractive effort until the power limit is reached. Then this maximum (constant) power is maintained until the tractive effort equals the resistance to motion (for a particular alignment resistance). During this acceleration phase, tractive effort decreases while at the same time the total resistance increases so that the acceleration force is reduced to zero. In the *speed holding* phase the speed is held constant by applying just enough traction to balance resistance. In the *coasting* regime power is turned off by which the train gradually decelerates due to the resistance to motion. Finally, controlled *braking* brings the train to standstill at the specified stop location. For small station spacings the maximum speed may not be reached before braking has to be applied, by which this regime is missing. Also the coasting regime may be excluded in the computation of the nominal (minimum) running time. However, coasting typically slightly increases running time at considerable energy savings.

The nominal running time on a track section is obtained by calculating a feasible speed-distance profile over the open track for given train and track alignment characteristics. The computation of distance as a function of speed requires numerical integration of $\int (v/a(v))dv$, where acceleration $a(v)$ is a nonlinear function of speed given by the force equilibrium equations over the various regimes and track characteristics. The associated running time as function of distance is subsequently obtained by numerical integration of $\int (1/v(s))ds$ over distance [214, 223].

3.2.2 Running Time Margin

A *running time margin* is generally added to the nominal running time, which serves several purposes. First, the running time margin admits *slower train speeds* conform circumstantial de-generated track conditions or lower train power than the design characteristics, see Figure 3.3.

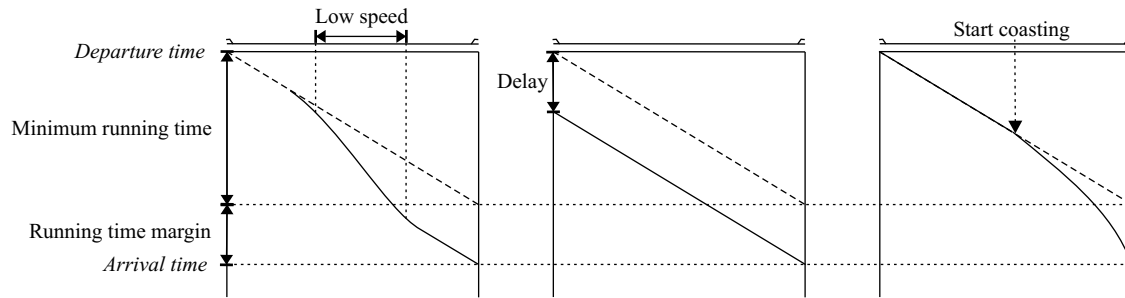


Figure 3.3 Time-distance diagrams demonstrating usage of running time margin: slow train (left); departure delay (middle); minimal energy consumption (right)

Recall that the nominal running time assumes a maximal speed profile in mild weather conditions. In practice conditions may occur that were not accounted for in the running time calculations. Moreover, conditions fluctuate for individual trains and time periods such as train mass, electrical current, weather (wet rails, hot rails, frozen joints, short sighting distance), rolling stock deterioration, rail wear, and driver behaviour. The running time margin hence allows a ‘slower’ speed profile that can be maintained by most trains even in worse conditions.

Second, the running time margin can be utilized as *recovery time* to reduce or eliminate departure delays, see Figure 3.3. If a train departs late the driver is supposed to run with maximal speed to the next station and thus reducing the delay at arrival through an actual running time that is smaller than scheduled. Departure delays at busy complex stations are quite common since early departures are prohibited and hence all departures are more or less ‘late’. Moreover, at transfer stations several trains are typically present around the same time to offer transfers. In the daily presence of arrival delays and extended dwell times conflicting inbound and outbound routes inevitably result in mutual hindrance and delayed route settings with departure delays as a consequence.

Third, the larger running time can be utilized for *energy-efficient* train running by applying a coasting regime [72, 104], see Figure 3.3. So if the margin is not completely needed for compensating slower acceleration or lower power, or for delay reduction, it is exploited for a considerable energy reduction resulting in cost-effective operations. The optimal switching location/time at which power is turned off depends on speed, delay, and remaining track alignment. The more a train is ahead of its schedule the earlier the coasting regime may start, to arrive exactly on-time with minimal energy consumption. The optimal speed profile can be computed in real-time by an onboard computer using optimal control theory, see e.g. Howlett & Pudney [104].

The running time margin is usually a percentage of the nominal running time. The Dutch Railways NS use a margin of 7% of the nominal running time [180]. The German Railways DB use margins ranging between 3% to 7% depending on traction type (electric, diesel), number of carriages, and speed limit [110, 99, 115]. The running time margin is uniformly distributed over each track section between two stops. In Germany, an exceptional running time margin is included on top of the standard margin in the annual timetable when large construction works are planned that inevitably lead to running time losses due to e.g. speed restrictions. These margins are however not spread evenly over the track sections but added just before large (transfer) stations [115]. Note that since the timetable is published in advance for an entire year also

the capacity utilization of large maintenance and construction works has to be incorporated in advance. In the Netherlands such running time supplements are added only when necessary by modification of the daily plan.

The total scheduled running time must satisfy some punctuality norm. For instance, NSR established for the year 2000 that 89% of the arriving trains at a station should arrive within 3 minutes of the scheduled arrival time. The nominal running time and 7% supplement is thus tacitly assumed to satisfy this norm, although this has not been justified by empirical data analysis.

3.3 Blocking times and Minimum Headway

Blocking time is the time interval in which a (block) section is exclusively allocated to a train and therefore blocked for other trains [95]. The blocking time for a running train is hence the virtual occupation time of a section and contains the following parts¹ (see Figure 3.4):

- the *switching time* to set up an interlocking route (0 s for automatic block signals and about 9 s for electronic interlocking),
- the *reaction time* of a train driver, which is the running time from the minimum sighting distance (in clear weather) to the approach signal at maximum speed (9 s),
- the *approaching time*, which is the running time from the approach signal to the main signal,
- the *block running time*, which is the running time between the block signals,
- the *clearing time*, which is the time between reaching the signal at the end of the block and the clearance of the block by the last train axle (depending on train length),
- the *switching time* to release the route interlocking (on open tracks this is equivalent to releasing the block signal at the block entrance).

Note that the approaching and block running time depend on block length and train speed. Hence blocking time is not necessarily equal for each fixed block on an open track, and the blocking times increase if a train runs slower than its design speed. Consequently blocking time is a stochastic variable.

Headway is the time interval between two consecutive trains. Scheduled headway is again partitioned in a minimum headway and a (headway) buffer time. The *minimum headway* is the time interval between two trains that enables the second train to run at unrestricted speed (by enabling proceed signals all the way).

We say that two routes are *conflicting* if they can not be used simultaneously. Conflicting routes occur at merging or crossing routes at junctions or station layouts, but also include opposing single-track routes, and a mutual route of two trains with different speeds or stopping characteristics where the leading train is slower than the following train.

In general, headway constraints may be classified as follows:

¹Generally also a safety margin is included corresponding to an overlap distance behind the signal. The overlap length ranges between 0 and 200 m for the various European railways [12]. In the Netherlands, overlap is not used except for movable bridges, so overlap is here generally 0 m.

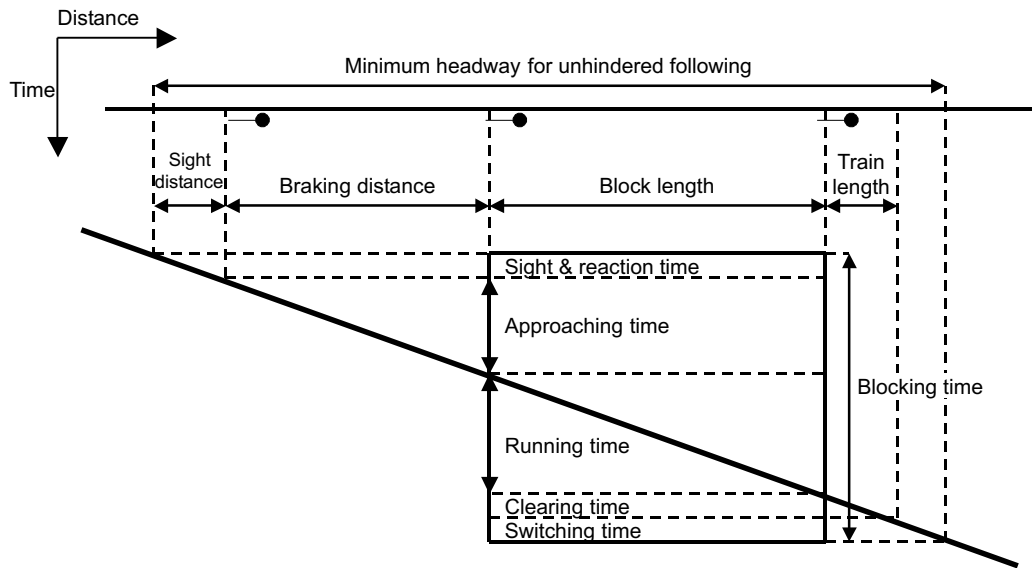


Figure 3.4 Blocking time for fixed block signalling

- *Arrival-arrival headway* between two arriving trains at a junction or on conflicting inbound routes at a station.
- *Departure-departure headway* between departing trains on conflicting outbound routes at a station or on a mutual open track.
- *Arrival-departure headway* between an arriving train on an inbound route and a departing train on a conflicting outbound route.
- *Departure-arrival headway* between a departing train on an outbound route and an arriving train on a conflicting inbound route.

In general, the minimum headway is determined by the blocking time of the mutual track sections and a (possible) running time to the conflicting sections. Hence, the minimum headway depends on speed, acceleration/braking characteristics, (block) section length, and — for headway at stations — the distance between the platform and the conflicting sections.

The minimum headway between trains on inbound and/or outbound routes at a station layout is the route blocking time of the first train with respect to the last conflicting section. This blocking time can be measured as the time interval between the route locking time and the (last) conflicting section release time of the first train, and the additional switching time to set up the route for the second train. Hence, the realized minimum headways can be determined using the infrastructure messages as obtained by TNV-Prepare from TNV-logfiles, cf. Chapter 4. Recall that TNV-Prepare collects the section occupation and clearance times on the inbound and outbound route of trains, the switch position lockings, and the aspect changes of the station entry and exit signals.

For fixed block systems the minimum headway between two trains running in sequence over an open track without overtaking facilities depends on the train speeds and block lengths. The following theorem is based on Dilli [57], who derived a general minimum headway equation for two sequential trains based on the running times to the successive blocks on the open track and their blocking times. Recall from Section 2.3.2 that the blocking time of a block section

includes the approaching time from the warning signal, which in the Netherlands is just the previous main signal. In this case, the minimum headway between two consecutive trains is defined by the following theorem.

Theorem 3.3.1 (Minimum headway on open track) *Consider a track between two stations that is divided into n blocks. Let $t_i^{(1)}$ and $t_i^{(2)}$ be the running time of the leading (first) and following (second) train to the sighting distance before block i , and b_i the blocking time of block i by the first train. Then the minimum headway is given as*

$$h^{\min} = \max_{i=1, \dots, n-1} (t_i^{(1)} - t_i^{(2)} + b_{i+1}). \quad (3.1)$$

If the sighting time is equal for both trains then t_i may be defined as just the running time to block i .

Proof: Let h^{\min} be the time interval between the departures of the first and second train. Consider any block i . The second train arrives at block i at $h^{\min} + t_i^{(2)}$ after departure of the first train. At this time the block must be free for an unhindered train run of the second train. The blocking time b_{i+1} is exactly the time difference from the moment that the first train is at sighting distance before block i to the signal release time after crossing block i and $i + 1$, see Figure 3.4. So after the blocking time the signal before block $i + 1$ shows a yellow aspect and that before block i shows a green aspect. We must thus have $h^{\min} + t_i^{(2)} \geq t_i^{(1)} + b_{i+1}$ or after rewriting

$$h^{\min} \geq t_i^{(1)} - t_i^{(2)} + b_{i+1}.$$

This must hold for any block i and hence the minimum headway is determined by the maximum over all blocks, which gives (3.1). If both sighting times (running time over the sighting distance) are equal then the difference is zero and hence the sighting time can be discarded in the running times to block i . \square

Feasibility of successive train paths on open tracks with fixed block signalling can be visualized by *blocking time diagrams* [158]. A blocking time diagram is a time-distance diagram showing the blocking times of the successive signals, see Figure 3.5. Theorem 3.3.1 can graphically be interpreted as shifting the blocking time graph of the second train to that of the first until it touches the other blocking time graph on at least one block, the *critical block*. Analogous blocking time diagrams exists for any (fixed or moving block) signalling system [158].

Blocking time depends on block length but also on train length and speed of the first train. So in general the critical block in the calculation of the minimum headway — the maximum in (3.1) — is by no means trivial. As seen in Figure 3.5 the critical block varies depending on the train order of slow and fast trains. If the first train is faster than the second then the critical running time difference $\Delta t = \max(t_i^{(1)} - t_i^{(2)}) < 0$. In Figure 3.5 this situation is illustrated by the first two trains. The first block is critical. The actual headway is increased by additional buffer time above the minimum headway. If the first train is slower then $\Delta t > 0$. This is illustrated by the second and third train in the figure. The one but last (the 8st) block is here critical. Note that the running time difference is a considerable part in the minimum headway. If both trains have the same speed then $\Delta t = 0$ and the critical block is (or are) the one with largest blocking time. In the figure the third and fourth train show this situation, where the second block is critical.

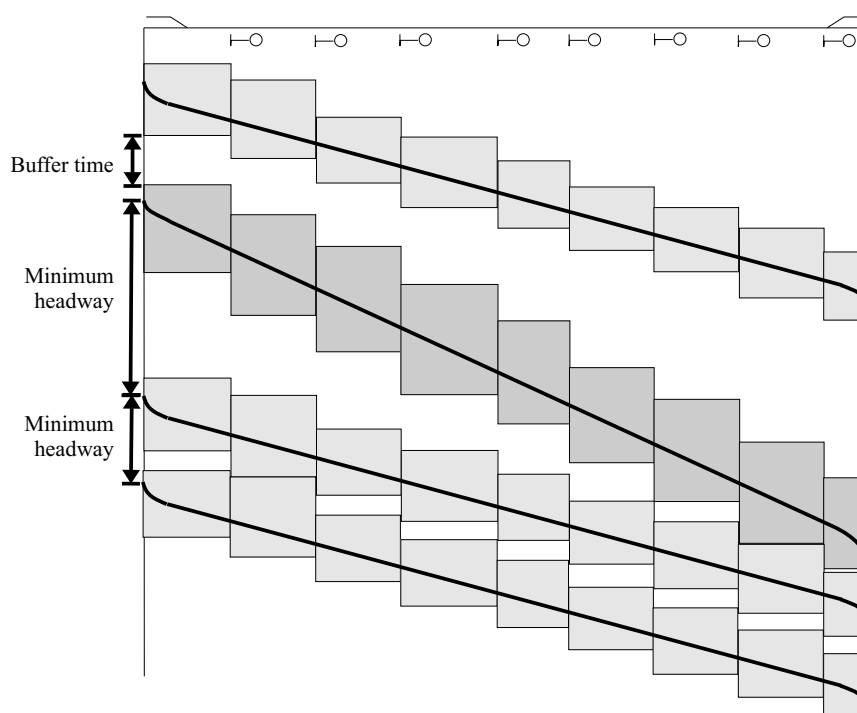


Figure 3.5 Blocking time diagram

The (headway) *buffer time* between two consecutive trains is just the scheduled headway minus the minimum headway, see Figure 3.5. The amount of buffer time (at the critical block) between two train paths determines how much a train may deviate from its scheduled path before it hinders the other train. Table 3.1 shows the generic headway norms used by the Dutch infrastructure manager ProRail in the capacity allocation procedures [215, 166]. These norms include buffer time.

Table 3.1 Headway norms incl. buffer time (source: [166])

Situation	headway (min)
Arrival/departure headway, 1st train passenger train	3
Arrival/departure headway, 1st train freight train	4
Arrival/departure headway, both trains minimum dwell time	4
Headway between two running freight trains	3
Headway at overtaking arriving-through train	2
Headway at overtaking through-departing train	2
Headway at crossing	3
Headway at crossing inbound route close to platform	4
Headway at crossing in station layout far from platform	5

3.4 Dwell Time

Scheduled dwell time at stations or at stops along the open track can be partitioned into several components, see Figure 3.6. The *minimum dwell time* is the necessary time for passengers to alight and board the train, and may sometimes also include a coupling or uncoupling time. The alighting and boarding time depends on train and infrastructure characteristics (number and width of doors, location of the platform accesses, platform width, level difference between platform and vehicle floor, gap between platform and vehicle) and passenger flows, and fluctuates over the day, see e.g. Fiedler [64]. In a periodic timetable a train line schedule is fixed and repeats with a regular interval (e.g. an hour). The scheduled dwell time is therefore also constant and must be determined carefully. A tight dwell time is a source of delay, whilst large dwell time means large travel time and high station capacity utilization. The time for opening the train doors is also included in the minimum dwell time.

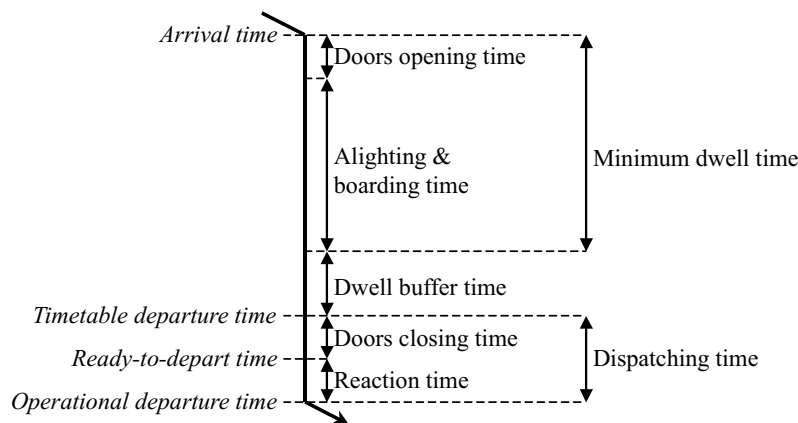


Figure 3.6 Dwell time components

The closing time of doors is usually also considered as a part of dwell time since doors are (or should be) closed while the train is still standing at the platform. However, passengers arriving on time at the departure platform must be able to get on the train, even if they arrive just before the published departure time. This presents a discrepancy in the definition of dwell time, although door closing time only takes a few seconds depending on train type. As shown in Figure 3.6 we distinguish between the scheduled departure time as communicated to the travellers and an operational departure time of the *working timetable* that is used by the railway employees. The operational dwell time covers the published dwell time but additionally includes a *dispatching time* for the departure procedure in which doors are closed and the driver prepares for departure or waits for permission to depart. Note that although published timetables are given in minutes, the operational timetable may be more detailed in, say, a tenth of a minute (6 seconds).

In current Dutch practice, minimum dwell time depends on train type, train length (composition), and station. Table 3.2 gives the minimum dwell time norms for short stops along the open track or small stations. These values are exclusive time loss due to braking from and acceleration to the design speed. At larger (transfer) stations dwell time depends heavily on traveller demand. The minimum dwell time is here adapted to local circumstances and is usually 1 or 2

Table 3.2 Minimum dwell times at short stops (source: [166])

Electric traction	Dwell time (min)
SGM II	0.3
Mat 64, SGM III, SM 90	0.5
IRM, DDAR	0.6
Mat 54, ICM, ICR, DDM	0.7
Diesel traction	
DE II/III, DH, DM 90	0.5

Table 3.3 Minimum (de)coupling times of Dutch passenger rolling stock (source: [166])

Trainset type	Coupling time (min)	Decoupling time (min)
Multiple units	3	2
Locomotive hauled coaches	8	5

min. When rolling stock has to be coupled or decoupled the minimum dwell time is the maximum of the passenger and rolling stock process time. The minimum (de)coupling times are given in Table 3.3. When transfers are scheduled the scheduled dwell time may be increased by synchronization time, see Section 3.7. The minimum dwell time of freight trains is at least 3 min [151, 215].

3.5 Transfer Time

The *minimum transfer time* between a feeder train service and a connecting service is the necessary time in which passengers are able to change trains (with high probability). The minimum transfer time includes alighting time, walking time (including possible orientation), and boarding time. It depends on individual walking speed and acquaintance with the station, the relative position of the arrival and departure platform (cross-platform, two platforms apart, etc.), the geography of the station (platform lengths, distances between platforms, widths of corridors and door-ways, presence of escalators, etc.), and the pedestrian flows and densities in the station and on the platforms. The underlying processes of the (minimum) transfer time are typically stochastic.

In current Dutch and German practice minimum transfer time is determined by some simple rules-of-thumb based on the relative platform positions, i.e., 2 min for a cross-platform transfer, 3 min for a transfer between trains at the same platform but at different platform-ends, 4 min when trains are one platform apart, and 5 min for trains that are two or more platforms apart. Depending on local station geography the minimum transfer time may differ from these guidelines [98, 150]. As a guide to travellers the published timetable booklet (*Spoorboekje*) [152] contains the (minimum) transfer times for the most important transfer stations.

Recent developments in pedestrian flow modelling allow accurate estimations of transfer (walking) times [43, 44]. These models have been developed to evaluate pedestrian behaviour and to support the design of efficient railway stations. However, the models could (and should) also be utilized in the estimation of minimum transfer times and the evaluation of timetable designs.

3.6 Layover Time

Layover time is the time a train spends at a terminal station. The *minimum layover time* depends on train type and possible shunting activities. For turning multiple units (EMUs or DMUs) that continue a train service in the opposite direction with the same driver the minimum layover time is given by the closing time of the cabin on one end, the walking time over the length of the train, and a preparation time for departure in the cabin on the other end. The minimum layover time of locomotive hauled coaches (additionally) depends on possible shunting and coupling activities of the locomotive and the possibilities of the station layout. Also the train composition may be rearranged which requires shunting activities. Table 3.4 gives the minimum layover time norms for various trainsets.

Table 3.4 Minimum layover times of passenger rolling stock (source: [166])

Rolling stock	Layover time (min)
Mat 54, Mat 64, SGM	$2 + 0.3 C + 0.5 U$
ICM, IRM, DDAR	$3 + 0.3 C + 1 U$
DDM	6 – 7
DE II/III	3 U
DH I/II	2 U
Locomotive hauled coaches	7 – 12

Note: U = number of units; C = number of cars within a unit

During a stay in terminals trains may also require cleaning, and toilets may be drained and provided with clean water. These activities are (largely) done in parallel to the technical processes. The maximum of the parallel terminal processes then determines the minimum layover time.

3.7 Synchronization Time

Scheduled dwell time may be increased further by so-called *synchronization time* to enable a transfer. Synchronization is the coordination of the departure of a train to arrivals of other trains to offer a connection for transferring passengers. Synchronization time is hence the additional time over the minimum dwell time that is necessary for the synchronization of the train departure to transferring passengers, see Figure 3.7. It is the time interval from the end of the minimum dwell time to the end of the transfer time relative to the arrival times of the connected train pair.

Synchronization time may effectively be used to compensate for arrival delays in which case it acts as dwell buffer time. On the other hand synchronization time may just be additional (dwell) waiting time if a tight arrival headway links the arrivals of the two connected trains. The effect of synchronization on performance hence depends on the ability of the synchronization time to neutralize arrival delays, see Section 3.8.2.

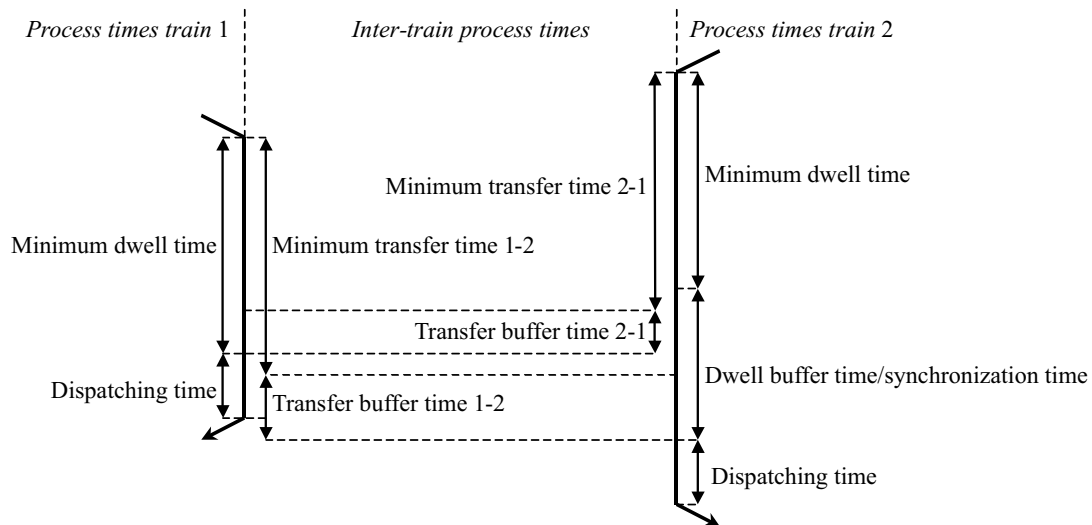


Figure 3.7 Process times in a bilateral transfer connection

3.8 Buffer Time versus Scheduled Waiting Time

3.8.1 Buffer Time

Scheduled dwell time may also contain *dwell buffer time*, which can be used to compensate for arrival delays and/or variations in alighting/boarding times. In the latter respect dwell buffer time is an alternative to running time margins. Note however that dwell time is desired as small as possible from a station capacity point of view. In practice, minimum dwell time is often larger than necessary (in off-peak hours) and can thus also partly be used to reduce arrival delays. In fact, there is no clear distinction between (or knowledge of) minimum dwell time and scheduled dwell time (incl. buffer time). Dwell buffer time can be defined as the difference between the (deterministic) scheduled dwell time and the (fluctuating) minimum dwell time. Viewed this way, in peak hours (with heavy traffic) there is in theory only small or no dwell buffer time, whereas during off-peak hours a larger part of the scheduled dwell time is dwell buffer time.

Transfer buffer time compensates for delayed feeder trains and thus reduces the probability of missing a connection. Note that even within the punctuality norm (say 89% arrival delay with a tolerance of 3 minutes), transfer buffer time is necessary to prevent train delays up to 3 min. Moreover, with the above norm 11% of the trains are accepted to be late for more than 3 min. The amount of buffer time should reflect the importance of a transfer, the arrival delay distribution, and the presence of a bottleneck on the route after the station (by which a departure delay is highly undesirable). Note that transfer buffer time presents additional slack above the running time margin of the feeder train to secure connections without dispatching effort. The amount of transfer time depends on the amount of dwell time and vice versa: if the arrival times are given, fixing the dwell time of the connecting train inevitably determines the transfer time from the feeder train. The analogue is valid if transfer time is fixed. If the scheduled transfer time is too tight and has to be adjusted this also increases the synchronization time and thus also the dwell time, see Figure 3.7.

The *layover buffer time* must guarantee stable train circulations in the sense that delays at de-

parture from a terminal should be minimized. Thus, layover buffer time must secure reliable layover times as opposed to relying on reserve rolling stock at the terminal. Allocating large buffer time at terminals is a convenient measure to secure stable train round trips. In contrast to dwell buffer time and running time margins layover buffer time does not increase passenger travel times, although of course it increases terminal platform occupation. As a guideline for stable train circulations NS prescribes a minimum layover time of 5 min for local trains and 20 min for long-distance trains [180]. These values include layover buffer time.

The round trip time of a train must be a multiple of the (train line) cycle time in order to fit the periodic timetable. The total buffer time in a round trip is therefore given as the amount of time that has to be added to the sum of all minimum process times (running time, dwell time, layover time) to gain a multiple of the cycle time. The freedom of allocation of this buffer time over the round trip depends on synchronization times and scheduled waiting times.

3.8.2 Scheduled Waiting Time

Scheduled waiting time is time loss in the timetable due to infrastructure restrictions. Because of conflicting train movements running time, dwell time, or transfer time may be forced to be longer than the minimum process time. This additional time is called scheduled waiting time. For instance, a transfer time may be forced to be larger than the minimum transfer time due to minimum headway constraints at arrival and departure. This additional time is called *scheduled transfer waiting time*. The minimum transfer time must be respected to allow passengers to transfer, whilst additional scheduled transfer waiting time is required because of train traffic constraints.

Scheduled waiting time differs from buffer time in that it can not be used as recovery time because of headway restrictions. Buffer time increases the operational dwell (or transfer) time for on-time and early arrivals, but in case of arrival delays the dwell (transfer) time may be reduced down to the minimum dwell (transfer) time. Hence, dwell (transfer) buffer time is flexible, whereas on the other hand scheduled waiting time is rigid. This is best explained by means of an example.

A typical occurrence of synchronization time is at bilateral transfer connections between trains that share a common (partial) route, see Figure 3.8. In this figure, train 2 arrives first and is overtaken by train 1 that arrives after a minimum (arrival) headway, stops for a minimum amount of time, and then departs before train 2. Only then train 2 may depart after a minimum (departure) headway. Note that if train 2 is late (and the train order is not changed) then also train 1 arrives late because of the minimum headway restriction. Subsequently, train 1 departs late and because of the departure minimum headway so does train 2. The dwell time of train 2, including the synchronization time, is thus rigid and does not contain buffer time.

Headway restrictions are a source for increased delay sensitivity. Figure 3.8 shows a situation in which the two connected trains are completely tied. Let us consider the comparable situations in which only the headway restrictions are relaxed (and the arrival and departure times stay fixed). If the minimum headway restriction at arrival is reduced (by e.g. a different signalling system) or removed (by e.g. a different platform allocation, four-track route, or a flyover to prevent conflicting routes) then slack is introduced: (part of) the synchronization time of train 2 is replaced by dwell buffer time and (part of) the scheduled transfer waiting time from train

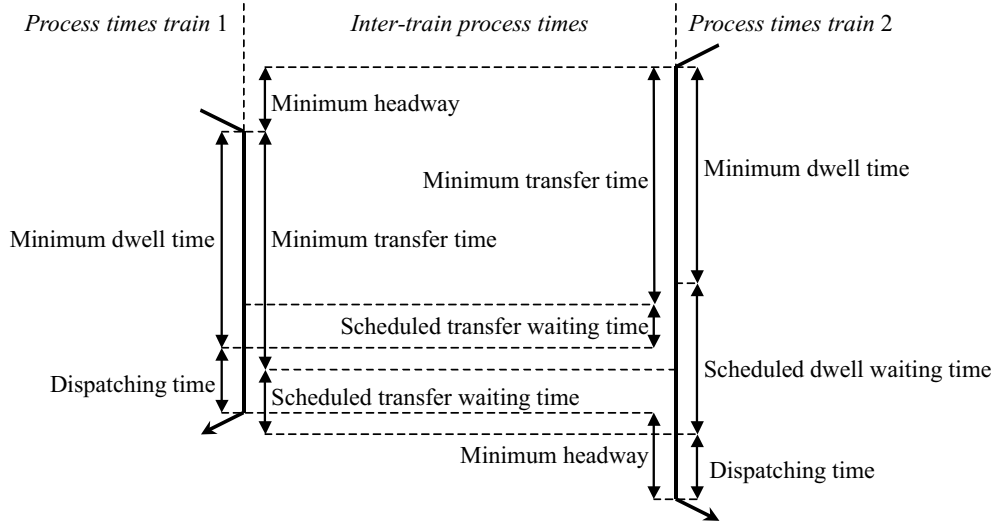


Figure 3.8 Scheduled dwell and transfer waiting time

2 to train 1 becomes transfer buffer time. Note that the scheduled transfer waiting time in the opposite direction (train 1 to 2) does not change. If the minimum departure headway is also decreased or removed then also (part of) the other scheduled transfer waiting time becomes transfer buffer time. If both headway restrictions are completely removed then the situation is reduced to Figure 3.7. If on the other hand only the departure headway is reduced or removed whilst the arrival headway is still respected then only (part of) the scheduled transfer waiting time from train 1 to 2 is replaced by transfer buffer time.

3.9 Literature Review of Railway Timetabling

A vast amount of literature is dedicated to railway timetabling [10, 38]. This section gives a review of the existing literature on the construction and evaluation of passenger railway timetables, with an emphasis on traffic *networks* of *scheduled* train services and thus on interactions and network dependencies between trains rather than on individual train schedules. We first consider the problem of constructing feasible timetables in Section 3.9.1. Section 3.9.2 deals with timetable optimization. Section 3.9.3 considers deterministic models for timetable performance evaluation including methods based on max-plus algebra. Section 3.9.4 considers stochastic models that can be used for timetable performance analysis. These methods are partitioned in timetable-independent queueing models (§3.9.4.1) and timetable-dependent stochastic delay propagation models (§3.9.4.2). Section 3.9.5 considers simulation models of network-wide timetables.

3.9.1 Timetable Feasibility

The construction of a railway timetable has long been an intensive time-consuming and manual task. With the advance of computer technology, many tedious routine tasks were automated, such as e.g. running time calculations. However, a completely automatic construction of railway

timetables is not as easy as it may seem. Scheduling trains involves sequencing of trains on open tracks and synchronizing trains at stations, which are combinatorial difficult problems. In fact, train scheduling belongs to the class of *NP-complete* problems [69], and so are related problems as line optimization, rolling stock assignment and crew scheduling. Hence, railway planning is still a computer-aided interactive affair that requires skills of experienced planners.

One of the main challenges in railway timetabling is the resolution of conflicting train paths. The basic philosophy in railway planning is that a timetable is conflict-free, or *feasible*, in the sense that train traffic is unhindered if each train adheres to the timetable. Feasibility of a timetable is visualized by *time-distance diagrams*, where the horizontal axis corresponds to a route of successive stations and the vertical axis corresponds to time (or vice versa). A train path is then drawn by connecting the scheduled arrival, departure and through times at successive stations. In this way the slope of a line between two points represents the average speed on the associated track. The slope of a fast train is less steep than that of a slow train, and a vertical line represents a stop. Two trains are conflicting if their paths intersect on a single-track section. Many timetable characteristics are clearly represented by time-distance diagrams, such as track occupancy, speed differences (different slopes), train intensity (number of trains), and distribution of scheduled headway at timetable points. Time-distance diagrams are the main tool in manual and computer-aided timetabling and still in use by planners and dispatchers.

Nowadays, running time calculations and drawing of time-distance diagrams are typically supported by computer software based on databases of rolling stock characteristics and the railway infrastructure. An example is the Dutch VPT-Planning system, see Chapter 2. More advanced computerized timetabling support systems are also able to automatically detect and interactively resolve conflicts. An example is the system SCAN (*Schedule ANalysis*) [113] for scheduling train traffic over single-track rail lines with partial double-track sections where trains can pass (opposite trains) or overtake.

Time-distance diagrams indicate train paths based on timetable points (junctions and stations) and scheduled event times (arrival, departure or through times), and as such do not accurately show the infrastructure occupation times. Hence, buffer times can only be roughly estimated, and conflicting routes in stations or critical blocks on open tracks may not be identified exactly. The traditional time-distance diagrams are therefore no longer sufficient to represent the infrastructure utilization in dense network timetables, where various rail lines meet at complex station layouts.

Brünger [23] developed the interactive scheduling system FAKTUS (*FAhrplanKonstrukTion und -UnterSuchung*), in which the relation between timetable and infrastructure utilization is captured by explicitly computing the *blocking times* of successive block sections at open tracks and routes in stations. In brief, a blocking time is the time interval that a track section is exclusively reserved for one train [95]. Assuming a fixed block system, the time-distance diagrams are enhanced by showing the blocking times associated to each train path. The distance axis now also specifies the trackside signals and route release points, and the blocking times of the successive sections takes the form of a block step function, cf. Figure 3.5. A conflict is now clearly visualized by overlapping blocks, which implies that a track section would be occupied by two trains simultaneously. Hence, in a feasible timetable the time-distance blocks do never overlap. The *minimum headway* between two departing or through trains is given by the minimum time interval between the two departures so that the block step function of the second train just touches that of the first train. Any additional time gap at this *critical block* is *buffer*

time. FAKTUS requires a detailed modelling of railway infrastructure, for which a separate module SPURPLAN was developed by Deutsche Bahn (DB) [23]. In SPURPLAN the railway infrastructure is modelled as a directed graph with node weights. The modules SPURPLAN and FAKTUS are integrated in the system RUT (*RechnerUnterstütztes Trassenmanagement*), which is now the standard timetable design tool of the German Railways (DB).

Schrijver & Steenbeek [184] use a combinatorial model for the computation of a feasible periodic timetable. Their *feasibility problem* is based on the *Periodic Event Scheduling Problem* (PESP) introduced by Serafini & Ukovich [188]. PESP is the problem to find a feasible solution to a system of *periodic time window constraints*. In this model the time differences between two periodic departure times $x_i, x_j \in [0, T)$ are constrained by time windows, i.e., $(x_j - x_i) \bmod T \in [l_{ij}, u_{ij}]$, where T is the period length (usually $T = 60$). The modulo operation represents that the *periodic (departure) events* repeat each T minutes. The modular constraints can be *lifted* to mixed-integer constraints by explicitly modelling the modulo operation as an integer multiple of the cycle time [183, 188]. Then the constraints take the form $x_j - x_i + z_{ij}T \in [l_{ij}, u_{ij}]$ with $z_{ij} \in \mathbb{Z}$. Using these integral variables PESP is reformulated as a mixed-integer programming (MIP) problem. Serafini & Ukovich [188] proved that PESP is NP-complete, see also Odijk [154] in the context of the timetable feasibility problem. Characteristic to the timetable feasibility problem is the large number of constraints with “wide” time windows, i.e., $[l_{ij}, u_{ij}]$ with $0 \ll u_{ij} - l_{ij} \leq T$ corresponding to minimum headway constraints. The constraint propagation algorithm developed in Serafini & Ukovich [188] does not perform well for these instances. Schrijver & Steenbeek [184] developed an alternative powerful constraint propagation algorithm, called CADANS (*Combinatorisch-Algebraïsch Dienstregeling Algoritme voor de Nederlandse Spoorwegen*), which is capable of computing feasible timetables (if they exist) for the national Dutch railway network in reasonable time (several seconds to 15 minutes depending on the constraints). Also several other algorithms have been developed. Odijk [153] developed a cutting plane algorithm, which was successfully applied to small instances (large stations). Wezel *et al.* [225] developed a genetic algorithm for quickly finding suboptimal solutions.

The performance of CADANS led to the development of the Dutch timetable design system DONS (*Designer Of Network Schedules*) by NSR and Railned (ProRail) to support railway planners in the construction of feasible timetables [101, 102]. The time window model is consistent with the practice of railway planners, who use guidelines for e.g. a minimum dwell time or transfer time and maximum waiting times that should not be exceeded. In the DONS interface planners give minimum and maximum values for all process times between train runs, such as dwell time, transfer time, coupling time, and layover time, as well as minimum (time) headway between two train arrivals, departures, or through times at conflict points. DONS transforms the specifications into periodic time window constraints and sends them to the solver CADANS. If CADANS finds a feasible timetable satisfying all the constraints the timetable is returned as a list of successive arrival and departure times for all train lines. If on the other hand no feasible timetable exists then CADANS gives a minimal set of conflicting constraints, which should be relaxed by the planner before a feasible solution can be found. These conflicting constraints also indicate bottlenecks in the timetable or infrastructure.

In CADANS complex station layouts are modelled as black boxes. Hence, local feasibility within station layouts is not taken into account. Therefore, a second module was developed to check whether the computed network timetable is feasible with respect to local infrastructure.

Zwaneveld [230] defined the problem of routing trains through a railway station as finding a feasible (or optimal) assignment of trains to station routes and platforms given the station layout and the arrival and departure times of trains. Typical constraints include capacity, interlocking system, and cross-platform connections. Zwaneveld *et al.* [231] show that this station routing problem can be modelled as a *weighted node packing problem* and present a branch-and-cut algorithm, combined with efficient preprocessing and valid inequalities techniques, that is able to solve the problem for all Dutch station instances. This algorithm is implemented in the system STATIONS as part of DONS [230].

3.9.2 Timetable Optimization

An optimal network timetable is a feasible timetable that optimizes some objective function. Hence, the timetable *optimization* problem can be seen as an extension to the timetable *feasibility* problem. Obviously, an optimal solution to the optimization problem is also a solution to the associated feasibility problem, but the reverse is generally not true. If the feasibility problem is NP-complete then so is the associated optimization problem. An added difficulty in the formulation of the optimization problem is the choice of an appropriate objective function. A typical objective is the minimization of passenger waiting time resulting in short transfer times at transfer stations.

Weigand [220, 222] considered the problem of minimizing passenger waiting time in periodic railway timetables. He used a graph-theoretic modelling approach by defining a directed (*transport chain*) graph from the train line data as follows: a node is defined for each train service between two (transfer) stations, and an arc between two nodes represents a station stop or passenger transfer. A weight is assigned to each node corresponding to the associated (fixed) running time, and arc weights correspond to minimum dwell/transfer times, which are interpreted as minimum waiting times. The variables are the additional “network caused” waiting times (buffer times) on the arcs. Weigand observed that in acyclic graphs network caused waiting time does not occur. However, if the graph contains cycles then at least one arc in each cycle must contain buffer time. The total buffer time on any cycle is determined by a cycle constraint: in a periodic timetable the oriented sum of running times (node weights), minimum waiting times (arc weights), and buffer times (variables) on the cycle must be a multiple of the timetable cycle time. Note that without loss of generality the node weights can be included in the arc weights, which transforms the transport chain graph to a traditional weighted digraph with arc weights only [81].

From graph theory it is well-known that a finite graph has a *fundamental cycle basis* of $\nu = m - n + c$ linear independent cycles, where m is the number of arcs, n the number of nodes, and c the number of strongly-connected components [16]. Any cycle can be generated by a combination of cycles from this basis, and if each fundamental cycle satisfies the cycle constraint then any cycle does. Hence, the (minimum) number of constraints on the buffer times in a periodic timetable is equal to this *cyclomatic number* ν . The resulting problem is a mixed integer program (MIP) with m continuous variables (the buffer times) and ν integers corresponding to the ν cycle constraints. The cost function is a weighted sum of buffer times, where the weights correspond to passenger volumes. Weigand [220, 222] described a heuristic in which all buffer time in each fundamental cycle is assigned to the cycle arc with minimal weight. This problem is equivalent to finding a maximum spanning tree, i.e., a spanning tree that maximizes the sum

of its arc weights (passenger flows). The arcs of this maximum spanning tree are then assigned zero buffer time and the nontree arcs get all buffer time. Since this solution is suboptimal, the algorithm proceeds by successively trying to improve the solution using a simplex method and exchanging basis variables for nonbasis variables until no more (one-step) improvement can be obtained. The heuristic performs well for small networks, but the computation time increases exponentially with the size of the network [220] and also the error relative to the optimal solution increases with network size [193].

Stemme [193] extended Weigand's MIP model with maximum waiting times on each arc of the (transport chain) graph. The cost function is again the weighted sum of buffer times over all arcs. Stemme also used the arc lower and upper bounds to compute a lower and upper bound on the integer variable associated to each fundamental cycle. Stemme [193] describes a branch-and-bound algorithm for solving this MIP problem to optimality. The method is applied to the Berlin underground network giving the optimal solution in 59 CPU minutes.

Nachtigall [141, 142] formalizes the MIP with cycle constraints and proves that the problem is NP-complete. A branch-and-bound procedure becomes more effective when inequalities are added to the constraint system that tighten the feasible (integer) region. Therefore, Nachtigall [142] derived two classes of facet-defining valid inequalities and developed two polynomial separation algorithms for generating strong cutting planes. These inequalities can be computed in a pre-processing step and added to the constraint system to tighten the feasible region. Nachtigall & Voget [143] also developed a *genetic algorithm* to find suboptimal solutions to the MIP-problem.

An alternative MIP-formulation is the time window constraint system of PESP and CADANS. Krsta [122, 123] used this constraint formulation including minimum headway constraints as in CADANS. The linear cost function is the weighted sum of synchronization times (dwell and transfer waiting times) in the network timetable. The weights are defined as the number of through (transfer) travellers at the stop (transfer), which are obtained from the traveller assignment model PROLOP [20] (cf. Section 2.2.3). Since the passenger flows depend on the waiting times in the timetable, Krsta proposes an iterative method of passenger assignment and timetable optimization. However, convergence of this iterative approach is not guaranteed. Krsta uses the commercial optimization software CPLEX to solve the MIP directly. Lindner [128] combined the PESP formulation of timetable constraints with line optimization constraints with the objective of minimizing the operational costs. For practical instances from the railways in the Netherlands (NS) and Germany (DB) the resulting MIP could not be solved directly by a commercial solver (CPLEX) within a day. Lindner therefore described several preprocessing techniques, valid inequalities and relaxations, and developed a branch-and-bound procedure to tackle the problem. In particular, reduction of the number of transfer constraints is necessary to solve practical instances within a few hours. For instance, the NS-intercity network and the DB-intercity network with 40 transfer constraints could only be solved in about 10 hours.

It is remarkable that the authors using the time window formulation include infrastructure constraints, whilst in the cycle constraint formulation infraconstraints are neglected. Nachtigall [142] proposed to indirectly include PESP-constraints in the problem formulation using a penalty term in the objective function. However, the MIP problems with cycle constraints and time window constraints are mathematically equivalent and correspond to different matrix representations of the same underlying digraph, as shown in Goverde [81]. In the time window

constraint system the (node) event times are the decision variables and the problem is formulated using the arc-node incidence matrix $M \in \{0, \pm 1\}^{m \times n}$ of the digraph as

$$l \leq Mx + zT \leq u, \quad z \in \mathbb{Z}^m,$$

where x is an n -dimensional vector of (departure) event times associated to the n nodes, l, u are m -dimensional vectors corresponding to the time-window bounds, and z is an m -dimensional integral vector. On the other hand, the cycle constraint system is defined in the arc tension vector $y \in [l, u]$ as decision variable and using the cycle-arc incidence matrix (or cycle matrix) $\Gamma \in \{0, \pm 1\}^{m-n+c}$ as

$$\Gamma y + zT = 0, \quad y \in [l, u], \quad z \in \mathbb{Z}^{m-n+c}.$$

In graph theory the event times x correspond to node *potentials* and the arc variables y to potential differences or *tensions* [174]. For fixed integers the problem relaxes to the *optimal* or *feasible differential problem*, which is a network programming problem solvable in $O(n^3)$ time [174]. Odijk [153] used this relaxation of PESP in a cutting plane algorithm. The equivalence between both formulations imply that solution algorithms and preprocessing approaches developed for one problem can also be applied to the other. The cycle constraint formulation contains less integer variables (m versus $m - n + c$) and is therefore favourable in direct solution approaches such as branch and bound. Peeters [159] developed an additional class of cutting planes for the MIP problem and did computational experiments to compare the window formulation and the cycle constraint formulation, which confirmed the latter as the best formulation from a solution algorithm point of view.

Most authors of the timetable optimization problem used a linear cost function to minimize the dwell and transfer times in the timetable [122, 136, 141, 193, 222]. This objective gives optimal timetables with minimal transfer times for high priority connections with large transfer flows in case of punctual railway operations. However, in case of delays this timetable is far from optimal: since high priority connections obtain tight transfer times arrival delays result in either missed connections for large amounts of passengers or in many secondary delays when trains wait for important connections. Goverde [81] therefore proposed an alternative objective of a weighted sum of separate convex cost functions of the buffer times. For instance, a cost measuring the risk of buffer time failure, depending on arrival delay parameters, can be used for connections where reliability is important to guarantee e.g. stable train circulations. The cost of a transfer connection is the mean transfer time, which depends on several parameters including mean arrival delay, frequency, and waiting time regulations. For punctual operation the convex functions reduce to the usual linear objective of the weighted sum of all buffer times. With respect to arrival delays, the risk and significance of missing connections are also measured. The distribution of buffer times in the resulting network timetable reflects the priorities between the individual buffer time performance costs. The convexity of the cost functions guarantees that a local optimal solution is also the global optimum. In general, optimization problems with nonlinear objective functions are harder to solve than linear optimization problems. On the other hand, the proposed cost functions penalize large buffer times at stops, connections, and turns, making upper bounds on these buffer times superfluous, which relaxes the feasibility problem [81].

Vromans [213] developed an interesting two-stage stochastic optimization model that combines timetable optimization and simulation. The timetable constraints are based on the MIP formulation of the periodic time-window constraints (see §3.9.1) with fixed integer vector (fixed train

orders), whereas $(\max, +)$ -recursive equations (written as linear inequalities) are used to simulate the timetable with respect to sampled process times. The method starts with a feasible periodic timetable and aims at optimally redistributing margins and buffer times over the timetable without changing the essential timetable structure (fixed train orders). In a first step random disturbances are assigned to the process times representing the process time realizations in consecutive timetable simulation periods. The process time realizations are used in the formulation of a (large-scale) linear programming problem including both the timetable constraints and the timetable simulation model; the event times are the decision variables and the objective is to minimize the (weighted) average delay. The solution to the LP problem is an improved periodic timetable that is optimized with respect to the sampled process times. Convergence with respect to the number of realizations has not been addressed (except for a simple special case). The model has been applied to a corridor of the Dutch Railways (in one direction).

A related model is the *schedule synchronization* problem in which the line schedules (running and dwell times) are fixed. The problem is to determine the optimal departure times of all lines at their starting station such that the costs of the resulting transfer times at stations where the lines meet are minimized. This optimization problem can be formulated as a binary integer program (BIP) [118] or an integer program (IP) [19]. However, infrastructure constraints can not be handled trivially in these formulations. Domschke [58] proved that the problem is NP-complete. Note that this problem can also be modelled using the time window (or PESP) constraints as a special case with fixed dwell times, which then also allows infrastructure constraints. In fact, Migom & Valaert [136] already developed a model resembling the time window constraints for the Belgian intercity network but were unable to solve it. They then fixed all dwell times and solved the remaining problem of finding the optimal departure times at the starting stations. The schedule synchronization formulation is mainly applied to road public transport networks (bus systems).

3.9.3 Deterministic Timetable Performance Evaluation Models

Braker [21] modelled the periodic timetable of the Dutch intercity network as a recursive system in max-plus algebra and analysed its periodic behaviour by solving an eigenvalue problem in max-plus algebra. The max-plus model is essentially given by precedence relations between departure events that model running times, dwell times and transfer times. The variables are the departure times which depend on preceding departures times and the scheduled departure times. The model can be described as a linear system in max-plus algebra of the form $x(k) = Ax(k-1) \oplus d(k)$, where $x(k)$ and $d(k)$ are vectors of the k th actual and scheduled departure times, respectively, and A is a matrix of transportation times corresponding to the precedence relations. The maximum eigenvalue can be interpreted as the minimal cycle time where all trains depart as early as possible and the associated eigenvector gives the earliest departure times. A necessary condition for a stable timetable is therefore that the timetable period length T exceeds the maximum eigenvalue λ , where the difference $T - \lambda$ is the available slack on a *critical circuit*. Van Egmond [207] used the max-plus model to compute the delay propagation of an initial delay. Subiono [196] extended Braker's approach to railway timetables of mixed train types (AR, IR, and IC), see also Olsder *et al.* [156].

The max-plus models of Braker and Subiono captured the essential interconnection structure of a periodic railway timetable and enabled the analysis of network performance and delay propagation over train synchronizations due to passenger transfers and logistic connections of rolling

stock and train crews. However, these max-plus models neglect headway restrictions imposed by the railway infrastructure and safety and signalling systems. Hence, the model results only give a lower bound to the system performance assuming that all timetable slack time acts as buffer time, i.e., the differences between scheduled and minimum station dwell/transfer times can be fully utilized for compensating delays. Note that additional constraints corresponding to infrastructure limitations may limit buffer times and show scheduled waiting times instead, cf. §3.8.

Van Egmond [208, 209] showed that blocking time diagrams can be described by a max-plus *heap* model and that the determination of capacity consumption of a given timetable (compressed sequence of blocking time graphs) equals an eigenvalue problem of the associated matrix. Van Egmond [208, 209] described a *heaps of pieces* [71] model as an *automaton* [71] over the max-plus algebra. The heap model consists of a finite set of fixed-blocks (resources, machines) and a set of train runs (tasks, jobs) specified by their time slots over the blocks corresponding to a blocking time diagram. More specifically, each train run between two stations is represented by the lower and upper contour of the associated blocking time graph, i.e., the lower (upper) contour of a train run is a vector with the i -th entry given by the start (end) of the blocking time of block i in the railway network. The contours define a block pattern called a *piece*. A *schedule* of an ordered sequence of pieces then corresponds to a heap obtained from piling up the pieces starting with a zero ground (all blocks are initially available), similar to a tetris game. The contour of a heap of pieces can be described by matrix multiplication over the max-plus algebra. A square matrix $\mathcal{M}(a)$ is assigned to each piece a as follows: if the piece (train run) uses both block i and j then $\mathcal{M}(a)_{ij}$ is the time interval from the start of the blocking time of block i (element i of the lower contour vector) to the end of block j (element j of the upper contour vector); if $i = j$ is not a block on the train route then $\mathcal{M}(a)_{ii} = 0$; and $\mathcal{M}(a)_{ij} = -\infty$ otherwise (i or j is not on the route). Reversely, a given matrix $\mathcal{M}(a)$ also uniquely defines the lower and upper contour vector of a piece a (up to a vertical shift). The matrix associated to a heap of pieces is given by max-plus multiplication of the matrices of the pieces in given sequence order. This matrix thus corresponds to the tightest schedule with zero buffer time between the train runs at the critical blocks. The upper contour is given by multiplying the heap matrix with the initial vector, and the height of the heap is the maximum of these vector elements, which corresponds to the minimum cycle time of the schedule of the trains in the specified order. The evolution of the upper contour of a heap of pieces by piling up pieces to the heap is given by multiplying the upper contour of the heap by the matrix of the new piece. For periodic schedules the minimum cycle time can be computed by solving the eigenvalue problem of matrix $\mathcal{M}(w)$ where w is the heap (schedule) obtained by concatenating the pieces in the schedule (of one period). The eigenvalue gives the minimum cycle time in the periodic regime. Van Egmond [208] also shows how buffer times can be incorporated in the heap model and how delays propagate over the trains in the schedule.

The max-plus heap model [208, 209] explicitly models the scheduled infrastructure utilization. However, this requires a detailed (microscopic) modelling of the signal locations at open tracks and routes over station layouts, and the determination of the associated running times. On the other hand, the recursive max-plus model [21] gives a macroscopic dynamic description of departure events at stations with only precedence relations between events that model running times, dwell times and transfer times, which are easily obtained from the railway timetable. An interesting question is whether it is possible to combine the two model approaches to obtain a model that describes a scheduled railway system over large networks including infrastructure

utilization but without the extensive input data and model dimension requirements of the heap model. This challenge is addressed in this thesis in the chapters 6–8.

A different approach to capacity assessment of periodic timetables is presented in the Swiss deterministic analytical system CAPRES (*CAPacité de RÉSeaux ferroviaires*) [42, 129]. Capacity utilization of a basic periodic timetable is here analysed by saturating the timetable with additional trains, while respecting all timetable constraints. Running times and dwell times are specified by a minimum and maximum value, which allows some flexibility in the saturation process. The saturated timetable depends on a list of extra trains and a saturation strategy that determines the order in which trains are added to the timetable during the saturation process. This approach is useful in assessing unused capacity (possible number of extra trains) and detecting bottlenecks (critical constraints that prevent addition of a train). CAPRES is used at SBB, RFF, and SNCF.

3.9.4 Stochastic Models of Railway Operations

A timetable that is feasible for punctual train services may still be sensitive to variations in running times and dwell times, and thus perform inadequately in daily practice where running and dwell times vary from trip to trip. Evaluating the performance of a railway timetable in the presence of process time variations is therefore an essential aspect in timetable design. Of particular interest is the propagation of delays over the scheduled train services and the ability of a timetable to reduce delays by built-in running time margins and buffer times.

3.9.4.1 Queueing Models

Queueing models can be used to estimate waiting times in railway operations given a random interarrival process. These models are capable of giving a (rough) prediction of bottlenecks and waiting times which can be translated to the amount of buffer time needed in a timetable with corresponding traffic intensity. Queueing models are mainly applied in strategic capacity assessment studies when details of the future timetable are still uncertain.

Schwanhäüßer and co-workers developed several queueing models to assess the capacity of railway infrastructure in terms of train mix, frequency of different train types, and mean interarrival times [186]. Schwanhäüßer [185] derived analytical solutions to the required mean buffer time on open-tracks such that an acceptable level of total delay is not exceeded. He modelled all possible delay propagations between *train pairs* assuming heterogeneous train traffic with random train orders, exponential interarrival times, and priority rules between different train types. The approach was implemented in the mid 1980s in the MS-DOS application STRELE (*Streckenleistungsfähigkeit*) [186].

Wakob [217] extended Schwanhäüßer's method to the assessment of scheduled waiting time at railway stations and adjacent open-tracks. The approach is based on a decomposition of the station layout into separate route sections, called TFKs (*TeilFahrstraßenKnoten*), that can only be claimed by one train at a time. The TFKs are modelled as single-server queues where the minimum headway acts as service time. The model assumes random train orders, Gamma-distributed interarrival times, and priorities between different train types. Moreover, Wakob assumes that the TFKs are independent and therefore neglects the interaction between train

movements over a sequence of TFKs, see also De Kort *et al.* [51]. Wakob's approach has been implemented in the MS-DOS software ALFA (*Analytische Leistungsfähigkeitsermittlung der FAhrstraßenknoten*) [186], and more recently in the tool ANKE (*Analytische NetzKapazitätsErmittlung*) [201], which is compatible to the infrastructure database SPURPLAN.

Wendler [224] developed several extensions to the queueing models of Schwanhäußer and Wakob based on conflicts between *train triples* and new approximation algorithms, which improve the modelling of TFKs and their interactions. However, the method again assumes random train orders and is thus still not valid for estimating delay propagation in periodic timetables, cf. Wendler [224, §5.3].

Meng [133] extended Schwanhäußer's delay propagation model to train connections in stations and derived analytical solutions for the required mean (dwell and transfer) buffer time at a railway station for Gamma-distributed interarrival times. Train arrival orders are again assumed random and the probability that two trains are connected is proportional to the relative train type combinations over all possibilities. Hence, Meng calculates the mean required buffer time over all trains in a station with respect to all possible future timetables and combinations of train connections. The method is therefore not valid for periodic timetables with fixed train orders.

Huisman *et al.* [105] developed a *product form queueing network* for (large-scale) railway networks. Instead of a detailed modelling of the infrastructure, the model mimics the service and waiting times from the traffic interconnection structure with three separate components: stations, junctions, and connecting open tracks. Only double-track (or multi-track) lines are considered, where each direction has its own tracks. Each track is modelled by two First-Come-First-Serve (FCFS) single-server queues connected by a tandem queue, which represent the train runs corresponding to a given train mix on the open track. The service time of the first and last FCFS queue corresponds to the minimum headway at departure and arrival, respectively, and the total service time of the tandem queue represents the free running time on the open track. The number of queues in the tandem and their service times are chosen such that the mean and variance of the total service time equals that of the free running time corresponding to the train mix. Stations are modelled by FCFS multi-server queues, where the number of servers corresponds to the number of platform tracks and the service time corresponds to the occupation time of a platform track. Hence, it is assumed that each train may use each platform track. Finally, junctions are modelled by either two FCFS single-server queues in case of a fly-over or by an *order-independent* single-server queue for level-crossings. All service times are assumed exponential and the arrivals into the network occur according to a Poisson process. Huisman *et al.* [105] proved that the steady-state distribution of this network is given by the product of the steady-state distributions of all isolated queues. For practical computations explicit expressions are derived for the mean waiting time of each component. This queueing approach again assumes random train orders independent of a periodic timetable.

3.9.4.2 Stochastic Delay Propagation Models

Kraft [121] developed a model for the knock-on delays on a main railway line with several merging and diverging lines operating under a periodic timetable. He considers various cases of headway distributions, including fixed headway, mixed headway, and stochastic headway (shifted exponential and Erlang). The first case corresponds to a railway line with one-way traffic running at a fixed regular interval. The second case occurs naturally when trains on

two or more railway lines merge. For instance, when two lines with equal frequency merge then traffic with twice this frequency results after the merging section, where the headway after merging equals the interarrival times at the merging section. If these interarrival times are equal, i.e., the arrival times of both lines have an offset of half their headway, then a regular headway results after merging. If a train is delayed before the merging section then the order of merging may be changed to minimize total delay propagation. The delay propagation depends on the location of a primary delay: at a merging line, on the main line, or at a diverging line. For railway networks with up to three merging routes and exponential primary delays Kraft derives analytical expressions for the mean total delay associated to the optimal merging orders. The model does not include opposing trains on single-track routes nor cyclic networks.

Weigand [220, 221] considers propagation of delays in scheduled (cyclic) train service networks with a periodic timetable. He assumes exponential delays characterized by two parameters: the mean delay and the fraction of delayed trains, the delay probability. Weigand considers one train run at a time between the departure from one station to that of the next, and iteratively derives analytical expressions of the change in the two delay (mean and probability) parameters. The delay evolution is subsequently derived as the sum of an initial departure delay, a primary delay at the open track corrected by a deterministic running time margin, and secondary connection delays at the next station due to waiting for delayed feeder trains corrected by buffer times. All these delays are assumed independent. The connection delay depends on the number of feeder trains and their arrival delays. If the resulting departure delay is positive then it is used as the initial delay in the calculation of the delay evolution of the next train run. This way the delay propagation of all trains in the network is iteratively calculated. Weigand [220] showed that if on the average the buffer times (including running time margins) exceed the individual primary delays then the system reaches a stable state with a constant mean level-of-delay. For cyclic networks this means that a stable state exists if on each circuit in the network the average buffer time exceeds the average primary delay.

Mühlhans [137] generalized the analytical stochastic model of Weigand by using general probability distributions for the primary delays and recursively deriving cumulative distribution functions (CDFs) for the evolution of delays. The delay evolution is the convolution of the initial departure delay and independent primary delays at several locations of a train run: running time extension at the open track, hindrance at the entrance of a station, dwell time extension, and hindrance at departure. Running time margin is used uniformly over the track and dwell buffer time is incorporated as a shift parameter that reduces the effect of hindrance at arrival and dwell time extension. If the train has to wait for delayed feeder trains then the convolution up to the departure hindrance is multiplied with the product of the individual arrival delay CDFs (shifted by the transfer buffer times) of the feeder trains. This corresponds to the assumption that all arrival delays are independent, in which case the CDF of the maximum delay is the product of the individual CDFs. Finally, the departure delay at the next segment is obtained by convolution with the CDF of the departure hindrance. The CDFs for each train run can be computed numerically, and in the special case of exponential primary delays Mühlhans [137] derived explicit solutions. The approaches of Weigand and Mühlhans only consider secondary delays due to waiting for connections at transfer stations. Delays due to hinder at conflict points or to following trains are implicitly modelled as part of the primary delay on the open track.

Carey [28] considers multiple train services on (unidirectional) single-track lines with stochastic running and dwell times defined by general probability density functions (PDFs) and determin-

istic minimum headway times at station arrivals and departures. Carey derives recursions for the successive PDFs of arrival and departure times for each train and station. The recursions include primary delays (incorporated in the running and dwell time distributions) and secondary delays due to headway conflicts of following trains, which Carey calls ‘knock-on delays’. Furthermore, Carey [28, 29] presents performance measures of travel time or schedule deviations based on the arrival and departure time PDFs which can be used to compare alternative timetables, such as expected arrival lateness (of any train at any served station), the probability of arriving x minutes late, and similar measures for departures. He also proves convexity properties of these cost measures with respect to scheduled arrival or departure times. Using these costs Carey formulates an optimization problem to compute optimal arrival and departure times with the restriction that train orders keep unchanged, which thus corresponds to optimizing the distribution of buffer times over the train line schedules. Carey proposes a cyclic coordinate method to solve the resulting unconstrained convex optimization problem. In a follow-up paper by Carey & Kwieciński [30] the stochastic model is extended to networks with train connections at transfer stations and two-aspect block signalling on open tracks. The latter paper also contains a simple example problem of optimizing the buffer times in a timetable of one train over a single line with five stops.

Higgins & Kozan [100] present an alternative numerical-analytical stochastic model of scheduled urban passenger train networks. The railway network is partitioned into blocks protected by signals, which permit only one train at a time. A minimum blocking time is assigned to each block. If a block contains a station (platform track) then its blocking time includes dwell time. On each block a train suffers a primary delay with certain probability, and recovers with a deterministic scheduled slack time (running time margin and buffer time). Secondary delay may occur due to platform conflicts, transfer connections, turns, fixed train orders (overtaking), and headway conflicts of following trains with different speeds when no overtaking track is available (knock-on delays). The model is a sum of implicit analytical expressions for the expected primary and secondary delay (with incorporated slack times) over all blocks and trains, and is solved by an *iterative refinement* algorithm. The model was applied to a real-life suburban train network in Brisbane, Australia, operated by Queensland Rail (QR). This network consists of 400 km track with 557 blocks operated by 6 train lines. The considered period is the morning peak with in total 157 trains and 148 connections. The model was validated by comparison with stochastic simulation, since historical train delay data was only limited available (percentage of passenger trains less than 3 and 5 minutes late). Primary delays were assumed to follow an Erlang distribution with shape parameter 3 and mean delay of 3 minutes for all blocks, whilst the delay probabilities were estimated depending on block type: no station (0.0001), busy station (0.08), and nonbusy station (0.002). The analytical model was solved in 1 minute and 35 seconds, whereas the simulation model (on the same PC) required 6000 iterations in 5.5 hours. The results of the analytical and simulation model were similar with an *average absolute relative error* of 8%. The analytical model was applied for an analysis of scheduled slack time in the network timetable.

Kaminsky [114] developed a pragmatic approach to compute the optimal headway (and buffer time) between two departing trains based on the performance criterium that a given percentage of delayed trains — Kaminsky uses 80% — does not propagate to the second train. First, the 80th-percentile of the departure delay of the first train is determined using data of the German train monitoring system RZÜ (Rechnergestützte ZugÜberwachung). In fact, Kaminsky uses an approximation by assuming exponential departure delays, which gives an explicit expression in

three parameters: the percentage of delayed trains, the mean delay of the delayed trains, and the desired quantile (0.8). Second, Kaminsky determines the critical block for the *minimum* running times and subsequently the running time margin in the *planned* running time up to this block, which is then subtracted from the percentile. The result gives the buffer time between the two trains. Hence, the method takes into account the infrastructure and block lengths, train speed difference, running time margins at each block, and empirical delay statistics, although it neglects a possible delay of the second train. For crossing train routes the critical block is the one containing the crossing, and for following trains it depends on the train order and speed difference: slow-fast, fast-slow, or equal speed. After determination of the optimal buffer time for each train pair the scheduled departure times are adjusted interactively by the timetable designer to represent the optimal buffer times as much as possible while maintaining the original train sequence and respecting network constraints.

3.9.5 Network Simulation

Simulation is a popular approach to analyse complex systems when no analytical tools are available. However, simulation is typically very time-consuming, which limits its application to scheduled railway traffic over large-scale railway networks. Hence, in practice railway planners are forced to concentrate on stations or rail corridors and thereby discarding network interdependencies. However, with the advance of computer power a number of simulation models have been developed which simulate railway traffic networks.

FASTA (*FAhrplan STAbilität*) [147] is a Swiss discrete-event macroscopic simulation system for stability analysis of periodic network timetables. The railway network is modelled as a directed graph where nodes correspond to stations or junctions and arcs correspond to the connecting tracks. Each arc is assigned an attribute specifying the number of tracks with their allowed traffic direction. Train routes are modelled as paths in the graph, where the exact running tracks are determined dynamically during simulation. Infrastructure constraints are modelled by minimum headway restrictions between trains and the model also considers train connections at stations. Running times can be stochastic. The output consists of the delays on different levels of aggregation.

In the Netherlands, the macroscopic simulation system SIMONE (SIMulation MOdel of NEtworks) has been developed for testing stability and robustness of railway timetables on a network level [134, 135]. SIMONE is compatible with the Dutch timetable design system DONS, by which simulation models are automatically generated from timetable and infrastructure information in the DONS-database. Additional parameters can be set for the stochastic behaviour of dwell times and running times and simple decision rules for solving train conflicts. The disturbances on dwell and running time create primary delays, which may cause conflicts with other trains resulting in secondary delays. Conflicts are modelled using minimum headway at conflict points and occupied platforms in stations. Stations are modelled as black boxes with platform groups assigned to each train line. If the platforms are all occupied then an arriving train has to wait before the station on the open track. The simulation output can be given in statistics for any selection of infrastructure and trains in different levels of aggregation from the entire network and all trains down to a specific station, track or train. Statistics include total delay, ratio between secondary and primary delay, punctuality (percentage of trains less than x minutes late), and percentage cancelled connections. One of the disadvantages of simulation,

in particular for large networks, is the large simulation time. A simulation experiment of the national Dutch network takes several days: one simulation run (20 simulated hours) already takes several hours (including warming-up), and about 50 repetitions are minimally necessary to obtain reliable statistics [210]. SIMONE is used at NSR and ProRail.

Microscopic simulation systems are based on a detailed modelling of infrastructure (including signalling systems), rolling stock and timetable, which enables an accurate computation of running times and blocking times. *Synchronous* microscopic simulation systems give a realistic simulation of railway operations where trains run according to the timetable and react accurately to the signalling system. Also dispatching rules are specified in these simulation models to mimic dispatchers and control centres. An example of a synchronous microscopic simulation system is the Swiss OpenTrack [106, 144].

RailSys [53, 169] is a software system that integrates a timetable and infrastructure manager with synchronous microscopic simulation and automatic dispatching. RailSys allows interactive timetable construction using visualization of blocking time diagrams like FAKTUS/RUT. Moreover, train path conflicts throughout the network are automatically detected and timetable simulation can be used to evaluate the impact of the timetable conflicts. In the microscopic simulation module the effect of (primary) stochastic dwell time delays and departure time delays can be simulated. The secondary delays are computed in the simulation according to the signalling system and timetable connections between trains. This way robustness of the constructed timetables can be evaluated. Recently, an automatic ‘slot search’ has been added capable of conflict-free fitting a new train path in an existing timetable [169].

Gröger [90, 91] developed the *asynchronous* microscopic simulation system BABSI (*BAhnBetriebsSimulation*) for automatic railway timetabling and timetable simulation. BABSI is based on asynchronous scheduling algorithms adopting the blocking time and infrastructure modelling approach of FAKTUS/SPURPLAN (RUT), see §3.9.1. In asynchronous scheduling, trains are ordered by priority and conflicts are hierarchically solved by priority class, i.e., for all trains of the same priority a feasible timetable is computed whilst discarding trains of lower priority and keeping train schedules of higher priority fixed. BABSI uses the asynchronous scheduling approach segmentwise, where the ends of a segment are determined for each train by a scheduled stop with overtaking opportunity. Conflicts are then resolved by asynchronously (re)scheduling all trains (of the same priority) segment by segment in chronological order, which may sometimes require backtracking to earlier conflict resolutions. In the simulation mode, BABSI assigns random delays to trains and subsequently simulates the railway operations where the automatic conflict resolution algorithms mimic the dispatchers. The simulation thus demonstrates the stability of a timetable by comparing the timetable with the simulation output (realized timetable in the simulation). The user can also specify an amount of buffer time that must be considered between the blocking times of the train paths during conflict resolution, which thus results in robust schedules. In the automatic timetabling mode, all train path requests are inserted into BABSI where all conflicts are solved automatically using the internal conflict resolution algorithms, which finally results in a feasible timetable. The behaviour of the conflict resolution algorithms — and thus the resulting feasible timetable — depends on parameters for priorities between the various measures to solve individual conflicts (rerouting, dwell time extension, running time extension, relocation of overtakings or passings, etc.) and rules for (dynamic) train priorities. The asynchronous automatic conflict resolution algorithms in BABSI were developed by Jacobs [108, 109] for the automatic rescheduling tool ASDIS

(*ASynchrone DISposition*) which is also based on the FAKTUS/SPURPLAN methodology.

3.10 Conclusions

Running times and dwell times are stochastic variables. Therefore, a robust timetable contains margins and buffer times to compensate for slight variations in process times. Also buffer times in transfer times and headway times between train pairs guarantee that small delays do not instantaneously result in secondary delays. Intermediate delays that can not be compensated by buffer times are the topic of operational rail traffic management. Large delays due to e.g. track obstruction are controlled by ad-hoc planning strategies. This latter category is beyond the scope of this thesis.

Process times in railway operations generally consist of a minimum process time and an additional buffer time. The calculation of minimum process times is either based on calculation models in normal conditions using mean values of parameters (running times) or by simple experience-based norms depending on local characteristics (dwell time, transfer time, headway). Ex-post evaluation of process times using feedback of realization data is not (a structural) part of the railway planning processes. Until recently the lack of accurate operations data did not allow such an analysis.

Running time margins are computed proportionally to the running times (7%) and mainly serve to compensate for worse (environmental) conditions than assumed in the running time calculation models. Utilization of the margins as recovery time for late departures is hence only moderately applicable. Statistical analysis of running times may be utilized to evaluate running time performance, test dependencies on e.g. departure delay, and improve current running times. Again, this requires availability of operations data.

This chapter furthermore gave an extensive review of existing approaches to construct feasible timetables and to evaluate networks timetables on stability and robustness to delay propagation. The existing railway timetable and operations models can be partitioned into microscopic and macroscopic models. Microscopic models are based on blocking times and require detailed modelling of infrastructure and signalling systems. Conflicting train paths are detected by overlapping blocking time graphs, and resolved interactively or automatically by shifting the overlapping blocking time graphs. Sophisticated software has been developed for timetable construction and simulation of railway operations based on these blocking time diagrams.

Macroscopic models are based on precedence relations between events using (periodic) time window constraints. Infrastructure and signalling systems are also modelled in an abstract way by minimum headway times between events. The resulting constraint system can be used in (mixed-integer) mathematical programming problems to find feasible timetables or to compute optimal timetables with respect to some given objective function. Existing mathematical programming software can be used to compute feasible timetables of large-scale networks.

The (microscopic and macroscopic) models used for the construction of railway timetables are deterministic. Stochastic elements are introduced for evaluation of the constructed timetables. For the microscopic models this leads to simulation models. For the macroscopic models also analytical approaches have been developed based on implicit recursions of distribution functions. The stochastic (analytical and simulation) models obviously require input in the form of

stochastic distributions for delays or process times. Some models assume simple (exponential) distributions, others work for any theoretical or empirical distribution functions. Empirical research on the required distributions is however rarely done, basically because of lack of data. A major drawback of both simulation and analytical stochastic models is the extensive amount of time needed to compute the output, even for medium-sized networks. In practice, railway planners therefore focus on smaller subnetworks and thereby discard network dependencies.

Deterministic max-plus algebra models provide an alternative to stochastic timetable evaluation (simulation) models. Models based on max-plus algebra compute performance properties inherent to the timetable structure and identify the critical processes in large-scale networks. There are both microscopic and macroscopic max-plus algebra models. The current macroscopic max-plus algebra models are only based on the timetable without consideration of infrastructure constraints. This thesis will remedy this shortcoming and make a connection to the mathematical programming models, i.e., the periodic time window constraints are reformulated in max-plus algebra which gives a $(\max, +)$ -recursive system that can be used to derive timetable properties corresponding to periodic steady-state solutions of the dynamic system and to compute delay propagation consistent with the timetable and infrastructure constraints.

The literature review justified the research objectives stated in Chapter 1 to fill gaps in the current knowledge and practice of railway timetabling. In particular, accurate data of railway operations is needed to validate distributions used in stochastic models and simulation tools (research objectives 1 & 2). Moreover, a good alternative to simulation for timetable performance evaluation of large-scale railway networks is still missing. This thesis is concerned with extending and improving the macroscopic max-plus algebra modelling and analysis approach to fill this important gap in the current timetable design process (research objective 3).

Chapter 4

TRAIN DETECTION DATA AND TNV-PREPARE

4.1 Introduction

Quality management is essential for securing quality and reliability of train services and requires regular evaluation of (railway) system performance. Although experienced planners usually have an idea of possible flaws or shortcomings in the timetable, its significance to the actual operations is unknown by a lack of quantitative support. Therefore, punctuality reports based on a day-by-day collection of operations data must be available on a regular basis requiring the automatic retrieval of operations data. Inadequate or deteriorating performance of certain train services is then revealed right from the start, by which instant action can be undertaken to identify and improve deficient processes.

In the Netherlands, ProRail Traffic Control maintains a database of scheduled and realized train event times, the *Vervoersgegevensbank* (VGB), from which punctuality reports are generated [46]. The realization data in VGB are received daily from the Traffic Control System VKL, see Section 2.3.7. The accuracy of these realization times is however in the order of minutes. This inaccuracy is mainly due to the mismatch of measurement location (at signals) and the timetable points at which the scheduled event times are specified (the middle of platform tracks). VKL uses *correction terms* to match the passage of the entry (exit) signal to the actual arrival (departure) at the platform. The correction terms are specified for each signal/platform pair (TNV-windows) and further depend on train activity (arrival, departure, or passage) only. A correction term is thus a constant value for all trains without consideration of train type, rolling stock characteristics, train length, speed at the signal, alternative routes, and stop position at the platform track. In particular, arrival times suffer from significant estimation errors because station entry signals are usually located far from the platform. Arrival time realizations may have an error of several minutes depending on the local situation. The error in departure and through realization times (which are related to exit signals) was about a minute, and since July 1, 2003 improved to about half a minute after removal of a filter in the registration process. The change in the registration procedure did however not improve the inaccuracy of arrival times which are dominated by the correction terms, see Goverde [83] for more details. The VGB is mainly used for statistics of aggregated data and has not been developed for accurate details of individual train activities.

In an international context similar problems have been revealed concerning automatic train data collection. In Germany, Hermann [99] used train describer data from the RZÜ (*Rechnerunterstützte ZugÜberwachung*) Frankfurt for a statistical delay analysis. He also found a discrepancy between measurement locations (at main signals) and timetable points (at platforms).

Hermann approximated the time difference by constant interpolation. In Switzerland, the train describer system SURF (*Système Unifié de Régulation Ferroviaire*) is used — apart from train monitoring — for punctuality analysis and even online checking of train positions accessible to passengers via the SBB website. Trains can be found by station or even by train number. The website shows the actual delay (deviation from schedule) and an estimated arrival and departure time at the desired station or at all stops on the train route. The data is also used by the timetable analysis tool *OpenTimeTable* (OTT) [200]. This tool compares and visualizes scheduled and realized arrival and departure times of daily train numbers in time-distance diagrams. The SBB measurements are also taken at main signals instead of the timetable points (platforms) and correction terms are used to estimate the remaining running time. However, the realization times of SBB have a high accuracy with an absolute error below 20 seconds, because SBB use correction terms differentiated by route, activity, and train type, and moreover locations of signals are optimized.

Feedback of operational data to the planning process is essential for improving punctuality and reliability of railway operations, see also Schaafsma [179]. The availability of accurate data of process time realizations enables the fine-tuning of scheduled process times, such as dwell times, running times, blocking times, headway at infra points, and route setting times. In railway systems small variations in process times may cause large delays if a train has to stop before a stop signal. Advanced statistical analysis of individual train runs and interactions between trains thus requires operational data with an accuracy in the order of seconds. Clearly, the accuracy of individual train event times in the VGB is too rough for such empirical analyses.

Accurate train movement and infrastructure data is available in TNV-logfiles recorded by TNV-systems, although these logfiles are not accessible for direct analysis. This chapter considers the developed software applications TNV-Prepare [84] and TNV-Filter [82]. TNV-Prepare has been developed to match infrastructure events to train numbers based on TNV-logfiles. This gives e.g. the passage times in seconds of (the front and back of) trains on section level in addition to TNV-position level. Moreover, since TNV-Prepare generates the entire trajectory at section level of incoming and outgoing routes, accurate speed estimates of approaching and departing trains can be computed resulting in reliable and accurate arrival and departure time estimates. For this latter estimation problem the accompanying TNV-Filter application has been developed.

The outline of this chapter is as follows. Section 4.2 explains the information contained in TNV-logfiles. The developed software application TNV-Prepare is introduced in Section 4.3 and TNV-Filter in Section 4.4. Finally, Section 4.5 gives conclusions and further recommendations.

4.2 TNV-Logfiles

TNV-systems were already introduced in Section 2.3.4. In brief, TNV-systems are the Dutch train describer systems that keep track of the progress of trains based on train numbers and infrastructure messages. One of the functionalities is to keep records of received signalling information and mutations in train number positions, which results in logfiles of about 25 MB ASCII-code per day for each of the 13 TNV areas. Originally, these logfiles were intended for maintenance only. In a later stadium the logfiles were used for investigation of accidents. For

13-SEP-1997	07:34:39	TNV_PLM	VTNR	1: Verplaatsing 1803 van EHV\$4/4S.1 naar EHV\$64/64S.0.
13-SEP-1997	07:34:43	TNV_PLM	VTNR	2: Invoer 1524 in EHV\$FGI/FGU.0.
13-SEP-1997	07:56:45	TNV_PLM	VTNR	3: Wis 1519 in EHV\$EGI/EGU.4.
13-SEP-1997	08:09:05	TNV_PLM	VTNR	4: Wijzig *00001 in EHV\$2/2S.0 naar 5221.
13-SEP-1997	08:12:58	TNV_PLM	VTNR	7: Generatie van *00001 bij verplaatsing van EHV\$18.
13-SEP-1997	08:26:55	TNV_PLM	VTNR	9: 6423 omgenummerd tot 6426 te EHV\$302S.
13-SEP-1997	08:27:23	TNV_PLM	VGRN\$TNV15	13: 821 is overgedragen aan VS_MT1.
13-SEP-1997	08:28:08	TNV_PLM	VGRN\$TNV12	14: 3625 ontvangen uit VS_AH1.
13-SEP-1997	08:29:06	TNV_DLM	VTNR	103: Elementmelding aangaande BTL\$1270T toestand: BZ_BEZET.
13-SEP-1997	08:29:07	TNV_DLM	VTNR	103: Elementmelding aangaande HMDN\$423AT toestand: BZ_ONBEZET.
13-SEP-1997	08:29:09	TNV_DLM	VTNR	103: Elementmelding aangaande BTL\$94 toestand: SEI_GA.
13-SEP-1997	08:29:25	TNV_DLM	VTNR	103: Elementmelding aangaande BTL\$1358 toestand: SEI_STOP.
13-SEP-1997	08:29:30	TNV_DLM	VTNR	103: Elementmelding aangaande BTL\$1351A toestand: LR_LINKS_V.
13-SEP-1997	08:29:38	TNV_DLM	VTNR	103: Elementmelding aangaande EHV\$21 toestand: LR_RECHTS_V.

Figure 4.1 Example lines in a TNV-logfile

this purpose, the TNV-logfiles were kept for about eight days on the hard disks of the various TNV-systems and then deleted. For the latter objective, the application *TNV-Replay* [162] was developed, which reads the recorded messages one at a time and visualizes the physical events (section occupations and clearances, signal aspects, point lockings, and TNV-positions) in a schematic view of the station layouts on a computer screen. This application is still in use, and is also exercised by traffic controllers to replay and analyse recent traffic situations.

A TNV-logfile contains a sequence of lines with an event logging on each line, see Figure 4.1. A logline includes a date and time stamp, a message code, and the message. The time stamp of a logged event is the time instant at which the event is logged and may hence differ from the actual event time by e.g. transmission delays. The time is given with a precision of a second, or even in decimals of a second. It is however arguable whether a precision of two decimals of a second is still accurate with respect to transmission delays.

The two types of messages in a logfile that are of interest are train number messages and infrastructure messages, see Table 4.1. These are considered in detail below.

4.2.1 Train Number Events

The progress of train numbers through a traffic control area can be derived from the TNV-logfiles by train number messages (code 1 to 14). These messages also demonstrate the operation of a TNV-system. Therefore, we here present an overview of the different messages.

Initial TNV-positions of a train number are obtained from code 2 and 4 messages. A code 2 insertion of a train number in a TNV-window is generated

- manually by a dispatcher at the origin station of a train line;
- automatically after receiving a train number from a TNV-system of a neighbouring traffic control area (code 14);
- after the automatic generation of a train number for an unknown train (code 7);
- after uncoupling and detected shunting movement of a train unit (code 8);
- manually after an incorrect train number deletion.

A code 4 train number change is generated

- automatically after an automatic train number renumbering (code 9);
- manually by a controller after identifying an unknown train that was given a temporary train number (code 7 message);

Table 4.1 Events logged in TNV-Logfiles (translated from Dutch)

Train number events generated by TNV-system		
<i>Code</i>	<i>Event</i>	<i>Message</i>
1	Step	1: Step of <code>trainnumber</code> from TNV-window to TNV-window.
2	Insertion	2: Inserted <code>trainnumber</code> in TNV-window.
3	Deletion	3: Deleted <code>trainnumber</code> in TNV-window.
4	Change	4: Changed <code>trainnumber</code> to <code>trainnumber</code> in TNV-window.
7	Generation	7: Generated <code>trainnumber</code> at step from TNV-window.
8	Derivation	8: <code>*trainnumber</code> derived from <code>trainnumber</code> in TNV-window.
9	Renumbering	9: Renumbered <code>trainnumber</code> to <code>trainnumber</code> in TNV-window.
13	Transfer	13: Transferred <code>trainnumber</code> to VKL-system.
14	Receiving	14: Received <code>trainnumber</code> from VKL-system.
Events received from safety system		
<i>Code</i>	<i>Event</i>	<i>Message</i>
103	Section occupied	103: Message from element <code>element</code> state: OCCUPIED.
103	Section cleared	103: Message from element <code>element</code> state: FREE.
103	Proceed signal	103: Message from element <code>element</code> state: GO.
103	Stop signal	103: Message from element <code>element</code> state: STOP.
103	Switch left	103: Message from element <code>element</code> state: LEFT.
103	Switch right	103: Message from element <code>element</code> state: RIGHT.

- after a shunting train gets ready at its departure platform track;
- after a terminating train changes train line;
- after an incorrect train renumbering.

A code 9 message is an automatic renumbering of a train number at terminals, where a train turns to operate the same line in reversed direction. A code 9 message is automatically followed by a code 4 train number change. A code 7 train number generation is automatically generated after an unknown train step from one to another TNV-window. Such a train number starts with an asterisk (e.g. *00001) and as soon as a controller has identified the correct train number, this temporary train number is changed into its standard train number by a manually generated code 4 train number change.

Once a train number position is known, code 1 messages give the train number steps over successive TNV-windows. A final TNV-position in a control area is given by either a code 9 train renumbering (followed by a code 4 train number change) or a code 3 deletion message. A code 3 deletion is either generated manually by a controller or automatically after a train number transfer to the TNV-system of a neighbouring traffic control area (code 13).

4.2.2 Infrastructure Events

TNV-systems receive messages from the safety and control systems, which are logged immediately after arrival. These messages correspond to a binary change in status of infrastructure elements, and all have code 103, see Table 4.1. A *section message* reports the occupation of a section or a track-free detection. A *signal message* announces that a signal has been set to a stop aspect (red light) or to a proceed aspect (yellow or green light). Finally, a *switch message* communicates a set and locked left or right position of a switch.

These infrastructure events can be associated to a train number that either directly causes the transitions by train detection (section entrance of the first train axle, section exit of the last train axle, automatic signal aspects), or indirect via the interlocking system (route setting and controlled signal aspects). However, an infrastructure message does *not* contain an explicit train number. Recall that a TNV-system operates over a wide area with many station layouts and open tracks. Over this entire area infrastructure messages are communicated to the TNV-system. Hence, a train number message is surrounded by many infrastructure messages and it is not a trivial task to find a train number associated to the infrastructure messages.

4.3 TNV-Prepare

From the TNV-logfiles the progress of train numbers over TNV-windows are easily derived. However, the occupancy of the underlying track circuits gives a much more accurate description of train movements. But track section messages are not matched to train numbers. Recall that TNV-windows usually cover several track circuits (sections) that detect the presence of a train. In this section we show that it is possible to match section occupations to train numbers by posterior analysis of the TNV-logfiles. This method has been implemented in the software tool TNV-Prepare.

TNV-Prepare was developed during 1998/2000 at the Transport and Planning Section of the Faculty of Civil Engineering and Geosciences of TU Delft. It is an empirical analysis tool that converts TNV-logfiles into tables of successive events on a route of a train line, including TNV-steps and state changes of sections, signals, and switches. In the sequel these tables are called *TNV-tables*. The program is written in Delphi and runs on MS Windows 95/98/2000/NT/XP/etc. operating systems.

TNV-Prepare consists of three main modules as depicted in Figure 4.2: The main module TNV-Prepare builds an internal database from TNV-logfiles and additional timetable and network inputs. The module TNV-Report takes care of the actual database search and generation of TNV-tables. Finally, the module TNV-View displays TNV-tables and exports tables to external formats.

4.3.1 The Internal Database

4.3.1.1 Infrastructure Modelling

Within TNV-Prepare, the rail infrastructure is implemented as a set of coupled and connected objects (infra elements). A railway network is basically built up from sections that act as separate train detection units —mostly track circuits. In TNV-Prepare a *section* is also the fundamental element. The model network is constructed in one direction only, by which a section may have up to two successor sections corresponding to a boundary section (zero successors), a track section (one successor), and a switch (two successors). A route over the network is hence always defined in one direction, where an additional toggle determines whether or not the route is run in reversed direction. This approach facilitates and speeds up the network building process.

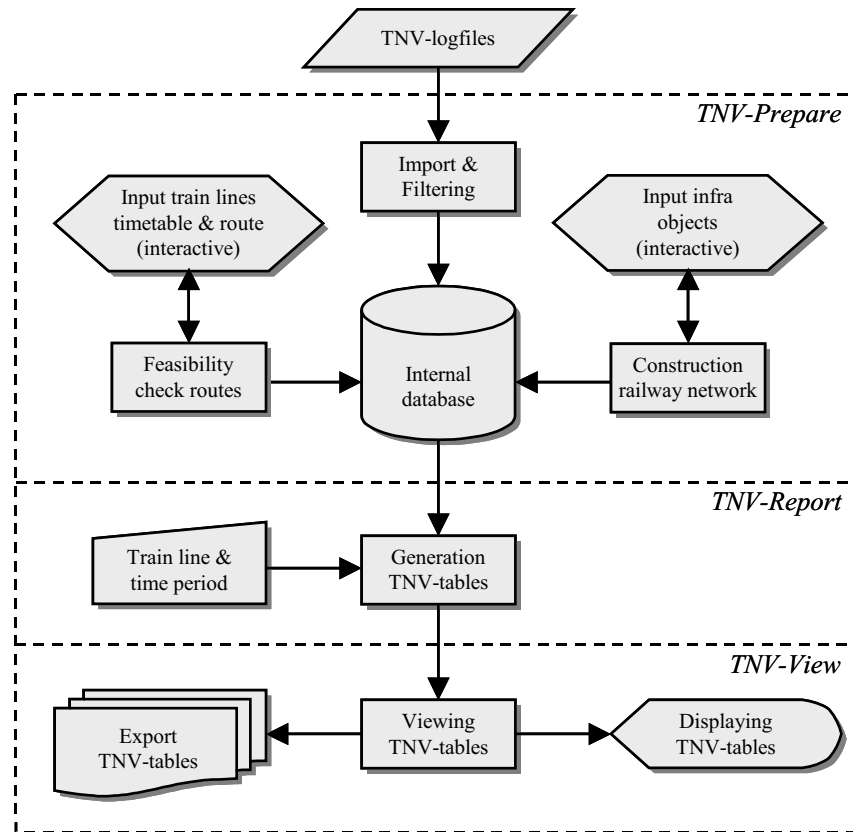


Figure 4.2 Architecture of TNV-Prepare

Additional objects may be assigned to a section according to a geographical or logical point of view: a switch, signal, and/or TNV-position. Coupling of these infra elements to sections requires schematic drawings of station layouts. In the Netherlands these drawings are available at ProRail (Railinfrabeheer), known as OKT-maps *Overzicht Takken en Knopen*. These maps are computer drawings generated by the system CARE [68].

A section may embed a *switch*, in which case it has two successors. A *signal* protects one or more routes defined as a sequence of sections. These routes have the first section in common and the signal hence corresponds to this section. A *TNV-position* is attached to the last section of a TNV-window. Recall that a TNV-step indicates which way a train is heading. So a TNV-position corresponds to a route from the first section after the former TNV-position to the last section of the current TNV-position. This last section hence determines the train target, whereas the TNV-step occurs at the entrance of the first section. It must be noted that in practice several routes—called route blocks—exist from the initial to the final section in a TNV-position. The actual set up route is nevertheless uniquely determined by the locked switch positions at the occurrence of the TNV-step.

4.3.1.2 Setting Up the Internal Database

The TNV-Prepare main module exhibits several functionalities as indicated in Figure 4.2. First, the import utility reads TNV-logfiles and stores the relevant information in an internal database to which the search algorithms apply. New TNV-logfiles can be added whenever they become

available.

Second, the rail infrastructure has to be defined. For each train line an initial and final TNV-position is interactively chosen. If a route between the TNV-positions has not yet been constructed an input session is initiated that determines the sections associated to the TNV-positions and the possible connecting sections in between. This way the rail infrastructure is built up from the parts of the user's interest only. The rail infrastructure will become more complete with each addition of a train line and/or route. Additional objects (switches and signals) can be assigned to a section separately using the object editing utility.

After defining the route the timetable information must be provided, including frequency, the planned arrival and departure time, the platform track section, and possible alternative route(s). Standard routes are constructed using the route editing utility, and can be defined in terms of predefined subroutes which relieves the manual input session. An added route is checked on feasibility with respect to the rail infrastructure, i.e., it has to be a sequence of connected sections. Routes may be defined for different periods in time according to changes in railway infrastructure, and also may depend on train number reflecting different standard platform allocations during the day.

The TNV-Prepare module also contains utilities to edit or add objects, and to view and edit timetable information. These functionalities can be used to adjust incorrect input or to reflect onto changes in the infrastructure or timetable. More details can be found in the TNV-Prepare user's guide [111].

4.3.2 Generation of TNV-Tables

4.3.2.1 Target Events

We are interested in the state changes of subsequent route objects caused by a running train (number), and possibly its immediate predecessor. The TNV-steps are of course the main search events that determine the (rough) train number positions in time. The state of the other infra elements are binary variables: a section is either occupied or free, a switch is either locked in left or right position, and a signal state is either stop or go —where the actual signal aspect also depends on the state of the next downstream signal. With respect to a particular train number TNV-Prepare searches for the *target events* as shown in Table 4.2.

Table 4.2 Objects and target events in TNV-Prepare

Object	Event 1	Event 2	Event 3
TNV-position	TNV-step		
Section	Last clearance	Occupation	Clearance
Signal	Last proceed	Stop	Proceed
Switch	Left position	Right position	

For a TNV-position the target event is a train number appearance in the TNV-window. Generally this corresponds to a TNV-step, but occasionally also a train number insertion or change may be relevant, e.g. for a first train departure from a terminal. A section has three target events: the occupation by the current train (first axle) and the clearance after the current train (last axle),

as well as the last clearance message before occupation by the current train. Note that this latter event corresponds to a preceding train but is worthwhile for capacity analysis. The target signal events are similar: the last proceed message before the approach of the current train, the stop message caused by the passing current train, and the next signal release message. The relevant switch events are the last switch lockings in left and right position before the current train crosses the associated switch section. The switch events are also interesting for capacity analysis.

4.3.2.2 The Main Search Algorithm

This section explains the search algorithm for the target events from TNV-logfiles. The train number events generated by a TNV-system (see Table 4.1) can be used to follow a train number through a railway network. Alternative routes may be possible within the same sequence of TNV-steps, and moreover trains of one train line may stop at different platforms from time to time, which is indicated by alternative TNV-positions and routes.

The TNV-Report module generates TNV-tables based on the data collected by the TNV-Prepare module. The search period for each train number can be restricted by setting two parameters δ_{in} and δ_{out} in order to increase the computation speed for finding the event times associated to objects along the route. For instance, a switch position may not have changed for hours and the exact switching time is then of no interest for the current train. The search period starts at δ_{in} minutes before the first TNV-message and ends at δ_{out} minutes after the last TNV-message of the route. The parameters δ_{in} and δ_{out} can be set between 0 and 10 minutes. If a route event has not been logged within this time period then the associated column entry in the TNV-table is left empty.

Figure 4.3 Input window for generating TNV-tables

The main search algorithm is shown in Figure 4.4. First the user selects a particular train line and a fixed period of interest (a day, a week, a month, etc.) in an input window, see Figure 4.3. Also several train lines and/or periods can be selected. The different jobs are then put in a queue and processed successively. This is convenient as the generation of a TNV-table may take a few minutes to a few hours depending on the PC-speed, the required period (from a day to several years) and route length (a local route within a station vs. a route over the entire traffic control area covering many stations). After the first job has been started intervention of the user is no longer required.

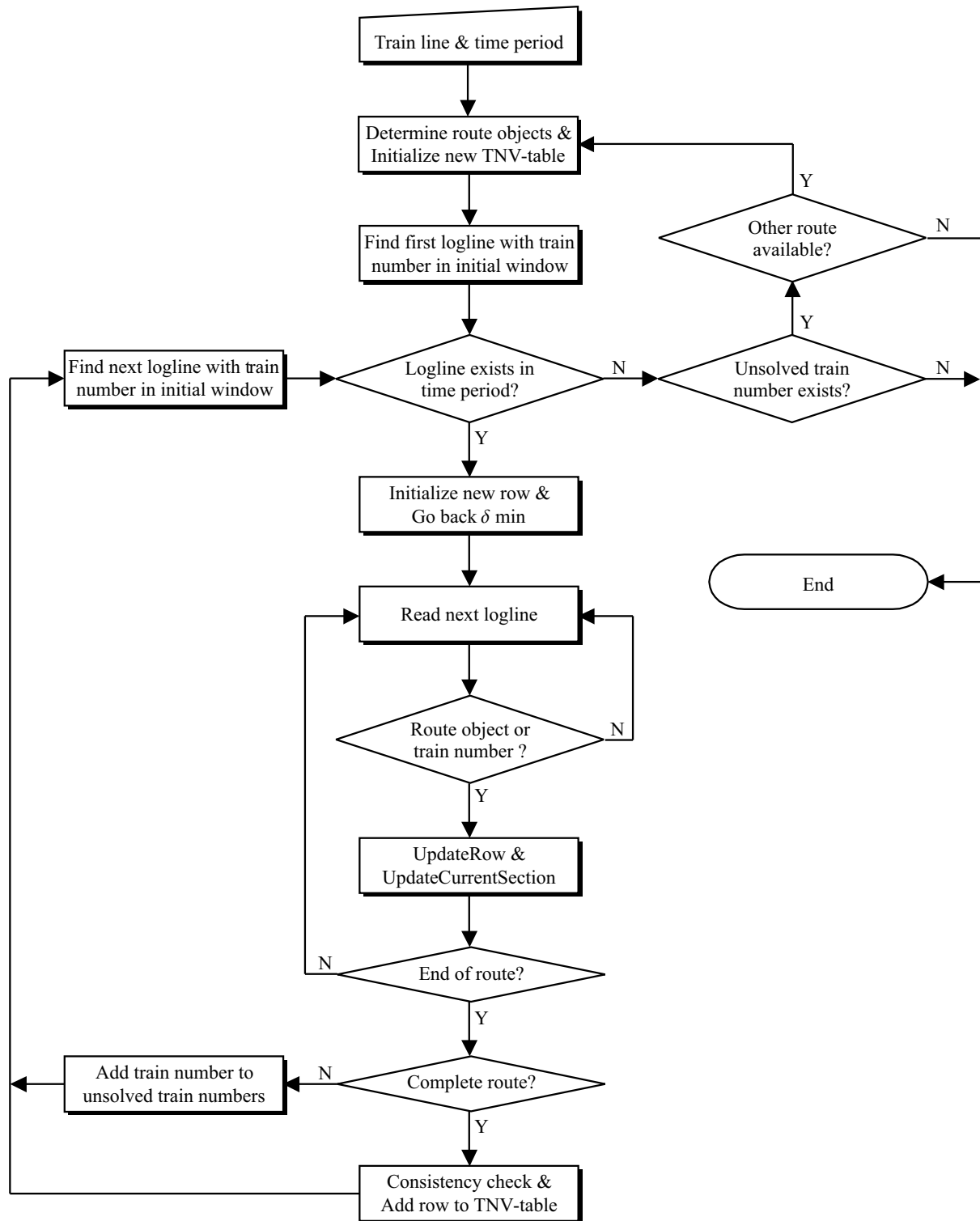


Figure 4.4 Search algorithm in TNV-Prepare

The program then reads the associated timetable information (hourly planned arrival and departure time, frequency, etc.) and selects a route. If alternative routes are available the order has been specified in TNV-Prepare. Next all route objects are determined and a new TNV-table is initialized, that is, columns are constructed for the events associated to each object, in the order of subsequent sections with respect to the train running direction.

The program then searches in the database for the first TNV-message of a train number corresponding to the current train line in the initial TNV-window. If this logline exists the inner-loop train number handling starts at the TNV-message logline. First, the current logline is set back for δ_{in} minutes — the start up time — which is necessary to find preceding events (last section clearances, last signal releases, et cetera). A new row of the TNV-table is initialized with the current date, train number, planned arrival time, and planned departure time. All other columns stay empty. The subsequent loglines are read and for each route object message the TNV-table row is updated using the procedure `UPDATEROW`, and a pointer is maintained to the current section by the procedure `UPDATECURRENTSECTION`, both explained in §4.3.2.3. If the end of the route is reached —marked by a TNV-step to a non-route TNV-position— a preset additional time δ_{out} is reserved for reading subsequent loglines in order to obtain possible additional section or signal releases. If the route has been completed the generated row is added to the TNV-table after a consistency check. Inconsistent event times are rejected resulting in empty entries at the particular columns in the TNV-tables, like lacking data. If on the other hand the train stepped out of the route to an alternative TNV-position then the generated row is completely rejected and the train number (and date) is added to a list of unsolved train numbers, which are handled later as exceptions with alternative routes. This terminates the inner-loop train number evaluation and the program proceeds with the next train number.

If no more train numbers are found or if the end of the period is reached, the list of unsolved train numbers is checked. If this list is not empty the program checks for another available route. If an alternative route exists the program starts all over but only with respect to the unsolved train numbers of which pointers to the associated initial TNV-window loglines have been memorized. If no more alternative route exists, the unsolved train numbers are stored in a log file to the TNV-table. If required, the routes of the unsolved trains can be traced and added to the database later using the TNV-Prepare train route analysis utility. On the other hand if the list of unsolved train numbers is empty then the program goes to the next train line in the queue or if the queue is empty the program terminates.

4.3.2.3 Inner Loop Update Procedures

The inner-loop procedures and `UPDATECURRENTSECTION` and `UPDATEROW` build the TNV-table step-by-step and keep track of the current section, respectively, while going to the successive loglines in the search period. Before describing these algorithms we first need some notation. A logline k in a TNV-logfile can be summarized as (t_k, o_k, e_k) , where t_k is the logtime (including date), o_k the object, and e_k the event in line k . For the infra elements the distinction between object (infra element) and event (state change) is clear and each object has two possible events, see Table 4.1. For a TNV-message we are only interested in the appearance of the current train number in the TNV-position. Recalling Table 4.1, an event is hence a train number step into the TNV-window (code 1), a train number insertion (code 2), or a train number change (code 4). Recall that code 7 and 14 messages are followed by a code 2 message and a code 9 is

followed by a code 4 message, and hence these codes may be used as checks. A train number removal (code 3) may identify the end of a route. A code 13 is again followed by a code 3 message and may thus also be used as a check.

The timetable information of a train line contains amongst others the scheduled arrival and departure time, and the route block from an initial TNV-position to a final TNV-position given as a sequence of sections including a platform section. Define for a given route the set of attached objects as $\mathcal{O} = \{\mathcal{O}_1 \cup \mathcal{O}_2 \cup \mathcal{O}_3 \cup \mathcal{O}_4\}$, where \mathcal{O}_1 is the set of TNV-positions, \mathcal{O}_2 the set of sections, \mathcal{O}_3 the set of signals, and \mathcal{O}_4 the set of switches along the route. Furthermore define the mapping

$$S : \mathcal{O} \rightarrow \mathcal{O}_2$$

that maps an object o_k to its associated section s_k , with the exception of $o_k \in \mathcal{O}_1$ which is mapped to the first section of the TNV-window. Note that the TNV-step occurs at the entrance of the first section of a new TNV-window.

A row in a TNV-table is built up from columns for each route object ordered by successive sections. The sequence of sections on a route defines a partial ordering, i.e., $s_1 < s_2$ means that section s_1 precedes section s_2 in the train running direction. Furthermore $s_2 = \sigma(s_1)$ denotes that s_2 is the successor of section s_1 . Each route object generates a number of columns equal to its associated number of events as given in Table 4.2. By $\text{event}(o_k, i)$ we denote the i th event (column) of object o_k , e.g. if o_k is a particular section s_k then $\text{event}(o_k, 3)$ is the third (clearance) column associated to $o_k = s_k$. The objects associated to a section (TNV-position, signal, and/or switch) are placed after the preceding section columns and before the next section.

Algorithm 4.3.1 shows the pseudo-code of `UPDATECURRENTSECTION`. An update of the current section is only applicable at a TNV-step or section occupation message only. The 1st line updates the current section if the logline is a TNV-step of the current train number. The current section then becomes the first section of the associated TNV-position. If the logline is the occupation of the successor of the current section then the current section is replaced by its successor (lines 2-3).

Algorithm 4.3.1 (`UPDATECURRENTSECTION`)

Input: TNV-logline.

Output: Current section.

```

1  if  $o_k \in \mathcal{O}_1$  then  $s \leftarrow S(o_k)$ ;                                //Logline is a TNV step
2  else if  $o_k \in \mathcal{O}_2$  then                                           //Logline is a section event
3      if [ $e_k = \text{occupied}$  and  $S(o_k) = \sigma(s)$ ] then  $s \leftarrow S(o_k)$ ;
```

Algorithm 4.3.2 shows the pseudo-code of the procedure `UPDATEROW`. The input is a logline (t_k, o_k, e_k) and the TNV-table row of the current train number. The algorithm considers subsequently the four possible object messages. Line 1 states that if the event is an input of the current train number into the TNV-position o_k then t_k is inserted as the event time in the TNV-position column. Lines 2–11 handle a route section event. If the logline is the occupation of section $o_k = S(o_k) = s_k$ and if the current section pointer s has not already passed this section then t_k is inserted as the event time in the occupation (2nd) column of object s_k (line 5). Additionally the clearance columns may have to be updated if these contain an event time

of a previous train (line 6–8). If the logline is a section clearance then t_k is inserted into an empty clearance (3rd) column of section object $o_k = s_k$ (line 10) provided that the section has already been occupied or the section lies before the current section s (line 9). If on the other hand the section has not yet been occupied and s_k precedes the current section s then the section clearance corresponds to a previous train and t_k is inserted in the 1st object column (line 11). Lines 12–21 take care of signal messages. The procedure is similar to a section message. Finally, lines 22–24 are concerned with switch messages. A switch message is only inserted if the switch lies after the current section (line 22), so that the final switching event is the last before entrance of the current train. If the logline is a switch locking in the left position then t_k is inserted in the 1st column of the switch object o_k (line 23), and otherwise it is inserted in the 2nd column (line 24).

Algorithm 4.3.2 (UPDATEROW)

Input: Logline (t_k, o_k, e_k) and current TNV-Table row.

Output: Updated TNV-table row with logged event.

```

1  if  $o_k \in \mathcal{O}_1$  then event( $o_k, 1$ )  $\leftarrow t_k$ ;                                //Logline is a TNV step
2  else if  $o_k \in \mathcal{O}_2$  then                                                //Logline is a section event
3      if  $e_k = \text{occupied}$  then
4          if  $s \leq S(o_k)$  then
5              event( $o_k, 2$ )  $\leftarrow t_k$ ;
6              if event( $o_k, 3$ )  $\neq \emptyset$  then
7                  event( $o_k, 1$ )  $\leftarrow$  event( $o_k, 3$ );
8                  event( $o_k, 3$ )  $\leftarrow \emptyset$ ;
9      else if [event( $o_k, 2$ )  $\neq \emptyset$  or  $S(o_k) < s$ ] then
10         if event( $o_k, 3$ ) =  $\emptyset$  then event( $o_k, 3$ )  $\leftarrow t_k$ ;
11         else event( $o_k, 1$ )  $\leftarrow t_k$ ;
12 else if  $o_k \in \mathcal{O}_3$  then                                                //Logline is a signal event
13     if  $e_k = \text{stop}$  then
14         if  $s \leq S(o_k)$  then
15             event( $o_k, 2$ )  $\leftarrow t_k$ ;
16             if event( $o_k, 3$ )  $\neq \emptyset$  then
17                 event( $o_k, 1$ )  $\leftarrow$  event( $o_k, 3$ );
18                 event( $o_k, 3$ )  $\leftarrow \emptyset$ ;
19         else if [event( $o_k, 2$ )  $\neq \emptyset$  or  $S(o_k) < s$ ] then
20             if event( $o_k, 3$ ) =  $\emptyset$  then event( $o_k, 3$ )  $\leftarrow t_k$ ;
21             else event( $o_k, 1$ )  $\leftarrow t_k$ ;
22 else if [ $o_k \in \mathcal{O}_4$  and  $S(o_k) \geq s$ ] then                                //Logline is a switch event
23     if  $e_k = \text{left}$  then event( $o_k, 1$ )  $\leftarrow t_k$ ;
24     else event( $o_k, 2$ )  $\leftarrow t_k$ ;

```

4.3.3 TNV-Tables

Generated TNV-tables can be displayed in the TNV-View module. Each row of a TNV-table corresponds to a train number at a particular day. The first four columns contain the date, train number, scheduled arrival time, and scheduled departure time. The next columns give the event times associated to consecutive elements on the train path.

Datum	TreinNr	Drg	Drg	256	256	256	EB1/EB1S.0	255T	255T	255T	255	255
		Aankomst	Vertrek	GA	STOP	GA		VRIJ	BEZET	VRIJ	LINKS	RECHTS
1997-9-19	1527	09:24	09:29	09:29:16	09:32:48	09:36:35	09:32:48	09:16:01	09:32:48	09:33:05		
1997-9-19	1531	10:24	10:29	10:21:57	10:32:55	10:35:56	10:32:55	10:18:09	10:32:55	10:33:12	10:12:51	10:30:02
1997-9-19	1535	11:24	11:29	11:28:05	11:30:50	11:34:34	11:30:50		11:30:50	11:31:09		
1997-9-19	1539	12:24	12:29	12:28:06	12:31:17	12:34:26	12:31:17	12:13:44	12:31:17	12:31:38		
1997-9-19	1543	13:24	13:29	13:28:10	13:31:45	13:35:05	13:31:45	13:17:38	13:31:45	13:32:03	13:15:36	13:28:06
1997-9-19	1547	14:24	14:29	14:11:04	14:31:16	14:34:57	14:31:16		14:31:16	14:31:32		
1997-9-19	1551	15:24	15:29	15:28:06	15:33:25	15:35:44	15:33:25		15:33:25	15:33:45		
1997-9-19	1555	16:24	16:29	16:27:27	16:36:13	16:38:00	16:36:13		16:36:13	16:36:32		
1997-9-19	1559	17:24	17:29	17:30:34	17:35:58	17:40:15	17:35:58	17:25:46	17:35:58	17:36:20		17:20:45
1997-9-19	1563	18:24	18:29	18:33:11	18:36:04	18:37:04	18:36:04		18:36:04	18:36:24		
1997-9-19	1567	19:24	19:29	19:30:12	19:32:09	19:35:58	19:32:09	19:29:57	19:32:09	19:32:29	19:26:51	19:30:06
1997-9-19	1571	20:24	20:29	20:28:30	20:32:14	20:37:14	20:32:14	20:28:01	20:32:14	20:32:31		

Figure 4.5 Event times of section EHV\$255T and associated objects in TNV-table

Figure 4.5 shows a part of a TNV-table as displayed by TNV-View. The first four columns show the date, train number, and scheduled arrival and departure time. The remaining successive columns correspond to signal 256 (columns 5-7), a TNV-step to position EHV\$EB1/EB1S.0 (column 8), section 255T (columns 9-11), and switch 255 (last two columns). All objects correspond to section 255T. Note that the empty cells in the columns associated to switch 255 imply that the switch position has not changed for about 20–30 minutes, which is the search period up to entering the associated section 255T depending on the parameter δ_{in} . Equivalently, an empty cell in the ‘last clearance’ column (column 9) of section 255T denotes that this section was cleared (and hence occupied) for more than 20–30 minutes before the current occupation.

TNV-View has several viewing and export options. Route events (columns) can be hidden leaving an overview of particular events. For instance, hiding all columns except section entries gives a view of the progress of a train over a route, see Figure 4.6. Hidden columns are also excluded when exporting files, by which output files are generated with various levels of detail for further analysis. Output formats include tab-delimited or comma-separated values (CSV) that can be opened by common spreadsheet and statistical programs. A special output format is also available that can be read by the TNV-filter tool to estimate speed profiles and platform arrival and departure times.

TNV-View also contains several basic spreadsheet functionalities to support visual inspection and comparison of TNV-tables. The heading row and the first four columns can be frozen when scrolling through the data cells. Several windows containing different TNV-tables can be viewed simultaneously. Moreover, these windows can be coupled and jointly scrolled to easily compare related TNV-tables. More details can be found in the TNV-Prepare user’s guide [111].

Datum	TreinNr	Drg	Drg	23BT	27BT	33BT	47AT	24T [°]	107AT	108AT	121BT	193BT
		Aankomst	Vertrek	BEZET	BEZET	BEZET	BEZET	BEZET	BEZET	BEZET	BEZET	BEZET
1997-9-15	1519	07:24	07:29	07:22:15	07:22:27	07:22:33	07:22:42	07:22:50	07:29:45	07:29:53	07:30:16	07:30:22
1997-9-15	1523	08:24	08:29	08:23:49	08:23:58	08:24:03	08:24:10	08:24:17	08:30:59	08:31:09	08:31:33	08:31:38
1997-9-15	1527	09:24	09:29	09:21:51	09:21:59	09:22:05	09:22:13	09:22:21	09:33:36	09:33:43	09:33:59	09:34:03
1997-9-15	1531	10:24	10:29	10:22:12	10:22:20	10:22:27	10:22:35	10:22:42	10:32:54	10:33:02	10:33:23	10:33:28
1997-9-15	1535	11:24	11:29	11:23:25	11:23:34	11:23:40	11:23:48	11:23:55	11:29:57	11:30:10	11:30:37	11:30:42
1997-9-15	1539	12:24	12:29	12:23:22	12:23:36	12:23:45	12:23:56	12:24:04	12:32:14	12:32:26	12:32:48	12:32:53
1997-9-15	1543	13:24	13:29	13:21:05	13:21:13	13:21:18	13:21:24	13:21:31	13:30:02	13:30:09	13:30:28	13:30:32
1997-9-15	1547	14:24	14:29	14:25:17	14:25:26	14:25:31	14:25:39	14:25:46	14:34:03	14:34:11	14:34:32	14:34:37
1997-9-15	1551	15:24	15:29	15:31:14	15:31:22	15:31:28	15:31:35	15:31:42	15:37:02	15:37:09	15:37:27	15:37:31
1997-9-15	1555	16:24	16:29	16:23:11	16:23:19	16:23:25	16:23:32	16:23:39	16:30:57	16:31:05	16:31:26	16:31:31
1997-9-15	1559	17:24	17:29	17:31:58	17:32:08	17:32:14	17:32:23	17:32:30	17:37:20	17:37:35	17:38:00	17:38:05
1997-9-15	1563	18:24	18:29	18:26:28	18:26:49	18:26:57	18:27:06	18:27:14	18:34:23	18:34:34	18:34:55	18:35:00

Figure 4.6 Subsequent section occupancy times in TNV-table

4.3.4 Accuracy and Reliability of TNV-Tables

The event times in the TNV-logfiles are the time instants at which the events are logged by the TNV-system. This logged event time may differ from the actual event time as a result of transmission delay or noise. However, a transmission delay is usually only a fraction of a second, and also the time necessary to log a received message is negligible. Note that event times are given in seconds and so the maximal precision is one second.

The degree of accuracy and reliability of the (logged) event times can be evaluated by several tests based on route logic. Two types of tests are distinguished: a consistency test, which is an integrated part of the TNV-Report module, and a synchronicity test. The tests have been applied on TNV-logfiles recorded during one week in Eindhoven. The sequel explains the tests and the results of the Eindhoven TNV-logfiles.

TNV-Report performs several *consistency tests* in its search algorithm based on route logic. A first test is based on the *chronological ordering* of events. For instance, successive sections on a route must be occupied consecutively, and also a section can only be cleared after the entrance of an adjacent section. TNV-Report detects and discards inconsistent data, which results in empty cells in the TNV-tables. Thus, the generated TNV-tables only contain consistent data with respect to the route logic. Note that the last section clearance before the passage of the current train usually corresponds to different trains. So the last clearances of successive sections may be caused by a train running in the opposite direction or by a crossing train route. These events should therefore not be compared with the route logic of the current train. Empty cells may also result from *missing events*. As an example, suppose that a TNV-step has been logged but a section of the previous TNV-position has not yet been occupied. Clearly, the train has passed the section but for some reason this has not been detected, transmitted, or recorded. TNV-Report only generates an event in a TNV-table if a logical test guarantees its consistency. Thus, a missing event results in one or more empty cells in the TNV-table.

Analysis of the generated TNV-tables of the Eindhoven TNV-logfiles shows that the number of empty cells caused by inconsistent data is negligible, even in periods of heavy (communication) traffic. Hence, the TNV-logfiles are highly complete and correctly represent the actual events in a consistent chronological order.

Also a *synchronicity test* can be applied to the TNV-tables that have been generated by TNV-Report. This post-analysis of the generated tables is based on the fact that synchronous events have equal occurrence times. A triple of synchronous events occurs at the first section of a TNV-position that is located near a signal, i.e., a stop signal, a section occupation, and a TNV-step. These events correspond to different processes that are triggered by a train entering the first section (track circuit) of a TNV-window. First, the signal changes to a stop aspect, which is then reported via the interlocking system to the TNV-System. Second, the section occupation is reported via the interlocking system to the TNV-System. And third, the TNV-step is generated by the TNV-System based on this received section occupation message.

This synchronicity has been tested on the TNV-tables that were generated from the Eindhoven TNV-logfiles. The logged event times of each triple were observed equal for all TNV-steps of any train at Eindhoven, with an occasional exception of one second delay of the TNV-step. These exceptions follow from the sequential triggering of processes where the most vital information is processed first. The generation of a TNV-step and its logging follows the section occupation logging. If the latter event is logged at the end of a clock-second, the next event is logged at the next clock-second. Likewise, the stop signal event time is received — and hence logged — by the TNV-system before the section occupation and TNV-step. Therefore, also the logged stop signal may occasionally differ one second from the other two events. Thus, from the test of the Eindhoven TNV-logfiles follows that the logged events have an accuracy of one second. It can be concluded that the computation time of a TNV-step is negligible, and the same holds for the recording time of an event. Moreover, it can be concluded that the transmission of messages from the signalling systems is free of noise.

In conclusion, tests of the Eindhoven TNV-logfiles prove that the logged event times equal the actual event times with an error smaller than one second, the events are recorded in the correct chronological order, and missing logged events are exceptional. The TNV-tables generated by TNV-Prepare/Report are thus highly complete and accurately represent the actual traffic processes.

4.4 TNV-Filter

4.4.1 Filtering of Train Paths through Stations

The actual arrival and departure times at a platform stop are in general not measured and hence not recorded automatically. The closest measured event to an arrival is the platform track section occupancy, or even more close, the clearance of the last section before the platform track section. Likewise, a departure can be approximated by the measured occupancy of the track section just after the platform track section. The running time before and after the stop on the platform track section may nevertheless be considerable depending on the local station layout (platform track section length) and stop location at the platform track.

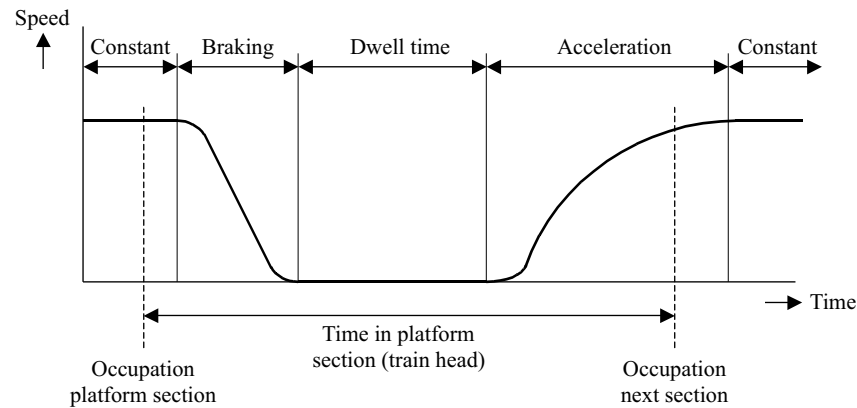


Figure 4.7 Activities on a platform track section

Within the occupation time of the platform track section several activities take place: braking until standstill at the stop location, opening of doors, boarding and alighting of passengers, waiting at the platform track, the departure procedure, acceleration after departure, and clearing the section after passage of the last train axle, see Figure 4.7. Let us define the arrival and departure time as the start and end of standstill at the platform, respectively. Then the arrival and departure time can be estimated from the platform section occupancy and the running times before and after standstill at the platform track section.

Figure 4.8 shows the running times of equivalent trains over the same route through Eindhoven over a distance of 435 meter from the entry signal to the platform section border. The data is obtained using TNV-Prepare and represents a typical picture of the running time distribution through a station. Clearly, trains run with different speeds to the platform and hence the arrival and departure time do not only depend on the passage time at the platform section borders but also on speed and deceleration/acceleration.

Filtering of a train path through a station therefore contains the following steps for arriving and departing trains:

- (i) Estimation of speed and acceleration/deceleration at the platform track section borders;
- (ii) Estimation of the stop position at the platform track, possibly depending on train length;
- (iii) Prediction of the running time at the platform track section before and after the stop position.

Section 4.4.2 describes a least-squares estimation method for finding the speed profile and filtered section passage times over the in- and outbound train route through the station, including the average accelerations on the sections. Here the filtered passage times are feasible with respect to train motion equations and correspond to the measured passage times after rounding. The running time estimations at the platform track are considered in Section 4.4.4.

4.4.2 Speed Profile Estimation

This section presents an approach to accurately estimate the train speed profile over a route through a station before and after the platform section. This result will then be used in the next section to establish running times on the platform section.

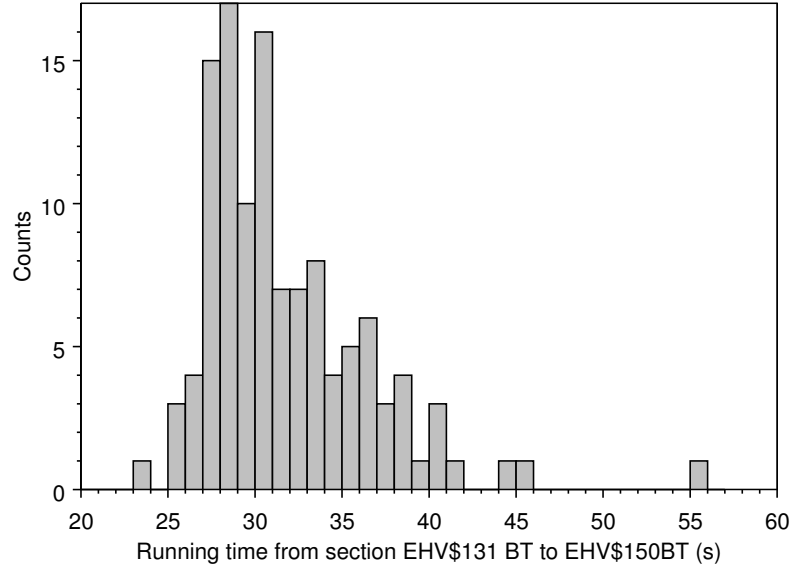


Figure 4.8 Histogram of running time from the entry signal to the platform section border in Eindhoven (IC1500 Heerlen-The Hague CS)

The speed on a train route through a station may vary due to e.g. coasting or active braking in view of a platform or speed restrictions due to switches or track curvature. Moreover, variation of, for example, train composition (train length) and driver behaviour causes a different speed profile even for trains of the same type. The average speed over a part of the route is hence not an applicable speed estimate. Furthermore, the data precision in seconds prevents using the average speed over just the last section as an estimate for the speed at the platform section border. Consider a track section of length l_k and passage times t_k and t_{k+1} of the first train axle on the subsequent section borders. The average speed on this section is

$$\hat{v}_k = \frac{l_k}{t_{k+1} - t_k}.$$

Let δ be the accuracy of the passage times. Then the actual passage time is uniformly distributed on $[t_i, t_i + \delta)$ for $i = k, k + 1$, and the absolute error of the speed estimate is the difference of the speed upper and lower bound, that is,

$$|\varepsilon_k| = \left(\frac{l_k}{t_{k+1} - t_k - \delta} \right) - \left(\frac{l_k}{t_{k+1} - t_k + \delta} \right) = \frac{2\delta l_k}{(t_{k+1} - t_k)^2 - \delta^2}. \quad (4.1)$$

As an example consider a track section of 50 m and assume that the passage times (of the first train axle) at the section borders are 16:05:30 and 16:05:35, respectively, with a precision of a second. Note that the accuracy of the measurements can never be higher than the precision, so in the best case we have $\delta = 1$. Since, we here have $t_{k+1} - t_k = 5$ s, the average section speed is $\hat{v}_k = 50/5 = 10$ m/s, and the absolute speed estimation error is $|\varepsilon_k| = (2 \cdot 50)/(5^2 - 1) = 100/24 = 4.17$ m/s by (4.1). The lower and upper bound on the speed estimate with respect to the precision is $\underline{v}_k = 50/6 = 8.33$ m/s and $\bar{v}_k = 50/4 = 12.5$ m/s, respectively. The minimal variance speed estimate is the middle of the error bounds $(8.33 + 12.5)/2 = 10.42$ m/s with a maximal error of $4.17/2 = 2.08$ m/s. This is an error of 20%.

The error bounds in (4.1) can also be used as bounds on the actual speed if the accuracy of the measurement is known. Reversely, (4.1) can be used to determine the measurement error if accurate speed estimates are obtained from an alternative method or if speed measurements are available.

The motion of a train is a dynamic process with three variables that change over time: the position of a train, its speed, and the acceleration (or deceleration for negative values). The variables are hence functions of time. In the sequel we assume that the section passage times and section lengths are available. The passage times of sections on a route are generated by TNV-Prepare. The section lengths must be provided by the railway infrastructure management. In the Netherlands the positions of insulation joints between track circuits (the section borders) are shown on OBE-maps from Railinfrabeheer. These maps used to be drawn by hand but are currently replaced by computer drawings using the system CARE [68].

Consider a train run over a route of n track sections and assume that the n section entrance times are available from (track circuit occupancy) measurements. The train dynamics on this route can be described by the discrete-time version of the Newton laws of motion

$$\begin{cases} x_{k+1} &= x_k + v_k(t_{k+1} - t_k) + \frac{1}{2}a_k(t_{k+1} - t_k)^2 \\ v_{k+1} &= v_k + a_k(t_{k+1} - t_k), \end{cases} \quad (4.2)$$

for $k = 1, \dots, n-1$. Here x_k is the (known) route position of the beginning of section k , v_k is the speed at this section boundary, a_k is the (average) acceleration on section k , and t_k is the measured passage (entrance) time of section k . The main problem here is that the passage times are only approximately known, i.e., the measurements are rounded to seconds and possibly have measurement errors. Therefore, the passage times are unknowns within some bounds. Note that if the passage times were known precisely then (4.2) is a system of $2n-2$ linear equations in the $2n-1$ variables $(a_1, \dots, a_{n-1}, v_1, \dots, v_n)$. In this case, the only variable to be determined is the initial speed v_1 : for given speed v_1 (4.2) is just a system of as many linear equations as variables. The problem then reduces to finding v_1 such that this linear system has a feasible solution. If on the other hand the train positions x_k are unknown instead of the passage times then (4.2) is a standard linear filtering problem, which can be solved by the Kalman filter, see e.g. Anderson and Moore [8]. For the specific problem at hand however a least-squares approach is pursued.

Consider the system (4.2) with known positions x_k . Note that this system is nonlinear in the passage times t_k . We are now faced with the problem to find variables v_k ($k = 1, \dots, n$), a_k ($k = 1, \dots, n-1$), and τ_k ($k = 1, \dots, n$) with $\tau_k \in [t_k, t_k + 1)$ such that

$$J_k(v_k, a_k, \tau_k, \tau_{k+1}; x_k) := x_k + v_k(\tau_{k+1} - \tau_k) + \frac{1}{2}a_k(\tau_{k+1} - \tau_k)^2$$

is equal to x_{k+1} for all $k = 1, \dots, n-1$. Note that x_k is a known parameter in $J_k(\cdot)$ and not a variable. There is some redundancy in (4.2): we only have to find the initial speed v_1 and actual passage time τ_k at the first section, and then subsequently in each step k must find appropriate variables a_k and τ_{k+1} , which then also fixes speed v_{k+1} by the second equation in (4.2). The decision variables can therefore be reduced to the $2n$ variables $(\tau_1, \dots, \tau_n, v_1, a_1, \dots, a_{n-1})$.

The problem can now be defined as a least-squares optimization problem that minimizes the sum of squared errors of $x_{k+1} - J_k(v_k, a_k, \tau_k, \tau_{k+1})$, while satisfying $\tau_k \in [t_k, t_k + 1)$ for all k . Instead of explicitly adding the passage time constraints to the optimization problem it is more

convenient from an algorithmic point of view to extend the objective function with additional terms that penalize large deviations from the actual passage times. We therefore consider the following least-squares optimization problem

$$\text{Minimize } \sum_{k=1}^{n-1} (x_{k+1} - J_k(v_k, a_k, \tau_k, \tau_{k+1}))^2 + \sum_{k=1}^{n-1} a_k^2 + \sum_{k=1}^{n-2} (a_{k+1} - a_k)^2 + \sum_{k=1}^n (\tau_k - t_k - \frac{1}{2})^2 \quad (4.3)$$

subject to

$$v_{k+1} = v_k + a_k(\tau_{k+1} - \tau_k), \quad k = 1, \dots, n-1. \quad (4.4)$$

The first term in the least-squares cost function penalizes the deviation of the section position x_{k+1} and the estimated train position at time τ_{k+1} given by $J_k(v_k, a_k, \tau_k, \tau_{k+1})$. The second term minimizes the necessary acceleration or deceleration. The third term expresses the assumption that the jumps in acceleration or deceleration are as small as possible. The fourth term penalizes the deviation of the actual passage time τ_k from the expected passage time $t_k + 1/2$. Recall that a rounded measurement t_k is in fact a uniformly distributed stochastic variable on $[t_k, t_k + 1)$ with mean $t_k + 1/2$. The constraint (4.4) implicitly determines the speeds v_k ($k = 2, \dots, n$) in terms of passage times and acceleration, and only serves for notational convenience. In the actual implementation these (equality) transformations are substituted directly in the definition of the cost function.

The terms in the cost function may also be weighted differently. Note that an absolute deviation of 1 second of the passage time estimates τ_k from the measurements is allowed. However a difference of 1 m/s² on an acceleration estimate is unacceptable. Therefore the acceleration terms can be multiplied by a weight of for instance 100. In this case a change in value of a passage time τ_k of 1 second is in the same order as a change of 0.01 m/s² in acceleration rate. Nevertheless, experiments showed good performance of the least-squares estimation with cost function (4.3) with no (or equal) weights.

If the estimated variables from the unconstrained least-squares problem exceed unrealistic limits then constraints on the variables must be added explicitly, which results in a constrained least-squares problem. In particular simple box constraints are applicable, i.e., where the decision variables are bounded individually from below and above.

Passage time bounds. Assume that the passage time measurements are only subject to round-off errors caused by the precision in seconds. Then we have the constraints

$$t_k \leq \tau_k < t_k + 1, \quad k = 1, \dots, n,$$

where t_k are the measured passage times in seconds. The bounds can be adjusted when additional measurement errors apply.

Acceleration and deceleration bounds. The acceleration and braking rates must satisfy the train characteristics. We therefore have the constraints

$$\underline{a} \leq a_k \leq \bar{a}, \quad k = 1, \dots, n-1,$$

where \bar{a} is the maximum characteristic acceleration and $\underline{a} = -d$ is the negative maximum characteristic braking rate d .

Speed restriction. Speed can be limited by the maximum speed of the train characteristics or by speed restrictions of the railway infrastructure (station layout or open track). We thus have

$$0 \leq v_1 \leq \bar{v},$$

where \bar{v} is the speed restriction on the first section. Recall that we do not consider all section speeds explicitly as variables. If we want to incorporate speed restrictions on each section separately the model must be slightly changed. A first possibility is to include all n speeds in the decision variables instead of the $n - 1$ acceleration rates. An alternative is to define a nonlinear constraint where the speed bounds are expressed in nonlinear constraints on acceleration and passage times. The latter option means however that no longer efficient least-square optimization algorithms can be used, but a nonlinear programming method must be pursued.

The solution to the speed estimation problem is now obtained as follows. First, (4.3) is solved by an unconstrained nonlinear least-squares algorithm. If one or more of the variables do not satisfy the above constraints then the constraints are added and the resulting problem is solved by a constrained nonlinear least-squares method. Unconstrained nonlinear least-squares problems are efficiently solved by the Gauss-Newton method or the Levenberg-Marquardt method [35, 55]. Constrained nonlinear least-square problems are computationally more involved. These problems are tackled by general constrained nonlinear minimization algorithms, which are adapted to take advantage of the special structure of the least squares cost function. In the Matlab Optimization Toolbox [35] a trust region method is used as developed by Coleman & Li [36]. This latter method requires at least as many terms in the cost function as variables. The variables that have to be estimated are each τ_k and a_k , and the initial speed v_1 . The problem thus has $2n$ variables and the cost function (4.3) exhibits $4n - 4$ terms. So the constrained problem can be solved by this method for $n \geq 2$, i.e., the considered route must contain at least measurements of 2 track sections, which is necessary anyway to estimate the average speed on one section. The 3rd term can be safely dropped but is included because it directs the (unconstrained) solution to more satisfying results by penalizing acceleration jumps. It is however only applicable if $n \geq 3$ so that at least the acceleration on two sections must be fit. Furthermore note that if the acceleration terms in the cost function are dropped then we only have $2n - 1$ terms and the constraint problem with variable bounds can not be solved (by the above method). If only the 2nd term (squared accelerations) is dropped then $3n - 3$ terms remain and the constrained problem can be solved if $n \geq 3$ (section) measurements are available. It can hence be concluded that for the method to really work at least 3 sections must be taken into account. Otherwise one just takes the average speed on one section based on the passage times at both section borders.

It should be noted that if some bounds are too tight, the constrained problem may be infeasible and the problem has no solution. If for instance the measurements have an error because of noise or transmission delays then the constraint system may be infeasible since the actual passage times τ_k may deviate more than one second from t_k . Note that a constant bias on all measurements has no effect on the estimates. So infeasibility only occurs when the measurements have fluctuating errors such as a transmission delay to only one or a few measurements. Thus, the least-squares problem with above additional constraints can also be used to check for possible measurement noise.

4.4.3 Train Length Estimation

The stop location on the platform tracks may depend on the train length. We therefore also want to be able to estimate the train length from the data. Train length can be estimated using three quantities at a fixed track position:

- passage time of the first train axle;
- passage time of the last train axle;
- (average) speed between the first and last axle passage.

Consider a section border between section k and $k + 1$. The passage time of the train head (or first axle) is measured as the time that section $k + 1$ gets occupied. On the other hand the passage time of the train rear (or last axle) is measured by the clearance time of section k . If the speed is known and constant during the passage of the section border then the train length ℓ , approximated as the difference between the first and last axle, is given as

$$\ell = v \cdot (s_k - t_{k+1}),$$

where v is the (average) speed at the section border, t_{k+1} is the entrance time of section $k + 1$, and s_k is the clearance time of section k .

The accuracy of this estimate depends on the accuracy of the three variables. If the passage times have an accuracy of 1 second, and we assume perfect knowledge of the average speed, then the estimation error of the train length is still $2v$. Furthermore, the average speed is also not known exactly. In the last section a method was presented to estimate the speed of the train front at each section border. Here we need the average speed during the entire passage of a train over a section border. As we have seen the speed profile is usually not constant during the train trip, and in particular at the approach and departure of a station. The average speed on the section border may be approximated by $(v_{k+1} + u_k)/2$, where v_{k+1} is the speed of the train front at the occupancy of section $k + 1$ and u_k is the speed of the train back at the clearance of section k . These two values must be estimated by e.g. the method of the last section. Still, the error in the speed estimate is not known and hence neither is the error of train length. This error may be decreased by taking the average of several train length estimates at subsequent sections.

The least-squares model of the last section can be extended to include train length estimation. We now must find the speed profile of both the front and rear of the train. The speed profile estimation of the train back is also obtained from the Newton laws of motion but with respect to the section clearance times, which are the passage times of the last axle of a train. The average acceleration based on track clearance times can only be obtained from the second section onwards since no passage time of the train back is available for the beginning of the first section. Define

$$I_k(u_k, b_k, \sigma_k, \sigma_{k+1}; x_{k+1}) := x_{k+1} + u_k(\sigma_{k+1} - \sigma_k) + \frac{1}{2}b_k(\sigma_{k+1} - \sigma_k)^2,$$

where σ_k is the filtered clearance time of section k , u_k is the speed at the end of section k estimated from the clearance times, and b_k is the average acceleration/deceleration at section $k + 1$. Then we must have $x_{k+2} = I_k(u_k, b_k, \sigma_k, \sigma_{k+1})$ for all $k = 1, \dots, n - 2$.

Consider again a route of n sections to which we have measurements of the occupations and clearances. The least-squares optimization problem is now given as

$$\begin{aligned}
 \text{Minimize } & \sum_{k=1}^{n-1} (x_{k+1} - J_k(v_k, a_k, \tau_k, \tau_{k+1}))^2 + \sum_{k=1}^{n-1} a_k^2 + \sum_{k=1}^{n-2} (a_{k+1} - a_k)^2 + \sum_{k=1}^n (\tau_k - t_k - \frac{1}{2})^2 \\
 & + \sum_{k=1}^{n-2} (x_{k+2} - I_k(u_k, b_k, \sigma_k, \sigma_{k+1}))^2 + \sum_{k=1}^{n-1} b_k^2 + \sum_{k=1}^{n-2} (b_{k+1} - b_k)^2 \\
 & + \sum_{k=1}^{n-1} (\sigma_k - s_k - \frac{1}{2})^2 + \sum_{k=1}^{n-1} (\ell - \frac{1}{2}(v_{k+1} + u_k) \cdot (\sigma_k - \tau_{k+1}))^2 \quad (4.5)
 \end{aligned}$$

subject to

$$\begin{aligned}
 v_{k+1} &= v_k + a_k(\tau_{k+1} - \tau_k), \quad k = 1, \dots, n-1 \\
 u_{k+1} &= u_k + b_k(\sigma_{k+1} - \sigma_k), \quad k = 1, \dots, n-2.
 \end{aligned}$$

Here t_k , τ_k , x_k , v_k , and a_k are as before, s_k is the measured clearance time of section k , σ_k is the filtered clearance time, u_k is the speed of the last axle at the exit of section k , b_k is the average acceleration/deceleration of the last axle at section $k+1$, and ℓ is the train length. In the cost function the first term is the squared error of the train front motion equations. The second term minimizes the necessary acceleration or deceleration of the train front. The third term expresses the assumption that the jumps in acceleration or deceleration are as small as possible. The fourth term penalizes the deviation of the actual passage time τ_k from the expected passage time $t_k + 1/2$. The fifth term is the squared error of the train back motion equations. The sixth term minimizes the acceleration or deceleration of the train back. The seventh term expresses the assumption that the jumps in acceleration or deceleration are as small as possible. The eighth term penalizes the deviation of the actual passage time σ_k of the train back from the expected passage time $s_k + 1/2$. And the final term is the squared error of the train length estimate. The two constraints are functional equations that are used in the definition of the cost function.

Problem (4.5) is an unconstrained nonlinear least-squares estimation problem. Like in the last section, the least-squares problem can be extended by weights in the cost function and additional bounding constraints. Observe that the last term couples the estimations based on the entrance times and the clearance times, which otherwise are two separable problems.

4.4.4 Running Time on Platform Tracks

In this section we derive analytical estimates for the running times on the platform track. The following information is assumed available:

- train passage time and speed at the platform section borders;
- train acceleration (deceleration) at the platform sections borders;
- train acceleration and deceleration characteristics;
- platform section length;
- stop location at the platform of the train front.

The platform section passage times are obtained by TNV-Prepare with an accuracy of one second. The estimation of train speed and acceleration is considered in the previous section. As

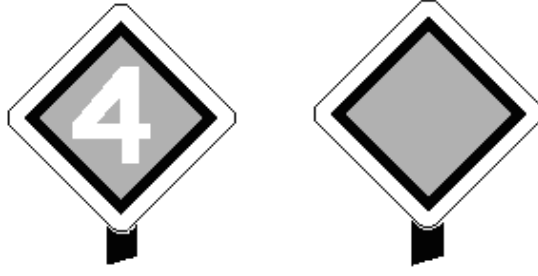


Figure 4.9 Signs (blue background) indicating the stop location at a platform track for a train with 4 coaches (left) and for any train irrespective of the number of coaches (right)

an estimate for the acceleration on the platform section border we use the average acceleration on the section before and after the platform section. Train characteristics and platform section lengths must be provided by the operators or railway infrastructure management. Recall that train lines are usually operated by trains of the same type with possible varying trainset compositions (number of train units) over different periods during the day.

The stop location at a platform depends on train composition and the location of stairways and escalators. If the platform access facilities are located at the end of the platform (with respect to the arriving train direction) then the stop location is invariant to train composition (length): each train (driver) runs as close as possible to the platform end, provided that the departure signal is not situated within less than 5 m from the end of the platform. On the other hand, if the access facilities are located at the beginning or the centre of the platform then the stop location generally depends on the train length. In the Netherlands, fixed trackside signs indicate the stop locations at the platform track, see Figure 4.9. If the stop location depends on train length then several signs indicate the relevant stop position for trains with a specified number of coaches. If the stop sign positions or the number of coaches are unknown at the time of analysis then train length estimation may be used to find the actual or approximate stop locations.

Let $v_0 > 0$ ($v_1 > 0$) be the estimated speed at the entrance (exit) of the platform section, a_0 (a_1) be the estimated average deceleration/acceleration on the section preceding (following) the platform section, and $d_{\max} < 0$ ($a_{\max} > 0$) be the maximum train-characteristic deceleration (acceleration) rate. Assume that l is the desired stop position (of the front of the train), measured from the entering platform section border and L is the platform section length. Then the following lemma applies.

Lemma 4.4.1 *The stop location $l \in (0, L)$ is feasible if*

$$\frac{v_0^2}{2|d_{\max}|} \leq l \leq L - \frac{v_1^2}{2a_{\max}}. \quad (4.6)$$

Proof: Consider the continuous Newton laws of motion $x(t) = x(0) + v(0) \cdot t + \frac{1}{2}a(t) \cdot t^2$ and $v(t) = v(0) + a(t) \cdot t$. For constant acceleration/deceleration $a(t) \equiv a \neq 0$ the 2nd equation gives time as function of speed by $t = (v(t) - v(0))/a$. Substitution in the 1st equation and rearranging gives the covered distance in terms of speed

$$x(t) = x(0) + \frac{v(t)^2 - v(0)^2}{2a}. \quad (4.7)$$

Now first consider the train arrival. The minimal braking distance is obtained by braking at maximum capacity $a = -|d_{\max}|$. Let $t = 0$ be the entrance time at the platform section, and so $x(0) = 0$ and $v(0) = v_0$. The minimal distance $x(t)$ necessary for braking to zero speed $v(t) = 0$ is now obtained from (4.7), which gives the lower bound on l . Now consider the train departure. Assume that the train departs at $t = 0$ with maximum acceleration a_{\max} from $x(0)$ to the platform section border $x(t) = L$. This strategy accelerates from $v(0) = 0$ to $v(t) = v_1$ over the shortest distance (and in minimal time). Substitution in (4.7) gives the upper bound on l . \square

In the sequel we assume that the bounds (4.6) in Lemma 4.4.1 are valid.

At the platform track section no more additional information is obtained from the safety systems. We therefore have to assume a certain braking and acceleration strategy and compute the running time on the platform track accordingly. First we explore the feasible and maximal speed profiles.

Let the *maximum-braking speed function* $v_{\text{dec}}^{\max} : [0, l] \mapsto \mathbb{R}_+$ and the *maximum-acceleration speed function* $v_{\text{acc}}^{\max} : [l, L] \mapsto \mathbb{R}_+$ be defined on the platform track section as

$$v_{\text{dec}}^{\max}(x) := \sqrt{2|d_{\max}|(l - x)} \quad \text{and} \quad v_{\text{acc}}^{\max} := \sqrt{2a_{\max}(x - l)}.$$

The area $\{(x, v) | 0 \leq x \leq l, 0 \leq v \leq v_{\text{dec}}^{\max}(x)\}$ is the area in the distance-speed plane from which the destination $(l, 0)$ can be reached. Likewise $\{(x, v) | l \leq x \leq L, 0 \leq v \leq v_{\text{acc}}^{\max}(x)\}$ is the area in the distance-speed plane that is reachable from the stop location, see Figure 4.10.

The following lemma gives the speed profile over the platform track section with minimum platform running time. Note that a straight line in the distance-speed plane from the platform entry to the stop location and again straight to the platform exit is not the fastest speed profile.

Lemma 4.4.2 *Let the bounds (4.6) in Lemma 4.4.1 be valid. The minimum platform running time before arrival with initial speed v_0 is*

$$t_{\text{in}}^{\min} = (u_0^{\max} - v_0)/a_{\max} + u_0^{\max}/|d_{\max}|$$

and the minimum platform running time after departure with final speed v_1 is

$$t_{\text{out}}^{\min} = (v_1 - u_1^{\max})/|d_{\max}| + u_1^{\max}/a_{\max},$$

where

$$u_0^{\max} = \sqrt{\frac{v_0^2|d_{\max}| + 2la_{\max}|d_{\max}|}{a_{\max} + |d_{\max}|}} \quad \text{and} \quad u_1^{\max} = \sqrt{\frac{v_1^2a_{\max} + 2(L-l)a_{\max}|d_{\max}|}{a_{\max} + |d_{\max}|}}.$$

Proof: The speed profile with minimum running time in the distance-speed plane from $(0, v_0)$ to $(l, 0)$ is given by accelerating with maximum acceleration until the maximum braking curve is reached, after which this curve is followed by constant braking with maximum braking rate, see Figure 4.10. Note that by this strategy the speed at each position is the highest possible. The switching position l_0 and associated speed can be found using (4.7). For the maximum acceleration phase we find $l_0 = (v^2 - v_0^2)/2a_{\max}$ and for the maximum braking phase we have

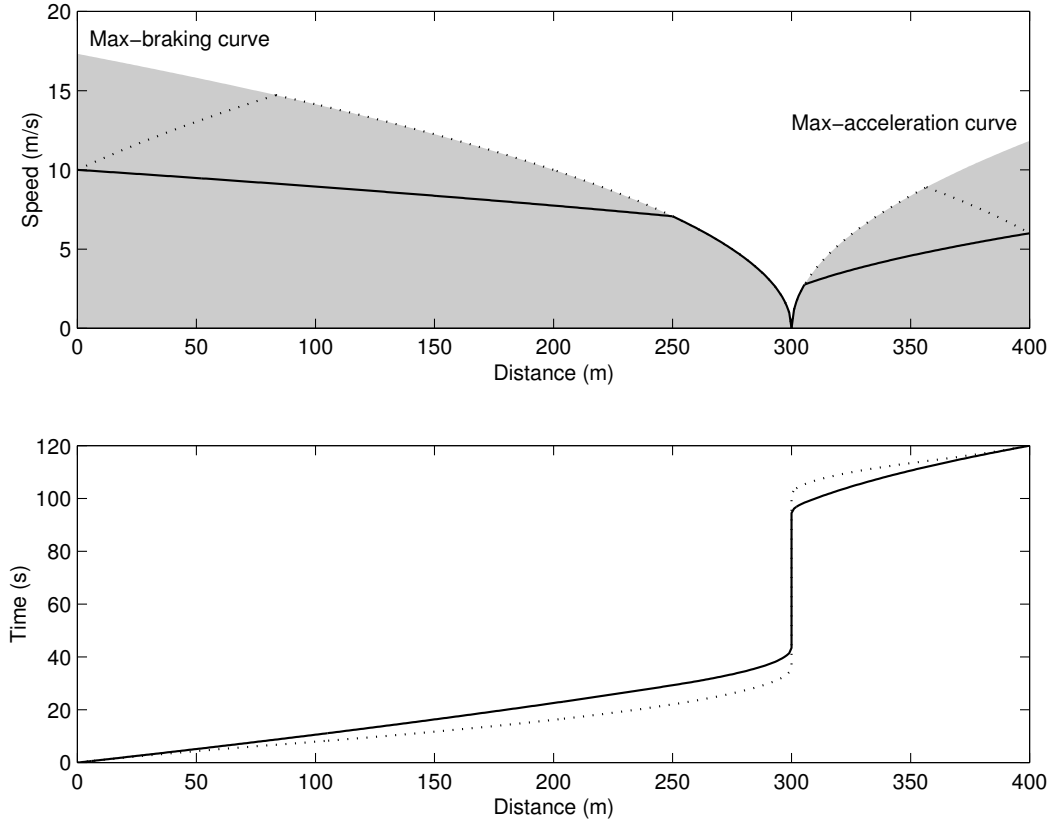


Figure 4.10 Speed-distance and time-distance diagrams of fastest (dashed) and predicted (solid) platform track curves. The dark area is the feasible speed-distance region ($l = 300\text{m}$, $d_{\max} = -0.5\text{m/s}^2$, $a_{\max} = 0.7\text{m/s}^2$)

$l - l_0 = v^2/2|d_{\max}|$. Substituting the first equation into the second and solving for v gives $v = u_0^{\max}$, which is hence the switching speed on the maximum braking curve. The running time is now given as the sum of the running time to the switching point $(u_0^{\max} - v_0)/a_{\max}$ and the braking time from the switching point $u_0^{\max}/|d_{\max}|$.

The speed profile with minimum running time in the distance-speed plane from $(l, 0)$ to (L, v_1) is given by following the maximum acceleration curve as far as possible and then braking with maximum braking rate to reach (L, v_1) , see Figure 4.10. Similar to the running time before arrival case, we find the switching speed u_1^{\max} , and the running time is then given as the sum of the running time on the maximum acceleration curve to the switching point u_1^{\max}/a_{\max} and the running time from the switching point to the platform end $(v_1 - u_1^{\max})/|d_{\max}|$. \square

Lemma 4.4.3 *Let the bounds (4.6) in Lemma 4.4.1 be valid. Then on the distance-speed plane $\{(x, v) | 0 \leq x \leq L, v \geq 0\}$ the following hold.*

- (i) *The distance-speed trajectory of a constant-deceleration motion with deceleration a_0 and initial speed v_0 intersects the maximum braking curve on $[0, l]$ if and only if $a_0 \geq -v_0^2/(2l)$.*
- (ii) *The distance-speed trajectory of a constant-acceleration motion through (L, v_1) with acceleration rate a_1 intersects the maximum acceleration curve on $[l, L]$ if and only if $a_1 \leq v_1^2/(2(L - l))$.*

Proof: First consider the deceleration curve. Since the bounds in Lemma 4.4.1 are valid $(0, v_0)$ lies in the feasible area, i.e., below the maximum deceleration curve. A train that runs from $x = 0$ with initial speed v_0 and constant deceleration $a_0 < 0$ reaches zero speed at $l_0 = -v_0^2/(2a_0)$. Hence, the distance-speed curve intersects the maximum braking curve only if $l_0 \geq l$. So we have $l \geq -v_0^2/(2a_0)$ which proves the first part for $a_0 < 0$. Now let $a_0 \geq 0$. Then the speed does not decrease and hence must reach the boundary of the feasible region, i.e., it intersects the maximum braking curve on $[0, l]$.

Now, consider the acceleration curve. The proof is similar to the first part. Because (4.6) is valid (L, v_1) lies below the maximum acceleration curve. Depending on a_1 the constant-acceleration curve through (L, v_1) either intersects the maximum acceleration curve or the zero-speed boundary on $l < x < L$ (recall $v_1 > 0$). The acceleration distance from zero speed to v_1 with constant acceleration $a_1 > 0$ is $v_1^2/(2a_1)$. So if $v_1^2/(2a_1) \geq L - l$ then the curve intersects the maximum acceleration curve. This proves the second part for $a_1 > 0$. Clearly, for $a_1 \leq 0$ the curve has downward or zero slope and must hence intersect the maximum braking curve on $[l, L]$ before reaching (L, v_1) . \square

Since no information is available of the processes on the platform section, we have to assume a certain procedure to approximate the platform speed profile.

Assumption 4.1 *Let a train enter a platform section with speed $v_0 > 0$ and deceleration a_0 , stop at stop location l , and exit the platform section with speed $v_1 > 0$ and acceleration a_1 . For the speed profile on the platform section the following is assumed.*

- (i) *A train runs nonstop to the stop location l with final maximum braking phase.*
- (ii) *Between the platform entrance and the final maximum braking phase the train runs with constant deceleration a_0 if $a_0 \geq -v_0^2/(2l)$ and with constant speed v_0 otherwise.*
- (iii) *A train departs with initial maximum acceleration phase and runs nonstop to the platform section exit.*
- (iv) *Between the initial maximum acceleration phase and the platform section exit the train runs with constant acceleration a_1 if $a_1 \leq v_1^2/(2(L - l))$ and with constant speed v_1 otherwise.*

Figure 4.10 shows the speed-distance and time-distance graph that satisfy Assumption 4.1. The following theorem states that the conditions in Assumption 4.1 define a unique feasible speed profile and gives analytical expressions for the associated platform running time estimates.

Theorem 4.4.1 *If (4.6) is valid the speed profile in Assumption 4.1 is feasible and uniquely determined. The associated inbound platform running time is*

$$t_{\text{in}}^r = \begin{cases} l/v_0 + v_0/(2|d_{\text{max}}|) & \text{if } d_{\text{max}} \leq a_0 \leq -v_0^2/(2l) \text{ or } a_0 = 0 \\ (u_0 - v_0)/a_0 + u_0/|d_{\text{max}}| & \text{if } -v_0^2/(2l) \leq a_0 < 0 \text{ or } a_0 > 0. \end{cases}$$

and the outbound platform running time is

$$t_{\text{out}}^r = \begin{cases} (L - l)/v_1 + v_1/(2a_{\text{max}}) & \text{if } v_1^2/(2(L - l)) \leq a_1 \leq a_{\text{max}} \text{ or } a_1 = 0 \\ (v_1 - u_1)/a_1 + u_1/a_{\text{max}} & \text{if } 0 < a_1 < v_1^2/(2(L - l)) \text{ or } a_1 < 0, \end{cases}$$

where

$$u_0 = \sqrt{\frac{v_0^2 |d_{\max}| + 2la_0 |d_{\max}|}{|d_{\max}| + a_0}} \quad \text{and} \quad u_1 = \sqrt{\frac{v_1^2 a_{\max} - 2(L-l)a_1 a_{\max}}{a_{\max} - a_1}}.$$

Proof: Feasibility follows from Lemma 4.4.1 and 4.4.3: From Lemma 4.4.3.(i) it follows that if the condition on a_0 is satisfied then the constant deceleration curve intersects the maximum braking curve, and at this switching point the deceleration rate is switched to maximum braking, which gives a uniquely defined continuous curve in the distance-speed plane. On the other hand, if the condition is not satisfied, the point $(0, v_0)$ still lies in the feasible region below the maximum braking curve by Lemma 4.4.1. The curve with constant speed v_0 hence must intersect the maximum braking curve at v_0 for a distance between 0 and l . At this switching point the constant speed phase switches to maximum braking, which uniquely defines a continuous curve in the distance-speed plane. An analogous reasoning holds for the departure speed profile. If the condition in Lemma 4.4.3.(ii) is valid a unique switching point exists to switch from the maximum acceleration curve to constant acceleration with rate a_1 . And if this condition is not valid then the maximum acceleration curve is followed until speed v_1 is reached at which the speed profile switches to a constant speed phase.

We now prove the correctness of the platform running time expression. First the running time before arrival. The expression clearly has a discontinuity at the point $a_0 = -v_0^2/2l$. Below this value a speed-holding/maximum-braking policy is pursued, i.e., $a(x) \equiv 0$ if $0 \leq x \leq l_0$ and $a(x) \equiv d_{\max}$ if $l_0 < x \leq l$, where l_0 is the switching location $l_0 = l - v_0^2/(2|d_{\max}|)$, which is the stop position l minus the maximum braking distance from v_0 to zero speed. The associated running time is the first part of the arrival running time expression. This running time represents the time to cover a distance l with constant speed v_0 and an additional time loss caused by braking with maximum capacity to zero speed from l_0 onward. Also note that the case $a_0 = 0$ is represented by this equation since this is exactly the speed-holding phase. The second part in the arrival running time expression represents the constant-deceleration/maximum-braking policy, i.e., $a(x) \equiv a_0$ if $0 \leq x \leq l_0$ and $a(x) \equiv d_{\max}$ if $l_0 < x \leq l$, where l_0 is now the switching location given by

$$l_0 = \frac{l|d_{\max}| - \frac{1}{2}v_0^2}{|d_{\max}| + a_0}.$$

The speed at this switching location is $v(l_0) = u_0$. Note that for $a_0 = 0$ the switching positions of both policies collide and $u_0 = v_0$. The associated running time is now the second part of the arrival running time expression. The first term is the switching time t_0 and the second term is the additional running time to brake with maximum capacity from $v(l_0) = u_0$ to zero speed.

The proof of the expression for the platform running time after departure is completely analogous to the arrival running time. The switching position in the second departure running time expression associated to the maximum-acceleration/constant-acceleration policy now is $l_0 = (\frac{1}{2}v_1^2 - (L-l)a_1)/(a_{\max} - a_1)$ with speed $v(l_0) = u_1$. \square

The following lemma states that the platform running times are smooth in $a_0 = 0$ and $a_1 = 0$. As a result the running time estimates do not show a sudden jump if the initial (final) acceleration varies around zero, i.e., the estimates are insensitive to parameter variations around zero.

Lemma 4.4.4 *Let $t_{\text{in}}^r(a_0)$ and $t_{\text{out}}^r(a_1)$ as defined in Theorem 4.4.1. The platform running time t_{in}^r is continuous in $a_0 = 0$ and t_{out}^r is continuous in $a_1 = 0$.*

Proof: The lemma is proved by application of the rule of l'Hôpital, which can be stated as follows: If f and g are differentiable in $x = 0$, $f(0) = g(0) = 0$, $g'(0) \neq 0$, and $\lim_{x \rightarrow 0} f'(x)/g'(x)$ exists, then $\lim_{x \rightarrow 0} f(x)/g(x) = \lim_{x \rightarrow 0} f'(x)/g'(x)$. Applying l'Hôpital's rule to the first term in $t_{\text{in}}^r(a_0)$ for $a_0 \rightarrow 0$ gives

$$\lim_{a_0 \rightarrow 0} \frac{-v_0 + \sqrt{v_0^2 |d_{\text{max}}| + 2la_0 |d_{\text{max}}|} / \sqrt{|d_{\text{max}}| + a_0}}{a_0} = \frac{l}{v_0} - \frac{v_0}{2|d_{\text{max}}|}.$$

Note that both the denominator and numerator on the left-hand side are zero in $a_0 = 0$, and the derivative of the denominator to a_0 is 1. Calculation of the derivative of the numerator to a_0 and substituting $a_0 = 0$ gives the right-hand side. Hence the conditions of l'Hôpital's rule are satisfied. The second term of $t_{\text{in}}^r(a_0)$ with $a_0 \rightarrow 0$ is calculated directly as $v_0/|d_{\text{max}}|$. Adding this to the expression for the first term derived above gives $t_{\text{in}}^r(0) = l/v_0 + v_0/(2|d_{\text{max}}|)$. Comparison with the first expression for $t_{\text{in}}^r(0)$ gives

$$\lim_{a_0 \rightarrow 0} t_{\text{in}}^r(a_0) = t_{\text{in}}^r(0).$$

The $t_{\text{out}}^r(a_1)$ case is proved completely analogously. □

4.4.5 Arrival and Departure Delays

Platform arrival and departure time estimates directly follow from the results of the previous sections. The arrival time is simply the sum of the measured platform entrance time and the remaining platform running time before standstill. Similar, the departure time is the platform exit time minus the platform running time after dwelling.

Theorem 4.4.2 *Let t_0 and t_1 be the entrance time and exit time of the train front (first axle) on the platform section, respectively, and t_{in}^r and t_{out}^r the platform running times as defined in Theorem 4.4.1. Then a feasible arrival time estimate \hat{a} and departure time estimate \hat{d} is given as*

$$\hat{a} = t_0 + t_{\text{in}}^r \quad \text{and} \quad \hat{d} = t_1 - t_{\text{out}}^r.$$

Furthermore, let a and d be the scheduled arrival time and scheduled departure time. Then the arrival delay estimate and departure delay estimate is given as

$$A = \hat{a} - a = t_0 + t_{\text{in}}^r - a \quad \text{and} \quad D = \hat{d} - d = t_1 - t_{\text{out}}^r - d.$$

Note that by the above delay definition a delay can either be early (negative delay) or late (positive delay). One may also be interested in arrival lateness only — when early arrivals are considered on time. Arrival lateness is then defined as $(A)^+ = (\hat{a} - a)^+ = (t_0 + t_{\text{in}}^r - a)^+$, where $(a)^+ = \max(a, 0)$. Note that early departures are not allowed and hence departures should always be punctual or (more or less) late.

The calculations in Section 4.4 have been implemented in the application TNV-Filter using the Matlab numerical computing environment. The input to TNV-Filter is a file containing date,

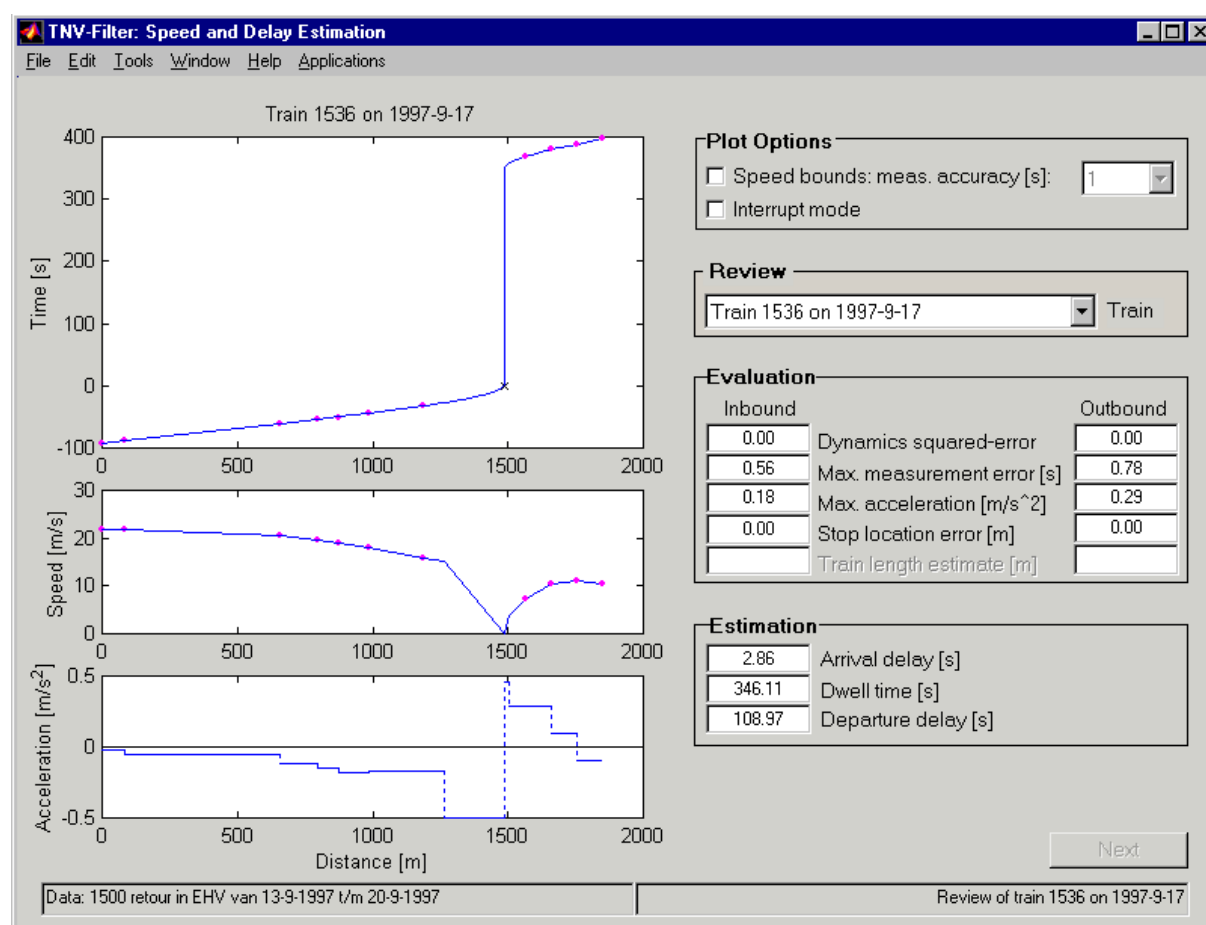


Figure 4.11 TNV-Filter graphical user interface

train number, and occupation and clearance times generated by TNV-Prepare (in the TNV-View export utility). Section lengths and parameters (train/track characteristics) are provided by input windows. The output is a file where each line contains subsequently date, train number, arrival delay, dwell time, and departure delay. Alternatively, arrival times and departure times may be included instead of the delays. TNV-Filter has a graphical user interface in which the speed profile and time-distance graphs are displayed, see Figure 4.11. Also some calculation statistics are shown measuring the goodness of fit. These statistics identify incorrect or irregular input to which no feasible output can be computed. The graphs provide an additional means for visual inspection. Hence, TNV-Filter also supports exploration of irregular behaviour, such as a stop on the inbound (outbound) route just before (after) the platform section.

4.5 Conclusions and Recommendations

Existing data collection and registration methods are not accurate enough for detailed analysis of railway operations. Until recently, feedback of precise operations data to the railway planning process was therefore not possible, although this feedback is essential for analysing and improving railway operations. However, train describer records (TNV-logfiles) contain invaluable data — with a precision and accuracy of a second — that can be traced back to train number

governed events using the developed software application TNV-prepare.

TNV-Prepare couples events of infra elements to train numbers, such as section occupations and releases on open tracks and through railway stations, triggered signal changes, and switch position lockings. From this information other interesting process times can easily be derived, such as blocking times, running times on (block) sections, headway at infra points, route setting times, et cetera.

The actual arrival and departure times at a platform stop are in general not recorded automatically. Therefore, the tool TNV-Filter has been developed that estimates arrival and departure times in (large) stations based on TNV-tables generated by TNV-Prepare. The speed trajectory and train length of each train entering or departing a station is estimated on the basis of section (track circuit) occupation and clearance times and scheduled train characteristics. Estimation errors due to round-off errors (passage times are given in seconds) and deceleration (acceleration) variations during the approach (departure) are filtered by means of a nonlinear least-squares method taking into account possible speed limits at e.g. signals and switches. Subsequently, the running time at the platform section before and after standstill are estimated from the filtered inbound and outbound speed profiles, known standard deceleration and acceleration characteristics per type of train, and stop location on the platform section (possibly depending on train length). This way, the arrival and departure times of each train at the platform tracks are determined with a precision in the order of a second.

From March 2000 the TNV-logfiles from each TNV-control area are no longer wasted after a few days, but centrally collected each day and saved on CD-ROM for (internal) analysis purposes. This archiving is done by AEA Technology Rail under license from ProRail, primarily for use with TNV-Replay. The saved format is more compact and differs slightly from the raw TNV-logfiles described in this chapter [83]. In July 2003 the import utility of TNV-Prepare was extended to handle this format as well.

Chapter 5

STATISTICAL ANALYSIS: THE EINDHOVEN CASE

5.1 Introduction

Until recently, empirical analysis of train delays dealt with delays of at least 3 minutes for practical reasons of operations control. However, modern train detection systems and computing facilities now enable much more precise measurements and hence also much more accurate data analysis opportunities, see Chapter 4. Analysis of realized process times is a crucial step in punctuality management since operations data contain invaluable information about process time variations – which should be small in a well-designed railway system – and train interactions. Analysis of realization data reveals tight headway times or the actual amount of buffer time at infrastructure bottlenecks and train connections.

Stations are the bottlenecks in a railway network as here trains of various lines meet and interact. Delayed and/or early trains result in potential conflicting train paths — controlled by the interlocking system — causing mutual hinder at conflict points. Delays measured at stations represent a mixture of primary and secondary delays. Arrival delays are *input delays* to a station area summarizing the train operations upstream to the station including the inbound routes. They are a mixture of primary running time disruptions on the preceding open track and e.g. a provoked low speed by following a slow train on the open track, and hinder at merging and crossing inbound routes. Disruptions in the dwelling process are a source of primary delays, e.g. extensive alighting and boarding time and a prolonged departure process. The measured departure delays are the result of arrival delays, disruption in the dwelling process, and secondary delays at departure resulting from e.g. conflicting outbound routes or waiting for delayed feeder trains.

Statistics of process time realizations and resulting delays are a means of timetable evaluation identifying tight process times and critical train interactions (transfer times, headway) or on the other hand quantifying available slack and buffer times. Moreover, regression analysis can be applied to evaluate potential dependencies between processes as a cause of delay propagation. Note that delay measurements at stations provide train delays associated to any possible primary or secondary source. Finding the explicit source(s) of these resulting delays is hard and requires monitoring information other than just delay measurements. Nevertheless, train dependencies and critical process times expose possible sources of delay and give directions to possible improvements in the timetable design.

The objective of this chapter is to find *structural* variations in process times caused by regular minor disruptions and interactions. Major incidents or accidents — leading to long-term damage or obstruction of rail tracks — are not structural and (should) occur only seldom, and are

thus discarded in the analysis. Trains affected by an uncommon event experience delays that are clearly not representative to the usual stochastic behaviour. These situations are the subject of incidence management rather than daily operations practice. From a statistical point of view these delays are usually identified as outliers.

In the Netherlands, passenger train services operate basically according to a periodic timetable, repeating the same arrival and departure times each hour, with the exception of additional passenger trains in rush hours and freight trains that are scheduled in between the regular train services. It is hence anticipated that the traffic processes are mainly variations on a repetitive pattern. This motivates an aggregation on train line level rather than analysing process times of individual train numbers.

This chapter considers a case study of a statistical analysis applied to Eindhoven station. Parts of this chapter have been published before in Goverde *et al.* [87] and Hansen & Goverde [93, 94], and presented at several congresses including the 9th WCTR [86] and WCRR 2001 [85]. Over the last years similar and other statistical analyses have been applied to various stations and corridors [145, 199, 228]. The results presented in this chapter on Eindhoven have also been found in the other studies.

TNV-logfiles in the traffic area Eindhoven were collected during one week in September 1997 and made available by Railinfrabeheer and Railverkeersleiding to TU Delft. Note that in 1997 TNV-logfiles were not maintained but could be saved on request. From the TNV-logfiles the train line specific event times at railway station Eindhoven were generated by TNV-Prepare and subsequently the platform arrival and departure times were obtained using the TNV-Filter program (Chapter 4). In total, 1846 trains had been recorded, of which about 30% IC-trains, 30% IR-trains and 40% local (AR) trains. Freight trains have been discarded in the analysis. The statistical analysis of this Eindhoven data has been done by means of the statistical software package S-Plus [131].

The chapter is outlined as follows. Section 5.2 presents the characteristics of station Eindhoven. Section 5.3 gives the derived punctuality statistics of Eindhoven. In Section 5.4 departure delays are predicted from arrival delays using regression analysis, whereas the remaining noise is attributed to human factors. Section 5.5 covers distribution assessment of the events and processes in Eindhoven. In the final section some conclusions are presented.

5.2 Railway station Eindhoven

Eindhoven is the main intercity transfer station in the southern part of the Netherlands, where train lines of four main directions meet: from Utrecht (and beyond) in the north, from Rotterdam in the west, Venlo in the east, and Heerlen in the south. Eindhoven has 6 platforms for passengers and connects 3 double-track railway routes. A double-track route from Utrecht and one from Rotterdam merge at Boxtel from which a double-track¹ route leads to Eindhoven. So the west- and northbound trains have a mutual double-track route between Eindhoven and Boxtel, see Figure 5.1.

¹In the mean time the corridor between Eindhoven and Boxtel has been upgraded to a four-track route as part of the Rail 21 programme. The four-track route became fully operational at the end of 2002

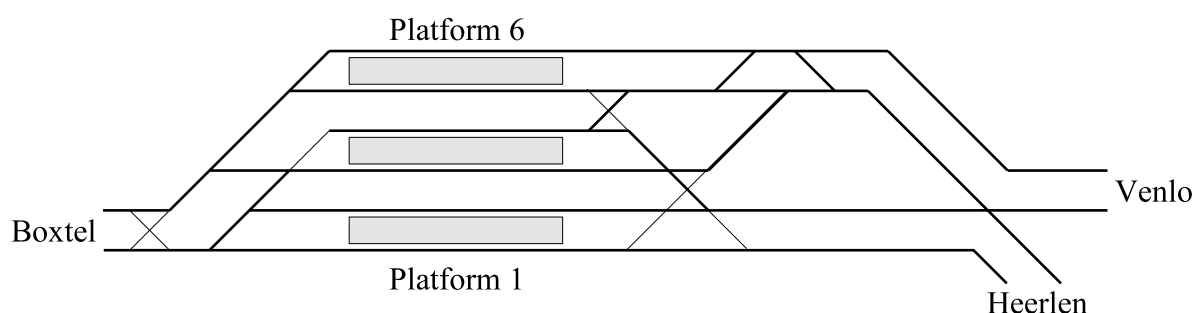


Figure 5.1 Station layout Eindhoven, shunting tracks not shown (1997)

Each (non-peak) hour 16 passenger trains arrive and depart in Eindhoven, that is, 4 trains from and in each direction. These trains correspond to 9 train lines, including

- 3 intercity (IC) train lines,
- 1 international (INT) train line,
- 2 interregional (IR) train lines, and
- 3 local (AR) train lines.

Eindhoven is the origin/destination station of 5 train lines (6 trains per hour) and 4 train lines stop in Eindhoven in both (forward and backward) directions (10 trains per hour), see Table 5.1. In rush hours, an extra passenger IR train line of 2 trains per hour is scheduled from/to the direction Utrecht, resulting in 10 passenger trains per hour between Eindhoven and Boxtel. Also additional freight trains pass Eindhoven on 4 through tracks. Between the long-distance train lines 6 cross-platform transfers are scheduled, see Section 5.3.4.

Table 5.1 Basic timetable and platform occupation in Eindhoven (1997/1998)

Train line	Frequency [train/hr]	Forward			Backward			Remark
		Track	A	D	Track	A	D	
IC800 Hlm-Mt	1	1	57	59	5	35	37	
IC900 Hlm-Ehv	1	2	27	-	5	-	07	
IC1500 Gvc-Hrl	1	1	24	29	6	05	09	
INT1800 Ehv-Koln	$\frac{1}{2}$	4	-	33	4	01	-	Even hours
IR1900 Rtd-Vl	1	2	54	59	6	35	39	
IR2700 Ehv-Vl	$\frac{1}{2}$	4	-	33	4	01	-	Odd hours
IR3500 Ut-Ehv	2	1	07	-	5	-	27	Peak hours
AR5200 Tbw-Dn	2	2	15	17	6	14	16	
AR6400 Ehv-Wrt	2	3	-	05	3	27	-	
AR9600 Ut-Ehv	2	3	20	-	3	-	12	

5.3 Punctuality Analysis

5.3.1 Arrival Delay

For all train lines the arrival times at Eindhoven have been obtained using TNV-Prepare and TNV-Filter. The resulting arrival delays are computed as the difference between the measured arrival times and the scheduled arrival times according to the published passenger train timetable (year plan) [152]. Hence, positive arrival delays correspond to late arrivals and negative values to early arrivals, as experienced by the passengers.

Table 5.2 Arrival delay statistics

Train line	N/O ¹	Mean	SD	Med.	F(180)	Skew	Late trains		
		[s]	[s]	[s]	[%]		Perc.	Mean	SD
							[%]	[s]	[s]
IC800 Hlm-Mt	109/2	83	100	83	83	0.4	76	122	81
IC800 Mt-Hlm	119/1	39	130	-6	86	1.0	46	148	115
IC900 Hlm-Ehv	116/0	138	144	98	66	0.9	84	171	133
IC1500 Gvc-Hrl	111/1	69	166	23	85	1.7	61	149	169
IC1500 Hrl-Gvc	99/3	49	85	43	93	0.5	71	88	67
INT1800 Koln-Ehv	58/2	63	97	53	86	0.7	66	112	80
IR1900 Rtd-Vl	109/0	24	118	-3	88	1.0	49	117	102
IR1900 Vl-Rtd	63/3	-46	82	-70	92	1.3	25	77	70
IR2700 Vl-Ehv	50/2	7	49	-3	96	0.8	50	48	39
IR3500 Ut-Ehv	15/2	85	124	98	69	0.2	80	132	94
AR5200 Dn-Tbwt	103/1	20	85	6	94	0.8	55	77	71
AR6400 Wt-Ehv	124/5	4	63	-16	100	1.0	40	81	74
AR9600 Ut-Ehv	139/4	-1	62	-16	96	1.1	41	62	53

¹N/O: Number of Measurements/Outliers

Table 5.2 shows a summary of the arrival delay statistics. During the one week measurement period several exceptional large arrival delays have been observed that deviated strongly from the bulk of the data, see for example Figure 5.2. These observations were identified as outliers and discarded in the remaining analysis (as denoted in the 2nd column of Table 5.2). This way the statistics are not distorted by outliers. The number of observations for the IR3500 Ut-Ehv is very small as these trains arrive from Utrecht in evening peak hours and at Sunday evening only. The statistics for this train line are hence only indicative, e.g. the 95% confidence interval of the mean arrival delay of the IR3500 Ut-Ehv trains is [10, 160] and the standard error is 34.4 seconds. In comparison the standard errors of the mean arrival delay of the other train lines range between 5.5 and 16.0 seconds. For a detailed account of the statistical procedures we refer to Goverde *et al.* [87].

The general view is that IC (and international) trains perform worse than IR and AR trains. The mean arrival delay per IC/INT line varies between $\frac{1}{2}$ and $1\frac{1}{2}$ min, with an exceptional inferior performance of the IC900 Hlm-Ehv trains that have a mean arrival delay of $2\frac{1}{2}$ min. The IR/AR trains have a considerable smaller mean arrival delay ranging basically from around 0 to $\frac{1}{2}$ min, and more than 50% of these trains arrive early. The westbound IR1900 Vl-Rtd trains even have a mean arrival of $\frac{3}{4}$ min early.

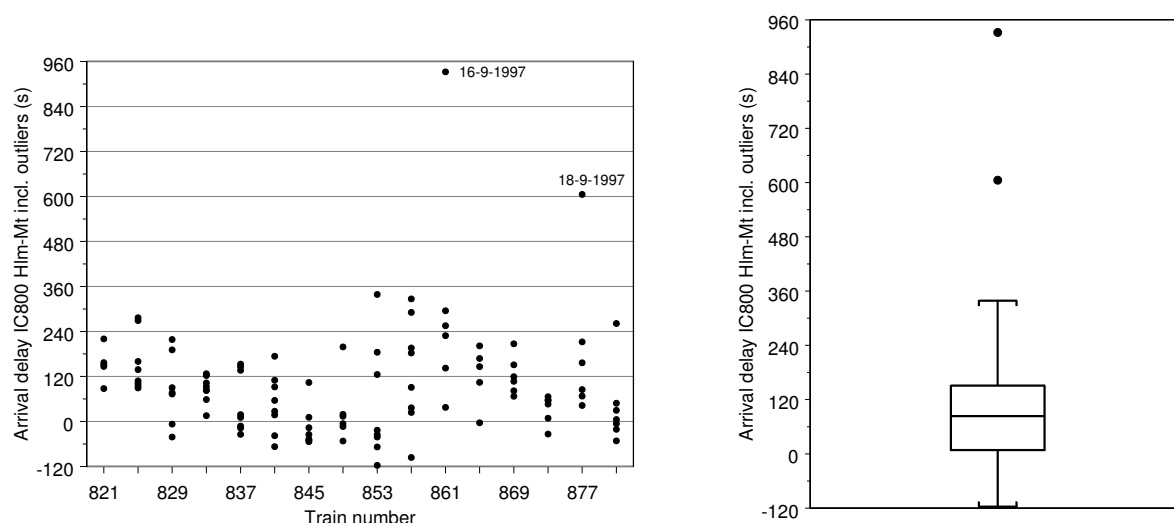


Figure 5.2 Arrival delay scatterplot (left) and boxplot (right) of the IC800 Hlm-Mt trains, identifying 2 outliers

The percentage of IC/INT trains arriving within 3 minutes after the scheduled arrival time ranges between 83% and 86%, with the exception of the westbound IC1500 Hrl-Gvc trains (93%), and the far worse performance of the IC900 Hlm-Ehv trains (66%). This percentage is considerably higher for AR/IR trains, which range between 88% and 100% (not counting the extra IR3500 trains). In 1997, NS aspired after 87% on time arrivals, where a train is considered late only if it is 3 minutes or more behind schedule. So this punctuality norm requires that $F(180) \geq 87\%$. In Eindhoven, all IC/INT train lines perform inadequate, except for the IC1500 Hrl-Gvc trains. The AR/IR trains on the other hand all perform satisfactory.

The statistics of late trains also show some notable facts. The percentage of IC/INT trains arriving late is significantly higher than that of the AR/IR trains, and so are the mean arrival delays of the late IC/INT trains. The mean arrival delay for late IC/INT trains ranges between $1\frac{1}{2}$ and 3 minutes. Only the IC800 Mt-Hlm trains are more often on time (or early) than late, although the mean arrival delay of the late trains is again considerable ($2\frac{1}{2}$ minutes). This suggests a bimodal behaviour where trains are either too early or too late, see Section 5.5.1. The same remarks apply to the IC1500 Gvc-Hrl trains. The IC900 Hlm-Ehv trains show again inferior performance with 84% trains arriving late with a mean delay of 3 minutes. In contrast, the AR/IR trains are more often on time (or early) than late and the late trains have a moderate mean arrival delay around 1 minute. The late IR1900 Rtd-Vl trains have an exceptional large arrival delay of 2 minutes, although only 49% is late. In this case the distribution is skewed to the right with a heavy tail, that is, although the data is centered around the scheduled arrival time also late arrivals occur of which the frequency slowly decreases with lateness. This also explains the large standard deviation (2 minutes) of this train line.

A general conclusion is that the arrival delays of IC/INT trains are worse than those of AR/IR trains, and eastbound trains from the Randstad perform worse than trains originating from the eastern part of the Netherlands.

5.3.2 Departure Delay

Table 5.3 shows the departure delay statistics of all train lines from Eindhoven during the observation period. The IR3500 train line now corresponds to extra trains from Eindhoven to Utrecht in the morning peak hours on working days, in the morning on Saturdays, in the afternoon on Fridays, and in the evening hours on Sundays. The amount of IC3500 Ehv-Ut observations is sufficient as the variation is only small; the standard error of the mean departure delay is 8.4 seconds. The mean departure standard error of all train lines ranges between 4.2 and 16.5 seconds [87].

Table 5.3 Departure delay statistics

Train line	N/O ¹	Mean [s]	SD [s]	Median [s]	F(180) [%]	Early [%]
IC800 Hlm-Mt	109/4	113	91	97	80	3
IC800 Mt-Hlm	119/2	120	104	71	78	1
IC900 Ehv-Hlm	128/3	100	84	73	84	0
IC1500 Gvc-Hrl	108/1	154	136	105	69	0
IC1500 Hrl-Gvc	99/3	120	69	108	78	0
INT1800 Ehv-Köln	56/1	123	103	89	77	0
IR1900 Rtd-Vl	109/0	117	94	100	78	2
IR1900 Vl-Rtd	63/3	90	58	78	96	0
IR2700 Ehv-Vl	55/0	154	122	111	69	0
IR3500 Ehv-Ut	34/5	45	45	32	98	0
AR5200 Tbwt-Dn	148/9	51	49	29	92	1
AR5200 Dn-Tbwt	103/1	83	81	52	88	0
AR9600 Ehv-Ut	210/1	98	100	61	84	1

¹N/O: Number of Measurements/Outliers

The IC/INT trains have a mean departure delay of 2 minutes, with the exception of the starting IC900 Ehv-Hlm trains ($1\frac{1}{2}$ min) and the large mean departure delay of the IC1500 Gvc-Hrl trains (3 min). The mean departure delay of the AR/IR trains is significantly smaller and ranges between 1 and $1\frac{1}{2}$ minute, with the exception of the IR1900 Rtd-Vl trains (2 min) and the IR2700 Ehv-Vl trains ($2\frac{1}{2}$ min).

Looking at the fraction of departure delays not exceeding 3 minutes, we see again that the IC/INT trains perform worse than the AR/IR trains. From the IC/INT trains the IC1500 Gv-Hrl has the worst punctuality (only 69% departs within 3 min after schedule), and the starting IC900 Ehv-Hlm trains perform best (84%). This percentage for the other IC/INT train lines ranges between 77% and 80%. In case of the AR/IR trains the IR2700 Ehv-Vl (69%) and IR1900 Rtd-Vl (78%) have the worst punctuality. Of the other AR/IR trains between 84% and 98% departs no later than 3 minutes. In 1997, the NS aimed at a minimum of 87% trains departing before 3 minutes after schedule. All IC/INT train lines fail to satisfy this norm, whereas 4 out of 7 AR/IR train lines meet the 87%-norm.

A critical observation is the departure performance of train lines starting in Eindhoven. The train line performing best is the IC900 Ehv-Hlm for the IC/INT lines, and the IR3500 Ehv-Ut for the AR/IR lines. On the other hand, the INT1800 Ehv-Köln is the worst performing IC/INT line (except for the much inferior IC1500 Gvc-Hrl), and the worst AR/IR lines also

start in Eindhoven including the most inferior performing IR2700 Ehv-VI line. Some of these late departure cases may be explained by conflicts with other (delayed) trains. In other cases, lack of personnel discipline appears the only explanation. In Section 5.4 we will see that the IC900 Ehv-Hlm trains – although departing relatively punctual – blocks the following IC1500 Hrl-Gvc trains.

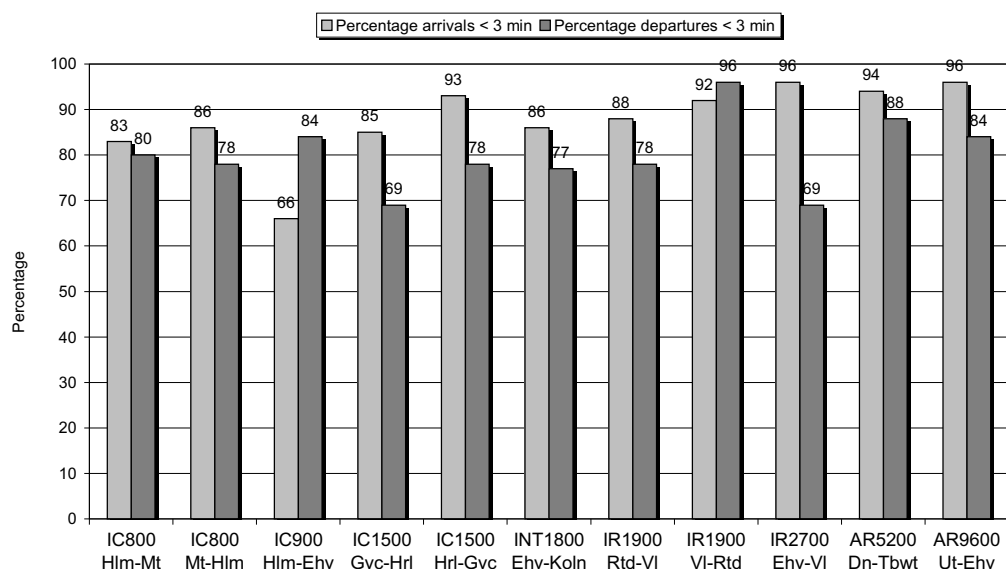


Figure 5.3 Arrival and departure punctuality

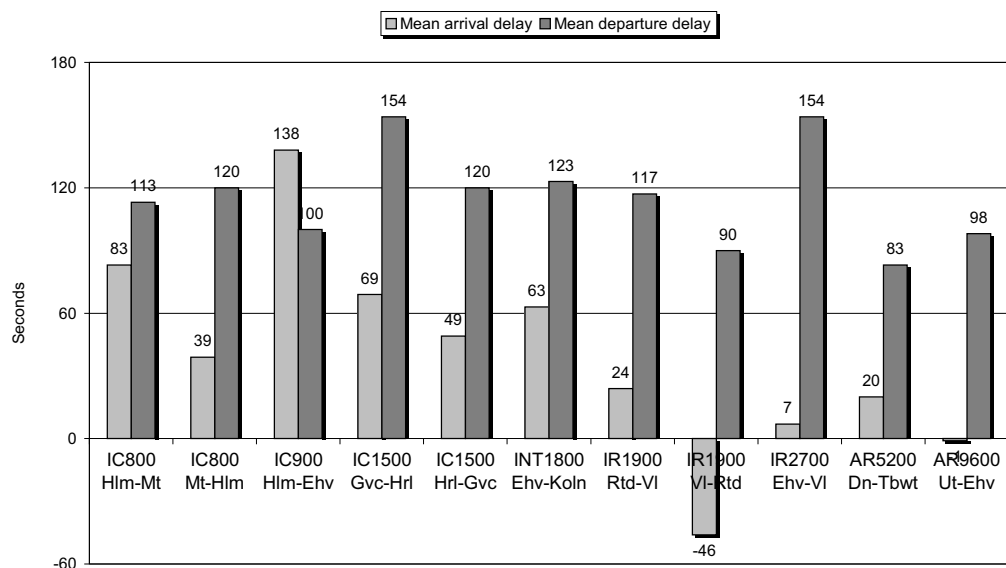


Figure 5.4 Mean arrival and departure delay

Let us now compare the arrival and departure statistics. Figure 5.3 shows the share of arrival delays and departure delays smaller than 3 minutes, whereas Figure 5.4 gives the mean arrival and departure delays for all train lines. Note that we discard the IR3500 line since the arrivals and departures of this line correspond to different periods (the evening and morning peak, respectively) and are obviously not related. These figures clearly show that punctuality and mean

delay at departure is generally worse than at arrival, with only two exceptions: the IC900 (which however turns in Eindhoven with 40 min layover time), and the IR1900 Vl-Rtd (of which 75% arrive early). Possible causes of this punctuality drop in Eindhoven are too tight dwell times or transfer times, and conflicting train movements. In the sequel of this chapter we will explore these delay enlargements by data analysis techniques. In particular, Section 5.4 investigates transfer connections using regression analysis.

As an example of a potential source of hindering we consider the following case. The INT1800 EHV-Koln and IR2700 EHV-Vl are scheduled to depart for Venlo from platform 4 at 33 each hour (recall that these lines run every other hour and together offer an hourly service to Venlo). However, at 35 each hour the IC800 Mt-Hlm is scheduled to arrive at platform 5 (to offer a cross-platform transfer). The outbound route from platform 4 to Venlo crosses the inbound route from Maastricht to platform 5 at a distance of 1500 meter from the platforms, i.e., at about 1 minute running time for both the inbound and outbound trains. The conflicting train routes are thus scheduled almost simultaneously, where the inbound intercity train has priority at the crossing over the departing INT/IR train. This scheduled situation is clearly critical: a slight delay of the arriving IC800 train already results in hindering the departing INT1800/IR2700 train. A similar hindrance situation over the same crossing occurs between the outbound IR1900 Rtd-Vl trains (departure from platform 2 in Eindhoven at 59) and the inbound IC1500 Hrl-Gvc trains (arrival at platform 6 in Eindhoven at 05), although here the outbound train is scheduled first. Tromp & Hansen [199] give a detailed analysis of this latter case.

5.3.3 Dwell Time

Four through train lines have a stop at Eindhoven in both directions resulting in dwell times for 8 train directions. Table 5.4 shows the dwell time statistics². The scheduled dwell times are 2 minutes (4 cases), 4 minutes (2 cases), and 5 minutes (2 cases). The mean and median dwell time are all considerable larger than scheduled in correspondence to Figure 5.4 that shows a delay increase during the stop in Eindhoven. Since early arrivals cause large dwell times, Table 5.4 also gives the dwell times for late trains only (see also Figure 5.5). Still the mean dwell time is significantly larger than scheduled with an average excess of 20 to 45 seconds. These figures are highly accurate since the confidence intervals of the mean dwell times are very tight. The mean standard errors range between 3.9 and 10.7 s for all trains per line, and the mean standard errors of dwell time for late trains range between 4.0 and 12.6 s (the larger standard errors correspond to 300 s scheduled dwell time) [87].

So even for late trains the mean dwell times still exceed the scheduled time for all train lines, although one expects the opposite if buffer time is available. It can be concluded that the scheduled dwell times are too tight and there is no buffer time available to compensate for arrival delays.

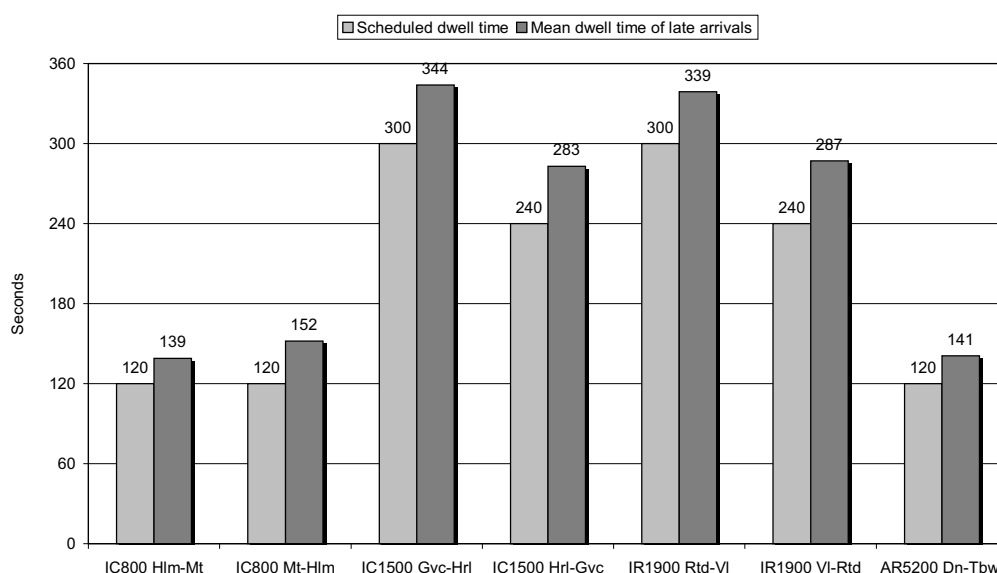
Exceeding the scheduled dwell time may have several causes. First, the amount of boarding and alighting passengers may be so excessive that the scheduled dwell time is not sufficient. A field analysis further showed that train drivers were not that concerned to depart as quick as possible [226]. Trains often departed 30 seconds or more behind schedule, even though no more

²There was a problem to recover the inbound route of the AR5200 Tbwt-Dn at the time of analysis, by which the associated dwell time is missing in the analysis

Table 5.4 Dwell time statistics

Train line	N/O ¹	Plan [s]	Mean [s]	SD [s]	Median [s]	Late trains		
						Perc. [%]	Mean [s]	SD [s]
IC800 Hlm-Mt	109/2	120	149	40	144	76	139	36
IC800 Mt-Hlm	119/2	120	201	60	197	46	152	34
IC1500 Gvc-Hrl	108/2	300	385	111	366	61	344	91
IC1500 Hrl-Gvc	99/3	240	311	67	305	71	283	50
IR1900 Rtd-VI	109/0	300	393	101	389	49	339	92
IR1900 VI-Rtd	63/5	240	377	75	379	25	287	31
AR5200 Dn-Tbwt	103/1	120	171	68	168	55	141	65

¹N/O: Number of Measurements/Outliers

**Figure 5.5** Dwell time of late trains

boarding of passengers took place. All this time the departure signal shows a proceed aspect so that the locked route blocks possible other traffic. Second, a delayed feeder train may be a source for delays when the connection is secured, see Section 5.4. Third, a route conflict may postpone the outbound route setting, see the discussion at the end of Section 5.3.2.

5.3.4 Transfer Time

Transfer connections are one of the major sources of secondary delays. Especially in the highly urbanized Netherlands, where intensive train services are coordinated in an integrated periodic timetable offering good connections between any pair of stations with (cross-platform) transfer opportunities between main lines when direct connections are not available. In Eindhoven, 6 cross-platform transfers are scheduled between train lines from all 4 directions.

Table 5.5 shows the transfer time statistics for *late feeder trains*. Note that these transfer times are crucial as the connecting train may wait or the connection might be cancelled. The third

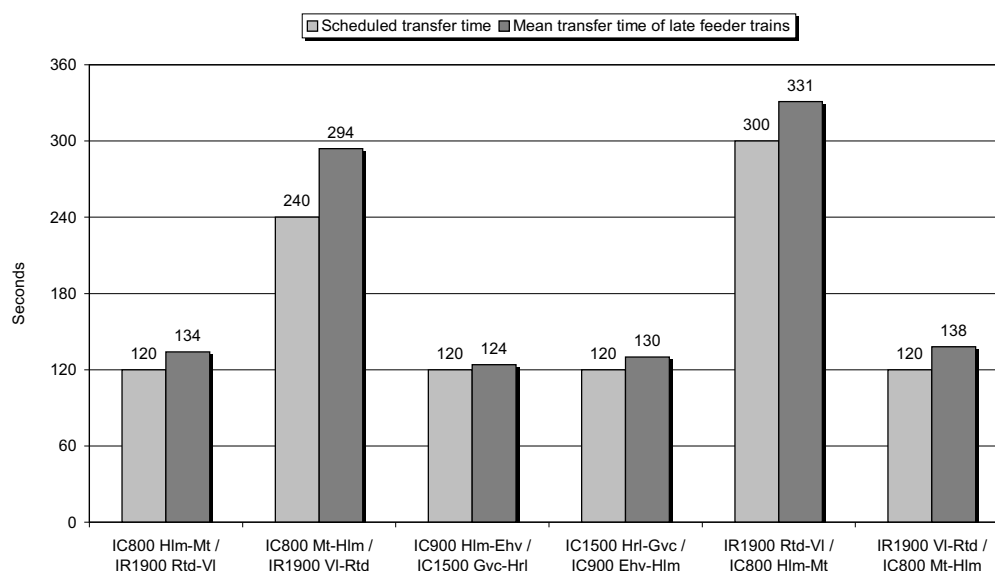
Table 5.5 Transfer time statistics

Feeder line	Connection	N/O/C ¹	Plan	Late feeder trains			
				Perc.	Mean	SD	Median
			[s]	[%]	[s]	[s]	[s]
IC800 Hlm-Mt	IR1900 Rtd-VI	102/6/2	120	80	134	41	128
IC800 Mt-Hlm	IR1900 VI-Rtd	60/4/1	240	32	294	36	292
IC900 Hlm-Ehv	IC1500 Gvc-Hrl	102/8/1	120	83	124	27	117
IC1500 Hrl-Gvc	IC900 Ehv-Hlm	95/8/3	120	69	130	37	128
IR1900 Rtd-VI	IC800 Hlm-Mt	102/6/0	300	49	331	70	314
IR1900 VI-Rtd	IC800 Mt-Hlm	63/4/3	120	21	138	32	140

¹N/O/C: Number of Measurements/Outliers/Cancelled Connections

column gives the number of total transfers, the number of outliers, and the number of cancelled connections (which are also included in the outliers). Only a fraction of the observed transfers is cancelled due to an extremely large arrival delay of the feeder train: the percentages of cancelled connections range from 0% to 5%. The confidence levels of the mean transfer times (for late feeder trains) are highly accurate. The mean standard errors range from 3.1 seconds to 10.2 seconds (the latter corresponds to the 300 seconds scheduled transfer time).

Four connections have a scheduled transfer time of 2 minutes. In these cases the mean transfer time is slightly larger. The other two connections have a larger scheduled transfer time, but still the mean transfer time exceeds the scheduled transfer time with a 1/2 minute for the 5 minute transfer time and 1 minute for the 4 minute transfer time. Figure 5.6 visualizes the mean transfer time (for the late feeder trains).

**Figure 5.6** Transfer time of late feeder trains

One would expect that if a train waits for transferring passengers of a late feeder train it would depart as soon as these passengers get on the train. However, we found that the mean transfer times from late feeder trains exceed the scheduled transfer time. Several explanations are possible, such as conflicting train movements (route settings) or headway constraints.

Another explanation is that the scheduled transfer time is too tight for a cross-platform in Eindhoven as a result of dense passenger flows. If the number of transferring passengers is large, also the alighting time from the feeder train and the boarding time in the connecting train gets large. Moreover, opposite passenger flows and waiting passengers at the platform hinder transferring passengers in both alighting and walking to the other train. In particular the 4 connections involving the IC800 and IR1900 trains may suffer from this phenomena: when the IC800 Hlm-Mt arrives the platform is already blocked by transferring passengers from the IR1900 train that arrived shortly before, as well as travellers originating from Eindhoven. For the northbound lines, the IC800 Mt-Hlm and IR1900 Vl-Rtd trains arrive at the same time and hence again transferring passengers in opposite directions cross each other, and they are also hindered by boarding travellers originating from Eindhoven and alighting passengers who are heading towards the escalator. A field analysis indeed showed crowding of waiting passengers at the platforms in Eindhoven [226].

The transfer connections may hence explain the delay increase in Eindhoven for the 6 train lines involved in interconnections. This is analysed in Section 5.4.

5.4 Regression Analysis

5.4.1 Introduction

The train interconnections at Eindhoven may explain (some of) the variation in a departure delay, which can be explored using regression analysis. Table 5.6 summarizes the cross-platform transfers at Eindhoven along with the transfer time from feeder to connecting train and the dwell time of the connecting train.

Table 5.6 Cross-platform transfers in Eindhoven

Feeder train line	Transfer time [s]	Connection	Dwell time [s]
IR1900 Rtd-Vl	300	IC800 Hlm-Mt	120
IC800 Hlm-Mt	120	IR1900 Rtd-Vl	300
IR1900 Vl-Rtd	120	IC800 Mt-Hlm	120
IC800 Mt-Hlm	240	IR1900 Vl-Rtd	240
IC900 Hlm-Ehv	120	IC1500 Gvc-Hrl	300
IC1500 Hrl-Gvc	120	IC900 Ehv-Hlm	-

Linear regression analysis aims at explaining the statistical behaviour of a certain dependent variable by a model of predictor (or independent) variables, see e.g. Rice (1988). In this section, we analyse the dependence of the departure delays of a pair of interconnected trains on their arrival delays. We consider a simple linear regression model

$$D_{\text{train 1}} = \beta_0 + \beta_1 f(A_{\text{train 1}}, A_{\text{train 2}}),$$

where the first (constant) term on the right-hand side is called the intercept and the second term consists of a function in the predictor variables (the arrival delays) multiplied by a slope parameter. Note that the model is linear in the unknown parameters β_0 and β_1 , but not necessarily in

the predictor variables. The function of the predictor variables in the regression models that we consider is either the arrival delay of one of the trains or the maximum of both arrival delays. The first case implies domination of the used arrival delay over the arrival delay of the other train. In the latter case, both trains propagate their arrival delay to the connecting train.

A positive intercept in the regression models denotes the average overload (or buffer for negative intercepts) to the scheduled dwell/transfer time when the arrival delays are zero. For a positive intercept and a positive slope smaller than one, the departure delays grow with the arrival delays but with a slower rate. So, from a certain arrival delay determined by the intercept and the slope,

$$\frac{\beta_0}{1 - \beta_1}, \quad (5.1)$$

the departure delay gets smaller than the (maximum) arrival delay. A small arrival delay thus results in an increased departure delay (the intercept dominates), whereas for a large arrival delay the (departure) delay is reduced although the delay will never settle to zero. The latter behaviour corresponds to the practice that trains with large arrival delays are given priority and stop only for a minimum necessary time. If the intercept is negative then the delay is decreased and even settles to zero for arrival delays below a value determined by the intercept and slope given as $-\beta_0/\beta_1$.

The quality of a linear regression fit is assessed by several test statistics. Multiple R^2 is the *squared multiple correlation coefficient*, which can be interpreted as the proportion of the variability of the dependent variable that can be explained by the independent variables. The *residual* is the difference of the observed and fitted values. The *residual standard error* (RSE) is therefore a measure of the variation between the observed and fitted values. The F -statistic should be as large as possible for a good fit, and the p-value close to zero. For more details on linear regression analysis we refer to e.g. Rice [172].

For the detection of possible outliers we applied robust LTS regression analysis, see Section 5.4.2. The outliers were then discarded in the linear regression analysis. The main results are summarized in Table 5.7 and detailed in the sequel. The cancelled connections mentioned in Table 5.7 are also contained in the outliers.

Table 5.7 Linear regression results transfer connections

Transfer	N/O/C ¹	R^2	RSE	F	β_0			β_1		
					Val.	SE	t	Val.	SE	t
IC800/IR1900 Hlm-Vl	102/11/2	0.86	31	526	41	4.2	9.6	0.76	0.033	23
IR1900/IC800 Rtd-Mt	102/2/0	0.92	36	1196	38	4.5	8.4	0.91	0.026	35
IC800/IR1900 Mt-Rtd	60/4/1	0.94	32	897	82	4.5	18.4	0.72	0.024	30
IR1900/IC800 Vl-Hlm	60/7/3	0.86	45	302	73	6.3	11.6	0.82	0.047	17
IC900/IC1500 Hlm-Hrl	102/8/1	0.94	30	1484	32	4.3	7.6	0.86	0.022	39
IC1500/IC900 Hrl-Hlm	95/8/3	0.81	25	359	46	4.7	9.9	0.85	0.045	19

¹N/O/C: Number of Measurements/Outliers/Cancelled Connections

5.4.2 Robust LTS Regression

Outliers may influence the results of regression analysis. Therefore, prior to fitting a simple linear regression model, we used a robust *least trimmed squares* (LTS) regression analysis to

identify possible outliers [176, 131]. As an example we show the procedure as applied to the regression analysis of the transfer connection from the IC800 Mt-Hlm to the IR1900 Vl-Rtd train line.

In LTS regression the cost function is the sum of the smallest q squared residuals, where q depends on the data size. The default value is $q = \max(\lfloor (n+p+1)/2 \rfloor, \lfloor 0.9n \rfloor)$, where n is the number of observations and p is the number of regression coefficients. For simple regression $p = 2$, so that in practice 90% of the number of observations is used for the LTS regression estimate. This corresponds to a 10% trimmed data set.

In our example the dependent variable is the IR1900 Vl-Rtd departure delay and the independent variable is the maximum of both arrival delays. The data contains 60 observations, and hence the LTS estimate is based on 54 observations. The LTS regression model is

$$D_{\text{IR1900 Vl-Rtd}} = 79 + 0.72 \max(A_{\text{IC800 Mt-Hlm}}, A_{\text{IR1900 Vl-Rtd}}).$$

We use this robust regression fit to identify possible outliers.

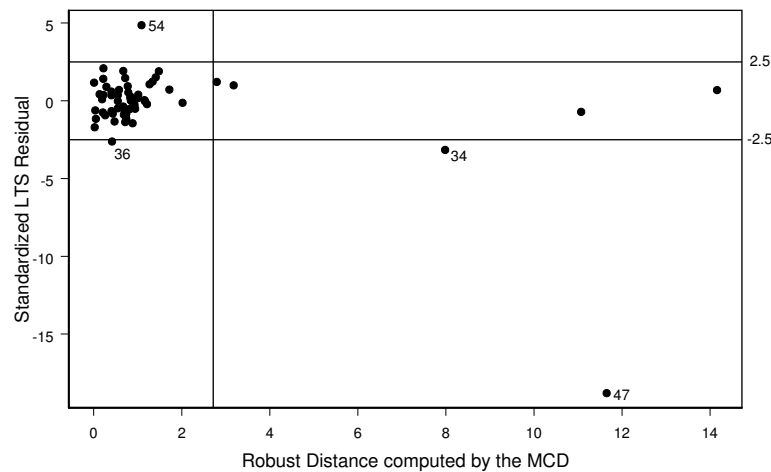


Figure 5.7 Diagnostic plot of LTS Residuals vs. robust distance

Figure 5.7 shows the diagnostic plot of the standardized LTS residuals versus the robust distances computed by the *minimum covariance determinant* (MCD) estimates [176, 131]. This plot allows to distinguish between regular observations, vertical outliers, good leverage points, and bad leverage points. The plot should be read as follows. The regular observations that behave according to the model are grouped in the left rectangle between the horizontal lines with LTS residuals -2.5 and 2.5 , and the vertical lines with MCD estimates 0 and 2.5. The four points at the right of this rectangle between the two horizontal lines are *good leverage points*: the arrival delays are much larger but the predictions still follow the model well. The points in the areas above and below the rectangle between the two horizontal lines are *regression outliers*: they generally cause a shift of the regression line in vertical direction. Finally, the points in the two areas at the right top and right bottom are *bad leverage points* that have a negative influence on the slope of the regression line.

The robust diagnostic plot in Figure 5.7 hence identifies 4 outliers. Observation 47 at the right bottom is the missed connection, which is clearly identified as a bad leverage point. The IC800

arrival delay is 836 s, whereas the IR1900 delay has only a small departure delay of 39 s. A second bad leverage point is observation 34, which corresponds to 577 s arrival delay of the IR1900 train and a departure delay of 388 s. Furthermore, two regression outliers are detected: Observation 36 consists of a 43 s arrival delay of the IC800 train and a departure delay of 20 s. And finally, observation 54 where both trains arrive early (63 s and 70 s, respectively) but the departure is 200 s delayed.

The next step is to remove the 4 outliers from the data and use a simple linear regression analysis on the remaining data to obtain a final regression fit. In Table 5.7 we see that the final regression fit is obtained as

$$D_{\text{IR1900 VI-Rtd}} = 82 + 0.72 \max(A_{\text{IC800 Mt-Hlm}}, A_{\text{IR1900 VI-Rtd}}),$$

which differs from the LTS regression fit only in the intercept with 3 seconds. Note that these regression coefficients may differ from the LTS regression estimate since the linear regression fit is based on more observations, assuming that the number of outliers does not exceed 10% of the total number of observations. Despite the relatively small number of observations ($60 - 4 = 56$) for the above regression fit, the fit performs remarkably well with an explained variation of $R^2 = 94\%$ and a residual standard error of $\text{RSE} = 32$ seconds. For an interpretation of the results see Section 5.4.4.

5.4.3 Transfers between IC800 Hlm-Mt and IR1900 Rtd-VI

The eastbound IR1900 and IC800 trains run in this order from Boxtel to Eindhoven over the same track. The IC800 trains are scheduled to arrive 3 minutes after the IR1900 trains after which 2 minutes later both trains depart in their respective directions. This timing allows a cross-platform transfer between both trains with a transfer time of 5 and 2 minutes, respectively.

The regression model that performs best in explaining the departure of the IC800 trains to Maastricht from the arrival delays is

$$D_{\text{IC800 Hlm-Mt}} = 38 + 0.91 A_{\text{IC800 Hlm-Mt}},$$

where $D_{\text{IC800 Hlm-Mt}}$ is the departure delay of the IC800 trains at Eindhoven in the direction Maastricht, and $A_{\text{IC800 Hlm-Mt}}$ its arrival delay, see Figure 5.8. This model explains 92% of the variation of the departure delay with a residual standard error of 36 seconds. Detailed regression results are presented in Table 5.7. Apparently, the departure of IC800 trains to Maastricht does not depend on the arrival of the feeder IR1900 trains from Rotterdam. Recall however that the IR1900 and IC800 trains approach Eindhoven in this order over the same double-track route from Boxtel. In all observations this order is respected, and hence a large IR1900 arrival delay also resulted in a large IC800 delay.

The regression model of the departure of the IR1900 trains to Venlo that performs best is

$$D_{\text{IR1900 Rtd-VI}} = 41 + 0.76 A_{\text{IC800 Hlm-Mt}},$$

which explains 86% of the variation of the departure delay with a residual standard error of 31 seconds, see Figure 5.8. Table 5.7 contains the detailed regression results. The departure time of the IC 1900 trains to Venlo also depends only on the arrival delay of the feeder IC 800 trains

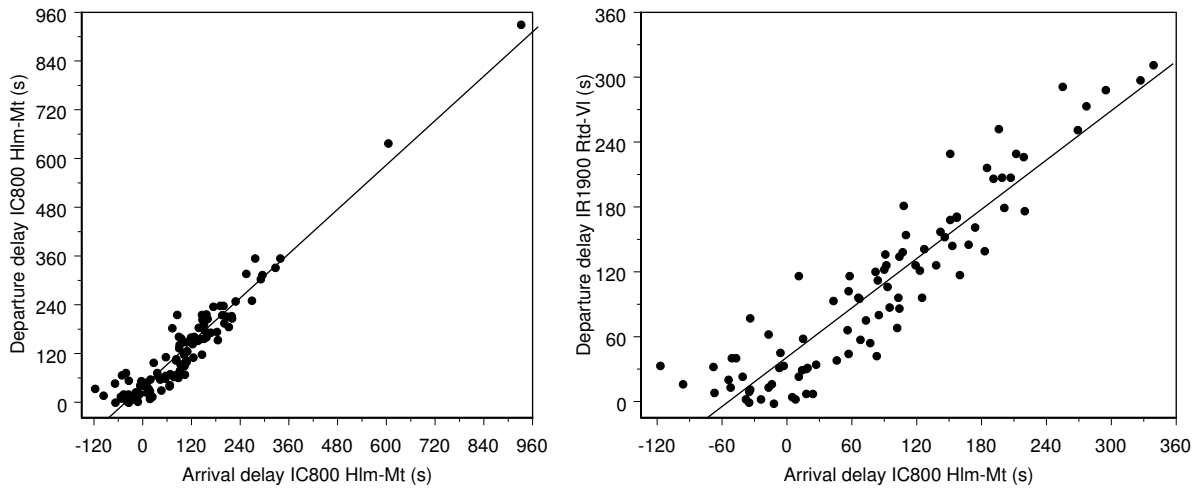


Figure 5.8 Linear regression model of departure delay IC800 Hlm-Mt (left) and departure delay IR1900 Rtd-Vl (right)

from Haarlem. Further analysis showed that in only 2 cases (out of 102) the IR 1900 trains did not wait for the IC800 trains. Hence, the arrival delay of IC800 — possibly obtained from the IR1900 before passing Boxtel — is (back-) propagated to the IR1900 by the transfer.

The large scheduled dwell time of the IR1900 trains (5 min) is obviously the result of a synchronization time to allow for a transfer with the IC800 train. Due to the infrastructure limitations between Boxtel and Eindhoven and the scheduled transfer, the large dwell time cannot be used as buffer time. The analogue is valid for the transfer time of 5 minutes from the IR1900 to the IC800 trains. Moreover, the dwell time of the IC800 train (2 min) and the transfer time of 2 min from the IC800 to the IR1900 trains are too tight and contain no buffer times, as can be seen from the positive intercepts of both regression models. The regression models both perform very well, i.e., the models explain most of the variation in the departure delay and the residual errors are small. It can be concluded that in this bilateral transfer connection the IC800 trains clearly dominate the departures.

5.4.4 Transfers between IC800 Mt-Hlm and IR1900 Vl-Rtd

The westbound IC800 and IR1900 trains are scheduled to arrive at the same time in Eindhoven to allow a cross-platform transfer. The IC800 train departs 2 minutes later, whereas the IR1900 train has to wait 2 additional minutes before it is allowed to depart over the same open track to Boxtel.

The linear regression model of the IC800 departure delays in the arrival delays is

$$D_{\text{IC800 Mt-Hlm}} = 73 + 0.82 \max(A_{\text{IC800 Mt-Hlm}}, A_{\text{IR1900 Vl-Rtd}}),$$

which explains 86% of the variation in the departure delays with a residual standard error of 45 seconds, see Figure 5.9. Details are given in Table 5.7. The regression model of the IR1900 departure delays in the arrival delays is

$$D_{\text{IR1900 Vl-Rtd}} = 82 + 0.72 \max(A_{\text{IC800 Mt-Hlm}}, A_{\text{IR1900 Vl-Rtd}}),$$

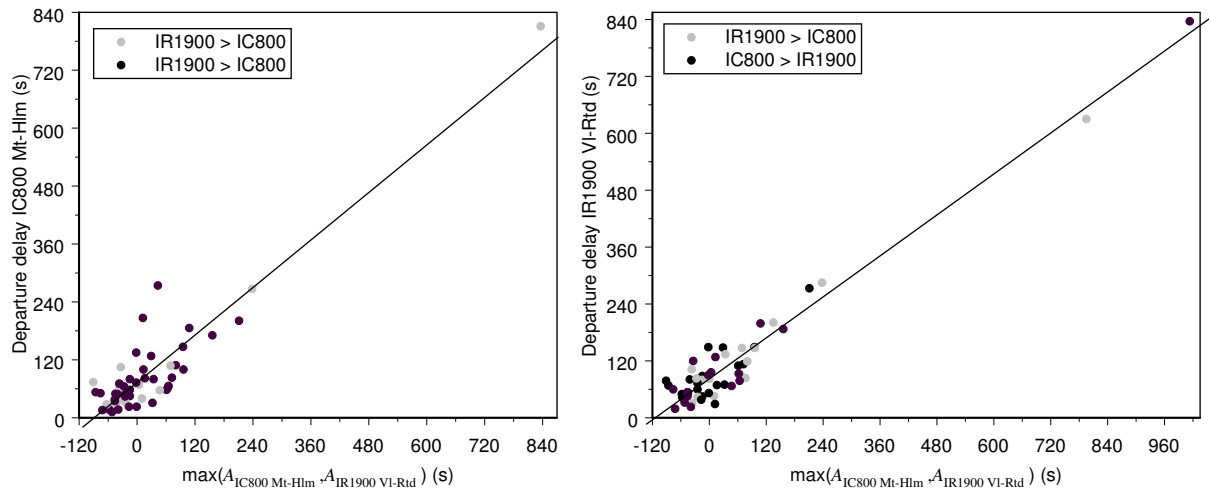


Figure 5.9 Linear regression model of departure delay IC800 Mt-Hlm (left) and departure delay IR1900 VI-Rtd (right)

which explains 94% of the IR1900 departure variation with a residual standard error of 32 seconds, see Figure 5.9. The complete regression results are found in Table 5.7.

From these regression models we see that the transfer connection in Eindhoven between the westbound IC800 and IR1900 trains results in a mutual dependence of the departure delays on the arrival delays. The departing route of the IC800 and IR1900 trains coincides from Eindhoven to Boxtel and is scheduled in this order. In only 3 cases (out of 60) this order is changed and the IR1900 train departs first, which results in a missed connection in only 1 of these cases. Moreover, in only 3 (other) cases the IC800 trains do not wait for a large delayed IR1900 train. In all other cases the transfer is secured and the departure order is respected from Eindhoven to Boxtel. Hence, the departure of the IC800 trains to Haarlem depends on the latest of both arrivals. This also holds for the departure of the IR1900 trains to Rotterdam, which depart after the IC 800 trains.

The dwell time of the IC800 trains and the transfer time from the IR1900 to the IC800 trains (both 2 min) are crucial. These process times are too tight as can be seen from the large intercept of the IC800 departure regression model. The larger dwell time of the IR1900 trains and the transfer time from IR1900 to IC800 (both 4 min) are not effective with respect to buffer time but result from the headway departure constraint, which requires a safety distance of (about) 2 minutes between the IC800 and IR1900 trains.

5.4.5 Transfer IC900 Hlm-Ehv to IC1500 Gvc-Hrl

The IC900 train line from Haarlem to Eindhoven turns in Eindhoven and departs 40 minutes later in backward direction. There is a scheduled transfer in Eindhoven to the IC1500 train line in the direction Heerlen. The IC1500 train is scheduled to arrive first, followed 3 minutes later by the IC900 train, after which the IC1500 departs 2 minutes later.

Regression analysis of the IC1500 departure delay in terms of the arrival delays gives the linear regression model

$$D_{IC1500 \text{ Gvc-Hrl}} = 32 + 0.86A_{IC900 \text{ Hlm-Ehv}},$$

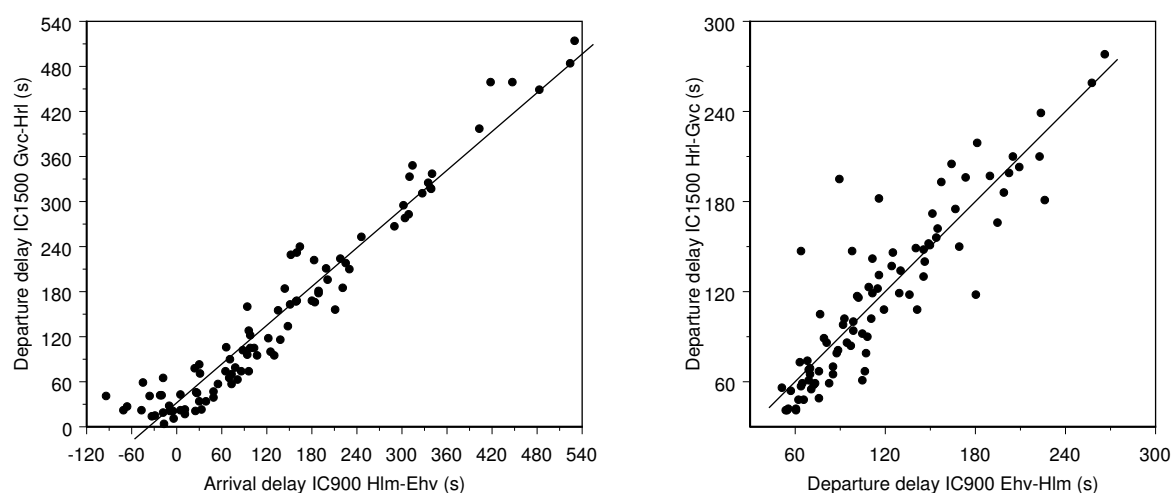


Figure 5.10 Linear regression model of departure delay IC1500 Gvc-Hrl (left) and IC1500 Hrl-Gvc (right)

which explains 94% of the variation in the IC1500 departure delay with a residual standard error of 30 seconds, see Figure 5.10. The complete regression results are given in Table 5.7.

The departure of the southbound IC1500 train depends on the arrival delay of the feeder IC900 train only. Again, both trains share the approaching route from Boxtel, where the IC900 trains are scheduled after the IC1500 trains. This order is changed in only 3 (out of 102) cases. In only 1 case an IC1500 train does not wait on a large delayed IC900 train. Hence the high dependence on the feeder train.

The large dwell time of the IC1500 trains (5 min) is not effective since when a IC1500 train is delayed then so is the IC900 - if the order from the Boxtel-Eindhoven corridor is respected - and at Eindhoven the IC1500 train waits on its turn for the IC900 to secure the transfer. The transfer time from IC900 to IC1500 (2 min) is slightly too tight as follows from the positive intercept in the regression model.

5.4.6 Transfer IC1500 Hrl-Gvc to IC900 Ehv-Hlm

The IC900 trains starting in Eindhoven for Haarlem have to wait for IC1500 trains from Heerlen with a tight transfer time of 2 minutes. It is expected that the transfer connection is the main bottleneck for a punctual departure. Only in 3 (out of 95) cases the IC900 train does not wait for a delayed IC1500 train. The variation in IC900 departure delays can however not be explained satisfactorily from regression analysis with the arrival delays of the feeder train as predictor variables.

Apparently, a large proportion of the starting IC900 trains are delayed independently of the transfer connection. The IC900 trains arrive at platform 2 and depart 40 minutes later from platform 5. In between, the train is parked on a shunting track. No other trains seem to interact structurally with the departure of the IC900 trains. The shunting process may be an explanation of the variation in departure times, including the personnel behaviour.

When considering the departure delay of both the IC900 trains and the IC1500 trains a clear dependence is seen, which is the result of the Eindhoven-Boxtel corridor. A simple regression model of the IC1500 departure delay in the IC900 departure delay is

$$D_{\text{IC1500 Hrl-Gvc}} = 46 + 0.85D_{\text{IC900 EHV-Hlm}},$$

which explains 81% of the IC1500 departure delay variation with a residual standard error of 25 seconds, see Figure 5.10. Details are presented in Table 5.7. The IC1500 trains are hindered by the IC900 trains, which are scheduled to depart first. The IC1500 train then departs after a minimum departure headway to respect the safety distance. This hindrance may explain the low departure punctuality of the IC1500 trains (78% departs within 3 min late), whereas the arrival punctuality is very high (93% arrives within 3 min late), see Figure 5.3. The low departure punctuality of the AR9600 EHV-Ut trains may be caused on its turn by the delayed IC1500 trains.

A possible improvement of this situation is changing the timetable order of the IC900 and IC1500 trains. This way the IC1500 trains do not have to wait for the starting IC900 trains. However, changing this order also implies changing the order of the IC800 and IR1900 trains to keep the regular interval timetable intact. Recall that the IC1500/IR1900 train lines and the IC800/IC900 train lines provide a bundled half hour service on a large part of their (mutual) route. Evidently, NSR also recognized this improvement, which has been realized in the 2001/2002 timetable [215]. Obviously, the problem is no longer actual since the release of the four-track route in 2002.

5.4.7 Stability

In the previous subsections the linear regression analyses of train pairs involved in a transfer connection showed a strong dependency of the departure delays in the arrival delays. The only exception being the last connection (from IC1500 Hrl-Gvc to IC900 EHV-Hlm), which is therefore discarded in the following.

The regression models of the five transfer connections are all similar in that the intercept is positive and the slope is between 0 and 1. Hence, for small arrival delays the intercept dominates resulting in an increase of delay, i.e., on the average the departure delay exceeds the arrival delay. However, from a certain threshold given by the ratio (5.1) the average departure delay gets smaller than the arrival delay and so the delay is stabilized.

The *stability ratios* are shown in Table 5.8 for the five train connections along with the regression parameters with a precision of four decimals. The stabilizing behaviour reveals a decrease

Table 5.8 Stabilizing ratios of the transfer connections

Transfer	β_0 [s]	β_1 -	$\beta_0/(1 - \beta_1)$ [s]
IC800/IR1900 Hlm-Vl	41.2396	0.7642	175
IR1900/IC800 Rtd-Mt	38.0116	0.9073	410
IC800/IR1900 Mt-Rtd	81.7479	0.7171	289
IR1900/IC800 Vl-Hlm	73.0933	0.8153	396
IC900/IC1500 Hlm-Hrl	32.4915	0.8629	237

in delay for arrival delays from 3 to 7 min for the various connections. So although the connections have no buffer time, the delay propagation exhibits a downward trend and the stability ratio quantifies the delay reducing behaviour for large arrival delays.

5.5 Probability Distributions

5.5.1 Arrival Delay

The empirical arrival delay probability density functions of the various train lines are mostly bell-shaped and (more or less) skewed to the right (having a longer right tail), see Figure 5.11. This is easily explained as follows. Most arrival times concentrate around a mean value, although some trains arrive early and other trains arrive more or less late. The early arrivals are however constrained to a certain minimum corresponding to arriving fast trains that departed from the preceding station without delay. On the other hand, late arrivals can get very large corresponding to a departure delay at the preceding station or a large running time due to e.g. a low speed or an unscheduled stop at the open track.

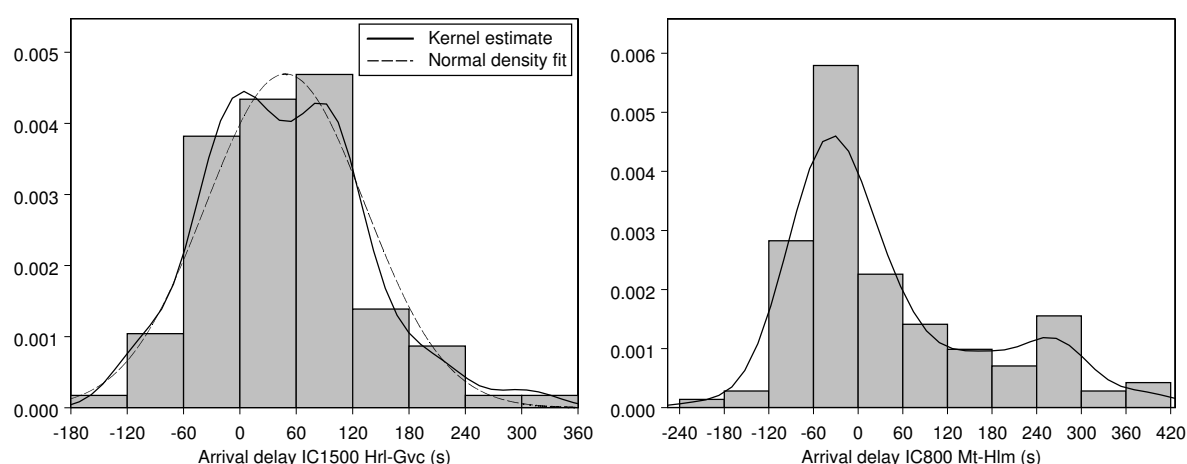


Figure 5.11 Arrival delay distribution. Left: IC1500 Hrl-Gvc histogram, kernel estimate, and normal density fit. Right: IC800 Mt-Hlm histogram and kernel estimate

Table 5.2 also gives the coefficient of skewness to each train line. A positive value implies skewness to the right. The skewness coefficients range between $+0.2$ and $+1.7$. When the skewness is small the arrival delay distribution is symmetric and may hence be approximated by a normal distribution. The hypothesis that the arrival delays follow a normal distribution is formally tested using the Kolmogorov-Smirnov (KS) goodness-of-fit test [131]. Table 5.9 shows the p-values of the KS-tests of single normality for the estimated parameters (mean and standard deviation) of the 13 train lines as given in Table 5.2. With a significance level of 5% the normality hypothesis is accepted for the arrival delays of 8 train lines, whereas the hypothesis is rejected for 5 train lines. The arrival delays of the latter train lines all have a coefficient of skewness of around $+1$, by which a skewed distribution may be more appropriate like a Weibull, Erlang, or lognormal distribution. Also the stronger composite hypothesis is tested that the arrival delays have a normal distribution with unknown parameters [172, 131]. The

Table 5.9 Arrival delay Kolmogorov-Smirnov goodness-of-fit tests

Train line	Normal KS-test p-value	Late trains Exponential KS-test p-value
IC800 Hlm-Mt	0.7350	0.0202
IC800 Mt-Hlm	0.0016	0.2819
IC900 Hlm-Ehv	0.0450	0.1204
IC1500 Gvc-Hrl	0.0010	0.2310
IC1500 Hrl-Gvc	0.8650	0.0320
INT1800 Köln-Ehv	0.7230	0.2881
IR1900 Rtd-VI	0.1602	0.8847
IR1900 VI-Rtd	0.1904	0.7979
IR2700 VI-Ehv	0.5856	0.5257
IR3500 Ut-Ehv	0.9899	0.6004
AR5200 Dn-Tbwt	0.2446	0.1923
AR6400 Wt-Ehv	0.0029	0.6493
AR9600 Ut-Ehv	0.0092	0.9582

KS-test of composite normality rejects the normal distribution for 3 more train lines (IR1900 Rtd-VI, IR1900 VI-Rtd, and AR5200 Dn-Tbwt) [87]. The associated skewness coefficients are again around +1. There is hence only strong statistical evidence for a good normal fit for the 5 train lines with the lowest coefficients of skewness.

Apart from the positive skewness another observation is that the arrival delay densities are more or less bimodal for about half of the train lines, see Figure 5.11. A possible explanation is that slightly delayed trains ‘loose’ their scheduled inbound route setting to a conflicting train and hence have to stop at the open track before a stop signal near the station, by which the delay is further increased. This premise is easily checked using the signal event times on the train route tables as generated by TNV-Prepare. Another alternative is to check the order of this arrival and the arrival/departure of possible conflicting trains. Tromp & Hansen [199] consider a particular case in Eindhoven (based on the same Eindhoven data set), where IR1900 Rtd-VI trains depart from platform 2 to Venlo and IC1500 Hrl-Gvc trains arrive 6 minutes later from Heerlen at platform 6. The outbound and inbound routes cross at about 2 minute running time distance from the platforms leaving a tight buffer time on the crossing.

Graphical means like a histogram and a kernel estimate clearly show any peculiarity in the shape of an empirical probability density, such as the bimodal shapes in Figure 5.11. In contrast, the distribution shape is hard to detect from (arrival delay) statistics only. This motivates using visual exploratory analysis of empirical distributions to find any structural data properties as a complement to computing basic statistics.

In the analysis of e.g. delay propagation and connection reliability late arrivals are of prime interest, whereas early arrivals are simply treated as ‘on time arrivals’. Therefore, we also consider the distribution of arrival lateness. The histogram and empirical density of arrival lateness suggest a good fit by a negative-exponential distribution, see Figure 5.12. This hypothesis is formally tested using the KS goodness-of-fit test of single exponentiality for the estimated parameter (1/mean), with the mean as given in Table 5.2. Table 5.9 shows the computed p-values for each train line. With a significance level of 5%, the exponential distribution of late arrival

delays is accepted for all train lines except the IC800 Hlm-Mt and the IC1500 Hrl-Gvc. The fraction of late arrivals for the latter two train lines is very high (76% and 71%, respectively), and so the empirical distribution looks like a normal distribution truncated to the left about a minute before the mode (mean delay). Recall that a normal distribution is a good model for all (early and late) arrival delays in case of these two train lines. Hence, the late arrival delays of these train lines constitute most trains instead of just the right tail.

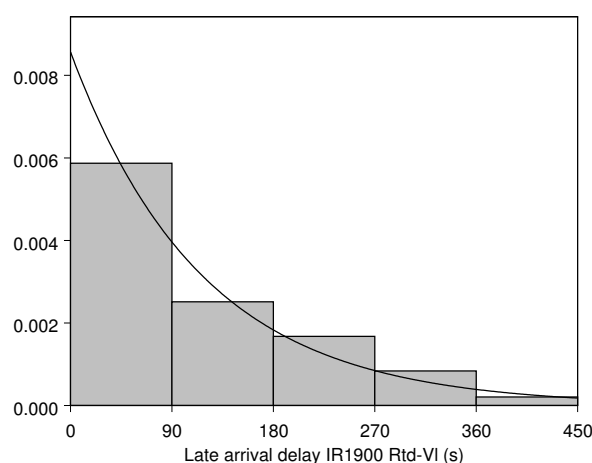


Figure 5.12 Late arrival delay distribution: IR1900 Rtd-VI histogram and exponential fit

From the Eindhoven data we conclude that in general an exponential distribution is a good model to train arrival lateness. Only when almost all trains are late this distribution may no longer be acceptable.

5.5.2 Departure Delay

Since early departures are prohibited, departure delays are expected to follow an exponential distribution, i.e., a train departs after the scheduled departure time with a random delay whose probability decreases as time elapses. The departure delay histograms also suggest a good exponential fit, see Figure 5.13. This hypothesis is formally tested by a Kolmogorov-Smirnov goodness-of-fit test of single exponentiality for the estimated parameter ($1/\text{mean}$) of the 13 train lines as given in Table 5.3. Table 5.10 shows the computed p-values. On a 5% significance level the hypothesis is accepted for all train lines, except for 3 lines: the IC1500 Hrl-Gvc, the IR1900 VI-Rtd, and the AR5200 Dn-Tbwt.

The 3 train lines for which the exponential departure delay model is rejected have in common that they depart close after another train over the Eindhoven-Boxtel track. In Section 5.4.6 we have already seen that the IC1500 Hrl-Gvc is hindered by the IC900 EHV-Hlm that is scheduled to depart 2 minutes before in the same direction to Boxtel. The IC1500 Hrl-Gvc departure delay is hence conditioned on the IC900 EHV-Hlm departure delay and the departure headway, by which the departure delay distribution does no longer represent a random delay. An analogous situation holds for the IR1900 VI-Rtd that is scheduled to depart 2 minutes after the IC800 Mt-Hlm through the corridor to Boxtel. Section 5.4.4 already showed the dependence between the IC800 Mt-Hlm and the IR1900 VI-Rtd trains through a bilateral transfer connection. The

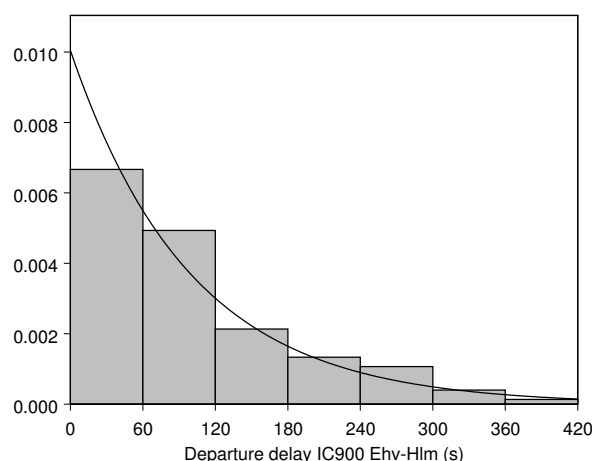


Figure 5.13 Departure delay distribution: IC900 Ehv-Hlm histogram and exponential fit

Table 5.10 Departure delay Kolmogorov-Smirnov goodness-of-fit tests

Train line	Exponential KS-test
	p-value
IC800 Hlm-Mt	0.1445
IC800 Mt-Hlm	0.0576
IC900 Hlm-Ehv	0.3214
IC1500 Gvc-Hrl	0.9113
IC1500 Hrl-Gvc	0.0000
INT1800 Ehv-Köln	0.1538
IR1900 Rtd-VI	0.1526
IR1900 VI-Rtd	0.0030
IR2700 Ehv-VI	0.7900
IR3500 Ehv-Ut	0.9962
AR5200 Tbwt-Dn	0.2257
AR5200 Dn-Tbwt	0.0032
AR9600 Ehv-Ut	0.8150

AR5200 Dn-Tbwt trains depart in schedule 4 minutes after the AR9600 Ehv-Ut trains over the same open track to Boxtel, which also may influence the departure delay distribution.

It can be concluded that an exponential distribution is in general a good stochastic model for train departure delays, as long as the departure is not restricted by some headway constraint of a closely scheduled train departing slightly sooner over the same route.

5.5.3 Dwell Time

The dwell time of an early train is larger than scheduled since an early departure is not allowed. On the other hand, late trains may have a dwell time smaller than scheduled if the composite process of alighting, boarding, and departing takes less time than scheduled. However, in Section 5.3.3 we have seen that the observed mean dwell time is significantly larger than scheduled, even when considering late trains only.

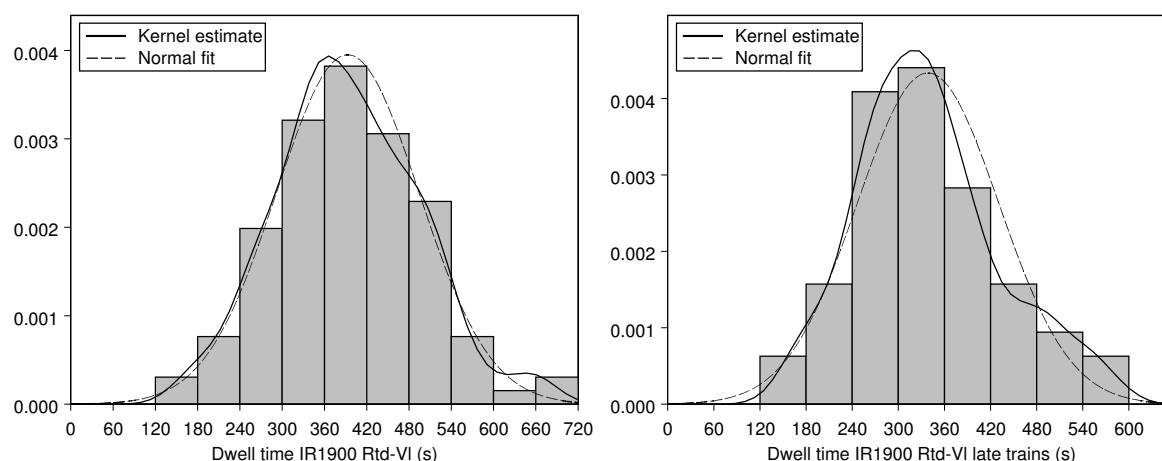


Figure 5.14 Dwell time distribution: IR1900 Rtd-VI histogram, kernel estimate, and normal density fit (left), and idem for late IR1900 Rtd-VI trains (right)

The histograms and kernel estimates of dwell time suggest a normal distribution, both for all trains and for late trains only, see Figure 5.14. The normal hypothesis is formally tested using the Kolmogorov-Smirnov test with the estimated parameters of Table 5.4. Table 5.11 shows the computed p-values. On a 5% significance level, a normal dwell time is accepted for all train lines, both in case of all trains and for the subset of late trains only. In general dwell time is thus evenly spread around a mean value that is larger than the scheduled dwell time.

Table 5.11 Dwell time Kolmogorov-Smirnov goodness-of-fit tests

Train line	Normal KS-test p-value	Late trains	Excess dwell time
		Normal KS-test p-value	Exponential KS-test p-value
IC800 Hlm-Mt	0.8454	0.6355	0.1831
IC800 Mt-Hlm	0.3073	0.6784	0.5
IC1500 Gvc-Hrl	0.5944	0.3157	0.3171
IC1500 Hrl-Gvc	0.5003	0.8201	0.0489
IR1900 Rtd-VI	0.9325	0.6711	0.5
IR1900 VI-Rtd	0.8429	0.7405	0.1403
AR5200 Dn-Tbwt	0.6027	0.0717	0.1633

Another interesting point is the distribution of dwell time excess of late trains. It appears that this extra dwell time above the scheduled dwell time follows a negative-exponential distribution, see Figure 5.15. This hypothesis is tested using the KS-test of *composite* exponentiality, which tests the hypothesis that the data is exponential with unknown parameter. The p-values are also shown in Table 5.11. On a 5% significance level, the exponential distribution is accepted by all train lines except for the IC1500 Hrl-Gvc, whose p-value is slightly smaller than the 5% significance level. Therefore, we also applied the KS-test of single exponentiality for given mean dwell time excess, which accepts the specified exponential distributions for all train lines including the IC1500 Hrl-Gvc. Hence, there is strong statistical evidence that an exponential distribution is a good model for the excess dwell time of late trains.

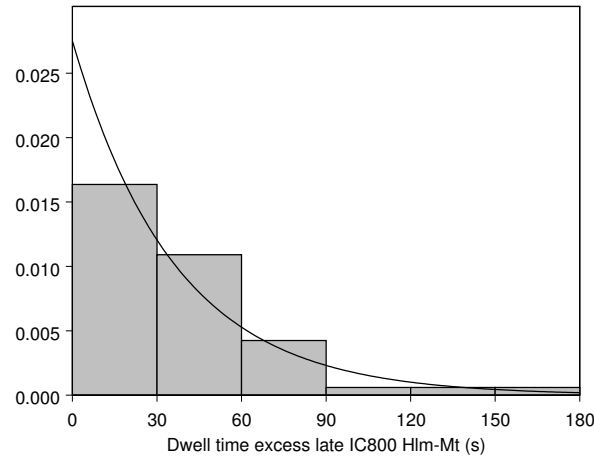


Figure 5.15 Distribution of the excess dwell time of late trains: IR800 Hlm-Mt histogram and exponential density fit

5.5.4 Transfer Time

The transfer time empirical distributions of each connection suggest good normal fits, although some are skewed to the right, see Figure 5.16. The hypothesis of a normal transfer time distribution has been tested formally using the KS-test of single normality. Table 5.12 shows the computed p-values. There is no statistical evidence to reject a normal distribution to the transfer time data on a 5% significance level, and this also holds for the subsets of late trains only. So a normal distribution is a good probabilistic model for the transfer time.

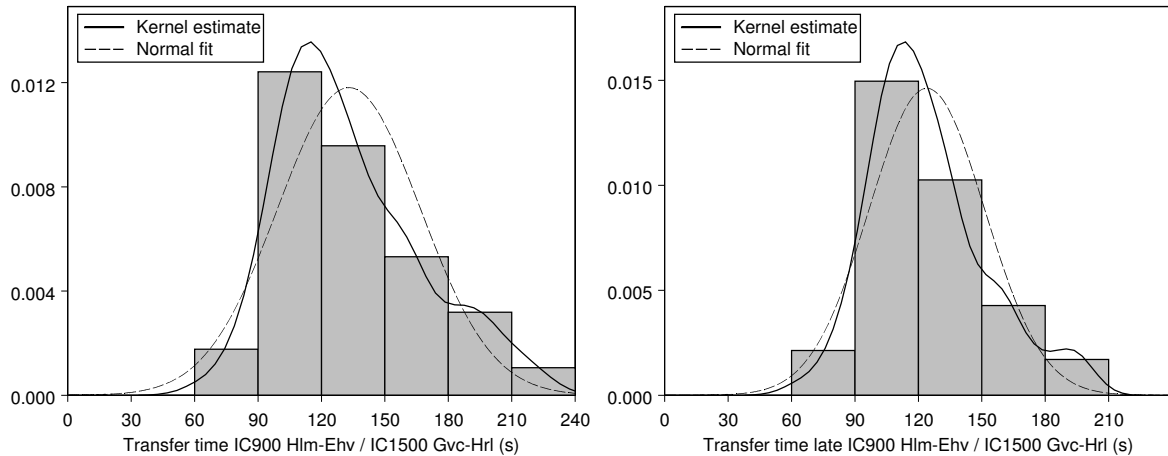


Figure 5.16 Transfer time distribution: IC900 Hlm-Ehv/IC1500 Gvc-Hrl histogram, kernel estimate, and normal density fit (left), and idem for late feeder trains (right)

5.6 Conclusions

Based on TNV-logfiles and the software tool TNV-Prepare (Chapter 4), train arrival and departure delays in Eindhoven have been analysed for a period of a week in September 1997. It has

Table 5.12 Transfer time Kolmogorov-Smirnov goodness-of-fit tests

Feeder line	Connection	Normal KS-test p-value	Late feeder trains
			Normal KS-test p-value
IC800 Hlm-Mt	IR1900 Rtd-VI	0.4171	0.0878
IC800 Mt-Hlm	IR1900 VI-Rtd	0.3896	0.9427
IC900 Hlm-Ehv	IC1500 Gvc-Hrl	0.2245	0.2566
IC1500 Hrl-Gvc	IC900 Ehv-Hlm	0.3069	0.7781
IR1900 Rtd-VI	IC800 Hlm-Mt	0.8789	0.5901
IR1900 VI-Rtd	IC800 Mt-Hlm	0.9849	0.9698

been shown that the mean dwell time of each train line is larger than scheduled, even when considering late trains only. As a result, the mean train delay increased in Eindhoven. IC/INT trains arrived on average about 1 minute late but the mean departure delays increased to about 2 minutes. The AR/IR trains arrived generally quite punctual but the mean departure delay increased to about $1\frac{1}{2}$ minute late. The exceptions on these general observations have even worse performance: The large mean arrival delay of the IC900 Hlm-Ehv trains (over 2 min), and the large mean departure delays of the IC1500 Gvc-Hrl and IR2700 Ehv-VI trains (over $2\frac{1}{2}$ min both).

The mean arrival and departure delays at Eindhoven are thus less than 3 minutes for each train line and the train are therefore not delayed according to the NS norm. However, looking at the fraction of trains that are less than 3 min late, we also see a significant punctuality drop from arrival to departure. About 85% IC/INT trains arrived less than 3 min late, whereas this percentage is less than 80% at departure. In 1997, NS had a desired punctuality norm of 87% trains less than 3 min late. Only 1 arriving IC train line satisfies this performance (the IC1500 Hrl-Gvc with 93%), and none of the departing IC/INT trains. The AR/IR arrivals on the other hand all satisfy the punctuality norm: here the percentage trains arriving within 3 min late ranges between 88% and 96%; with the exception of the extra peak hour trains IR3500 Ut-Ehv (69%). The AR/IR departures are again less punctual: 4 AR/IR train lines have an acceptable percentage trains departing less than 3 min late ranging from 88% to 98%; for the other 3 departing AR/IR train lines this percentage is 84% or lower.

The decrease in punctuality at Eindhoven could be explained by simple linear regression models. A range of different factors were found to be responsible for departure delays, including

- Departing trains of 3 eastbound train lines are mainly delayed by a cross-platform transfer in Eindhoven, in combination of running over the same open track from Boxtel to Eindhoven in fixed order (IC800 Hlm-Mt, IC1500 Gvc-Hrl, IR1900 Rtd-VI);
- Departing trains of 3 westbound train lines are mainly delayed by a cross-platform transfer connection in Eindhoven, followed by running over the same open track to Boxtel in fixed order (IC800 Mt-Hlm, IC1500 Hrl-Gvc, IR1900 VI-Rtd);
- Departing trains of 2 train lines are hindered by arriving trains that cross the outbound route (INT1800 Ehv-Koln, IR2700 Ehv-VI);
- Starting trains seem a major source of primary delay (IC900 Ehv-Hlm);
- Departing trains are hindered by delayed preceding trains on the open track to Boxtel (AR9600 Ehv-Ut).

For the scheduled dwell and transfer buffer times of the interconnected trains we moreover obtain the following conclusions:

- A transfer connection of two trains that arrive over the same open track in fixed order results in a large dwell time (synchronization time) for the first arriving train and also in a large transfer time for transferring passengers of this train. However, these large dwell and transfer times do not contain effective buffer time for arrival delay compensation.
- A transfer connection of two trains just before a common open track results in a large dwell time (synchronization time) for the last departing train, without effective buffer time.

A generic conclusion is that the function of Eindhoven as a transfer station in combination with the Eindhoven-Boxtel corridor results in large scheduled dwell and transfer times that still lack buffer time, and hence enforces a strong source of delay propagation. During the last few years the corridor between Boxtel and Eindhoven has been upgraded to four-tracks, which became fully operational at the end of 2002. The above results indicate that this infrastructure construction leads to a considerable capacity improvement, shorter dwell (and travel) times, and increased punctuality. An ex-post analysis of the new situation would be interesting to quantify the gains of this infrastructure investment.

Chapter 6

TIMED EVENT GRAPHS

6.1 Introduction

Train arrivals at main stations initiate several concurrent activities: alighting and boarding of passengers, passenger transfers to connecting trains departing in different directions, and exiting passengers walking to their final destination or continuing their journey in another transport mode. Likewise, train departures synchronize activities of through, starting and transferring passengers. Rolling stock connections show similar structures: trains from different directions may be coupled to continue as one combined train or a train may be decoupled after which the front and back continue in different directions. The railway infrastructure and safety and signalling systems cause a different kind of synchronization between trains on conflicting routes which must run in sequence over the shared infrastructure in some decided order.

The main complexity in railway timetable design is due to settling of concurrency by choosing certain priority rules such as specifying routing and/or train sequence orders [154, 231]. The theory developed in the forthcoming may then be used to evaluate the consequences of these choices in terms of performance. When the timetable has been settled by a higher-level scheduling policy the resulting railway traffic system is mainly characterized by trains running concurrently over partially shared tracks and synchronization of trains at stations and junctions. The dynamics of such traffic systems can be modelled by *timed event graphs* [11], a subclass in the theory of *Petri nets* [139, 218]. In these discrete-event systems the state evolution depends on causal relations between activities and discrete events in contrast to conventional dynamical systems where dynamics are governed by difference or differential equations [189].

Various classes of Petri nets have been used for modelling and analysing railway systems, see e.g. Ren & Zhou [170], Sakaguchi & Tomii [177], Van der Aalst & Odijk [205] and Zhu [229]. In general, simulation can be used to derive properties of highly complex Petri net models. In the special case of timed event graphs a rich analytical theory has been developed to prove structural and behavioural properties [139] as well as performance properties [11, 32]. In this chapter we will be concerned with modelling timed event graphs and deriving structural and behavioural properties. Performance evaluation is based on a state-space representation of timed event graphs which gives a linear system description in *max-plus algebra*. This will be the topic of Chapters 7 and 8.

In the sequel we assume that a basic network timetable structure has already been designed in an earlier stage of the planning process and analyse the properties of the resulting structure. We thus assume full knowledge of the timetable (arrival and departure times of all train lines), minimum process times (running times and dwell times of all train lines, passenger transfer times between train lines at transfer stations, layover times of train circulations at line terminals, connection times of rolling stock connections (coupling/decoupling times), and transfer

times of train crews or other logistic connections), and minimum headway times between train paths. This information determines all train interconnections, infrastructure restrictions and train orders at conflict points. The strength or vulnerability of the imposed timetable structure furthermore depends on the amount and distribution of process time supplements and buffer times over the timetable.

The outline of this chapter is as follows. Section 6.2 formally introduces Petri nets and the special subclass of timed event graphs. Section 6.3 explains how timed event graphs can be used to model typical railway system issues, including timetable and infrastructure structures. Section 6.4 is concerned with behavioural properties of timed event graphs. Section 6.5 describes the synthesis of a timed event graph based on the railway timetable and (global) infrastructure data. Conclusions are given in Section 6.6.

6.2 Petri Nets and Timed Event Graphs

6.2.1 Basic Definitions

A *Petri net* is a special bipartite directed graph introduced by Petri [161] as a general graphical and mathematical modelling tool for describing relations between conditions and events. Since this pioneering work many authors contributed to the development of the Petri net theory, see the excellent review and tutorial paper by Murata [139]. Event graphs are a subclass of Petri nets which are able to efficiently describe synchronization structures in networks. As opposed to general Petri nets event graphs cannot model choice or decisions, in favour of superior analytical and computational power. In particular, the state representation of timed event graphs corresponds to linear systems in *max-plus algebra*, which will be the topic of Chapter 7 and 8. This section formally defines the structure of timed event graphs.

Definition 6.2.1 (Petri net) A Petri net is a tuple $PN = (\mathcal{T}, \mathcal{P}, \mathcal{E}, \mu)$, where

- (i) $\mathcal{T} = \{t_1, \dots, t_n\}$ is a finite set of transitions;
- (ii) $\mathcal{P} = \{p_1, \dots, p_m\}$ is a finite set of places;
- (iii) $\mathcal{P} \cap \mathcal{T} = \emptyset$ and $\mathcal{P} \cup \mathcal{T} \neq \emptyset$;
- (iv) $\mathcal{E} \subseteq \mathcal{T} \times \mathcal{P} \cup \mathcal{P} \times \mathcal{T}$ is a set of arcs from transitions to places and vice versa;
- (v) $\mu \in \mathbb{N}_0^m$ is an initial marking of the places.

Graphically, places are depicted as circles and transitions as rectangles or bars. The initial marking is represented by drawing $\mu(p_k) = \mu_k$ dots (tokens) in the circle representing place p_k , see Figure 6.1. A transition is called an *input transition* to a place if there is an arc from the transition to the place and an *output transition* if the arc is reversed. Analogously, a place adjacent to a transition is called an *incoming place* if there is an arc from the place to the transition and an *outgoing place* if the arc is reversed.

Definition 6.2.2 (Event graph) An event graph is a Petri net in which each place has exactly one input and one output transition.

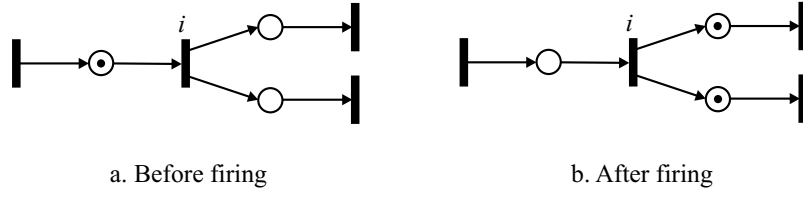


Figure 6.1 Transition firing rule in a timed event graph

In an event graph each place together with its incoming and outgoing arc can be interpreted as an arc itself, connecting the input and output transition directly. An event graph can thus be represented as a weighted digraph $\mathcal{G} = (\mathcal{T}, \mathcal{P}, \mu)$, with node set $\mathcal{T} = \{1, \dots, n\}$ and arc set $\mathcal{P} \subseteq \mathcal{T} \times \mathcal{T}$ where each place $p_k \in \mathcal{P}$ corresponds to a *marked arc* $p_k = (j, i, \mu_k)$, $1 \leq k \leq m$. An event graph is therefore also known as a marked graph [139]. In the sequel, we will denote an event graph by its marked graph representation $\mathcal{G} = (\mathcal{T}, \mathcal{P}, \mu)$.

A *timed Petri net* has an additional deterministic time delay attached to places (holding times) or to transitions (firing times), reflecting processing times in places and durations of transition firings, respectively. In an event graph time delay may be associated freely to either its transitions or its places, since either form can easily be transformed to the other [11, §2.5.2]. Without loss of generality, we therefore assume that time delays are associated to places corresponding to the interpretation of places as processes that obviously are time-consuming.

Definition 6.2.3 (Timed event graph) A timed event graph is a quadruple $\mathcal{G} = (\mathcal{T}, \mathcal{P}, \mu, w)$, where $(\mathcal{T}, \mathcal{P}, \mu)$ is an event graph and $w \in \mathbb{R}_+^m$ a weight vector of holding times associated to the places.

A timed event graph is a discrete event dynamic system (DEDS), where transitions correspond to events and places represent processes. A token in a place represents an active process, and the holding time of a place is the minimum time that a token is occupied in the place. The distribution of tokens over places represents the state of the system, and the dynamic behaviour of the modelled system can be studied by the movements of tokens over the places governed by the occurrence of events obeying the following rule, see Figure 6.1.

Definition 6.2.4 (Firing rule) A marking μ in a timed event graph $\mathcal{G} = (\mathcal{T}, \mathcal{P}, \mu, w)$ dynamically changes according to the following two-step firing rule:

- (i) A transition i is enabled if each incoming place contains a token and the associated holding times have elapsed;
- (ii) A firing of an enabled transition i removes one token from each incoming place and adds one token to each outgoing place.

We also say that a transition is *firable* if each incoming place contains at least one token. The firing rule also explains the difference between a marking and a holding time of a place, the latter being the minimum time that a token must spend in a place before enabling the outgoing transition.

A transition without predecessors is called a *source* transition. A transition without successors is called a *sink* transition. A sink transition consumes tokens but does not produce any. An

autonomous event graph is an event graph without sources. A *loop* is a place $p_j = (i, i)$, where i is both input and output transition to the place p_j . In a loop a token is simultaneously removed and added to p_j , but the new token becomes available to the output transition only after again the holding time has elapsed.

Remark The first four properties in Definition 6.2.1 define a *net* $\mathcal{N} = (\mathcal{T}, \mathcal{P}, \mathcal{E})$, which is a bipartite directed graph (V, E) with node set $V = \mathcal{T} \cup \mathcal{P}$ that is partitioned in two kinds of elements called transitions and places, respectively. The marking defined by the 5th property together with the firing rule extends the net to a place/transition net or *Petri net* $PN = (\mathcal{N}, \mu)$. An event graph is also called a *decision-free* Petri net or *marked graph* [139]. It is decision-free in the sense that the flow of tokens through a place is generated by only one input transition and there is no choice between more than one output transition. Note that if a place has two output transitions then a decision must be made about which transition is fired. If one of the transitions fires, the token is removed from the place and the other transition is no longer enabled. In an event graph this situation is not applicable since each place has exactly one input and output transition. \square

A timed event graph may also be thought of as a bivalued directed multigraph $\mathcal{G} = (\mathcal{T}, \mathcal{P}, \mu, w)$, where both weights are associated to the arcs. In this digraph, the nodes correspond to transitions, the arcs to places, the first arc weight to the initial marking, and the second arc weight to the holding time. This means that a timed event graph can be stored in a computer using efficient weighted digraph representations and manipulated by standard data structures. For small dense networks a (weighted) adjacency or incidence matrix representation can be used, whereas for large-scale sparse networks an arc list, adjacency list or forward/reverse star representation may be used [3, 39]. We will generally represent a timed event graph $\mathcal{G} = (\mathcal{T}, \mathcal{P}, \mu, w)$ as a (marked) *arc list*

$$p_k = (\text{in}(p_k), \text{out}(p_k), \mu(p_k), w(p_k)), \quad 1 \leq k \leq m,$$

where $\text{in}(p_k)$ is the input transition of p_k , $\text{out}(p_k)$ the output transition, $\mu(p_k) = \mu_k$ the initial marking, and $w(p_k) = w_k$ the holding time. The transitions are just numbered from $1, \dots, n$. This representation takes only $O(m)$ storage place. The *adjacency list* representation of a timed event graph is a list (or array) of the transitions, where each transition points to a list of all its outgoing places. This representation takes $O(n+m)$ storage place and is useful when traversing the timed event graph. In general, there may be multiple places between a pair of transitions. Nevertheless, without loss of generality we may assume that parallel places with the same input and output transition have different markings. Indeed, if two or more parallel places have the same initial marking then the one with the highest holding time dominates the others and so the places can be combined to a single place with the maximum holding time. In Chapter 7 we will also introduce a matrix representation of a timed event graph that will be useful for algebraic manipulations.

6.2.2 Building Blocks of Timed Event Graphs

The topology of event graphs allows sequential and parallel processes that are connected by three primitive transitions:

- (i) **Sequential transitions** model a succession of processes or stages of processes, which each consume some holding time before the next stage is enabled, see Figure 6.2.a. An

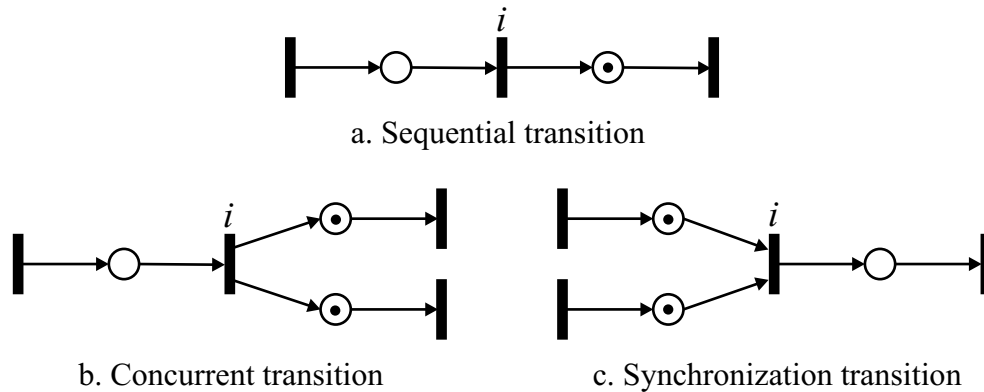


Figure 6.2 Primitive transitions in a (timed) event graph

example is a sequence of train runs and stops that are enabled by an alternating sequence of train arrivals and departures.

- (ii) **Concurrent transitions** initiate several concurrent processes simultaneously, see Figure 6.2.b. An example is the arrival of a train, which enables transfer flows to several connecting trains.
- (iii) **Synchronization transitions** model events that are enabled by two or more parallel processes, see Figure 6.2.c. An example is the departure of a train that has to wait for several feeder trains.

From these three building blocks complex interconnection structures can be built as explained in the next section. The main restriction in the modelling power of timed event graphs stems from the requirement that places are not allowed to have more than one input and output transition (Definition 6.2.2). Indeed, as already remarked in the last section, this condition implies that all firing sequences are fixed a priori, by which the Petri net is conflict-free or decision-free. This is exactly what we aim for: a timetable structure is unambiguously modelled by a timed event graph, and therefore the properties of the (timed event graph) model depend on the characteristics of the timetable design only. Note that a railway timetable structure should be *feasible* (or conflict-free) and implicitly represents a wide range of design choices (train orders on open tracks, speed differences, connections, etc.).

Places correspond to processes and dependencies between events, such as train runs, train stops, transfer flows at stations, and headway between trains on conflicting routes. The interpretation of a place depends on the interpretation of its input and output transition. Viewed in isolation of its environment, a place is just a precedence relation from its input to its output transition. Its particular implication becomes only clear in perspective to the overall interconnection structure. This is in contrast to high-level *coloured Petri nets* (CPNs), where different types (“colours”) of tokens are identified [218]. We will not pursue this approach, since our main interest is the powerful analysis properties of timed event graphs and their max-plus state-space representation.

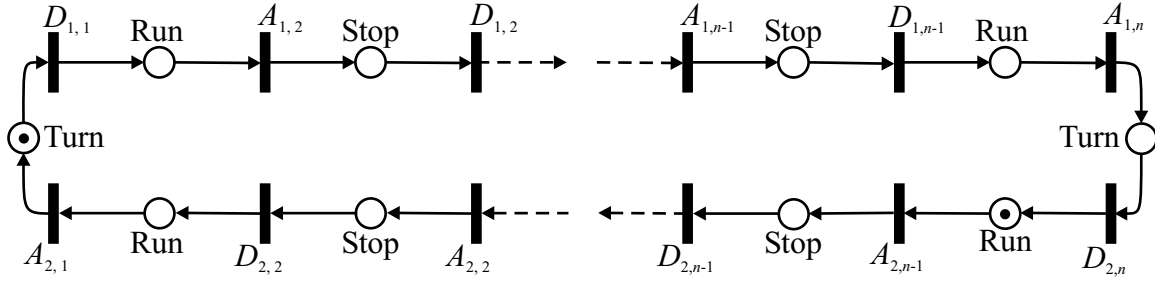


Figure 6.3 Timed event graph of a train circulation

6.3 Basic Modelling Approach of Railway Systems

This section presents the modelling potential of timed event graphs to railway systems. Along the way we touch a range of structural and behavioural issues that are analysed in Section 6.4, and in the next chapters in the framework of max-plus algebra.

6.3.1 Train Circulations

A timed event graph is a discrete event dynamic system, where the transitions are the discrete events. From an analysis point of view, only events have to be modelled that interact with other events in a nontrivial way. In particular, series compositions can be collapsed into one process. The remaining variables are then arrival and departure events of train lines at stations (or timetable points).

In the sequel, we denote by $D_{i,j}$ the departure of train line L_i from station S_j , and likewise $A_{i,j}$ denotes the arrival of train line L_i at station S_j . A train line is then modelled as a sequence of runs and stops over the railway network from an origin terminal to a destination terminal. Passenger train lines are usually operated in both directions which are modelled by two separate train lines. If trains turn at the terminals and proceed in the opposite direction, then a layover time at both terminals completes the train circulations, see Figure 6.3, where line 2 denotes the return direction of line 1. In this figure the identification of transitions and places is for illustrational purpose only.

A train *run* is modelled by a place between a departure transition and an arrival transition. This place can be interpreted as the occupation of the open track between two stations by a train of a specified train line. The holding time of the place is the *running time* between the stations. The presence of a token means that a train is running on the open track. A *stop* is modelled by a place between an arrival and a departure transition. The holding time is the associated *minimum dwell time*, which may depend on train line and station. This place can be interpreted as the platform track occupation of a given train line. The presence of a token means that the train is standing at the platform track.

The initial marking of the places in a train circulation must be consistent with the line cycle time (1/frequency) and the timetable (if any). The determination of a consistent initial marking is considered in Section 6.5. Also more advanced rolling stock assignments are possible. At line ends, rolling stock may switch train lines because of a more efficient rolling stock assignment. Also coupling or decoupling units at intermediate stations along the route may be applicable if

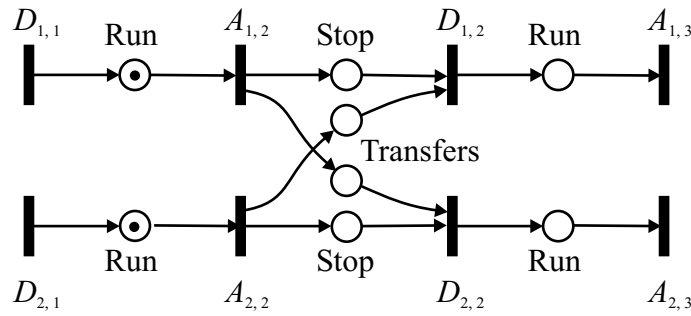


Figure 6.4 Timed event graph of a train interconnection structure

e.g. the passenger load is not equal over the entire route. This leads to interconnections between train lines, which is considered in the next section.

The absence of tokens in a place modelling a train run does not mean that the associated open track or platform track is free! If another train line runs over the same track, then this is modelled as a separate place. Hence, a given open track is free if and only if all places associated to this open track have zero tokens. The simultaneous presence of two trains on the same open track within a specified minimum headway is implicitly prevented by precedence constraints in the topology of the timed event graph. This is explained in Section 6.3.3.

Likewise, the absence of tokens in a place modelling a train stop does not mean that the associated platform track is free. If another train line stops at the same platform then this is modelled as a separate place, and the platform track is free if and only if all places associated to this platform have zero tokens. The model interconnection structure guarantees that an occupied platform is blocked for other trains, except when explicitly modelled otherwise, such as for the coupling of two train units.

A place may contain more than one token. For instance, several trains of the same line may run on an open track at some time distance apart. The tokens then act according to the *first-in first-out* (FIFO) principle, i.e., overtaking in a place is not allowed. Moreover, a transition fires only once at a time. The holding time of each token starts immediately after being fired into the place. Hence, multiple tokens in a place enable the output transition at different time instances. In Section 6.4 we will consider behavioural properties of a timed event graph, such as boundedness of the number of tokens in a place and the cycle time between two transition firings.

6.3.2 Train Synchronizations

The interconnection structure between train lines at shared stations may arise from passenger transfers or logistic connections. The latter include coupling or decoupling of train units, turns at terminals, and crew transfers. Figure 6.4 illustrates two interconnected train lines through a bilateral passenger transfer. The places between the events have three different interpretations: a running train, a dwelling train, and transferring passengers. From an event graph point of view these processes just represent several stages in a transport chain, which must satisfy some precedence constraints.

A *transfer* is modelled by a place between an arrival transition of a feeder line and a departure transition of the connecting line. The holding time is the *minimum transfer time*. This place is

interpreted as a passenger flow from the feeder train to the connecting train. The presence of a token implies that the feeder train has arrived. The absence of tokens means that the connecting train has departed.

The topology of the timed event graph in Figure 6.4 models a bilateral transfer of two train lines. The upper sequence $D_{1,1} \rightarrow A_{1,2} \rightarrow D_{1,2} \rightarrow A_{1,3}$ models the subsequent events of train line 1. The lower sequence $D_{2,1} \rightarrow A_{2,2} \rightarrow D_{2,2} \rightarrow A_{2,3}$ does the same for train line 2. The (transfer) places connecting the two lines represent the actual transfers and model the dependence of both departures $D_{1,2}$ and $D_{2,2}$ on the arrivals $A_{1,2}$ and $A_{2,2}$. The stop place ensures the causality that a train cannot depart before it has arrived, and the transfer place secures that the connection waits for its feeder train.

6.3.3 Headway Constraints

Figure 6.5 shows an event graph that models a minimum time separation and fixed firing order between two transitions (here transitions i and j). The ordering mechanism between transitions i and j is provided by a circuit over the places p_{ij} and p_{ji} containing exactly one token. The output transition of the place containing the token is enabled first. In the case of Figure 6.5 place p_{ij} with output transition i contains the token and hence i is enabled as soon as the holding times of all incoming places have been completed, whereas j is only enabled after i has fired and subsequently the holding time of p_{ji} has elapsed. The minimum time separation between transitions i and j is thus controlled by the holding times in places p_{ij} and p_{ji} .

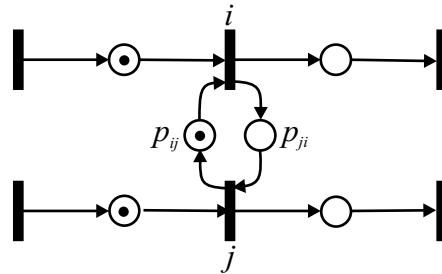


Figure 6.5 Minimum headway structure in timed event graphs

This *minimum headway structure* can be used to model a fixed order and time separation at conflicting routes imposed by railway infrastructure and safety and signalling systems. A conflicting route typically occurs at stations, crossings, merging or diverging junctions, and overtaking sections at open tracks. The following practical cases can be identified:

- **Arrival headway** between two arriving trains over conflicting inbound routes at a station layout.
- **Departure headway** between two departing trains over conflicting outbound routes at a station layout or to a shared open track.
- **Arrival/Departure headway** of two trains over a conflicting inbound and outbound route at a station layout.
- **Overtaking** of a slow train by a fast following train at an overtaking track or station stop.
- **Meeting and passing** of opposite trains at a meet-and-pass section or station on a single-track route.

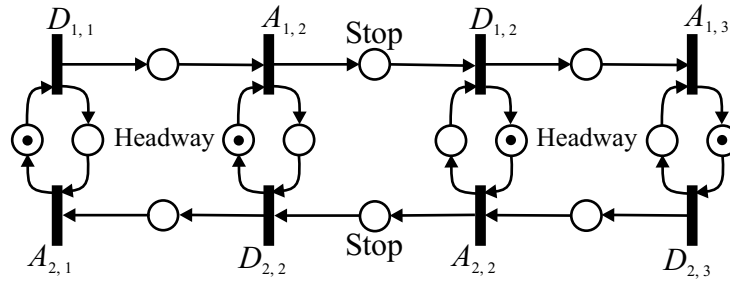


Figure 6.6 Timed event graph model of a meet-and-pass station of opposite train traffic over a single-track route

Headway constraints are bilateral interactions between pairs of trains. Headway (time) generally includes running time to the approach signal protecting the conflict point and blocking time of the conflicting route sections, see Section 3.3. An arrival headway constraint is formulated in terms of a pair of arrival transitions giving a sequence ordering and time separation of two arriving trains at a station according to interlocking of inbound routes. A departure headway constraint relates to a pair of departing trains that share a track section in either a station layout or a junction some distance away from the departure station(s). In the latter case the running time to and over the junction is a major part of the headway. An arrival/departure headway constraint acts on an arrival and a departure transition. The minimum headway from the arriving train is based on interlocking of the inbound route. The headway in the other direction depends on whether the departure takes place at the same station of the arriving train or another station. In the former case the headway is based on interlocking of the outbound route. In the latter case the running time from the departure station to and over the conflict point constitutes a major part of the headway.

Figure 6.6 shows an example of a meet-and-pass structure. Trains of line 1 and 2 run in opposite directions over a single-track. At station S_2 the trains meet and pass, i.e., a train that has arrived at this station must wait for the arrival of the opposite train before it is allowed to depart. The holding time of e.g. the place from $A_{1,2}$ to $D_{2,2}$ represents the switching time of the outbound route setting after the release of the critical point section by the opposite inbound train.

Example 6.1 The behavioural properties of a timed event graph depend on its topology and initial marking. In particular the infrastructure constraints narrow the flexibility of concurrent processes. This example examines in detail the token dynamics or *token game* of an overtaking station.

Figure 6.7 shows an extension to the interconnection example of Figure 6.4, where intercity trains (line 2) overtake local trains (line 1) during the stop at station S_2 . So the two train lines run over the same open track and the running order is changed at station S_2 . The holding times of the places are also shown. The minimum dwell time of both train lines at S_2 is 1 minute. The scheduled transfers at station S_2 from line L_1 to L_2 and vice versa, have 2 minutes minimum transfer time. Trains that approach or depart station S_2 must respect a minimum headway of 2 minutes, which is a common infrastructure restriction.

The flow of tokens in the timed event graph of Figure 6.7 is completely deterministic for the specified initial marking in the headway circuits. Figure 6.8 shows the successive stages of the markings in the timed event graph that are reachable from the initial marking. At each

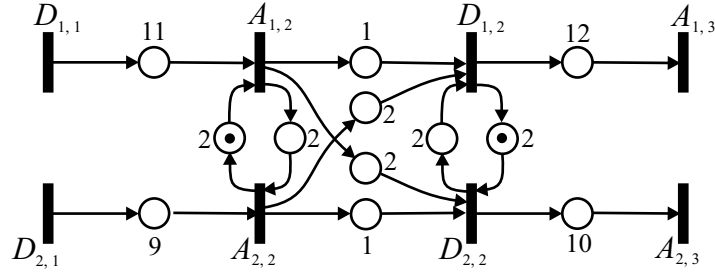


Figure 6.7 Minimum headway structure in a timed event graph model of an overtaking station

stage the active places are indicated together with the transitions that will be enabled next. We assume that the transitions $D_{1,2}$ and $D_{2,1}$ have just been fired. Hence, in the initial marking (Figure 6.8.a) trains of both lines approach station S_2 .

Because of the arrival headway constraint, a local train (of the upper line L_1) must arrive first, followed by an intercity train (of the lower line L_2) with a minimum headway of 2 minutes. In the mean time, the transferring passengers from the local train have already arrived at the intercity platform and are ready to board right after the arrival of the intercity. The intercity has to depart first after 1 minute minimum dwell time. Only 2 minutes after this departure the local train is also allowed to depart because of the departure headway constraint. One minute earlier the transferring passengers from the intercity train have already boarded the local train. If the transitions fire as early as possible then the local train has 5 minutes dwell time, including a scheduled dwell waiting time of 4 minutes caused by the overtaking intercity. The transfer times are 3 minutes in both directions, and thus both contain 1 minute scheduled transfer waiting time. The intercity has only 1 minute dwell time. The firing sequence at station S_2 is thus prescribed as $A_{1,2} \rightarrow A_{2,2} \rightarrow D_{2,2} \rightarrow D_{1,2}$. \square

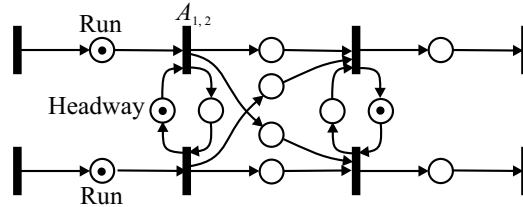
Example 6.1 showed that capacity utilization not only depends on the minimum process times but is also strongly determined by the interconnection structure and initial marking, and in particular the scheduled order at conflicting train routes.

6.4 Behavioural Properties

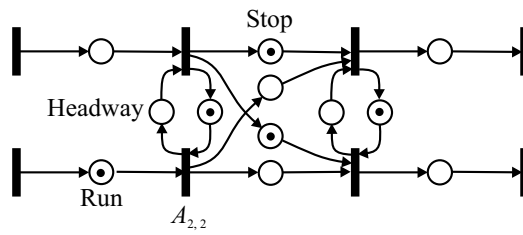
The *behavioural properties* of a timed event graph describe the possible dynamic behaviour of tokens in the timed event graph with respect to the initial marking. In fact, the token dynamics of an autonomous timed event graph for a given initial marking is completely deterministic (since it is decision-free). In Section 6.3.3 we showed that a token game obtained from executing the timed event graph gives a visualization of the possible firing sequences. This is an example of a discrete-event simulation. In this section we present analytical methods to *prove* behavioural properties of a timed event graph.

6.4.1 Liveness

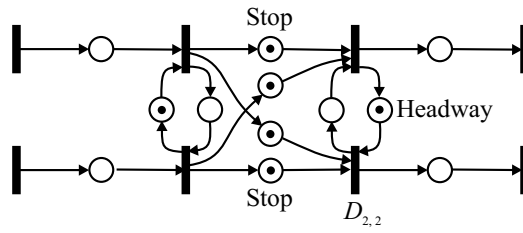
A first question that comes into mind is how to decide whether or not all transitions are fireable. This is related to a *deadlock* situation where the system state prohibits any occurrence of events. Clearly, such a state should be avoided.



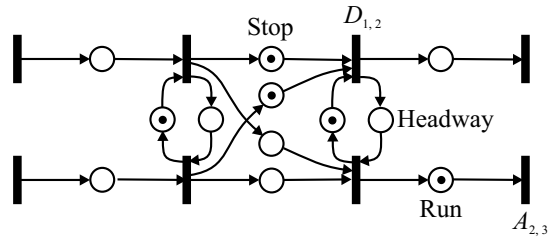
a. Train 1 arrives, Train 2 is still running



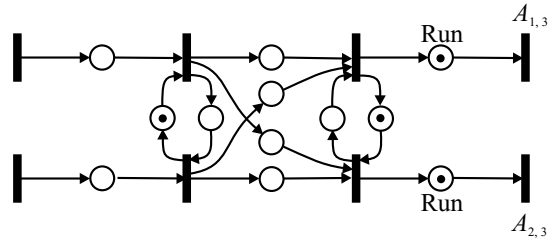
b. Train 1 is dwelling and transferring passengers walk to platform train 2, Train 2 arrives



c. Both trains are dwelling, Transfers between both trains, Train 2 may depart when ready



d. Train 2 has departed, Train 1 may depart when minimum headway has elapsed



e. Both trains have departed

Figure 6.8 Token flow in a timed event graph of an overtaking station

Definition 6.4.1 (Liveness) *A transition is live if it is firable at the initial marking or can get firable through some firing sequence from the initial marking. An event graph is live for an initial marking if all its transitions are live. An event graph that is not live is called deadlocked.*

The most well-known example of deadlock is a single-track route occupied by a train heading for a meet-and-pass station of which all platforms are occupied by opposite trains. Another example of a deadlocked scheduled railway system occurs when a train waits for a feeder train that never arrives. Note that if this train also has connections at following stations these connecting trains eventually also keep on waiting, and so on. Finally, no train in the railway system (or a strongly connected subsystem) will ever be able to depart.

A *circuit* in an event graph is a directed path of transitions and places where the first and last transition coincides. The following basic lemma states that the number of tokens on a circuit in an event graph does not change by firing [37].

Lemma 6.4.1 *The number of tokens in any circuit of an event graph \mathcal{G} is invariant to any firing sequence.*

Proof: Consider any circuit in an event graph. A token in a place on the circuit can only be generated and consumed by transitions that also belong to the circuit since in an event graph each place has only one input and one output transition. Moreover, if a transition in the circuit is fired then a token is removed from the incoming place but simultaneously added to the outgoing place in the circuit, by which the number of tokens in the circuit does not change after firing. \square

Commoner *et al.* [37, Th. 1] proved the following necessary and sufficient condition for an event graph to be live, which provides a simple liveness test of an event graph.

Theorem 6.4.1 (Liveness) *An event graph $\mathcal{G} = (\mathcal{T}, \mathcal{P}, \mu_0)$ is live if and only if each circuit contains at least one token in the initial marking μ_0 .*

Proof: If a circuit of an event graph has zero tokens in the initial marking then this circuit remains free of tokens by Lemma 6.4.1. But then the transitions on this circuit will never be enabled. Therefore, each circuit in the initial marking should have at least one token to be live. Conversely, assume there exists a transition i that is not live. Then i must have an incoming place without tokens and this place must be restrained from tokens by any firing sequence. This means that the input transition of this incoming place may never be enabled. Since the number of places in an event graph is finite, backtracking on token-free incoming places either ends in a source (which is firable by convention), or at a circuit which contains a marked place by the condition in the theorem. This contradicts that i is not live. \square

Note that a live marking remains live after firing as a consequence of Theorem 6.4.1 and Lemma 6.4.1

6.4.2 Reachability

Firing an enabled transition changes the distribution of tokens (marking) in an event graph according to the firing rule in Definition 6.2.4. A sequence of firings thus results in a sequence

of markings. We are now interested in determining whether a certain desired or undesired marking can be reached, or more general, in determining the possible markings that can be reached from an initial marking.

Definition 6.4.2 (Reachability, reachable set) A marking μ is reachable from a marking μ_0 if there exists a firing sequence transforming μ_0 to μ . The reachable set of an event graph $\mathcal{G} = (\mathcal{T}, \mathcal{P}, \mu_0)$ is the set of all possible markings reachable from the initial marking μ_0 , and is denoted as $R(\mu_0)$.

The topological structure of a timed event graph can be characterized in terms of its incidence matrix. Let $\mathcal{G} = (\mathcal{T}, \mathcal{P}, \mu_0, w)$ be a timed event graph. A matrix representation \mathcal{G} is the transition-place incidence matrix $M \in \{0, \pm 1\}^{n \times m}$ defined as

$$[M]_{ij} = \begin{cases} 1 & \text{if } \text{out}(p_j) = i \\ -1 & \text{if } \text{in}(p_j) = i \\ 0 & \text{otherwise.} \end{cases}$$

From the firing rule immediately follows that the negative entries in row i correspond to the incoming places from which a token is removed if transition i fires, and the positive entries correspond to the outgoing places to which a token is added. Each column j has two nonzeros corresponding to the input and output transition of place p_j . The incidence matrix M equals the node-arc incidence matrix of the underlying digraph where each place p_j is identified with an arc from transition $\text{in}(p_j)$ to $\text{out}(p_j)$.

The marking evolution over an event graph can be described by a dynamic equation of successive markings. Let $\mu(k)$ be the marking after k transition firings in an event graph $(\mathcal{T}, \mathcal{P}, \mu_0)$ with incidence matrix $M \in \{0, \pm 1\}^{n \times m}$. The firing vector $\sigma(k) \in \{0, 1\}^n$ denotes the enabled transitions that fire simultaneously at the k th firing, i.e., $\sigma_i(\cdot) = 1$ if i fires and $\sigma_i(\cdot) = 0$ otherwise. A necessary and sufficient condition for transition i to be enabled at marking $\mu = (\mu_1, \dots, \mu_m)^\top \in \mathbb{N}_0^m$ is

$$\mu_j \geq (-M)_{ij} \quad \text{for all } j = 1, \dots, m.$$

In particular this inequality must be valid for all j associated to predecessor places p_j of transition i for which $(M)_{ij} = -1$. The inequality is trivially satisfied for all other p_j . The marking dynamic equation in an event graph is given by

$$\mu(k) = \mu(k-1) + M^\top \sigma(k), \quad k \in \mathbb{N},$$

where $\mu(0) = \mu_0$ and M^\top is the transposed incidence matrix. Now suppose that a marking μ is reachable from the initial marking μ_0 through a feasible firing sequence $\{\sigma(1), \sigma(2), \dots, \sigma(l)\}$. Then marking $\mu = \mu(l)$ is determined by

$$\mu = \mu_0 + M^\top y, \tag{6.1}$$

where $y = \sum_{k=1}^l \sigma(k) \in \mathbb{N}_0^n$ is the firing count vector, i.e., y_i is the number of times that i must fire to reach μ from μ_0 . Hence, a necessary condition for a marking μ to be reachable is that there exists a valid firing count vector y satisfying (6.1). However, (6.1) is not a sufficient condition, since y may not correspond to a legal firing sequence, i.e., a firing sequence that

satisfies the firing rule. In particular, both μ and y are constrained to be nonnegative integral vectors.

A necessary and sufficient condition for a reachable marking is obtained in terms of the *fundamental cycle matrix* of an event graph. The following is a straightforward generalization of graph theoretic concepts to event graphs. Basic references on graph theory are Berge [16] and Bollobás [18]. A *cycle* in an event graph is a sequence of transitions and places, where the first and last transition coincide. In a cycle the orientation of places may be arbitrary. Recall that a *circuit* is a cycle in which all places are oriented in the same direction. An *elementary cycle* is a cycle where each transition occurs only once, i.e., a cycle having no subcycles. In the sequel, we will always assume that a cycle is elementary. A cycle is represented by its *place incidence vector* $\gamma = (\gamma_1, \dots, \gamma_m)^\top \in \{0, \pm 1\}^m$, defined as $\gamma_k = 1$ if p_k is a forward place w.r.t. the cycle orientation, $\gamma_k = -1$ if p_k is a backward place, and $\gamma_k = 0$ otherwise. The sum of two cycles is again a cycle and indeed the set of all cycles is a subspace of \mathbb{R}^m with dimension $\nu = m - n + c$, where c is the number of strongly-connected components of the event graph.

A *cycle basis* is a set of *independent cycles* that spans the *cycle space*, i.e., each cycle in the event graph can be obtained by a linear combination of the cycles in the cycle basis. A cycle basis is obtained by the following graph algorithm. First, assume that $\mathcal{G} = (\mathcal{T}, \mathcal{P})$ is strongly connected, i.e., $c = 1$. Then there exists a *spanning tree* $\mathcal{S} = (\mathcal{T}, \mathcal{P}_{\mathcal{S}})$ over the transitions of \mathcal{G} with $\mathcal{P}_{\mathcal{S}} \subseteq \mathcal{P}$. By definition, a spanning tree does not contain cycles and adding a nontree place $p_k \in \mathcal{P} \setminus \mathcal{P}_{\mathcal{S}}$ generates a cycle in \mathcal{G} with a path on the spanning tree from the output transition of the nontree place to its input transition. The number of places in a spanning tree is $n - 1$ as any additional place gives a cycle. Hence, the number of nontree places is $m - (n - 1) = m - n + 1$. Each cycle generated by a nontree place and a path on a spanning tree is called a *fundamental cycle*. The orientation of a fundamental cycle is defined by the direction of the nontree place. The set of $m - n + 1$ fundamental cycles form a *fundamental cycle basis*. Note that a fundamental cycle basis is not unique but depends on the choice of the spanning tree. Now consider the general case of an event graph with c components. Then we may consider each strongly-connected component separately, or equivalently, find a *spanning forest* \mathcal{F} with $n - c$ places. The number of places in $\mathcal{G} - \mathcal{F}$ is the cyclomatic number $\nu = m - n + c$, and each of these places generates a fundamental cycle associated to the spanning forest \mathcal{F} . From this algorithm follows that the dimension of the cycle space is ν since each fundamental cycle contains exactly one unique place that is not contained in any other fundamental cycle.

Above we presented an algorithm for finding a fundamental cycle basis. By definition each cycle can be represented by a linear combination of these fundamental cycles. The (fundamental) *cycle matrix* of an event graph is now the cycle-place incidence matrix $\Gamma \in \{0, \pm 1\}^{\nu \times m}$, where each row is the incidence vector of a fundamental cycle,

$$[\Gamma]_{ij} = \begin{cases} 1 & \text{if } p_j \text{ is a forward place in fundamental cycle } i \\ -1 & \text{if } p_j \text{ is a backward place in fundamental cycle } i \\ 0 & \text{otherwise.} \end{cases}$$

Recall that the direction of a place on a cycle depends on the orientation of the cycle.

Murata [138] proved a necessary and sufficient condition for a reachable marking using a circuit theoretic analogy. We give a new simple proof based on polyhedral theory [181]. We need the following important definition. A matrix A is called *totally unimodular* if the determinant of

each square submatrix of A takes values in $\{0, \pm 1\}$. The following lemma is a basic result in polyhedral theory [181, §19.1].

Lemma 6.4.2 *Let $A \in \{0, \pm 1\}^{m \times n}$ be a totally unimodular matrix and $b \in \mathbb{Z}^n$ an integral vector. Then the polyhedron $\{x \in \mathbb{R}^m \mid x \geq 0, Ax = b\}$ is integral, that is, all of its extreme points are integral vectors.*

We can now prove the following theorem.

Theorem 6.4.2 (Reachability) *Let $\mathcal{G} = (\mathcal{T}, \mathcal{P}, \mu_0)$ be a live (timed) event graph. Then a marking μ is reachable from the initial marking μ_0 if and only if*

$$\Gamma\mu = \Gamma\mu_0, \quad (6.2)$$

where Γ is the fundamental cycle matrix of \mathcal{G} .

Proof: If μ is reachable from μ_0 then there must be a legal firing sequence with firing count vector y satisfying (6.1), or equivalently

$$M^\top y = \Delta_\mu \quad (6.3)$$

where $\Delta_\mu = \mu - \mu_0$. This means that the vector Δ_μ is a linear combination of the columns of M^\top (or rows of M), or equivalently, Δ_μ is an element in the range of M^\top . From linear algebra it is well-known [195] that (6.3) has a solution y iff Δ_μ is orthogonal to the kernel of M , i.e., $\xi^\top \Delta_\mu = 0$ for all $\xi \in \{\xi \in \{0, \pm 1\}^m \mid M\xi = 0\}$. From graph theory it is known that the rank of an incidence matrix M is $n - c$, where c is the number of strongly-connected components of the (event) graph, and the dimension of its kernel is the cyclomatic number $\nu = m - n + c$. In fact the kernel of an incidence matrix is the *cycle space* spanned by ν independent cycles [16, Ch. 4]. Now, the cycle matrix Γ is the matrix where each row corresponds to an independent cycle from a cycle basis of the graph \mathcal{G} . Hence, the rows of Γ span the kernel of M , and therefore $\Gamma\Delta_\mu = 0$ is a necessary condition for the existence of a solution y to (6.3).

Conversely, let $\mu \in \{\mu \in \mathbb{R}^m \mid \mu \geq 0, \Gamma\mu = \Gamma\mu_0\}$. It is well-known that a cycle matrix Γ is totally unimodular. Moreover, since both μ_0 and Γ are integral, also $\Gamma\mu_0$ is integral. From Lemma 6.4.2 then follows that there is an integral vector μ such that $\Gamma\mu = \Gamma\mu_0$. Therefore, $\Delta_\mu = \mu - \mu_0$ is integral. It is also well-known that an incidence matrix M (and its transpose M^\top) is totally unimodular. Then again by Lemma 6.4.2 $\{y \in \mathbb{R}^n \mid y \geq 0, M^\top y = \Delta_\mu\}$ is an integral polyhedron. Hence, the condition $\Gamma\mu = \Gamma\mu_0$ is sufficient for the existence of an integral vector $y \geq 0$ satisfying (6.3). \square

The roles of μ_0 and μ in (the proof of) Theorem 6.4.2 can be interchanged. Hence we obtain the following.

Corollary 6.4.1 *Let $\mathcal{G} = (\mathcal{T}, \mathcal{P}, \mu_0)$ be a live (timed) event graph. Two markings μ_0 and μ are mutually reachable if and only if (6.2) holds.*

Commoner *et al.* [37] proved a necessary and sufficient condition for a reachable marking μ in the case of a live and strongly-connected event graph. In a strongly-connected (event) graph

(a basis of) the set of all cycles can be generated from (a basis of) the set of all circuits and vice versa [16]. Therefore the following result of Commoner *et al.* [37, Th.11] is a corollary to Theorem 6.4.2.

Corollary 6.4.2 *Let $\mathcal{G} = (\mathcal{T}, \mathcal{P}, \mu_0)$ be a live and strongly-connected (timed) event graph. Then a marking μ is reachable from the initial marking μ_0 if and only if the token count on each (directed) circuit in $\mathcal{G} = (\mathcal{T}, \mathcal{P}, \mu)$ is equal to that of $\mathcal{G} = (\mathcal{T}, \mathcal{P}, \mu_0)$.*

The reachable set of an event graph is now completely described by the following corollary to Theorem 6.4.2.

Corollary 6.4.3 (Reachable set) *The reachable set of a live event graph $\mathcal{G} = (\mathcal{T}, \mathcal{P}, \mu_0)$ is*

$$R(\mu_0) = \{\mu \in \mathbb{N}_0^m \mid \Gamma\mu = \Gamma\mu_0\},$$

where Γ is a fundamental cycle matrix of \mathcal{G} .

Thus, for any marking μ_0 all timed event graphs $\mathcal{G} = (\mathcal{T}, \mathcal{P}, \mu, w)$ with initial marking $\mu \in R(\mu_0)$ are equivalent in the sense that they are interchangeable by some legal firing sequence. Hence, all behavioural properties of a timed event graph $\mathcal{G} = (\mathcal{T}, \mathcal{P}, \mu_0, w)$ are invariant to changing the initial marking in any marking $\mu \in R(\mu_0)$.

6.4.3 Periodicity

A (timed) event graph $\mathcal{G} = (\mathcal{T}, \mathcal{P}, \mu_0)$ is *consistent* if there exists a finite firing sequence from μ_0 back to μ_0 in which each transition fires at least once. Formally, this is defined as follows.

Definition 6.4.3 (Consistency) *A (timed) event graph $\mathcal{G} = (\mathcal{T}, \mathcal{P}, \mu_0)$ is consistent if there exists a positive firing count vector $y \in \mathbb{N}^n$ such that $M^\top y = 0$, where M is the incidence matrix of \mathcal{G} .*

Consistency is indifferent to loops in the event graph since any firing of the associated transition both removes and adds a token to the place in the loop. Hence, consistency can be defined without loss of generality in terms of incidence matrices although they do not represent loops.

Definition 6.4.4 (Synchronousness) *A consistent event graph is called synchronous if the transitions of any firing sequence transforming μ_0 back to itself are fired the same (nonzero) number of times.*

Lemma 6.4.3 (Synchronousness) *A strongly-connected (timed) event graph $\mathcal{G} = (\mathcal{T}, \mathcal{P}, \mu_0)$ is synchronous.*

Proof: If marking μ_0 is reachable from μ_0 then (6.1) with $\mu = \mu_0$ gives $M^\top y = 0$. The rows of M^\top have exactly two nonzeros 1 and -1 , and so $y = (1, \dots, 1)^\top \in \mathbb{N}^n$ is a solution to $M^\top y = 0$. Moreover, the (transposed) incidence matrix M (M^\top) of a strongly-connected digraph has rank $n - 1$, and therefore the kernel of M^\top has dimension 1. Hence, the only vectors satisfying $M^\top y = 0$ are multiples of $y = (1, \dots, 1)^\top \in \mathbb{N}^n$, which spans the kernel. \square

Synchronousness is more restrictive than consistency: the latter requires the existence of a firing sequence returning to the initial marking, whereas synchronousness assumes that in such a firing sequence all transitions have fired the same time. A consistent timed event graph exhibits a periodic behaviour if a suitable sequence of firings is repeated. This is the basis of a periodic timetable which in fact determines such a suitable order of train departures.

The cycle time of an event is the asymptotic steady-state interval between two successive occurrences of the event. Formally, this is defined as follows.

Definition 6.4.5 (Cycle time) Consider a timed event graph $\mathcal{G} = (\mathcal{T}, \mathcal{P}, \mu_0, w)$. Let $x_i(k)$ be the time at which transition $i \in \mathcal{T}$ fires for the k -th time. Then the cycle time χ_i is defined for each transition $i \in \mathcal{T}$ by

$$\chi_i = \lim_{k \rightarrow \infty} \frac{x_i(k)}{k}.$$

If all transitions have the same cycle time then we say that the timed event graph is *periodic*. For any (closed) path ξ denote by $w(\xi)$ and $\mu(\xi)$ the weight and marking of the path, respectively. Hence,

$$w(\xi) = \sum_{p_k \in \xi} w_k \quad \text{and} \quad \mu(\xi) = \sum_{p_k \in \xi} \mu_k.$$

Theorem 6.4.3 (Periodicity) A live strongly-connected timed event graph $\mathcal{G} = (\mathcal{T}, \mathcal{P}, \mu_0, w)$ is periodic and the common cycle time equals the maximum cycle mean η defined as

$$\eta = \max_{\xi \in C} \frac{w(\xi)}{\mu(\xi)}, \quad (6.4)$$

where C is the set of all elementary circuits in \mathcal{G} .

Proof: By liveness of \mathcal{G} each transition is fireable by some firing sequence from the initial marking. Moreover, because \mathcal{G} is strongly connected it is synchronous by Lemma 6.4.3 and therefore each transition has fired the same number of times before a next cycle of firings starts. Hence, \mathcal{G} is periodic and the cycle time is determined by the transitions on a circuit with the largest mean weight, which is given by (6.4). \square

If a (departure) transition in a strongly-connected event graph is deadlocked then the entire system is deadlocked, i.e., the cycle time is undefined. On the other hand if the strongly-connected event graph is live then the system is periodic. In the next chapter we will give an efficient algorithm to compute the minimum cycle time as the solution of an eigenvalue problem in the max-plus algebra.

6.4.4 Boundedness

A synchronous timed event graph also implies that the event graph is bounded.

Definition 6.4.6 (Boundedness) A place p is said to be k -bounded, with $k \in \mathbb{Z}_+$, if the number of tokens in p never exceeds k for any marking reachable from the initial marking μ_0 . A (timed) event graph is called k -bounded if each of its places is k -bounded. A place (or event graph) is said to be bounded if it is k -bounded for some integer $k > 0$.

In a strongly-connected timed event graph each place is by definition contained in a circuit and by Lemma 6.4.1 the number of tokens in a place can never exceed the minimum number of tokens in any circuit over this place. Hence, a strongly-connected timed event graph is bounded. However, a stronger result is valid when the timed event graph is in its periodic steady-state.

Theorem 6.4.4 *Let $\mathcal{G} = (\mathcal{T}, \mathcal{P}, \mu_0)$ be a live strongly-connected (timed) event graph, and $k = \max_i(\mu_{0,i})$ the maximum initial marking of any place. Then \mathcal{G} is asymptotically $(k+1)$ -bounded.*

Proof: Since \mathcal{G} is strongly connected by definition each place belongs to at least one circuit. Moreover, by Theorem 6.4.3 each transition has the same cycle time. Therefore, in each period a place obtains one token from its input transition and passes one token to its output transition. So the number of tokens in a place can be at most the initial number plus one. Hence, the number of tokens in each place is at most $k + 1$, and so \mathcal{G} is $(k + 1)$ -bounded. \square

6.5 Synthesis of Scheduled Railway Systems

The basic modelling approach has already been introduced in Section 6.3. Here we give an algorithm to construct a timed event graph associated to a periodic network timetable, and prove the behavioural properties of the constructed timed event graph.

6.5.1 Input Data

To model a train service network as a timed event graph input data must be available on the timetable, train lines, connections between train lines, and headway constraints. The timetable contains the arrival and departure times of each train line at the stations they serve. Train line information includes routes, served stations, frequency, running times, minimum dwell times, and minimum layover times (if applicable). Information on connections includes train pairs and station and the minimum transfer or connection times. The data of headway constraints contains pairs of train events and conflict point, and the minimum headway in both directions that has to be respected at the conflict point.

In Section 6.3 we considered both arrival and departure events. However, since we are concerned with deterministic running times, the arrival times of train runs are trivially expressed in their departure times. Therefore we may concentrate on departure times only without loss of generality. Note that this reduces the number of modelled transitions by a factor two.

Timetable Points

We adopt a macroscopic view of a railway network consisting of timetable points and tracks between these points. A *timetable point* is a location on the railway network where interacting or conflicting events may occur. Examples of timetable points are main railway stations, intermediate stops on the open track, crossings, merging and diverging junctions, shunting yards, freight yards, and movable bridges. Timetable points are denoted by variables S_i and can be interpreted as (virtual) stations. The set of all timetable points is denoted by $\mathcal{S} = \{S_1, \dots, S_{|\mathcal{S}|}\}$. The timetable points can be defined in a file `TimetablePointData` where each row characterizes a timetable point as

$$\text{TimetablePointData}(i) = (S_i, x_i, y_i, \text{type}_i),$$

where S_i is the station name, x_i and y_i are the coordinates with respect to a map of the railway network, and $type_i$ is the type of the timetable point. We distinguish between the following types: intercity station (IC), interregional station (IR), regional station (AR), freight or shunting yard (F), junctions (J), and movable bridges (BR). Like the coordinates, the timetable point types are essentially only used for visualizing the railway network. Different types of timetable points may be visualized by different objects or objects of different size. In the PETER software (see Chapter 8) passenger stations are visualized by circles of varying size (IC>IR>AR), freight and shunting yards by squares, and junctions/bridges by dots.

By definition all events on a railway network occur at timetable points. Routes over timetable points are implicitly determined by line constraints as considered below. Conflicting routes and platform capacity within railway stations are also implicitly modelled by headway constraints as considered below. Headway conflicts on the open tracks are only considered at timetable points. Signals and blocks on open tracks are thus not explicitly included in the model. Nevertheless, because we assume deterministic running times feasibility at the open track is ensured by headway constraints at the beginning and end of the open track (departure and arrival headway constraints) and possible headway constraints at intermediate timetable points.

This macroscopic modelling of the railway network by headway constraints has the advantage that the timed event graph is independent of particular safety and signalling systems. Hence, the modelling approach is applicable for hybrid railway networks with a mixture of any fixed block and moving block signalling systems.

Line Data

A train line is determined by a sequence of *line segments* between successive timetable points on the line route. Timetable points are either stations where the train line stops or intermediate passing points. The former generates *arrival* and *departure* events, whilst the latter gives *passage* or *through* events. The through events are included to define possible headway constraints. For instance, an intercity train may have a scheduled overtake of a regional train at a local station without stopping. The minimum headway constraints between the dwelling train and through train are then defined between the arrival and departure event of the regional train and the passage event of the intercity train. If for instance the intercity train is delayed then the minimum headway constraint between the intercity passage event and the local departure event guarantees that the regional train waits for the passage of the intercity train.

Train lines with a frequency $f > 1$ per timetable cycle time are modelled by f separate train lines. Likewise, train lines operated in both forward and return direction are modelled by two different train lines. For instance, consider the Dutch railway timetable with cycle time $T = 60$ minutes and the regional train line 6300 from The Hague CS to Haarlem and vice versa that is operated twice per hour in both directions. We model this by 4 train lines named $63xy$ using a digit $x \in \{0, 1\}$ for the forward (0) or return (1) direction and a digit $y \in \{1, \dots, f\}$ for the subsequent trains starting from the terminals within one timetable period. Hence, 6301 is the train line from The Hague CS to Haarlem corresponding to the first departure from The Hague CS at 06 each hour, 6302 is the train line departing from The Hague CS 30 minutes later at 36 each hour, 6311 is the train line from Haarlem to The Hague CS departing from Haarlem at 03 each hour, and 6312 is the train line Haarlem–The Hague departing from Haarlem at 33 each hour.

The train lines are defined in a file `LineData`. The rows in this file contain the successive train

line segments of the train lines, where each row i contains the following objects:

$$\text{LineData}(i) = (L_i, S_i^1, S_i^2, A_i, d_i, t_i^{\text{run}}, t_i^{\text{min}}),$$

with L_i the train line number, S_i^1 the origin station of the line segment, S_i^2 the destination station of the line segment, $A_i \in \{S, P, E\}$ the activity type at the destination S_i^2 being either a *stop* (S), a *passage* (P) or an ending E, $d_i \in [0, T)$ the scheduled event time at the origin S_i^1 , $t_i^{\text{run}} \geq 0$ the running time from S_i^1 to S_i^2 , and $t_i^{\text{min}} \geq 0$ the minimum process time at S_i^2 . For a stop activity the minimum process time t_i^{min} corresponds to the minimum dwell time at S_i^2 . For a passage activity $t_i^{\text{min}} = 0$. The event at the destination station is either an arrival or passage depending on the activity A_i . Likewise, the scheduled event time d_i at the origin is either a departure time or a through time depending on the activity at S_i^1 .

By definition the successive rows in LineData satisfy the following continuity assumption:

$$\text{if } L_i = L_{i+1} \text{ then } S_i^2 = S_{i+1}^1.$$

So, if two successive rows i and $i + 1$ correspond to the same train line then the destination station of row i is the origin station of row $i + 1$. Hence, LineData consists of blocks of subsequent rows corresponding to a train line route from one terminal to the other. We furthermore assume that all train lines start with a departure from a terminal and the last line segment of each train line is an end. Hence,

$$\text{if } L_i \neq L_{i+1} \text{ then } A_i = E.$$

Turns are assumed to be part of the synchronization constraints, which facilitates the description of complex train circulations over different train lines.

Synchronization Data

At transfer stations train lines may be synchronized to allow passenger or crew transfers or rolling stock connections. Likewise, at terminal stations trains may turn to continue in the opposite direction or switch to another train line. These synchronization constraints are defined in a file SynchData, where each row k corresponds to a single transfer, connection or turn from one train line to another characterized by the following objects:

$$\text{SynchData}(k) = (L_k^1, L_k^2, S_k, t_k^{\text{min}}),$$

with L_k^1 the feeder train line number, L_k^2 the connecting train line number, S_k the shared connection station, and $t_k^{\text{min}} \geq 0$ the minimum transfer, connection or layover time at S_k .

Each synchronization constraints is defined from an arrival event of the feeder train to the departure event of the connecting train, both at the same station S_k . Hence, there is no need to further specify the event types of the train lines in a synchronization constraint.

Headway Data

Finally, HeadwayData contains a list of minimum headway constraints between train lines. Each row k corresponds to a minimum headway constraint and contains the following objects:

$$\text{HeadwayData}(k) = (L_k^1, S_k^1, L_k^2, S_k^2, h_k, E_k^1, E_k^2),$$

where L_k^1 and L_k^2 are the conflicting train line numbers with origin station S_k^1 and S_k^2 , respectively, $h_k \geq 0$ is the minimum headway time from the first train to the second train, and the

event types $E_k^1, E_k^2 \in \{D, A\}$ denote whether the headway constraint must be evaluated at the outbound route of a departure (D) from the origin station or at the inbound route of an arrival (A) at the destination station of each line segment. For example, $(L_1^1, S_1^1, L_1^2, S_1^2, 2, A, D)$ is an AD-headway constraint, where the departure of train 2 must respect a 2 minute minimum headway after the arrival of train 1 (in a periodic pattern). For through trains the arrival and departure time are equivalent and combined in the passage time. However, note that an arrival over the incoming route of a through train refers to the destination station at the end of a line segment and therefore equals the departure over the outbound route at the origin station of the *next* line segment.

6.5.2 Timed Event Graph Construction

Based on the input data defined in the previous section we construct the timed event graph in three steps. First, the train line sequences are generated. Second, train lines are connected by events with synchronization constraints, and third, train lines are interconnected between event pairs with headway constraints. We first define the data structure of the timed event graph.

Transitions are stored as a list with four elements

$$\mathcal{T}(i) = (L_i, S_i, E_i, d_i) \quad (6.5)$$

where L_i is the train line of event i , S_i is the timetable point, $E_i \in \{A, D, P, E\}$ the event type, and d_i the scheduled event time. The event type is either an arrival (A), departure (D), passage (P), or termination/ending (E), and depending on the event type the event time is an arrival, departure, through or termination time. Furthermore, a line end corresponds to one of three situations: a turn to operate a train line in the opposite direction, a switch to operate on another train line or a run out of the modelled area. Note that the triple (L_i, S_i, E_i) uniquely identifies an event whilst the event time d_i gives additional information about the timetable. Moreover, if two distinct transitions (L_i, S_i, E_i) and (L_j, S_j, E_j) satisfy $L_i = L_j$ and $S_i = S_j$ then either $E_i = A$ and $E_j = D$ or vice versa.

Places are stored as a list of four elements

$$p_k = (\text{in}(p_k), \text{out}(p_k), \mu(p_k), w(p_k)) \quad (6.6)$$

corresponding to the input transition, output transition, initial marking, and holding time of place p_k . The input and output transition $\text{in}(p_k)$ and $\text{out}(p_k)$ are represented by an integer corresponding to an index of the transition list. So, $\text{in}(p_k) = i$ implies a link to transition $\mathcal{T}(i) = (L_i, S_i, E_i, d_i)$. The data structure (6.6) is a simple *arc list* representation of a timed event graph. We may also obtain an *adjacency list* representation by extending the transition list (6.5) with one more object corresponding to (a link to) a list of all places p_k with $\text{in}(p_k) = i$. For more information on data structures we refer to e.g. Aho *et al.* [2] or Cormen *et al.* [39].

We use the notation $d_i \in [0, T)$ for the scheduled event time associated with transition i , and T is the cycle time (or period length) of the timetable (usually $T = 60$ minutes). If the scheduled event times are given in whole minutes then obviously $d_i \in \{0, 1, \dots, T - 1\}$.

Algorithm 6.5.1 gives the basic algorithm for constructing the timed event graph. Here we used the ceiling function $\lceil a \rceil$ giving the least integer larger than or equal to a real number a . Line 1

Algorithm 6.5.1 (TIMEDEVENTGRAPHCONSTRUCTION)**Input:** LineData, SynchData and HeadwayData.**Output:** Arc list of timed event graph $(\mathcal{T}, \mathcal{P}, \mu, w)$.

```

1   $\mathcal{T} \leftarrow \emptyset; \mathcal{P} \leftarrow \emptyset; i \leftarrow 1; n \leftarrow 1;$  //Step 1. Train lines
2  while LineData( $i$ ) exists do
3       $\mathcal{T}(n) \leftarrow (L_i, S_i^1, D, d_i);$  //Add line start event
4      while  $A_i \neq E$  do
5          if  $A_i = P$  then
6               $\mathcal{T}(n+1) \leftarrow (L_{i+1}, S_{i+1}^1, P, d_{i+1});$  //Add through event
7               $\mu \leftarrow \lceil (t_i^{\text{run}} + d_i - d_{i+1})/T \rceil;$ 
8               $\mathcal{P} \leftarrow \mathcal{P} \cup \{(n, n+1, \mu, t_i^{\text{run}})\};$  //Add run place
9               $n \leftarrow n+1;$ 
10             elseif  $A_i = S$  then
11                  $a \leftarrow d_i + t_i^{\text{run}} \pmod T;$ 
12                  $\mathcal{T}(n+1) \leftarrow (L_{i+1}, S_{i+1}^1, A, a);$  //Add arrival event
13                  $\mathcal{T}(n+2) \leftarrow (L_{i+1}, S_{i+1}^1, D, d_{i+1});$  //Add departure event
14                  $\mu_1 \leftarrow \lceil (t_i^{\text{run}} + d_i - a)/T \rceil;$ 
15                  $\mu_2 \leftarrow \lceil (t_i^{\text{min}} + a - d_{i+1})/T \rceil;$ 
16                  $\mathcal{P} \leftarrow \mathcal{P} \cup \{(n, n+1, \mu_1, t_i^{\text{run}})\};$  //Add run place
17                  $\mathcal{P} \leftarrow \mathcal{P} \cup \{(n+1, n+2, \mu_2, t_i^{\text{min}})\};$  //Add stop place
18                  $n \leftarrow n+2;$ 
19              $i \leftarrow i+1;$ 
20              $a \leftarrow d_i + t_i^{\text{run}} \pmod T;$ 
21              $\mathcal{T}(n+1) \leftarrow (L_i, S_i^2, E, a);$  //Add terminal event
22              $\mu \leftarrow \lceil (t_i^{\text{run}} + d_i - a)/T \rceil;$ 
23              $\mathcal{P} \leftarrow \mathcal{P} \cup \{(n, n+1, \mu, t_i^{\text{run}})\};$  //Add run place
24              $n \leftarrow n+1;$ 
25              $i \leftarrow i+1;$ 
26   $k \leftarrow 1;$  //Step 2. Synchronization
27  while SynchData( $k$ ) exists do
28      find  $i = (L_k^1, S_k^1, A)$  and  $j = (L_k^2, S_k^2, D);$ 
29       $\mu \leftarrow \lceil (t_k^{\text{min}} + d_i - d_j)/T \rceil;$ 
30       $\mathcal{P} \leftarrow \mathcal{P} \cup \{(i, j, \mu, t_k^{\text{min}})\};$  //Add synchronization place
31       $k \leftarrow k+1;$ 
32   $k \leftarrow 1;$  //Step 3. Headway constraints
33  while HeadwayData( $k$ ) exists do
34      find  $i = (L_k^1, S_k^1, E_i)$  with  $E_i \in \{D, P\};$ 
35      find  $j = (L_k^2, S_k^2, E_j)$  with  $E_j \in \{D, P\};$ 
36      if  $E_k^1 = A$  then  $i \leftarrow i+1;$ 
37      if  $E_k^2 = A$  then  $j \leftarrow j+1;$ 
38       $\mu \leftarrow \lceil (h_k + d_i - d_j)/T \rceil;$ 
39       $\mathcal{P} \leftarrow \mathcal{P} \cup \{(i, j, \mu, h_k)\};$  //Add headway place
40       $k \leftarrow k+1;$ 

```

initializes the lists \mathcal{T} and \mathcal{P} of transitions and places, respectively, as well as the two counters i and n . The counter i points at the current row in `LineData` and n denotes the current size of the transition list. Lines 2–25 generate all transitions and places corresponding to a train line from terminal to terminal. Each train line starts with a departure event from a terminal (line 3). For a passage activity lines 5–9 generate a through event and a place from the previous transition to this new transition corresponding to a train run. Likewise, for a stop activity lines 10–18 generate an arrival and a departure event and two cascade places from the previous transition over the two new transitions corresponding to a train run and stop, respectively. The algorithm iterates over the inner loop of line 5–19 until the current input row contains an end activity. Lines 20–24 generate a terminal event and a place corresponding to the train run on the final line segment of the current line. The algorithm then proceeds with the next train line in the outer loop (line 2), and this procedure repeats until the last row of `LineData` has been reached.

The synchronization constraints are considered in lines 26–31. For each row k in `SynchData` the corresponding arrival and departure transitions are connected by a place with holding time equal to the minimum transfer/connection/layover time.

Finally, lines 32–40 generate the places corresponding to minimum headway constraints. Some explanation is in order to the procedure of finding the correct transitions in lines 34–37. If the event type is $E_k^1 = D$ then the associated transition may either be a departure or through event at station S_k^1 . Note that either (L_k^1, S_k^1, D) or (L_k^1, S_k^1, P) may exist but not both since an (outbound) event is either a departure or a passage. On the other hand, if the event type is $E_k^1 = A$ then the associated transition is either an arrival, through or terminal event at the next timetable point after S_k^1 on the route of line L_k^1 . To locate the corresponding transition in the transition list \mathcal{T} observe that an arrival, passage or terminal event at the destination station of a line segment in the transition list \mathcal{T} is the successor of the departure or passage at the origin station of this line segment, i.e., if the latter transition is located in $\mathcal{T}(i)$ then the former transition is located in $\mathcal{T}(i + 1)$. The analogue holds for event E_k^2 .

We assume that the input data is such that the timed event graph generated by Algorithm 6.5.1 satisfies the following condition.

Assumption 6.1 *On any circuit ξ with weight $w(\xi) = 0$ there is at least one place $p_k = (j, i, l, 0) \in \xi$ such that $d_i \neq d_j$.*

This assumption is no limitation in practice but guarantees that each circuit has at least one proper precedence relation that determines a firing sequence order. Given this assumption the timed event graph constructed by Algorithm 6.5.1 satisfies the following basic behavioural properties.

Theorem 6.5.1 (Initial marking) *Let $(\mathcal{T}, \mathcal{P}, \mu, w)$ be the timed event graph constructed by Algorithm 6.5.1, where the initial marking in each place $p_k = (i, j, \mu_k, w_k) \in \mathcal{P}$ is defined by*

$$\mu_k = \left\lceil \frac{w_k + d_i - d_j}{T} \right\rceil, \quad (6.7)$$

with $d \in [0, T)^n$ the scheduled departure time vector (modulo T). Then $\mathcal{G} = (\mathcal{T}, \mathcal{P}, \mu, w)$ is live and μ is the minimal marking such that each event i is firable at time d_i with cycle time T .

Proof: First note that the initial marking equation (6.7) defines nonnegative markings $\mu_k = \lceil (w_k + d_i - d_j)/T \rceil \geq 0$ only, since $(w_k + d_i - d_j)/T > (w_k - T)/T \geq -T/T = -1$. We next prove that each circuit of the constructed timed event graph contains at least one token and therefore by Theorem 6.4.1 the timed event graph is live. Consider first any circuit ξ with at least one place $p_k \in \xi$ with $w_k > 0$ and thus $w(\xi) > 0$. Then

$$\begin{aligned} \sum_{p_k \in \xi} \mu_k &= \sum_{p_k \in \xi} \lceil (w_k + d_{\text{in}(p_k)} - d_{\text{out}(p_k)})/T \rceil \\ &\geq \left\lceil \sum_{p_k \in \xi} (w_k + d_{\text{in}(p_k)} - d_{\text{out}(p_k)})/T \right\rceil = \left\lceil \frac{1}{T} \sum_{p_k \in \xi} w_k \right\rceil > 0. \end{aligned} \quad (6.8)$$

Now consider the case $w(\xi) = 0$, i.e., $w_k = 0$ for all $p_k \in \xi$. Then

$$\sum_{p_k \in \xi} \mu_k = \sum_{p_k \in \xi} \lceil (w_k + d_{\text{in}(p_k)} - d_{\text{out}(p_k)})/T \rceil = \sum_{p_k \in \xi} \lceil (d_{\text{in}(p_k)} - d_{\text{out}(p_k)})/T \rceil \geq 1$$

by Assumption 6.1. We next prove that (6.7) is the minimal marking for which the timed event graph is executable with a cycle time T and firing instants $d_i \pmod T$. Consider any place $p_k = (i, j)$. If transition i fires at time instant $d_i \in [0, T)$ then the token added to p_k is available to j at time instant $d_i + w_k$. The timetable requires that j fires at time instants $d_j + l \cdot T$ ($l \in \mathbb{N}_0$) and so at these time instants a token should be available in p_k . The token fired by i is only available after a number of cycles given by

$$\begin{aligned} \mu_k &= \min\{l \in \mathbb{N}_0 \mid d_j + lT \geq d_i + w_k\} \\ &= \min\{l \in \mathbb{N}_0 \mid l \geq (d_i + w_k - d_j)/T\}. \end{aligned} \quad (6.9)$$

Thus, the initial marking of p_k must contain at least this amount of tokens to be able to fire at the scheduled time instants before the first token from transition i becomes available. The minimal marking $l \in \mathbb{N}_0$ in (6.9) is exactly the right-hand side of (6.7). \square

It is interesting to look at the strongly-connected components in the timed event graph constructed by Algorithm 6.5.1. Rolling stock is often exclusively allocated to one train line in both directions, i.e., trains turn at the terminal stations and continue in the opposite direction. In other cases rolling stock alternates between train lines at a common terminal station. Hence, rolling stock circulations ‘close’ the train lines by which each complete train line is contained in at least one strongly-connected component. Moreover, bidirectional transfers between train lines at a mutual transfer station connect two components into one larger component, and likewise headway constraints between two train lines in both directions also combine strongly-connected components. It is therefore not surprising that the timed event graph may be largely strongly connected with separate components only at some disconnected regional railway lines. The strongly-connected components have several behavioural properties as stated in the following theorem.

Theorem 6.5.2 *Let $(\mathcal{T}, \mathcal{P}, \mu, w)$ be the timed event graph constructed by Algorithm 6.5.1 and let p be the maximum initial marking in any place, $p = \max_k \mu_k$. If $\mathcal{G} = (\mathcal{T}, \mathcal{P}, \mu, w)$ is strongly connected then it is autonomous, live, $(p + 1)$ -bounded and periodic with a cycle time smaller than or equal to T .*

Proof: By definition of strongly connectedness each transition in the event graph is contained in a circuit and thus has an incoming place, which implies that \mathcal{G} is autonomous. Liveness follows directly from Theorem 6.5.1. By Theorem 6.4.3 and strongly connectedness, \mathcal{G} is periodic and the cycle time equals the maximum cycle mean η . Let ξ be an arbitrary circuit. If $w(\xi) = 0$ for all circuits ξ then trivially $T \geq \eta = 0$. On the other hand, if $w(\xi) > 0$ then $T \geq (\sum_{p_k \in \xi} w_k) / (\sum_{p_k \in \xi} \mu_k)$ by (6.8) and therefore also $T \geq \eta$. Finally, \mathcal{G} is $p + 1$ -bounded by Theorem 6.4.4. \square

In the timed event graph of Algorithm 6.5.1 the timetable is implicitly incorporated in the determination of the initial marking, cf. (6.7) and the timed event graph is executable with respect to the timetable d , although the transitions do not wait for the scheduled departure times before firing. Instead the transitions fire as early as the initial marking and holding times allow. By Theorem 6.5.2 the strongly-connected components then operate periodically with cycle time smaller than T after possibly some transient behaviour. This will be detailed in Chapter 8.

The timed event graph can be forced into a periodic behaviour in accordance with the periodic timetable by explicitly including the latter into the model. This essentially means that the transitions do not fire as early as possible but wait for their scheduled event time. Hence, the timetable realizes additional buffer times between successive departures. Moreover, if the timed event graph is not connected then inclusion of the timetable also has a coordinating function between the various strongly-connected components.

The periodic timetable with cycle time T can be implemented in the timed event graph as follows. First, add a *loop* to the timed event graph consisting of transition $n + 1$ which is both input and output transition to a place $p_{n+1, n+1} = (n + 1, n + 1)$ with one initial token and holding time $w_{n+1} = T$. Hence, transition $n + 1$ fires with a cycle time T and may be interpreted as a clock that synchronizes the start of the next period for all transitions. Second, add a place $p_{i, n+1} = (n + 1, i)$ for all $i = 1, \dots, n$. The place $p_{i, n+1}$ has zero initial tokens and the holding time is defined as $w_{i, n+1} = d_i$, where $d_i \in [0, T)$ is the timetable event time of transition i . If transition $n + 1$ fires at time instant $t = 0$ then each i in the timed event graph is enabled at $x_i(k) = d_i + k \cdot T$ for $k \in \mathbb{N}_0$. Thus, the resulting (autonomous) *scheduled timed event graph* $\bar{\mathcal{G}}$ is given in arc list representation as

$$\bar{\mathcal{G}} = \mathcal{G} \cup \{(n + 1, n + 1, 1, T)\} \cup \{(n + 1, i, 0, d_i) | i = 1, \dots, n\}. \quad (6.10)$$

This corresponds to the timed event graph $\bar{\mathcal{G}} = (\bar{\mathcal{T}}, \bar{\mathcal{P}}, \bar{\mu}, \bar{w})$, where

$$\begin{aligned} \bar{\mathcal{T}} &\doteq \mathcal{T} \cup \{n + 1\}, \\ \bar{\mathcal{P}} &\doteq \mathcal{P} \cup \{(n + 1, n + 1)\} \cup \{(n + 1, i) | i = 1, \dots, n\}, \\ \bar{\mu} &\doteq (\mu^\top, 1, 0, \dots, 0)^\top \in \mathbb{Z}_+^{m+1+n}, \\ \bar{w} &\doteq (w^\top, T, d^\top)^\top \in \mathbb{R}_+^{m+1+n}. \end{aligned}$$

Theorem 6.5.3 (Scheduled timed event graph) *Let $\bar{\mathcal{G}} = (\bar{\mathcal{T}}, \bar{\mathcal{P}}, \bar{\mu}, \bar{w})$ be the scheduled timed event graph defined in (6.10) and let p be the maximum initial marking in any place, $p = \max_k \bar{\mu}_k$. Then $\bar{\mathcal{G}}$ is autonomous, live, $(p + 1)$ -bounded, and periodic with cycle time T .*

Proof: By construction transition $n + 1$ is a predecessor to all transitions, including $n + 1$ itself, and therefore $\bar{\mathcal{G}}$ is autonomous. The original timed event graph \mathcal{G} is live by Theorem 6.5.1. The

event graph $\bar{\mathcal{G}}$ differs from \mathcal{G} by one additional transition $n + 1$, a place $(n + 1, n + 1)$, and places from the new transition $n + 1$ to each other transition. The loop $(n + 1, n + 1)$ contains one token and transition $n + 1$ has no other incoming places, by which the new transition $n + 1$ is live. Furthermore, the loop $(n + 1, n + 1)$ is the only new circuit generated by the new places. Hence, $\bar{\mathcal{G}}$ is live. By Theorem 6.5.2 all strongly-connected subgraphs of \mathcal{G} are periodic with cycle time not exceeding T . The added places from $n + 1$ to all original transitions do not change the strongly-connected components. Hence, the components in $\bar{\mathcal{G}}$ are those of \mathcal{G} plus the additional loop $(n + 1, n + 1)$. Moreover, transition $n + 1$ has cycle time T and has access to all other transitions. Therefore, any transition in $\bar{\mathcal{G}}$ is slowed down to the cycle time of $n + 1$, i.e., the complete timed event graph is synchronous with cycle time T . Finally, $\bar{\mathcal{G}}$ is $(p + 1)$ -bounded since each transition in $\bar{\mathcal{G}}$ has the same cycle time and so each place receives at most one token before again consuming a token during one period. Note that the loop $(n + 1, n + 1)$ is 1-bounded and $p > 0$ since $\bar{\mathcal{G}}$ is live. \square

In the scheduled event graph (6.10) we incorporated the timetable integrally over all transitions. However, in general only departures must be strictly adhered to, whilst arrivals and passages are also allowed to be early. Hence, we can alternatively add the timetable places to departure events only, i.e.,

$$\mathcal{G}' = \mathcal{G} \cup \{(n + 1, n + 1, 1, T)\} \cup \{(n + 1, i, 0, d_i) | i \in \mathcal{D}\}, \quad (6.11)$$

where

$$\mathcal{D} \doteq \{i \in \mathcal{T} \mid E_i = \mathcal{D}\}.$$

Each arrival, through or terminal event at the destination station of a line segment has a predecessor in \mathcal{T} corresponding to the departure event at the origin station of this line segment. Therefore, the proof of Theorem 6.5.3 is also valid for the timed event graph \mathcal{G}' and so Theorem 6.5.3 also holds for \mathcal{G}' instead of $\bar{\mathcal{G}}$.

Comparing Theorem 6.5.2 and 6.5.3, we see that an integrated periodic timetable has an impact on the properties of a timed event graph comparable to strongly connectedness. In Chapter 8 we will study the performance properties of a timed event graph — including the dependence on the internal structure of strongly-connected components — in terms of its max-plus state-space realization using the max-plus algebraic eigenvalue theory that will be introduced in Chapter 7.

6.5.3 Event Domain Description

The timed event graph can alternatively be described in the *event domain*, where the variables are the event times associated to the transitions $i \in \mathcal{T}$. Let $x_i(k)$ denote the k th occurrence time of event i (e.g. departure i of train line L_i from station S_i). We assume that all trains run at an integrated regular interval T (usually $T = 60$ minutes). If the discrete event system is synchronous, the counter k represents the period (hour) in which the event occurs. If a train line has a frequency $f > 1$ trains per cycle time T then the f trains in a basic period are modelled by separate train lines with a cycle time T each. Without loss of generality we furthermore assume that the first timetable period is $[0, T)$, the 2nd period is $[T, 2 \cdot T)$, and in general the k th period is $[(k - 1) \cdot T, k \cdot T)$.

Consider a timed event graph $\mathcal{G} = (\mathcal{T}, \mathcal{P}, \mu, w)$. Then each place $p \in \mathcal{P}$ with $\text{out}(p) = i$ generates a constraint on the event time $x_i(k)$ given by

$$x_i(k) \geq x_{\text{in}(p)}(k - \mu(p)) + w(p),$$

since i may only fire for the k th time if the activity initiated by event $\text{in}(p)$ in $\mu(p)$ periods before has been completed. Denote by Π_i the set of incoming places to transition i , so

$$\Pi_i \doteq \{p \in \mathcal{P} \mid \text{out}(p) = i\}.$$

Then if transitions fire as soon as they are enabled, we obtain the following equation for the event times

$$x_i(k) = \max_{p \in \Pi_i} (x_{\text{in}(p)}(k - \mu(p)) + w(p)) \quad \text{for all } i \in \mathcal{T}. \quad (6.12)$$

If events are not allowed to occur before their scheduled event times then additional *timetable* constraints must be taken into account defined as

$$x_i(k) \geq d_i(k) \quad \text{for all } i \in \mathcal{T},$$

where $d_i(k)$ is the *scheduled event time* of event i in period k . In a periodic timetable with cycle time T the scheduled event time of event i over successive periods $k \in \mathbb{N}$ is given by $d_i(k) = d_i(0) + k \cdot T$, where $d_i(0)$ is an initial scheduled departure time. The general dynamic event time equations of the scheduled timed event graph then becomes

$$x_i(k) = \max \left(\max_{p \in \Pi_i} (x_{\text{in}(p)}(k - \mu(p)) + w(p)), d_i(k) \right) \quad \text{for all } i \in \mathcal{T}. \quad (6.13)$$

The dynamic equations (6.12) and (6.13) are the state-space realizations of the (homogeneous) timed event graph and scheduled timed event graph, respectively. This description is used in the performance evaluation of timed event graphs, see Chapter 8. It is interesting to note that the discrete-event dynamic equations (6.12) and (6.13) are nonlinear because of the maximum operation. Nevertheless, the equations become linear when evaluated in the appropriate algebra, the so-called *max-plus algebra*, where the fundamental operations are the maximum and sum, see Chapter 7.

Example 6.2 Consider the timed event graph of Figure 6.7. The line constraints are

$$\begin{aligned} A_{1,2}(k) &\geq D_{1,1}(k) + 11 \\ D_{1,2}(k) &\geq A_{1,2}(k) + 1 \\ A_{1,3}(k) &\geq D_{1,2}(k) + 12 \\ A_{2,2}(k) &\geq D_{2,1}(k) + 9 \\ D_{2,2}(k) &\geq A_{2,2}(k) + 1 \\ A_{2,3}(k) &\geq D_{2,2}(k) + 10, \end{aligned}$$

the transfer constraints are

$$\begin{aligned} D_{1,2}(k) &\geq A_{2,2}(k) + 2 \\ D_{2,2}(k) &\geq A_{1,2}(k) + 2 \end{aligned}$$

and the headway constraints are given by

$$\begin{aligned} A_{1,2}(k) &\geq A_{2,2}(k - 1) + 2 \\ A_{2,2}(k) &\geq A_{1,2}(k) + 2 \\ D_{1,2}(k) &\geq D_{2,2}(k) + 2 \\ D_{2,2}(k) &\geq D_{1,2}(k - 1) + 2. \end{aligned}$$

From these constraints we obtain the following discrete-event dynamic system description in the event domain:

$$\begin{aligned}
A_{1,2}(k) &= \max(D_{1,1}(k) + 11, A_{2,2}(k - 1) + 2) \\
D_{1,2}(k) &= \max(A_{1,2}(k) + 1, A_{2,2}(k) + 2, D_{2,2}(k) + 2) \\
A_{1,3}(k) &= D_{1,2}(k) + 12 \\
A_{2,2}(k) &= \max(D_{2,1}(k) + 9, A_{1,2}(k) + 2) \\
D_{2,2}(k) &= \max(A_{2,2}(k) + 1, A_{1,2}(k) + 2, D_{1,2}(k - 1) + 2) \\
A_{2,3}(k) &= D_{2,2}(k) + 10.
\end{aligned}$$

Now suppose that a train on line L_1 departs from station S_1 at 0 and a train of line L_2 follows after 5 minutes, i.e., $D_{1,1}(1) = 0$ and $D_{2,1}(1) = 5$. Moreover, assume that these are the first two trains of a day and therefore no events have occurred for $k < 1$ which can be modelled by taking the event times $x(0)$ sufficiently small, or in particular we may take initially $A_{2,2}(0) = -\infty$ and $D_{1,2}(0) = -\infty$. Then we can simply compute the event times from the recursions above, evaluated in the appropriate order, giving

$$\begin{aligned}
A_{1,2}(1) &= \max(D_{1,1}(1) + 11, A_{2,2}(0) + 2) = \max(0 + 11, -\infty + 2) = 11 \\
A_{2,2}(1) &= \max(D_{2,1}(1) + 9, A_{1,2}(1) + 2) = \max(5 + 9, 11 + 2) = 14 \\
D_{2,2}(1) &= \max(A_{2,2}(1) + 1, A_{1,2}(1) + 2, D_{1,2}(0) + 2) = \max(14 + 1, 11 + 2, -\infty + 2) = 15 \\
D_{1,2}(1) &= \max(A_{1,2}(1) + 1, A_{2,2}(1) + 2, D_{2,2}(1) + 2) = \max(11 + 1, 14 + 2, 15 + 2) = 17 \\
A_{2,3}(1) &= D_{2,2}(1) + 10 = 15 + 10 = 25 \\
A_{1,3}(1) &= D_{1,2}(1) + 12 = 17 + 12 = 29.
\end{aligned}$$

If the successive departure times $D_{1,1}(k)$ and $D_{2,1}(k)$ from station S_1 are given for each $k \geq 1$ then we can analogously compute the successive event times for each period $k \in \mathbb{N}$. \square

6.6 Conclusions

A railway timetable and the shared infrastructure utilization generate train interdependencies that leads to scheduled waiting times and delay propagation during operations. In general, a timetable represents a (cyclic) network structure of train circulations and synchronization of trains at main railway stations imposed by passenger transfers, rolling stock connections or crew transfers, and in addition the railway infrastructure and safety and signalling systems cause headway restrictions between successive trains. This intrinsic network structure and the train traffic dynamics within this structure can be modelled and analysed by a graphical and mathematical structure called *timed event graphs*.

Structural properties of timed event graphs concern the topology or interconnection structure. We showed how the primitive structures of timed event graphs (sequential, concurrent and synchronization transitions) can be connected to model typical timetable structures and infrastructure restrictions. Structural properties are independent of the initial marking. On the other hand, behavioural properties of timed event graphs are those characteristics that depend on the initial marking. We showed that timed event graphs have a tendency of becoming periodic driven by the circulation of tokens over circuits in the timed event graph.

This chapter also described the input data necessary for the synthesis of a timed event graph that models the essential features of a scheduled railway system. Line data contains the line schedules and train process times, synchronization data contains passenger and logistic connections between train lines, and headway data consists of all headway restrictions between event pairs corresponding to conflicting train routes. An algorithm has been presented for systematically constructing a timed event graph based on this input data. The timetable and process times contained in the timetable, synchronization data and headway data have been used to derive a consistent initial marking. So far, the analysis of the timetable structure has been mainly structural and behavioural. The next step is performance related issues which will be considered in Chapter 8 after explaining the fundamental mathematics in Chapter 7.

Chapter 7

MAX-PLUS ALGEBRA

7.1 Introduction

This chapter deals with max-plus algebra. Max-plus algebra is a particular example of an idempotent semiring, or dioid, originating from the 1960s as a formal algebraic structure for solving a range of path problems in graph theory. Many graph algorithms are equivalent to classical algorithms for solving linear systems of equations when formulated in the appropriate algebra [75]. Cuninghame-Green [40] gave a first systematic treatment of max-plus algebra showing many counterparts to linear algebra with interpretations in path problems over graphs. In 1985, Cohen *et al.* [32] showed that timed event graphs can be represented by (recursive) linear systems in max-plus algebra and explained how the periodic steady-state behaviour of these discrete-event systems are characterized by solving an eigenproblem in max-plus algebra. This led to a renewed interest in max-plus algebra accumulating to a max-plus linear system theory of discrete-event dynamic systems as presented in Baccelli *et al.* [11], in analogy to linear system theory of dynamic systems governed by differential and difference equations. Current research issues include the geometric description of max-plus semimodules, see e.g. Cohen *et al.* [34].

This chapter introduces max-plus algebra, its connection to path problems, and the eigenproblem of max-plus matrices. The eigenstructure of *irreducible* max-plus matrices is well-known [11, 40]. Gaubert [70] developed a full description of the eigenstructure of *reducible* max-plus matrices. Cochet-Terrasson *et al.* [31] introduced a generalized eigenproblem of max-plus polynomial matrices and described the max-plus policy iteration algorithm for solving this problem. A max-plus polynomial matrix can be viewed as a formal representation of a timed event graph. The paper of Cochet-Terrasson *et al.* [31] therefore motivated the approach in this chapter to develop a complete description of the generalized eigenstructure of reducible max-plus polynomial matrices. In Chapter 8 we will use the polynomial matrix in the state-space description of the timed event graph. Hence, a polynomial matrix is not only a formal representation of timed event graphs but can also be used to describe the firing dynamics of the timed event graph.

The outline of this chapter is as follows. Section 7.2 defines the max-plus semiring as well as polynomials and matrices over this semiring, which are themselves also semirings. The relation between max-plus matrices and precedence graphs is explained, as well as that of max-plus polynomial matrices and timed event graphs. Section 7.3 is concerned with max-plus semimodules, which represent the counterpart of vector spaces in max-plus algebra. Section 7.4 considers the eigenproblem of max-plus matrices and extends this theory to the generalized eigenproblem of max-plus polynomial matrices. This section also explains the max-plus policy iteration algorithm. Longest path algorithms are considered in Section 7.5. Finally, Section 7.6 presents some conclusions.

7.2 Max-Plus Semirings

7.2.1 Basic Definitions: Semirings, Semifields, Dioids

Max-plus algebra is one of the main examples of algebraic structures called dioids or idempotent semirings. This subsection formally defines these structures before zooming into the particular class of max-plus algebra. More background on classical algebra can be found in e.g. Lang [127].

First, let us recall some basic algebra, see also Table 7.1. A *semigroup* (S, \cdot) is a nonempty set S equipped with a binary operation \cdot which is *associative*:

$$\forall a, b, c \in S : a \cdot (b \cdot c) = (a \cdot b) \cdot c.$$

A *monoid* (S, \cdot) is a semigroup containing a *neutral element* $e \in S$, such that

$$\forall a \in S : a \cdot e = e \cdot a = a.$$

A *group* (S, \cdot) is a monoid wherein each element has an *inverse element*:

$$\forall a \in S, \exists a^{-1} : a \cdot a^{-1} = a^{-1} \cdot a = e.$$

A semigroup (monoid, group) (S, \cdot) is *commutative* or *abelian* if

$$\forall a, b \in S : a \cdot b = b \cdot a.$$

A monoid or group may also be denoted by (S, \cdot, e) to indicate the neutral element explicitly.

Table 7.1 Properties of algebraic structures (S, \cdot)

	Associative	Neutral element	Inverse	Commutative	Idempotent
Semigroup	✓	-	-	-	-
Monoid	✓	✓	-	-	-
Semilattice	✓	-	×	✓	✓
Group	✓	✓	✓	-	×

Legend: ✓ = characteristic; – = optional; × = prohibitive

Definition 7.2.1 (Semiring) A semiring (S, \oplus, \otimes) is a nonempty set S equipped with two binary operations called *addition* (\oplus) and *multiplication* (\otimes) satisfying the following conditions:

- (i) (S, \oplus, ε) is a commutative monoid, where ε is called the *zero element*.
- (ii) (S, \otimes, e) is a monoid, where e is called the *unit (or identity) element*.
- (iii) *Multiplication is (left- and right-) distributive over addition:*

$$\forall a, b, c \in S : a \otimes (b \oplus c) = (a \otimes b) \oplus (a \otimes c) \text{ and } (a \oplus b) \otimes c = (a \otimes c) \oplus (b \otimes c).$$

- (iv) *The zero element is absorbing:*

$$\forall a \in S : a \otimes \varepsilon = \varepsilon \otimes a = \varepsilon. \quad (7.1)$$

A semiring may also be denoted by $(S, \oplus, \otimes, \varepsilon, e)$ to indicate the zero and unit element explicitly.

If (S, \otimes) is also commutative then (S, \oplus, \otimes) is a *commutative semiring*. From the definition directly follows that any semiring has at least one element, namely the zero element ε . Moreover, if a semiring (S, \oplus, \otimes) has more than one element, $|S| > 1$, then it contains both a zero and unit element and $e \neq \varepsilon$ by the absorption law. Indeed, for all $a \in S$ we have $a \otimes e = a$ (e is the identity) and $a \otimes \varepsilon = \varepsilon$ (ε is absorbing), whence if $e = \varepsilon$ then we must have $a = \varepsilon$ or equivalently $S = \{\varepsilon\}$. This proves that $e = \varepsilon$ if and only if $|S| = 1$. Furthermore, the neutral elements are unique, since if both e and e' are a zero element then $e = e \oplus e' = e'$. Likewise, if ε and ε' are both a unit element, then $\varepsilon = \varepsilon \otimes \varepsilon' = \varepsilon'$.

Definition 7.2.2 (Semifield) A semifield $(S, \oplus, \otimes, \varepsilon, e)$ is a semiring in which $(S \setminus \{\varepsilon\}, \otimes, e)$ is a group.

In a commutative semifield $(S, \oplus, \otimes, \varepsilon, e)$ each nonzero element has a (multiplicative) inverse, i.e., $\forall a \in S \setminus \{\varepsilon\}, \exists a^{-1} : a \otimes a^{-1} = a^{-1} \otimes a = e$. In general we may distinguish between a right- and left-inverse, but in a *commutative* semifield they coincide. Obviously, ε is not invertible since the zero element ε in a semiring is absorbing. This is similar to the ordinary field of real numbers, where 0 has no multiplicative inverse. The inverse multiplicative operation is called *division* and is denoted by \oslash .

Definition 7.2.3 (Idempotency, dioid) Let (S, \oplus, \otimes) be a semiring. An element $a \in S$ is called (additively) idempotent if $a \oplus a = a$. A semiring (S, \oplus, \otimes) is idempotent if $\forall a \in S : a \oplus a = a$. An idempotent semiring is also called a dioid.

A commutative idempotent semigroup (S, \oplus) is also called a *semilattice* [40], cf. Section 7.2.7. Hence, addition in an idempotent semiring (or dioid) can also be characterized as a semilattice with zero element. An example of an idempotent operation is the pairwise maximum operation, since $\max(a, a) = a$ for any $a \in \mathbb{R}$.

Proposition 7.2.1 An idempotent semiring (semigroup, monoid) has exactly one additive invertible element, which is the zero element ε .

Proof: Assume that a has an additive inverse b such that $a \oplus b = \varepsilon$. Then $a = a \oplus \varepsilon = a \oplus a \oplus b = a \oplus b = \varepsilon$ and likewise $b = \varepsilon \oplus b = a \oplus b \oplus b = a \oplus b = \varepsilon$. Thus, $a = b = \varepsilon$. \square

Idempotency thus prevents the existence of (additive) inverse elements, and therefore an idempotent semiring (semifield) can *not* be embedded in a ring (field), wherein addition is a group. Semirings may therefore be classified into two essentially different classes according to whether or not addition is idempotent. An example of a semiring (in fact, a semifield) that is not idempotent is $\mathbb{R}_+ = ([0, \infty), +, \cdot, 0, 1)$, the nonnegative real numbers with conventional addition and multiplication. Clearly, this semiring can be extended to a ring (or field) by adding the negative real numbers. Such semirings therefore correspond to the nonnegative elements of a ring, which can be *symmetrized* with negative elements. In contrast, addition in idempotent semirings (or dioids) is neither invertible nor can be made invertible in the classic sense, since idempotent addition simply does not allow the existence of inverse elements (other than the trivial zero

element) because of Proposition 7.2.1. Therefore, alternative notions of inversion have been developed for solving linear equations (and monotone functional equations) over a dioid based on residuation theory of (semi)lattices [11, 40]. We will not deliberate this here any further, but refer to Cuninghame-Green [40] and Baccelli *et al.* [11] for details.

Definition 7.2.4 (Subsemiring) Let $(S, \oplus, \otimes, \varepsilon, e)$ be an (idempotent) semiring. A subset $T \subseteq S$ is a subsemiring of $(S, \oplus, \otimes, \varepsilon, e)$ if

- (i) $\varepsilon \in T$ and $e \in T$.
- (ii) T is closed under addition and multiplication, i.e., $\forall a, b \in T : a \oplus b \in T$ and $a \otimes b \in T$.

A subsemiring T of a semiring $(S, \oplus, \otimes, \varepsilon, e)$ inherits the addition and multiplication of the latter and $(T, \oplus, \otimes, \varepsilon, e)$ is itself a semiring. If $(S, \oplus, \otimes, \varepsilon, e)$ is idempotent (or commutative) then so are its subsemirings.

7.2.2 The (max,+)-Semifield

Max-plus algebra is the study of the algebraic structure $\mathbb{R}_{\max} \doteq (\mathbb{R} \cup \{-\infty\}, \oplus, \otimes)$ of the set $\mathbb{R} \cup \{-\infty\}$ equipped with two binary operations called addition (\oplus) and multiplication (\otimes), which are defined for all $a, b \in \mathbb{R} \cup \{-\infty\}$ by

$$a \oplus b \doteq \max(a, b), \quad a \otimes b \doteq a + b. \quad (7.2)$$

The algebraic structure $\mathbb{R}_{\max} = (\mathbb{R} \cup \{-\infty\}, \oplus, \otimes)$ is a *semifield*. In the forthcoming, the scalar operations \oplus and \otimes will always mean the (max, +) operations defined by (7.2).

Proposition 7.2.2 $\mathbb{R}_{\max} = (\mathbb{R} \cup \{-\infty\}, \oplus, \otimes, \varepsilon, e)$, with $\oplus = \max$, $\otimes = +$, zero element $\varepsilon = -\infty$ and unit element $e = 0$ is a commutative idempotent semifield.

Proof: The proposition is easily verified by checking the axioms. □

$\mathbb{R}_{\max} = (\mathbb{R} \cup \{-\infty\}, \max, +)$ is known as the (max, +)-*semiring* or (max, +)-*semifield*. In literature also the names *path algebra* [75] and *schedule algebra* [73] are used corresponding to applications to path and schedule problems over directed graphs. In the sequel, we will use the notation $\varepsilon = -\infty$ and $e = 0$ to emphasize the special meaning of these elements in \mathbb{R}_{\max} . We also denote by $\mathbb{R}_{\varepsilon} \doteq \mathbb{R} \cup \{\varepsilon\}$ the set of real numbers extended by ε . Because of distributivity, \otimes has priority over \oplus and so we also just write ab instead of $a \otimes b$, as is also common in conventional algebra. Since the zero element in \mathbb{R}_{\max} is ε we will also refer to a *nonzero* element as a *finite* element. Division in \mathbb{R}_{\max} is defined for all $a \in \mathbb{R}_{\varepsilon}$ and $b \in \mathbb{R}$ by

$$a \oslash b \doteq a - b.$$

A power $a^{\otimes l}$ in max-plus algebra is defined by repeated multiplication of l factors, i.e., for all $a \in \mathbb{R}_{\max}$ and $l \in \mathbb{N}$

$$a^{\otimes l} \doteq \underbrace{a \otimes \cdots \otimes a}_{l \text{ times}} = l \cdot a,$$

where \cdot is the conventional multiplication. The superscript \otimes may be omitted if there is no confusion that the power must be evaluated in max-plus algebra. Powers of $a \in \mathbb{R}_{\max}$ are not restricted to integers but can more generally be defined by $a^{\otimes l} \doteq l \cdot a$ for any real number $l \in \mathbb{R}$, and by convention $\varepsilon^{\otimes 0} = e$. Products of powers satisfy $a^k \otimes a^l = a^{k \otimes l}$, since $a^k a^l = k \cdot a + l \cdot a = (k + l) \cdot a = a^{k \otimes l}$. A (positive) power of a sum satisfies $(a \oplus b)^k = a^k \oplus b^k$ for all $k \in \mathbb{N}$, since $(a \oplus b)^k = k \cdot \max(a, b) = \max(k \cdot a, k \cdot b) = a^k \oplus b^k$. By induction this identity is easily generalized to a power of a finite series of elements $a_i \in \mathbb{R}_{\max}$ as

$$\left(\bigoplus_{i=1}^n a_i \right)^k = \bigoplus_{i=1}^n a_i^k \quad \text{for all } k \in \mathbb{N}.$$

The notation of the inverse a^{-1} should not be confused with the power of a to -1 , although incidentally $a^{\otimes -1} = -a$ is the inverse of $a \neq \varepsilon$.

The following examples illustrate the arithmetics in \mathbb{R}_{\max} .

$$\begin{array}{lll} 2.4 \oplus 3 & = & 3 \\ 2 \oplus -3 & = & 2 \\ e \oplus 3 & = & 3 \\ -2 \oplus -3 & = & -2 \\ \varepsilon \oplus 3 & = & 3 \end{array} \quad \begin{array}{lll} 2.4 \otimes 3 & = & 5.4 \\ 2 \otimes -3 & = & -1 \\ e \otimes 3 & = & -3 \\ -2 \otimes -3 & = & -5 \\ \varepsilon \otimes 3 & = & \varepsilon \end{array} \quad \begin{array}{lll} 4 \oplus 8 \otimes -3 & = & 5 \\ 3^{-8} & = & -24 \\ 2 \otimes 4^{-3} \otimes 5 & = & -5 \\ (2 \oplus 3)^2 & = & 6 \\ (-1 \oplus -4)^3 & = & -3. \end{array}$$

If we are interested in integers only we may also work in the dioid $\mathbb{Z}_{\max} = (\mathbb{Z} \cup \{\varepsilon\}, \oplus, \otimes)$. \mathbb{Z}_{\max} is a subsemiring of \mathbb{R}_{\max} and therefore itself an idempotent semiring (see Definition 7.2.4), which is easily proved as follows. Clearly, $\varepsilon, e \in \mathbb{Z}_{\max}$ and for any two integers $a, b \in \mathbb{Z}$ also $a \oplus b = \max(a, b)$ and $a \otimes b = a + b$ is an integer. Furthermore, $a \oplus \varepsilon = a$ and $a \otimes \varepsilon = \varepsilon$. The multiplicative inverses $a^{-1} = -a$ of all nonzero elements are also contained in \mathbb{Z} . Hence, \mathbb{Z}_{\max} is a commutative idempotent semifield. Another subsemiring of \mathbb{R}_{\max} (and of \mathbb{Z}_{\max}) is $(\mathbb{N} \cup \{0, \varepsilon\}, \oplus, \otimes)$, which is a commutative idempotent semiring, but not a semifield.

7.2.3 Max-Plus Polynomials

In this section we look at polynomials over the $(\max, +)$ -Semiring.

Definition 7.2.5 (Max-plus polynomial) A (formal) max-plus polynomial in an indeterminate X is a finite sum $\bigoplus_{l=0}^p a_l X^l$ for some integer $p \in \mathbb{N}$ and $a_l \in \mathbb{R}_{\max}$. The set of max-plus polynomials is denoted as $\mathbb{R}_{\max}[X]$.

The elements a_l of a polynomial $f = \bigoplus_{l=0}^p a_l X^l \in \mathbb{R}_{\max}[X]$ are called the *coefficients* of f . The *support* of a polynomial f is the index set of the finite coefficients of f , denoted as $\text{supp}(f) = \{0 \leq l \leq p \mid a_l > \varepsilon\}$. The *degree* of a polynomial $f \in \mathbb{R}_{\max}[X]$ is the highest power of X (or highest index) with $a_l > \varepsilon$, and denoted as $\deg(f) = \bigoplus_{l \in \text{supp}(f)} l$. Two polynomials $\bigoplus_{l=0}^p a_l X^l$ and $\bigoplus_{l=0}^p b_l X^l$ are equal if and only if $a_l = b_l$ for all $l = 0, \dots, p$.

On the set of formal max-plus polynomials $\mathbb{R}_{\max}[X]$ we define addition and multiplication as follows. Let $f = \bigoplus_{l=0}^p a_l X^l$ and $g = \bigoplus_{l=0}^q b_l X^l$. The sum \oplus of two polynomials is defined

componentwise, i.e.,

$$f \oplus g = \bigoplus_{l=0}^{\deg(f) \oplus \deg(g)} (a_l \oplus b_l) X^l. \quad (7.3)$$

If the support of the polynomials f and g differs then we treat the missing coefficients as ε . Note that the degree of $h = f \oplus g \in \mathbb{R}_{\max}[X]$ is the maximal degree of f and g , $\deg(h) = \deg(f) \oplus \deg(g) = \max(\deg(f), \deg(g))$. The product \otimes of two polynomials is defined according to the *sup-convolution* rule:

$$f \otimes g = \bigoplus_{l=0}^{\deg(f) \otimes \deg(g)} \left(\bigoplus_{i \otimes j = l} a_i \otimes b_j \right) X^l. \quad (7.4)$$

The degree of the product of two polynomials is the product of the degree of its factors, $\deg(f \otimes g) = \deg(f) \otimes \deg(g) = \deg(f) + \deg(g)$.

It is easily verified that the set of polynomials $\mathbb{R}_{\max}[X]$ with addition and multiplication as defined in (7.3) and (7.4), respectively, satisfies the axioms of a semiring with the constant polynomials ε and e acting as zero and unit, respectively. Note that the neutral elements can be understood as the polynomials of degree 0, i.e., $\varepsilon = \varepsilon X^0$ and $e = e X^0$. More generally, we define the set $S[X]$ of polynomials in the indeterminate X over a semiring (S, \oplus, \otimes) with addition and multiplication defined by (7.3) and (7.4) evaluated over S . The proof of the following theorem is a straightforward exercise in checking the axioms of a semiring.

Theorem 7.2.1 *Let $(S, \oplus, \otimes, \varepsilon, e)$ be an (idempotent) semiring. Then the algebraic structure $(S[X], \oplus, \otimes, \varepsilon, e)$ of polynomials over S with addition \oplus and multiplication \otimes as defined in (7.3) and (7.4), respectively, is an (idempotent) semiring.*

In particular, the sets of max-plus polynomials $\mathbb{R}_{\max}[X]$ and $\mathbb{Z}_{\max}[X]$ are idempotent semirings.

The definition of polynomial addition and multiplication is consistent with algebraic manipulations in \mathbb{R}_{\max} when considering the indeterminate as a variable in \mathbb{R}_{\max} . By the following proposition we may *substitute* an element $x \in \mathbb{R}_{\max}$ for the indeterminate X . Hence, to each polynomial $f \in \mathbb{R}_{\max}[X]$ we can associate a *polynomial function* $f : \mathbb{R}_{\max} \rightarrow \mathbb{R}_{\max}$ defined by $f(x) = \bigoplus_{l=0}^p a_l x^l$.

Theorem 7.2.2 *Let $(S[X], \oplus, \otimes, \varepsilon, e)$ be a polynomial semiring over a commutative semiring S . Then for any $x \in S$ the valuation mapping $\varphi : f \mapsto f(x)$ is a homomorphism from $S[X]$ into S .*

Proof: We must prove that $\varphi(f \oplus g) = \varphi(f) \oplus \varphi(g)$ and $\varphi(f \otimes g) = \varphi(f) \otimes \varphi(g)$. We may assume without loss of generality that two polynomials have the same degree by taking any missing coefficients equal to ε . So let $f(X) = \bigoplus_{i=0}^p a_i X^i$ and $g(X) = \bigoplus_{j=0}^p b_j X^j$. Then for

addition we have

$$\begin{aligned}
\varphi(f) \oplus \varphi(g) &= f(x) \oplus g(x) \\
&= \left(\bigoplus_{i=0}^p a_i x^i \right) \oplus \left(\bigoplus_{j=0}^p b_j x^j \right) \\
&= a_0 \oplus a_1 x \oplus \dots \oplus a_p x^p \oplus b_0 \oplus b_1 x \oplus \dots \oplus b_p x^p \\
&= (a_0 \oplus b_0) \oplus (a_1 x \oplus b_1 x) \oplus \dots \oplus (a_p x^p \oplus b_p x^p) \quad (\text{by associativity}) \\
&= (a_0 \oplus b_0) \oplus (a_1 \oplus b_1)x \oplus \dots \oplus (a_p \oplus b_p)x^p \quad (\text{by distributivity}) \\
&= \bigoplus_{l=0}^p (a_l \oplus b_l) x^l \\
&= (f \oplus g)(x) \quad (\text{by (7.3)}) \\
&= \varphi(f \oplus g).
\end{aligned}$$

For multiplication we have

$$\begin{aligned}
\varphi(f) \otimes \varphi(g) &= f(x) \otimes g(x) \\
&= \left(\bigoplus_{i=0}^p a_i x^i \right) \otimes \left(\bigoplus_{j=0}^p b_j x^j \right) \\
&\stackrel{\text{distr.}}{=} a_0 \left(\bigoplus_{j=0}^p b_j x^j \right) \oplus a_1 x \left(\bigoplus_{j=0}^p b_j x^j \right) \oplus \dots \oplus a_p x^p \left(\bigoplus_{j=0}^p b_j x^j \right) \\
&\stackrel{\text{comm.}}{=} a_0 \left(\bigoplus_{j=0}^p b_j x^j \right) \oplus a_1 \left(\bigoplus_{j=0}^p b_j x^{j+1} \right) \oplus \dots \oplus a_p \left(\bigoplus_{j=0}^p b_j x^{j+p} \right) \\
&= \bigoplus_{i=0}^p \left(a_i \otimes \left(\bigoplus_{j=0}^p b_j x^{i+j} \right) \right) \\
&= \bigoplus_{i=0}^p \bigoplus_{j=0}^p (a_i \otimes b_j) x^{i+j} \\
&= \bigoplus_{l=0}^{p \otimes p} \bigoplus_{i \otimes j = l} (a_i \otimes b_j) x^{i \otimes j} \\
&\stackrel{(7.4)}{=} (f \otimes g)(x) \\
&= \varphi(f \otimes g).
\end{aligned}$$

Here the third equality follows from distributivity of multiplication over addition and in the fourth equality we used the multiplicative commutativity assumption of S . \square

The valuation homomorphism $\varphi : \mathbb{R}_{\max}[X] \rightarrow \mathbb{R}_{\max}$ is not an isomorphism, since e.g. the two polynomials $X^2 \oplus X \oplus e$ and $X^2 \oplus e$ are different by definition, but for the associated polynomial functions we have $x^2 \oplus x \oplus e = \max(2x, x, 0) = \max(2x, 0) = x^2 \oplus e$ for all $x \in \mathbb{R}_{\max}$.

7.2.4 Max-Plus Matrices

In this section we consider matrices over the $(\max, +)$ -semiring. The scalar max-plus operations are extended to matrices in a standard way. Let $\mathbb{R}_{\max}^{m \times n}$ be the set of $m \times n$ matrices with entries in \mathbb{R}_{\max} . Then matrix addition \oplus is defined componentwise for $A, B \in \mathbb{R}_{\max}^{m \times n}$ as

$$[A \oplus B]_{ij} = a_{ij} \oplus b_{ij} = \max(a_{ij}, b_{ij}), \quad (7.5)$$

and matrix multiplication \otimes is defined for matrices $A \in \mathbb{R}_{\max}^{m \times n}$ and $B \in \mathbb{R}_{\max}^{n \times r}$ as

$$[A \otimes B]_{ij} = \bigoplus_{k=1}^n a_{ik} \otimes b_{kj} = \max_{k=1, \dots, n} (a_{ik} + b_{kj}), \quad (7.6)$$

where $A = (a_{ij})$ and $B = (b_{ij})$. The matrix of all entries equal to ε acts as a zero matrix, i.e., $A \oplus \mathcal{E}_{m \times n} = \mathcal{E}_{m \times n} \oplus A = A$ for all $A \in \mathbb{R}_{\max}^{m \times n}$, where $\mathcal{E}_{m \times n}$ is the $m \times n$ matrix with all elements equal to ε . For square matrices the square matrix defined as $[E]_{ii} = e$ and $[E]_{ij} = \varepsilon$ for $j \neq i$ acts as an identity matrix. The set of square matrices $\mathbb{R}_{\max}^{n \times n}$ is an idempotent semiring by the following theorem.

Theorem 7.2.3 *Let $(S, \oplus, \otimes, \varepsilon, e)$ be an (idempotent) semiring. Then the algebraic structure $(S^{n \times n}, \oplus, \otimes)$ of square matrices over S is an (idempotent) semiring for addition defined as $[A \oplus B]_{ij} = a_{ij} \oplus b_{ij}$ and multiplication defined as $[A \otimes B]_{ij} = \bigoplus_{k=1}^n a_{ik} \otimes b_{kj}$. The zero matrix \mathcal{E} and identity matrix E are given as*

$$\mathcal{E}_{n \times n} \doteq \begin{bmatrix} \varepsilon & \cdots & \varepsilon \\ \vdots & & \vdots \\ \varepsilon & \cdots & \varepsilon \end{bmatrix} \quad \text{and} \quad E_{n \times n} \doteq \begin{bmatrix} e & & \varepsilon \\ & \ddots & \\ \varepsilon & & e \end{bmatrix}.$$

Proof: The axioms in Definition 7.2.1 are easily verified, and so is idempotency. In particular $\mathcal{E}_{n \times n}$ is absorbing since $A \otimes \mathcal{E}_{n \times n} = \mathcal{E}_{n \times n} \otimes A = \mathcal{E}$ for all $A \in S^{n \times n}$. \square

The zero matrix $\mathcal{E}_{n \times n}$ is also denoted as \mathcal{E} , where the dimension is chosen appropriately, and likewise the identity matrix $E_{n \times n}$ is also denoted as E . Obviously, since $S^{n \times n}$ is a semiring we can simply denote the zero and unit as ε and e , respectively. However, for the sake of clarity we will restrict the notation ε and e to scalar semirings and \mathcal{E} and E to matrix semirings. Note that S can be viewed as a special case of $S^{n \times n}$ with $n = 1$. There is no ambiguity in using the same symbols \oplus and \otimes for both scalar operations and matrix operations, since they relate to two different objects (scalars and matrices).

For square matrices a *matrix power* is defined recursively by

$$A^{\otimes 0} = E, \quad A^{\otimes l} = A \otimes A^{\otimes l-1} \quad \text{for all } l \in \mathbb{N}.$$

So e.g. $A^{\otimes 3} = A \otimes A^{\otimes 2} = A \otimes A \otimes A$. We will also just write $A^l = A^{\otimes l}$ when it is clear from the context that we are working in max-plus algebra. Multiplication of two matrix powers over the same matrix satisfies $A^k \otimes A^l = A^{k \oplus l}$. Matrix powers in max-plus algebra have a special meaning in terms of paths in graphs as we will see in Section 7.2.5

The *transpose* of a matrix $A = (a_{ij})$ is defined as $A^\top = (a_{ji})$. A *permutation matrix* $P \in \mathbb{R}_{\max}^{n \times n}$ is an identity matrix with possibly some exchanged rows (or columns). Hence, each column (row) of a permutation matrix is a *unit vector* e_i with entry e at row (column) i and ε elsewhere. A permutation matrix satisfies $P \otimes P^\top = E$ and therefore each permutation matrix has an inverse $P^{-1} = P^\top$. The set of all permutation matrices in $\mathbb{R}_{\max}^{n \times n}$ is a group for matrix multiplication, but it is *not* a (sub)semiring because there is no zero matrix (\mathcal{E} is no permutation matrix). Premultiplying a matrix $A \in \mathbb{R}_{\max}^{n \times n}$ by P results in exchanging the rows of A , whereas postmultiplying by P rearranges the columns of A . For example, if P is obtained by swapping row i and j of E then row (column) i and j of A will be swapped by the product PA (respectively AP). The matrix $P^\top AP$ is a simultaneous permutation of rows and columns of A corresponding to a coordinate transformation. The mapping $A \rightarrow P^\top AP$ is a *similarity transformation*.

Example 7.1 Let $A \in \mathbb{R}_{\max}^{3 \times 3}$ and assume we want a coordinate transformation such that the indices $(1, 2, 3)$ are exchanged to $(3, 1, 2)$, by which e.g. a_{12} becomes a_{31} . This is obtained by a transformation $P^\top A P$ with $P = [e_3 \ e_1 \ e_2]$. For example, if

$$A = \begin{bmatrix} 11 & 12 & 13 \\ 21 & 22 & 23 \\ 31 & 32 & 33 \end{bmatrix} \quad \text{and} \quad P = \begin{bmatrix} \varepsilon & e & \varepsilon \\ \varepsilon & \varepsilon & e \\ e & \varepsilon & \varepsilon \end{bmatrix}$$

then

$$\begin{aligned} P^\top \otimes A \otimes P &= \begin{bmatrix} \varepsilon & \varepsilon & e \\ e & \varepsilon & \varepsilon \\ \varepsilon & e & \varepsilon \end{bmatrix} \otimes \begin{bmatrix} 11 & 12 & 13 \\ 21 & 22 & 23 \\ 31 & 32 & 33 \end{bmatrix} \otimes \begin{bmatrix} \varepsilon & e & \varepsilon \\ \varepsilon & \varepsilon & e \\ e & \varepsilon & \varepsilon \end{bmatrix} \\ &= \begin{bmatrix} \varepsilon & \varepsilon & e \\ e & \varepsilon & \varepsilon \\ \varepsilon & e & \varepsilon \end{bmatrix} \otimes \begin{bmatrix} 13 & 11 & 12 \\ 23 & 21 & 22 \\ 33 & 31 & 32 \end{bmatrix} \\ &= \begin{bmatrix} 33 & 31 & 32 \\ 13 & 11 & 12 \\ 23 & 21 & 22 \end{bmatrix}. \end{aligned}$$

Note that the matrix elements are rearranged but not changed. □

An $r \times q$ *block matrix* is a matrix that is partitioned into $r \times q$ rectangular submatrices, called blocks. In particular, locations of zero blocks (submatrices containing zeros only) are of combinatorial and computational interest. A matrix with a particular useful block structure is a lower *block triangular matrix*

$$A = \begin{bmatrix} A_{11} & & \mathcal{E} \\ \vdots & \ddots & \\ A_{r1} & \cdots & A_{rr} \end{bmatrix},$$

with *square* blocks A_{ii} on the diagonal, and zero blocks $A_{ij} = \mathcal{E}$ for $j > i$ for all $1 \leq i \leq r$. Analogously, an upper block triangular matrix has only zeros below the block diagonal. Matrices having the same block (triangular) structure are called *conformable* block matrices. Note that block triangular matrices are square matrices because their diagonal blocks are square.

Proposition 7.2.3 *The set of conformable (lower or upper) block triangular matrices in $\mathbb{R}_{\max}^{n \times n}$ is a subsemiring of $\mathbb{R}_{\max}^{n \times n}$.*

Proof: Clearly, \mathcal{E} and E are lower and upper block triangular, since all off-diagonal elements are zero. The structure of zero entries is clearly preserved under (componentwise) addition. Multiplication of two conformable $r \times r$ block matrices A and B with square diagonal blocks yields a matrix C with the same block partitioning, determined by $C_{ij} = \bigoplus_{k=1}^r A_{ik} \otimes B_{kj}$, $1 \leq i, j \leq r$. Note that the block multiplications are well-defined since by the square diagonal blocks the number of columns of each block A_{ik} equals the number of rows of B_{kj} . Now, if A and B are lower block triangular matrices then $A_{ik} = \mathcal{E}$ for $k > i$ and $B_{kj} = \mathcal{E}$ for $k < j$, and therefore $A_{ik} B_{kj} = \mathcal{E}$ whenever $i < k$ or $k < j$. Hence, $C_{ij} = \bigoplus_{k=j}^i A_{ik} \otimes B_{kj}$ if $j \leq i$ and $C_{ij} = \varepsilon$ for $j > i$, which is exactly the lower block triangular structure. The proof for upper block triangular matrices is similar, but can also be derived as follows. If A and B are

conformable upper block triangular matrices then their transposes A^\top and B^\top are lower block triangular matrices, which we just proved to be closed under matrix addition and multiplication. Hence, $A \oplus B = (A^\top \oplus B^\top)^\top$ and $A \otimes B = (B^\top \otimes A^\top)^\top$ are transpositions of lower block triangular matrices, which are again upper block triangular. \square

Definition 7.2.6 (Reducibility, Irreducibility) A matrix $A \in \mathbb{R}_{\max}^{n \times n}$ is called reducible if there exists a permutation matrix P such that $P^\top A P$ is lower block triangular, i.e.,

$$P^\top A P = \begin{bmatrix} A_{11} & \mathcal{E} \\ A_{21} & A_{22} \end{bmatrix}, \quad (7.7)$$

where A_{11} and A_{22} are square matrices. If a matrix is not reducible it is called irreducible.

Note that any (finite) sum and product of a reducible matrix is again a reducible matrix because of Proposition 7.2.3. For instance, the l th power of (7.7) for any integer $l \in \mathbb{N}$ is

$$(P^\top A P)^l = \begin{bmatrix} A_{11} & \mathcal{E} \\ A_{21} & A_{22} \end{bmatrix}^l = \begin{bmatrix} A_{11}^l & \mathcal{E} \\ \bigoplus_{k=0}^{l-1} A_{22}^k A_{21} A_{11}^{l-k-1} & A_{22}^l \end{bmatrix}.$$

It will be useful to extend the internal matrix operations (addition and multiplication) by *scalar multiplication*, defined as componentwise multiplication by a scalar of the underlying semiring. So on any matrix semiring $S^{n \times n}$ we define $[cA]_{ij} = c \otimes a_{ij}$ for all $c \in S$ and $A = (a_{ij}) \in S^{n \times n}$. This extended structure is called a semialgebra. As is common in conventional linear algebra we will be using the same symbol for scalar-matrix multiplication as for multiplication of scalars and matrices. The context defines without ambiguity how the operation should be interpreted.

Definition 7.2.7 (Semialgebra) A semialgebra over a semiring (S, \oplus, \otimes) is a set X equipped with two internal binary operations $\oplus : X \times X \rightarrow X$ (addition) and $\otimes : X \times X \rightarrow X$ (multiplication), and an external operation $\otimes : S \times X \rightarrow X$ (scalar multiplication), satisfying the following conditions:

- (i) $(X, \oplus, \otimes, \varepsilon_X, e_X)$ is a semiring;
- (ii) Scalar multiplication satisfies

$$\forall a, b \in S, \forall x \in X : (a \otimes b) \otimes x = a \otimes (b \otimes x) \quad \text{and} \quad e \otimes x = x.$$

- (iii) Scalar multiplication is distributive over addition:

$$\forall a, b \in S, \forall x, y \in X : a \otimes (x \oplus y) = a \otimes x \oplus a \otimes y \quad \text{and} \quad (a \oplus b) \otimes x = a \otimes x \oplus b \otimes x.$$

- (iv) The zero ε_X is absorbing:

$$\forall a \in S, \forall x \in X : a \otimes \varepsilon_X = \varepsilon \otimes x = \varepsilon_X.$$

We also denote the zero and unit elements of a semialgebra over a semiring simply as ε and e , or in the case of a matrix semialgebra by \mathcal{E} and E . If the semialgebra has an idempotent addition then it is called an *idempotent semialgebra*.

Proposition 7.2.4 *A semialgebra (X, \oplus, \otimes) over an idempotent semiring (S, \oplus, \otimes) is an idempotent semialgebra.*

Proof: For the idempotent unit element $e \in S$ we have $x \oplus x = e \otimes x \oplus e \otimes x = (e \oplus e) \otimes x = e \otimes x = x$ for all $x \in X$. \square

Theorem 7.2.4 *Let $(S, \oplus, \otimes, \varepsilon, e)$ be an (idempotent) semiring. Then the algebraic structure $(S^{n \times n}, \oplus, \otimes)$ of square matrices over S is an (idempotent) semialgebra for addition defined as $[A \oplus B]_{ij} = a_{ij} \oplus b_{ij}$, multiplication defined as $[A \otimes B]_{ij} = \bigoplus_{k=1}^n a_{ik} \otimes b_{kj}$, and scalar multiplication defined as $[c \otimes A]_{ij} = c \otimes a_{ij}$ with $A, B \in S^{n \times n}$ and $c \in S$. The zero matrix is \mathcal{E} and the identity matrix is E .*

Proof: We already know from Theorem 7.2.3 that if S is an (idempotent) semiring then so is $S^{n \times n}$. The remaining axioms easily follow from the semiring properties of S and the fact that scalar multiplication is defined componentwise. Let $c, d \in S$ and $A = (a_{ij}), B = (b_{ij}) \in S^{n \times n}$. Then by associativity of multiplication in S we have $[(c \otimes d)A]_{ij} = (c \otimes d) \otimes a_{ij} = c \otimes (d \otimes a_{ij}) = c \otimes [dA]_{ij}$. By distributivity of S we obtain $[c(A \oplus B)]_{ij} = c \otimes (a_{ij} \oplus b_{ij}) = c \otimes a_{ij} \oplus c \otimes b_{ij} = [cA]_{ij} \oplus [cB]_{ij}$, and likewise $[(c \oplus d)A]_{ij} = (c \oplus d) \otimes a_{ij} = c \otimes a_{ij} \oplus d \otimes a_{ij} = [cA]_{ij} \oplus [dA]_{ij}$. Finally, $[c \otimes \mathcal{E}]_{ij} = c\varepsilon = \varepsilon$, $[\varepsilon \otimes A]_{ij} = \varepsilon \otimes a_{ij} = \varepsilon$, and $[e \otimes A]_{ij} = e \otimes a_{ij} = a_{ij} = [A]_{ij}$. \square

In particular, $\mathbb{R}_{\max}^{n \times n}$ is an idempotent semialgebra over \mathbb{R}_{\max} , and so multiplication of a matrix $A \in \mathbb{R}_{\max}^{n \times n}$ by a scalar $c \in \mathbb{R}_{\max}$ is well-defined. Likewise for $\mathbb{Z}_{\max}^{n \times n}$.

7.2.5 Precedence Graphs and Path Matrices

A square max-plus matrix can be viewed as the adjacency matrix of a weighted directed graph (or digraph). A weighted digraph is denoted by (V, E, w) , where V is the set of vertices (or nodes), $E \subseteq V \times V$ is the set of arcs, and $w \in \mathbb{R}^{|E|}$ is a vector of arc weights.

Definition 7.2.8 (Precedence graph) *The precedence graph $G(A)$ associated to a matrix $A \in \mathbb{R}_{\max}^{n \times n}$ is a weighted digraph $G = (V, E, w)$ with $V = \{1, \dots, n\}$ and an arc $(j, i) \in E$ with weight $w(j, i) = a_{ij}$ for each $a_{ij} \neq \varepsilon$.*

Hence, $a_{ij} = \varepsilon$ implies that there is no arc from j to i in the digraph $G(A)$. By definition, the precedence graph is a *simple* digraph, i.e., there is at most one arc (i, j) from any node i to j . As a corollary, any simple weighted digraph $G = (V, E, w)$ is the precedence graph of a square matrix $A \in \mathbb{R}_{\max}^{|V| \times |V|}$ with entry $a_{ij} = w(j, i)$ for each arc $(j, i) \in E$, and $a_{ij} = \varepsilon$ otherwise. For digraphs with multiarcs (multigraphs) we may also associate a square matrix $A \in \mathbb{R}_{\max}^{|V| \times |V|}$ by defining a_{ij} as the maximum weight of parallel arcs from j to i , i.e., $a_{ij} = \bigoplus_l w_l(j, i)$, where $w_l(j, i)$ is the weight of the l th parallel arc from j to i . However, the one-to-one correspondence between the digraph and its associated max-plus matrix is now lost: only the maximum arc weights are stored in the max-plus matrix.

In the sequel, we need some terminology of graph theory. An arc (i, j) is an ordered pair of nodes, where i is its tail and j its head. A *path* in a digraph is a sequence of adjacent arcs $\xi = (\xi_1, \dots, \xi_m)$ such that the head of ξ_i is the tail of ξ_{i+1} for $i = 1, \dots, m-1$. Hence, all arcs on a path have the same orientation. The length $l(\xi)$ of a path ξ is the number of arcs it contains,

so if $\xi = (\xi_1, \dots, \xi_m)$ then $l(\xi) = m$. In a weighted digraph the *path weight* is the product of arc weights, i.e., $w(\xi) = \bigotimes_{\xi_i \in \xi} w_i$, where w_i is the weight of arc ξ_i . Note that this corresponds to the conventional sum of arc weights. By convention, a path of length 0 has weight 0. A path of length 0 corresponds to staying at a node, and should not be confused with a loop from a node to itself, which has length 1.

A matrix power in max-plus algebra has a special meaning in terms of paths in digraphs. By definition (7.6) of matrix multiplication, we have $[A^2]_{ij} = \max_{k=1, \dots, n} (a_{ik} + a_{kj})$, which equals the largest weight of all paths with exactly two arcs from j to i . In general, A^m is the matrix of the maximum weights of all paths with length m , i.e.,

$[A^m]_{ij}$ is the maximum weight of all paths from j to i with m arcs.

Now, let $A^{(m)} \doteq \bigoplus_{l=0}^m A^l$ be the matrix of the maximum weights of all paths with length smaller than or equal to m , i.e.,

$[A^{(m)}]_{ij}$ is the maximum weight of all paths from j to i with at most m arcs.

The following proposition shows that the matrices $A^{(m)}$ can also be determined by a max-plus matrix power.

Proposition 7.2.5 *For any $A \in \mathbb{R}_{\max}^{n \times n}$ and any $m \in \mathbb{N}$*

$$\bigoplus_{l=0}^m A^l = (E \oplus A)^m. \quad (7.8)$$

Proof: Clearly, for $m = 1$ we have $E \oplus A = A^0 \oplus A^1$. Now assume that (7.8) holds for $m = k$ then it also holds for $m = k + 1$, since

$$\begin{aligned} (E \oplus A)^{k+1} &= (E \oplus A) \otimes (E \oplus A)^k \\ &= (E \oplus A) \otimes \bigoplus_{l=0}^k A^l && \text{(induction step)} \\ &= \bigoplus_{l=0}^k (A^l) \oplus \bigoplus_{l=0}^k (AA^l) && \text{(by distributivity)} \\ &= \bigoplus_{l=0}^k (A^l) \oplus \bigoplus_{l=1}^{k+1} (A^l) \\ &= E \oplus \bigoplus_{l=1}^k (A^l) \oplus \bigoplus_{l=1}^k (A^l) \oplus A^{k+1} \\ &= E \oplus \bigoplus_{l=1}^k (A^l) \oplus A^{k+1} && \text{(by idempotency)} \\ &= \bigoplus_{l=0}^{k+1} A^l. \end{aligned}$$

Hence, by induction (7.8) is valid for all $m \in \mathbb{N}$. □

Let

$$A^+ \doteq \bigoplus_{l=1}^{\infty} A^l = A \oplus A^2 \oplus A^3 \oplus \dots \quad (7.9)$$

Then $[A^+]_{ij}$ is the maximum path weight from j to i over all paths of any length (> 0). Therefore, A^+ is also called the (longest) *path matrix*¹. The entry $[A^+]_{ii}$ is the maximum path weight

¹In the min-plus semiring $(\mathbb{R}^{n \times n} \cup \{\infty\}, \min, +)$ this matrix is known as the *shortest path matrix*

from i back to i over paths with length at least one. A related matrix sum is the (Kleene) *star* of A , defined as

$$A^* \doteq \bigoplus_{l=0}^{\infty} A^l = E \oplus A \oplus A^2 \oplus \dots \quad (7.10)$$

The matrix A^* is also known as the quasi-inverse or matrix closure of A [73]. The matrices A^* and A^+ are equal except possibly for the diagonal elements. Consider a node i in the precedence graph $G(A)$. If i is not contained in any circuit then $[A^+]_{ii} = \varepsilon$. If on the other hand i is contained in circuits with negative weight only then $[A^+]_{ii} < e$. In both cases $[A^*]_{ii} = e$.

The closure A^* for any matrix $A \in \mathbb{R}_{\max}^{n \times n}$ satisfies a range of properties that follow immediately from its definition. In particular, $A^+ = AA^*$ and $A^* = E \oplus A^+ = E \oplus AA^*$. Furthermore, from (7.10) and (additive) idempotency of $\mathbb{R}_{\max}^{n \times n}$ follows $A^*A^* = A^*$, which means that A^* is both additive and multiplicative idempotent.

In general, the infinite sums in (7.9) and (7.10) do not have to converge. However, the following proposition gives a necessary and sufficient condition for finite convergence of these infinite sums.

Proposition 7.2.6 *Let $A \in \mathbb{R}_{\max}^{n \times n}$ be such that the associated precedence graph $G(A)$ has no circuits with positive weight. Then the limits A^* and A^+ exist and are reached by the finite sums*

$$A^* = \bigoplus_{l=0}^{n-1} A^l \quad \text{and} \quad A^+ = \bigoplus_{l=1}^n A^l. \quad (7.11)$$

Proof: In a digraph with n nodes, any path from node j to i , $j \neq i$, of length n or more necessarily consists of an elementary path with length strictly less than n and one or more circuits. Since by assumption any circuit has nonpositive weight, the inclusion of a circuit to an elementary path will never increase the path weight, by which follows that the maximum-weight path between any two distinct nodes has length at most $n - 1$. Moreover, a path from any node i to itself is by definition a circuit and thus has nonpositive weight by assumption. Therefore, for all i, j there is an integer $l \in \{0, \dots, n - 1\}$ such that $[A^l]_{ij} \geq [A^m]_{ij}$ for all integers $m \geq n$. Hence,

$$\bigoplus_{l=0}^{n-1} A^l \geq A^m \quad \text{for all } m \geq n, \quad (7.12)$$

proving the finite convergence of A^* . Note that by the assumption on the circuit weights the diagonal entries of A^* are all e . In the case of A^+ , a diagonal entry $[A^+]_{ii}$ corresponds to the maximum-weight circuit over i . Clearly this must be an elementary circuit by the same reasoning as above. An elementary circuit in a digraph of n nodes has at most n nodes, whence $\bigoplus_{l=1}^n A^l \geq A^m$ for all $m \geq n + 1$. \square

If $A \in \mathbb{R}_{\max}^{n \times n}$ satisfies the condition of Proposition 7.2.6, i.e., $G(A)$ has no positive-weight circuits, then in particular $A^* = (E \oplus A)^m$ for any $m \geq n - 1$ because of (7.12) and Proposition 7.2.5.

By definition an acyclic graph has no circuits and we therefore obtain the following corollary to Proposition 7.2.6.

Corollary 7.2.1 *If $A \in \mathbb{R}_{\max}^{n \times n}$ has an acyclic precedence graph $G(A)$ then A^* and A^+ exist and are defined by (7.11).*

The matrices A^+ and A^* can be computed by efficient graph algorithms due to the equivalence to the all-pairs longest (or shortest) path problem. The well-known *Floyd-Warshall algorithm* [66, 39] computes A^+ in $O(n^3)$ time using a special implementation of the repeated max-plus matrix multiplication, see Section 7.5.1. For large sparse matrices the repeated shortest path algorithm of Johnson [112, 39] is even more efficient, see Section 7.5 for more details. If we have computed A^+ then we also have $A^* = E \oplus A^+$, by simply setting each negative diagonal entry to 0, since $[A^*]_{ii} = e \oplus [A^+]_{ii} = \max(0, a_{ii}^+)$.

Lemma 7.2.1 *Let $A, P \in \mathbb{R}_{\max}^{n \times n}$, where P is a permutation matrix. Then*

$$(P^\top AP)^+ = P^\top A^+ P \quad \text{and} \quad (P^\top AP)^* = P^\top A^* P.$$

Proof: A permutation matrix P satisfies $PP^\top = P^\top P = E$ and therefore $(P^\top AP)^2 = P^\top APP^\top AP = P^\top A^2 P$. By induction we obtain $(P^\top AP)^l = P^\top A^l P$ for any integer $l \geq 1$, and thus

$$(P^\top AP)^+ = \bigoplus_{l=1}^{\infty} (P^\top AP)^l = \bigoplus_{l=1}^{\infty} P^\top A^l P = P^\top \otimes \left(\bigoplus_{l=1}^{\infty} A^l \right) \otimes P = P^\top A^+ P.$$

The proof of $(P^\top AP)^* = P^\top A^* P$ is similar, with the additional term $(P^\top AP)^0 = E = P^\top P = P^\top EP = P^\top A^0 P$. \square

A directed graph $G(A)$ is *strongly connected* if there is a path from any node j to any node i in $G(A)$. In terms of the matrix A this means that for all indices $1 \leq i, j \leq n$ there exists an integer $l \in \mathbb{N}$ such that $[A^l]_{ij} > \varepsilon$, or using the path matrix we simply have $A^+ > \varepsilon$. The following proposition gives a graph interpretation of an irreducible matrix A . We assume that $n \geq 2$.

Proposition 7.2.7 *Let $A \in \mathbb{R}_{\max}^{n \times n}$ with associated precedence graph $G(A)$. Then A is irreducible if and only if $G(A)$ is strongly connected.*

Proof: We prove the contraposition that A is reducible if and only if $G(A)$ is not strongly connected. First, assume that $G(A) = (V, E)$ is not strongly connected. Then there exists a nonempty subset of nodes $W \subset V$, such that no arcs go from W to $V \setminus W$. Without loss of generality, we may assume that the nodes are numbered such that the last $|W|$ nodes correspond to W . But then A has the block triangular form (7.7), where A_{11} corresponds to the arcs in the component $(V \setminus W)$, A_{22} to the arcs between nodes in W , and the block $A_{12} = \mathcal{E}$ corresponds to $a_{ij} = \varepsilon$ for $(j, i) \in W \times (V \setminus W)$.

Conversely, assume that A is reducible. Then there exists a permutation matrix P , such that $P^\top AP$ has block triangular form (7.7). By Proposition 7.2.3 this block triangular structure is preserved for any sum and power, whence $(P^\top AP)^+ = \bigoplus_{l=1}^{\infty} (P^\top AP)^l$ is also block triangular and so is $P^\top A^+ P$ by Lemma 7.2.1. Thus, $A^+ \not> \varepsilon$ and so $G(A)$ is not strongly connected. \square

7.2.6 Polynomial Matrices and Timed Event Graphs

Since $\mathbb{R}_{\max}[X]$ and $\mathbb{R}_{\max}^{n \times n}$ are idempotent semirings we can also consider square matrices with entries in $\mathbb{R}_{\max}[X]$, or polynomials with square matrices as coefficients. This leads to the idempotent semiring $\mathbb{R}_{\max}^{n \times n}[X]$ of max-plus polynomial matrices, which will play a central role in the theory of max-plus linear systems of Chapter 8.

Definition 7.2.9 (Polynomial matrix) A polynomial matrix in an indeterminate X over a semiring S is a finite sum

$$\mathcal{A} = \bigoplus_{l=0}^p A_l \otimes X^l \quad (7.13)$$

for some integer $p \in \mathbb{N}$ and matrix coefficients $A_l \in S^{n \times n}$. The set of $n \times n$ polynomial matrices is denoted as $S^{n \times n}[X]$.

In particular, $\mathbb{R}_{\max}^{n \times n}[X]$ is the set of max-plus polynomial matrices in an indeterminate X over the semiring \mathbb{R}_{\max} with elements $\bigoplus_{l=0}^p A_l \otimes X^l$, where $A_l \in \mathbb{R}_{\max}^{n \times n}$.

Theorem 7.2.5 Let (S, \oplus, \otimes) be an (idempotent) semiring. Then the set $S^{n \times n}[X]$ of square polynomial matrices over S is an (idempotent) semiring for addition defined as

$$\mathcal{A} \oplus \mathcal{B} = \bigoplus_{l=0}^{\deg(\mathcal{A}) \oplus \deg(\mathcal{B})} (A_l \oplus B_l) X^l \quad (7.14)$$

and multiplication defined as

$$\mathcal{A} \otimes \mathcal{B} = \bigoplus_{l=0}^{\deg(\mathcal{A}) \otimes \deg(\mathcal{B})} \bigoplus_{r \otimes s = l} (A_r \otimes B_s) X^l. \quad (7.15)$$

The zero and unit elements in $S^{n \times n}[X]$ are the zero matrix \mathcal{E} and identity matrix E .

Proof: If S is an (idempotent) semiring then $S^{n \times n}$ is an (idempotent) semiring by Theorem 7.2.3. The addition defined in (7.14) is simply the polynomial addition over the (idempotent) matrix semiring $S^{n \times n}$ and the multiplication (7.15) is just polynomial multiplication over $S^{n \times n}$. Hence, Theorem 7.2.1 can be applied, by which $S^{n \times n}[X]$ is an (idempotent) semiring. The zero and identity matrix can be interpreted as the constant polynomial matrices $\mathcal{E}X^0$ and EX^0 . \square

In Definition 7.2.9 a polynomial matrix is defined as a polynomial with matrix coefficients. An alternative definition of a polynomial matrix is a matrix $\mathcal{A} \in (\mathbb{R}_{\max}[X])^{n \times n}$ with polynomial entries $\mathcal{A}_{ij} = \bigoplus_{l=0}^p a_{ij}^{(l)} X^l$, where $a_{ij}^{(l)} \in \mathbb{R}_{\max}$ for all $1 \leq i, j \leq n$ and $0 \leq l \leq p$. In fact, we will show that the algebraic structures $\mathbb{R}_{\max}^{n \times n}[X]$ and $(\mathbb{R}_{\max}[X])^{n \times n}$ are indistinguishable or *isomorphic*, by which it is mathematically justified to interpret a polynomial matrix either as a polynomial with matrix coefficients or as a matrix with polynomial entries. For example,

$$\mathcal{A} = \begin{bmatrix} \varepsilon & e \\ 3 & e \end{bmatrix} \oplus \begin{bmatrix} \varepsilon & e \\ e & 2 \end{bmatrix} X = \begin{bmatrix} \varepsilon & e \oplus X \\ 3 \oplus X & e \oplus 2X \end{bmatrix}.$$

Theorem 7.2.6 *Let (S, \oplus, \otimes) be an (idempotent) semiring. Then the set $(S[X])^{n \times n}$ of square matrices \mathcal{A} with polynomial entries $\mathcal{A}_{ij} = \bigoplus_{l=0}^p a_{ij}^{(l)} X^l$ in an indeterminate X over S is an (idempotent) semiring for addition defined as*

$$(\mathcal{A} \oplus \mathcal{B})_{ij} = \mathcal{A}_{ij} \oplus \mathcal{B}_{ij} = \bigoplus_{l=0}^{\deg(\mathcal{A}_{ij}) \oplus \deg(\mathcal{B}_{ij})} (a_{ij}^{(l)} \oplus b_{ij}^{(l)}) X^l, \quad (7.16)$$

and multiplication as

$$(\mathcal{A} \otimes \mathcal{B})_{ij} = \bigoplus_{k=1}^n (\mathcal{A}_{ik} \otimes \mathcal{B}_{kj}) = \bigoplus_{k=1}^n \bigoplus_{l=0}^{\deg(\mathcal{A}_{ik}) \otimes \deg(\mathcal{B}_{kj})} \bigoplus_{r \otimes s = l} (a_{ik}^{(r)} \otimes b_{kj}^{(s)}) X^l. \quad (7.17)$$

The zero and unit elements in $(S[X])^{n \times n}$ are the zero matrix \mathcal{E} and identity matrix E .

Proof: If S is an (idempotent) semiring then $S[X]$ is also an (idempotent) semiring by Theorem 7.2.1. The addition defined in (7.16) is simply the (componentwise) matrix addition over the (idempotent) semiring $S[X]$ and the multiplication (7.17) is just matrix multiplication over $S[X]$. Hence, Theorem 7.2.3 can be applied, by which $S^{n \times n}[X]$ is an (idempotent) semiring. \square

Note the similarity between the proof of Theorem 7.2.6 and that of Theorem 7.2.5. $S^{n \times n}[X]$ is the semiring of polynomials with matrix coefficients and $(S[X])^{n \times n}$ is the semiring of matrices with polynomial entries. The resulting semiring structure is algebraically equivalent as presented in the following theorem.

Theorem 7.2.7 *Let (S, \oplus, \otimes) be an (idempotent) semiring. Then the (idempotent) semirings $S^{n \times n}[X]$ and $(S[X])^{n \times n}$ are isomorphic.*

Proof: Define the mapping $\psi : S^{n \times n}[X] \rightarrow (S[X])^{n \times n}$ as

$$\psi \left(\bigoplus_{l=0}^p A_l X^l \right) = \mathcal{A} \quad \text{with} \quad \mathcal{A}_{ij} = \bigoplus_{l=0}^p [A_l]_{ij} X^l \quad \text{for all } 1 \leq i, j \leq n.$$

It is easily seen that ψ is bijective and maps each entry of a matrix coefficient uniquely onto a coefficient of a polynomial matrix entry, i.e., $[A_l]_{ij} = a_{ij}^{(l)}$ for all $1 \leq i, j \leq n$ and $0 \leq l \leq p$. Hence, the inverse mapping $\psi^{-1} : (S[X])^{n \times n} \rightarrow S^{n \times n}[X]$ is well-defined. Addition (7.14) on $(S[X])^{n \times n}$ is exactly (7.16) by identifying $[A_l]_{ij} = a_{ij}^{(l)}$, i.e., $\mathcal{A} \oplus \mathcal{B} = \psi(\psi^{-1}(\mathcal{A}) \oplus \psi^{-1}(\mathcal{B}))$. Likewise, multiplication (7.17) is just the elementwise formulation of (7.17) with $[A_l]_{ij} = a_{ij}^{(l)}$, that is, $\mathcal{A} \otimes \mathcal{B} = \psi(\psi^{-1}(\mathcal{A}) \otimes \psi^{-1}(\mathcal{B}))$. Then clearly ψ is an isomorphism from $S^{n \times n}[X]$ to $(S[X])^{n \times n}$ and so $(S[X])^{n \times n}$ is isomorphic to $S^{n \times n}[X]$. Moreover, this isomorphism also implies that $(S[X])^{n \times n}$ is an (idempotent) semiring if and only if $S^{n \times n}[X]$ is. \square

Because of Theorem 7.2.7 we may identify by both $S^{n \times n}[X] \cong (S[X])^{n \times n}$ the $n \times n$ polynomial matrix semiring in an indeterminate X over the semiring S .

In particular, $\mathbb{R}_{\max}^{n \times n}[X]$ and $\mathbb{Z}_{\max}^{n \times n}[X]$ are idempotent semirings, with addition and multiplication understood as matrix addition and multiplication over the semiring $\mathbb{R}_{\max}[X]$. As an example in $\mathbb{R}_{\max}^{2 \times 2}[X]$ we have

$$\begin{bmatrix} 2 & X \\ e \oplus 1X & X^2 \end{bmatrix} \oplus \begin{bmatrix} 3X & 1X \\ 3 & 1 \oplus 2X \end{bmatrix} = \begin{bmatrix} 2 \oplus 3X & 1X \\ 3 \oplus 1X & 1 \oplus 2X \oplus X^2 \end{bmatrix}$$

and

$$\begin{bmatrix} 2 & X \\ e \oplus 1X & X^2 \end{bmatrix} \otimes \begin{bmatrix} 3X & 1X \\ 3 & 1 \oplus 2X \end{bmatrix} = \begin{bmatrix} 5X & 3X \oplus 2X^2 \\ 3X \oplus 4X^2 & 1X \oplus 2X^2 \oplus 2X^3 \end{bmatrix}.$$

Analogous to a max-plus polynomial function associated to a max-plus polynomial, we associate a *matrix polynomial function* $A : \mathbb{R}_{\max} \rightarrow \mathbb{R}_{\max}^{n \times n}$ to each matrix polynomial $\mathcal{A} \in \mathbb{R}_{\max}^{n \times n}[X]$ by substituting an element $x \in \mathbb{R}_{\max}$ for the indeterminate X .

Theorem 7.2.8 *Let $(S^{n \times n}[X], \oplus, \otimes, \mathcal{E}, E)$ be the semiring of polynomial matrices over a commutative semiring S . Then for any $x \in S$ the valuation mapping $\varphi : \mathcal{A} \mapsto A(x)$ is a homomorphism from $S^{n \times n}[X]$ into $S^{n \times n}$.*

Proof: The proof is analogous to that of Theorem 7.2.2 by showing that $\varphi(\mathcal{A} \oplus \mathcal{B}) = \varphi(\mathcal{A}) \oplus \varphi(\mathcal{B})$ and $\varphi(\mathcal{A} \otimes \mathcal{B}) = \varphi(\mathcal{A}) \otimes \varphi(\mathcal{B})$ hold entrywise. Without loss of generality we assume that all polynomial entries have the same degree by taking any missing coefficients equal to ε . So let $\mathcal{A}_{ij} = \bigoplus_{l=0}^p a_{ij}^{(l)} X^l$ and $\mathcal{B}_{ij} = \bigoplus_{l=0}^p b_{ij}^{(l)} X^l$. Then for addition we have

$$\begin{aligned} \varphi(\mathcal{A}) \oplus \varphi(\mathcal{B}) &= A(x) \oplus B(x) \\ &= \left(\bigoplus_{i=0}^p A_i x^i \right) \oplus \left(\bigoplus_{j=0}^p B_j x^j \right) \\ &= A_0 \oplus A_1 x \oplus \dots \oplus A_p x^p \oplus B_0 \oplus B_1 x \oplus \dots \oplus B_p x^p \\ &= (A_0 \oplus B_0) \oplus (A_1 x \oplus B_1 x) \oplus \dots \oplus (A_p x^p \oplus B_p x^p) \quad (\text{by associativity}) \\ &= (A_0 \oplus B_0) \oplus (A_1 \oplus B_1)x \oplus \dots \oplus (A_p \oplus B_p)x^p \quad (\text{by distributivity}) \\ &= \bigoplus_{l=0}^p (A_l \oplus B_l) x^l \\ &= (A \oplus B)(x) \\ &= \varphi(\mathcal{A} \oplus \mathcal{B}). \end{aligned}$$

For multiplication we have

$$\begin{aligned} \varphi(\mathcal{A}) \otimes \varphi(\mathcal{B}) &= A(x) \otimes B(x) \\ &= \left(\bigoplus_{i=0}^p A_i x^i \right) \otimes \left(\bigoplus_{j=0}^p B_j x^j \right) \\ &\stackrel{\text{distr.}}{=} A_0 \left(\bigoplus_{j=0}^p B_j x^j \right) \oplus A_1 x \left(\bigoplus_{j=0}^p B_j x^j \right) \oplus \dots \oplus A_p x^p \left(\bigoplus_{j=0}^p B_j x^j \right) \\ &\stackrel{\text{comm.}}{=} A_0 \left(\bigoplus_{j=0}^p B_j x^j \right) \oplus A_1 \left(\bigoplus_{j=0}^p B_j x^{1+j} \right) \oplus \dots \oplus A_p \left(\bigoplus_{j=0}^p B_j x^{p+j} \right) \\ &= \bigoplus_{i=0}^p \left(A_i \otimes \left(\bigoplus_{j=0}^p B_j x^{i+j} \right) \right) \\ &= \bigoplus_{i=0}^p \bigoplus_{j=0}^p (A_i \otimes B_j) x^{i \otimes j} \\ &= \bigoplus_{l=0}^{p \otimes p} \bigoplus_{i \otimes j = l} (A_i \otimes B_j) x^l \\ &= (A \otimes B)(x) \\ &= \varphi(\mathcal{A} \otimes \mathcal{B}). \end{aligned}$$

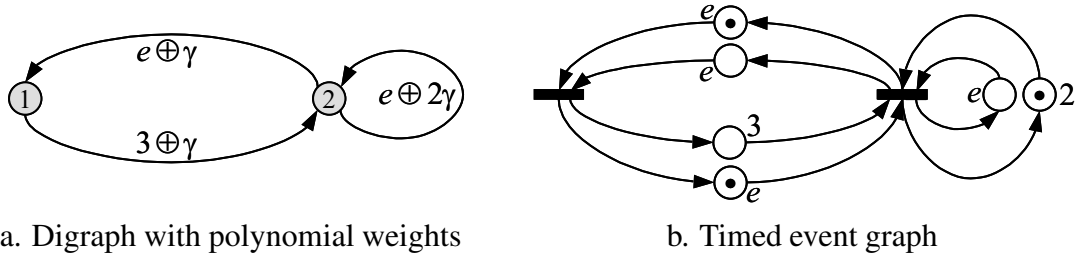


Figure 7.1 Graph representations of a max-plus polynomial matrix

Here the third equality follows from distributivity of multiplication over addition and in the fourth equality we used the scalar multiplication of a matrix and the multiplicative commutativity assumption of S . \square

Viewed as a matrix with polynomial entries the valuation homomorphism is consistent with the internal multiplication in $(S[X])^{n \times n}$. However, the evaluation in a polynomial with matrix coefficients requires scalar multiplication of the matrix coefficients. Hence, in the latter case we need to consider $S^{n \times n}$ as a semialgebra, with scalar multiplication as external product.

Theorem 7.2.8 is a generalization of Theorem 7.2.2, which corresponds to the special case that $n = 1$. Note that a matrix (semi)ring $S^{n \times n}$ is in general not (multiplicative) commutative, except for the scalar case $n = 1$. Hence, the condition of Theorem 7.2.2 is not satisfied for a polynomial semiring $S^{n \times n}[X]$ over a semiring $S^{n \times n}$ for $n > 1$. However, Theorem 7.2.8 shows that commutativity of the base semiring S is sufficient for the valuation mapping to be a homomorphism, as a consequence of mapping the indeterminate to a scalar.

A polynomial matrix $\mathcal{A} \in \mathbb{R}_{\max}^{n \times n}[X]$ is associated to a timed event graph $\mathcal{G}(\mathcal{A}) = (\mathcal{T}, \mathcal{P}, \mu, w)$, analogous to a precedence graph associated to a matrix $A \in \mathbb{R}_{\max}^{n \times n}$, cf. Section 7.2.5.

Definition 7.2.10 (Graph representation of a polynomial matrix) A polynomial matrix $\mathcal{A} \in \mathbb{R}_{\max}^{n \times n}[X]$ corresponds to the timed event graph $\mathcal{G}(\mathcal{A}) = (\mathcal{T}, \mathcal{P}, \mu, w)$ with transitions (nodes) $\mathcal{T} = \{1, \dots, n\}$ and a place (marked arc) $(j, i) \in \mathcal{P}$ with initial marking $\mu(j, i) = l$ and holding time $w(j, i) = [A_l]_{ij}$ for each $[A_l]_{ij} \neq \varepsilon$.

According to this definition each matrix coefficient A_l of a polynomial matrix \mathcal{A} defines a precedence graph $G(A_l)$ corresponding to a subgraph of $\mathcal{G}(\mathcal{A})$ where each place has l tokens. Of particular interest is the subgraph $G(A_0)$, which must be acyclic for a live timed event graph, cf. Section 6.4. If on the other hand we look at a polynomial matrix as a matrix of polynomials then each nonzero (finite) polynomial entry $[\mathcal{A}]_{ij} = [A_0]_{ij} \oplus [A_1]_{ij}X \oplus [A_2]_{ij}X^2 \oplus \dots \oplus [A_p]_{ij}X^p$ defines multiple places (or a multiarc) from node j to i corresponding to the polynomial support $\text{supp}([\mathcal{A}]_{ij})$. Hence, a polynomial arc weight translates into $|\text{supp}([\mathcal{A}]_{ij})|$ parallel marked arcs according to the interpretation of \oplus as synchronization mechanism, see Figure 7.1.

All definitions on matrices $A \in \mathbb{R}_{\max}^{n \times n}$ also hold for polynomial matrices $\mathcal{A} \in \mathbb{R}_{\max}^{n \times n}[X]$. Matrix powers \mathcal{A}^l , finite series $\bigoplus_{l=0}^m \mathcal{A}^l$, \mathcal{A}^+ , \mathcal{A}^* , etc. have the same meaning as before but are now interpreted in terms of timed event graphs. For example, $[\mathcal{A}^+]_{ij}$ is the longest path from transition j to i with respect to the holding times of the places. The other way around, precedence graphs of max-plus matrices $A \in \mathbb{R}_{\max}^{n \times n}$ may be viewed as timed event graphs where

all arcs have the same marking. Permutation matrices $P \in \mathbb{R}_{\max}^{n \times n}[X]$ are the same as in $\mathbb{R}_{\max}^{n \times n}$ (like the identity matrix), and $P^\top \mathcal{A} P$ is just a coordinate transformation of the indices of the matrix \mathcal{A} . A reducible polynomial matrix is defined analogous to Definition 7.2.6 as a polynomial matrix \mathcal{A} that can be written in lower block triangular form by an appropriate coordinate transformation, where now of course blocks are rectangular polynomial submatrices. In fact, (ir)reducibility is a combinatorial matrix property that only depends on the support of the matrix, $\text{supp}(\mathcal{A}) = \{(j, i) \mid [\mathcal{A}]_{ij} \neq \varepsilon\}$, that is, the pattern of nonzero entries. The support is preserved by the valuation homomorphism for finite values of the variable X . Hence, $\mathcal{A} \in \mathbb{R}_{\max}^{n \times n}[X]$ is (ir)reducible if and only if $A(e) \in \mathbb{R}_{\max}^{n \times n}$ is, or any $A(x)$ with fixed $x \in \mathbb{R}_{\max} \setminus \{\varepsilon\}$ for that matter, where $A(x)$ is the valuation homomorphism of \mathcal{A} in x . In particular, $\mathcal{G}(\mathcal{A})$ is strongly connected if and only if $A(e)$ is irreducible. Indeed, for fixed $x = e$ the polynomial matrix function reduces to a max-plus matrix, where the associated precedence graph is obtained from the timed event graph by replacing the multiple places from a transition j to i by a single arc from node j to i with weight $a_{ij} = \max_{l=0, \dots, p} [A_l]_{ij}$. Note that strongly connectedness is invariant to (the weights of) parallel places. An algebraic characterization of an irreducible square polynomial matrix $\mathcal{A} \in \mathbb{R}_{\max}^{n \times n}[X]$ is that for all i, j there exists an integer $m \in \mathbb{N}$, such that $[\mathcal{A}^m]_{ij} \neq \varepsilon$, or such that $[A^m(e)]_{ij} \neq \varepsilon$. This corresponds to strongly connectedness of the associated timed event graph, i.e., a path exists between any two transitions.

7.2.7 Partially Ordered Semirings

Definition 7.2.11 (Partial order, total order) A binary relation \leq on a set $S \neq \emptyset$ is called a partial order on S if the following axioms are satisfied for all $a, b, c \in S$:

- (i) Reflexivity: $a \leq a$.
- (ii) Antisymmetry: if $a \leq b$ and $b \leq a$ then $a = b$.
- (iii) Transitivity: if $a \leq b$ and $b \leq c$ then $a \leq c$.

A partial order is called a total order if it additionally satisfies

- Comparability: for all $a, b \in S$, either $a \leq b$ or $b \leq a$.

If \leq is a partial order on S then (S, \leq) is called a partially ordered set. Likewise, if \leq is a total order on S then (S, \leq) is called a totally ordered set.

Given a partially ordered set (S, \leq) , we define $a \geq b$ as the equivalence of $b \leq a$. If $a \leq b$ and $a \neq b$ we also write $a < b$, and similarly $a > b \Leftrightarrow (b \leq a \wedge a \neq b)$.

Definition 7.2.12 (Partially ordered semiring) Let $(S, \oplus, \otimes, \varepsilon, e)$ be a semiring and (S, \leq) a partially ordered set. Then $(S, \oplus, \otimes, \leq)$ is called a partially ordered semiring if the following monotony laws are satisfied for all $a, b, c \in S$:

- (i) Additive monotony: if $a \leq b$ then $a \oplus c \leq b \oplus c$.
- (ii) Multiplicative monotony: if $a \leq b$ and $\varepsilon \leq c$ then $a \otimes c \leq b \otimes c$ and $c \otimes a \leq c \otimes b$.

If moreover \leq is a total order on S then $(S, \oplus, \otimes, \leq)$ is called a totally ordered semiring.

Thus, in a partial ordered semiring the order is preserved under addition and multiplication. The nonnegativity condition $c \geq \varepsilon$ in the multiplicative monotony law of Definition 7.2.12 is redundant if ε is a least or *bottom element* of S , i.e., an element that is smaller than any other element of S . In the $(\max, +)$ -semiring the zero is $\varepsilon = -\infty$, which is obviously a least element with respect to the natural ordering of an idempotent semiring.

Theorem 7.2.9 (Natural ordering) *An idempotent semiring (S, \oplus, \otimes) is naturally partially ordered by*

$$a \leq b \Leftrightarrow a \oplus b = b. \quad (7.18)$$

Proof: First, we prove that (7.18) defines a partial order. By idempotency $a \oplus a = a$ for all $a \in S$ and hence $a \leq a$ (reflexivity). If $a \oplus b = b$ and $b \oplus a = a$ then by commutativity of addition $b = a \oplus b = b \oplus a = a$ (antisymmetry). Finally, if $a \oplus b = b$ and $b \oplus c = c$ then by associativity $a \oplus c = a \oplus (b \oplus c) = (a \oplus b) \oplus c = b \oplus c = c$ (transitivity).

We now prove the monotony laws of addition and multiplication. If $a \oplus b = b$ then for all $c \in S$ we have $(a \oplus c) \oplus (b \oplus c) = (a \oplus b) \oplus (c \oplus c) = b \oplus c$, where we used commutativity, associativity and idempotency of addition. The multiplicative monotony law follows from distributivity of multiplication over addition: if $a \oplus b = b$ then $(a \otimes c) \oplus (b \otimes c) = (a \oplus b) \otimes c = b \otimes c$ for all $c \in S$, including $c = \varepsilon$, which is well-defined since ε is absorbing. Analogously, $(c \otimes a) \oplus (c \otimes b) = c \otimes (a \oplus b) = c \otimes b$. \square

By definition a zero element in a semiring S satisfies $\varepsilon \oplus a = a$ for all $a \in S$, and therefore $\varepsilon \leq a$ for all $a \in S$ with the natural order (7.18). Thus, we have the following corollary.

Proposition 7.2.8 (Nonnegativity) *Let (S, \oplus, \otimes) be an idempotent semiring with the natural partial order \leq defined by (7.18). Then all elements $a \in S$ are nonnegative, i.e., $\varepsilon \leq a$ for all $a \in S$.*

In lattice theory the zero element ε is called a *bottom element* of S [11]. In particular, matrices over the max-plus algebra are nonnegative by definition. As a consequence, the spectral analysis of matrices in $\mathbb{R}_{\max}^{n \times n}$ resembles the classical theory of nonnegative matrices $A \in \mathbb{R}_+^{n \times n}$, as we will see in Section 7.4.

By Theorem 7.2.9 idempotent semirings have a natural order relation, which is preserved under the addition and multiplication operations of the semiring. In particular, on the semirings encountered so far we have the following natural orders.

- (i) $(\mathbb{R}_{\max}, \leq)$ is a *totally ordered semifield*, where the total order \leq is consistent with the natural order of the real numbers (\mathbb{R}, \leq) .
- (ii) $(\mathbb{R}_{\max}^{n \times n}, \leq)$ is a partially ordered semiring, where $A \leq B$ is defined elementwise as $a_{ij} \leq b_{ij}$ for all $1 \leq i, j \leq n$ with the (scalar) natural order of $(\mathbb{R}_{\max}, \leq)$. We write $A < B$ if $a_{ij} < b_{ij}$ for all $1 \leq i, j \leq n$. This order is not total as is easily seen by a counterexample. Let

$$A = \begin{bmatrix} 1 & 1 \\ \varepsilon & 1 \end{bmatrix}, \quad B = \begin{bmatrix} 1 & 2 \\ \varepsilon & 1 \end{bmatrix}, \quad C = \begin{bmatrix} 1 & 1 \\ \varepsilon & 2 \end{bmatrix}.$$

Then we have $A \leq B$ and $A \leq C$, but $B \not\leq C$ and $C \not\leq B$.

- (iii) $(\mathbb{R}_{\max}[X], \leq)$ is a partially ordered semiring, where $\bigoplus_{l=0}^p a_l X^l \leq \bigoplus_{l=0}^q b_l X^l$ is defined elementwise by $a_l \leq b_l$ for all $0 \leq l \leq p \oplus q$. If the polynomials do not have the same support then the nonexistent coefficients are understood to be zero (ε). For example, $2 \oplus 2X \oplus 2X^3 \leq 2 \oplus 2X \oplus 1X^2 \oplus 2X^3$, but $2 \not\leq 2X$ and $2X \not\leq 2$, so \leq is a partial order but not a total order.
- (iv) $(\mathbb{R}_{\max}^{n \times n}[X], \leq)$ is a partially ordered semiring, where $\bigoplus_{l=0}^p A_l X^l \leq \bigoplus_{l=0}^q B_l X^l$ is defined elementwise as $[A_l]_{ij} \leq [B_l]_{ij}$ for all $1 \leq i, j \leq n$ and $0 \leq l \leq p \oplus q$. For example, let

$$\mathcal{A} = \begin{bmatrix} X^2 & X \\ \varepsilon & 3X \oplus 2X^2 \end{bmatrix}, \quad \mathcal{B} = \begin{bmatrix} X^2 & 1X \\ \varepsilon & 3X \oplus 2X^2 \end{bmatrix}, \quad \mathcal{C} = \begin{bmatrix} X^2 & X \\ e & 3X \oplus 2X^2 \end{bmatrix}.$$

Then $\mathcal{A} \leq \mathcal{B}$ and $\mathcal{A} \leq \mathcal{C}$, but $\mathcal{B} \not\leq \mathcal{C}$ and $\mathcal{C} \not\leq \mathcal{B}$.

A partially ordered set (S, \leq) is called a *sup-semilattice* (or *join-semilattice*) if the supremum (or least upper bound) $\sup(a, b)$ exists for all $a, b \in S$. Hence, each subsemiring S of \mathbb{R}_{\max} is a sup-semilattice, since $a \oplus b = \max(a, b) = \sup(a, b)$ exists for each $a, b \in S \subseteq \mathbb{R}_{\max}$ by Definition 7.2.4 of a subsemiring.

7.3 Max-Plus Semimodules

7.3.1 Semimodules over the $(\max, +)$ -Semiring

The analogue of a vector space over a field or a module over a ring in conventional algebra [127] is a *semimodule* over a semiring. The elements of a semimodule are vectors with elements in a semiring, where addition is defined componentwise and where vectors can be multiplied by an element of the semiring, see e.g. Dudnikov & Samborskiĭ [59] and Golan [73].

Definition 7.3.1 (Semimodule) A (left) semimodule (V, \oplus) over the semiring $(S, \oplus, \otimes, \varepsilon, e)$ is a set V equipped with an internal addition \oplus , and an external multiplication \otimes defined on $S \times V$ to V , satisfying the following axioms:

- (i) (V, \oplus) is a commutative monoid, where the zero is denoted as ε_V .
- (ii) The external multiplication satisfies

$$\forall a, b \in S, \forall x \in V : (a \otimes b) \otimes x = a \otimes (b \otimes x) \quad \text{and} \quad e \otimes x = x.$$

- (iii) The external multiplication is distributive over addition:

$$\forall a, b \in S, \forall x, y \in V : a \otimes (x \oplus y) = a \otimes x \oplus a \otimes y \quad \text{and} \quad (a \oplus b) \otimes x = a \otimes x \oplus b \otimes x.$$

- (iv) The zero ε_V is absorbing:

$$\forall a \in S, \forall x \in V : a \otimes \varepsilon_V = \varepsilon \otimes x = \varepsilon_V.$$

A right-semimodule is defined similarly for external multiplication from the right, i.e., $\otimes : V \times S \rightarrow V$. A semimodule (V, \oplus) over an idempotent semiring $(S, \oplus, \otimes, \varepsilon, e)$ is an *idempotent semimodule*, since $x \oplus x = e \otimes x \oplus e \otimes x = (e \oplus e) \otimes x = e \otimes x = x$ for all $x \in V$,

cf. Proposition 7.2.4. An idempotent semimodule over an idempotent semiring is also called a *moduloid* [11].

An important class of semimodules is the set $S^n = S \times \cdots \times S$ of vectors with entries in a semiring S and pointwise addition and scalar multiplication.

Theorem 7.3.1 *Let $(S, \oplus, \otimes, \varepsilon, e)$ be an (idempotent) semiring and $n \in \mathbb{N}$. Then (S^n, \oplus) of n -dimensional vectors over (S, \oplus, \otimes) is an (idempotent) (left) semimodule for componentwise addition $[x \oplus y]_i = x_i \oplus y_i$ and external (left) multiplication $[c \otimes x]_i = c \otimes x_i$ for all $x, y \in S^n$ and $c \in S$. The zero vector is $\varepsilon = (\varepsilon, \dots, \varepsilon)^\top \in S^n$.*

Proof: The semiring properties are inherited by addition and scalar multiplication on the semimodule as they are both defined componentwise. Hence, if (S, \oplus) is associative, commutative, and/or idempotent then so is (S^n, \oplus) , and if ε is an absorbing zero of (S, \oplus, \otimes) then the vector with each component equal to ε is an absorbing zero of (S^n, \oplus, \otimes) . Likewise, the 2nd semimodule axiom directly follows from associativity and the unit e of (S, \otimes) , and distributivity of scalar multiplication over addition is a consequence of distributivity in (S, \oplus, \otimes) . \square

A right-semimodule (S^n, \oplus) over (S, \oplus, \otimes) is defined analogously by componentwise right-sided scalar multiplication $[x \otimes c]_i = x_i \otimes c$. If S is commutative then these left- and right-semimodules are equivalent and we just say that (S^n, \oplus) is a semimodule over (S, \oplus, \otimes) .

In particular, \mathbb{R}_{\max}^n is an idempotent semimodule (moduloid) of vectors over \mathbb{R}_{\max} equipped with componentwise addition

$$\begin{bmatrix} x_1 \\ \vdots \\ x_n \end{bmatrix} \oplus \begin{bmatrix} y_1 \\ \vdots \\ y_n \end{bmatrix} \doteq \begin{bmatrix} x_1 \oplus y_1 \\ \vdots \\ x_n \oplus y_n \end{bmatrix} = \begin{bmatrix} \max(x_1, y_1) \\ \vdots \\ \max(x_n, y_n) \end{bmatrix}$$

and two-sided scalar multiplication

$$a \otimes \begin{bmatrix} x_1 \\ \vdots \\ x_n \end{bmatrix} \doteq \begin{bmatrix} a \otimes x_1 \\ \vdots \\ a \otimes x_n \end{bmatrix} = \begin{bmatrix} a + x_1 \\ \vdots \\ a + x_n \end{bmatrix} = \begin{bmatrix} x_1 \otimes a \\ \vdots \\ x_n \otimes a \end{bmatrix} \doteq \begin{bmatrix} x_1 \\ \vdots \\ x_n \end{bmatrix} \otimes a,$$

with $x, y \in \mathbb{R}_{\max}^n$ and $a \in \mathbb{R}_{\max}$.

Definition 7.3.2 (Subsemimodule) *Let (V, \oplus) be a semimodule over a semiring (S, \oplus, \otimes) . A nonempty subset $W \subseteq V$ is a subsemimodule of (V, \oplus, ε) if it is closed under addition and external multiplication: $ax \oplus by \in W$ for all $x, y \in W$ and $a, b \in S$.*

Let ε_V be the zero of a semimodule V over a semiring $(S, \oplus, \otimes, \varepsilon, e)$. Then $\varepsilon_V \in W$ for any subsemimodule W of V , since $W \neq \emptyset$ and if $x \in W$ then also $\varepsilon \otimes x = \varepsilon_V \in W$ by definition of a subsemimodule. Hence, a subsemimodule is itself again a semimodule.

7.3.2 Linear and Weak Independence

In this section we consider semimodules of vectors over \mathbb{R}_{\max} . We will show that the usual notion of linear independence of a set of vectors is no longer satisfactory in \mathbb{R}_{\max}^n and introduce

the concept of *weak independence* as proposed by Wagner [216], which allows an intrinsic notion of dimension and basis of semimodules.

Let $X = \{x_i\}_{i \in I}$ be a family of vectors of \mathbb{R}_{\max}^n . A *linear combination* of elements of X is a finite sum $\bigoplus_{i \in I} c_i x_i$, where $\{c_i\}_{i \in I}$ is a family of elements of \mathbb{R}_{\max} with *finite support*, i.e., the set $\text{supp}(I) = \{i \in I \mid c_i \neq \varepsilon\}$ is finite. The elements c_i are called the *coefficients* of the linear combination. The set of all linear combinations of vectors $\{x_i\}_{i \in I} = X \subset \mathbb{R}_{\max}^n$ is a subsemimodule of \mathbb{R}_{\max}^n called the *span* of X and denoted as $\text{span}(X)$. If $M = \text{span}(X)$ we say that X is a *generating family* or *spanning set* of the semimodule M . A semimodule $M \subset \mathbb{R}_{\max}^n$ is *finitely generated* if it has a finite generating family $X = \{x_1, \dots, x_m\} \subset M$. In this case, $M = \text{span}(x_1, \dots, x_m)$ with

$$\text{span}(x_1, \dots, x_m) \doteq \left\{ \bigoplus_{i=1}^m c_i x_i \mid c_1, \dots, c_m \in \mathbb{R}_{\max} \right\}.$$

A family $\{x_i\}_{i \in I}$ of \mathbb{R}_{\max}^n is *linearly independent* if for all families $\{a_i\}_{i \in I}$ and $\{b_i\}_{i \in I}$ in \mathbb{R}_{\max} with finite support

$$\bigoplus_{i \in I} a_i x_i = \bigoplus_{i \in I} b_i x_i \quad \text{implies} \quad a_i = b_i \text{ for all } i \in I.$$

A linearly independent generating family $\{x_i\}_{i \in I}$ is a *basis* and a semimodule that admits a basis is called a *free semimodule*. The *dimension* of a free semimodule is the cardinality of its basis, with the convention that if the basis is not finite then the dimension is infinite. By definition, each vector x in a free semimodule M with basis $\{x_i\}_{i \in I}$ can be written uniquely as $x = \bigoplus_{i \in I} c_i x_i$ for some family $\{c_i\}_{i \in I}$ of \mathbb{R}_{\max} with finite support.

For any $n \in \mathbb{N}$ the semimodule \mathbb{R}_{\max}^n is a finitely-generated free semimodule with dimension n . A basis is given by the n unit vectors $\{e_1, \dots, e_n\}$, where the j th unit vector is defined as $e_j = (\delta_{1j}, \dots, \delta_{nj})^\top$ with δ_{ij} the *Kronecker delta* translated to max-plus algebra:

$$\delta_{ij} = \begin{cases} e & \text{if } i = j \\ \varepsilon & \text{if } i \neq j. \end{cases}$$

For example, any $x \in \mathbb{R}_{\max}^4$ can be written uniquely as

$$x = c_1 \begin{bmatrix} e \\ \varepsilon \\ \varepsilon \\ \varepsilon \end{bmatrix} \oplus c_2 \begin{bmatrix} \varepsilon \\ e \\ \varepsilon \\ \varepsilon \end{bmatrix} \oplus c_3 \begin{bmatrix} \varepsilon \\ \varepsilon \\ e \\ \varepsilon \end{bmatrix} \oplus c_4 \begin{bmatrix} \varepsilon \\ \varepsilon \\ \varepsilon \\ e \end{bmatrix}.$$

with $c_i \in \mathbb{R}_{\max}$, $1 \leq i \leq 4$. A finitely-generated free semimodule is also called a finite-dimensional free semimodule or finite free semimodule.

However, in a semimodule this notion of linear independence is too strong. For instance, consider the semimodule $M = \text{span}(x_1, x_2) \subset \mathbb{R}_{\max}^2$ with $x_1 = (1, e)^\top$ and $x_2 = (e, \varepsilon)^\top$. Then $\{x_1, x_2\}$ is a minimal finite generating family of M . For example, the vector $(3, e)^\top$ is uniquely determined by the linear combination $(3, e)^\top = (1, e)^\top \oplus 3(e, \varepsilon)^\top$. But $\{x_1, x_2\}$ is not a basis of M , since e.g. $x_1 \oplus c_2 x_2 = x_1$ for all $c_2 \in [\varepsilon, 1]$.

Wagner [216] introduced an alternative definition of *weak independence* as follows.

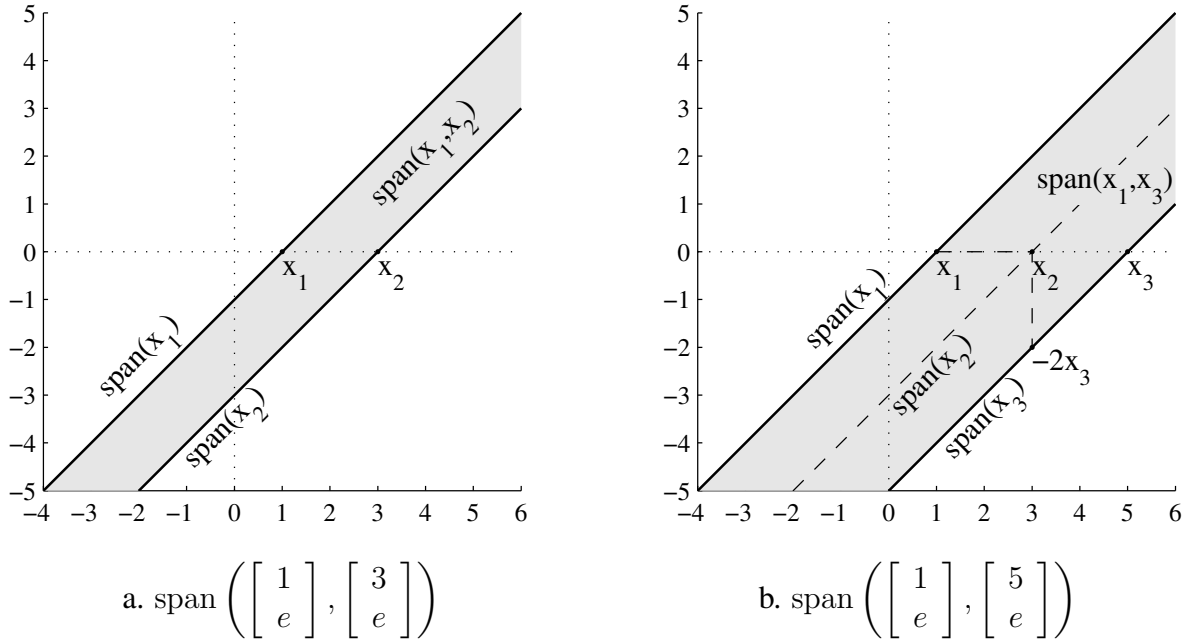


Figure 7.2 Semimodules in \mathbb{R}_{\max}^2 spanned by two weakly-independent finite vectors

Definition 7.3.3 (Weak independence, weak dependence) A vector $y \in \mathbb{R}_{\max}^n$ is weakly dependent on a set $X = \{x_i\}_{i \in I}$ with $x_i \in \mathbb{R}_{\max}^n$ if y can be written as a linear combination

$$y = \bigoplus_{i \in I} a_i x_i$$

for some coefficients $a_i \in \mathbb{R}_{\max}$, $i \in I$. Otherwise, y is weakly independent on X . A nonempty set $X = \{x_i\}_{i \in I}$ is weakly independent if each $x_j \in X$ is weakly independent on $X \setminus \{x_j\}$, and X is weakly dependent otherwise.

In conventional vector spaces weak independence is equivalent to linear independence, but in semimodules over \mathbb{R}_{\max} (or over any other proper semiring) weak independence does not imply linear independence.

A weakly-independent generating family is a *weak basis*. Wagner [216] proved that each weak basis of a semimodule has the same cardinality, which therefore justifies the definition of *weak dimension* of a finitely-generated semimodule as the cardinality of its weak basis. The following theorem was proved by Wagner [216] and states that each finitely-generated semimodule $M \subset \mathbb{R}_{\max}^n$ has a weak basis.

Theorem 7.3.2 Let $M \subset \mathbb{R}_{\max}^n$ be a finitely-generated semimodule. If x_1, \dots, x_m are weakly independent vectors of M and $M = \text{span}(x_1, \dots, x_m)$, then M has weak dimension m and $\{x_1, \dots, x_m\}$ is a weak basis of M .

A weak basis of a semimodule M is thus both a *minimal spanning set* — a smallest set of vectors that still spans the semimodule — and a *maximal weakly-independent set* — a largest set of vectors of M that still is weakly independent.

Example 7.2 Consider the semimodule $M_1 = \text{span}(x_1, x_2) \subset \mathbb{R}_{\max}^2$ with $x_1 = (1, e)^\top$ and

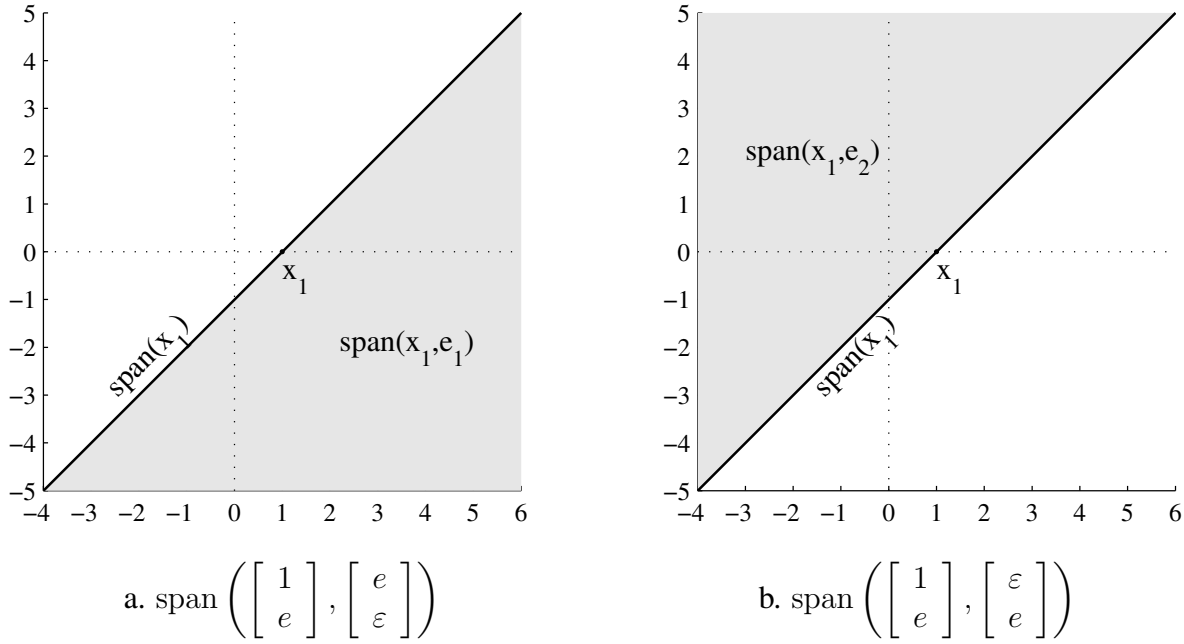


Figure 7.3 Semimodules in \mathbb{R}_{\max}^2 spanned by a finite vector and a unit vector

$x_2 = (3, e)^\top$. Clearly, x_1 and x_2 are weakly independent. Hence, $\{x_1, x_2\}$ is a weak basis of M and its weak dimension is 2. Figure 7.2.a shows the generated semimodule. Each vector $x_i \in \mathbb{R}_{\max}^2$ generates a one-dimensional line through x_i with slope 1, and two weakly-independent vectors span a 2-dimensional strip bounded by the lines generated by x_1 and x_2 , respectively.

Let $x_3 = (5, e)^\top$ and consider $M_2 = \text{span}(x_1, x_2, x_3) \subset \mathbb{R}_{\max}^2$ with x_1 and x_2 as above. Now, $x_2 = x_1 \oplus -2x_3$, whence x_2 is weakly dependent on $\{x_1, x_3\}$, see Figure 7.2.b. Hence, $\{x_1, x_3\}$ is a weak basis of M_2 , the weak dimension is again 2, and $M_2 = \text{span}(x_1, x_3)$.

Now consider the semimodule $M_3 = \text{span}(x_1, e_1) \subset \mathbb{R}_{\max}^2$ with $x_1 = (1, e)^\top$ as before and the unit vector $e_1 = (e, \varepsilon)^\top$. Clearly, $\{x_1, e_1\}$ is weakly independent and by definition spans M_3 . Hence, $\{x_1, e_1\}$ is a weak basis of M_3 and its weak dimension is 2. Figure 7.3.a shows the semimodule $\text{span}(x_1, e_1)$. It is the halfspace bounded above by the line through x_1 with slope 1, that is, the boundary corresponding to the one-dimensional semimodule $\text{span}(x_1)$. The difference with the former examples is that the second basis vector has a zero entry, and therefore has no full support, by which the semimodule is only bounded at one side.

The semimodule M_4 generated by x_1 and the other unit vector $e_2 = (\varepsilon, e)^\top$ is the 2-dimensional semimodule $\text{span}(x_1, e_2)$ bounded below by $\text{span}(x_1)$, see Figure 7.3.b. The remaining case is the free semimodule $M_5 = \text{span}(e_1, e_2) = \mathbb{R}_{\max}^2$ spanned by the two unit vectors. \square

Example 7.2 gave a complete description of the geometry of subsemimodules of \mathbb{R}_{\max}^2 , which can take four different forms: (i) a line with slope 1 corresponding to a one-dimensional subsemimodule; (ii) a two-dimensional strip bounded by two lines corresponding to two finite weakly-independent vectors; (iii) a two-dimensional halfspace bounded by one line corresponding to a finite vector and a (partially finite) unit vector; and (iv) the two-dimensional free semimodule spanned by two weakly-independent unit vectors. Mairesse [130] gives a geometric description of subsemimodules in \mathbb{R}_{\max}^3 using an orthogonal projection to the hyperspace orthogonal to the vector $(1, 1, 1)^\top$.

7.3.3 Linear Mappings

Any max-plus matrix $A \in \mathbb{R}_{\max}^{m \times n}$ can be identified with a *linear map* $A : \mathbb{R}_{\max}^n \rightarrow \mathbb{R}_{\max}^m$ defined by $A : x \mapsto Ax$. These linear maps will be the main topic in the remainder of this thesis.

Definition 7.3.4 (Linear map) *Let V, W be two idempotent semimodules over \mathbb{R}_{\max} . Then a mapping $f : V \rightarrow W$ is called a linear map from V to W if for all $x, y \in V$ and for all $c \in \mathbb{R}_{\max}$, we have*

- Additivity: $f(x \oplus y) = f(x) \oplus f(y)$,
- Homogeneity: $f(cx) = cf(x)$.

Because of homogeneity a linear map f maps the origin to the origin: with $c = \varepsilon$ we have for all $x \in V$: $f(\varepsilon \otimes x) = f(\varepsilon_n) = \varepsilon \otimes f(x) = \varepsilon_m$. If V and W are finitely-generated free semimodules over \mathbb{R}_{\max} with dimension n and m , i.e., $V = \mathbb{R}_{\max}^n$ and $W = \mathbb{R}_{\max}^m$, then the linear map $f : V \rightarrow W$ can be represented by a matrix $A \in \mathbb{R}_{\max}^{m \times n}$ as $f(x) = Ax$. Conversely, any matrix $A \in \mathbb{R}_{\max}^{m \times n}$ can be identified with a linear map $A : \mathbb{R}_{\max}^n \rightarrow \mathbb{R}_{\max}^m$ defined by $A : x \mapsto Ax$. Note that $A(x \oplus y) = Ax \oplus Ay$ and $A(cx) = cAx$ for all $x, y \in \mathbb{R}_{\max}^n$ and $c \in \mathbb{R}_{\max}$.

The *image* of a matrix (map) $A : \mathbb{R}_{\max}^n \rightarrow \mathbb{R}_{\max}^m$ is defined as

$$\text{im}(A) = \{Ax \mid x \in \mathbb{R}_{\max}^n\} \subseteq \mathbb{R}_{\max}^m.$$

Hence, the image of a matrix map is the subsemimodule generated by the columns of A , also called the *column space* or *range* of A . Indeed, we may write $Ax = \bigoplus_{i=1}^n [A]_{\cdot i} x^{(i)}$ where $[A]_{\cdot i}$ is the i th column of A and $x = (x^{(1)}, \dots, x^{(n)})^\top$. The number of weakly-independent columns of A is called the *weak column rank* of A and thus $\text{im}(A)$ is a finitely-generated semimodule with weak dimension equal to the weak column rank.

The image of a given matrix $A \in \mathbb{R}_{\max}^{m \times n}$ consists of m -dimensional vectors and so $\text{im}(A)$ is a subsemimodule of \mathbb{R}_{\max}^m . However, the weak dimension of $\text{im}(A)$ may exceed m if $n > m \geq 3$, which is distinct from conventional linear algebra. In general, there are max-plus semimodules $V \subset \mathbb{R}_{\max}^m$ of arbitrary large weak dimension as a result of the following theorem. For a proof see Cuninghame-Green [40, Theorem 16.4] or Cuninghame-Green & Butkovič [41].

Theorem 7.3.3 (Cuninghame-Green [40]) *Let $m \geq 3$. Then for any $n \in \mathbb{N}$ there exist n finite (weakly) independent vectors $v_1, \dots, v_n \in \mathbb{R}_{\max}^m$.*

In their proof of this theorem Cuninghame-Green & Butkovič [41] show that the vectors $v_i = (e, c_i, c_i^{-1})^\top = (e, c_i, -c_i)^\top \in \mathbb{R}_{\max}^3$ with distinct $c_i \in \mathbb{R}$, $i = 1, \dots, n$, are (weakly) independent. In particular, we may take $c_i = i$ for $i \in \mathbb{N}$. Then for all $n \in \mathbb{N}$ the max-plus matrix $A \in \mathbb{R}_{\max}^{3 \times n}$ defined as

$$A = \begin{bmatrix} e & e & \cdots & e \\ e & 1 & \cdots & n-1 \\ e & -1 & \cdots & -(n-1) \end{bmatrix},$$

has weak column rank n . This generalizes to matrices with row dimension $m \geq 3$, by simply adding rows with value e (like the first row above). The above also implies that the weak

column rank of a max-plus matrix may differ from its weak row rank — the weak dimension of the semimodule generated by the (independent) rows of A — including square matrices.

The *kernel* of a matrix $A \in \mathbb{R}_{\max}^{m \times n}$ may be defined as $\ker(A) = \{x \in \mathbb{R}_{\max}^n \mid Ax = \varepsilon\} \subseteq \mathbb{R}_{\max}^n$, see Golan [73]. However, this generally gives a trivial kernel: if A has no zero columns then $\ker(A) = \{\varepsilon\}$. Cohen *et al.* [33] give an alternative definition of the kernel, see also Cohen *et al.* [34]. Nevertheless, the dimension theory of max-plus matrices is still an open research topic and far from the elegant fundamental dimension theorem of conventional linear algebra [195].

In the next section we will consider invariant subsemimodules of square matrices $A \in \mathbb{R}_{\max}^{n \times n}$, that is, vectors $v \in \text{im}(A)$ satisfying $Av = v$ or more generally vectors $v \in \text{im}(A)$ satisfying $A \otimes v = \lambda \otimes v$ for some $\lambda \in \mathbb{R}_{\max}$. Finding all such vectors is the *max-plus eigenproblem* which is well-understood and considered in detail in the next section.

7.4 Max-Plus (Generalized) Eigenproblems

7.4.1 Introduction

The *eigenproblem* associated to a square matrix $A \in \mathbb{R}_{\max}^{n \times n}$ is the problem of finding a scalar $\lambda \in \mathbb{R}_{\max}$ and a nonzero vector $v \in \mathbb{R}_{\max}^n \setminus \{\varepsilon\}$, such that

$$A \otimes v = \lambda \otimes v. \quad (7.19)$$

If a solution (λ, v) exists then $\lambda = \lambda(A)$ is called an *eigenvalue*, v is a (right) *eigenvector* of A associated to the eigenvalue λ , and (λ, v) is an *eigenpair* of A . The set of all eigenvalues is the *spectrum* of A , denoted as $\text{spec}(A) = \{\lambda \in \mathbb{R}_{\max} \mid \exists v \neq \varepsilon : Av = \lambda v\}$. The *eigenstructure* of a square matrix is the spectrum and the associated eigenvectors.

The case that $\lambda = \varepsilon$ is an eigenvalue of a matrix $A \in \mathbb{R}_{\max}^{n \times n}$ is the least interesting and is dealt with in the following lemma.

Lemma 7.4.1 *A max-plus matrix $A \in \mathbb{R}_{\max}^{n \times n}$ has a zero eigenvalue $\lambda = \varepsilon$ if and only if A has a zero column.*

Proof: If the i th column of A is zero, $[A]_{\cdot i} = \varepsilon$, then $[A]_{\cdot i} e_i = \varepsilon$, where $e_i \in \mathbb{R}_{\max}^n$ is the i th unit vector. Thus, $\lambda = \varepsilon$ is an eigenvalue of A with eigenvector $e_i \neq \varepsilon$. Conversely, suppose $\lambda = \varepsilon$ is an eigenvalue of A with associated eigenvector $v \neq \varepsilon$. Then there is an entry $v_i > \varepsilon$ and because v must satisfy $Av = \varepsilon$ it follows that $[A]_{\cdot i} = \varepsilon$. \square

In the sequel assume that $\lambda > \varepsilon$. Then the inverse λ^{-1} exists since \mathbb{R}_{\max} is a semifield, and we may multiply both sides of (7.19) by λ^{-1} to obtain the reformulation $\lambda^{-1} \otimes A \otimes v = v$. Using the polynomial matrix $\mathcal{A} = AX \in \mathbb{R}_{\max}^{n \times n}[X]$ evaluated at $x = \lambda^{-1}$, the eigenproblem can be rewritten as the fixed-point problem $A(\lambda^{-1}) \otimes v = v$. This motivates the following definition of the *generalized eigenproblem* of square max-plus polynomial matrices $\mathcal{A} = \bigoplus_{l=0}^p A_l X^l \in \mathbb{R}_{\max}^{n \times n}[X]$: find a nonzero scalar $\lambda \in \mathbb{R}_{\max} \setminus \{\varepsilon\}$ and a nonzero vector $v \in \mathbb{R}_{\max}^n \setminus \{\varepsilon\}$, such that

$$A(\lambda^{-1}) \otimes v = v. \quad (7.20)$$

Clearly, for $\mathcal{A} = AX$ we retain the original eigenproblem (7.19) with the extra condition $\lambda > \varepsilon$. Another way to interpret (7.20) is that (e, v) is an eigenpair of $A(\lambda^{-1})$. For $\mathcal{A} = AX$ this interpretation reads $(A\lambda^{-1})v = \lambda^{-1}Av = \lambda^{-1}\lambda v = ev$. In the forthcoming, we will consider the generalized eigenproblem for square max-plus polynomial matrices, which embeds the eigenproblem of square matrices as a special case.

In max-plus algebra any (polynomial) matrix is nonnegative, cf. Section 7.2.7. As a result, many concepts from the Perron-Frobenius theory of nonnegative matrices [14, 17] also apply to matrices in max-plus algebra, see e.g. Cuninghame-Green [40], Baccelli *et al.* [11] and Bapat [13]. The max-plus (generalized) eigenproblem is fundamental to the max-plus linear system theory to be developed in Chapter 8. Therefore, this section gives an in-depth account of the (generalized) eigenproblem, which cumulates in the celebrated *policy iteration* algorithm of Cochet-Terrasson *et al.* [31] that solves max-plus generalized eigenproblems in ‘no time’ even for large-scale matrices.

7.4.2 Eigenstructure of Irreducible Matrices

We start this section with a fundamental theorem that states that an irreducible max-plus polynomial matrices has a unique eigenvalue which has a nice interpretation in terms of the cycle time of the associated timed event graph. An alternative proof is given in Baccelli *et al.* [11, Theorem 3.28].

Theorem 7.4.1 (Generalized eigenvalue) *Let $\mathcal{A} = \bigoplus_{l=0}^p A_l X^l \in \mathbb{R}_{\max}^{n \times n}[X]$ be an irreducible polynomial matrix with acyclic $G(A_0)$. Then \mathcal{A} has a unique generalized eigenvalue $\lambda > \varepsilon$ and finite eigenvectors $v > \varepsilon$ such that $A(\lambda^{-1}) \otimes v = v$, and λ is equal to the maximum cycle mean of the associated timed event graph $\mathcal{G}(\mathcal{A})$,*

$$\eta = \max_{\xi \in C} \frac{w(\xi)}{\mu(\xi)}, \quad (7.21)$$

where C is the set of all elementary circuits in $\mathcal{G}(\mathcal{A})$, $w(\xi)$ is the weight of circuit ξ , and $\mu(\xi)$ is the number of tokens in circuit ξ .

Proof: The irreducibility of \mathcal{A} implies that $\mathcal{G}(\mathcal{A})$ is strongly connected and so by definition contains circuits, and the acyclic assumption on $G(A_0)$ implies that each circuit in $\mathcal{G}(\mathcal{A})$ contains at least one token, $\mu(\xi) \geq 1$ for all $\xi \in C$. Hence, the maximum cycle mean η defined in (7.21) is well-defined and finite. We next prove that this means that also any eigenvector $v \in \mathbb{R}_{\max}^n$ is finite. Assume v is only partially finite and let $v = (\varepsilon, u)^\top$ be a partitioning of v with $u > \varepsilon$. Partitioning \mathcal{A} accordingly gives

$$\begin{bmatrix} A_{11}(\lambda^{-1}) & A_{12}(\lambda^{-1}) \\ A_{21}(\lambda^{-1}) & A_{22}(\lambda^{-1}) \end{bmatrix} \otimes \begin{bmatrix} \varepsilon \\ u \end{bmatrix} = \begin{bmatrix} \varepsilon \\ u \end{bmatrix},$$

and therefore $A_{12}(\lambda^{-1}) \otimes u = \varepsilon$, which implies $A_{12}(\lambda^{-1}) = \varepsilon$ since by assumption $u > \varepsilon$. However, this contradicts the irreducibility of \mathcal{A} and we conclude that v must be finite.

It remains to prove that λ equals the maximum cycle mean η . In conventional notation the generalized eigenproblem becomes

$$\max_{j=1, \dots, n} (w_{ij} - \mu_{ij}\lambda + v_j) = v_i \quad \text{for all } i = 1, \dots, n, \quad (7.22)$$

where

$$\mu_{ij} = \mu_{ij}(\lambda) = \arg \max_{l=0,\dots,p} ([A_l]_{ij} - l\lambda) \quad \text{and} \quad w_{ij} = [A_{\mu_{ij}}]_{ij}.$$

Note that the maximal polynomial term (or marked arc) depends on λ . From (7.22) we obtain

$$w_{ij} + v_j - v_i \leq \mu_{ij}\lambda \quad \text{for all } 1 \leq i, j \leq n,$$

where equality holds for at least one pair (j, i) for each $1 \leq i \leq n$. The terms $v_j - v_i$ vanish by summation over any circuit ξ and therefore

$$\lambda \geq \frac{\sum_{(j,i) \in \xi} (w_{ij} + v_j - v_i)}{\sum_{(j,i) \in \xi} \mu_{ij}} = \frac{\sum_{(j,i) \in \xi} w_{ij}}{\sum_{(j,i) \in \xi} \mu_{ij}} = \frac{w(\xi)}{\mu(\xi)} \quad \text{for all } \xi \in C. \quad (7.23)$$

Now consider the (saturation) graph $G^s(A(\lambda^{-1})) = (V^s, E^s)$ with node set $V^s = \{1, \dots, n\}$ and arc set $E^s = \{(j, i) \mid w_{ij} - \mu_{ij}\lambda + v_j = v_i\}$. This graph contains a circuit because each node i has at least one incoming arc by (7.22). Furthermore, each circuit ξ_0 in $G^s(A(\lambda^{-1}))$ satisfies $w(\xi_0)/\mu(\xi_0) = \lambda$ and by (7.23) it follows that λ is the maximum cycle mean, and therefore unique. \square

In the special case of $\mathcal{A} = AX$ the condition on A_0 is redundant and the token count on any circuit is just the circuit length. Hence, we obtain the following corollary to Theorem 7.4.1.

Corollary 7.4.1 (Eigenvalue) *Let $A \in \mathbb{R}_{\max}^{n \times n}$ be an irreducible matrix. Then A has a unique eigenvalue $\lambda > \varepsilon$ and finite eigenvectors $v > \varepsilon$ such that $A \otimes v = \lambda \otimes v$, and λ is equal to the maximum cycle mean of the associated precedence graph $G(A)$,*

$$\eta = \max_{\xi \in C} \frac{w(\xi)}{l(\xi)}, \quad (7.24)$$

where C is the set of all elementary circuits in $G(A)$, $w(\xi)$ is the weight of circuit ξ , and $l(\xi)$ is the length of circuit ξ .

The theorem presented here as corollary 7.4.1 is the analogue in max-plus algebra of the Perron-Frobenius theorem for nonnegative matrices [17, 187]. It is one of the classical results in max-plus algebra, see Gondran & Minoux [74], Cuninghame-Green [40, Chapter 25], Baccelli *et al.* [11, Theorem 3.23] and Bapat [13]. Theorem 7.4.1 is a generalization of this result to max-plus polynomial matrices.

In the first-order case $\mathcal{A} = AX$ the maximum cycle mean (7.24) can alternatively be written in matrix notation as

$$\lambda = \bigoplus_{k=1}^n (\text{tr}(A^k))^{1/k},$$

where the *trace* of a matrix $A = (a_{ij}) \in \mathbb{R}_{\max}^{n \times n}$ is defined as

$$\text{tr}(A) = \bigoplus_{i=1}^n a_{ii}.$$

A *critical circuit* is a circuit with maximum cycle mean. By Theorem 7.4.1 and Corollary 7.4.1 the (generalized) eigenvalue depends on the critical circuits in the underlying (timed event)

graph. A graph may contain several critical circuits, which by definition have the same (maximum) cycle mean. The nodes of a critical circuit are called *critical nodes*. Of course, a critical node may be contained in many circuits but at least one of them has a cycle mean equal to the maximum cycle mean.

In the sequel our main concern is the polynomial function $A(x)$ valuated at a fixed scalar $\nu^{-1} \in \mathbb{R}_{\max}$. The resulting matrix will henceforth be denoted as

$$A_\nu \doteq A(\nu^{-1}) = \bigoplus_{l=0}^p A_l \nu^{-l},$$

where $\nu \in \mathbb{R}_{\max}$ is a fixed scalar. We also write $A_\nu^+ = [A(\nu^{-1})]^+$, $A_\nu^* = [A(\nu^{-1})]^*$, et cetera. Note that $A_\nu \in \mathbb{R}_{\max}^{n \times n}$ and if $\nu = \lambda$ is a generalized eigenvalue of $\mathcal{A} \in \mathbb{R}_{\max}^{n \times n}[X]$ with eigenvector v then (e, v) is an eigenpair of A_λ , since $A_\lambda \otimes v = A(\lambda^{-1}) \otimes v = v$.

Lemma 7.4.2 *Let $\mathcal{A} \in \mathbb{R}_{\max}^{n \times n}[X]$ be an irreducible polynomial matrix with generalized eigenvalue $\lambda(\mathcal{A})$, $\nu \in \mathbb{R}_{\max} \setminus \{\varepsilon\}$ a finite scalar, and $A_\nu = A(\nu^{-1}) = \bigoplus_{l=0}^p A_l \nu^{-l} \in \mathbb{R}_{\max}^{n \times n}$. Then $\lambda(A_\nu) \leq e$ if and only if $\nu \geq \lambda(\mathcal{A})$.*

Proof: First note that since $\lambda(\mathcal{A})$ exists, A_0 must be acyclic by Theorem 7.4.1. We next prove that $\lambda(A_\nu)$ is a decreasing function of ν . Let $\nu_1 \geq \nu_2$. Then $c \otimes \nu_1^{-l} < c \otimes \nu_2^{-l}$ for any $c > \varepsilon$ and $l \in \mathbb{N}$, and so we have $[A(\nu_1^{-1})]_{ij} = \bigoplus_{l=0}^p [A_l]_{ij} \otimes \nu_1^{-l} \leq \bigoplus_{l=0}^p [A_l]_{ij} \otimes \nu_2^{-l} = [A(\nu_2^{-1})]_{ij}$, where equality holds iff $[A_0]_{ij} \geq \bigoplus_{l=1}^p [A_l]_{ij} \otimes \nu_2^{-l}$ (which includes the trivial case $[A(\nu^{-1})]_{ij} = \varepsilon$). Hence, each polynomial entry $[A(\nu^{-1})]_{ij}$ is a nonincreasing function of ν , and moreover each polynomial entry $[A(\nu^{-1})]_{ij}$ with degree 1 or higher is decreasing in ν . Because A_0 is acyclic, each circuit in $G(A_\nu)$ contains at least one arc with a polynomial weight of degree one or higher, and therefore all circuit weights and cycle means in $G(A_\nu)$ are decreasing in ν . The generalized eigenvalue $\lambda(A_\nu)$ is then a (strictly) decreasing function of ν by Theorem 7.4.1.

For $\nu = \lambda(\mathcal{A})$ we have $A_\lambda v = A(\lambda^{-1})v = v$ for some (generalized) eigenvector v and so A_λ has eigenvalue e . Hence, for any $\nu \geq \lambda$ we have $\lambda(A_\nu) \leq \lambda(A_\lambda) = e$, and so $\nu \geq \lambda$ is a sufficient condition. Moreover, if $\lambda(A_\nu) > e = \lambda(A_\lambda)$ then $\nu < \lambda$, and therefore $\nu \geq \lambda(\mathcal{A})$ is also a necessary condition. \square

Theorem 7.4.2 (Generalized eigenvectors) *Let $\mathcal{A} \in \mathbb{R}_{\max}^{n \times n}[X]$ be an irreducible polynomial matrix with generalized eigenvalue λ . Then any column i of A_λ^+ such that $[A_\lambda^+]_{ii} = e$ is a generalized eigenvector of \mathcal{A} associated to λ .*

Proof: Let (λ, v) be a generalized eigenpair of \mathcal{A} . Then (e, v) is an eigenpair of A_λ and the precedence graph $G(A_\lambda)$ is strongly connected with maximum cycle mean equal to e . The longest path matrix $A_\lambda^+ = \bigoplus_{l=1}^n A_\lambda^l$ is well-defined by Proposition 7.2.6, and by irreducibility $A_\lambda^+ > \varepsilon$. Let ξ_0 be a critical circuit of $G(A_\lambda)$ and i be any node on ξ_0 . Then any path from i to itself in $G(A_\lambda)$ has weight at most e , and since i belongs to ξ_0 , there is at least one such path with weight e . Hence, $[A_\lambda^+]_{ii} = e$ and therefore the i -th column of A_λ^+ is equal to that of A_λ^* . Let $v = [A_\lambda^+]_{\cdot i} = [A_\lambda^*]_{\cdot i}$, where $A_{\cdot i}$ denotes the i -th column of matrix A . Then

$$A_\lambda \otimes v = A_\lambda \otimes [A_\lambda^+]_{\cdot i} = A_\lambda \otimes [A_\lambda^*]_{\cdot i} = [A_\lambda \otimes A_\lambda^*]_{\cdot i} = [A_\lambda^+]_{\cdot i} = v,$$

which proves that $(\lambda, [A_\lambda^+]_{\cdot i})$ is a generalized eigenpair of \mathcal{A} . \square

The indices i satisfying the condition in Theorem 7.4.2 are exactly the critical nodes of the precedence graph $G(A_\lambda)$, i.e., the nodes on a critical circuit of $G(A_\lambda)$.

In the case of a square max-plus matrix $A \in \mathbb{R}_{\max}^{n \times n}$ with eigenvalue $\lambda \in \mathbb{R}_{\max} \setminus \{\varepsilon\}$ we have $[A_\lambda]_{ij} = [A \otimes \lambda^{-1}]_{ij} = a_{ij} - \lambda$. Clearly, the support of A , $\text{supp}(A) = \{(j, i) \mid a_{ij} > \varepsilon, 1 \leq i, j \leq n\}$, is preserved in A_λ . Furthermore, the precedence graphs $G(A)$ and $G(A_\lambda)$ are equal except for the arc weights, and in particular the critical circuits in both graphs are the same, with the maximum cycle means $\eta(A) = \lambda$ and $\eta(A_\lambda) = e$. Hence, we have the following corollary to Theorem 7.4.2.

Corollary 7.4.2 (Eigenvectors) *Let $A \in \mathbb{R}_{\max}^{n \times n}$ be an irreducible matrix with eigenvalue λ . Then any column i of $[\lambda^{-1}A]^+$ such that $[\lambda^{-1}A]_{ii}^+ = e$ is an eigenvector of A associated to λ .*

If $v_1, v_2 \in \mathbb{R}_{\max}^n$ are two generalized eigenvectors of \mathcal{A} corresponding to the generalized eigenvalue $\lambda \in \mathbb{R}_{\max}$ then for any $c_1, c_2 \in \mathbb{R}_{\max}$ also $c_1 v_1 \oplus c_2 v_2$ is a generalized eigenvector of \mathcal{A} corresponding to λ , since

$$\begin{aligned} A(\lambda^{-1}) \otimes (c_1 v_1 \oplus c_2 v_2) &= A(\lambda^{-1}) \otimes (c_1 v_1) \oplus A(\lambda^{-1}) \otimes (c_2 v_2) \\ &= c_1 (A(\lambda^{-1}) \otimes v_1) \oplus c_2 (A(\lambda^{-1}) \otimes v_2) \\ &= c_1 v_1 \oplus c_2 v_2. \end{aligned}$$

This argument is easily expanded to any linear combination of generalized eigenvectors. In general, the generalized eigenvectors corresponding to a generalized eigenvalue λ of a polynomial matrix $\mathcal{A} \in \mathbb{R}_{\max}^{n \times n}[X]$ span a subsemimodule of \mathbb{R}_{\max}^n :

$$\mathcal{V}(\lambda) = \{v \in \mathbb{R}_{\max}^n \mid A(\lambda^{-1})v = v\} = \bigoplus_{i \in I} c_i [A_\lambda^+]_{\cdot i}$$

with $c_i \in \mathbb{R}_{\max}$ and $I = \{1 \leq i \leq n \mid [A_\lambda^+]_{ii} = e\}$. This semimodule is called the *eigensemimodule* of \mathcal{A} corresponding to the generalized eigenvalue λ or also simply the *eigenspace* of $\lambda(\mathcal{A})$. Unlike the classical Perron-Frobenius theory where an irreducible nonnegative matrix has a unique eigenvector (up to a constant multiple), the dimension of the eigenspace of a max-plus (polynomial) matrix depends on the interconnection structure of the critical circuit(s) of $G(A_\lambda)$.

Lemma 7.4.3 *Let $\mathcal{A} \in \mathbb{R}_{\max}^{n \times n}[X]$ be an irreducible polynomial matrix with generalized eigenvalue λ . If the precedence graph $G(A_\lambda)$ has a unique critical circuit then all generalized eigenvectors associated to λ are weakly dependent, and the one-dimensional eigenspace is given by $\mathcal{V}(\lambda) = \text{span}([A_\lambda^+]_{\cdot i})$ for any index $i \in \{1 \leq i \leq n \mid [A_\lambda^+]_{ii} = e\}$.*

Proof: By Theorem 7.4.2 we know that the set $\mathcal{V}(\lambda)$ of generalized eigenvectors is generated by the critical columns of A_λ^+ . By definition $[A_\lambda^+]_{\cdot i}$ is a critical column if and only if i is contained in a critical circuit of $G(A_\lambda)$, i.e., $[A_\lambda^+]_{ii} = e$. It remains to prove that under the condition of a unique critical circuit all generalized eigenvectors are proportional and thus weakly dependent. In general, $[A_\lambda^+]_{lj} \geq [A_\lambda^+]_{li}[A_\lambda^+]_{ij}$ for each $1 \leq l \leq n$, with strict equality only if the longest path from j to l passes node i . If i, j are any two nodes on a critical circuit of $G(A_\lambda)$ then $[A_\lambda^+]_{ji}[A_\lambda^+]_{ij} = [A_\lambda^+]_{jj} = e$. Therefore, for all $1 \leq l \leq n$

$$[A_\lambda^+]_{li}[A_\lambda^+]_{ij} \leq [A_\lambda^+]_{lj} = [A_\lambda^+]_{lj}[A_\lambda^+]_{ji}[A_\lambda^+]_{ij} \leq [A_\lambda^+]_{li}[A_\lambda^+]_{ij}$$

and so $[A_\lambda^+]_{\cdot j} = [A_\lambda^+]_{\cdot i} [A_\lambda^+]_{ij} = [A_\lambda^+]_{ij} [A_\lambda^+]_{\cdot i}$, which proves that $[A_\lambda^+]_{\cdot j}$ and $[A_\lambda^+]_{\cdot i}$ are weakly dependent for any pair of indices i and j on the same critical circuit. \square

If there is more than one critical circuit then the eigenspace may be generated by several weakly-independent generalized eigenvectors. The general result requires the notion of the *critical graph*.

Definition 7.4.1 (Critical graph) Let $\mathcal{A} \in \mathbb{R}_{\max}^{n \times n}[X]$ be a polynomial matrix with generalized eigenvalue λ . The critical graph $G^c(A_\lambda) = (V^c, E^c)$ is the digraph with node set $V^c = \{1 \leq i \leq n \mid [A_\lambda^+]_{ii} = e\}$ and arc set $E^c = \{(j, i) \mid [A_\lambda]_{ij} > \varepsilon, i, j \in V^c\}$.

Note that the critical graph $G^c(A_\lambda) = (V^c, E^c)$ is a cyclic subgraph of the precedence graph $G(A_\lambda) = (V, E)$, with $V^c \subseteq V$ and $E^c = E \cap (V^c \times V^c)$. If λ is known the critical graph can be computed using Algorithm 7.5.3 of Section 7.5.3. This algorithm computes the diagonal of the matrix A_λ^+ . Selecting all diagonal entries equal to e gives the node set V^c and subsequently E^c is determined by selecting all arcs (j, i) corresponding to $[A_\lambda]_{ij} \neq \varepsilon$ with both $j, i \in V^c$.

If $G^c(A_\lambda)$ is not strongly connected then the node set can be decomposed into *critical classes* K_i^c associated to the strongly-connected components, $V^c = K_1^c \cup \dots \cup K_c^c$, where c is the number of components, and $K_i^c \cap K_j^c = \emptyset$ for $i \neq j$. The next theorem characterizes the eigenspace of an irreducible max-plus (polynomial) matrix by its weak basis.

Theorem 7.4.3 (Eigenspace) Let $\mathcal{A} \in \mathbb{R}_{\max}^{n \times n}[X]$ be an irreducible polynomial matrix with generalized eigenvalue λ . If the critical graph $G^c(A_\lambda)$ has c connected components then the eigenspace $\mathcal{V}(\lambda) \subseteq \mathbb{R}_{\max}^n$ of generalized eigenvectors associated to λ is a finitely-generated semimodule of weak dimension c , given by

$$\mathcal{V}(\lambda) = \text{span}([A_\lambda^+]_{\cdot i_1}, \dots, [A_\lambda^+]_{\cdot i_c}), \quad (7.25)$$

where the indices are arbitrarily selected from each critical class $i_k \in K_k^c$ for all $k = 1, \dots, c$.

Proof: By Theorem 7.4.2 we know that the set $\mathcal{V}(\lambda)$ of generalized eigenvectors is generated by the critical columns of A_λ^+ , and by Lemma 7.4.3 the generalized eigenvectors from the same critical classes are weakly dependent. We now prove that a maximal weakly independent set of generalized eigenvectors is obtained by selecting one critical column of A_λ^+ for each critical class K_1^c, \dots, K_c^c , which then constitutes a weak basis of $\mathcal{V}(\lambda)$. Let $I = \{i_1, \dots, i_c\}$ be a representative set of indices from each class K_1^c, \dots, K_c^c . Then we must prove that for each $i \in I$ the vector $[A_\lambda^+]_{\cdot i}$ is weakly independent on the set $\{[A_\lambda^+]_{\cdot k} \mid k \in I \setminus \{i\}\}$. We argue by contradiction. Suppose

$$[A_\lambda^+]_{\cdot i} = \bigoplus_{k \in I \setminus \{i\}} c_k \otimes [A_\lambda^+]_{\cdot k} \quad (7.26)$$

for some coefficients $c_k \in \mathbb{R}_{\max}$, $k \in I \setminus \{i\}$. Concentrating on the i th row of (7.26) we have $[A_\lambda^+]_{ii} = \bigoplus_{k \in I \setminus \{i\}} c_k [A_\lambda^+]_{ik} = e$, since i is a critical node. Hence, there must be at least one index $j \in I \setminus \{i\}$ with $c_j = [A_\lambda^+]_{ij}^{-1}$, such that $e = c_j [A_\lambda^+]_{ij} = [A_\lambda^+]_{ij}^{-1} [A_\lambda^+]_{ij}$. Then by (7.26) we have $[A_\lambda^+]_{\cdot i} \geq [A_\lambda^+]_{ij}^{-1} [A_\lambda^+]_{\cdot j}$. In particular, on the j th row this gives $[A_\lambda^+]_{ji} \geq [A_\lambda^+]_{ij}^{-1} [A_\lambda^+]_{jj} = [A_\lambda^+]_{ij}^{-1} e = [A_\lambda^+]_{ij}^{-1}$. However, in general we have $[A_\lambda^+]_{ij} [A_\lambda^+]_{ji} \leq e$ or equivalently $[A_\lambda^+]_{ji} \leq [A_\lambda^+]_{ij}^{-1}$ with equality only if i and j are on the same critical circuit. But by construction i and j correspond to distinct critical classes and we thus have a contradiction. \square

Theorem 7.4.3 is a generalization of the eigensemimodule for irreducible square max-plus matrices $A \in \mathbb{R}_{\max}^{n \times n}$ as described by Gondran & Minoux [74], Cuninghame-Green [40], and Baccelli *et al.* [11, Theorem 3.101].

We end this section with a relaxation of the generalized eigenproblem that will be useful in the sequel. Consider a polynomial matrix $\mathcal{A} \in \mathbb{R}_{\max}^{n \times n}[X]$ and a fixed scalar $T \in \mathbb{R}_{\max}$. A vector $u \in \mathbb{R}_{\max}^n \setminus \{\varepsilon\}$ satisfying the inequality $A(T^{-1}) \otimes u \leq u$ is called a generalized *subeigenvector* of \mathcal{A} associated to T . If this inequality is satisfied for some subeigenvector then T is called a generalized *supereigenvalue* of \mathcal{A} .

Theorem 7.4.4 (Subeigenvector) *Let $\mathcal{A} \in \mathbb{R}_{\max}^{n \times n}[X]$ be an irreducible polynomial matrix with generalized eigenvalue $\lambda(\mathcal{A})$, and $T > \varepsilon$ a finite scalar. Then there exists a finite vector $u > \varepsilon \in \mathbb{R}_{\max}^n$ such that*

$$A(T^{-1}) \otimes u \leq u \quad (7.27)$$

if and only if $T \geq \lambda(\mathcal{A})$. Moreover, $T = \lambda(\mathcal{A})$ if and only if $A(T^{-1}) \otimes u = u$.

Proof: We first prove sufficiency of the condition $T \geq \lambda(\mathcal{A})$ for the existence of some vector $u \in \mathbb{R}_{\max}^n$ such that (7.27) holds. So assume $T \geq \lambda(\mathcal{A})$. Then $A_T = A(T^{-1})$ has eigenvalue smaller than or equal to e by Lemma 7.4.2 and if (7.27) is valid for some u then $A(T^{-1})^k u = A(T^{-1})^{k-1} A(T^{-1}) u \leq A(T^{-1})^{k-1} u$ for any $k \in \mathbb{N}$, and so by induction $A(T^{-1})^k \otimes u \leq u$. Now suppose that at least one entry of u is zero, say $u_i = \varepsilon$. Then for any $k \in \mathbb{N}$

$$\bigoplus_{j=1}^n [A(T^{-1})^k]_{ij} u_j \leq u_i. \quad (7.28)$$

Since $u \neq \varepsilon$ there is an entry $u_j > \varepsilon$ for some $1 \leq j \leq n$, and because $A(T^{-1})$ is irreducible there exists a $k \in \mathbb{N}$ such that $[A(T^{-1})^k]_{ij} > \varepsilon$ for this j . But then the left-hand side of (7.28) is finite and therefore $u_i > \varepsilon$. This contradicts the hypothesis $u_i = \varepsilon$, and so we must have $u > \varepsilon$.

Conversely, assume there is a vector $u > \varepsilon$ satisfying (7.27). Then the inverse u_i^{-1} exists for each $1 \leq i \leq n$ and therefore (7.28) can be written as $\bigoplus_{j=1}^n [A(T^{-1})^k]_{ij} u_j u_i^{-1} \leq e$. In particular, for all $1 \leq i \leq n$ and $k \in \mathbb{N}$ we obtain $[A(T^{-1})^k]_{ii} \leq e$, and therefore $\bigoplus_{k=1}^n [A(T^{-1})^k]_{ii} = [A(T^{-1})^+]_{ii} \leq e$ for all $1 \leq i \leq n$. This implies that $A_T = A(T^{-1})$ has maximum cycle mean smaller than or equal to e , or $\lambda(A_T) \leq e$. By Lemma 7.4.2 we thus have $T \geq \lambda(\mathcal{A})$, which proves the necessity of this condition. \square

In the special case $\mathcal{A} = AX$, the inequality becomes $Au \leq Tu$, which was also proved by Gaubert [70, Lemma IV.1.3.8]. In this case, Theorem 7.4.4 is the max-plus algebra analogue of the Subinvariance Theorem of nonnegative matrices, see e.g. Seneta [187, Theorem 1.6]. Theorem 7.4.4 is a generalization to max-plus polynomial matrices.

7.4.3 State Classification and the Reduced Graph

The eigenstructure of a *reducible* (polynomial) matrix depends on the interconnection structure of the associated (timed event) graph, and in particular on accessibility relations between events. Again there is a strong connection to the theory of nonnegative matrices. Rothblum [175] generalized the Perron-Frobenius theorem to *reducible* square nonnegative matrices motivated

by the theory of Markov chains, see also Berman & Plemmons [17]. Gaubert [70] considered the analogous generalization of the Perron-Frobenius theorem to square max-plus matrices, see also Bapat [13]. In this section and the next we will develop the theory for max-plus polynomial matrices and associated timed event graphs, which generalizes the theory of max-plus matrices and their precedence graphs. The present section introduces a classification of events similar to state classification of Markov chains [17, 175].

Let $\mathcal{A} \in \mathbb{R}_{\max}^{n \times n}[X]$ be a max-plus polynomial matrix with associated timed event graph $\mathcal{G}(\mathcal{A}) = (\mathcal{T}, \mathcal{P}, \tau, \mu)$, where $\mathcal{T} = \{1, \dots, n\}$ corresponds to the indices of \mathcal{A} . We say that event j has access to event i , denoted as $j \rightarrow i$, if there is a path from j to i in $\mathcal{G}(\mathcal{A})$, or equivalently, if there is an integer $l \geq 0$ such that $[\mathcal{A}^l]_{ij} > \varepsilon$. If both j has access to i and i has access to j then we say that j and i communicate, denoted as $j \leftrightarrow i$, where by convention each event communicates with itself ($\forall i \in \mathcal{T} : i \leftrightarrow i$). Communication is an *equivalence relation* on the set of events \mathcal{T} (or on the index set of \mathcal{A}).

Definition 7.4.2 (Equivalence relation) A binary relation \leftrightarrow on a set $\mathcal{T} \neq \emptyset$ is an equivalence relation on \mathcal{T} if the following axioms are satisfied for any $i, j, k \in \mathcal{T}$:

- (i) Reflexivity: $i \leftrightarrow i$.
- (ii) Symmetry: if $i \leftrightarrow j$ then $j \leftrightarrow i$.
- (iii) Transitivity: if $i \leftrightarrow j$ and $j \leftrightarrow k$ then $i \leftrightarrow k$.

For any $i \in \mathcal{T}$ the associated set of communicating events $\{j \in \mathcal{T} \mid j \leftrightarrow i\}$ is called an *equivalence class* (or a class). Note that a class corresponds to a strongly-connected component in the corresponding (timed event) graph. It is well-known that an equivalence relation partitions a set in (nonempty disjoint) equivalence classes $\mathcal{T} = \mathcal{T}_1 \cup \dots \cup \mathcal{T}_c$, where $\mathcal{T}_i \cap \mathcal{T}_j = \emptyset$ if $\mathcal{T}_i \neq \mathcal{T}_j$ and c is the number of communication classes [15]. If \mathcal{T}_j and \mathcal{T}_i are two classes and an event in \mathcal{T}_j has access to an event in \mathcal{T}_i then all events in class \mathcal{T}_j have access to all events in \mathcal{T}_i and we say that class \mathcal{T}_j has access to class \mathcal{T}_i , denoted as $\mathcal{T}_j \rightarrow \mathcal{T}_i$. By definition, if class \mathcal{T}_j has access to class \mathcal{T}_i and vice versa then $\mathcal{T}_j = \mathcal{T}_i$. A class is called *initial* if no other class has access to it, and it is called *final* if it has access to no other class. Each square max-plus (polynomial) matrix has at least one initial and one final class.

The interconnection structure between the communication classes of a polynomial matrix \mathcal{A} or its associated event set \mathcal{T} is visualized by the *reduced graph* [2, 11].

Definition 7.4.3 (Reduced graph) Let $\mathcal{A} \in \mathbb{R}_{\max}^{n \times n}[X]$ be a polynomial matrix with associated timed event graph $\mathcal{G}(\mathcal{A}) = (\mathcal{T}, \mathcal{P}, \tau, \mu)$ and let $\mathcal{T} = \bigcup_{i=1}^c \mathcal{T}_i$ be a partitioning in communication classes. Then the reduced graph $G_{\text{red}}(\mathcal{A}) = (V_{\text{red}}, E_{\text{red}})$ is the acyclic digraph with node set $V_{\text{red}} = \{\mathcal{T}_1, \dots, \mathcal{T}_c\}$ and arc set $E_{\text{red}} = \{(\mathcal{T}_j, \mathcal{T}_i) \mid \mathcal{T}_j \rightarrow \mathcal{T}_i, i \neq j, 1 \leq i, j \leq c\}$.

Each class in the timed event graph is thus contracted to a node in the reduced graph and the arcs in the reduced graph represent the accessibility relations between classes. The reduced graph is also known as the *component graph* [39] and in Markov chain theory as the *communication graph* [17].

The accessibility relation defines a partial order (see Definition 7.2.11) on the communication

classes according to

$$\mathcal{T}_j \preceq \mathcal{T}_i \Leftrightarrow \mathcal{T}_j \rightarrow \mathcal{T}_i.$$

We also denote by $\mathcal{T}_j \succeq \mathcal{T}_i$ the equivalence of $\mathcal{T}_i \preceq \mathcal{T}_j$. If $\mathcal{T}_j \preceq \mathcal{T}_i$ and $\mathcal{T}_j \neq \mathcal{T}_i$ then we also write $\mathcal{T}_j \prec \mathcal{T}_i$, and similarly $\mathcal{T}_j \succ \mathcal{T}_i$ iff $\mathcal{T}_i \preceq \mathcal{T}_j$ and $\mathcal{T}_j \neq \mathcal{T}_i$. An alternative interpretation of $\mathcal{T}_j \preceq \mathcal{T}_i$ is that \mathcal{T}_j precedes or equals \mathcal{T}_i in the reduced graph, and likewise $\mathcal{T}_j \prec \mathcal{T}_i$ means \mathcal{T}_j precedes \mathcal{T}_i . Similarly $\mathcal{T}_j \succeq \mathcal{T}_i$ (respectively $\mathcal{T}_j \succ \mathcal{T}_i$) means that \mathcal{T}_j succeeds (or equals) \mathcal{T}_i in the reduced graph.

A (polynomial) matrix is *irreducible* if it has only one class. Hence, in an irreducible matrix all events communicate, which is consistent with Proposition 7.2.7. Note that each communication class corresponds to the events (transitions, nodes) in a strongly-connected component of the associated (timed event) graph, and the number of classes c is just the number of strongly-connected components. Hence, finding all classes in a (polynomial) matrix is equivalent to finding all strongly-connected components in a (timed event) graph, which is solvable in linear $O(n + m)$ time by Tarjan's algorithm [198] based on depth-first search, see also Cormen *et al.* [39]. Here, $n = |\mathcal{T}|$ is the number of events (number of rows) and $m = |\mathcal{P}|$ is the number of places (marked arcs, nonzero entries).

Let $\mathcal{A} \in \mathbb{R}_{\max}^{n \times n}[X]$ be a reducible max-plus polynomial matrix with c classes. Then, possibly after a suitable coordinate transformation $P^\top \mathcal{A} P$, \mathcal{A} takes the form of a lower block triangular (polynomial) matrix with irreducible square diagonal blocks, called the *Frobenius normal form*:

$$\mathcal{A} = \begin{bmatrix} \mathcal{A}_{11} & & \mathcal{E} \\ \vdots & \ddots & \\ \mathcal{A}_{c1} & \cdots & \mathcal{A}_{cc} \end{bmatrix}. \quad (7.29)$$

Here $\mathcal{A}_{ii} \in \mathbb{R}_{\max}^{n_i \times n_i}[X]$ are irreducible square blocks corresponding to the classes \mathcal{T}_i with cardinality $n_i = |\mathcal{T}_i|$, and obviously $n_1 \otimes \cdots \otimes n_c = n$. Expressed in the Frobenius normal form, a class \mathcal{T}_j has access to \mathcal{T}_i if and only if $\mathcal{A}_{ij} \neq \mathcal{E}$, where $\mathcal{A}_{ij} \in \mathbb{R}_{\max}^{n_i \times n_j}[X]$ is the block to the left of \mathcal{A}_{ii} and below \mathcal{A}_{jj} . If $\mathcal{A}_{ij} = \mathcal{E}$ for all blocks at the left of \mathcal{A}_{ii} then \mathcal{T}_i is an initial class, and if $\mathcal{A}_{ij} = \mathcal{E}$ for all blocks below \mathcal{A}_{jj} then \mathcal{T}_j is final. In particular \mathcal{A}_{11} is an initial class and \mathcal{A}_{cc} is a final class. A block \mathcal{A}_{ii} (and associated class) is called *isolated* if it is both initial and final. An isolated class has no access to any other class nor does any other class have access to an isolated class. An empty row corresponds to an initial class of a single (source) event, and likewise an empty column corresponds to a final class of a single (sink) event.

Example 7.3 Consider the polynomial matrix in Frobenius normal form

$$\mathcal{A} = \left[\begin{array}{cc|cc|c} \varepsilon & 30X & \varepsilon & \varepsilon & \varepsilon \\ 28 & 55X & \varepsilon & \varepsilon & \varepsilon \\ \hline \varepsilon & 5 & 40X & \varepsilon & \varepsilon \\ 3 & \varepsilon & \varepsilon & \varepsilon & 25X \\ \varepsilon & \varepsilon & 20 & 25 & \varepsilon \\ \hline \varepsilon & 5 & \varepsilon & \varepsilon & 58X \end{array} \right],$$

where the block structure is emphasized by solid lines. The associated timed event graph $\mathcal{G}(\mathcal{A}) = (\mathcal{T}, \mathcal{P}, \tau, \mu)$ is shown in Figure 7.4. \mathcal{A} has four classes (depicted by the dashed boxes in Figure 7.4): an initial class $\mathcal{T}_1 = \{1, 2\}$, a transient class $\mathcal{T}_2 = \{3\}$, and two final classes

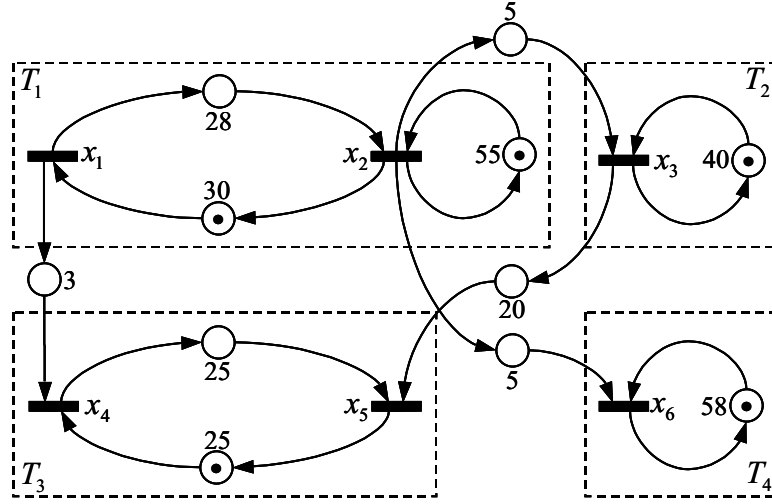


Figure 7.4 Timed event graph and communication classes

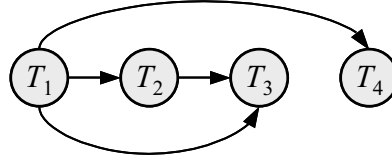


Figure 7.5 Reduced graph

$\mathcal{T}_3 = \{4, 5\}$ and $\mathcal{T}_4 = \{6\}$. Figure 7.5 shows the reduced graph, which clearly visualizes the accessibility relations between the communication classes. \mathcal{T}_1 has access to all classes and \mathcal{T}_2 has access to \mathcal{T}_3 (and itself). Since the other two classes are final they have only access to themselves. We thus have $\mathcal{T}_1 \prec \mathcal{T}_2 \prec \mathcal{T}_3$ and $\mathcal{T}_1 \prec \mathcal{T}_4$. This example also shows that the induced partial order between communication classes is not total, since e.g. $\mathcal{T}_2 \not\prec \mathcal{T}_4$ and $\mathcal{T}_4 \not\prec \mathcal{T}_2$. \square

7.4.4 Eigenstructure of Reducible Matrices

The spectrum of reducible square max-plus (polynomial) matrices depends on the (generalized) eigenvalues of the communication classes and the interconnection structure of the reduced graph. We start this section with the observation that the spectrum of a (polynomial) matrix is invariant to a similarity transformation.

Lemma 7.4.4 *Let $\mathcal{A} \in \mathbb{R}_{\max}^{n \times n}[X]$ be a polynomial matrix and $P \in \mathbb{R}_{\max}^{n \times n}$ a permutation matrix. Then $\lambda \in \text{spec}(\mathcal{A})$ if and only if $\lambda \in \text{spec}(P^\top \mathcal{A} P)$.*

Proof: The generalized eigenequation of $P^\top \mathcal{A} P$ is defined as $P^\top \mathcal{A}(\lambda^{-1}) P v = v$. Premultiplying both sides of this matrix equation by the permutation matrix P just reorders the rows of the matrix equation, but leaves the n generalized eigenequations unchanged. Thus,

$$P^\top \mathcal{A}(\lambda^{-1}) P v = v \quad \Leftrightarrow \quad P P^\top \mathcal{A}(\lambda^{-1}) P v = P v \quad \Leftrightarrow \quad \mathcal{A}(\lambda^{-1}) P v = P v.$$

Here we used the identity $P P^\top = E$ for any permutation matrix P . Hence, if (λ, v) is a generalized eigenvalue of $P^\top \mathcal{A} P$ then $(\lambda, P v)$ is a generalized eigenpair of \mathcal{A} , and vice versa. Or

equivalently, if (λ, u) is a generalized eigenpair of \mathcal{A} then $(\lambda, P^\top u)$ is a generalized eigenvalue of $P^\top \mathcal{A} P$, and vice versa. \square

Without loss of generality we thus may assume that a reducible (polynomial) matrix is in Frobenius normal form (7.29), where the event set (or index set) $\mathcal{T} = \{1, \dots, n\}$ is partitioned into c classes $\mathcal{T} = \bigcup_{i=1}^c \mathcal{T}_i$. The number of events in class \mathcal{T}_i is denoted as $n_i = |\mathcal{T}_i|$, with $\bigotimes_{i=1}^c n_i = n$.

Each class \mathcal{T}_i corresponds to an irreducible polynomial submatrix $\mathcal{A}_{ii} \in \mathbb{R}_{\max}^{n_i \times n_i}[X]$ of \mathcal{A} and thus has a unique generalized eigenvalue $\lambda(\mathcal{A}_{ii})$ by Theorem 7.4.1. However, this class generalized eigenvalue may be dominated by a preceding class with larger generalized eigenvalue. Moreover, if the class has access to a class with larger generalized eigenvalue then its generalized eigenvalue is not contained in the spectrum of the full matrix \mathcal{A} , as we will see below.

For any subset $I \subseteq \mathcal{T}$ let $\Gamma(I)$ be the set of events that are accessible from I , i.e.,

$$\Gamma(I) \doteq \{j \in \mathcal{T} \mid \exists i \in I : i \rightarrow j\}.$$

A subset $I \subseteq \mathcal{T}$ is a *closed set* if $I = \Gamma(I)$.

Lemma 7.4.5 *Let $\mathcal{A} \in \mathbb{R}_{\max}^{n \times n}[X]$ be a polynomial matrix and let $\mathcal{T} = \bigcup_{i=1}^c \mathcal{T}_i$ be a partitioning of the event set in communication classes. Then $K_i = \Gamma(\mathcal{T}_i)$ is a closed set for each $1 \leq i \leq c$.*

Proof: For any class $\mathcal{T}_i \subseteq \mathcal{T}$ the set $\Gamma(\mathcal{T}_i) \neq \emptyset$ since $\mathcal{T}_i \subseteq \Gamma(\mathcal{T}_i)$ for all $1 \leq i \leq c$. Furthermore, if $\mathcal{T}_i \preceq \mathcal{T}_j$ then by definition $\mathcal{T}_j \subset \Gamma(\mathcal{T}_i)$. Hence, $K_i = \Gamma(\mathcal{T}_i)$ contains all classes accessible from \mathcal{T}_i and is thus a closed set for each $1 \leq i \leq c$. \square

The following theorem was proved by Gaubert [70] for square max-plus matrices $A \in \mathbb{R}_{\max}^{n \times n}$.

Theorem 7.4.5 (Generalized eigenpair) *Let $\mathcal{A} \in \mathbb{R}_{\max}^{n \times n}[X]$ be a polynomial matrix in Frobenius normal form with c classes,*

$$\mathcal{A} = \begin{bmatrix} \mathcal{A}_{11} & & \mathcal{E} \\ \vdots & \ddots & \\ \mathcal{A}_{c1} & \cdots & \mathcal{A}_{cc} \end{bmatrix}.$$

Then λ is a generalized eigenvalue of \mathcal{A} if and only if there exists a class \mathcal{T}_i such that $\lambda = \lambda(\mathcal{A}_{ii})$ and

$$\lambda(\mathcal{A}_{ii}) = \bigoplus_{\mathcal{T}_j \subseteq \Gamma(\mathcal{T}_i)} \lambda(\mathcal{A}_{jj}). \quad (7.30)$$

Moreover there exists a generalized eigenvector $v = (v^1, \dots, v^n)^\top \in \mathbb{R}_{\max}^n$ associated to $\lambda(\mathcal{A}) = \lambda(\mathcal{A}_{ii})$ with support $\Gamma(\mathcal{T}_i)$, given by

$$v^j = \begin{cases} [A_\lambda^+]_{jl} & \text{if } j \in \Gamma(\mathcal{T}_i) \\ \varepsilon & \text{otherwise,} \end{cases} \quad (7.31)$$

for any $l \in \mathcal{T}_i$ with $[A_\lambda^+]_{ll} = e$.

Proof: Assume that $\lambda = \lambda(\mathcal{A}_{ii})$ is a generalized eigenvalue of \mathcal{A} but (7.30) is violated. Hence, there exists a class $\mathcal{T}_k \subset \Gamma(\mathcal{T}_i)$ with $\lambda(\mathcal{A}_{kk}) > \lambda(\mathcal{A}_{ii})$. Let the generalized eigenvector $v \in \mathbb{R}_{\max}^n$ associated to λ be partitioned conform the block partitioning of \mathcal{A} , i.e., $v = (v_1, \dots, v_c)^\top \in \mathbb{R}_{\max}^n$ with $v_j \in \mathbb{R}_{\max}^{|\mathcal{T}_j|}$, $1 \leq j \leq c$. Then the k th block row of the generalized eigenequation $A(\lambda^{-1}) \otimes v = v$ becomes

$$\bigoplus_{j \neq k} A_{kj}(\lambda^{-1}) \otimes v_j \oplus A_{kk}(\lambda^{-1}) \otimes v_k = v_k,$$

and therefore in particular $A_{kk}(\lambda^{-1})v_k \leq v_k$, which implies that v_k is a subeigenvector of \mathcal{A}_{kk} associated to $\lambda = \lambda(\mathcal{A}_{ii})$. Then by Theorem 7.4.4 we must have $\lambda \geq \lambda(\mathcal{A}_{kk})$, but this contradicts the assumption $\lambda(\mathcal{A}_{kk}) > \lambda(\mathcal{A}_{ii})$. Thus, (7.30) is a necessary condition.

Conversely, assume (7.30) is valid. By Lemma 7.4.5 the set $K_i = \Gamma(\mathcal{T}_i) \subseteq \mathcal{T}$ is closed. Hence, possibly after a similarity transformation, \mathcal{A} can be written in block triangular form

$$\mathcal{A} = \begin{bmatrix} \mathcal{A}_{[\bar{K}_i|\bar{K}_i]} & \mathcal{E} \\ \mathcal{A}_{[\bar{K}_i|K_i]} & \mathcal{A}_{[K_i|K_i]} \end{bmatrix},$$

where $\bar{K}_i = \mathcal{T} \setminus K_i$ is the complement of K_i in \mathcal{T} , and $\mathcal{A}_{[I|J]} \in \mathbb{R}_{\max}^{I \times J}[X]$ denotes the submatrix of \mathcal{A} corresponding to row index set I and column index set J . Assume (λ, v) is a generalized eigenpair of the principle submatrix $\mathcal{A}_{[K_i|K_i]}$ with $v \in \mathbb{R}_{\max}^{K_i}$. Then $(\varepsilon, v)^\top \in \mathbb{R}_{\max}^n$ is a generalized eigenvector of \mathcal{A} associated to λ , since

$$\begin{bmatrix} A_{[\bar{K}_i|\bar{K}_i]}(\lambda^{-1}) & \mathcal{E} \\ A_{[\bar{K}_i|K_i]}(\lambda^{-1}) & A_{[K_i|K_i]}(\lambda^{-1}) \end{bmatrix} \begin{bmatrix} \varepsilon \\ v \end{bmatrix} = \begin{bmatrix} \varepsilon \\ A_{[K_i|K_i]}(\lambda^{-1})v \end{bmatrix} = \begin{bmatrix} \varepsilon \\ v \end{bmatrix}. \quad (7.32)$$

Hence, we may restrict ourselves to the generalized eigenvalue of the principle submatrix $\mathcal{B} = \mathcal{A}_{[K_i|K_i]} \in \mathbb{R}_{\max}^{K_i \times K_i}[X]$ of \mathcal{A} . Because of (7.30), λ is the maximum generalized eigenvalue of \mathcal{B} . Let $B_\lambda = B(\lambda^{-1})$. Then B_λ has eigenvalue e and so the precedence graph $G(B_\lambda)$ has no circuits with positive weight. By Proposition 7.2.6 the matrices B_λ^+ and B_λ^* are then well-defined, and by definition $B_\lambda[B_\lambda^*]_{\cdot l} = [B_\lambda^+]_{\cdot l}$ for any $1 \leq l \leq |K_i|$. If l is contained in a critical circuit of $\mathcal{G}(\mathcal{B})$ then $[B_\lambda^+]_{ll} = e$, and so $[B_\lambda^+]_{\cdot l} = [B_\lambda^*]_{\cdot l}$. Hence, for any critical index l the vector $[B_\lambda^+]_{\cdot l}$ is an eigenvector of B_λ associated to the eigenvalue e , and therefore also a generalized eigenvector of \mathcal{B} associated to λ , since $B(\lambda^{-1})[B_\lambda^+]_{\cdot l} = B_\lambda[B_\lambda^+]_{\cdot l} = [B_\lambda^+]_{\cdot l}$. This proves that (7.30) is also a sufficient condition.

It remains to prove that (7.31) defines a generalized eigenvector v of \mathcal{A} . From (7.32) and the fact that $K_i = \Gamma(\mathcal{T}_i)$ is closed it follows that a generalized eigenvector v associated to $\lambda = \lambda(\mathcal{A}_{ii})$ exists with $\text{supp}(v) = K_i = \Gamma(\mathcal{T}_i)$. Consider again the generalized eigenvector $[B_\lambda^+]_{\cdot l}$ of \mathcal{B} . If \mathcal{A} is already in the form (7.32) then we simply have $v = (\varepsilon, [B_\lambda^+]_{\cdot l})^\top = [A_\lambda^+]_{\cdot l}$. If the form (7.32) is obtained after a similarity transformation $P^\top \mathcal{A} P$ then we have $v = P^\top \otimes (\varepsilon, [B_\lambda^+]_{\cdot l})^\top$, analogous to the proof of Lemma 7.4.4, which is exactly (7.31). \square

Corollary 7.4.3 *Let $\mathcal{A} \in \mathbb{R}_{\max}^{n \times n}[X]$ be a polynomial matrix in Frobenius normal form (7.29) with c classes. Then the set of all generalized eigenvalues of \mathcal{A} is characterized by*

$$\text{spec}(\mathcal{A}) = \left\{ \lambda(\mathcal{A}_{ii}) \in \mathbb{R}_{\max} \mid \lambda(\mathcal{A}_{ii}) = \bigoplus_{\mathcal{T}_j \subseteq \Gamma(\mathcal{T}_i)} \lambda(\mathcal{A}_{jj}), 1 \leq i \leq c \right\}. \quad (7.33)$$

Classes that satisfy the condition in Theorem 7.4.5 are obviously of particular importance, and will be called *principle* in the sequel. So if $\mathcal{A} \in \mathbb{R}_{\max}^{n \times n}[X]$ is a polynomial matrix in Frobenius normal form (7.29) then \mathcal{T}_i is a *principle class* if $\lambda(\mathcal{A}_{ii}) \geq \lambda(\mathcal{A}_{jj})$ for all $\mathcal{T}_j \in \Gamma(\mathcal{T}_i)$. A class with (generalized) eigenvalue equal to the maximum (generalized) eigenvalue is called *basic*, and any other class is *nonbasic*. Clearly, all basic classes are principle. Moreover, all final classes are trivially principle. Thus, we have the following corollary to Theorem 7.4.5

Corollary 7.4.4 *Let $\mathcal{A} \in \mathbb{R}_{\max}^{n \times n}[X]$ be a polynomial matrix in Frobenius normal form with c classes $\mathcal{T}_1, \dots, \mathcal{T}_c$. Then*

- (i) $\lambda_0 = \bigoplus_{i=1}^c \lambda(\mathcal{A}_{ii}) \in \text{spec}(\mathcal{A})$.
- (ii) $\lambda(\mathcal{A}_{ii}) \in \text{spec}(\mathcal{A})$ for each final class $\mathcal{T}_i \subseteq \mathcal{T}$.

Remark Theorem 7.4.5 is formulated according to the convention in max-plus algebra that the ij -th entry of a (polynomial) matrix corresponds to the (marked) arc (j, i) in the precedence graph (timed event graph) [11]. In conventional graph theory an arc (j, i) corresponds to the ji -th entry of the adjacency matrix [16, 18]. The ‘reversed arc’ convention in max-plus algebra enables a familiar linear system equation $x(k) = Ax(k-1)$ with column vectors $x(\cdot)$, as opposed to a dynamic equation $y(k) = y(k-1)M$ for row vectors $y(\cdot)$ (which is however customary in Markov chain theory). The “reverse” statement of the theorem is the following: the set of eigenvalues is determined by the maximum eigenvalue of all classes that are accessible from a given class [13, 31]. \square

According to Theorem 7.4.5 any principle class \mathcal{T}_i of a (polynomial) matrix, or its index set, defines a (generalized) eigenvector with finite entry v^j only if j is accessible from class \mathcal{T}_i , in which case it is the weight of a longest path from a selected critical node $l \in \mathcal{T}_i$ to j in the precedence graph $G(A_\lambda)$. If the critical graph $G^c(A_{[\mathcal{T}_i|\mathcal{T}_i]}(\lambda^{-1}))$ restricted to the nodes of class \mathcal{T}_i has several disconnected critical circuits then \mathcal{T}_i defines several weakly-independent (generalized) eigenvectors associated to the generalized eigenvalue $\lambda(\mathcal{A}) = \lambda(\mathcal{A}_{ii})$, analogous to an irreducible (polynomial) matrix. However, these (generalized) eigenvectors have the same support. More important are (generalized) vectors resulting from distinct principle classes with the same (generalized) eigenvalue, which have access to different classes conform the precedence ordering in the reduced graph.

Define for each $\lambda \in \text{spec}(\mathcal{A})$ the set of principle classes with eigenvalue λ as

$$\mathcal{K}(\lambda) = \left\{ \mathcal{T}_i \mid \lambda(\mathcal{A}_{ii}) = \lambda, \lambda(\mathcal{A}_{ii}) = \bigoplus_{\mathcal{T}_j \subseteq \Gamma(\mathcal{T}_i)} \lambda(\mathcal{A}_{jj}), 1 \leq i \leq c \right\}. \quad (7.34)$$

Then the events that are accessible from any principle class with generalized eigenvalue $\lambda \in \text{spec}(\mathcal{A})$ is

$$K_\lambda = \Gamma(\mathcal{K}(\lambda)) = \bigcup_{\mathcal{T}_k \in \mathcal{K}(\lambda)} \Gamma(\mathcal{T}_k) = \{1 \leq j \leq n \mid \exists \mathcal{T}_k \in \mathcal{K}(\lambda) : \mathcal{T}_k \rightarrow j\}. \quad (7.35)$$

Theorem 7.4.6 (Eigenspace) *Let $\mathcal{A} \in \mathbb{R}_{\max}^{n \times n}[X]$ be a polynomial matrix in Frobenius normal form with c classes $\mathcal{T}_1, \dots, \mathcal{T}_c$, $\lambda \in \text{spec}(\mathcal{A})$, and define $\bar{A}_\lambda = A_{[K_\lambda|K_\lambda]}(\lambda^{-1}) \in \mathbb{R}_{\max}^{K_\lambda \times K_\lambda}$. If the*

critical graph $G^c(\bar{A}_\lambda)$ has v strongly-connected components with index sets K_1^c, \dots, K_v^c then the eigenspace $\mathcal{V}(\lambda) \subseteq \mathbb{R}_{\max}^n$ of generalized eigenvectors associated to λ is a finitely-generated semimodule of weak dimension v with weak basis $\{v_{i_1}, \dots, v_{i_v}\}$ defined as

$$v_{i_k}^j = \begin{cases} [A_\lambda^+]_{ji_k} & \text{if } j \in K_\lambda \\ \varepsilon & \text{otherwise,} \end{cases} \quad (7.36)$$

where the indices $i_k \in K_k^c$ are arbitrarily selected from each critical component for all $k = 1, \dots, v$.

Proof: The classes in K_λ have maximum generalized eigenvalue λ corresponding to the principle classes in $\mathcal{K}(\lambda)$. Therefore, analogous to Lemma 7.4.2 $\bar{A}_\lambda = A_{[K_\lambda|K_\lambda]}(\lambda^{-1}) \in \mathbb{R}_{\max}^{K_\lambda \times K_\lambda}$ has maximum eigenvalue e . For all (critical) nodes i on a critical circuit of a principle class, we then have $[\bar{A}_\lambda^+]_{ii} = [A_\lambda^+]_{ii} = e$ and therefore the critical graph $G^c(\bar{A}_\lambda)$ is the union of the critical graphs of the principle classes. Moreover, the critical circuits of different principle classes are by definition separate components in the critical graph, and so there are $v \geq c$ number of components in the critical graph. From Theorem 7.4.3 it then follows that the generalized eigenvectors associated to the nodes in the critical graph $G^c(\bar{A}_\lambda)$ span the eigensemimodule $\mathcal{V}(\lambda)$, i.e.,

$$\mathcal{V}(\lambda) = \bigoplus_{i \in I} c_i v_i \quad \text{with} \quad I = V^c = \{1 \leq i \leq n \mid [A_\lambda^+]_{ii} = e\},$$

where $c_i \in \mathbb{R}_{\max}$ and the vectors v_i are defined by (7.36). Recall that K_λ is the union of $\Gamma(\mathcal{T}_k)$ over the principle classes $\mathcal{T}_k \in \mathcal{K}(\lambda)$ by (7.35), whence (7.36) coincides with (7.31). It remains to prove that a weak basis of $\mathcal{V}(\lambda)$ is obtained by selecting an arbitrary node i_k from each component K_k^c in $G^c(\bar{A}_\lambda)$, $1 \leq k \leq v$.

We first prove that generalized eigenvectors of different classes are weakly independent. Consider the accessibility relations between the classes $\mathcal{T}_1, \dots, \mathcal{T}_c$ conform the reduced graph associated to \mathcal{A} , see Section 7.4.3. We are interested in the principle classes $\mathcal{T}_i \in \mathcal{K}(\lambda)$ and their descendants in the reduced graph, which are exactly the classes accessible from the principle classes in $\mathcal{K}(\lambda)$, i.e., $\Gamma(\mathcal{K}(\lambda)) = K_\lambda$. For any sequence $\mathcal{T}_{k_1} \prec \mathcal{T}_{k_2} \prec \mathcal{T}_{k_3}$ in the reduced graph we have $\Gamma(\mathcal{T}_{k_1}) \supset \Gamma(\mathcal{T}_{k_2}) \supset \Gamma(\mathcal{T}_{k_3})$. Now, consider any principle class $\mathcal{T}_k \in \mathcal{K}(\lambda)$, which generates a generalized eigenvector v_{i_k} with support $\Gamma(\mathcal{T}_k)$ by (7.36). Then there does not exist a linear combination of generalized eigenvectors associated to the other principle classes in $\mathcal{K}(\lambda) \setminus \mathcal{T}_k$ with the same support, which is proved as follows. For any preceding class $\mathcal{T}_j \prec \mathcal{T}_k$ in the reduced graph we have $\Gamma(\mathcal{T}_k) \subset \Gamma(\mathcal{T}_j)$, and in particular $\mathcal{T}_j \not\subseteq \Gamma(\mathcal{T}_k)$. Thus, a generalized vector associated to a preceding class has larger support than v_{i_k} and a linear combination including such a vector will also have larger support unless the associated coefficient is ε . On the other hand, for all succeeding classes $\mathcal{T}_j \succ \mathcal{T}_k$ in the reduced graph we have $\Gamma(\mathcal{T}_k) \supset \Gamma(\mathcal{T}_j)$, and in particular $\mathcal{T}_k \not\subseteq \Gamma(\mathcal{T}_j)$ for all $\mathcal{T}_j \succ \mathcal{T}_k$. Hence, v_{i_k} cannot be written as a linear combination of generalized eigenvectors associated to classes succeeding \mathcal{T}_i . This proves that v_{i_k} is weakly independent of the generalized eigenvectors from other (principle) classes.

Finally, if a class has more than one component in the critical graph then the generalized eigenvectors associated to each component have the same support but are weakly independent, which is proved as follows. Partition the vectors according to $v = (v_{[\mathcal{T}_k]}, v_{[\bar{\mathcal{T}}_k]})$, where $\bar{\mathcal{T}}_k = \mathcal{T} \setminus \mathcal{T}_k$. By Theorem 7.4.3 the partial vectors corresponding to \mathcal{T}_k are weakly independent, and they remain weakly independent regardless of a dimension expansion. \square

By Theorem 7.4.6 a generalized eigenvector associated to a generalized eigenvalue $\lambda \in \text{spec}(\mathcal{A})$ has maximum support $K_\lambda = \cup_{\mathcal{T}_i \in \mathcal{K}(\lambda)} \Gamma(\mathcal{T}_i)$. In particular we have the following.

Corollary 7.4.5 *Let $\mathcal{A} \in \mathbb{R}_{\max}^{n \times n}[X]$ be any reducible polynomial matrix. Then \mathcal{A} has a finite generalized eigenvector $v > \varepsilon$ if and only if all initial classes are basic.*

A consequence of this corollary (or of Theorem 7.4.6) is that if a polynomial matrix has several distinct generalized eigenvalues with maximum generalized eigenvalue λ_0 then all generalized eigenvectors associated to some $\lambda \in \text{spec}(\mathcal{A})$ with $\lambda < \lambda_0$ have zero entries ε .

Example 7.4 Consider the following matrices in $\mathbb{R}_{\max}^{2 \times 2}$:

$$A = \begin{bmatrix} 4 & \varepsilon \\ \varepsilon & 5 \end{bmatrix}, \quad B = \begin{bmatrix} 4 & \varepsilon \\ 2 & 5 \end{bmatrix}, \quad C = \begin{bmatrix} 4 & 2 \\ \varepsilon & 5 \end{bmatrix}.$$

All three matrices are reducible and have 2 classes, $\mathcal{T}_1 = \{1\}$ and $\mathcal{T}_2 = \{2\}$. Matrix A consists of two isolated classes with eigenvalue $\lambda(A_{11}) = 4$ and $\lambda(A_{22}) = 5$. Hence, $\text{spec}(A) = \{5, 4\}$. The unit vector $(\varepsilon, e)^\top$ is an eigenvector associated to $\lambda_0(A) = 5$ and $(e, \varepsilon)^\top$ is an eigenvector associated to $\lambda_1(A) = 4$. Matrix B has the same classes as A , but now class $\mathcal{T}_1 = \{1\}$ has access to class $\mathcal{T}_2 = \{2\}$ with $\lambda(B_{11}) = 4 < 5 = \lambda(B_{22})$, and therefore by Theorem 7.4.5 the local eigenvalue $\lambda(B_{11})$ is not an eigenvalue of B . Hence, B has only one eigenvalue, $\text{spec}(B) = \{5\}$, corresponding to the final basic class $\mathcal{T}_2 = \{2\}$ and an associated eigenvector is the unit vector $(\varepsilon, e)^\top$. Matrix C has two classes $\mathcal{T}_1 \succ \mathcal{T}_2$ with $\lambda(C_{11}) = 4$ and $\lambda(C_{22}) = 5$. Both class eigenvalues are eigenvalues of C by Corollary 7.4.4, since \mathcal{T}_1 is final and \mathcal{T}_2 has maximum eigenvalue. Indeed, the final class \mathcal{T}_1 trivially satisfies Theorem 7.4.5 because $\Gamma_1 = \mathcal{T}_1 = \{1\}$. For class \mathcal{T}_2 we obtain $\Gamma_2 = \{1, 2\}$, and therefore $\lambda(C_{22}) = 5 \geq \lambda(C_{11}) \otimes \lambda(C_{22}) = 4 \otimes 5 = 5$. Hence, $\text{spec}(C) = \{5, 4\}$ by Theorem 7.4.5. Two distinct eigenpairs of C are $(4, (\varepsilon, e)^\top)$ and $(5, (3, e)^\top)$. The latter eigenpair also illustrates Corollary 7.4.5. Moreover, since $B = C^\top$, this example also proves that in max-plus algebra we can have $\text{spec}(B) \neq \text{spec}(B^\top)$ in contrast to conventional linear algebra. \square

Example 7.5 Consider again the polynomial matrix $\mathcal{A} \in \mathbb{R}_{\max}^{6 \times 6}[X]$ of Example 7.3 with associated timed event graph shown in Figure 7.4. The generalized eigenvalues of the four irreducible classes can be computed using Theorem 7.4.1. \mathcal{T}_1 has two circuits with maximum cycle mean $\eta_1 = (28 \otimes 30)^1 \oplus 55 = \max(28 + 30, 55) = 58$; \mathcal{T}_2 has one circuit with cycle mean $\eta_2 = 40$; \mathcal{T}_3 has one circuit with cycle mean $\eta_3 = (25 \otimes 25)^1 = 50$; and \mathcal{T}_4 has one circuit with cycle mean $\eta_4 = 58$. Using Theorem 7.4.5 we obtain $\text{spec}(\mathcal{A}) = \{58, 50\}$. The maximum generalized eigenvalue is $\lambda_0 = \bigoplus_{i=1}^4 \eta_i = 58$ corresponding to the initial basic class \mathcal{T}_1 and the final basic class \mathcal{T}_4 . The other generalized eigenvalue 50 corresponds to the nonbasic final class \mathcal{T}_3 . Class \mathcal{T}_2 with generalized eigenvalue 40 does not contribute to $\text{spec}(\mathcal{A})$, since $\mathcal{T}_2 \prec \mathcal{T}_3$ and $\lambda(\mathcal{A}_{22}) = 40 \leq \lambda(\mathcal{A}_{33}) = 50$. Hence, the generalized eigenvalue of \mathcal{T}_2 is “disguised” by the accessibility relations between the communication classes.

We next determine the generalized eigenvectors associated to the maximum generalized eigenvalue $\lambda_0(\mathcal{A}) = 58$. First, we compute the valuated polynomial function $A_{\lambda_0} = A(58^{-1}) =$

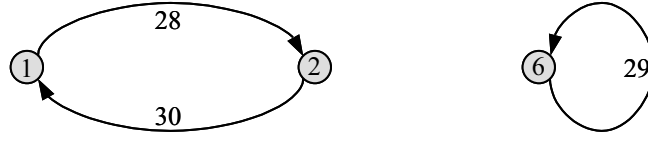


Figure 7.6 Critical graph of Example 7.5

$A(-58)$ and its associated longest path matrix:

$$A_{\lambda_0} = \begin{bmatrix} \varepsilon & -28 & \varepsilon & \varepsilon & \varepsilon & \varepsilon \\ 28 & -3 & \varepsilon & \varepsilon & \varepsilon & \varepsilon \\ \hline \varepsilon & 5 & -18 & \varepsilon & \varepsilon & \varepsilon \\ 3 & \varepsilon & \varepsilon & \varepsilon & -33 & \varepsilon \\ \hline \varepsilon & \varepsilon & 20 & 25 & \varepsilon & \varepsilon \\ \hline \varepsilon & 5 & \varepsilon & \varepsilon & \varepsilon & e \end{bmatrix} \quad \text{and} \quad A_{\lambda_0}^+ = \begin{bmatrix} e & -28 & \varepsilon & \varepsilon & \varepsilon & \varepsilon \\ 28 & e & \varepsilon & \varepsilon & \varepsilon & \varepsilon \\ 33 & 5 & -18 & 7 & \varepsilon & \varepsilon \\ 20 & -8 & -13 & -8 & -33 & \varepsilon \\ 53 & 25 & 20 & 25 & -8 & \varepsilon \\ 33 & 5 & \varepsilon & \varepsilon & \varepsilon & e \end{bmatrix}.$$

By Theorem 7.4.6 the columns of the longest path matrix with diagonal entries equal to e are generalized eigenvectors of \mathcal{A} associated to the maximum eigenvalue $\lambda_0 = 58$, which are here the columns 1, 2 and 6 of $A_{\lambda_0}^+$. The first two columns are obviously weakly dependent, since $[A_{\lambda_0}^+]_{\cdot 1} = 28 \otimes [A_{\lambda_0}^+]_{\cdot 2}$. Figure 7.6 shows the critical graph $G^c(A_{\lambda_0})$ which clearly consists of two strongly-connected components $V^c = K_1^c \cup K_2^c$, with $K_1^c = \{1, 2\}$ and $K_2^c = \{6\}$. By Theorem 7.4.6 the eigenspace associated to λ_0 is generated by the remaining two weakly independent vectors and is therefore

$$\mathcal{V}(\lambda_0) = c_1 \otimes \begin{bmatrix} e \\ 28 \\ 33 \\ 20 \\ 53 \\ 33 \end{bmatrix} \oplus c_2 \otimes \begin{bmatrix} \varepsilon \\ \varepsilon \\ \varepsilon \\ \varepsilon \\ \varepsilon \\ e \end{bmatrix}. \quad (7.37)$$

This eigenspace is a two-dimensional subsemimodule of \mathbb{R}_{\max}^6 .

The generalized eigenvectors associated to the second generalized eigenvalue $\lambda_1 = 50$ is by Theorem 7.4.6 obtained from the principal submatrix $\bar{A}_{\lambda_1} = A_{[\mathcal{T}_3|\mathcal{T}_3]}(\lambda_1^{-1})$ and its associated longest path matrix,

$$\bar{A}_{\lambda_1} = \begin{bmatrix} \varepsilon & -25 \\ 25 & \varepsilon \end{bmatrix} \quad \text{and} \quad \bar{A}_{\lambda_1}^+ = \begin{bmatrix} e & -25 \\ 25 & e \end{bmatrix}.$$

Both diagonal entries of $\bar{A}_{\lambda_1}^+$ are zero and therefore both columns of $\bar{A}_{\lambda_1}^+$ correspond to generalized eigenvectors. The columns belong to the same circuit and therefore are weakly dependent, $[\bar{A}_{\lambda_1}^+]_{\cdot 1} = 25 \otimes [\bar{A}_{\lambda_1}^+]_{\cdot 2}$. Applying Theorem 7.4.6 a generalized eigenvector associated to $\lambda_1 = 50$ is $(\varepsilon, \varepsilon, \varepsilon, e, 25, \varepsilon)^T$ and the eigenspace $\mathcal{V}(\lambda_1)$ associated to $\lambda_1 = 50$ is the one-dimensional subsemimodule of \mathbb{R}_{\max}^6 spanned by this generalized eigenvector. \square

7.4.5 The Cycle Time Vector

The maximal performance of a periodic system is determined by the slowest component in the interconnection structure. Therefore we define the *cycle time vector* $\chi = (\chi_1, \dots, \chi_n)^T$ where

each χ_i equals the maximal generalized eigenvalue of the irreducible classes that have access to event i . For a polynomial matrix \mathcal{A} in Frobenius normal form with c classes $\mathcal{T}_1, \dots, \mathcal{T}_c$ this gives

$$\chi_i = \bigoplus_{\mathcal{T}_k \rightarrow i} \lambda(\mathcal{A}_{kk}) \quad \text{for all } 1 \leq i \leq n. \quad (7.38)$$

Moreover, we define a generalized *eigenmode* of a polynomial matrix \mathcal{A} as a pair (χ, v) of a cycle time vector χ and an associated *bias* vector v that satisfies for all $1 \leq i \leq n$:

$$v_i = \bigoplus_{j=1}^n \bigoplus_{l=0}^p ([A_l]_{ij} \otimes \chi_j^{-l} \otimes v_j).$$

If $\mathcal{A} \in \mathbb{R}_{\max}^{n \times n}[X]$ is an irreducible polynomial matrix then the bias vector is equivalent to the eigenvector, and this is also true for reducible polynomial matrices with a constant cycle time vector, i.e., when the initial classes are also basic. In the general reducible case however the cycle time vector may have different entries. If the bias vector is partitioned accordingly then the partial bias vectors augmented with zero entries are generalized eigenvectors corresponding to the various cycle time entries. Hence, if $I \subseteq \{1, \dots, n\}$ is an index set of equal cycle time entries then this cycle time is a generalized eigenvalue of \mathcal{A} with associated generalized eigenvector $x \in \mathbb{R}_{\max}^n$ given by $x_i = v_i$ if $i \in I$ and $x_i = \varepsilon$ if $i \notin I$. The generalized eigenmode thus corresponds to the worst-case generalized eigenstructure of the system.

In the forthcoming we will assume that each event i has a predecessor. Hence, the timed event graph has no source events, or equivalently, the polynomial matrix has no zero rows. Moreover, we assume that each circuit has at least one token, i.e., $G(A_0)$ is acyclic.

Definition 7.4.4 (Nondegeneracy) A polynomial matrix $\mathcal{A} = \bigoplus_{l=0}^p A_l X^l \in \mathbb{R}_{\max}^{n \times n}[X]$ is called nondegenerate if

- (i) Each row has at least one finite entry, or formally, for all $1 \leq i \leq n$ there exists $1 \leq j \leq n$ and $0 \leq l \leq p$, such that $[A_l]_{ij} \neq \varepsilon$,
- (ii) $G(A_0)$ is acyclic, i.e., $\text{tr}(A_0^+) = \bigoplus_{i=1}^n [A_0^+]_{ii} = \varepsilon$.

For the eigenproblem of a square max-plus matrix the acyclicity condition on $G(A_0)$ is superfluous, since this case corresponds to $\mathcal{A} = A_1 X$, and therefore $A_0 = \mathcal{E}$. Hence, in this case nondegeneracy is equivalent to the requirement that A has no empty rows.

Lemma 7.4.6 A polynomial matrix $\mathcal{A} = \bigoplus_{l=0}^p A_l X^l \in \mathbb{R}_{\max}^{n \times n}[X]$ is nondegenerate if and only if its associated timed event graph $\mathcal{G}(\mathcal{A})$ is autonomous and live.

Proof: By definition an autonomous timed event graph has no source transitions and therefore each transition i must have an incoming place (j, i, l) , or equivalently, each row i of the associated polynomial matrix must have at least one finite entry $[A_l]_{ij} \neq \varepsilon$. By Theorem 6.4.1 a timed event graph is live if and only if there are no circuits with zero tokens or equivalently iff $G(A_0)$ has no circuits. Hence, $[A_0^\ell]_{ii} = \varepsilon$ for all $1 \leq i, \ell \leq n$, or equivalently, $[A_0^+]_{ii} = \varepsilon$ for all $1 \leq i \leq n$, which can be abbreviated to the condition $\text{tr}(A_0^+) = \bigoplus_{i=1}^n [A_0^+]_{ii} = \varepsilon$. \square

The nondegeneracy condition on a polynomial matrix is a necessary and sufficient condition for the existence of a finite cycle time vector, that is, it guarantees that each transition i has a finite cycle time $\varepsilon < \chi_i < \infty$. This is formally stated in the following theorem.

Theorem 7.4.7 *Let $\mathcal{A} = \bigoplus_{l=0}^p A_l X^l \in \mathbb{R}_{\max}^{n \times n}[X]$ be a nondegenerate polynomial matrix. Then \mathcal{A} has a finite cycle time vector $\chi > \varepsilon$, and the entry χ_i is equal to the maximum cycle mean over all classes that have access to i for all $1 \leq i \leq n$.*

Proof: The timed event graph $\mathcal{G}(\mathcal{A})$ is finite with n transitions and $m \leq n \cdot n \cdot p + n - 1$ places, where the worst-case bound corresponds to full matrices A_l for $1 \leq l \leq p$ and $|\text{supp}(A_0)| = n - 1$ corresponding to a maximum spanning tree with zero tokens. Recall that a maximum spanning tree is the most dense simple graph that has no cycles. From the nondegeneracy condition follows that each transition has an incoming place and because the event graph is finite this means that each transition has an upstream circuit. Moreover, nondegeneracy of \mathcal{A} implies that $G(A_0)$ is acyclic and therefore by Theorem 7.4.1 the generalized eigenvalue of each class equals the (finite) maximum cycle mean of the associated strongly connected component. By definition (7.38) each cycle time entry χ_i is the maximal generalized eigenvalue over all classes that have access to i , which is thus equivalent to the maximum of all (maximum) cycle means of those classes. Hence, each event i has at least one upstream circuit and the maximum cycle mean over all upstream circuits defines the cycle time entry χ_i for all $1 \leq i \leq n$. \square

7.4.6 The Policy Iteration Algorithm

An efficient algorithm to compute the (generalized) eigenstructure of a max-plus (polynomial) matrix is the *policy iteration algorithm* developed by Cochet-Terrasson *et al.* [31] based on Howard's multichain policy iteration algorithm for Markov decision processes with average reward [103], which is well-known in the fields of dynamic programming and stochastic control, see e.g. Puterman [168].

The policy iteration algorithm applies to nondegenerate irreducible and reducible polynomial matrices. In the irreducible case it computes the generalized eigenvalue, an associated generalized eigenvector, and an optimal policy from which a critical circuit is easily determined. In the reducible case the policy iteration algorithm computes for each transition the maximal generalized eigenvalue that has access to it, and an associated eigenvector with maximal support. Hence, the algorithm computes the generalized eigenmode (χ, v) of a nondegenerate polynomial matrix \mathcal{A} and moreover is generally applicable without prior knowledge on the class structure of the polynomial matrix.

In the sequel we will utilize the adjacency list representation (6.6) of the places (or marked arcs) $p_k = (j, i, l) \in \mathcal{P}$, $1 \leq k \leq m$, which unambiguously identifies all places in the timed event graph associated to the finite polynomial matrix entries $[A_l]_{ij}$. Recall that this is a sparse (polynomial) matrix notation. Define for each event $i \in \mathcal{T}$ the set $\Pi_i \subseteq \mathcal{P}$ of incoming places as

$$\Pi_i \doteq \{p_k \in \mathcal{P} \mid \text{out}(p_k) = i\} = \{(j, i, l) \mid [A_l]_{ij} \neq \varepsilon, 1 \leq j \leq n, 0 \leq l \leq p\}.$$

Then the *generalized eigenproblem* is to find a generalized eigenmode (χ, v) , such that for all

$$1 \leq i \leq n$$

$$\chi_i = \bigoplus_{(j,i,l) \in \Pi_i} \chi_j = \max_{(j,i,l) \in \Pi_i} \chi_j, \quad (7.39a)$$

$$v_i = \bigoplus_{(j,i,l) \in \Pi_i} ([A_l]_{ij} \otimes \chi_j^{-l} \otimes v_j) = \max_{(j,i,l) \in \Pi_i} ([A_l]_{ij} - l \cdot \chi_j + v_j). \quad (7.39b)$$

We will refer to (7.39a) as the *first-order optimality equation* and to (7.39b) as the *second-order optimality equation*. The key to the policy iteration algorithm is a policy. A *policy* is a vector function $\pi : \mathcal{T}^n \rightarrow \mathcal{P}^n$ that maps each transition to one of its incoming places, i.e.,

$$\pi_i = p_k \in \Pi_i \quad \text{for all } i \in \mathcal{T}.$$

An entry $\pi_i \in \Pi_i$ is also simply called the policy of transition i . The holding time, initial marking, input transition, and output transition of a policy π_i are denoted as $w(\pi_i)$, $\mu(\pi_i)$, $\text{in}(\pi_i)$, and $\text{out}(\pi_i)$, respectively. A polynomial matrix representation of a policy π is $\mathcal{A}^\pi = \bigoplus_{l=0}^p A_l^\pi X^l$, where each row i has exactly one finite entry $[A_l]_{ij} > \varepsilon$ conform

$$[A_l^\pi]_{ij} = \begin{cases} w(\pi_i) & \text{if } \text{in}(\pi_i) = j \text{ and } \mu(\pi_i) = l \\ \varepsilon & \text{otherwise.} \end{cases}$$

Let $\mathcal{P}^\pi = \{\pi_1, \dots, \pi_n\} \subseteq \mathcal{P}$ be the set of places in the policy π . A *policy graph* is the timed event graph $\mathcal{G}(\mathcal{A}^\pi) = (\mathcal{T}, \mathcal{P}^\pi, \mu(\pi), w(\pi))$ associated to a policy π , which is a simple subgraph of $\mathcal{G}(\mathcal{A})$ with each transition $1 \leq i \leq n$ having indegree one, that is, each transition has exactly one incoming place. By the following lemma the number of circuits in a policy graph $\mathcal{G}(\mathcal{A}^\pi)$ is finite.

Lemma 7.4.7 *Let $\mathcal{G}(\mathcal{A}^\pi)$ be a timed event graph associated to a policy π . Then each connected component of $\mathcal{G}(\mathcal{A}^\pi)$ contains one and only one circuit.*

Proof: By definition of a policy each place has a unique output transition and therefore $\mathcal{G}(\mathcal{A}^\pi)$ does not contain parallel places. Hence, $\mathcal{G}(\mathcal{A}^\pi)$ is a simple (timed event) graph. From graph theory it is well-known that a connected (timed event) graph with n nodes (transitions) and no cycles has exactly $n - 1$ arcs (places), corresponding to a spanning tree; any additional arc (place) will generate a circuit, and furthermore deleting any arc (place) will make the graph no longer connected [16, Ch. 16]. As an immediate consequence, if $\mathcal{G}(\mathcal{A}^\pi)$ is connected and contains n places then it has exactly 1 circuit. Now, suppose $\mathcal{G}(\mathcal{A}^\pi)$ has c components. Then it contains a forest of c trees spanning the components. A straightforward extension of the above shows that this spanning forest has $n - c$ places: assume that the trees have n_1, \dots, n_c transitions, respectively, with $\sum_{i=1}^c n_i = n$. Then each tree contains $n_i - 1$ places, and together they possess $\sum_{i=1}^c (n_i - 1) = n - c$ places. In a policy each transition must have an incoming place, whilst a (finite) tree contains by definition a transition without predecessor. Hence, each tree in the forest needs at least one additional place, which generates exactly one circuit in each of the c components. \square

The proof of Lemma 7.4.7 also reveals the structure of a policy (timed event) graph $\mathcal{G}(\mathcal{A}^\pi)$: each component consists of a ‘base’ circuit with possibly some outgoing paths or trees. This topology guarantees that each transition has an incoming place, and furthermore, corresponds to the timed event graph with the least number of places with this property. This structure also has the following consequence.

Lemma 7.4.8 *Let $\mathcal{A}^\pi \in \mathbb{R}_{\max}^{n \times n}[X]$ be a polynomial matrix associated to a policy π . Then \mathcal{A}^π has a finite cycle time vector $\chi > \varepsilon$, which is uniquely determined.*

Proof: By Lemma 7.4.7 each transition i in the policy graph $\mathcal{G}(\mathcal{A}^\pi)$ has one and only one upstream circuit, and therefore the cycle time χ_i of transition i is uniquely determined by the cycle mean of this circuit. This holds for all transitions in the same connected component which therefore share the same unique cycle time. Note that here a component is not *strongly* connected, except for the trivial case that the circuit covers all transitions. The connected components are a partitioning of $\mathcal{T} = \{1, \dots, n\}$ and therefore the direct sum of the cycle time vector components gives a cycle time vector of full support. \square

Finding a generalized eigenmode of a policy polynomial matrix is called *policy evaluation*. Policy evaluation involves finding the circuits and connected components, computing the cycle mean of the circuits, and computing an associated generalized eigenvector. Lemma 7.4.7 suggest a simple procedure to find all circuits in the policy event graph: starting from an arbitrary transition just follow the associated policies backwards until an already visited transition is revisited. This transition, say s , then obviously lies on a circuit. By Lemma 7.4.7 this is the only circuit in the component of the policy graph containing s . Hence, the cycle mean of this circuit is the unique generalized eigenvalue χ for all events accessible from s in $\mathcal{G}(\mathcal{A}^\pi)$. By Theorem 7.4.5 the associated entries of the generalized eigenvector are given by the longest path weights in $G(\mathcal{A}_\chi^\pi)$ from s to all accessible events, which can efficiently be computed using a *breadth-first search* (BFS) algorithm [39]. In BFS the transitions are visited in topological order from s , by which the value of $v_{\text{in}(\pi(i))}$ is determined before reaching transition i and therefore v_i can be computed directly by $v_i = w(\pi_i) - \mu(\pi_i) \cdot \chi_{\text{in}(\pi_i)} + v_{\text{in}(\pi_i)}$.

A given policy π^k with generalized eigenmode (χ^k, v^k) is optimal iff it satisfies the optimality conditions (7.39a–7.39b). So a policy π^k can be improved if there exists a place $p = (j, i, l) \in \Pi_i$ with $\chi_j^k > \chi_i^k$ for some transition $1 \leq i \leq n$, conform the first-order optimality condition (7.39a). In this case transition i can be connected to a component with higher cycle time. Let

$$\pi_i^{k+1} = \arg \max_{(j,i,l) \in \Pi_i} \chi_j^k.$$

Then if $\chi_i^{k+1} \neq \chi_i^k$ at least one transition is improved under the new policy. However, if $\chi_i^{k+1} = \chi_i^k$ then we must still check the second-order optimality condition (7.39b). If for any transition i there is a predecessor j over a place with l tokens such that $v_i^k < [A_l]_{ij} - l \cdot \chi_j^k + v_j^k$ then π_i^k is not optimal, and an improved policy is found by

$$\pi_i^{k+1} = \arg \max_{(j,i,l) \in \Pi_i} ([A_l]_{ij} - l \cdot \chi_j^k + v_j^k).$$

The *policy iteration algorithm* computes the maximum generalized eigenmode of a polynomial matrix $\mathcal{A} \in \mathbb{R}_{\max}^{n \times n}[X]$ by exploiting the efficient computation of the generalized eigenmode of a policy graph and successively improving policies until an optimal policy has been found. In general, the policy iteration algorithm starts with an arbitrary policy—select any incoming place for each transition—and then iterates between a *policy evaluation* step which computes a generalized eigenmode corresponding to a given policy, and a *policy improvement* step which tries to improve the current policy. If no more improvement can be found, the generalized

Algorithm 7.4.1 (POLICYITERATION)

Input: Adjacency list $\{(\text{in}(p), \text{out}(p), \mu(p), w(p))\}_{p \in \mathcal{P}}$ of nondegenerate polynomial matrix $\mathcal{A} \in \mathbb{R}_{\max}^{n \times n}[X]$.

Output: Generalized eigenmode (χ, v) of \mathcal{A} .

```

1   $k \leftarrow 0$ ; improved  $\leftarrow 1$ ; for  $i \leftarrow 1$  to  $n$  do  $v_i^0 \leftarrow -\infty$ ; //Initialization
2  for each  $p \in \mathcal{P}$  do //Heuristic for initial policy
3      if  $\mu(p) > 0$  then if  $w(p)/\mu(p) > v_{\text{out}(p)}^0$  then  $v_{\text{out}(p)}^0 \leftarrow w(p)/\mu(p)$ ;  $\pi_{\text{out}(p)}^1 \leftarrow p$ ;
4      else if  $w(p) > v_{\text{out}(p)}^0$  then  $v_{\text{out}(p)}^0 \leftarrow w(p)$ ;  $\pi_{\text{out}(p)}^1 \leftarrow p$ ;
5  while improved do //Main loop (policy iteration)
6       $k \leftarrow k + 1$ ;  $c \leftarrow 0$ ; for  $i \leftarrow 1$  to  $n$  do component( $i$ )  $\leftarrow 0$ ; //New iteration
7      for  $j \leftarrow 1$  to  $n$  do //Policy evaluation
8          if component( $j$ ) = 0 then //New component
9               $c \leftarrow c + 1$ ;  $s \leftarrow j$ ;
10             while component( $s$ ) = 0 do component( $s$ )  $\leftarrow c$ ;  $s \leftarrow \text{in}(\pi_s^k)$ ;
11              $w_c \leftarrow w(\pi_s^k)$ ;  $\mu_c \leftarrow \mu(\pi_s^k)$ ;  $i \leftarrow \text{in}(\pi_s^k)$ ;
12             while  $i \neq s$  do  $w_c \leftarrow w_c + w(\pi_i^k)$ ;  $\mu_c \leftarrow \mu_c + \mu(\pi_i^k)$ ;  $i \leftarrow \text{in}(\pi_i^k)$ ;
13              $\chi_s^k \leftarrow w_c/\mu_c$ ;  $v_s^k \leftarrow v_s^{k-1}$ ; //New cycle mean
14             Use breadth-first search to visit all events  $i$  accessible from  $s$  in  $\mathcal{G}(\mathcal{A}^{\pi^k})$  and let
15              $\chi_i^k \leftarrow \chi_s^k$ ;  $v_i^k \leftarrow w(\pi_i^k) - \mu(\pi_i^k) \cdot \chi_s^k + v_{\text{in}(\pi_i^k)}^k$ ; component( $i$ )  $\leftarrow c$ ;
16     improved  $\leftarrow 0$ ; //Policy improvement
17     for  $i \leftarrow 1$  to  $n$  do  $\chi_i^{k+1} \leftarrow \chi_i^k$ ;  $v_i^{k+1} \leftarrow v_i^k$ ;  $\pi_i^{k+1} \leftarrow \pi_i^k$ ;
18     if  $c > 1$  then for each  $p \in \mathcal{P}$  do //First order improvement
19         if  $\chi_{\text{in}(p)}^k > \chi_{\text{out}(p)}^{k+1}$  then  $\chi_{\text{out}(p)}^{k+1} \leftarrow \chi_{\text{in}(p)}^k$ ;  $\pi_{\text{out}(p)}^{k+1} \leftarrow p$ ; improved  $\leftarrow 1$ ;
20     if not improved then //Second order improvement
21         if  $c = 1$  then for each  $p \in \mathcal{P}$  do
22             if  $v_{\text{out}(p)}^{k+1} < w(p) - \mu(p) \cdot \chi_{\text{in}(p)}^k + v_{\text{in}(p)}^k$  then
23                  $v_{\text{out}(p)}^{k+1} \leftarrow w(p) - \mu(p) \cdot \chi_{\text{in}(p)}^k + v_{\text{in}(p)}^k$ ;  $\pi_{\text{out}(p)}^{k+1} \leftarrow p$ ; improved  $\leftarrow 1$ ;
24             else for each  $p \in \mathcal{P}$  do
25                 if  $\chi_{\text{in}(p)}^k = \chi_{\text{out}(p)}^k$  and  $v_{\text{out}(p)}^{k+1} < w(p) - \mu(p) \cdot \chi_{\text{in}(p)}^k + v_{\text{in}(p)}^k$  then
26                      $v_{\text{out}(p)}^{k+1} \leftarrow w(p) - \mu(p) \cdot \chi_{\text{in}(p)}^k + v_{\text{in}(p)}^k$ ;  $\pi_{\text{out}(p)}^{k+1} \leftarrow p$ ; improved  $\leftarrow 1$ ;
27 return  $(\chi^k, v^k)$  //Terminate

```

eigenmode of the policy satisfies both optimality conditions (7.39a–7.39b) and a solution to the generalized eigenproblem has been found.

Algorithm 7.4.1 gives the pseudo-code of the policy iteration algorithm using the adjacency list representation of the (sparse) polynomial matrix, i.e., a list

$$\{(\text{in}(p), \text{out}(p), \mu(p), w(p)) \mid p \in \mathcal{P}\} = \{(j, i, l, [A_l]_{ij}) \mid [A_l]_{ij} \neq \varepsilon\},$$

where the transitions are integers $\{1, \dots, n\}$. Lines 1–4 initialize the main variables. The counter k keeps track of the number of iterations, improved is a boolean variable that terminates the algorithm if at the end of a main iteration improved = 0, and v^0 is an initial value for the eigenvector. We refer to an entry v_i also as the *value* of transition i . Lines 2–4 define an initial policy using a greedy heuristic: the initial policy π_i^1 for transition i is set to the largest 'mean

weight' of all incoming places, i.e.,

$$\pi_i^1 \in \arg \max_{(j,i,l) \in \Pi_i} \frac{[A_l]_{ij}}{\max(1, l)},$$

with the convention that for the degenerate case $l = 0$ the 'mean weight' is set to $[A_l]_{ij}$ as in the case $l = 1$. This is implemented by checking for each place whether the actual value of the output transition can be improved using the 'mean weight' of the current place. This choice for the initial policy is customary but any other initial policy could be used as well.

Lines 5–27 contain the main loop of the algorithm which iterates until no more improvement is found (line 5), in which case the optimal policy has been found and the current eigenmode (χ^k, v^k) is returned as output of the algorithm (line 27). Line 6 updates the iteration counter, resets the number of found connected components c to 0, and initializes the variable component to 0 for all transitions. At the end of the k th iteration c is the number of connected components of policy π^k and $\text{component}(i)$ is the component of transition i .

Lines 7–15 implement the policy evaluation step, which computes the eigenmode of the policy component by component. For each transition j if $\text{component}(j) = 0$ then j has not yet been visited in iteration k and so a new component has been found (lines 7–8). Line 9 updates the component counter and initializes transition s to the current transition. Line 10 finds a critical transition using the policies to search the policy graph backwards starting from the current transition and labelling all visited transitions by updating the variable component until an already labelled transition is revisited, indicating that a circuit has been found containing the updated transition s . Lines 11–13 compute the cycle mean of the current component. Line 11 initializes two variables w_c and μ_c by the weight and marking of the policy of s , and line 12 walks backwards over the policies in the circuit updating the path weight and marking from s until s is revisited. Line 13 then sets the cycle time χ_s^k to the cycle mean computed by dividing the computed circuit weight by the circuit token count, and sets the value v_s^k to the value of s in the last iteration. The particular choice of the initial value v_s^k is customary and useful for analysis of the algorithm but could be set to any arbitrary value, in particular $v_s^k = 0$. Lines 14–15 visit all transitions accessible from s using breadth-first search, setting the cycle time equal to the computed cycle mean, the eigenvector value to the value of s plus the mean path weight from s , and component to the current component. Hence, together with transition j each transition in the same component has also been visited and evaluated before the algorithm returns to line 7, and therefore these transitions will be skipped in line 8. So if there is only one connected component in the k th policy then all transitions will be visited in the first iteration of line 7, and therefore all remaining iterations in line 7 will terminate directly in line 8. On the other hand, if there is a transition that has not yet been visited then there is at least one more component in the policy and the first unvisited transition that satisfies the condition of line 8 starts a new policy evaluation iteration for the next component.

Lines 16–26 implement the policy improvement step. Lines 16–17 reset the boolean variable improved to zero, and copies the current cycle time vector, eigenvector and policy. If more than one component has been found in the policy evaluation step then a first-order improvement may be found (lines 18–19). In this case for each place is checked whether the input transition has a higher cycle time than the output transition, and if so, the output transition is connected to the component with higher cycle time and an improved policy has been found for this transition. Note that in the comparison of cycle times (line 19) the updated cycle time of

the output transition is used which secures that only places with higher input cycle time than in the last improvement are accepted for a further improvement. If no first-order improvement has been found or if all transitions are already contained in one component then lines 20–26 check whether a second-order improvement can be found. If there is only one component in the current policy then for each place it is simply checked whether a higher value of the output transition can be obtained using this place instead of the actual policy, and if so, the value of the output transition is improved and a new policy has been found for this transition (lines 21–23). In the case of more than one component under the current policy the second-order improvement is only applicable to places with the same cycle time in both its input and output transition, in which case the same improvement procedure is applied as in the case of one component (lines 24–26). Note that since the first-order improvement must have been passed without improvement we know that if the cycle time of the input and output transition are not equal then the output transition is accessible from a transition with higher cycle time than the input transition. If an improved policy has been found for any of the transitions then at the end of the policy improvement routine $\text{improved} = 1$ and a new iteration starts from line 5, otherwise the algorithm terminates and returns the current generalized eigenmode (χ^k, v^k) as the solution.

Cochet-Terrasson *et al.* [31] proved the following theorem.

Theorem 7.4.8 *Let $\mathcal{A} = \bigoplus_{l=0}^p A_l X^l \in \mathbb{R}_{\max}^{n \times n}[X]$ be a nondegenerate polynomial matrix. Then the policy iteration algorithm converges to the optimal policy in a finite number of iterations, and $\lambda_0 = \bigoplus_{i=1}^n \chi_i$ is the maximum generalized eigenvalue of \mathcal{A} .*

Proposition 7.4.1 *Let $\mathcal{A} = \bigoplus_{l=0}^p A_l X^l \in \mathbb{R}_{\max}^{n \times n}[X]$ be a nondegenerate polynomial matrix. Then the policy iteration algorithm terminates in $I \cdot O(m)$ computation time, where m is the number of finite entries $[A_l]_{ij}$ and I is the number of iterations of the algorithm.*

Proof: The worst-case computational complexity of Algorithm 7.4.1 can be estimated as follows. The initialization step takes $O(n)$ to initialize v^0 (line 1) and $O(m)$ to compute the initial policy by checking all m places once (lines 2–4). Hence, the initialization takes $O(n) + O(m) = O(m)$ time. We now estimate the time complexity of one iteration of the main loop (lines 5–26). Starting a new iteration takes $O(n)$ time to reset the variable component for each transition. Policy evaluation only searches the policy graph, which has n transitions and also just n places. Consider one iteration of policy evaluation (lines 8–15). Let n_j denote the number of transitions (and places) in component $1 \leq j \leq c$, with c the total number of connected components in the policy. Line 10 searches the component backwards until a transition has been encountered twice. Hence, an upper bound for the number of transitions that have been visited before a transition is revisited is n_j . In lines 11–12 all transitions in the circuit contained in the component are visited, which can be at most n_j transitions corresponding to the case that the component is one big circuit. Lines 14–15 search all transitions in the component using BFS, which takes $O(n_j)$ time. Evaluating one component in a policy graph thus takes $3 \cdot O(n_j) = O(n_j)$ time. Hence, the iterations of line 7 take $(n-c) \cdot O(1) + \sum_{j=1}^c O(n_j) = O(n-c) + O(n) = O(n)$ time, where the first term corresponds to the $n - c$ cases that a transition of an already evaluated component is checked in line 8 which takes just $O(1)$ time. The policy improvement routine takes $O(m)$ time, since now all places are checked. If the policy has just one connected component then each place is checked in lines 21–23, which thus takes $O(m)$ time. If the policy has several components then first each place is checked for first-order improvements in

lines 18–19, taking $O(m)$ time, and if no improvements have been found then each place is checked again for the condition of the second-order improvements, which takes again $O(m)$ time. Hence, the worst-case situation takes $2 \cdot O(m) = O(m)$ time. The time complexity for the entire algorithm can thus be estimated as $O(m) + I \cdot (O(n) + O(m)) = I \cdot O(m)$, where I is the number of iterations of the main loop. \square

Cochet-Terrasson *et al.* [31] argue that the average value of the number I of iterations of the algorithm is small, and their experiments suggest that on the average $I = O(\log n)$. A worst-case bound for the number of iterations I is still an open problem. Nevertheless, extensive experiments conducted by Dasdan *et al.* [47, 49, 50] show that the policy iteration algorithm outperforms all other known algorithms for computing the maximum cycle mean. In Section 7.4.7 we briefly review the best known other maximum cycle mean algorithms and their running time bounds.

Example 7.6 Reconsider the polynomial matrix of Example 7.3 with the timed event graph of Figure 7.4. The maximal generalized eigenproblem is to find vectors $\chi, v \in \mathbb{R}_{\max}^6$, $v \neq \varepsilon$, such that

$$\chi_i = \bigoplus_{j \rightarrow i} \chi_j$$

and

$$\begin{bmatrix} \varepsilon & 30\chi_2^{-1} & \varepsilon & \varepsilon & \varepsilon & \varepsilon \\ 28 & 55\chi_2^{-1} & \varepsilon & \varepsilon & \varepsilon & \varepsilon \\ \varepsilon & 5 & 40\chi_3^{-1} & \varepsilon & \varepsilon & \varepsilon \\ 3 & \varepsilon & \varepsilon & \varepsilon & 25\chi_5^{-1} & \varepsilon \\ \varepsilon & \varepsilon & 20 & 25 & \varepsilon & \varepsilon \\ \varepsilon & 5 & \varepsilon & \varepsilon & \varepsilon & 58\chi_6^{-1} \end{bmatrix} \otimes \begin{bmatrix} v_1 \\ v_2 \\ v_3 \\ v_4 \\ v_5 \\ v_6 \end{bmatrix} = \begin{bmatrix} v_1 \\ v_2 \\ v_3 \\ v_4 \\ v_5 \\ v_6 \end{bmatrix}.$$

This example illustrates the working of the policy iteration algorithm. Note that the timed event graph has no parallel places, by which we may identify a place $p_k = (j, i, \mu(p_k), w(p_k))$ by its input and output transition, and a policy $\pi_i = p_k$ of a transition i is also completely determined by its input transition $\text{in}(\pi_i) = j$ — the predecessor transition of i . Figure 7.7 summarizes the successive policies and corresponding generalized eigenmodes of each iteration, which will be detailed below. The numbering of the transitions in the policy graphs of Figure 7.7 are consistent with Figure 7.4, so transition 1 is at the upper-left and transition 6 is at the lower-right.

Initialization. The degree of all polynomial entries is either zero or one, and therefore the initial eigenvector is determined as the maximal polynomial coefficient in each row, $v^0 = (30, 55, 40, 25, 25, 58)^\top$, and the initial policy is given by the associated column indices $\text{in}(\pi^1) = (2, 2, 3, 5, 4, 6)^\top$. The policy graph is shown in the top row of Figure 7.7. The bold bias values are determined in the 1st policy evaluation phase.

Policy evaluation of π^1 . The policy graph has 4 connected components. The first component has the loop around transition 2 as base circuit. This circuit is found by the algorithm by walking backwards over the policies. Starting with transition 1 this gives $\text{in}(\pi_1^1) = 2$ and $\text{in}(\pi_2^1) = 2$. Now we encountered transition 2 twice and so we have found a circuit. The cycle mean is $\chi_2^1 = w(\pi_2^1)/\mu(\pi_2^1) = 55/1 = 55$ and the value of root transition 2 is set to the initial value, $v_2^1 = v_2^0 = 55$. The only transition accessible from transition 2 is transition 1. Hence, we set $\chi_1^1 = \chi_2^1 = 55$ and $v_1^1 = 30 - 1 \cdot 55 + 55 = 30$. The next unlabelled transition is transition 3. The associated component consists of only one transition and a loop, so $\chi_3^1 = 40/1 = 40$ and

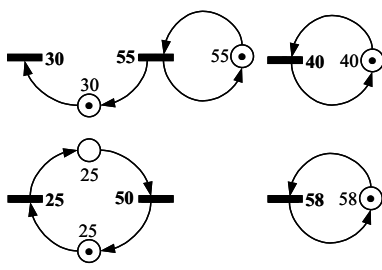
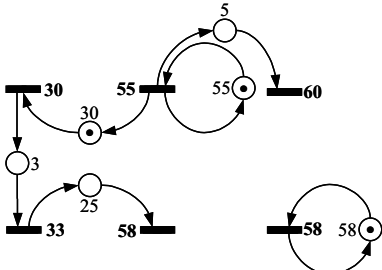
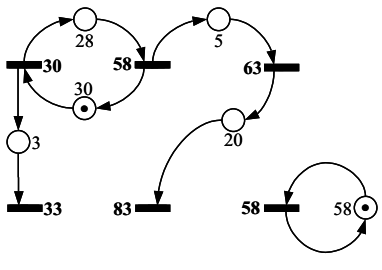
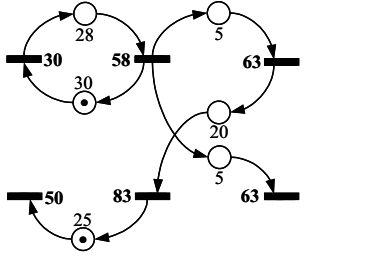
Policy π^k	Predecessor $\text{in}(\pi^k)$	Cycle time χ^k	Eigenvector v^k	Policy graph $\mathcal{G}(\mathcal{A}^{\pi^k})$
π^1	$\begin{bmatrix} 2 \\ 2 \\ 3 \\ 5 \\ 4 \\ 6 \end{bmatrix}$	$\begin{bmatrix} 55 \\ 55 \\ 40 \\ 50 \\ 50 \\ 58 \end{bmatrix}$	$\begin{bmatrix} 30 \\ 55 \\ 40 \\ 25 \\ 50 \\ 58 \end{bmatrix}$	
π^2	$\begin{bmatrix} 2 \\ 2 \\ 2 \\ 1 \\ 4 \\ 6 \end{bmatrix}$	$\begin{bmatrix} 55 \\ 55 \\ 55 \\ 55 \\ 55 \\ 58 \end{bmatrix}$	$\begin{bmatrix} 30 \\ 55 \\ 60 \\ 33 \\ 58 \\ 58 \end{bmatrix}$	
π^3	$\begin{bmatrix} 2 \\ 1 \\ 2 \\ 1 \\ 3 \\ 6 \end{bmatrix}$	$\begin{bmatrix} 58 \\ 58 \\ 58 \\ 58 \\ 58 \\ 58 \end{bmatrix}$	$\begin{bmatrix} 30 \\ 58 \\ 63 \\ 33 \\ 83 \\ 58 \end{bmatrix}$	
π^4	$\begin{bmatrix} 2 \\ 1 \\ 2 \\ 5 \\ 3 \\ 2 \end{bmatrix}$	$\begin{bmatrix} 58 \\ 58 \\ 58 \\ 58 \\ 58 \\ 58 \end{bmatrix}$	$\begin{bmatrix} 30 \\ 58 \\ 63 \\ 50 \\ 83 \\ 63 \end{bmatrix}$	

Figure 7.7 The successive policies and generalized eigenmodes of Example 7.6

$v_3^1 = v_3^0 = 40$. The next unlabelled transition is transition 4 with $\text{in}(\pi_4^1) = 5$ and $\text{in}(\pi_5^1) = 4$. Hence, the circuit of the third component is $(4, 5, 4)$. Starting from transition 4 the cycle mean is computed as $\chi_4^1 = (w(\pi_4^1) + w(\pi_5^1))/(\mu(\pi_4^1) + \mu(\pi_5^1)) = (25 + 25)/(1 + 0) = 50$ and the bias value is $v_4^1 = v_4^0 = 25$. Transition 5 is accessible from transition 4 and so $\chi_5^1 = \chi_4^1 = 50$ and $v_5^1 = 25 - 0 \cdot 50 + 25 = 50$. The final unlabelled transition is transition 6 which forms a component of its own with a loop having cycle mean $\chi_6^1 = 58/1$ and the bias value is simply set as $v_6^1 = v_6^0 = 58$. We thus computed the generalized eigenmode (χ^1, v^1) of π^1 .

Policy improvement of π^1 . Two first-order improvements can be computed. Transition 3 (with $\chi_3^1 = 40$) has transition 2 as a predecessor with higher cycle time and so $\chi_3^2 = \chi_2^1 = 55$. Likewise, transition 4 ($\chi_4^1 = 50$) is connected to transition 1 with higher cycle time $\chi_4^2 = \chi_1^1 = 55$. Also transition 5 ($\chi_5^1 = 50$) is improved because $\chi_4^2 = 55 > \chi_5^1 = 50$, but the new policy is just the improved old one, so the policy of transition 5 is maintained by predecessor 4 although the cycle time is updated to $\chi_5^2 = \chi_4^2 = 55$. We thus found the improved policy $\text{in}(\pi^2) = (2, 2, 2, 1, 4, 6)^\top$.

Policy evaluation of π^2 . The policy graph is shown in the 2nd row of Figure 7.7. There are 2 components. The circuit of the first component is again the loop around transition 2 with cycle mean $\chi_2^2 = 55/1 = 55$ and the bias value of transition 2 is set to $v_2^2 = v_2^1 = 55$. Transition 2 has three successors: transition 1 and 3, and transition 2 itself which has already been labelled. Hence, we set $\chi_1^2 = 55$ and $v_1^2 = 30 - 1 \cdot 55 + 55 = 30$, and $\chi_3^2 = 55$ and $v_3^2 = 5 - 0 \cdot 55 + 55 = 60$. Transition 3 has no successors but transition 1 has, so we follow the path from transition 1 to transition 4 and set $\chi_4^2 = 55$ and $v_4^2 = 3 - 0 \cdot 55 + 30 = 33$. Transition 4 has transition 5 as successor and so we proceed setting $\chi_5^2 = 55$ and $v_5^2 = 25 - 0 \cdot 55 + 33 = 58$. Now all transition accessible from transition 2 have been visited, and we proceed to the next unlabelled transition. This is transition 6 which is still isolated and so again $\chi_6^2 = 58$ and $v_6^2 = v_6^1 = 58$.

Policy improvement of π^2 . There are no first-order improvements, but two second-order improvements can be found. Transition 2 has predecessor 1 with $v_2^2 = 55 < 28 - 0 \cdot 55 + 30 = 58$ and thus an improved policy is $\text{in}(\pi_2^3) = 1$. Likewise, for transition 5 we find the improved policy $\text{in}(\pi_5^3) = 3$ since $v_5^2 = 58 < 20 - 0 \cdot 55 + 60 = 80$. At the end of the 2nd policy improvement we thus have the improved policy $\text{in}(\pi^3) = (2, 1, 2, 1, 3, 6)^\top$.

Policy evaluation of π^3 . The policy graph is shown in the 3rd row of Figure 7.7. There are two components. The circuit of the first component is $(1, 2, 1)$ with cycle mean $\chi_1^3 = (28 + 30)/(0 + 1) = 58$. Visiting all transition from transition 1 we find the generalized eigenmode as in the third row of Figure 7.7. Transition 6 is still an isolated component with cycle time 58.

Policy improvement of π^3 . Again no first-order improvement is found, but there are two second-order improvements. For transition 4 we find the improved policy $\text{in}(\pi_4^4) = 5$ since $v_4^3 = 33 < 25 - 1 \cdot 58 + 83 = 50$. For transition 6 we find the improved policy $\text{in}(\pi_6^4) = 2$ because $v_6^3 = 58 < 5 - 0 \cdot 58 + 58 = 63$. We thus found the improved policy $\text{in}(\pi^4) = (2, 1, 2, 5, 3, 2)^\top$.

Policy evaluation of π^4 . The policy graph (Figure 7.7, 4th row) is connected, with circuit $(1, 2, 1)$. The cycle mean is $\chi_1^4 = (28 + 30)/(0 + 1) = 58$ and the value for the root transition is set to $v_1^4 = v_1^3 = 30$. The bias vector is obtained by adding the root value v_1^4 to the mean path weights of the paths from root transition 1 to all transitions giving $v^4 = (30, 58, 63, 50, 83, 63)^\top$. Since all transitions are accessible from a single root transition the cycle time vector is $\chi^4 = (58, 58, 58, 58, 58, 58)^\top$.

Policy improvement of π^4 . We can skip the first-order improvement step, since π^4 consists of only one connected component and therefore all transitions have the same cycle time. Second-order improvements can be found neither, which means that π^4 is an optimal policy and (χ^4, v^4) is a generalized eigenmode.

Since all transitions have the same cycle time $\lambda_0 = 58$ is the maximum generalized eigenvalue by Theorem 7.4.8. Comparing the computed generalized eigenvector v^4 with the eigensemi-module (7.37) as computed in Example 7.5, we see that $v^4 \in \mathcal{V}(\lambda_0)$ with $c_1 = 30$. \square

The policy iteration algorithm computes the maximum generalized eigenvalue $\lambda_0 = \bigoplus_{i=1}^n \chi_i$ and one particular associated generalized eigenvector given by

$$x_i = \begin{cases} v_i & \text{if } \chi_i = \lambda_0 \\ \varepsilon & \text{otherwise.} \end{cases}$$

If one is interested in determining all classes and eigenpairs of a polynomial matrix \mathcal{A} then the theory of Section 7.4.4 must be applied. This requires the following main steps:

1. Determine the Frobenius normal form (7.29) of \mathcal{A} , i.e., compute the classes (strongly-connected components) of \mathcal{A} and the reduced graph $G_{\text{red}}(\mathcal{A})$,
2. Apply the policy iteration algorithm to each irreducible principle submatrix of \mathcal{A} corresponding to the classes,
3. Compute the principle classes (7.34) and determine the spectrum (7.33) of \mathcal{A} ,
4. Compute the critical graph and apply Theorem 7.4.6 to construct the generalized eigensemi-module $\mathcal{V}(\lambda)$ for each $\lambda \in \text{spec}(\mathcal{A})$.

7.4.7 Alternative Eigenproblem Algorithms

In the operations research literature several algorithms have been developed related to the max-plus (generalized) eigenproblem. The problem of computing the maximum (or minimum) cycle mean in a weighted digraph (precedence graph) is generally known as the *maximum mean cycle problem* (or minimum mean cycle problem) [3], which thus corresponds to the eigenvalue of a max-plus matrix. The more general problem of computing the maximum (or minimum) cycle mean in a biweighted or marked graph (timed event graph) is known as the maximum (minimum) profit-to-time ratio cycle problem or briefly the *maximum ratio cycle problem* [3], which corresponds to finding the generalized eigenvalue of a max-plus polynomial matrix. Note that the maximum mean cycle problem is a special case of the maximum ratio cycle problem (corresponding to a unit initial marking) and hence any algorithm for the latter more general problem also solves the former problem. Conversely, any algorithm for the maximum mean cycle problem can also be used for the maximum ratio cycle problem after a transformation from the (higher-order) timed event graph to a canonical precedence graph, see Section 8.2.5.

Karp's algorithm [116] is the first and most well-known polynomial algorithm for the maximum cycle mean problem. It is based on Karp's theorem [116]: If $A = (a_{ij}) \in \mathbb{R}_{\max}^{n \times n}$ is irreducible then the maximum cycle mean in the (strongly connected) precedence graph $G(A) = (V, E)$ is given by

$$\lambda = \max_{i=1, \dots, n} \min_{k=0, \dots, n-1} \frac{[A^n]_{ij} - [A^k]_{ij}}{n - k} \quad \text{for any } 1 \leq j \leq n,$$

where the matrix powers are evaluated in max-plus algebra, see also Baccelli *et al.* [11, Theorem 2.19]. To evaluate this expression we must compute the j th columns (for arbitrary j) of the matrices A^k for $k = 0, \dots, n$, which are just the single-origin longest path weights from origin j over paths with length k . Karp's algorithm [116] uses the dynamic programming algorithm

$$[A^k]_{ij} = \max_{(l,i) \in \Pi(i)} (a_{il} + [A^{k-1}]_{lj}) \quad \text{for all } i, k = 1, \dots, n,$$

with initial conditions $[A^0]_{jj} = e$ and $[A^0]_{ij} = \varepsilon$ for all $i \neq j$, and where $\Pi(i) = \{(l, i) \mid a_{il} \neq \varepsilon, 1 \leq l \leq n\}$ denotes the set of incoming arcs of i . The resulting algorithm runs in $\Theta(nm)$ time. Dasdan & Gupta [48] propose a breadth-first search (BFS) variant of Karp's algorithm. At each level k only nodes $l \in V_k = \{l \in V \mid [A^k]_{lj} \neq \varepsilon\}$ have to be considered in the computation of the finite entries $[A^{k+1}]_{ij}$, since $[A^{k+1}]_{ij} > \varepsilon$ iff $i \in \text{succ}(l)$ for some $l \in V_k$. Hence, at level k the path weight $[A^{k+1}]_{ij}$ is updated for each successor $i \in \text{succ}(l)$ of the nodes $l \in V_k$. Dasdan & Gupta's algorithm also runs in $O(nm)$ time for worst-case instances. Braker [21] extended Karp's algorithm to find the generalized eigenvalue of polynomial matrices $\mathcal{A} = \bigoplus_{l=1}^p A_l X^l$ without zero-order terms, i.e., the maximum cycle ratio in timed event graphs with at least one token in each place. Experiments by Braker [21] showed that the *extended Karp algorithm* applied to polynomial matrices (corresponding to timed event graphs) outperforms Karp's algorithm applied to the augmented matrix obtained by transformation of the timed event graph to the canonical precedence graph (without considering the additional time to compute this augmented matrix). For other variants of Karp's algorithm, see Dasdan *et al.* [49, 50].

Karp & Orlin [117] developed two parametric longest (shortest) path algorithms which essentially find the generalized eigenvalue λ of an irreducible first-order max-plus polynomial matrix $\mathcal{A} = \bigoplus_{l=0}^1 A_l X^l$. They define a digraph where each arc k has a *parametric arc weight* $w_k - \lambda \mu_k$ with $\mu_k \in \{0, 1\}$ and parameter $\lambda \in \mathbb{R}$. The problem then translates to finding the maximal (minimal) λ such that the graph has no positive (negative) weight circuits. Karp & Orlin give an $O(nm \log n)$ (and also an $O(n^3)$) algorithm for solving this cycle ratio problem. Young *et al.* [227] give a Fibonacci heap implementation of Karp & Orlin's algorithm that runs in $O(nm + n^2 \log n)$ time. Moreover, the algorithm of Young *et al.* [227] applies to reducible digraphs with generalized parametric arc weights $w_k - \lambda \mu_k$ with $\mu_k \in \{0, p\}$, which thus corresponds to general reducible max-plus polynomial matrices $\mathcal{A} = \bigoplus_{l=0}^p A_l X^l$. Young *et al.* [227] showed that in the special case of the maximum (minimum) cycle mean problem, i.e., $\mu_k = 1$ for all arcs k , their parametric path algorithm runs in worst-case time $O(nm + n^2 \log n)$ and *expected time* $O(m + n \log n)$.

The *power algorithm* [22, 190, 197] computes both the eigenvalue and an eigenvector for an irreducible matrix $A \in \mathbb{R}_{\max}^{n \times n}$. For any $x(0) \neq \varepsilon$ iterate $x(k) = A \otimes x(k-1)$, $k \geq 1$, until $x(p) = c \otimes x(q)$ for some integers $p > q \geq 0$ and real $c \in \mathbb{R}$. Then $\lambda = c/(p-q)$ is the unique eigenvalue and $v = \bigoplus_{j=1}^{p-q} \lambda^{p-q-j} \otimes x(q+j-1)$ is an eigenvector. The computation time of the power algorithm depends on the length of the transient behaviour before the vector $x(k)$ reaches the periodic regime. Soto y Koelemijer [190] shows that the power algorithm takes $O(c_A^2 n + c_A m)$ time and $O(c_A n)$ space, where $c_A = c(A, x(0))$ is the length of the transient regime, which may become arbitrary large for some matrices A (with small $\lambda_0(A) - \lambda_1(A)$ where $\lambda_1(A)$ is the second largest cycle mean) and 'bad' choices of $x(0)$. Note, however, that if $x(0)$ happens to be an eigenvector then only $p-q$ iterations are needed. If A is a state matrix corresponding to a periodic timetable as in the next chapter then the timetable vector d_0 is a

Table 7.2 Maximum mean cycle and ratio algorithms

Algorithm	Running time	Space	Marking	Red.	Eigenvector
Karp [116]	$\Theta(nm)$	$\Theta(n^2)^\dagger$	1	no	no
BFS Karp [48]	$O(nm)$	$\Theta(n^2)^\dagger$	1	no	no
Extended Karp [21]	$O(nm)$	$\Theta(n^2)^\dagger$	$1, \dots, p$	no	no
Parametric path algorithm [227]	$O(nm + n^2 \log n)$	$O(m)$	$0, \dots, p$	yes	no
Power algorithm [22, 197]	$O(c_A^2 n + c_A m)$	$O(c_A n)$	1	no	yes
Policy iteration [31]	$O(Im)$	$O(n)$	$0, \dots, p$	yes	yes

[†]A two-pass implementation runs in $\Theta(n)$ space [49, 50]

good choice for the initial vector $x(0)$, since d_0 either lies in the eigensemimodule of A (and thus is an eigenvector) or it is close to some eigenvector with some additional slack time on the critical circuit(s) and on critical paths from the critical circuit(s). Hence, the power algorithm may be very efficient in the evaluation of railway timetables, although it requires preprocessing to find the irreducible classes and to transform a timed event graph to an equivalent one with unit initial marking.

Table 7.2 summarizes the (best) mentioned algorithms for the maximum cycle mean and ratio problems. The successive columns give the algorithm name/characteristic and source, running time complexity, space complexity (in addition to the storage of the input graph which requires $O(m)$ space for an adjacency list representation), initial marking, applicability to reducible matrices, and whether or not an eigenvector is computed. Note that a unit initial marking implies a maximum mean cycle algorithm, whereas also some (recursive) maximum ratio cycle algorithms require at least one token all places. Dasdan *et al.* [49, 50] report on extensive experiments on a large number of maximum mean cycle algorithms and conclude that the policy iteration algorithm outperformed all other algorithms. Dasdan [47] reports on extensive experiments for maximum ratio cycle algorithms and concludes that the policy iteration algorithm and the parametric longest path algorithm were competitive and both outperformed the other algorithms. These papers also give various improvements on the implementation of the tested algorithms. The experiments by Dasdan *et al.* [49, 50] and Dasdan [47] included all algorithms considered here except for the Power algorithm and the extended Karp algorithm. Soto y Koelemeijer [190] compared the policy iteration algorithm and the power algorithm and showed that the former outperforms the latter for worst-case matrices and arbitrary initial vectors $x(0)$ in the power algorithm.

In conclusion, the policy iteration algorithm is the most general and efficient algorithm to solve large-scale (reducible) max-plus generalized eigenproblems. The parametric path algorithm may also be used if finding an eigenvector is not crucial. The other algorithms are less efficient and require preprocessing to find the strongly-connected components and transform a timed event graph to one with a unit marking (except for the extended Karp's algorithm), although these preprocessing steps can be implemented efficiently in linear running time (see also §8.2.5). The power algorithm is easy to implement and can be used for small (strongly connected, unit marking) timed event graphs, and so are (variants of) Karp's algorithm if computing an eigenvector is not necessary.

The complete solution of the (generalized) eigenproblem also requires all critical circuits and eigenvectors associated to the disconnected components in the critical graph. Most algorithms

can easily be extended to give one critical circuit, but finding all critical nodes requires more effort. Olsder *et al.* [155] describe an algorithm for computing the maximum eigenvalue and all critical nodes of a max-plus matrix $A \in \mathbb{R}_{\max}^{n \times n}$ containing at least one circuit. The algorithm uses the Floyd-Warshall procedure (see §7.5.1) to detect positive weight circuits of the parametric matrix $A_\lambda = \lambda^{-1}A = (a_{ij} - \lambda)$ for increasing values of λ until $\lambda = \lambda_0(A)$. Starting with a lower bound for λ (e.g., $\lambda = \min\{a_{ij} \mid a_{ij} > \varepsilon\}$) the Floyd-Warshall procedure is applied to A_λ ; if a positive diagonal entry $[A_\lambda^k]_{ii}$ is computed then λ is reset to the cycle mean of this circuit (obtained by backtracking on the predecessor vector) and the Floyd-Warshall procedure is restarted on the updated matrix A_λ . If the Floyd-Warshall procedure terminates without detecting a positive circuit then $\lambda = \lambda_0(A)$ and the critical nodes are those i with $[A_\lambda^+]_{ii} = 0$. Olsder *et al.* [155] then describe how to obtain finite eigenvectors from the longest path matrix A_λ^+ under the assumption that all nodes are accessible from a critical circuit (that is, the initial classes of A are basic, see Corollary 7.4.5).

The most efficient approach to compute all critical nodes associated to the maximum generalized eigenvalue λ_0 of a polynomial matrix $\mathcal{A} \in \mathbb{R}_{\max}^{n \times n}[X]$ proceeds in two stages: first compute the maximum generalized eigenvalue λ_0 using the policy iteration algorithm (or any other fast algorithm) and subsequently compute the *diagonal* of the longest path matrix $[A(\lambda_0^{-1})]^+$ using the ALLLONGESTCIRCUITS algorithm presented in §7.5.3. If the policy iteration algorithm returns a cycle time vector with entries $\chi_i \neq \lambda_0$ then we may restrict the computation of the diagonal to the principle submatrix $[A_{[K_0|K_0]}(\lambda_0^{-1})]^+$ where $K_0 = \{1 \leq i \leq n \mid \chi_i = \lambda_0\}$. Finally, a basis of the eigensemimodule associated to λ_0 is obtained by computing the columns $[A_{\lambda_0}^+]_{\cdot j}$ for a selected node j from each component in the critical graph, see Theorem 7.4.6. The latter is a single-origin longest path problem from origin j , see §7.5.2. Note that the policy iteration algorithm is more efficient to compute λ_0 than repeated application of an all-pair longest path algorithm as in Olsder *et al.* [155], and moreover, a repeated single-origin longest path algorithm for the selected critical nodes is much more efficient than computing the complete longest path matrix.

7.5 Longest Path Algorithms

7.5.1 All-Pair Longest Paths

A necessary and sufficient condition for the existence of finite longest paths in finite digraphs is that the graph has no positive-weight circuits. In the sequel we will assume that this condition is satisfied. In general, all path algorithms can easily be extended to detect positive-weight circuits and return an error message if such a circuit is detected [3, 39]. Recall that a precedence graph $G(A)$ has a positive circuit iff the maximum eigenvalue (or maximum cycle mean) $\lambda_0(A) > e$. We will only call a longest path algorithm for max-plus matrices with maximum eigenvalue not exceeding e , for ‘normalized’ max-plus matrices $A_{\lambda_0} = \lambda_0^{-1}A$, or valuated polynomial matrices $A_\nu = A(\nu^{-1}) = \bigoplus_{l=0}^p A_l \nu^{-l}$ with $\nu \geq \lambda_0$, which all satisfy the condition of nonpositive-weight circuits.

Algorithm 7.5.1 gives the well-known Floyd-Warshall algorithm for computing the longest path matrix A^+ [66, 219, 39]. The algorithm iteratively computes the longest path weight from each node j to i using paths over ‘internal’ nodes $1, \dots, k$ only. Thus, in the k -th (outer) iteration

Algorithm 7.5.1 (FLOYDWARSHALL)**Input:** Matrix $A \in \mathbb{R}_{\max}^{n \times n}$.**Output:** Longest path matrix $D = (d_{ij}) = A^+$.

```

1   $D \leftarrow A$ ;
2  for  $k = 1$  to  $n$  do
3      for  $i = 1$  to  $n$  do
4          if  $d_{ik} > \varepsilon$  then                                //Proceed to next  $i$  if  $d_{ik} = \varepsilon$ 
5              for  $j = 1$  to  $n$  do
6                   $d_{ij} \leftarrow d_{ij} \oplus d_{ik} \otimes d_{kj}$ ;
7  return  $D$                                                     //Terminate

```

the algorithm checks for each origin j whether the weight of the current path to each i can be increased by going over node k . The algorithm takes $O(n^3)$ time and space. The Floyd-Warshall algorithm is robust and very general: it applies to digraphs with arbitrary arc weights, it computes the longest path weights between any pair of nodes, if a node i is not accessible from a node j then the returned associated path weight is ε , and positive-weight circuits are simply detected by a positive diagonal entry d_{jj} .

The Floyd-Warshall algorithm is easy to implement and well-suited for small graphs and for dense graphs. For (large-scale) sparse graphs however a repeated single-origin longest path algorithm is more efficient in both time and space complexity. If all arcs have nonpositive weight a longest path matrix A^+ can be computed in $O(nm + n^2 \log n)$ time by repeatedly applying a Fibonacci heap implementation of Dijkstra's (label-setting) algorithm using each node as an origin once [3, 39, 67]. Moreover, if we are interested only in some particular entry $[A^+]_{ij}$ or only a few complete rows or columns of A^+ then Dijkstra's algorithm is also the most efficient. However, if $G(A)$ contains both positive and negative arc weights (in conventional sense) then Dijkstra's algorithm cannot be used (directly). In this case we can use the Bellman-Ford (label-correcting) algorithm to compute a row or column of the longest path matrix, which takes $O(nm)$ time [3, 39]. Also the computation of a single entry $[A^+]_{ij}$ takes $O(nm)$ time using a label-correcting algorithm. For large-scale sparse matrices with both positive and negative entries the longest path matrix can also be computed by Johnson's algorithm [112]. Johnson's algorithm first uses the Bellman-Ford algorithm to transform the graph (in $O(nm)$ time) into one with nonpositive arc weights only, and then applies Dijkstra's algorithm repeatedly using each of the n nodes as an origin once, which takes $n \cdot O(m + n \log n) = O(nm + n^2 \log n)$ time using a Fibonacci heap implementation [3, 39, 67]. Johnson's algorithm thus also runs in $O(nm + n^2 \log n)$ time, although it needs more overhead compared to repeatedly applying Dijkstra's algorithm directly to a matrix with nonpositive weights only. Note that for sparse matrices $m \ll n^2$ and thus $nm \ll n^3$, whence a repeated single-origin longest path algorithm is more efficient than Floyd-Warshall for sparse graphs.

7.5.2 Single-Origin Longest Paths

The Floyd-Warshall algorithm is an example of a *label-correcting path algorithm*. Path algorithms are iterative algorithms that maintain so-called (node) distance labels (longest path weights from the origin) in each iteration. The algorithms are classified into two groups: label-setting and label-correcting algorithms [3, 39]. A label-correcting path algorithm updates the

tentative distance labels in each iteration until the last iteration at which they all become permanent and are proved optimal. In contrast, a label-setting algorithm finds one optimal distance label in each iteration. Label-setting algorithms are variants of Dijkstra's path algorithm [56] and are restricted to graphs with nonpositive arc weights (or acyclic graphs) only. Label-correcting algorithms, such as the Bellman-Ford algorithm, are more general and apply to graphs with arbitrary arc weights.

In the current and the next section we focus on Dijkstra's label-setting algorithm for three main reasons. First, label-setting algorithms have a better worst-case time complexity and thus are likely to be faster for large-scale networks. Second, Dijkstra's algorithm returns an optimal path weight at each iteration and can thus be terminated prematurely if the path or all paths of interest have been found. This feature is exploited in the algorithm for finding all critical circuits in Section 7.5.3. Third, Dijkstra's algorithm finds an optimal path in each iteration by *nondecreasing weight*, by which the algorithm can be terminated if path weights exceed some threshold value. This latter property is useful in the computation of the recovery matrix in Section 8.5.

A single-origin longest path algorithm over a precedence graph $G(A) = (V, E)$ computes the maximum-weight paths and the corresponding weights from a specified origin node s to all nodes accessible from s , i.e., the column $[A^+]_{\cdot s}$ where $[A^+]_{is} = \varepsilon$ if there is no path from s to i in the precedence graph $G(A)$. The vast literature on path algorithms is mainly devoted to networks where the origin is a *source* (a node with indegree zero) and the problem is accordingly commonly referred to as the single-source shortest path (SSSP) problem. Maximum-weight or critical circuits are however crucial in our study of timed event graphs and max-plus linear systems. We therefore emphasize advanced initialization schemes of common path algorithms which are necessary to find the longest path (circuit) from an origin i back to i along with the longest paths to all other accessible nodes. Furthermore, our discussion of path algorithms and data structures distinguishes from the customary literature on two more points: (1) Algorithms and data structures are usually formulated in terms of shortest-path problems over graphs with no negative circuits; (2) The usual representation of arcs in adjacency lists is reversed.

Dijkstra's algorithm [56, 3, 39] iteratively determines a longest path tree with root s in a graph $G = (V, E)$ with nonpositive arc weights using a greedy strategy. The algorithm maintains a *candidate list* $H \subset V$ of nodes to be selected next and a vector of tentative distance labels $v = (v_1, \dots, v_n)$, which give lower bounds on the longest path weights from origin node s to nodes $i \in V$. At the end of the algorithm v_i is the *distance* or longest path weight from s to node i for each $i \in V$. The original algorithm starts by initializing $v_s = e$, $v_i = \varepsilon$ for all $i \in V \setminus \{s\}$, and $H = \{s\}$. A node i is *unlabelled* if $v_i = \varepsilon$, which means that node i has not yet been reached by the algorithm. An iteration of Dijkstra's algorithm consists of two steps: *node selection* and *scanning* (also called relaxation or reaching):

- (i) *Node selection*: Select a node $j \in H$ with maximal distance label

$$v_j = \bigoplus_{i \in H} v_i$$

and remove j from the candidate list H .

- (ii) *Scanning*: For each outgoing arc $(j, i) \in E$ such that $v_i < v_j \otimes a_{ij}$ set

$$v_i = v_j \otimes a_{ij}$$

and add i to H if it is not already in H .

During the course of the algorithm, each node is in one of three states: unlabelled, labelled, or scanned. Initially s is labelled and all other nodes are unlabelled. The algorithm repeats the node selection and scanning operations until there are no more labelled nodes (every node accessible from the origin has been scanned).

The nonpositive arc weights and greedy node selection strategy guarantees that a node, once scanned, will never be updated again which is easily seen by induction over the iterations: if at the beginning of an iteration node j is selected for scanning its label v_j is maximal over all labelled nodes in H (and all unlabelled nodes) and in particular $v_j \geq v_i$ for all its successors $i \in \text{succ}(j)$. Any label update in the scanning operation of j satisfies $v_i = v_j \otimes a_{ij} \leq v_j$ since $a_{ij} \leq e$ for all nodes $i \in \text{succ}(j)$, whence at the end of this iteration v_j is still maximal over H . Hence, the distance label of each scanned node becomes permanent, i.e., a longest path to the scanned node has been found. Dijkstra's algorithm thus scans each node accessible from s exactly once (after it is selected for scanning) and builds a longest path tree by adding in each iteration an outgoing arc towards a node with maximum distance label. This also implies an important property of Dijkstra's algorithm: the distances (longest path weights) are computed iteratively in monotonously nonincreasing order.

With the original initialization Dijkstra's algorithm does not compute the longest path from the origin s back to s , if circuits over s exist, because it initially sets $v_s = 0$ which is an upper bound for any circuit weight by the condition that all arcs must be nonpositive. Hence, Dijkstra's algorithm does not compute column s of the longest path matrix A^+ but that of the matrix star A^* instead, cf. Section 7.2.5. Since we are interested in A^+ we must still find the longest circuit from s to s , if one exists. Since $A^+ = AA^*$ we can simply run Dijkstra's algorithm and subsequently compute $v_s = \bigoplus_{(i,s) \in E} a_{si} \otimes v_i$. A more effective approach is obtained by running Dijkstra with the alternative initialization:

$$v_i = \begin{cases} a_{is} & \text{if } i \in \text{succ}(s) \\ \varepsilon & \text{otherwise} \end{cases} \quad \text{and} \quad H = \text{succ}(s).$$

After this initialization $v_s = a_{ss}$ and so initially $s \in H$ iff the graph contains a loop around s . Otherwise, $v_s = \varepsilon$ until a predecessor of s is selected and scanned (provided s has at least indegree one). Because the graph has no positive circuits the longest distance satisfies $v_s \leq 0$. Hence, whenever s is scanned $v_i \geq a_{is} \geq v_s \otimes a_{is}$ for all successors $i \in \text{succ}(s) = \{i \in V \mid (s, i) \in E\}$ and so s is a leaf in the longest path 'tree'. With this initialization the algorithm no longer grows a longest path tree rooted at s but a forest with multiple 'roots'. Nevertheless, the adjusted algorithm correctly computes the longest path weights from the (invisible) origin s via its successors $\text{succ}(s)$ to all nodes accessible from $\text{succ}(s)$ (and thus from s in the original graph).

Algorithm 7.5.2 gives the pseudocode of the (adjusted) Dijkstra's algorithm. If only distances above some threshold value δ are required then the algorithm can be terminated as soon as in line 4 a node j is selected with label $v_j > \delta$. Hence, the statements in lines 5–9 become conditional and are expanded by **if** $v_j > \delta$ **then** $H \leftarrow \emptyset$; **else** lines 5–9.

The computational effort of Dijkstra's algorithm depends on the implementation of the candidate list H . The proper data structure is a *priority queue* where nodes are ordered by their

Algorithm 7.5.2 (SINGLEORIGINLONGESTPATH)

Input: Matrix $A \in \mathbb{R}_{\max}^{n \times n}$ (adjacency list representation), origin node $s \in \{1, \dots, n\}$.
Output: Path weights from s in list $v = [A^+]_s$.

```

1  for  $i \leftarrow 1$  to  $n$  do  $v_i \leftarrow \varepsilon$ ;                                //Initialization
2  for  $i \in \text{succ}(s)$  do  $v_i \leftarrow a_{is}$ ;  $H \leftarrow H \cup \{s\}$ ;
3  while  $H \neq \emptyset$  do                                                //Main loop
4       $j \leftarrow \arg \max\{v_j \mid j \in H\}$ ;                                //Node selection
5       $H \leftarrow H \setminus \{j\}$ ;
6      for each  $i \in \text{succ}(j)$  do                                            //Scanning
7          if  $v_i < v_j + a_{ij}$  then
8               $v_i \leftarrow v_j + a_{ij}$ ;
9              if  $i \notin H$  then  $H \leftarrow H \cup \{i\}$ ;
10 return  $v$                                                                 //Terminate

```

distance label [2, 39, 67]. A priority queue is an ordered list with (in this case) the maximal node(s) at the top. Selecting a node with maximal distance (line 4) from a priority queue then reduces to returning the node at the top of the queue. However, the ordering in a priority queue must be maintained when deleting a selected node (line 5), updating a node label (line 8), and inserting a new node (line 9).

A *heap* is a data structure that implements a priority queue and supports among others the following operations [2, 39]:

- **MAKEHEAP**: returns a new empty heap,
- **INSERT**(i, H): inserts a new labelled node i to the heap H ,
- **DELETEMAX**(H): returns a maximum labelled node and deletes it from the heap,
- **INCREASELABEL**(i, d_i, H): increases the label of node i in H to d_i .

These heap operations of course maintain the order between nodes. A heap can be interpreted as a rooted tree where the maximal node is the root and each other node in the tree has a label not exceeding that of its parent. Note that we do not need an operation that checks whether a node is already in the heap (line 9) since this simply follows from the state of the node when it is updated: unlabelled nodes must be inserted in the heap and labelled nodes are increased in the heap. Heap operations typically take $O(\log |H|)$ time corresponding to the depth of the heap (tree), where $|H|$ is the heap size. For instance, *binary heaps* and *binomial heaps* need $O(\log |H|)$ time for all heap operations except **MAKEHEAP** which takes $O(1)$ time [39]. Using these heaps the SINGLEORIGINLONGESTPATH algorithm runs in $O(m \log n)$ time. Fibonacci heaps take $O(\log |H|)$ for **DELETEMAX** and $O(1)$ for all other heap operations [39, 67]. A Fibonacci heap implementation of SINGLEORIGINLONGESTPATH runs in $O(m + n \log n)$ time. Codes of heap data structures can be found in e.g. Cormen *et al.* [39].

7.5.3 All Critical Circuits

If we are interested in the diagonal of the longest path matrix A^+ only, we must repeatedly call Dijkstra's Algorithm 7.5.2 for all origins $s \in V$. However, we can speed up the single-origin longest path computations by proceeding to the next origin as soon as the longest path weight

Algorithm 7.5.3 (ALLLONGESTCIRCUITS)**Input:** Precedence graph $G(A) = (V, E)$ (adjacency list representation).**Output:** Maximum circuit weight over each node in list $d = ([A^+]_{ii})$.

```

1   $E' \leftarrow \emptyset;$  //Preprocessing
2  for each  $(j, i) \in E$  do
3      if  $j \neq i$  then  $E' \leftarrow E' \cup \{(j, i)\};$ 
4  component  $\leftarrow$  STRONGLYCONNECTEDCOMPONENT( $V, E'$ );
5  for  $i \leftarrow 1$  to  $n$  do  $d_i \leftarrow \varepsilon;$ 
6  for  $s \leftarrow 1$  to  $n$  do //Outer loop
7      if component( $s$ ) = 0 then
8          if  $s \in \text{succ}(s)$  then  $d_s \leftarrow a_{ss};$ 
9      else if  $d_s = \varepsilon$  then //Unknown circuit weight
10         for  $i \leftarrow 1$  to  $n$  do  $v_i \leftarrow \varepsilon; \pi_i \leftarrow \varepsilon;$  //Start Single Origin Longest Path
11         for  $i \in \text{succ}(s)$  do  $v_i \leftarrow a_{is}; \pi_i \leftarrow s; H \leftarrow H \cup \{s\};$ 
12         while  $H \neq \emptyset$  do //Inner loop
13              $j \leftarrow \arg \max \{v_j \mid j \in H\};$  //Node selection
14             if  $v_j = v_s$  then //Maximum circuit weight
15                  $d_s \leftarrow v_s; H \leftarrow \emptyset;$ 
16                 if  $v_s = 0$  then //Critical node
17                      $j \leftarrow \pi(s);$ 
18                     while  $j \neq s$  do //Critical circuit
19                         if  $d_j = \varepsilon$  then  $d_j \leftarrow 0;$ 
20                          $j \leftarrow \pi(j);$ 
21             else
22                  $H \leftarrow H \setminus \{j\};$ 
23                 for each  $i \in \text{succ}(j)$  do //Scanning
24                     if  $v_i < v_j + a_{ij}$  then
25                          $v_i \leftarrow v_j + a_{ij}; \pi_i \leftarrow j;$ 
26                         if  $i \notin H$  then  $H \leftarrow H \cup \{i\};$ 
27 return  $d$  //Terminate

```

to s has been found, i.e., when s is selected for scanning. Moreover, we can clearly skip each $s \in V$ with indegree zero and immediately set $[A^+]_{ss} = \varepsilon$, i.e., we can skip empty rows of A . More generally, we can skip each node that is not contained in some strongly-connected component. Furthermore, we do not have to store the entire path matrix in memory but just the finite diagonal entries and one distance vector at a time, which reduces the space complexity from $O(n^2)$ to $O(n)$.

The strongly-connected components of a digraph can efficiently be computed in linear $O(n+m)$ time and $O(m)$ space using variants of depth-first search, see Tarjan [198] and Cormen *et al.* [39] for two alternative algorithms. We refer to these references for the code of STRONGLYCONNECTEDCOMPONENT which we will use as a subroutine.

Algorithm 7.5.3 shows the pseudocode of ALLLONGESTCIRCUITS that computes the diagonal of the longest path matrix A^+ of a matrix $A \in \mathbb{R}_{\max}^{n \times n}$. The algorithm starts with a preprocessing step in lines 1–4 that computes the strongly-connected components of the precedence graph where loops are discarded. The call to STRONGLYCONNECTEDCOMPONENT returns a vector component where an entry component(s) = 0 implies that there is no circuit over s except

maybe for a loop (s, s) (which was discarded in the computation of the strongly-connected components). Line 5 initializes the circuit weight vector d ; an entry $d_i = \varepsilon$ implies that either there is no circuit over node i or (while the algorithm has not finished) the maximum circuit weight over node i has not yet been determined. Lines 6–26 contain the main loop that iterates over each origin $s \in V$. Lines 7–8 immediately short-cut an iteration if $\text{component}(s) = 0$ in which case d_s is either the weight of a loop over s or $d_s = \varepsilon$ if there is no such loop. Note that if there is a loop but no other circuit over s then it is unnecessary to compute the longest path weights from s (or from its successors) which in the worst-case takes computation of the complete longest path trees rooted at the other successors $j \in \text{succ}(s) \setminus \{s\}$ before s is scanned. Line 9 checks whether the maximum circuit weight over the current origin s is still unknown. If here $d_s \neq \varepsilon$ then s already must have been identified as a critical node on some critical circuit in a previous iteration and so we can skip this iteration ($d_s = 0$). On the other hand, if here $d_s = \varepsilon$ then a circuit over s must exist and the maximum weight has still to be determined, because $\text{component}(s) \neq 0$. Lines 10–26 are essentially the single-origin longest path algorithm (Algorithm 7.5.2) extended by lines 14–21 that cut off the single-origin longest path algorithm as soon as the maximum circuit weight over the origin has been found. Note that if $v_s = v_j$ for a selected node $j \in H$ then $s \in \max\{v_j \mid j \in H\}$ and so $v_s = v_j$ is the maximal distance of s from s , regardless whether or not $j = s$ (in case of a tie). Moreover, in the case that a critical circuit has been found ($v_s = 0$) lines 16–20 activate a backward walk over the critical circuit using the predecessor vector π and thereby setting any undetermined entry d_j to the critical circuit weight 0. If on the other hand the distance of the selected node j exceeds the label of s then j is removed from the candidate list and scanned, after which the next node is selected in a new iteration of the inner loop (lines 12–26).

Theorem 7.5.1 *Let $A \in \mathbb{R}_{\max}^{n \times n}$ with maximum eigenvalue $\lambda_0(A) \leq e$. Then Algorithm ALLLONGESTCIRCUITS computes the diagonal of the longest path matrix A^+ in $O(n \cdot S(n, m))$ time and using $O(m)$ space, where $S(n, m)$ is the worst-case running time of a single-origin longest path algorithm.*

Proof: If $\lambda_0(A) \leq e$ then the precedence graph $G(A) = (V, E)$ has no positive circuits and therefore the longest paths/circuits have finite length. The preprocessing step requires $O(m)$ time to copy the arc list E to E' and excluding the loops. Algorithm STRONGLYCONNECTEDCOMPONENT takes $O(n + m)$ time and $O(m)$ space. Lines 6–26 are essentially the single-source longest path algorithm taking $S(n, m)$ time plus lines 7–8 which adds $O(1)$ time and the inner-loop line 14 which adds $O(1)$ time to each iteration of the inner loop. Hence, these lines do not change the complexity bound of $S(n, m)$. The algorithm maintains four n -dimensional arrays component , d , v and π , and the data structure of the list H . Note that each iteration of the outer loop reapplies v for the distances from the current root s . \square

If A has both positive and negative entries then we may apply the approach of Johnson [39, 112] to compute reduced arc weights using a single-origin longest path algorithm for general arc weights once (e.g. Bellman-Ford) and then apply algorithm ALLLONGESTCIRCUITS to the reweighted graph with nonpositive arcs.

7.6 Conclusions

In this chapter we introduced max-plus algebra and several algorithms for solving eigenproblems and longest path problems in max-plus algebra. In particular, we introduced max-plus matrices and their associated precedence graphs, as well as max-plus polynomial matrices and their formal connection to timed event graphs. We explained linear dependence and independent vectors in semimodules, stressed the differences with vector spaces over classical fields, and gave a geometric description of vectors in max-plus semimodules.

We explained the (generalized) eigenproblem of max-plus (polynomial) matrices and showed the connection with the topological structure of the associated graphs. We showed how the nodes of the precedence (or timed event) graphs can be partitioned into classes with a unique eigenvalue which equals the (maximum) cycle mean of the critical circuit(s), and gave a full description of the corresponding eigenspaces (eigensemimodules). We furthermore presented the efficient policy iteration algorithm for solving the (generalized) eigenproblem and developed an algorithm for finding all critical circuits. Moreover, we considered efficient implementations of single-origin longest path algorithms.

The max-plus algebra theory and numerical algorithms developed in this chapter will be used in the next chapter on max-plus linear systems, which relates max-plus algebra to the performance analysis of timed event graphs — and railway timetables in particular.

Chapter 8

RAILWAY TIMETABLE STABILITY ANALYSIS

8.1 Introduction

The issue of railway traffic stability is rapidly gaining attention in Europe because of the increasingly saturated railway infrastructure where a slightly delayed train may cause a domino effect of secondary delays over the entire network. European railways are typically operated according to a predetermined (master) timetable, which represents a conflict-free coordination of train paths and includes slack time to manage train delays. From a system point of view the timetable can be understood as a steady state for the train traffic. Traffic stability then refers to the possibility and effort necessary of returning to the steady state after disruptions. The system response to disruptions is highly complicated due to complex cyclic train interdependencies generated by infrastructure restrictions (e.g. conflicting routes or a fast train getting stuck behind a leading slow train on an open track), timetable constraints (passenger connections at transfer stations), and logistics (rolling stock circulations and train personnel schedules). In this chapter we develop an analytical approach to analyse timetable stability based on max-plus algebra.

In Chapter 6 we have seen how scheduled railway systems can be modelled as timed event graphs and considered a number of structural and behavioural properties of timed event graphs. The present chapter is devoted to the dynamic behaviour over time or *performance evaluation* of timed event graphs based on the state-space representation of timed event graphs in the event domain, which was already briefly introduced in Section 6.5.3. The state-space description of timed event graphs is a system of $(\max, +)$ -recursive equations — recursive equations involving maximum and sum operations — and are thus nonlinear in a classical sense. However, formulated in max-plus algebra the state-space equations show a linear dynamic system and can be analysed using the theory developed in Chapter 7.

The approach taken in this chapter concentrates on network timetable evaluation in a deterministic setting in accordance to the design choices of e.g. train orders at conflicting routes and the deterministic design times (running times, dwell times, transfer times, minimum headway times, etc.) used in the construction of the timetable. A max-plus state matrix captures this timetable structure and the eigenstructure of this matrix reveals the interconnected components, associated cycle times and available recovery times, which can all be computed by efficient polynomial algorithms. Moreover, because bottlenecks of the systems are explicitly revealed — through the notion of critical circuits — this approach provides an efficient way not only to evaluate the performance but also to assess certain design choices made at earlier stages in the timetable design process. We propose transparent stability and robustness criteria and associated performance indicators and are able to identify critical processes or resources in the

timetable or infrastructure. The approach has been implemented in the computer application PETER (Performance Evaluation of Timed Events in Railways) which is also introduced and demonstrated in this chapter. PETER has been developed as a decision support to railway planners for evaluating and improving timetable designs and infrastructure utilization. Because of efficient numerical algorithms and implementations PETER enables a real-time environment to analyse large-scale periodic railway timetables.

The application oriented literature on max-plus algebra and timed event graphs typically deals with the analysis of irreducible first-order models of the form $x(k) = Ax(k-1) \oplus Bu(k)$, although in first instance the derived models contain higher-order and/or zero-order dynamics. Hence, more general order models are first transformed to the canonical first-order representation and analysed accordingly. In particular, topological and behavioural properties are analysed separately from performance properties. The first-order models indeed allow an elegant analysis avoiding some complications arising from especially the zero-order dynamics. In practice however the zero-order dynamics do represent essential behavioural properties that can only be analysed in full potential if explicitly available in the model. Moreover, the analyses usually assume irreducibility (strongly connectedness) without consideration of accessibility relations in general reducible systems. The first-order representations thus contain some simplifying assumptions that do no justice to the original problem. In this chapter we deal with general higher-order max-plus linear systems and propose a formal *polynomial matrix representation* of both the higher-order state matrix and associated timed event graph. We use this approach to model periodic railway timetables as *scheduled max-plus linear systems* and develop a generic max-plus system analysis theory that has been proved valuable in evaluating railway timetables on stability and robustness.

The chapter is outlined as follows. Section 8.2 introduces max-plus linear systems and proposes a general linear state-space representation of (scheduled) timed event graphs. Section 8.3 considers a spectral analysis of the linear system and defines an appropriate notion of timetable stability. Timetable realizability is considered in Section 8.4. Section 8.5 defines a notion of timetable robustness based on recovery times in the timetable. Section 8.6 deals with delay propagation and shows how any initial delay scenario may propagate over time and the network given the timetable structure. PETER is briefly introduced in Section 8.7, and illustrated in a case-study of the Dutch national railway timetable in Section 8.8. Section 8.9 ends this chapter with some conclusions.

8.2 Max-Plus Linear Systems

8.2.1 First-Order State-Space Equations

A max-plus linear system is a linear system description of a discrete-event dynamic system evaluated over the $(\max, +)$ -semiring, where the state dynamics can be described by recursive equations in max-plus algebra. The canonical (first-order) max-plus linear system is

$$\begin{cases} x(k) = Ax(k-1) \oplus Bu(k), & x(0) = x_0 \\ y(k) = Cx(k). \end{cases} \quad (8.1)$$

Here $x(\cdot) \in \mathbb{R}_{\max}^n$ is the *state vector*, $u(\cdot) \in \mathbb{R}_{\max}^r$ the *input vector* and $y(\cdot)$ an *output vector*. The state, input, and output vectors depend on a counter $k \in \mathbb{N}$ which numbers the subsequent

occurrences of events. The system matrices (A, B, C) are the *state matrix* $A \in \mathbb{R}_{\max}^{n \times n}$, the *input matrix* $B \in \mathbb{R}_{\max}^{n \times r}$, and the *output matrix* $C \in \mathbb{R}_{\max}^{s \times n}$. We consider only constant system matrices, so A , B , and C are invariant to k . Then for given system matrices the system evolution $\{x(k)\}_{k \in \mathbb{N}}$ and output sequence $\{y(k)\}_{k \in \mathbb{N}}$ is completely determined by the initial condition x_0 and the input sequence $\{u(k)\}_{k \in \mathbb{N}}$. If $C = E$, the identity matrix, then the output vector is just the state vector. The state vector $x = (x_1, \dots, x_n)^\top$ corresponds to events $1, \dots, n$ that occur at discrete times. Hence the term *discrete events*. The state vector $x(k)$ is the vector of *event times* associated to the k th occurrence of the events. So, $x_i(k)$ is the time instant at which event i takes place for the k th time.

A *homogeneous* max-plus linear system has no inputs, i.e., $B = \mathcal{E}$. In this case the recursive state equation is

$$x(k) = A \otimes x(k-1), \quad x(0) = x_0. \quad (8.2)$$

The evolution of a homogeneous first-order max-plus linear system can be calculated analytically for a given state matrix and initial condition. Substituting $k = 1$ in (8.2) simply gives $x(1) = Ax_0$, for $k = 2$ we obtain $x(2) = Ax(1) = A \otimes Ax_0 = A^2x_0$, and by a repeated argument we obtain

$$x(k) = A^k \otimes x_0 \quad \text{for all } k \in \mathbb{N}.$$

The behaviour of the homogeneous system depends on the eigenvalues of A and the initial state vector x_0 . Section 8.3 is devoted to this *spectral analysis*. It will be shown that the asymptotic behaviour of the successive event times is periodic and independent of the initial condition, although the initial condition determines the length of the transient behaviour before reaching the periodic regime [11, 190].

The inhomogeneous term $Bu(k)$ is used to control or regulate the system behaviour into a desired state evolution. In railway systems or public transport systems the (departure) events are generally regulated by a timetable, which specifies the earliest allowed departure times. A regular interval or *periodic timetable* with cycle time T is modelled itself by the homogeneous first-order max-plus linear system

$$d(k) = d(k-1) \otimes T, \quad d(0) = d_0,$$

where $d(\cdot) \in \mathbb{R}_{\max}^n$ is the *timetable vector* and $d_0 \in \mathbb{R}_{\max}^n$ is an initial timetable vector. Note that the right-hand side is a matrix multiplication of an $n \times 1$ -dimensional vector $d(k-1)$ and a scalar T giving the $n \times 1$ -dimensional vector $d(k)$. Alternatively, we could express this equation using the right-hand side $\text{diag}(T, \dots, T) \otimes d(k-1)$ with the diagonal matrix $\text{diag}(T, \dots, T) = T \otimes E \in \mathbb{R}_{\max}^{n \times n}$, or by the scalar-vector product $T \otimes d(k-1)$. The solution to this *timetable system* is

$$d(k) = T^k \otimes d_0 \quad \text{for all } k \in \mathbb{N}. \quad (8.3)$$

By defining $B = E \in \mathbb{R}_{\max}^{n \times n}$, the identity matrix, and $u(k) = d(k)$ we obtain $Bu(k) = d(k)$ which fits the framework (8.1). By convention we use the inhomogeneous term $d(k)$ directly for scheduled max-plus linear systems. An alternative representation that clearly visualizes the periodicity of the timetable is obtained by defining $B = d_0 \in \mathbb{R}_{\max}^{n \times 1}$ and $u(k) = T^k$, which again fits the inhomogeneous state equation (8.1). Here, the *clock event* $u(k)$ gives the starting time of the k th period with respect to the initial timetable vector d_0 . Nevertheless, we use the former representation which also allows aperiodic timetables.

The canonical state-space equations of a *scheduled max-plus linear system* with periodic timetable are therefore

$$x(k) = A \otimes x(k-1) \oplus d(k), \quad x(0) = x_0, \quad d(k) = d_0 \otimes T^k. \quad (8.4)$$

Here $x(k)$ and $d(k)$ are the k th actual and scheduled event time vectors, respectively.

8.2.2 Higher-Order State-Space Equations

The general state-space representation of a timed event graph $\mathcal{G} = (\mathcal{T}, \mathcal{P}, \mu, w)$ is the higher-order max-plus linear system

$$\begin{cases} x(k) = \bigoplus_{l=0}^p A_l x(k-l) \oplus Bu(k), & x(1-p) = x_{1-p}, \dots, x(0) = x_0 \\ y(k) = Cx(k). \end{cases} \quad (8.5)$$

Here the parameter p is called the *order* of the system which equals the highest initial marking of any place, $p = \bigoplus_{i=1}^m \mu_i$. The system matrices $A_l \in \mathbb{R}_{\max}^{n \times n}$ correspond to the places $p_h = (j, i, \mu_h, w_h)$ in the timed marked graph \mathcal{G} with initial marking $\mu_h = l$, i.e.,

$$[A_l]_{ij} = \begin{cases} w_h & \text{if } p_h = (j, i, l) \in \mathcal{P} \\ \varepsilon & \text{otherwise.} \end{cases} \quad (8.6)$$

Note that the first-order max-plus linear system (8.1) is a special case of (8.5) with all places having a unit initial marking, i.e., $A_1 = A$ and $A_0 = \mathcal{E}$. Thus, (8.1) is a *pure* first-order linear system without zero-order terms. In Section 8.2.5 we will show that any p th order linear system can be transformed into a pure first-order representation.

We now return to the timed event graph model $\mathcal{G} = (\mathcal{T}, \mathcal{P}, \mu, w)$ of a scheduled railway system as derived in Chapter 6. Each place $p_h \in \mathcal{P}$ with output transition $\text{out}(p_h) = i$ corresponds to a constraint in the event domain

$$x_i(k) \geq x_{\text{in}(p_h)}(k - \mu_h) \otimes w_h,$$

cf. Section 6.5.3. If transitions fire as soon as they are enabled the event times are given by

$$x_i(k) = \bigoplus_{p \in \Pi_i} x_{\text{in}(p_h)}(k - \mu_h) \otimes w_h \quad \text{for all } i \in \mathcal{T}, \quad (8.7)$$

where Π_i is the set of incoming places to transition i . Defining the matrices A_l by (8.6) then (8.7) becomes

$$x_i(k) = \bigoplus_{l=0}^p \bigoplus_{j=1}^n [A_l]_{ij} \otimes x_j(k-l) \quad \text{for all } 1 \leq i \leq n$$

which in vector notation is the p th order max-plus linear system

$$x(k) = \bigoplus_{l=0}^p A_l \otimes x(k-l).$$

where $x(k) = (x_1(k), \dots, x_n(k))^T$. If the events wait for their scheduled event times then the event times are given by the p th order inhomogeneous state-space equation

$$x(k) = \bigoplus_{l=0}^p A_l \otimes x(k-l) \oplus d(k), \quad (8.8)$$

where $d(k) = (d_1(k), \dots, d_n(k))^T$ is the *timetable vector* in period k . For a periodic timetable with cycle time T the timetable vectors are defined by (8.3), which equals $d_i(k) = d_i(0) \otimes T^k = d_i(0) + k \cdot T$ as in Section 6.5.3.

The general state-space equations of a *scheduled max-plus linear system* with periodic timetable are therefore

$$\begin{cases} x(k) &= \bigoplus_{l=0}^p A_l x(k-l) \oplus d(k) \\ y(k) &= Cx(k) \\ d(k) &= d_0 \otimes T^k. \end{cases} \quad (8.9)$$

In general the events in a railway system may be partitioned in departures, arrivals, passages and terminal events, cf. Chapter 6. Usually, only the departure events are prohibited to depart early, whilst arrival, through and terminal events may be early, that is, these latter events do not have to wait for their scheduled event time before arriving at or passing through a station. The (initial) timetable vector may thus be partitioned as $d_0 = (d_0^1, \varepsilon)^T$, where d_0^1 corresponds to the departure events. Likewise, the output vector may be defined to give e.g. the departure events only. Assuming that the events are ordered with the events of interest numbered first as $1, \dots, n_1$ then $C = [E \ \mathcal{E}] \in \mathbb{R}_{\max}^{n_1 \times n}$ yields the desired output vector $y(\cdot) \in \mathbb{R}_{\max}^{n_1}$.

The general p th order state-space equations (8.9) include an implicit zero-order term and appear therefore no longer purely recursive. However, from a timed event graph perspective it is clear that the zero-order dynamics merely correspond to transitions that fire in the same period as the predecessor transitions and thus still satisfy some precedence order. This will be explained in detail in Section 8.6. The system dynamics are therefore completely determined by (8.9) when given initial states $x(l)$ for $l = 1 - p, \dots, 0$. In Section 8.2.5 we also discuss a simple transformation that removes the zero-order terms from the state-space representation.

8.2.3 Polynomial Matrix Representation

An alternative formulation of a higher-order max-plus linear system (8.9) can be obtained using a shift operator. Let γ be the *backward-shift* operator defined on a discrete-event dynamic variable $x(k)$ as

$$\gamma x(k) = x(k-1).$$

A backward-shift over $l \geq 1$ periods is denoted by γ^l and corresponds to l successive applications of the backward shift γ , that is, $\gamma^l x(k) = x(k-l)$ for any integer $l \geq 1$. This is consistent with the recursion $\gamma^l x(k) = \gamma^{l-1} \gamma x(k) = \gamma^{l-1} x(k-1)$ for all $l \in \mathbb{N}$ with the convention that $\gamma^0 = e$. Using the shift operator the scheduled max-plus linear system (8.9) can be rewritten as

$$x(k) = \bigoplus_{l=0}^p A_l x(k-l) \oplus d(k) = \bigoplus_{l=0}^p A_l \gamma^l x(k) \oplus d(k) = A(\gamma) x(k) \oplus d(k), \quad (8.10)$$

where $A(\gamma) = \bigoplus_{l=0}^p A_l \gamma^l$ is a polynomial matrix in the shift operator γ . A polynomial matrix may thus be used both as a formal representation of a timed event graph, see Section 7.2.6, and

as a shift operator in the max-plus linear system state representation. In the sequel, we will also denote by $(j, i, l) \in \text{supp}(A(\gamma)) = \{(j, i, l) | [A_l]_{ij} \neq \varepsilon\}$ a place $(j, i) \in \mathcal{P}$ with l tokens.

A first-order max-plus linear system is one for which $A(\gamma) = A\gamma$, in which case $A(\gamma)x(k) = A\gamma x(k) = Ax(k-1)$. Hence, a first-order system satisfies the dynamic state-space equation $x(k) = Ax(k-1)$, or in the scheduled case $x(k) = Ax(k-1) \oplus d(k)$.

8.2.4 Autonomous Max-Plus Linear Systems

As previously defined a *homogeneous* higher-order max-plus linear system is a linear system with zero input matrix $B = \mathcal{E}$,

$$x(k) = \bigoplus_{l=0}^p A_l \otimes x(k-l) = A(\gamma) \otimes x(k). \quad (8.11)$$

A homogeneous linear system (8.11) is related to an *autonomous* linear system. An autonomous timed event graph is one that has no source transitions, which means that the polynomial matrix representation $A(\gamma)$ has no zero rows. The general scheduled max-plus linear system (8.8) however allows source events which simply fire according to the timetable. In a homogeneous system source transitions may be defined to fire unconditionally. Nevertheless, system performance is determined by the internal events of the cyclic interconnection structure of the timed event graph. Here, an *internal event* is an event contained in some circuit or accessible from an upstream circuit.

Definition 8.2.1 (Autonomous linear system) A homogeneous max-plus linear system $x(k) = A(\gamma)x(k) = \bigoplus_{l=0}^p A_l x(k-l)$ is called autonomous if the polynomial state matrix $A(\gamma)$ has no zero row, or formally, $\forall 1 \leq i \leq n, \exists 1 \leq j \leq n$ such that $[A(\gamma)]_{ij} \neq \varepsilon$.

An autonomous system thus corresponds to a timed event graph that has no incoming paths or trees.

The timetable subsystem of a scheduled max-plus linear system can be interpreted as an *open-loop control system*, where the periodic timetable is defined a priori. Consider the scheduled max-plus linear system (8.9). Then, given an initial timetable vector d_0 and initial state vectors $x_l, 1-p \leq l \leq 0$, this system may be viewed as an *autonomous* max-plus linear system defined by

$$\tilde{x}(k) = \begin{bmatrix} A(\gamma) & d_0 \\ \varepsilon & T\gamma \end{bmatrix} \otimes \tilde{x}(k), \quad y(k) = [C \quad \varepsilon] \otimes \tilde{x}(k), \quad (8.12)$$

with initial conditions

$$\tilde{x}(0) = \begin{bmatrix} x_0 \\ e \end{bmatrix} \text{ and } \tilde{x}(l) = \begin{bmatrix} x_l \\ \varepsilon \end{bmatrix} \text{ for } 1-p \leq l \leq -1,$$

where $\tilde{x} = (x, x_{n+1})^\top \in \mathbb{R}_{\max}^{n+1}$ is an augmented state vector with $x_{n+1}(k)$ the starting time of the k th period. Note that $x_{n+1}(k) = T^k = k \cdot T$. The autonomous linear system (8.12) is equivalent to the scheduled linear system (8.9) in the sense that the output sequence $\{y(k)\}_{k \in \mathbb{N}}$ is equal for both system realizations. Note that (8.12) is the state-space realization of the scheduled timed event graph (6.10) of Theorem 6.5.3.

8.2.5 First-Order Representations

The max-plus linear systems (8.8) and (8.11) are p th order systems which admit implicit (zero-order) terms. This section shows that any p th order max-plus linear system can be transformed into an equivalent pure first-order linear system (without zero-order terms).

A fundamental result in max-plus algebra is the solution of an implicit equation $x = Ax \oplus b$ is given by $x = A^*b$, provided A^* exists [11, §3.2.3]. The next lemma states a special case of this result which we will be using in the sequel at several occasions.

Lemma 8.2.1 *Let $A \in \mathbb{R}_{\max}^{n \times n}$ be such that $G(A)$ is an acyclic graph. Then for any vector $b \in \mathbb{R}_{\max}^n$ the implicit equation $x = Ax \oplus b$ has solution $x = A^*b$.*

Proof: Because $G(A)$ is acyclic $A^* = \bigoplus_{l=0}^{n-1} A^l$ is well-defined by Corollary 7.2.1. By recursive substitution we obtain

$$\begin{aligned}
 x &= Ax \oplus b \\
 &= A(Ax \oplus b) \oplus b = A^2x \oplus Ab \oplus b \\
 &= A^2(Ax \oplus b) \oplus Ab \oplus b = A^3x \oplus A^2b \oplus Ab \oplus b \\
 &\vdots \\
 &= A^n x \oplus \left(\bigoplus_{l=0}^{n-1} A^l \right) b \\
 &= A^*b.
 \end{aligned}$$

The last equality follows from the acyclicity of $G(A)$ which implies that $A^l = \mathcal{E}$ for all $l \geq n$, since any path with length n or more includes a circuit (in a finite graph with n nodes). \square

Now consider again the higher-order linear system $x(k) = \bigoplus_{l=0}^p A_l x(k-l) \oplus d(k)$. Recall that $G(A_0)$ is the precedence graph associated to A_0 . If this graph has a circuit then the classes accessible by events from this circuit are deadlocked. Hence, a necessary (and sufficient) condition for a live timed event graph associated to the max-plus system (8.8) or (8.11) is that $G(A_0)$ is acyclic. Moreover, this condition assures the existence of A_0^* . Before presenting the main result of this section we need the following lemma.

Lemma 8.2.2 *Let $x(k) = \bigoplus_{l=0}^p A_l \otimes x(k-l) \oplus d(k)$ be a scheduled max-plus linear system. If $G(A_0)$ is acyclic then*

$$A_0^* \otimes d(k) = d(k).$$

Proof: Because $G(A_0)$ is acyclic A_0^+ and A_0^* are finitely generated by Corollary 7.2.1. Moreover, since $G(A_0)$ has no circuits $[A_0^+]_{ii} = \varepsilon$ for all $1 \leq i \leq n$ and therefore $[A_0^*]_{ii} = [E \oplus A_0^+]_{ii} = e$ for all $1 \leq i \leq n$. From the marking formula (6.7) of Theorem 6.5.1 all paths $\xi \in P_{ij}$ in $G(A_0)$ from node j to i with weight $w(\xi)$ must satisfy $d_i(k) \geq w(\xi) \otimes d_j(k)$ otherwise some arc on the path would have had a token which contradicts that the path lies on $G(A_0)$. Hence, $d_i(k) \geq [A_0^+]_{ij} \otimes d_j(k)$ and

$$\bigoplus_{j=1}^n [A_0^*]_{ij} \otimes d_j(k) = e \otimes d_i(k) \oplus \bigoplus_{j \neq i} [A_0^+]_{ij} \otimes d_j(k) = d_i(k)$$

for each $1 \leq i \leq n$, which proves $A_0^*d(k) = d(k)$. \square

In the sequel we say that two max-plus linear systems are *equivalent* if the state trajectories $\{x(k)\}_{k \in \mathbb{N}}$ of both systems are equal.

Theorem 8.2.1 (Elimination of implicit terms) *Let $x(k) = \bigoplus_{l=0}^p A_l \otimes x(k-l) \oplus d(k)$ be a scheduled max-plus linear system. If $G(A_0)$ is acyclic and the initial conditions are given by $x(l) = x_l$ for $1-p \leq l \leq 0$ then this system is equivalent to*

$$x(k) = \bigoplus_{l=1}^p A_0^* A_l x(k-l) \oplus d(k). \quad (8.13)$$

Proof: Rewrite the higher-order linear system equation as

$$x(k) = \bigoplus_{l=0}^p A_l x(k-l) \oplus d(k) = A_0 x(k) \oplus \left(\bigoplus_{l=1}^p A_l x(k-l) \oplus d(k) \right).$$

This is an implicit equation in $x(k)$ and because $G(A_0)$ is acyclic we can apply Lemma 8.2.1, which gives

$$\begin{aligned} x(k) &= A_0^* \otimes \left(\bigoplus_{l=1}^p A_l x(k-l) \oplus d(k) \right) \\ &= \bigoplus_{l=1}^p A_0^* A_l x(k-l) \oplus A_0^* d(k) \\ &= \bigoplus_{l=1}^p A_0^* A_l x(k-l) \oplus d(k). \quad (\text{by Lemma 8.2.2}) \end{aligned}$$

With the initial conditions x_{1-p}, \dots, x_0 the recursive equations (8.13) completely determine the state trajectory $\{x(k)\}_{k \in \mathbb{N}}$. Note that the original state-space equations (8.8) also allow an additional initial vector $x(1)$. This initial condition is excluded for the transformed system description, see Section 8.6. \square

The interpretation of Theorem 8.2.1 is that places with zero initial tokens are contracted to the last predecessor with a nonzero number of initial tokens, i.e., places with zero tokens are removed from the graph and a new place is added from the input transition of the last upstream place(s) having nonzero initial tokens. The holding time of the new place given as $[\bar{A}_l]_{ij}$ is then the weight of the original path from transition j to i with the first place on this path having l tokens and the remaining places having zero tokens.

Removing the zero-order term using Theorem 8.2.1 may generate sinks in the associated timed event graph, see Figure 8.1. If a transition has only zero-token outgoing places then it becomes a sink after removal of the zero-token places. These transitions may subsequently be removed from the graph. So for any transition i with zero-token outgoing places only the state x_i is removed from the state vector x . The resulting reduced state vector is denoted as $\hat{x} \in \mathbb{R}^{\hat{n}}$, where \hat{n} is the number of transitions with nonzero-token outgoing places. Accordingly, the

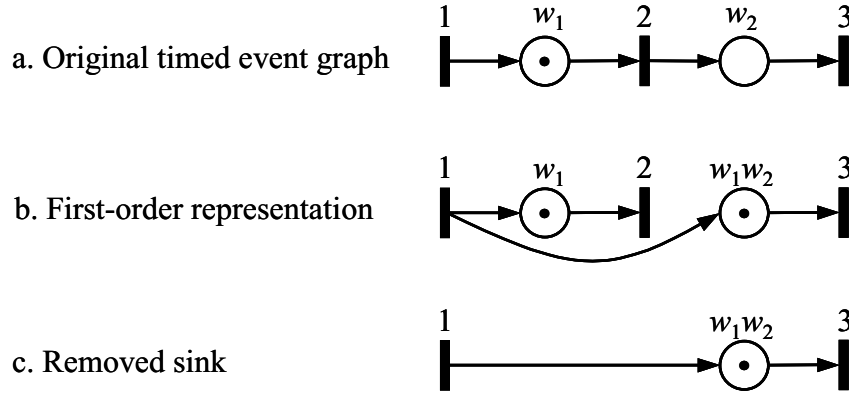


Figure 8.1 Elimination of implicit zero-order terms

associated row j and column j are removed from the matrices \bar{A}_l to obtain the reduced matrices $\hat{A}_l \in \mathbb{R}_{\max}^{\hat{n} \times \hat{n}}$.

Any live higher-order linear system can be represented as a canonical first-order linear system using state-space augmentation, which is a well-known technique in system theory.

Lemma 8.2.3 (State-space augmentation) *Any purely recursive max-plus linear system $x(k) = \bigoplus_{l=1}^p A_l \otimes x(k-l) \oplus d(k)$ with initial conditions $x(l) = x_l$, $1-p \leq l \leq 0$, can be written in first-order representation*

$$\tilde{x}(k) = \tilde{A} \otimes \tilde{x}(k-1) \oplus \tilde{d}(k), \quad \tilde{x}(0) = \tilde{x}_0, \quad (8.14)$$

for some augmented state-space.

Proof: We will give a constructive proof. Assume $x(\cdot), d(\cdot) \in \mathbb{R}_{\max}^n$ and $A_l \in \mathbb{R}_{\max}^{n \times n}$ for $1 \leq l \leq p$, and let $\tilde{n} = p \cdot n$. Define the *augmented* state and timetable vector $\tilde{x}(\cdot), \tilde{d}(\cdot) \in \mathbb{R}_{\max}^{\tilde{n}}$ and state matrix $\tilde{A} \in \mathbb{R}_{\max}^{\tilde{n} \times \tilde{n}}$ by

$$\tilde{x}(k) = \begin{bmatrix} x(k) \\ x(k-1) \\ \vdots \\ x(k-p+1) \end{bmatrix}, \quad \tilde{A} = \begin{bmatrix} A_1 & A_2 & \cdots & A_p \\ E & \mathcal{E} & \cdots & \mathcal{E} \\ & \ddots & \ddots & \vdots \\ \mathcal{E} & & E & \mathcal{E} \end{bmatrix} \quad \text{and} \quad \tilde{d}(k) = \begin{bmatrix} d(k) \\ \varepsilon \\ \vdots \\ \varepsilon \end{bmatrix}.$$

Then (8.14) with initial condition $\tilde{x}_0 = (x_0, \dots, x_{1-p})^\top$ is equivalent to the higher-order system $x(k) = \bigoplus_{l=1}^p A_l \otimes x(k-l) \oplus d(k)$ with initial conditions $x(0) = x_0, \dots, x(1-p) = x_{1-p}$. \square

Lemma 8.2.3 is visualized in Figure 8.2. Each place with $l > 1$ tokens is expanded to l places with one token each by adding $l-1$ sequential transitions. The first place maintains the original holding time and the remaining $l-1$ places get zero holding time. These places can be viewed as fictitious stops at dummy stations. The introduction of additional transitions leads to an increased dimension of the state vector, which is referred to as state-space augmentation.

Theorem 8.2.2 (First-order representation) *Let $x(k) = \bigoplus_{l=0}^p A_l \otimes x(k-l) \oplus d(k)$ be a scheduled max-plus linear system with initial conditions $x(l) = x_l$, $1-p \leq l \leq 0$, and acyclic*

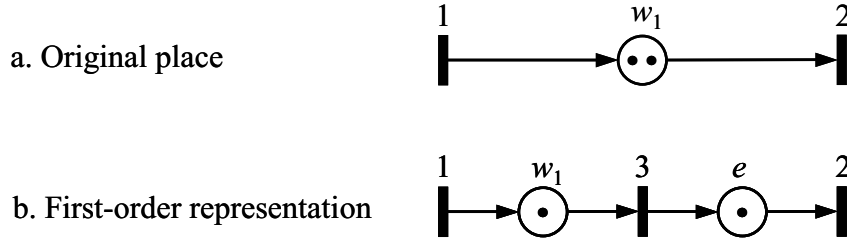


Figure 8.2 State-space augmentation

$G(A_0)$. Then it has a first-order representation $\tilde{x}(k) = \tilde{A} \otimes \tilde{x}(k-1) \oplus \tilde{d}(k)$ with initial condition $\tilde{x}(0) = \tilde{x}_0$ for some augmented state-space.

Proof: If $G(A_0)$ is acyclic then by Theorem 8.2.1 we have $x(k) = \bigoplus_{l=0}^p A_l \otimes x(k-l) \oplus d(k) = \bigoplus_{l=1}^p A_0^* A_l \otimes x(k-l) \oplus d(k)$. By Lemma 8.2.3 this system admits a first-order representation with state matrix

$$\tilde{A} = \begin{bmatrix} A_0^* A_1 & A_0^* A_2 & \cdots & A_0^* A_p \\ E & \mathcal{E} & \cdots & \mathcal{E} \\ & \ddots & \ddots & \vdots \\ \mathcal{E} & & E & \mathcal{E} \end{bmatrix}$$

and the augmented state vector, timetable vector, and initial condition are as in the proof of Lemma 8.2.3. \square

8.3 Max-Plus Spectral Analysis

8.3.1 Timetable Stability and Critical Circuits

The polynomial state matrix $A(\gamma)$ of a max-plus linear system reflects the structure of the railway traffic network including train interconnections, train orders, safety and infrastructure restrictions, train line cycle times (regular intervals), and timing constraints. The maximum max-plus generalized eigenvalue of this polynomial matrix equals the minimum cycle time in which the traffic system can satisfy the intrinsic requirements of a given timetable, i.e., running as early as possible while respecting all train orders, connections, and minimum headways. This minimum cycle time is determined by the worst-case sequence of blocking times or the critical circuit in the *compressed timetable*, which corresponds to the given timetable after removing all buffer times or slack contained therein. The compressed timetable is explicitly computed as part of the eigenproblem and is given by the associated eigenvector. Hence, the eigenvector contains the earliest realizable event times given all the timetable and infrastructure constraints. All circuits without any slack under the compressed timetable are called critical. The critical circuits thus determine the minimum cycle time of the network and also the remaining degree of freedom (departure time flexibility) for all trains that are not contained in a critical circuit.

A periodic timetable is called stable if a delay of any train can be compensated for by time reserves in the timetable, which prevents that a delay keeps circulating over the network. Or formally, for any $x(k_0) > d(k_0)$ there exists a $K > k_0$ such that $x(k) = d(k)$ for all $k \geq K$.

In particular this implies that for each event i a delay $z_i(k_0) = x_i(k_0) - d_i(k_0)$ in some period k_0 must have been (partially) absorbed before it recurs to a next occurrence of this event $x_i(k)$ with $k > k_0$. We thus obtain the following definition of stability.

Definition 8.3.1 (Stability) *A scheduled max-plus linear system is stable if each circuit in the associated timed event graph contains some positive buffer time.*

Stability can therefore be tested by computing the maximal generalized eigenvalue as presented in the following theorem.

Theorem 8.3.1 (Stability) *Let $A(\gamma) = \bigoplus_{l=0}^p A_l \gamma^l \in \mathbb{R}_{\max}^{n \times n}[\gamma]$ be a polynomial matrix with maximum generalized eigenvalue λ_0 . Then the scheduled max-plus linear system (8.9) is stable if and only if*

$$\lambda_0 < T.$$

If $\lambda_0 = T$ the system is called critical, and if $\lambda_0 > T$ the system is unstable.

Proof: By Theorem 7.4.1 the maximum eigenvalue λ_0 equals the maximum cycle mean over all circuits in the network. If $\lambda_0 < T$ then even the critical circuit(s) have some average buffer time $T - \lambda_0 > e$, and therefore all circuits have at least $T - \lambda_0 > e$ average buffer time. Note that the total buffer time on a circuit ξ is $\mu(\xi) \cdot T - w(\xi) \leq \mu(\xi) \cdot T - \mu(\xi) \cdot \lambda_0 = \mu(\xi) \cdot (T - \lambda_0)$, which is positive only if $T > \lambda_0$. Finally, notice that since λ_0 exists $G(A_0)$ must be acyclic and therefore there are no circuits with zero tokens. Hence, we only consider stability for live systems. \square

Theorem 8.3.1 states that the timetable cycle time should exceed the minimum possible one, that is, the maximum eigenvalue is the *minimum cycle time*. Hence, the maximum eigenvalue allows a stability test: if λ_0 exceeds the timetable cycle time T then the system is unstable. Instability here means that there is no slack on the critical circuit by which delays that reach the critical circuit can never settle, i.e., all trains on the critical circuit will get delayed and possibly propagate this delay to other trains in the network. If $\lambda_0 < T$ is close to T then delays on the critical circuit will settle only slowly and the system will become unstable in case of (temporary) process time prolongations on the critical circuit.

Stability thus depends on the eigenstructure of the (polynomial) state matrix of the homogeneous max-plus linear system $x(k) = \bigoplus_{l=0}^p A_l x(k-l) = A(\gamma)x(k)$. It is insightful to revisit and interpret the eigenproblem with respect to the dynamic system equations. Recall from Chapter 7 (Sections 7.4.5 and 7.4.6) that the associated generalized eigenmode (χ, v) satisfies the conditions (7.39a–7.39b) which we repeat here for convenience:

$$\chi_i = \max_{(j,i,l) \in \Pi_i} \chi_j \quad \text{and} \quad v_i = \max_{(j,i,l) \in \Pi_i} ([A_l]_{ij} - l \cdot \chi_j + v_j) \quad \text{for all } i = 1, \dots, n. \quad (8.15)$$

Here χ_j is the cycle time of event j with $\lambda_0 = \bigoplus_{j=1}^n \chi_j$. We now interpret v as an event time vector. Then (8.15) implies that each event i must wait for the latest preceding activity with process time $[A_l]_{ij}$ that was initiated l periods of length χ_j ago at event time $v_j - l \cdot \chi_j$. If $A(\gamma)$ is irreducible — the timed event graph $G(A(\gamma))$ is strongly-connected — all cycle times are constant $\chi_i \equiv \lambda_0$ corresponding to the minimal cycle time of all events. The eigenvector v then corresponds to the earliest possible event times where the events cycle at their minimal

cycle time λ_0 . In case of delayed events the system may thus ‘accelerate’ with cycle time λ_0 until the delays have settled. Note that delayed events consume timetable slack and buffer times and fire as early as possible until they again meet their schedule. In the reducible case delayed events of distinct classes may cycle at different cycle times in accordance to the available slack in the different components. Thus, events of nonbasic classes (with cycle time $\chi_j < \lambda_0$, see Section 7.4.4) settle quicker than events of basic classes, whilst critical events on a critical circuit take longest to settle.

The (maximum) eigenvalue is a unique characteristic of the state matrices of a max-plus linear system. Hence, the maximum eigenvalue is a performance indicator of the traffic scenario characterized by the timetable, infrastructure, and signalling system. In particular, like the state matrices the eigenvalue depends on the line frequencies, line schedules (running times, minimum dwell times), traffic mix (speed differences) and train orders on the open tracks, minimum headways, minimum layover times at terminals, minimum transfer times of passenger connections, and minimum (de-)coupling times of rolling stock connections.

8.3.2 Network Throughput

A performance indicator related to stability is capacity utilization. An indicator for network capacity utilization of a periodic railway system is the *network throughput* defined as (using conventional division)

$$\rho = \lambda_0/T,$$

where λ_0 is the minimum cycle time and T the timetable cycle time. For a stable railway system we have $0 < \rho \leq 1$, where $\rho = 1$ corresponds to the saturated case in which the mean cycle time of trains on the critical circuit is exactly (a multiple of) T . If $\rho < 1$ the system operates below its maximum (theoretical) performance and hence contains buffer time to compensate for delays. Clearly, the network throughput represents a trade-off between stability and capacity utilization. The higher this measure the more effective the train circulations but the less slack is available for delay recovery.

In current daily railway practice throughput is a more recognizable quantity than the minimum cycle time. For instance a throughput of 70% implies that the infrastructure on the worst-case circuit is utilized for 70% and the remaining 30% is buffer time to avoid or reduce hindrance. Network throughput refers to the throughput of the critical circuit. A large throughput on this circuit does not necessarily mean that the throughput on any corridor (which can be seen as a subnetwork) is also this high. It is therefore also relevant which transportation links make up the critical circuit, and how the critical cycle time relates to the cycle times of train lines and corridors or other subnetworks. The cycle times, and hence throughputs, of train lines are easily obtained when connections and headway are discarded: the circuits are then exactly the train line circulations (assuming layover times are included).

8.3.3 Stability Margin

The difference $\Delta_1 = T - \lambda_0$ gives the average amount of slack on the critical circuit(s) and hence is a measure of robustness or sensitivity to delays. In particular, Δ_1 is the marginal

increase of each *active* holding time such that the timetable becomes critical, i.e., Δ_1 is the solution to

$$\max_{\xi \in C} \frac{w(\xi) + \mu(\xi) \cdot \Delta_1}{\mu(\xi)} = \max_{\xi \in C} \frac{w(\xi)}{\mu(\xi)} + \Delta_1 = \lambda_0 + \Delta_1 = T.$$

Another indicator of robustness is the *stability margin* Δ_2 defined as the maximum simultaneous increase of all process times such that the train network can still be operated with cycle time T , or formally, Δ_2 is the solution to the problem $(\Delta_2 \otimes A(T^{-1})) \otimes v = v$. Note the difference with $\Delta_1 = T - \lambda$ which is defined relative to the marking in each place. Hence, Δ_1 relates to the number of trains (tokens) on each circuit whereas Δ_2 takes all stops (events) into account. The stability margin Δ_2 can be computed by solving an auxiliary eigenvalue problem as presented in the following theorem.

Theorem 8.3.2 (Stability margin) *Let (8.9) be a stable scheduled max-plus linear system. Then the stability margin Δ_2 is given by $\Delta_2 = \nu^{-1}$, where ν is the solution of the eigenvalue problem $A_T \otimes v = \nu \otimes v$.*

Proof: The stability margin Δ_2 is the implicit least solution of $(\Delta_2 \otimes A_T) \otimes v = e \otimes v$. The max-plus matrix $\Delta_2 \otimes A_T$ corresponds to the precedence graph $G(A_T)$ where each arc weight is increased by Δ_2 . Hence, by Theorem 7.4.1 we have

$$\max_{\xi \in C} \frac{w(\xi) - \mu(\xi) \cdot T + l(\xi) \cdot \Delta_2}{l(\xi)} = \max_{\xi \in C} \frac{w(\xi) - \mu(\xi) \cdot T}{l(\xi)} + \Delta_2 = e,$$

with solution $\Delta_2 = -\max_{\xi \in C} (w(\xi) - \mu(\xi) \cdot T) / l(\xi)$, which is exactly the inverse of the solution ν to the eigenvalue problem $A_T \otimes v = \nu \otimes v$. Hence $\Delta_2 = \nu^{-1} = -\nu$. \square

In first-order linear systems $x(k) = Ax(k-1)$ the number of places and tokens on each circuit ξ is the same, $l(\xi) = \mu(\xi)$, and therefore $\Delta_2 = \Delta_1$. In a first-order state-space representation the number of events is thus reduced to the number of initial tokens.

8.4 Timetable Realizability

In this section we focus on the timetable system $\{d(k)\}_{k \in \mathbb{N}}$. Hence, we assume that $A(\gamma)$ is a given polynomial state matrix and derive conditions on the timetable vectors $d(k)$ such that the scheduled max-plus linear system

$$x(k) = A(\gamma)x(k) \oplus d(k) \quad \text{for all } k \in \mathbb{N} \quad (8.16)$$

is well-defined. We will concentrate on periodic timetables that satisfy the first-order state equations $d(k) = d(k-1) \otimes T$, $d(0) = d_0$. From Section 8.2.1 we know that the solution of this timetable system is

$$d(k) = d_0 \otimes T^k, \quad k \in \mathbb{N}.$$

The characteristic parameters of a periodic timetable are thus the initial timetable vector d_0 and the cycle time T . If required the timetable sequence may be extended to the left by allowing periods $k \in \mathbb{Z}$.

A timetable only makes sense if the system is able to operate according to the timetable. This means that for each marked arc $(j, i, l) \in \text{supp}(A(\gamma))$

$$d_i(k) \geq [A_l]_{ij} \otimes d_j(k - l) \quad \text{for all } k \in \mathbb{Z}. \quad (8.17)$$

Timetables satisfying this condition are called *realizable* [21].

Definition 8.4.1 (Timetable realizability) A sequence $\{d(k)\}_{k \in \mathbb{Z}}$ is called a *realizable timetable* for the scheduled max-plus linear system (8.16) if

$$d(k) \geq A(\gamma)d(k) \quad \text{for all } k \in \mathbb{Z}. \quad (8.18)$$

The scheduled system (8.16) is called *realizable* if it has a *realizable timetable*.

Theorem 8.4.1 (Realizable periodic timetable) A periodic timetable $d(k) = d_0 \otimes T^k$, $k \in \mathbb{Z}$, is *realizable* for a scheduled max-plus linear system $x(k) = A(\gamma)x(k) \oplus d(k)$ if and only if d_0 is a generalized subeigenvector of $A(\gamma)$ associated to T , i.e.,

$$d_0 \geq A(T^{-1}) \otimes d_0. \quad (8.19)$$

Proof: Assume $d(\cdot)$ is a *realizable periodic timetable*. Then for all $k \in \mathbb{Z}$

$$d(k) \geq A(\gamma)d(k) = \bigoplus_{l=0}^p A_l d(k - l) = \bigoplus_{l=0}^p A_l d_0 T^{k-l} = \bigoplus_{l=0}^p A_l T^{-l} d_0 T^k = A(T^{-1})d(k).$$

In particular, for $k = 0$ we obtain inequality (8.19). Hence, for a periodic timetable the conditions (8.18) and (8.19) are equivalent. \square

By Theorem 8.4.1 any finite (sub)eigenvector of the polynomial state matrix $A(\gamma)$ associated to T is a *realizable timetable* to the scheduled system (8.16). Moreover, a *realizable timetable* is never unstable as stated in the following Theorem.

Theorem 8.4.2 A scheduled max-plus linear system with a *realizable periodic timetable* $d(k) = d_0 \otimes T^k$ for $k \in \mathbb{Z}$ is either *stable* or *critical*, i.e., $T \geq \lambda_0$.

Proof: By Theorem 8.4.1 a periodic timetable is *realizable* iff $d_0 \in \mathbb{R}_{\max}^n$ is a subeigenvector of $A(\gamma)$ associated to T . Then by Theorem 7.4.4 we must have $T \geq \lambda_0$, where λ_0 is the maximal generalized eigenvalue of $A(\gamma)$, and finally by Theorem 8.3.1 the system is *stable* except for the critical case $T = \lambda_0$. \square

The inequality (8.18), or equivalently (8.17), implies that a *realizable timetable* contains some nonnegative slack time in each process from one event to another. For a periodic timetable we can rewrite (8.17) as $d_i(k) \geq d_j(k) + [A_l]_{ij} - l \cdot T$ for all $k \in \mathbb{Z}$, or equivalently

$$d_i(k) - d_j(k) - [A_l]_{ij} + l \cdot T \geq 0 \quad \text{for all } k \in \mathbb{Z}. \quad (8.20)$$

The actual slack time from j to i may be less because of a tighter process (sequence) from event j to i . This is the topic of Section 8.5. Also note that a *realizable timetable* implies that when

all trains are able to depart according to schedule at some period then this will also be realized for any future period.

The derivation of a scheduled max-plus linear system and in particular the determination of the initial marking typically assumes a feasible timetable, cf. Algorithm 6.5.1 and Theorem 6.5.1. However, the (process time) input data for the timed event graph construction may differ from the process times applied during evaluation. The construction is based on the scheduled process times. Once the system has been generated the process times may be adjusted without changing the initial marking. For robustness studies the running times may be decreased by their running time margins and for capacity tests the minimum headway times can be reset to the capacity allocation norms. Realizability of the adjusted system is then no longer trivial.

8.5 Timetable Robustness

8.5.1 The Recovery Matrix

A timetable generally contains slack to recover from delays after disruptions. Slack time can be incorporated within scheduled process times (running time margins) or between train movements (buffer times). Moreover, a sequence of train runs embraces an accumulation of slack times. Timetable robustness against delay propagation is therefore determined by accessibility relations between events and the amount of available slack time on paths from one event to another. Since in general multiple paths exist between pairs of timetable events we are interested in the *critical path* from one event to another that has the least accumulated slack time over all possible paths. This is the topic of this section.

In this section we assume that $d(\cdot)$ is a *periodic timetable* with cycle time T and finite initial timetable vector $d_0 > \varepsilon$, and consider the scheduled max-plus linear system

$$x(k) = A(\gamma)x(k) \oplus d(k), \quad d(k) = d_0 \otimes T^k \quad \text{for all } k \in \mathbb{N}. \quad (8.21)$$

We write $d_0 = (d_1^0, \dots, d_n^0)^\top$. By definition, if $d_i(k) \in [0, T)$ for some $1 \leq i \leq n$ then $d_j(k) \in [0, T)$ for all $1 \leq j \leq n$. Moreover, each two events in a periodic timetable have a regular interval, i.e., for all $1 \leq i, j \leq n$ event time differences satisfy $d_i^0 - d_j^0 = d_i(k) - d_j(k)$ for all $k \in \mathbb{Z}$. Without loss of generality, we may assume that $d_0 \in [0, T)^n$ denotes the timetable vector over the basic period $[0, T)$.

In the sequel, we refer to the *slack time* of two adjacent events as the sum of process time margin and buffer time. Recovery time will be used in a more wide sense as follows [207].

Definition 8.5.1 (Recovery matrix) *The recovery matrix $R = (r_{ij})$ is the $n \times n$ dimensional matrix of (cumulative) recovery times, where r_{ij} is the minimum total slack time over all paths from event j to i in the timed event graph $\mathcal{G}(A(\gamma))$ associated to the scheduled max-plus linear system (8.21).*

An alternative interpretation of the recovery matrix is that r_{ij} is the largest delay of $x_j(k)$ in some period $k \in \mathbb{N}$ that will not reach $x_i(m)$ for all $m \geq k$. If there is no path from event j to i then delays of event j will never reach i and so $r_{ij} = \infty$. The recovery matrix thus takes

values from the extended set $\bar{\mathbb{R}}_{\max} \doteq \mathbb{R}_{\max} \cup \{\infty\}$, or from $[e, \infty)$ if the timetable is realizable, cf. (8.20). In fact, the recovery matrix is defined as a *shortest path problem* which corresponds to the so-called *min-plus algebra* $\mathbb{R}_{\min} = (\mathbb{R} \cup \{\infty\}, \min, +)$, which is an idempotent semiring dual to the max-plus algebra. We will however stay within the framework of the (extended) max-plus algebra by using the identity $\min(a, b) = -\max(-a, -b)$ for all $a, b \in \bar{\mathbb{R}}_{\max}$, where by convention $-\varepsilon = \infty$.

The following theorem characterizes the entries of a recovery matrix [207, 89].

Theorem 8.5.1 *Let (8.21) be a stable scheduled max-plus linear system. Then the associated recovery matrix $R = (r_{ij}) \in \bar{\mathbb{R}}_{\max}^{n \times n}$ is defined by*

$$r_{ij} = d_i^0 - d_j^0 - [A_T^+]_{ij}, \quad (8.22)$$

where $r_{ij} = \infty$ if there is no path from j to i in the timed event graph $\mathcal{G}(A(\gamma))$.

Proof: By the stability assumption $T > \lambda$ and therefore $A_T^+ = A^+(T^{-1}) = [\bigoplus_{l=0}^p A_l T^{-l}]^+$ is well-defined. By definition, the entry r_{ij} is the minimal cumulative slack over all paths from j to i in $\mathcal{G}(A(\gamma))$. Let P_{ij} be the set of all paths from j to i , and for any path $\xi \in P_{ij}$ denote by $w(\xi)$ the weight of path ξ and by $\mu(\xi)$ the initial marking on path ξ . Then for all $k \in \mathbb{N}$

$$\begin{aligned} r_{ij} &= \min_{\xi \in P_{ij}} [d_i(k + \mu(\xi)) - d_j(k) - w(\xi)] \\ &= \min_{\xi \in P_{ij}} [(d_i^0 + (k + \mu(\xi)) \cdot T) - (d_j^0 + k \cdot T) - w(\xi)] \\ &= \min_{\xi \in P_{ij}} [d_i^0 - d_j^0 - w(\xi) + \mu(\xi) \cdot T] \\ &= d_i^0 - d_j^0 - \max_{\xi \in P_{ij}} [w(\xi) - \mu(\xi) \cdot T] \\ &= d_i^0 - d_j^0 - [A_T^+]_{ij}. \end{aligned}$$

If there is no path from j to i then $[A_T^+]_{ij} = \varepsilon$, and by convention $r_{ij} = d_i^0 - d_j^0 - [A_T^+]_{ij} = d_i^0 - d_j^0 - \varepsilon = \infty$. \square

Theorem 8.5.1 shows that a recovery time depends on the cycle time $T \in \mathbb{R}_+$, the polynomial state matrix $A(\gamma) \in \mathbb{R}_{\max}^{n \times n}[\gamma]$, and the scheduled event times of the origin j and destination i , but *not* on the exact timetable of intermediate events. In the proof of Theorem 8.5.1 we used stability but did not need realizability. If a timetable is unrealizable then recovery times may be negative, i.e., there exist paths $j \rightarrow i$ such that $r_{ij} < 0$. Nevertheless, if the timetable is (partially) unrealizable but stable it can still be robust when the recovery times are positive for almost all connected event pairs in $G(A_T)$. Of course, the unrealizable arcs will always generate a (small) delay but depending on the slack of adjacent arcs this delay may be absorbed quickly which prevents delay propagation over large areas. Unrealizable train runs may formally occur in the timetable when infrastructure conflicts are not solved in the timetable design. This occurs for instance in the flexible time-window philosophy of dynamic railway traffic management [179]: route conflicts are solved by dispatchers in short-term rescheduling depending on the actual train positions during operation, e.g. on basis of a first-come first-served (FCFS) principle.

By Theorem 8.5.1 computation of the recovery matrix R involves solving an (all-pair) longest path problem over the graph $G(A_T)$. If A_T is stable then $G(A_T)$ does not contain positive

(weight) circuits, which is a necessary condition for the existence of finite longest paths. Nevertheless, $G(A_T)$ generally contains positive arc weights (in conventional sense). For example, for each $(j, i) \in \text{supp}(A_0)$ we have $[A_T]_{ij} = \bigoplus_{l=0}^p [A_l T^{-l}]_{ij} = [A_0]_{ij} \oplus \bigoplus_{l=1}^p [A_l T^{-l}]_{ij} \geq [A_0]_{ij} \geq e$. We can use the Floyd-Warshall algorithm to compute the longest path matrix A_T^+ in $O(n^3)$ time [3, 39]. However, the matrices $A_T \in \mathbb{R}_{\max}^{n \times n}$ are typically very large and sparse, i.e., $m \ll n^2$, where m is the number of finite matrix entries (arcs). In this case, it is more efficient to solve the all-pair longest path problem by a repeated single-origin (or single-destination) longest path algorithm. Implementations of Dijkstra's label-setting algorithm [56, 3, 39] are particularly efficient in both running time and memory usage. However, Dijkstra's longest path algorithm is restricted to graphs with nonpositive arc weights only¹

If $d_0 > \varepsilon$ is a realizable timetable then we can use the timetable vector d_0 to compute nonpositive *reduced arc weights* while leaving the longest paths invariant.

Lemma 8.5.1 (Slack Matrix) *Let (8.21) be a realizable scheduled max-plus linear system and define the slack matrix $S = (s_{ij}) \in \mathbb{R}_{\max}^{n \times n}$ by*

$$s_{ij} = d_j^0 - d_i^0 + [A_T]_{ij}. \quad (8.23)$$

Then S satisfies

- (i) $s_{ij} \leq e$ for all $1 \leq i, j \leq n$,
- (ii) the precedence graph $G(S)$ has no positive-weight circuits,
- (iii) $[S^+]_{ij} = d_j^0 - d_i^0 + [A_T^+]_{ij}$ for all $1 \leq i, j \leq n$.

Proof: The realizability assumption implies $d_i^0 \geq d_j^0 + [A_T]_{ij}$ and therefore $s_{ij} = d_j^0 - d_i^0 + [A_T]_{ij} \leq e$ for all $1 \leq i, j \leq n$, which proves (i). By (i) the graph $G(S)$ has nonpositive arc weights only and therefore the weight of each path or circuit in $G(S)$ will also be nonnegative, which proves property (ii). From Proposition 7.2.6 and property (ii) follows that S^+ exists and is given by $S^+ = \bigoplus_{l=1}^n S^l$. Also $A_T^+ = A(T^{-1})^+$ is well-defined which is proved as follows. By Corollary 8.4.2 we have $T \geq \lambda_0(A(\gamma))$ and therefore $\lambda_0(A_T) \leq e$. Hence, the maximum cycle mean of $G(A_T)$ is at most e and so all circuits in $G(A_T)$ must have nonpositive weight, by which $A_T^+ = \bigoplus_{l=1}^n A_T^l$ using Proposition 7.2.6. It remains to prove that the equality (iii) is valid. Obviously, $s_{ij} = \varepsilon$ iff $[A_T]_{ij} = \varepsilon$. Hence, the precedence graph $G(S)$ equals $G(A_T)$ except for an arc reweighting. Now, let P_{ij} be the set of all paths from j to i in $G(S)$. Then the path weight $w(\xi)$ of any path $\xi = (j = i_0, i_1, \dots, i_l = i) \in P_{ij}$ of some length $l = l(\xi)$ satisfies

$$w(\xi) = \sum_{k=1}^{l(\xi)} s_{i_k i_{k-1}} = \sum_{k=1}^{l(\xi)} \left(d_{i_{k-1}}^0 - d_{i_k}^0 + [A_T]_{i_k i_{k-1}} \right) = d_j^0 - d_i^0 + \sum_{k=1}^{l(\xi)} [A_T]_{i_k i_{k-1}}.$$

Hence, the weight of a path ξ in $G(S)$ equals its weight in $G(A_T)$ plus a constant term $d_j^0 - d_i^0$ that only depends on the initial and final node of the path. Since $\xi \in P_{ij}$ was arbitrary, this holds for all paths from j to i of any length and in particular for the maximum-weight paths, which proves (iii). \square

¹Recall that the discussion of path algorithms and data structures in the max-plus algebra setting distinguishes from the common literature on two points: (1) Algorithms and data structures are usually formulated in terms of shortest-path problems over graphs with no negative circuits. (2) The usual representation of arcs in adjacency matrices or lists is reversed

Theorem 8.5.2 *If the scheduled max-plus linear system (8.21) is realizable then the recovery matrix $R = (r_{ij})$ is well-defined by $r_{ij} = -[S^+]_{ij}$.*

Proof: The theorem follows immediately from Theorem 8.5.1 and Lemma 8.5.1(iii). \square

As a consequence of Theorem 8.5.2 the recovery matrix R can be computed as the solution to a longest path problem over a graph with nonpositive arc weights only. For this problem any longest (or shortest) path algorithm can be used. The best worst-case running time is $O(nm + n^2 \log n)$ obtained by repetitively using a Fibonacci heap implementation of Dijkstra's algorithm [67]. However, for large networks computing and storing the complete recovery matrix takes much computing time and storage space. Note that even if the matrix A_T is sparse this will generally not be the case for the recovery matrix R . In particular if A_T is irreducible then R is a full matrix and thus needs a storage space of $O(n^2)$.

In practice we are only interested in special parts of the matrix R which can better be computed on demand rather than precomputing and storing the full recovery matrix in advance. In particular we are interested in only a limited number of rows or columns or in the diagonal of the recovery matrix R , which have different practical interpretations. We next have a closer look at the interpretation of the matrix entries depending on their location in the matrix.

8.5.2 Delay Impact Vectors

Each j th column of the recovery matrix gives the recovery time from event j to all other events in the timetable. Hence, column j represents the *impact* that a delay of event j will have on future train events. An entry r_{ij} is the maximum delay of event j that can be compensated before reaching event i . If event j has a delay $z_j(k) \geq 0$ in some period k then event i will be delayed by $z_i(m) = \max(z_j(k) - r_{ij}, 0)$ at some period $m \geq k$, i.e., if $z_j(k) \leq r_{ij}$ then the delay will have been absorbed before reaching event i and otherwise event i will suffer a delay of $z_j(k) - r_{ij} \geq 0$.

A column j of the recovery matrix can thus be interpreted as a *delay impact vector*. The finite entries of this vector correspond to the events that are accessible from j and the values represent the impact that a delay of event j will have. Of special interest are recovery times below some threshold value δ , which specifies an *impact region* at level δ :

$$I_\delta(j) \doteq \{i \mid r_{ij} \leq \delta, 1 \leq i \leq n\}.$$

For example, the impact region $I_3(j)$ gives a neighbourhood of less than 3 minutes recovery time from event j .

The delay impact vector and associated impact regions give a quick insight view on the impact of individual delayed events. Since a delay impact vector is just a column of the recovery matrix it can be computed by the SINGLEORIGINLONGESTPATH algorithm of Section 7.5.2 for the origin j in $O(n_j \log n_j)$ time, where $n_j \leq n$ is the number of events accessible from j .

8.5.3 Delay Sensitivity Vectors

Each i th row of the recovery matrix gives the recovery time to event i from all other events in the timetable. Hence, row i represents the *sensitivity* of event i on delays of preceding events.

In this case, event i will receive a delay $z_i(m) = \max(z_j(k) - r_{ij}, 0)$ from a previous event j that was delayed by $z_j(k)$ in some period $k \leq m$. So again, if $z_j(k) \leq r_{ij}$ then the delay will have been absorbed before reaching event i and otherwise event i will suffer a delay of $z_j(k) - r_{ij} \geq 0$.

A row i of the recovery matrix can thus be interpreted as a *delay sensitivity vector*. The finite entries of this vector correspond to the events that have access to i and the values represent the sensitivity of event i on these preceding events. A critical set of events can be defined for which the recovery times to i are below some threshold value δ . This results in a *sensitivity region* at level δ :

$$S_\delta(i) \doteq \{j \mid r_{ij} \leq \delta, 1 \leq j \leq n\}.$$

For example, the sensitivity region $S_3(i)$ gives a neighbourhood of less than 3 minutes recovery time to event i .

The delay sensitivity vector and associated sensitivity regions quantify the vulnerability of an event on preceding events. A delay sensitivity vector is a row of the recovery matrix and can be computed by a *single-destination longest path algorithm*, or equivalently by a single-origin longest path algorithm in the graph $G(A_T)$ obtained by reversing all arcs. Hence, a sensitivity vector can be computed by the SINGLEORIGINLONGESTPATH algorithm of Section 7.5.2 for $G(A^T)$ and the origin i in $O(n_i \log n_i)$ time, where $n_i \leq n$ is the number of events that have access to i .

8.5.4 Circulation Recovery Times

Each diagonal entry of the recovery matrix gives the recovery time over all possible paths from an event i back to event i . The diagonal thus represents the *circulation recovery times* of all events in the timetable. The circulation recovery time is an absolute robustness measure for each periodic event separately and represents the maximum delay that can be absorbed by available slack in the timetable. Any larger delay will backfire (in reduced form) over some path (circuit) in the timetable.

The main issue in stability analysis is the circulation of delays over the network. If a delay keeps circulating over a circuit then all trains on this circuit keep departing delayed. In the spectral analysis of Sections 7.4 and 8.3 we considered critical circuits that have the smallest average amount of slack. The circulation recovery time gives a *second-order* stability test. In first instance an event is critical if it is part of a critical circuit with minimal stability margin. Recall that the stability margin is an integrated measure for all events on a critical circuit. In contrast, the circulation recovery time may vary for all critical events on the critical circuit(s). Hence, of all critical events the events with minimal circulation recovery time are the most jeopardizing to stability.

The circulation recovery times of all events are exactly the diagonal entries of the recovery matrix. Thus, the circulation recovery vector can be computed by the ALLLONGESTCIRCUITS algorithm of Section 7.5.3.

8.6 Delay Propagation

8.6.1 Introduction

The recovery matrix $R = (r_{ij})$ consists of the maximum delays that can be recovered between any two pairs of events in the network. So if an initial delay of a train j exceeds the recovery time r_{ij} then the delay will propagate to train i . Nevertheless, from the recovery matrix we still do not know *when* this train will be delayed and whether the train is delayed more than once by cyclic delay propagation or by initial delays of different trains. Hence, the recovery matrix gives a quick insight in the impact and sensitivity of delays but does not facilitate detailed propagation of delays over time and the network.

A *delay propagation* model explicitly computes the propagation of initial delays over space and time. Given any combination of initial delays a delay propagation model determines all arrival and departure delays of each train at each station over each subsequent period and thus also the *settling time* (or more precisely the settling period) after which all delays have been absorbed by available timetable slack. The max-plus dynamic equations provide an effective delay propagation model, which will be discussed in this section.

This delay propagation model can be applied to derive stability tests. An appropriate measure is for instance the *stability quotient* defined as the number of periods needed before an initial delay of some fixed value settles, see Pachl [158, §6.6]. For example, the German Railways recommend a stability quotient less than 2 for an initial delay of 10 minutes, which implies that any delay of 10 minutes should be completely compensated for within two timetable periods [158].

The delay propagation model can also be used for computing the optimal train waiting times and passenger delays [79, 96, 52]. Furthermore, several variants can be computed where for instance all trains wait for delayed feeder trains, transfer connections are cancelled, or reserve rolling stock can be assigned at line ends. The delay propagation is then computed for a number of models with different state matrices corresponding to removed or adjusted connections (arcs) which are compared with respect to some objective function.

8.6.2 The Delay Propagation Model

Assume $d_0 > \varepsilon$ and consider the scheduled max-plus linear system with a special output vector $z(k)$ containing the delays in period k :

$$\begin{cases} x(k) = A(\gamma)x(k) \oplus d(k), & k \in \mathbb{N} \\ d(k) = d_0 \otimes T^k, & k \in \mathbb{N} \\ z(k) = D^{-1}(k) \otimes x(k), & k \in \mathbb{N} \\ x(1^-) = x_1, x(l) = x_l, & 1 - p \leq l \leq 0, \end{cases} \quad (8.24)$$

where $D^{-1}(k) = \text{diag}(d_1^{-1}(k), \dots, d_n^{-1}(k))$. Hence, $z(k)$ is the *delay vector* of events scheduled in period k with entries

$$z_i(k) = d_i^{-1}(k) \otimes x_i(k) = x_i(k) \otimes d_i^{-1}(k) = x_i(k) - d_i(k).$$

Note that the dynamic state-space equation implies $x(k) \geq d(k)$ and therefore $z_i(k) \geq e$ for all $1 \leq i \leq n$. The inverse matrix is well-defined for any diagonal matrix $D \in \mathbb{R}_{\max}^{n \times n}$ with finite

diagonal entries. Hence as the notation suggests $D^{-1}(k)$ is the inverse matrix of the diagonal matrix

$$D(k) = \text{diag}(d(k)) = \begin{bmatrix} d_1(k) & & \mathcal{E} \\ & \ddots & \\ \mathcal{E} & & d_n(k) \end{bmatrix} = T^k \otimes \begin{bmatrix} d_1^0 & & \mathcal{E} \\ & \ddots & \\ \mathcal{E} & & d_n^0 \end{bmatrix}.$$

The initial conditions may be given in terms of the initial delay vectors $z_1, z_0, \dots, z_{1-p} \in \mathbb{R}_+^n$ of delays that reach events in the first (current) timetable period or beyond. The initial state vectors are then computed as $x_l = D(l) \otimes z_l$ for $1-p \leq l \leq 1$, where $D(l) = \text{diag}(d(l)) = T^l \otimes \text{diag}(d_0)$ is the left-continuation of the timetable system to the last periods $l = 1, 0, \dots, 1-p$. If we are only interested in a subset of delays or if $d_0 \not\geq \varepsilon$ then we may define the delay vector with respect to a suitable output vector $y(k) = C \otimes x(k)$ as $z(k) = D^{-1}(k) \otimes y(k)$, where $D(\cdot)$ is a diagonal matrix of the scheduled event times corresponding to the outputs $y_i(\cdot)$.

Particular attention must be given to the initial state vector x_1 . Assume that at some reference time t_0 (e.g. the current time) we know or have a prediction of the delays of all events scheduled up to t_0 . Without loss of generality we assume that t_0 occurs in the first period of the max-plus model, $t_0 \in [0, T)$. Then the initial conditions to the max-plus linear system (8.24) are the event time vectors of the last p periods x_{1-p}, \dots, x_0 such that $x(l) = x_l$ for $l = 1-p, \dots, 0$, and an initial vector x_1 that *partially* determines the state $x(1)$ for the events scheduled up to t_0 . Writing $x_1 = (x_1^1, \dots, x_n^1)^\top$, we have $x_i(1) = x_i^1$ for those events $1 \leq i \leq n$ that have a scheduled event time $d_i(1) \in [0, t_0]$, since these event times are known at time t_0 by assumption. The event times of the remaining events i are still unknown at time t_0 and depend on both the delayed events of preceding processes that were initiated before time t_0 as well as on the delay propagation within (the second part of) the first period over (t_0, T) . Since we have no information on the event times scheduled after t_0 they are given an initial estimate $x_i^1 = d_i(1)$, corresponding to the scheduled event times, and we thus have $x_i(1) \geq x_i^1$ for all i with $d_i(1) > t_0$. Hence, we denote by $x(1^-) = x_1$ the partially known state vector at time t_0 .

The general p th-order state-space equations contain (many) zero-order terms. Theoretically, we can eliminate these implicit terms from the dynamic model and obtain a purely recursive state-space realization, see Section 8.2.5. However, we then also loose the possibility of taking into account initial delays in the first period. Moreover, this procedure aggregates the propagation of delays within a timetable period. We will therefore keep the zero-order terms in the max-plus model to correctly represent and compute the propagation of delays over all events.

The following theorem gives a recursive procedure for computing the delay propagation that correctly incorporates the partial initial state vector x_1 of the first period. Recall that the (transitive closure) matrix A_0^* of a matrix A_0 with acyclic precedence graph can be computed in linear $O(n + m)$ time using a topological ordering algorithm [3].

Theorem 8.6.1 *Consider a realizable scheduled max-plus linear system (8.24) with acyclic $G(A_0)$ and initial state vectors x_l , $1-p \leq l \leq 1$. Then the state trajectory $\{x(k)\}_{k \in \mathbb{N}}$ is recursively determined by $x(1-p) = x_{1-p}, \dots, x(0) = x_0$,*

$$x(1) = A_0^* \otimes \left(x_1 \oplus \bigoplus_{l=1}^p A_l x_{1-l} \right) \oplus d(1)$$

and

$$x(k) = \bigoplus_{l=1}^p A_0^* A_l x(k-l) \oplus d(k) \quad \text{for all } k \geq 2.$$

Proof: The general state-space equations can be written as the implicit equation

$$x(k) = A_0 x(k) \oplus x(k^-) \oplus d(k),$$

where $x(k^-)$ is the state vector in period k before the zero-order propagation of delays within this period. Then by Lemma 8.2.1 we obtain

$$x(k) = A_0^* (x(k^-) \oplus d(k)) = A_0^* x(k^-) \oplus A_0^* d(k) = A_0^* x(k^-) \oplus d(k), \quad (8.25)$$

where in the last equality we used the result $A_0^* d(k) = d(k)$ of Lemma 8.2.2. For $k = 1$ the tentative state vector $x(1^-)$ consists of both the initial delays x_1 and the delays propagated from previous periods, $x(1^-) = x_1 \oplus \bigoplus_{l=1}^p A_l x_{1-l}$. Substitution in (8.25) gives the expression for $x(1)$. For $k \geq 2$ we have $x(k^-) = \bigoplus_{l=1}^p A_l x(k-l)$. Substitution in (8.25) and using distributivity gives the required result. \square

For any initial delay scenario the evolution of the system can be computed by the recursive procedure of Theorem 8.6.1. If the system is stable all delays will be absorbed after some settling period k_s depending on the particular initial delay scenario. To determine the settling time note that if in some period k a delayed transition fires over a marked arc with p tokens then this delayed token will become available after p periods. Hence, from the state vectors we may conclude that all delays have settled if in p consecutive periods no delays have occurred. The settling period k_s is thus given by

$$k_s = \min\{k \in \mathbb{N} \mid x(k+l) = d(k+l) \text{ for } 1 \leq l \leq p\}.$$

The output delay vectors $\{z(k)\}_{k=1-p}^{k_s}$ give all explicit delays. The delays in the first period can be partitioned around t_0 into $z(1) = z(1^-) + z(1^+)$. If $d_i(1) \leq t_0$ then $z_i(1) = z_i(1^-) = z_1^i$ and $z(1^+) = z(1) - z_1 = z_1 - z_1 = 0$, and if $d_i(1) > t_0$ then $z_i(1^-) = z_1 = 0$ and $z(1^+) = z(1) - z_1 = z(1)$. Aggregated output is easily obtained from these vectors, for example

- Total secondary delay:

$$\bigotimes_{i=1}^n \left(z_i(1^+) \otimes \bigotimes_{k=2}^{k_s} z_i(k) \right),$$

- Maximum secondary delay:

$$\bigoplus_{i=1}^n \left(z_i(1^+) \oplus \bigoplus_{k=2}^{k_s} z_i(k) \right),$$

- Ratio total secondary/initial delay:

$$\frac{\bigotimes_{i=1}^n \left(z_i(1^+) \otimes \bigotimes_{k=2}^{k_s} z_i(k) \right)}{\bigotimes_{i=1}^n \left(z_i(1^-) \otimes \bigotimes_{k=1-p}^0 z_i(k) \right)}.$$

Other statistics that can be obtained are e.g. the settling period, average secondary delay, number of delayed trains, and number of stations with delays.

8.6.3 A Bucket-Based Delay Propagation Algorithm

Theorem 8.6.1 gives a simple recursive procedure to compute the propagation of any initial delay scenario. For large-scale networks however this procedure is arguably not very efficient in both computation time and memory usage. In practice the matrices A_0, \dots, A_p are very sparse which can be exploited to effectively compute delay propagation in large-scale networks. In particular an adjacency list representation of the associated timed event graph can be used. Moreover, events that are not delayed can simply be discarded as they will not contribute to delaying a successor.

In the forthcoming we need the concept of a topological ordered graph. A *topological order* of nodes $i \in V$ in a graph $G = (V, E)$ is a numbering of nodes such for all arcs $(j, i) \in E$ we have $j < i$. If G is the precedence graph of a max-plus matrix $A \in \mathbb{R}_{\max}^{n \times n}$ then $V = \{1, \dots, n\}$ is topologically ordered if and only if A is strictly lower triangular, i.e., $a_{ij} = \varepsilon$ for all $j \geq i$ (and so $a_{ij} \neq \varepsilon$ iff $j < i$). In a topological ordered graph each path has an ascending numbering of nodes. Topological sorting of an acyclic graph can be done in linear $O(n + m)$ time using depth-first search [2, 39]. For any acyclic digraph $G = (V, E)$ topological sorting returns a permutation vector ord such that $\text{ord}(j) < \text{ord}(i)$ for each arc $(j, i) \in E$. Given this mapping $\text{ord} : V \rightarrow \{1, \dots, n\}$ the adjacency lists of G are easily rearranged in increasing order using two-level bucket sort on the set $\{(\text{ord}(j), \text{ord}(i)) \mid (j, i) \in E\}$, which also takes linear $O(n + m)$ time. Finally, the permutation ord simply maps an event set Z to the topological ordering and the inverse permutation ord^{-1} defined by $\text{ord}^{-1}(j) = \{i \mid \text{ord}(i) = j\}$ maps the topological ordered numbering back to the original numbering. Algebraically, the permutation ord defines a permutation matrix P such that the matrix $\tilde{A} = P^\top A P$ is strictly lower triangular.

Theorem 8.6.2 *Let (8.24) be a realizable scheduled max-plus linear system with arbitrary initial delay vectors z_{1-p}, \dots, z_1 and let $G_0 = (V_0, E_0) \subseteq G(A_0)$ be the acyclic graph with arc and node set defined as*

$$\begin{aligned} E_0 &= \{(j, i) \mid [A_0]_{ij} = e \text{ and } d_i^0 = d_j^0\} \\ V_0 &= \{1 \leq i \leq n \mid \exists j : (i, j) \in E_0 \text{ or } (j, i) \in E_0\}. \end{aligned}$$

Then a legal firing sequence for computing the delay propagation $\{z(k)\}_{k \in \mathbb{N}}$ is obtained by firing delayed events in order of their scheduled event times and breaking ties in topological order for events $i \in V_0$ and randomly otherwise.

Proof: First note that if $V_0 \neq \emptyset$ then G_0 is an acyclic digraph and thus a topological order of the nodes in V_0 exists. Furthermore, in G_0 all arcs have weight 0, each path consists of nodes sharing a common scheduled event time, and G_0 has no isolated nodes, i.e., nodes without a predecessor nor a successor. Let $i \in \mathcal{T} = \{1, \dots, n\}$ be an arbitrary event and assume first that $i \notin V_0$. The event time $x_i(k)$ in any period $k \in \mathbb{N}$ can be computed only if the event times of all (direct) predecessors are available. If $d_i(k)$ is the associated scheduled event time then each predecessor j associated to some place (j, i, l) has a scheduled event time $d_j(k - l) < d_i(k)$ because the timetable is realizable. Hence, the scheduled order equals the precedence order. If for some $j \in \mathcal{T}$ we have $d_i(k) = d_j(k)$ then j cannot be a predecessor of i and vice versa since this would violate the condition $d_j(k - l) < d_i(k)$. Hence, all events with equal scheduled event time can be computed independently and thus in random order. Now suppose $i \in V_0$. Then there may exist a predecessor $j \in V_0$ with $[A_0]_{ij} = e$ and $d_j(k) = d_i(k)$. If so, then the event

time $x_j(k)$ of this predecessor must be computed before $x_i(k)$ can be computed. Analogously, since also $j \in V_0$ the event time of any predecessor $s \in V_0$, if one exists, must be computed prior to $x_j(k)$, et cetera. Hence, by sorting the events in V_0 upstream of i , if any, in topological order the correct precedence order is obtained for computing the event times one at a time. Note that since $G(A_0)$ is acyclic also $G_0 = (V_0, E_0) \subseteq G(A_0)$ is acyclic and therefore each upstream path to any node $i \in V_0$ is finite, and in particular i itself may be a source in G_0 . \square

Corollary 8.6.1 *Let (8.24) be a realizable scheduled max-plus linear system. If $G(A_0)$ has (conventional) positive-weight arcs only then a legal firing sequence for computing $\{z(k)\}_{k \in \mathbb{N}}$ is obtained by firing delayed events in order of their scheduled event times and breaking ties randomly.*

Proof: If $[A_0]_{ij} > e$ for all $(j, i) \in \text{supp}(A_0)$ then $E_0 = V_0 = \emptyset$ and the result follows directly from Theorem 8.6.2. \square

Let $G = (V, E)$ be a directed graph and assume $G' = (V', E')$ is an *acyclic* subgraph of G with $V' \doteq \{i \in V \mid \exists j \in V : (i, j) \in E' \text{ or } (j, i) \in E'\}$. Then we say that the node set V is *topologically ordered with respect to* $G' = (V', E')$ if the node subset $V' \subset V$ is topologically ordered. Hence, given a polynomial matrix $A(\gamma) = \bigoplus_{l=0}^p A_l \gamma^l \in \mathbb{R}_{\max}^{n \times n}[\gamma]$ with acyclic $G(A_0)$ and a permutation matrix P corresponding to a topological reordering of nodes in $G(A_0)$, the similarity transformation $\tilde{A}(\gamma) = P^\top A(\gamma) P$ gives a polynomial matrix associated to the timed event graph $\mathcal{G}(\tilde{A}(\gamma))$ where the transitions are topologically ordered with respect to $G(A_0)$.

If the events of $\mathcal{G}(A(\gamma))$ are topologically ordered with respect to $G(A_0)$ then so they are for $G_0 \subseteq G(A_0)$. Hence, we have the following corollary to Theorem 8.6.2.

Corollary 8.6.2 *Let (8.24) be a realizable scheduled max-plus linear system and assume that the nodes are topologically ordered with respect to the acyclic graph $G(A_0)$. Then a legal firing sequence that computes the delay propagation $\{z(k)\}_{k \in \mathbb{N}}$ is obtained by firing delayed events in order of their scheduled event times and breaking ties in ascending index order, i.e., given a set of delayed events $Z \doteq \{(i, k, z_i(k)) \mid z_i(k) > e\}$ select the next delayed event i according to*

$$(j, k, z_j(k)) = \arg \min \{j \mid (j, k, z_j(k)) \in \arg \min \{d_i(k) \mid (i, k, z_i(k)) \in Z\}\},$$

where $d_i(k) = d_i^0 + k \cdot T$.

In general, topological sorting of an acyclic digraph $G(A_0)$ can be done very fast, as discussed above, and therefore we may sort the events of $\mathcal{G}(A(\gamma))$ with respect to $G(A_0)$ instead of the subgraph G_0 , if the latter has still to be determined. Moreover, sorting nodes with regard to $G(A_0)$ is independent of the holding times and initial timetable and therefore robust to variations in the finite entries of A_0 and the timetable vector d_0 . On the other hand, if we can establish that $V_0 = \emptyset$ then any numbering of events is trivially ‘topologically sorted’. A sufficient condition for $V_0 = \emptyset$ is that A_0 has no entries with value e . Another less restrictive sufficient condition is that any entry of A_0 with value e has different timetable values of the associated nodes, i.e., $d_i^0 \neq d_j^0$ for all (j, i) such that $[A_0]_{ij} = e$. Note that since A_0 is acyclic the diagonal has no finite entries. In the following we assume that either $V_0 = \emptyset$ or that the events are topologically sorted with respect to either G_0 or $G(A_0)$.

Theorem 8.6.2 and its Corollary 8.6.2 suggest a graph algorithm where delayed events are maintained in *buckets* of equal scheduled event time. Here, a *bucket* B_t is a linked list (of variable size) of all delayed events $(i, k, z_i(k))$ with scheduled event time $d_i(k) = t$. The buckets themselves are elements of an array $B = (B_t)$, or more precisely, B is an array of lists (or headers for lists) indexed by scheduled event time. A new delayed event $(i, k, z_i(k))$ with scheduled event time $d_i(k)$ is inserted in bucket $B_{d_i(k)}$ and an existing delayed event can be found by searching for it in the bucket indexed by the associated scheduled event time. This approach of sorting events is known as *bucket sort* or *binsort* [2]. We here tacitly assume that the scheduled event times are specified in whole minutes, which is generally true for departure times in railway timetables. If the indices of array B are restricted to nonnegative integers then it is convenient to choose the initial timetable vector d_0 such that $d_0 \in [(p-1) \cdot T, p \cdot T)^n$, where p is the order of the max-plus linear system. Then $d_i(1-p) = d_i^0 + (1-p) \cdot T \in [0, T)$ for all $1 \leq i \leq n$ and thus any delayed event $(i, k, z_i(k))$, $k \geq 1-p$, has at least scheduled event time 0.

Algorithm 8.6.1 gives the pseudocode for computing the propagation of any initial delay scenario in a scheduled max-plus linear system — or equivalently in the associated timed event graph. The required input is an adjacency list of the timed marked graph $\mathcal{G}(A(\gamma))$, the initial timetable vector $d_0 \in [(p-1) \cdot T, p \cdot T)^n$, the cycle time T , and a list of initial delays. We assume that the initial delayed events are specified by tuples of the form

$$(i, k, z_i(k)) \in Z_0 \doteq \{(i, k, z_i(k)) \mid z_i(k) > e, 1-p \leq k \leq 1\}, \quad (8.26)$$

where $i \in \mathcal{T} = \{1, \dots, n\}$ is the delayed event number, $k \in \mathbb{Z}$ the period in which the delay occurs, and $z_i(k) > 0$ is the delay.

Algorithm 8.6.1 uses two counters t and d_{\max} denoting the current scheduled event time and the maximum scheduled event time of delayed events encountered so far, respectively. Initially, t (d_{\max}) is set to a very large (negative) value (line 1). Then each initial delay is sorted in buckets and the counters t and d_{\max} are updated according to the scheduled event times of the sorted delayed events (lines 2–5). At the end of the initialization B_t is the nonempty bucket of smallest index, t the smallest scheduled event time amongst the initial delayed events, and $B_{d_{\max}}$ the nonempty bucket with largest index. The main program (lines 6–19) contains an outer and an inner loop. The outer loop iterates over the counter t and stops as soon as t exceeds d_{\max} which implies that all buckets are empty. The algorithm then terminates by returning the computed delay list Z , which contains all initial and secondary delayed events in scheduled order (line 20). For each current value of the counter t the inner loop (lines 7–18) is called, which explores the delayed events within bucket B_t . If bucket B_t is empty the program returns to the outer loop, increases the current scheduled event time t by one and starts a next iteration. On the other hand, if B_t is nonempty then the event with minimal index j is selected (line 8), deleted from the bucket and added to the final list of delays (line 9). Lines 10–18 scan each outgoing arc of j . If the current delay $z_j(k)$ exceeds the slack on an outgoing arc then the delay is propagated to the successor event and one of three options occurs: if the scheduled event time $d_i(k)$ of the successor i is larger than any scheduled event time encountered so far then d_{\max} is updated, the bucket array B is expanded with empty buckets up to $B_{d_i(k)}$, and the new (reduced) delay is inserted into $B_{d_i(k)}$ (lines 14–15). Otherwise, if the successor i is already in bucket $B_{d_i(k)}$ then the delay is updated (lines 16–17), and if i is not yet in the bucket then it is inserted (line 18). If the adjacency list of event j is exhausted, a new iteration of the inner-loop starts by finding the next event in bucket B_t or establishing that the bucket has become empty.

Algorithm 8.6.1 (DELAYPROPAGATION)

Input: Timed event graph $\mathcal{G}(A(\gamma))$ (adjacency list), realizable timetable $d_0 = (d_1^0, \dots, d_n^0)^\top$, cycle time T , initial delay list Z_0 .
Output: Delay list Z .

```

1   $t \leftarrow \infty$ ;  $d_{\max} \leftarrow \varepsilon$ ;                                     //Initialization
2  for each  $(i, k, z_i(k)) \in Z_0$  do
3       $d \leftarrow d_i^0 + k \cdot T$ ;
4       $B_d \leftarrow B_d \cup \{(i, k, z_i(k))\}$ ;
5       $t \leftarrow \min(t, d)$ ;  $d_{\max} \leftarrow \max(d_{\max}, d)$ ;
6  while  $t \leq d_{\max}$  do                                             //Main loop
7      while  $B_t \neq \emptyset$  do                                     //Inner loop
8           $(j, k, z_j(k)) \leftarrow \arg \min\{j \mid (j, k, z_j(k)) \in B_t\}$ ; //Delay selection
9           $B_t \leftarrow B_t \setminus \{(j, k, z_j(k))\}$ ;  $Z \leftarrow Z \cup \{(j, k, z_j(k))\}$ ;
10         for each place  $(j, i, l, [A_l]_{ij}) \in \text{succ}(j)$  do
11              $d \leftarrow d_i^0 + (k + l) \cdot T$ ;
12              $z \leftarrow t + [A_l]_{ij} + z_j(k) - d$ ;
13             if  $z > 0$  then                                           //Propagate
14                 if  $d > d_{\max}$  then
15                      $d_{\max} \leftarrow d$ ;  $B_d \leftarrow \{(i, k + l, z)\}$ ;
16                 else if  $(i, k + l, \cdot) \in B_d$  then
17                     if  $z_i(k + l) < z$  then  $z_i(k + l) \leftarrow z$ ;
18                 else  $B_d \leftarrow B_d \cup \{(i, k + l, z)\}$ ;
19          $t \leftarrow t + 1$ ;
20 return  $Z$                                                          //Terminate

```

The bucket implementation of the delay propagation algorithm is particular efficient if the scheduled event times are more or less evenly distributed from a finite discrete set (in each period). In general, railway timetables of large-scale networks show a rather uniform distribution of scheduled event times because of the diverse running times over the various stretches between station stops. Figure 8.3 shows the hourly scheduled departure times in the national Dutch railway timetable of the year 2000/2001 as a function of events (left) and the associated histogram (right). In this periodic timetable 2423 departure events are scheduled in each hour with scheduled departure times ranging from 0 to 59 minute. The plots indeed suggest that the events are quite evenly spread over the integers $[0, 59]$, which is also confirmed by formal statistical tests. This uniform distribution of scheduled departure times over the events stems from the large number of events of the large-scale network and the ‘random’ scheduled process times of the trains running over the network which depend on different station distances and varying operational characteristics of trains and infrastructure. The histogram at the right in Figure 8.3 also shows that in this case the size of a bucket will never exceed 57 events, where this upper bound corresponds to the (rare) case that in some period all events over the network with scheduled departure time 46 are delayed. The bucket implementation is therefore an effective way to decompose the list of delayed events during the course of the algorithm for quick access.

The efficiency of Algorithm 8.6.1 can be improved even more by an appropriate data structure of the buckets. In particular, each bucket should be implemented as an ordered list with respect to increasing event number or more generally as a *priority queue*. The buckets have a dynamic size and the maximum size differs from bucket to bucket. Most buckets contain only a few events

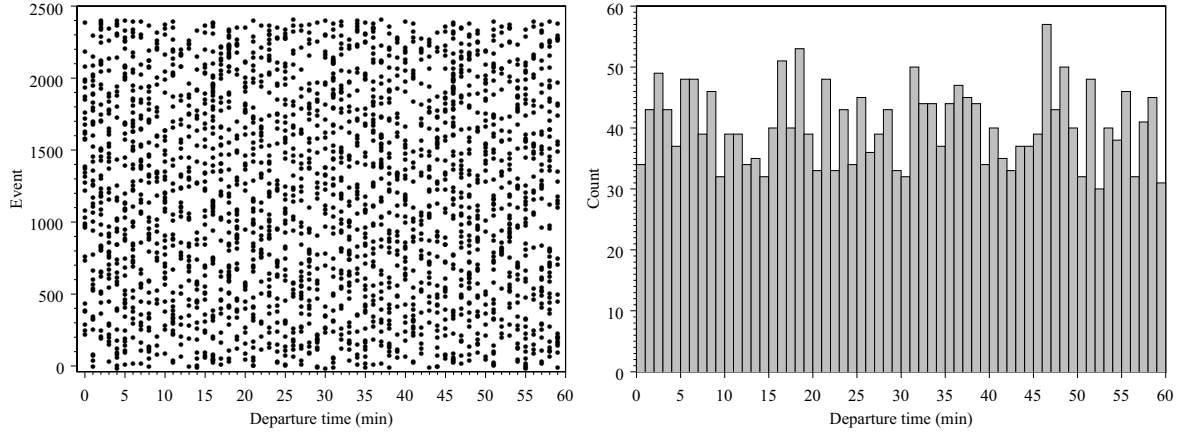


Figure 8.3 Departure time distribution in the Dutch railway timetable 2000/2001. Function of event number (left) and histogram (right)

and even “full” buckets have limited size as discussed in the last paragraph. Furthermore, the total number of events — and therefore the range of the event numbering — can be very large. Given these characteristics, a linked ordered (or linear) list is the preferred data structure for each bucket [119]. In a linked ordered list finding the minimal element in a bucket B_t (cf. line 8) just reduces to returning the first element in B_t , which takes $O(1)$ time, and so does deleting this minimal element from the ordered list (line 9). Finding a given event by its number (line 16) or establishing that the event is not yet in the list takes $O(n_t)$ time, where n_t is the maximal size of bucket t . When an event has been located in a bucket updating the delay takes $O(1)$ time. On the other hand, as soon as the list search meets a higher-numbered event it is known that the current event is not yet in the list and so it is inserted between the located higher-numbered event and its predecessor (line 18) in $O(1)$ time.

The linked linear list implementation of the buckets improves finding, updating and inserting items in a bucket as opposed to an unordered list regardless of the event selection method (line 8). Hence, even if events in a bucket may be selected randomly, cf. Corollary 8.6.1, the ordered list implementation of the buckets is the preferred data structure. More advanced *heap* data structures [2, 39] can be used if the size of buckets are likely to become very large, say exceeding 100. From the above discussion follows that a linked ordered list should be used if $n/T < 100$ and the scheduled event times are approximately uniformly distributed over $[0, T - 1]$. A heap implementation of the buckets may become more efficient if the ratio of number of events and cycle time n/T is very large or event times are scheduled disproportionally to some special values and many and/or large initial delays are introduced.

Theorem 8.6.3 *Let (8.24) be a stable scheduled max-plus linear system with realizable timetable $d(k) = d_0 T^k$ for $k \in \mathbb{Z}$, and either $V_0 = \emptyset$ or the nodes are topologically ordered with respect to $G_0 = (V_0, E_0)$. Then the delayed event set Z is finite and Algorithm 8.6.1 computes the delay propagation $\{z(k)\}_{k \in \mathbb{N}}$ for any initial delay scenario $\{z_{1-p}, \dots, z_1\}$ in finite time.*

Proof: If the max-plus linear system is stable, $\lambda_0(A(\gamma)) < T$, then by definition each circuit in the timed event graph $\mathcal{G}(A(\gamma))$ contains some positive buffer time and therefore each delay is strictly decreasing over each circuit, whence the total number of delays $|Z|$ is finite. The algorithm proceeds by scanning each delayed event exactly once as an immediate consequence

of Theorem 8.6.2 and its Corollary 8.6.2 and therefore terminates after a finite number of iterations. Note that a topological order of the nodes of $G(A_0)$ also implies a topological order with respect to $G_0 = (V_0, E_0)$ and is thus also covered by the theorem. \square

In practice Algorithm 8.6.1 has a fast pseudolinear running time in the number of (initial and secondary) delayed events $|Z|$ because: (1) the algorithm only scans delayed events, (2) each delayed event is scanned exactly once, (3) the number of successors checked for delay propagation in each scan is limited by the maximum outdegree over all nodes which is typically very small (< 10), (4) the buckets B_t are typically small ($n_t = |B_t| < 100$) and finding an event in an (ordered) bucket or detecting its absence takes on the average $\log(n_t) < 10$ comparisons, whereas all other bucket operations take $O(1)$ time.

8.7 PETER

8.7.1 Introduction

PETER is a strategic and tactical planning support system for the evaluation of periodic railway timetables on network stability and effective capacity utilization. PETER is an acronym of *Performance Evaluation of Timed Events in Railways*. The software PETER contains an implementation of the timed event graph and max-plus linear system theory presented in this thesis. The core of the PETER software is the implementation of an automatic (max-plus) model building procedure and efficient state-of-the-art numerical algorithms for analysing the model, which are well-documented in this thesis. For the programming and development of a user-friendly human-machine interface (HMI) suitable for railway planners it was decided to cooperate with the software firm ORTEC [88], who are specialized in planning software and, amongst others, developed and maintain the Dutch railway timetable design system DONS for the Dutch Railways (NSR) and ProRail. PETER has a modular system architecture written in Delphi for the operating systems MS Windows 95 and higher. The policy iteration algorithm of the critical circuit analysis is a callable routine implemented in C. The modular design facilitates future enhancements.

PETER has been developed to support railway professionals in their task of designing, evaluating and improving railway timetables. The graphical user interface (GUI) enables non-mathematical users to apply automated advanced mathematical modelling and analysis techniques while maintaining focus on timetabling decisions (input parameters) and interpretation of computational results. The tool relieves the tedious task of ‘pencil and paper’ calculations and allows visualization of complex (cyclic) network interdependencies which are inherently present in the railway timetable but hard to grasp without computer-aided support.

The main strength of PETER is the analytical max-plus analysis approach which in combination with efficient numerical graph algorithms enables a *real-time* computational environment for the evaluation of *large-scale* network timetables. Moreover, a graphical network visualization allows an insightful representation of results which helps users to focus on critical components and prevents them from drowning in an overkill of output which is a serious concern when analysing large-scale networks. PETER is also compatible with DONS. All analysis methods in PETER are hence available to quickly evaluate timetable structures generated by DONS, which is a further major contribution to the computer-aided timetable design in the Netherlands.

This section briefly outlines the features of PETER. In Section 8.8 the application of PETER — and the max-plus analysis approach in general — is demonstrated in a case study of the national Dutch railway timetable.

8.7.2 Input Data

PETER automatically builds a max-plus linear system model and the network visualization based on the following input data:

- Timetable points: name (abbreviation), coordinates and type (intercity stations (IC), interregional stations (IR), regional stops (AR), freight or shunting yards (F), junctions (J), and movable bridges (BR)),
- Train lines: line number, route, stops, nominal running times, minimum dwell times, frequency,
- Timetable: scheduled arrival, departure and through times,
- Connections: passenger transfers and minimum transfer times,
- Rolling stock circulations: turns or other rolling stock connections and minimum layover or (de-)coupling times,
- Logistics: crew transfers and minimum transfer times (optional),
- Infrastructure and safety system: minimum headway times between train events.

Section 6.5 gave a description of the generic input data file format. Timetable points are given in the `TimetablePointData`, train lines and timetable data are combined in the `LineData`, `SynchData` contain the connection, rolling stock circulation and logistics data, and the infrastructure and safety system data are given in the `HeadwayData`. In PETER these data are imported from a combined ASCII *generic input file*. Process times can be specified up to a second using decimal or time format (min:sec), e.g. 63 minutes and 15 seconds is specified in decimals by 63.25 and in time format by 63:15. This generic format is easily generated by standard text editors or spreadsheets. Networks can also be created within PETER using the build-in editors and saved in the generic format. For fast access the internal data structure of PETER and the computed results can also be saved from computer memory to a binary file.

PETER automatically constructs the max-plus model and draws the network view based on the input data. A build-in editor can also be used to edit data. When data has been edited it is checked on feasibility before PETER builds a new max-plus model. The modular system architecture of PETER enables easy extension of functionalities. As an example, a module has been developed that directly imports data files from the Dutch timetable design tool DONS, see Section 3.9.1. The DONS data is given in three data files: `TimetablePoints` contains the data of the timetable points. `Constraints` is the input data file prepared via the DONS interface that is used by CADANS to compute a feasible timetable (or a minimal set of conflicting constraints). Recall from Section 3.9.1 that CADANS is the kernel of DONS that computes a feasible timetable from a set of periodic time window constraints corresponding to the *periodic event scheduling problem* (PESP). `Constraints` thus contains these PESP constraints in a prescribed ASCII format. Finally, `Timetable` is an output file of CADANS containing a feasible timetable in some prescribed ASCII format.

PETER also contains several options to quickly analyse the impact of parameter variations. By simply selecting a toggle we may individually exclude all layover times, passenger transfers,

rolling stock connections, infrastructure constraints and/or any train line to see its influence on the timetable characteristics. Also a uniform running time margin (percentage) for each individual train line can be set which is then applied integrally over all line segments. Of course each line segment may also be given a dedicated running time margin in seconds.

8.7.3 Functionalities

PETER evaluates the performance of periodic railway timetables using the following three complementary functionalities:

1. *Critical circuit analysis*: identification and quantification of the critical cycles in the network with the least mean slack,
2. *Recovery time analysis*: identification and quantification of the least total slack available over all paths between any pair of train events,
3. *Delay propagation*: identification and quantification of the propagation of initial delay scenarios over time and space.

Together these functionalities give insight in the stability and robustness of a railway timetable structure with a main emphasis on the interconnection structure of train paths and decoupled subsystems (network connectivity), mean slack available on circuits in the network (network stability), and the distribution of time supplements and buffer times over the timetable (robustness). In the next subsections we will give a brief overview of the functionalities.

8.7.3.1 Critical Circuit Analysis

In PETER the max-plus spectral analysis has been called *critical circuit analysis* which might be more appealing to the intended users. Moreover, we may think of spectral analysis as the mathematical method to find the critical circuits and their components which are analysed subsequently by the users of PETER to improve (or establish) system performance — the critical circuit analysis. Critical circuit analysis can be viewed as the cyclic variant of the critical path method (CPM) in network analysis which concentrates on acyclic graphs and is a well-known method in project management (PERT, Project Evaluation Review Technique). The name spectral analysis would be more appealing to engineers since it (correctly) suggests a method for analysing the steady-state periodic solutions of the (max-plus) linear system. Hence, critical circuit analysis is made possible by the spectral analysis detailed in Section 8.3 using the (generalized) eigenvalue theory of Section 7.4. The generalized eigenproblem is solved in PETER by the policy iteration algorithm which gives the cycle time vector and an eigenvector, as well as the critical circuits and the components accessible from the critical circuits.

The primary results of the spectral analysis are shown in a separate window. In top a summary is presented of the maximum cycle time, maximum throughput, maximum stability margin, the number of components, and a most critical circuit (departure event list). Next, the spectral results are presented in tabular form for all departure events (line segments). Note that in PETER departures are the main events whereas all other events (arrivals, through and terminal events) are considered dummy events whose characteristics depend on the preceding departures. The departures are ordered by line segment number and each row corresponds to one departure. The

successive columns correspond to the line segment, scheduled departure time, a boolean showing whether the event is critical (yes/no), the cycle time, the eigenvector value, stability margin, circulation recovery margin, and a boolean showing whether the event is cyclic (yes/no). The latter boolean variable states whether an event is or is not contained in some circuit. If an event is not cyclic there are three options. First, the event is accessible by some circuit. In this case the cycle time and eigenvector entry are computed directly by the policy iteration algorithm. On the other hand, if the event has no upstream circuit but has access to some circuit then its cycle time and eigenvector entry are computed using a critical path to its cyclic successors (starting at a circuit node and computing backwards on the incoming trees). Third, if an event has no up- or downstream circuits — the event is part of a tree — then its cycle time and eigenvector entry are undefined.

The critical components are also available in a separate window. All components associated to some critical circuit(s) are shown ordered by cycle time. Each component is specified by four columns giving subsequently the cycle time, throughput, stability margin, and the (first) events on (one of) the critical circuits. By right-clicking on a component row three options become available: the details of the critical circuit in tabular form, a network visualization of the component and its critical circuits, or a time-distance diagram of the critical events and processes. The details of a critical circuit contain the successive departure events (line segments) along with the scheduled departure time at the origin, the arrival time at the destination, the connection time at the destination, connection type (stop, turn, transfer, coupling, headway), eigenvector value, and circulation recovery time.

The network view shows all critical circuits on the railway network. All tracks contained in a critical circuit are shown in shades of red (or in a black-and-white view, shades of grey). If the network contains several components with different cycle times the colours of the separate critical circuits are scaled accordingly with the maximum cycle time bright red and the least critical cycle time shown in white. It is also possible to view a single component accessible from some critical circuit. In this case the critical circuit is shown in red and all tracks accessible from the selected critical circuit are shown in black. This gives an insightful view of the impact region of critical events on the critical circuits.

As an example, Figure 8.4 shows the network view of the critical circuits of the Dutch railway timetable, see Section 8.8. The network is zoomed into the area of interest. There are 4 critical circuits. The most critical circuit has cycle time $\lambda_0 = 58:01$ and runs from The Hague HS (Gv) at the top-left corner, via Dordrecht (Ddr) in the middle, to Roosendaal (Rsd) at the bottom-left and Eindhoven (Ehv) at the bottom-right. The critical circuit of the least critical component ($\lambda_3 = 51:56$) is shown in white on the left of Schiedam (Sdm). The 2nd critical component ($\lambda_1 = 55:02$) runs between Gouda (Gd) and Alphen aan den Rijn (Apn) and its critical circuit is shown in a lighter shade of red. Finally, the critical circuit of the third critical component ($\lambda_2 = 52:26$) is shown in very light red from The Hague CS (Gvc) to Zoetermeer (Ztm) and to Rotterdam Hofplein near Rotterdam CS (Rtd). For more details, see Section 8.8.

The identification of critical circuits supports decisions to improve system stability by suggesting changes in the critical processes of the critical circuits. Possible actions are changing train orders, adding (or moving) a train to one of the critical processes, or improving the critical process time by e.g. faster train units, shorter dwell times (increased door-widths), shorter transfer times (cross-platform transfers), or infrastructure investments. Of course the amount of necessary slack depends on the reliability of individual or joint process times in the circuit. Moni-

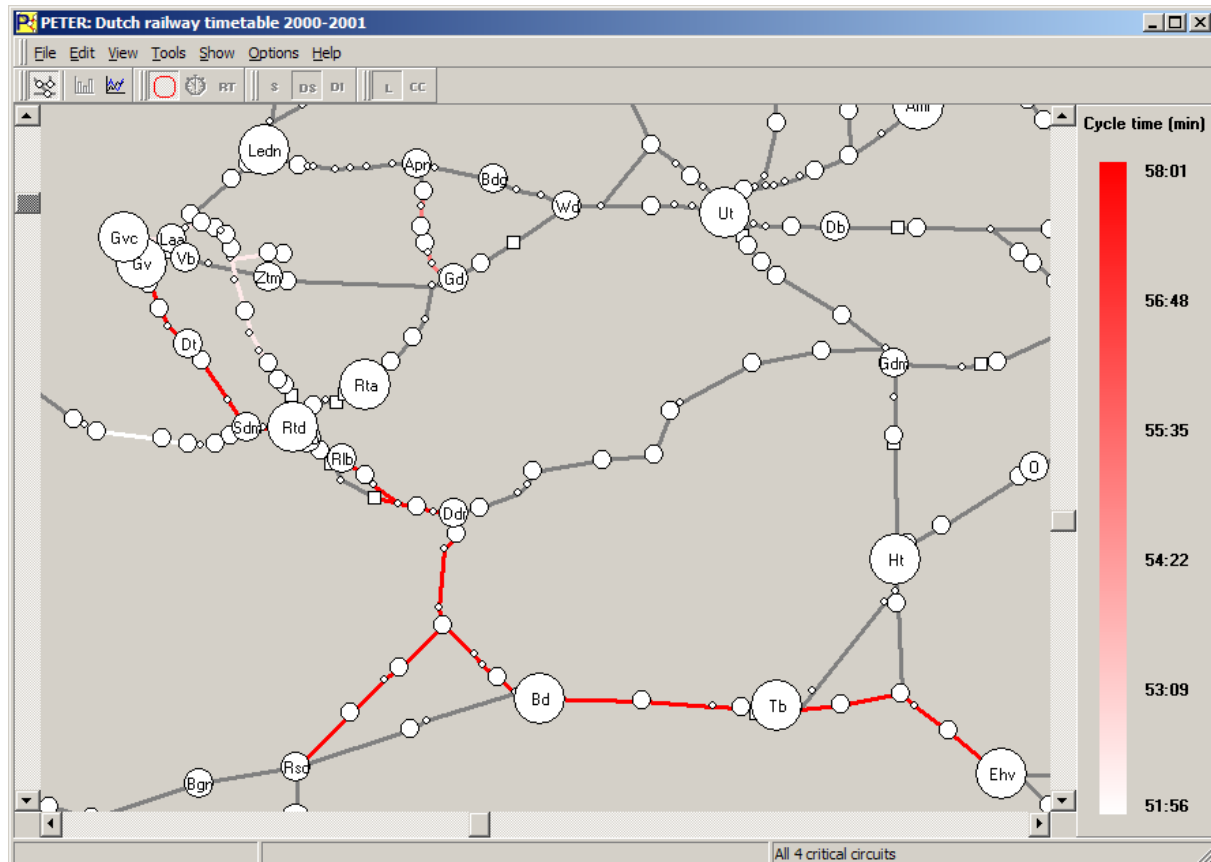


Figure 8.4 Four critical circuits in a model of the Dutch railway timetable

toring and managing schedule adherence of the identified critical processes is another means of improving system performance.

8.7.3.2 Recovery Time Analysis

Recall from Section 8.5 that the recovery time from one departure event to another is the minimum cumulative slack time over all possible paths in the interconnection network from the first event to the other. The recovery times include slack supplied within scheduled process times (e.g. running time margins) and buffer times between train paths. The theory behind the recovery time analysis has been considered in Section 8.5 using the longest path theory and algorithms of Section 7.5.

In PETER the recovery matrix is computed for all departure events. Still, the recovery matrix gives an overkill of information since all events accessible from each event leads to a recovery time entry. The main challenge therefore is to represent this information to a user in an accessible way. In Section 8.5 we already distinguished between rows, columns and the diagonal of the recovery matrix corresponding to delay sensitivity, delay impact and circulation recovery time, respectively. As already mentioned in the previous section, the circulation recovery time of each departure event is included in the list of primary results together with the results of the spectral analysis. In contrast to the circulation recovery times, the delay impact and delay sensitivity of some event i are vectors corresponding to all events accessible from i or having

access to i , respectively.

Projecting the delay impact and sensitivity vectors on the railway network gives an insightful network view of the delay impact regions and sensitivity regions of a selected event. In this network view the timetable points and interconnecting tracks are coloured according to the least (worst-case) recovery time over all events (line segments). The colour scheme runs continuously from black (0 min recovery time), via red (5 min), orange (10 min), yellow (15 min), light yellow (20 min) to white (25 min and higher). For example, Figure 8.7 on page 255 shows the delay impact of departure R6300 Gvc-Laa of regional train line R6300 The Hague CS-Haarlem departing from The Hague CS (Gvc) to the next local stop The Hague Laan van NOI (Laa). All stations and tracks coloured in black to red² contain events accessible from R6300 Gvc-Laa with recovery time 5 minutes or less corresponding to an impact region at level 5 minutes. The impact region at level 10 reaches all stations and tracks up to colour orange, et cetera. All timetable points and tracks shown in white are either not accessible from the selected event or contain only events with at least 25 minutes recovery time from the selected event.

The delay impact/sensitivity from/to a selected event can also be shown in tabular view or in a bar chart, either ordered by event name or by increasing recovery time. In the latter case the most critical events with respect to the least recovery time are shown first. The ordering by event name (line segment) gives a clear view in the change in recovery time over consecutive line segments.

The large amount of events in a delay impact/sensitivity vector may be managed by setting a *recovery threshold* parameter. If this parameter is set to, say, 15 minutes then only events with recovery time up to 15 minutes are shown, corresponding to the delay impact and sensitivity regions at level 15 minutes. In practice very large delays are managed by cancelling connections, changing train orders, running reserve rolling stock or even cancelling trains. Hence, from some threshold value the timetable is no longer respected and exact recovery times are therefore no longer relevant. From a performance evaluation viewpoint recovery times exceeding some threshold correspond to robust event pairs. Given a selected event, all accessible events with a large delay impact (sensitivity) above some threshold value can be considered outside any impact (sensitivity) region of the selected event.

8.7.3.3 Delay Propagation

Delay propagation is based on the algorithms of Section 8.6. The initial delays can be inserted manually or imported from a delay file. Manually inserted initial delays can also be saved to a generic delay file for future usage. The delay files enable easy access to a range of initial scenarios for delay propagation. The generic delay file is an ASCII file *InitialDelays* containing a list of all initial delays specified by event, period and delay, corresponding to the delay list (8.26).

The delay propagation is computed for any set of initial delays, the *initial delay scenario*, according to the active max-plus model (respecting the toggles that may exclude some constraint groups or train lines). The computed delays are classified into three types:

- *Initial delay*: defined in the initial delay scenario,

²For black and white view look at the legend at the right in Figure 8.7

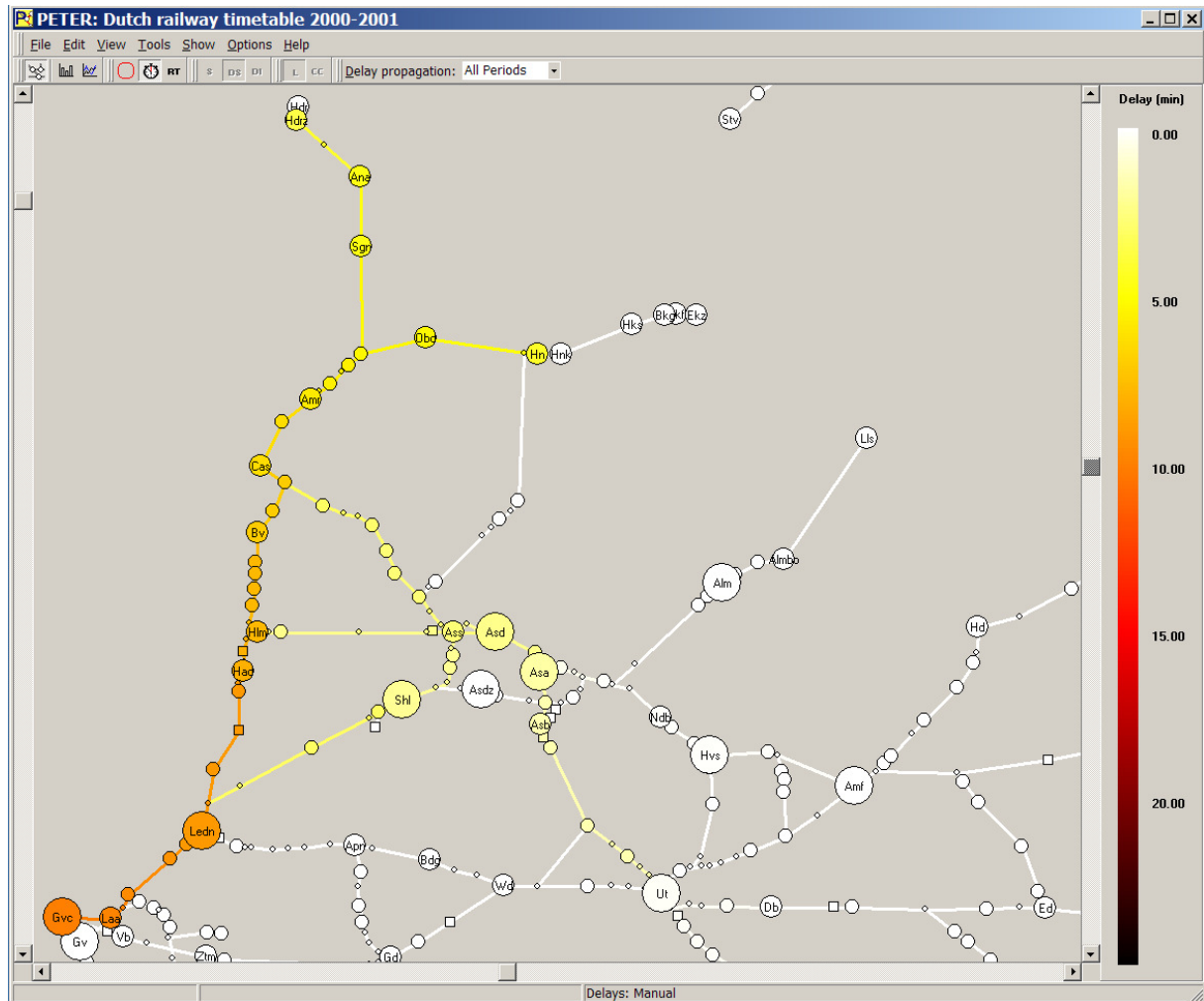


Figure 8.5 Delay propagation of 10 minutes initial delay of the R6300 Gvc-Hlm at The Hague CS (PETER network visualization)

- *Secondary delay*: a propagated delay from one train line to another.
- *Consecutive delay*: the receding delay propagation over successive segments of a train line following an initial or secondary delay.

Delay propagation over turning trains are also considered as secondary delays. The output can be shown in tabular form and visualized in the network view, and can be saved to an output file for further processing.

A pop-up window shows the results in tabular form starting with a summary. The summary gives a number of aggregated results: total initial delay, total secondary delay, cumulative secondary delay (including consecutive delays), number of secondary delayed trains, number of reached stations, average primary delay, average secondary delay, average total delay, and settling period. This summary is followed by a list of all delays in order of scheduled event time. Each row represents one delay and contains a number of columns: line segment (event), scheduled departure time, timetable period, delay, and delay type (initial, secondary, consecutive). The contents of this window can also be saved to an output file.

The network visualization consists of a projection of the delays to the network, similar to the recovery impact. Figure 8.5 shows an example of the network visualization, see §8.8 for details.. In this network view the timetable points and interconnecting tracks are coloured with respect to the maximum (worst-case) delay over all events (line segments). The colour scheme runs continuously from white (0 minutes delay), via yellow (5 min), orange (10 min), red (15 min), dark red (20 min) to black (25 min and higher). Note that the colour scheme is the reversed of the recovery times, so that again black is critical and white is harmless. The delay propagation can be visualized all at once, or by successive timetable periods which thus shows an animation of the delay propagation over the consecutive periods. The latter visualization starts with the initial delays, then the delay propagation in period zero, the first period, etc., until the settling period.

8.8 Case Study: The Dutch National Railway Timetable

8.8.1 Model Variants

This section presents the results of a case-study of the Dutch national railway timetable. The max-plus linear system model is based on a DONS variant of the Dutch 2000/2001 railway timetable in the morning peak. The model contains all train lines and freight paths scheduled in the morning peak including the intercity (IC), interregional (IR), and regional (R) lines of NS Reizigers, the regional lines of Syntus in the east of the Netherlands, the regional lines of No-ordNed in the north, the high-speed line (HST) from Amsterdam to Belgium, the international (INT) lines to Germany, and the freight (F) train paths. Table 8.1 summarizes the model. The dummy events correspond to arrival, through and terminal events.

Table 8.1 Summary of the Dutch national 2000/2001 railway timetable model

DONS timetable model		
Timetable points	729	stations, stops, shunting yards, junctions, movable bridges
Train line segments	7183	2062 stops, 281 turns, 4760 runs, 80 ends
Connections	259	198 transfers, 61 rolling stock connections
Headway constraints	87776	arrivals, departures, in/outbound, crossings, meets, overtaking
Max-plus linear system		
Nodes (transitions)	3536	1677 departure events, 1859 dummy events
Arcs (places)	25472	1677 line segments, 259 synchronization, 23536 infra
Tokens	12429	305 train runs, 90 connections, 105 turns, 11929 headway order
Order	2	13043 0-token places, 12193 1-token places, 236 2-token places

We consider two model variants distinguished by the amount of running time margin. In the *basic* variant we consider scheduled running times and in the *margins* variant we assume minimum running times implying that running time margins are used for delay reduction. Since the actual running time margins were not available we approximated them by subtracting 7% of the scheduled running times according to the capacity allocation norms, although in practice the default margins are slightly higher due to rounding running times to whole minutes. Furthermore, the DONS model did not always specify minimum layover times of turning trains. In those

Table 8.2 Spectral analysis results basic and margins timetable

Basic		Margins		Component / critical circuit (CC)
λ	Δ_2	λ	Δ_2	
60:00	0:00	58:01	0:11	Main network CC: Various
58:00	0:06	55:02	0:15	Line Gouda–Alphen aan den Rijn CC: R9500 Gouda–Boskoop–Gouda
55:00	0:22	51:56	0:35	Line Rotterdam CS–Hoek van Holland CC: R4200 Rotterdam CS–Maassluis West–Rotterdam CS
54:48	0:21	52:26	0:31	Lines The Hague CS–Zoetermeer/Rotterdam Hofplein CC: R13300, R13400, R13700, R13500, R13600

cases we used a default value of 5 minutes and assumed that any remaining layover time could be utilized as buffer time in case of delays. The minimum headway times in the DONS model utilized at infrastructure conflict points are based on the Dutch capacity allocation norms which range between 2 and 4 minutes depending on the route conflict and train types, see Chapter 3.

8.8.2 Critical Circuit Analysis

Table 8.2 shows the results of the spectral analysis of the *basic timetable*. The network is almost entirely connected with various critical circuits of maximum cycle mean $\lambda_0 = 60$. Hence, the basic timetable is critical implying that on the critical circuits no spare time is available other than the (unknown) process time margins and buffer times contained in the running times and minimum headways. The network contains three additionally strongly-connected components that are uncoupled from the main network component, see Table 8.2. The second critical component is the regional train line R9500 running on a single-track route between Gouda and Alphen aan den Rijn. The critical circuit has cycle mean $\lambda_1 = 58$ minutes and is compiled of the trip from Gouda to Boskoop just before Alphen where the train meets its opposite train, the minimum headway to the opposite train, the trip from Boskoop back to Gouda, and the turn in Gouda. The third component is the partial single-track route between Rotterdam CS and Hoek van Holland, where the train circulation of the R4200 between Rotterdam and Maassluis West (about 2/3 to the Hoek van Holland) is critical with cycle mean $\lambda_2 = 55$. The fourth component is a suburban subnetwork consisting of the Hofpleinlijn (The Hague CS–Rotterdam Hofplein) and the Zoetermeerlijn (The Hague CS–Zoetermeer); the critical circuit has cycle mean $\lambda_3 = 54:48$ minutes and consists of 66 arcs representing a mixed sequence of all running 5 regional train lines including 46 stops, 4 turns and 16 infrastructure constraints (arcs).

The *margins timetable* differs from the basic timetable by the incorporation of running time margins. Table 8.2 (3rd and 4th column) summarizes the results of the spectral analysis. We see the same four components as in the basic variant but smaller maximum cycle means. The critical circuits in the three smaller components have not changed, although the order of the cycle means of the last two components has changed reflecting that the amount of running time in the train line circulation of the R4200 is larger than in the critical circuit of the other component. The effect of the 7% running time margin is also apparent in the most critical component, which now contains 2 minutes average slack time. Moreover, this component now contains a unique critical circuit containing 10 trains running between The Hague HS to Breda and back, see

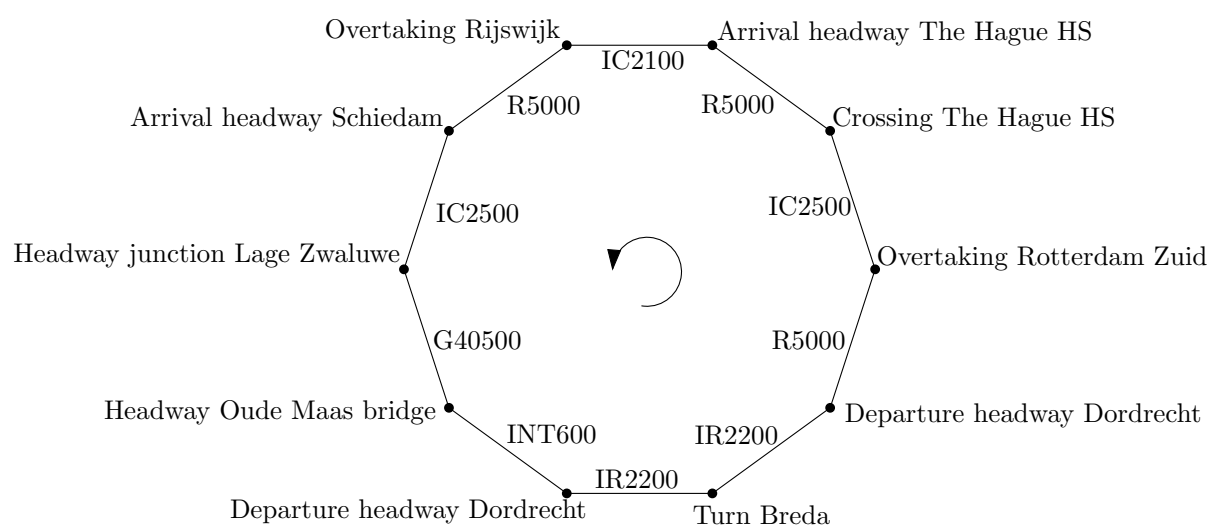


Figure 8.6 The critical circuit of the margins timetable

Figure 8.6. The nodes in Figure 8.6 represent critical events between the successive trains on the critical circuit. Intermediate stops of the trains are not shown. Figure 8.4 on page 248 shows the four critical circuits in the network visualization. In the sequel, we only consider the margins timetable.

Table 8.3 Spectral analysis results showing dependence on constraint types

Variant	λ (min)	ρ	Δ_2 (min)	r_{ii} (min)	Components
complete	58:01	0.97	00:11	5:57	4
no transfers	58:01	0.97	00:11	5:57	10
no turns	58:00	0.97	00:12	2:53	16
no turns/transfers	57:57	0.97	00:14	2:53	26
no infra	57:26	0.96	00:17	7:40	70
no infra/transfers	57:26	0.96	00:17	7:40	70
no infra/turns	57:26	0.96	00:17	7:40	3
no infra/turns/transfers	57:26	0.96	00:17	7:40	3

By definition λ_0 dominates the cycle times in all strong components accessible from the critical strong component. We next investigate the influence of passenger transfers, turns and infrastructure constraints on network connectivity, see Table 8.3. The columns show the timetable variant, eigenvalue, throughput, stability margin, the minimal circulation recovery time on the critical circuit(s) and the number of components, respectively. The first row is the reference model including all constraint types corresponding to Table 8.2. When discarding transfer constraints the number of components increases from 4 to 10. This shows that a number of components are only coupled by passenger transfers. The new decoupled components are 5 regional lines in the north (NoordNed) and 1 in the east (Syntus). Note that we do not discard rolling stock connections since they are considered hard connections that can not be cancelled. Discarding turning trains results in a decoupling of 12 additional components. Hence, availability of spare rolling stock at line ends could be helpful to reduce delay propagation. Discarding both transfers and

Table 8.4 Delay propagation of initial delay R6300 The Hague CS–Haarlem

Variant	Initial delay (min)	Total delay (min)	Trains	Sec delay (min)	Stations	Settling period
complete	10	489:48	29	61:22	37	3
no transfers	10	408:44	14	32:25	34	3
no turns	10	333:53	25	54:21	36	3
no turns/transfers	10	247:10	10	24:46	33	3
no infra	10	160:21	0	0	10	3
no infra/transfers	10	160:21	0	0	10	3
no infra/turns	10	70:06	0	0	9	0
no infra/turns/transfers	10	70:06	0	0	9	0
complete	11	715:29	53	101:27	55	4
complete	12	1064:01	83	169:53	85	4

turns leads to a decoupling of 26 components. This shows that transfers and turns connect distinct components, which suggest that cancelling transfers and allocating spare rolling stock can help reducing delay propagation to different directions. Table 8.3 also suggests that reduction of transfer times or layover times does not contribute much in decreasing the maximal eigenvalue. The infrastructure constraints on the other hand have a large impact on the eigenvalue as well as on the number of components. Train lines are thus mostly interconnected because of shared infrastructure. Finally, the drastic decrease in the number of components when discarding both infrastructure constraints and turns can be explained by the removal of circuits of train circulations and shared infrastructure. Finally, it must be realized that the critical circuits identified after discarding some arcs are also present in the general model but they are dominated by a more critical circuit that has access to these underlying components.

8.8.3 Delay Propagation and Recovery Time Analysis

Table 8.4 shows the propagation of a single initial delay of the regional line R6300 from The Hague CS (Gvc) to Haarlem (Hlm) over the margins timetable. Again we investigated the dependence of the constraint types on performance. In the reference variant (top row) we see the domino-effect of a local 10 minute initial delay of the R6300 Gvc-Hlm, see Figure 8.5. This delay propagates to 29 other trains and reaches 37 stations before it settles in 3 periods. The 489:48 minutes total delay is the cumulative delay of all train departures. The secondary delay denotes the propagation of delays to a new train line and does not measure the departure delays of these delayed trains on subsequent stations.

Cancelling passenger transfers halves the reached trains and almost halves the amount of secondary delay, although the total delay is still considerable. Allocating spare rolling stock at the line ends on the other hand leads to a small reduction of reached trains and secondary delays but in a considerable decrease of total delay. This shows the large impact of layover buffer times on stability. Management of both transfers and turns gives ‘the best of both worlds’ and seems to strengthen each other, confirming the result of the spectral analysis. The neglect of infrastructure constraints clearly shows that they are responsible for most of the delay propagation. The last two rows in Table 8.4 relate again to the complete model but with an initial delay of

11 and 12 minutes. This clearly shows how an additional delay of 1 minute has an exponential impact on delay propagation. Or conversely, it pays to prevent each minute of initial delay.

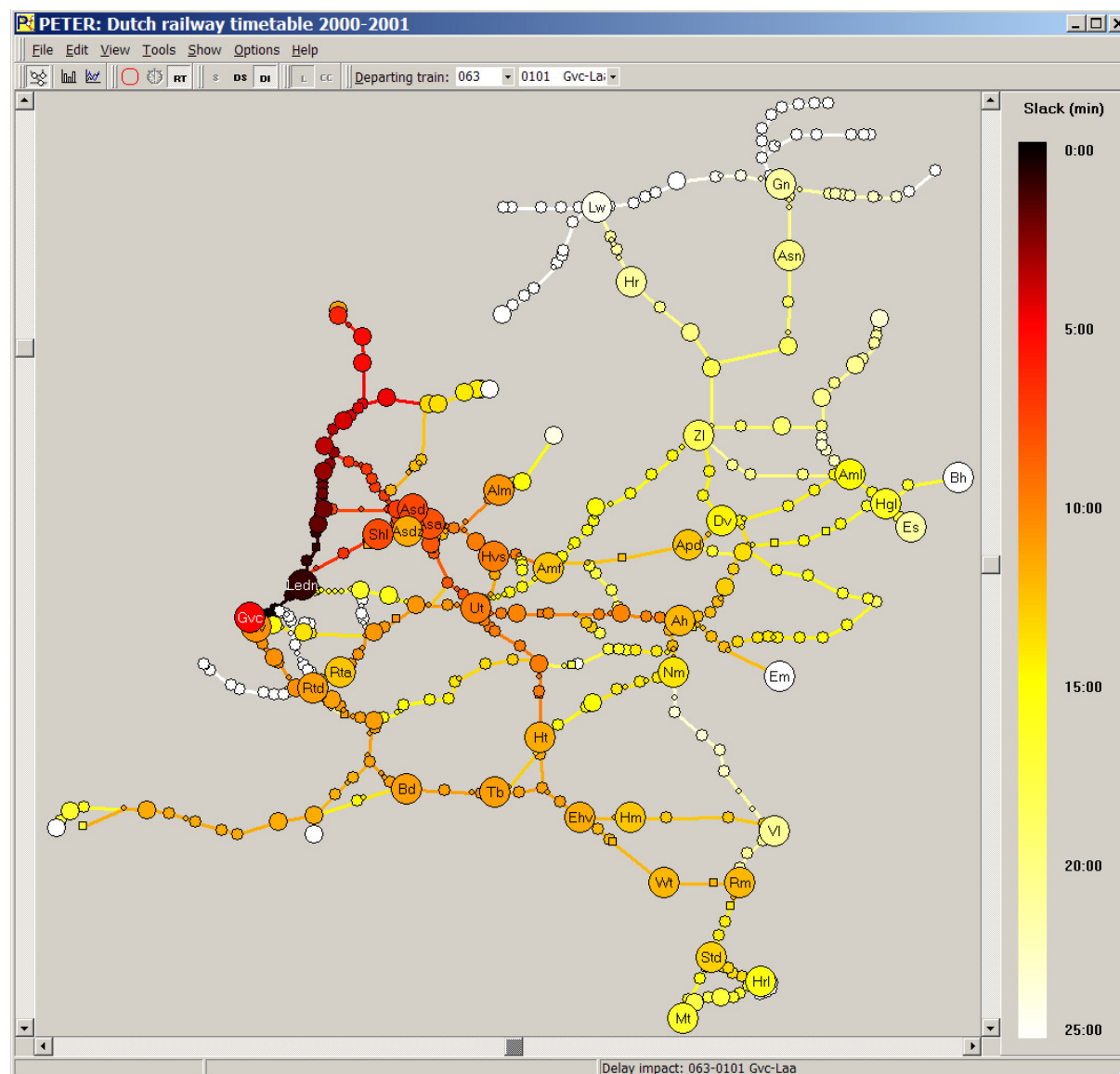


Figure 8.7 Delay impact (recovery times) of the R6300 The Hague CS-Haarlem (PETER network visualization): black denotes zero recovery time, white is more than 25 minutes recovery time or unconnected

Figure 8.7 shows the PETER network visualization of the delay impact vector (recovery times) of the departure of the R6300 Gvc-Hlm. The station colours denote how much recovery time is present from the departure of the R6300 to the worst-case trains on the various stations. Black implies zero recovery time and white implies either more than 25 minutes recovery time or that there is no path from the R6300 Gvc-Hlm. The stations coloured black to orange correspond to the stations reached in the reference variant of 10 minutes initial delay (top column of Table 8.4). The last two rows of Table 8.4 correspond to lighter shades of orange, see the legend in Figure 8.7.

The results of the delay propagation and recovery times shown here depend on the parameters (process times) of the DONS model. In particular, the minimum headway times are given by the headway norms, which however also include buffer time. Hence, the results are too conservative. More realistic minimum headways can be obtained by empirical data or using blocking time calculations. This was however beyond the scope of this case study.

8.9 Conclusions

Railway timetables have an intrinsic structure that can be conveniently modelled using max-plus algebra. It has been shown how polynomial matrices in max-plus algebra provide a direct link between timed event graphs and their max-plus state-space representations. A discrete-event systems theory has been developed to analyse these max-plus linear systems on stability, realizability, robustness, and delay propagation. The analysis methods are based on efficient algorithms including the solution to a generalized eigenproblem, shortest (or longest) path algorithms, and a dedicated delay propagation algorithm. Using these algorithms many valuable performance indicators can be computed, including network performance indicators (minimum cycle time, throughput, stability margin), recovery times (delay impact vectors, delay sensitivity vectors, circulation recovery times), and delay propagation statistics (total secondary delay, number of delayed trains, average secondary delay, settling period).

The max-plus eigenproblem provides several useful quantitative and qualitative characteristics of the railway timetable and its operational behaviour. A simple stability test is obtained by comparing the maximum eigenvalue (minimum cycle time) to the timetable period length (e.g. an hour). Obviously, the timetable cycle time must exceed the maximum eigenvalue otherwise the timetable is unrealizable, that is, it cannot be operated within the intended timetable period length. Only if the maximum eigenvalue is smaller than the basic timetable period it can be expected that the traffic network is stable, meaning that initial delays settle within a finite number of periods. The higher the difference between the minimum and intended cycle time the more stable the traffic network becomes. In addition, a stability margin can be computed by an auxiliary (max-plus) eigenproblem in which the timetable slack is explicitly evaluated. This stability margin gives the minimum slack time of each train run during a basic timetable period. This margin corresponds to a circuit with the least mean slack time, where the mean is taken over the number of trains (tokens) in the circuit. This circuit may differ from the critical circuit depending on the number of trains in the circuits: the higher the train count the less the share of slack time to each train.

The max-plus modelling and analysis algorithms have been implemented in the software tool PETER (Performance Evaluation of Timed Events in Railways). The algebraic approach combined with efficient graph theoretic algorithms allows real-time analysis of large-scale networks. The main functionalities of PETER have been explained and demonstrated with a case study of the Dutch railway timetable.

Chapter 9

CONCLUSIONS

9.1 Main Conclusions

9.1.1 Analysis of Train Detection Data

One of the main contributions of this PhD research conform the first research objective is the development of the software application *TNV-Prepare*, which converts TNV-logfiles to tables of train number and infrastructure events collected by train line and realized route. In these *TNV-tables* each daily train number has been coupled to the occupation and release time of the successive track sections on the realized train route, as well as relevant signal aspect changes and switch lockings. All recorded event times have a precision of one second and are checked on route-logic consistency by *TNV-Prepare*, thus guaranteeing the reliability of the information in the *TNV-tables*. The coupling of infrastructure data from the safety and signalling systems to train numbers enables an accurate quantitative analysis of train movements and station infrastructure utilization, including realized track occupation times, blocking times, and minimum headway times between train pairs, which was not possible before the development of *TNV-Prepare*.

Arrival and departure times at platform tracks are not detected directly by the safety and signalling systems. Nevertheless, ‘rough’ estimates of arrival times and departure times of scheduled events at platform tracks are available in the *TNV-tables* by means of the release time of the section directly before the platform track section (last train axle enters the platform section) and the occupation time of the successor section (first train axle leaves the platform track), respectively. The error in these arrival/departure time estimates range between a few seconds to a maximum of 30 seconds depending on the length of the platform track section, the train length, and the stop position on the platform track. These estimates are thus rather accurate and in particular improve the current automatic registration by the Dutch traffic control system VKL, which is based on far measurement points (at signals) using static tables of correction times to bridge the running time to/from the platform stop position. If additionally section lengths (and preferably also stop positions) are available, then the supplementary tool *TNV-Filter* can be used to improve the arrival/departure time estimates to a maximal error of a few seconds by fitting speed profiles through the station route and thus obtaining the actual speed and acceleration/deceleration rates at the platform section borders, which are used in estimating the remaining running time at the platform section. Thus, *TNV-Prepare* — in combination with *TNV-Filter* — also enables accurate estimates and analysis of dwell times, transfer times and running times, see Figure 9.1.

The data in TNV-logfiles made accessible via application of *TNV-Prepare* have been shown to be invaluable for detailed analysis of train punctuality, detection of train interdependencies,

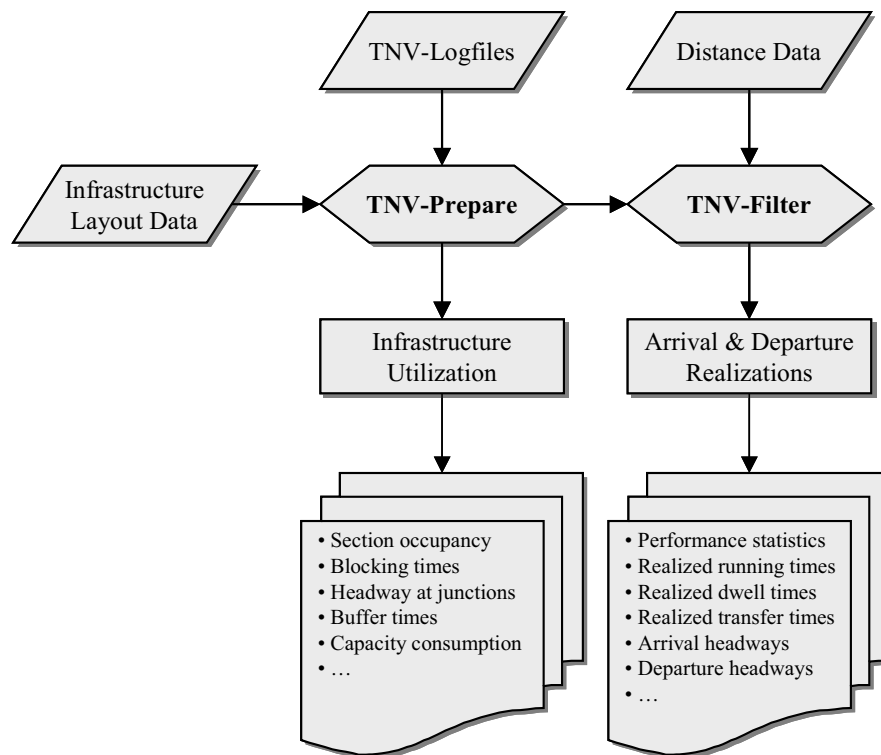


Figure 9.1 Flow chart of train detection data analysis

and quantification of hinder and secondary delays. The second research objective has been fulfilled by a case study of the railway station Eindhoven. The application of TNV-Prepare at Eindhoven showed a significant drop in punctuality from arrival to departure for all train lines dwelling at Eindhoven (with only one exception). Also the mean delay increased for all train lines stopping at Eindhoven, even when considering late trains only. This suggests a structural lack of buffer time in the dwell and transfer times and between the various train paths at Eindhoven. Regression analysis showed that the scheduled transfer connections were a main source of delay propagation. Conflicting train routes between arriving and departing trains were responsible for further secondary delays. This station thus proved to be a main source of secondary delays, which must be compensated for by running time margins and dwell buffer times at subsequent train runs and stops.

The case-study in Eindhoven has also been used for fitting and testing theoretical probability distributions of (arrival and departure) delays and dwell times for all 13 train lines, and transfer times for the 6 main cross-platform transfer connections. The dwell times and cross-platform transfer times in Eindhoven fit well to a normal distribution, also when considering late train arrivals only. Furthermore, dwell time excess for late trains fits well to an exponential distribution. The departure delays in Eindhoven also generally fit well to an exponential distribution, except when the departure follows closely after another departure in the same direction which occurs in 3 out of 13 cases in Eindhoven. The probability distributions of arrival delays in Eindhoven are more complicated. A normal distribution is formally accepted in 5 out of 13 cases. All empirical arrival delay distributions have a (more or less) positive skewness coefficient, which suggests that a skewed distribution may be more appropriate. However, 6 out of 13 empirical distributions are bimodal suggesting a mixture of distributions. The bimodal distributions may

be explained by hinder of arriving trains due to conflicting train routes by which the distribution is a mixture of hindered and unhindered arrivals. The arrivals can be partitioned into early and late arrivals. When considering late train arrivals only an exponential distribution fits well to the (late) arrival delays, except in 2 out of 13 cases of which the majority of trains arrive late. These 2 cases showed a good normal fit for all (early and late) arrivals.

Identification of small but structural primary and secondary delays is essential for improving railway operations and timetables. Structural shortcomings in a timetable often generate only small delays (less than 60 seconds) but a cumulation of small delays leads to large delays at possibly distant locations which become hard to explain. In the current practice where delays below 3 minutes are not recognized as such it is impossible to find the real sources of delays by which unnecessary drastic measures are applied to repair symptoms rather than actual problems. A periodic assessment of railway operations at stations and corridors with potential risk of delay propagation is therefore recommended to find and resolve sources of structural timetable conflicts. An important cause of timetable fragility is the quality and precision of some timetabling base data, such as assumptions on power supply, driver behaviour, alighting/boarding time, et cetera, used to compute e.g. running times, dwell times and minimum headway. Feedback from operational realization data thus is a necessary means to relieve this problem and match planning more closely to realization.

9.1.2 Timetable Stability Analysis

The third research objective was developing an analytical approach to evaluate and quantify critical network dependencies on capacity utilization and timetable stability. To this end, we adopted the max-plus algebra modelling approach and extended it by including headway constraints conform minimum headway relations imposed by the railway infrastructure. Moreover, the resulting constraint system resembles that of DONS — the Dutch timetable design system for computing feasible periodic timetables — which facilitates the compatibility between the timetable construction and timetable evaluation.

We showed that a periodic railway timetable has an inherent structure that can be modelled efficiently as a timed event graph, or equivalently, a linear system in max-plus algebra. The max-plus linear system model contains all timetable and headway constraints of interdependent event pairs. We emphasized the importance of the zero-order dynamics and showed that an effective description of a general (higher-order) max-plus linear system can be obtained using a polynomial state matrix, which yields a direct state-space representation in the event domain of the associated timed event graph. Performance evaluation of the max-plus linear system is achieved by computing the generalized eigenstructure of the (polynomial) state matrix for which the remarkably fast policy iteration algorithm is available. The eigenstructure explicitly quantifies the decoupled components and minimal cycle times of all events and moreover identifies the critical events and processes. The maximum generalized eigenvalue defines the minimum cycle time attainable for the given interconnection structure, which corresponds to the capacity consumption within a timetable period. The ratio of the maximum eigenvalue and the timetable period length gives the network throughput, and the difference between the timetable cycle time and the maximum eigenvalue is a measure of the stability margin within a basic timetable period. All these measures are related to the critical circuits in the network structure, which correspond to (closed) sequences of consecutive timetable events that are interrelated by

either timetable relations or conflicting routes. The identified critical events and processes give directions for further analysis to improve the timetable.

Supplementary to the eigenstructure analysis, the recovery times between all event pairs can be computed in the so-called recovery matrix using any available shortest (or longest) path algorithms. The diagonal entries of this recovery matrix are the circulation recovery times indicating for each event the minimum total slack over any recurrent path, which is a clear robustness measure. Also the columns and rows of the recovery matrix show explicitly the tightness between events over all paths in the network and thus identify the impact and sensitivity of delays in the network. Robustness against explicit initial delay scenarios can furthermore be computed by a very effective bucket-based delay propagation algorithm, yielding the settling period of the initial delays or any other individual or aggregated measure of the initial and secondary delays.

The max-plus analysis approach has been implemented in the software tool PETER (Performance Evaluation of Timed Events in Railways), which enables railway planners to use powerful mathematical techniques in the evaluation of periodic timetables. One of the main advantages of PETER over other existing software for evaluating railway timetables is its computational performance. Properties of large-scale timetables are computed in real-time which makes it a perfect tool for comparing a large number of different timetable variants or studying a timetable design in much detail using predefined initial delay scenarios. Moreover, we believe that the deterministic model conform the timetable design (deterministic process times, fixed train orders) is appealing to timetable designers who show a reluctant response to simulation tools.

The compatibility of PETER to DONS enables an automatic import of data. However, the minimum headway times used in DONS are mainly very simplified. Headway design norms may be used for the construction of a timetable, which then consist of the minimum headway time and some buffer time. For a realistic evaluation in PETER the amount of buffer time within these headway times must be known to prevent conservative results. It is however unknown how much buffer time is contained in the headway times used in DONS as this is typically location dependent and must be calculated by hand. Realistic minimum headway times can be obtained by either microscopic blocking time calculations or empirical train detection data. In the Netherlands, blocking time models are (still) not used in the railway planning practice. On the other hand, reliable empirical data on infrastructure utilization is now available by means of the tool TNV-Prepare which can thus be applied to derive realistic minimum headway times.

9.2 Recommendations and Future Research

9.2.1 Train Detection Data and Railway Operations Quality Management

TNV-Prepare requires manual input of railway infrastructure and routes, which is an undesirable tedious task when the tool is applied on a wider scale. The infrastructure modelling utility in TNV-Prepare can however be adapted to import infrastructure configuration data files from the system CARE [68] that also provides the configuration data in the TNV-systems. Each time the configuration data of a TNV-system is updated also the TNV-Prepare infrastructure must be updated. This guarantees a synchronization between the configuration data in the TNV-systems and TNV-Prepare, by which the infra elements and route blocks contained in the TNV-logfiles

are automatically recognized by TNV-Prepare. The configuration data in the TNV-Replay application [162] — also based on TNV-logfiles — is maintained in the same way. Ideally the configuration files also contain section lengths by which TNV-Filter is analogously automatically configured. ProRail is still developing an *Infra-atlas* that will contain up-to-date geographical data of station layouts, although it remains yet unclear whether length information of track sections will be completely available and maintained after local infrastructure modifications.

Recent developments in the format of TNV-logfiles authorized by ProRail ICT-Services for another project (monitoring of switch loads) also allow new improvements in the applicability of TNV-Prepare in both scale and time. The recording module of TNV-systems has been customized to include the reserved route block in each logged train number step message, where a route block is a list of sections and switches within a TNV-position. These new TNV-logfiles are known as VTL-files (*Verbeterde TNV-Logfiles*). This TNV software update has been gradually installed over the 13 TNV-systems during 2004–2005. The extra information in combination with the configuration files of the route blocks simplifies the search algorithm of TNV-Prepare considerably and consequently decreases the necessary computation time to couple train numbers to infrastructure events drastically, hence enabling a real-time and national generation of ‘TNV-tables’ over complete train line routes from terminal to terminal. Moreover, the system TROTS (TRain Observation and Tracking System) which is currently being developed to replace the TNV-systems will be able to provide accurate event time realizations. Availability of reliable train realization data in the near future is therefore no longer an issue.

Future effort must be directed towards usage of the empirical data in daily practice. As already discussed the data should be used for a regular comparison of planning with its realization to improve small structural conflicts in the timetable. More specific, dwell times and transfer times at (key) transfer stations should be evaluated and where necessary improved. Until now, these process times are mainly based on (historical) rules of thumb which have hardly been adjusted over the last decades although the traffic intensity changed considerably. Now we have the data available we can set this straight. Also train running times should be evaluated and in particular the used running time margins, which may depend on local conditions and circumstances. Internationally, different running time supplements are advised for the various train line types. Data analysis will reveal whether a differentiation of running time margins is worthwhile. Moreover, the existing running time calculation methods (such as in DONS and VPT-Planning) can be verified and possibly calibrated using the realization data, which will improve the realizability of the timetable. Finally, accurate determination of minimum headway times has been structurally neglected in the Netherlands, and therefore there is also no knowledge on existing buffer time between train paths at conflict points. Data analysis will reveal the realized minimum headways and thus buffer times between events. In combination with blocking time theory tight headway times without any average buffer time can easily be detected and consequently robustness of operations can be improved considerably by adding buffer time corresponding to the local variations in headway.

Deterioration and unavailability of infrastructure (signals, switches, tracks) and other technical equipment (rolling stock, dispatching and control systems) also have a main impact on the dispunctuality of railway operations. These primary sources of disruptions and delays can evidently not be detected from TNV-data. Nevertheless, a variety of registration systems are in use for logging incidents and equipment failures. A link between these systems and the TNV-data via train numbers, location and time of breakdowns, will provide the necessary information

to identify primary delays associated to recorded disruptions. Moreover, the secondary delays (and cancellations) resulting from the diagnosed primary delays can subsequently be determined from the TNV-data which thus reveals the impact of a disruption on operations. Knowing the impact of various disruptions may help to improve accurate disruption management.

9.2.2 Max-Plus Algebra

The max-plus algebra approach — and the tool PETER — could be an effective instrument to the capacity allocation process of infrastructure managers. In particular in the Netherlands where capacity requests of train operators are submitted as basic hour patterns (BHPs), which are nothing else than periodic timetables with a cycle time of one hour that can effectively be modelled and analysed in max-plus algebra as we have seen in this thesis. The infrastructure manager must coordinate the various BHP requests and test the resulting integrated BHP on feasibility and stability. The current practice at ProRail Capacity Allocation is still largely manual with the support of VPT-Planning (VPT-BUP), which however does not include conflict detection or evaluation functionalities other than the graphical means of time-distance graphs (no blocking times) and basic platform occupation diagrams. Possible extensions of PETER to be even more beneficial are an interface with VPT-BUP files to read VPT-BUP files and an automatic conflict detection mechanism. The latter implies that conflicting train paths are detected and minimum headways between conflicting train routes are computed. To this end, some additional data is required on the infrastructure usage. In the near future VPT-BUP will be replaced by PTI (*Planning & Toewijzing Infrastructuur*) which is currently under development. An interface to PTI is therefore also advisable.

This thesis considered deterministic max-plus linear systems for effective analysis of large-scale railway timetables. Future extensions may be directed towards introducing stochastic elements without sacrificing the computing time too much. This may lead to for instance sensitivity analysis of the timetable parameters (process times) to further identify critical events and processes. A more serious stochastic extension is changing the order of scheduled events, which is typically one of the most effective actions to reduce delay propagation. The problem of finding critical train orders is however linked to the NP-hard problems of sequencing and scheduling. Nevertheless, we may effectively evaluate the impact on performance of changing selected events. Another extension is the unavailability of resources by which the system must change to a different mode (state matrix). Current research on this topic includes (max-plus) *Taylor series approximations* [97] and — from a control point of view — *switching* max-plus linear systems [204].

Another research direction is railway timetable optimization. The max-plus delay propagation model may be used in a two-stage stochastic optimization model that combines timetable optimization and evaluation [213]. However, this optimization problem does not change the critical circuits but only the distribution of slack over the (critical) processes. Even more challenging is the question whether we can use the max-plus model to construct timetables in addition to evaluation and improving. For scheduled public transport this question can be answered confirmative: from the transportation times a max-plus model (or timed event graph) can be constructed and the eigenvector of the state matrix gives a most effective timetable for running regularly with a cycle time exceeding the eigenvalue. The performance of this initial timetable can successively be improved using *marking optimization* [126, 167] where tokens (vehicles)

can be added or redistributed over the timed event graph to optimize some objective function. In railway systems the shared use of infrastructure causes the difficulty that decisions have to be made on the order of trains over conflicting train routes. This ordering problem makes the problem typically NP-hard: in the worst-case all combinations of train orders must be evaluated before finding the optimal solution. The problem complexity is likely equivalent to the NP-complete periodic event scheduling problem (PESP). However, a different problem formulation may guide an efficient solution algorithm in practice. Heuristic design criteria may help to find good solutions. The stochastic max-plus model extensions may also guide the timetable optimization process [97].

BIBLIOGRAPHY

- [1] Abbink, E., Van den Berg, B., Kroon, L.G., and Salomon, M., “Allocation of Railway Rolling Stock for Passenger Trains”, *Transportation Science*, vol. 38, no. 1, pp. 33–41, 2004.
- [2] Aho, A.V., Hopcroft, J.E., and Ullman, J.D., *Data Structures and Algorithms*, Addison-Wesley, Reading, 1983.
- [3] Ahuja, R.K., Magnanti, T.L., and Orlin, J.B., *Network Flows: Theory, Algorithms, and Applications*, Prentice-Hall, New Jersey, 1993.
- [4] Alfieri, A., Groot, R., Kroon, L.G., and Schrijver, A., “Efficient Circulation of Railway Rolling Stock”, ERIM Report Series ERS-2002-110-LIS, Erasmus University Rotterdam, Rotterdam, 2002.
- [5] Allan, J., Brebbia, C.A., Hill, R.J., Sciutto, G., and Sone, S. (eds.), *Computers in Railways IX*, WIT Press, Southampton, 2004.
- [6] Allan, J., Hill, R.J., Brebbia, C.A., Sciutto, G., and Sone, S. (eds.), *Computers in Railways VII*, WIT Press, Southampton, 2000.
- [7] Allan, J., Hill, R.J., Brebbia, C.A., Sciutto, G., and Sone, S. (eds.), *Computers in Railways VIII*, WIT Press, Southampton, 2002.
- [8] Anderson, B.D.O. and Moore, J.B., *Optimal Filtering*, Prentice-Hall, Englewood Cliffs, 1979.
- [9] Andrews, H.I., *Railway Traction: The Principles of Mechanical and Electrical Railway Traction*, Studies in Mechanical Engineering, vol. 5, Elsevier, Amsterdam, 1996.
- [10] Assad, A.A., “Models for Rail Transportation”, *Transportation Research Part A*, vol. 14, no. 3, pp. 205–220, 1980.
- [11] Baccelli, F.L., Cohen, G., Olsder, G.J., and Quadrat, J.P., *Synchronization and Linearity: An Algebra for Discrete Event Systems*, Wiley, Chichester, 1992.
- [12] Bailey, C. (ed.), *European Railway Signalling*, Institution of Railway Signal Engineers (IRSE), A&C Black, London, 1995.
- [13] Bapat, R.B., “A Max Version of the Perron-Frobenius Theorem”, *Linear Algebra and its Applications*, vol. 275–276, pp. 3–18, 1998.
- [14] Bapat, R.B. and Raghavan, T.E.S., *Nonnegative Matrices and Applications*, Cambridge University Press, Cambridge, 1997.
- [15] Berge, C., *Topological Spaces*, Oliver & Boyd, London, 1963. Reprint by Dover, Mineola, 1997.
- [16] Berge, C., *The Theory of Graphs*, Methuen, London, 1966. Reprint by Dover, Mineola, 2001.
- [17] Berman, A. and Plemmons, R.J., *Nonnegative Matrices in the Mathematical Sciences*, Classics in Applied Mathematics, vol. 9, SIAM, Philadelphia, 1994.
- [18] Bollobás, B., *Modern Graph Theory*, Graduate Texts in Mathematics, vol. 184, Springer, New York, 1998.
- [19] Bookbinder, J.H. and Désilets, A., “Transfer Optimization in a Transit Network”, *Transportation Science*, vol. 26, no. 2, pp. 106–118, 1992.

- [20] Bouma, A. and Oltrogge, C., "Linienplanung und Simulation für öffentliche Verkehrswegen in Praxis und Theorie", *Eisenbahntechnische Rundschau (ETR)*, vol. 43, no. 6, pp. 369–378, 1994.
- [21] Braker, J.G., *Algorithms and Applications in Timed Discrete Event Systems*, PhD thesis, Delft University of Technology, Delft, 1993.
- [22] Braker, J.G. and Olsder, G.J., "The Power Algorithm in Max Algebra", *Linear Algebra and its Applications*, vol. 182, pp. 67–89, 1993.
- [23] Brünger, O., *Konzeption einer Rechnerunterstützung für die Feinkonstruktion von Eisenbahnfahrplänen*, Dissertation, Veröffentlichungen des Verkehrswissenschaftlichen Institutes der RWTH Aachen, Heft 51, Aachen, 1995.
- [24] Bussieck, M., *Optimal Lines in Public Rail Transport*, PhD thesis, Technische Universität Braunschweig, Braunschweig, 1998.
- [25] Bussieck, M.R., Kreuzer, P., and Zimmermann, U.T., "Optimal Lines for Railway Systems", *European Journal of Operational Research*, vol. 96, no. 1, pp. 54–63, 1997.
- [26] Bussieck, M.R., Winter, T., and Zimmermann, U.T., "Discrete Optimization in Public Rail Transport", *Mathematical Programming*, vol. 79, no. 3, pp. 415–444, 1997.
- [27] Caprara, A., Fischetti, M., Toth, P., Vigo, D., and Guida, P.L., "Algorithms for Railway Crew Management", *Mathematical Programming*, vol. 79, pp. 125–141, 1997.
- [28] Carey, M., "Reliability of Interconnected Scheduled Services", *European Journal of Operational Research*, vol. 79, no. 1, pp. 51–72, 1994.
- [29] Carey, M., "Ex Ante Heuristic Measures of Schedule Reliability", *Transportation Research Part B*, vol. 33, no. 7, pp. 473–494, 1999.
- [30] Carey, M. and Kwieciński, A., "Properties of Expected Costs and Performance Measures in Stochastic Models of Scheduled Transport", *European Journal of Operational Research*, vol. 83, no. 1, pp. 182–199, 1995.
- [31] Cochet-Terrasson, J., Cohen, G., Gaubert, S., Mc Gettrick, M., and Quadrat, J.-P., "Numerical Computation of Spectral Elements in Max-Plus Algebra", In: *IFAC Conference on System Structure and Control*, Nantes, France, 1998.
- [32] Cohen, G., Dubois, D., Quadrat, J.-P., and Viot, M., "A Linear-System-Theoretic View of Discrete-Event Processes and Its Use for Performance Evaluation in Manufacturing", *IEEE Transactions on Automatic Control*, vol. AC-30, no. 3, pp. 210–220, 1985.
- [33] Cohen, G., Gaubert, S., and Quadrat, J.-P., "Linear Projectors in the Max-Plus Algebra", In: *Proceedings of the 5th IEEE Mediterranean Conference on Control and Systems*, Paphos, Cyprus, 21–23 July, 1997.
- [34] Cohen, G., Gaubert, S., and Quadrat, J.-P., "Max-Plus Algebra and System Theory: Where We Are and Where to Go Now", *Annual Reviews in Control*, vol. 23, pp. 207–219, 1999.
- [35] Coleman, T., Branch, M.A., and Grace, A., *Optimization Toolbox User's Guide*, Version 2, The MathWorks, Natick, 1999.
- [36] Coleman, T.F. and Li, Y., "An Interior Trust Region Approach for Nonlinear Minimization Subject to Bounds", *SIAM Journal on Optimization*, vol. 6, pp. 418–445, 1996.
- [37] Commoner, F., Holt, A.W., Even, S., and Pnueli, A., "Marked Directed Graphs", *Journal of Computer and System Sciences*, vol. 5, pp. 511–523, 1971.
- [38] Cordeau, J.-F., Toth, P., and Vigo, D., "A Survey of Optimization Models for Train Routing and Scheduling", *Transportation Science*, vol. 32, no. 4, pp. 380–404, 1998.

- [39] Cormen, T.H., Leiserson, C.E., and Rivest, R.L., *Introduction to Algorithms*, MIT Press, Cambridge, 1990.
- [40] Cuninghame-Green, R.A., *Minimax Algebra*, Lecture Notes in Economics and Mathematical Systems, vol. 166, Springer, Berlin, 1979.
- [41] Cuninghame-Green, R.A. and Butkovič, P., “Bases in Max-Algebra”, *Linear Algebra and its Applications*, vol. 389, pp. 107–120, 2004.
- [42] Curchod, A. and Lucchini, L., “CAPRES: General Description of the Model”, Document ITEP 788/6, École Polytechnique Fédérale de Lausanne (EPFL), Lausanne, 2001.
- [43] Daamen, W., “A Quantitative Assessment on the Design of a Railway Station”, In: Allan *et al.* [7], pp. 191–200, 2002.
- [44] Daamen, W., *Modelling Passenger Flows in Public Transport Facilities*, PhD thesis, TRAIL Thesis Series, no. T2004/6, Delft University Press, Delft, 2004.
- [45] Dam, A. and Kieft, S., *Prolop, toedelings- en vergelijkingsmodel: Overzicht werking, in- en output*, NS Reizigers Marketingonderzoek & Advies, Utrecht, 1998.
- [46] Damen, A., “Uitvoeringstijden treinactiviteiten in Vervoersgegevensbank VKL”, Intern rapport, NS Verkeersleiding, Utrecht, 1997.
- [47] Dasdan, A., “Experimental Analysis of the Fastest Optimum Cycle Ratio and Mean Algorithms”, *ACM Transactions on Design Automation of Electronic Systems*, vol. 9, no. 4, pp. 385–418, 2004.
- [48] Dasdan, A. and Gupta, R.K., “Faster Maximum and Minimum Mean Cycle Algorithms for System Performance Analysis”, *IEEE Transactions on Computer-Aided Design of Integrated Circuits and Systems*, vol. 17, no. 10, pp. 889–899, 1998.
- [49] Dasdan, A., Irani, S.S., and Gupta, R.K., “An Experimental Study of Minimum Mean Cycle Algorithms”, Technical report 98-32, University of California, Irvine, 1998.
- [50] Dasdan, A., Irani, S.S., and Gupta, R.K., “Efficient Algorithms for Optimum Cycle Mean and Optimum Cost to Time Ratio Problems”, In: *Proceedings of the 36th ACM/IEEE Design Automation Conference (DAC)*, pp. 37–42, ACM Press, New York, 1999.
- [51] De Kort, A.F., Heidergott, B., Van Egmond, R.J., and Hooghiemstra, G., *Train Movement Analysis at Railway Stations: Procedures & Evaluation of Wakob’s Approach*, TRAIL Series in Transportation Science, no. S99/1, Delft University Press, Delft, 1999.
- [52] De Schutter, B., Van den Boom, T., and Hegyi, A., “A Model Predictive Control Approach for Recovery from Delays in Railway Systems”, *Transportation Research Record*, vol. 1793, pp. 15–20, 2002.
- [53] Demitz, J., Hübschen, C., and Albrecht, C., “Timetable Stability – Using Simulation to Ensure Quality in a Regular Interval Timetable”, In: Allan *et al.* [5], pp. 549–562, 2004.
- [54] Den Brok, M. and Vissers, R., “VPT, a New Systems Architecture for Planning and Control of Train Traffic in The Netherlands”, In: Murthy *et al.* [140], pp. 19–26, 1994.
- [55] Dennis, J.E., “Nonlinear Least Squares”, In: Jacobs, D. (ed.), *State of the Art in Numerical Analysis*, pp. 269–312, Academic Press, London, 1977.
- [56] Dijkstra, E.W., “A Note on Two Problems in Connexion with Graphs”, *Numerische Mathematik*, vol. 1, pp. 269–271, 1959.
- [57] Dilli, G., “Der Wandernde Engpaß und sein Gefolge”, *Eisenbahntechnische Rundschau (ETR)*, vol. 3, no. 1, pp. 1–11, 1954.
- [58] Domschke, W., “Schedule Synchronization for Public Transit Networks”, *OR Spektrum*, vol. 11, no. 1, pp. 17–24, 1989.

- [59] Dudnikov, P.I. and Samborskiĭ, S.N., “Endomorphisms of Finitely Generated Free Semi-modules”, In: Maslov, V.P. and Samborskiĭ, S.N. (eds.), *Idempotent Analysis*, Advances in Soviet Mathematics, vol. 13, pp. 65–85, American Mathematical Association (AMS), Providence, 1992.
- [60] European Commission, “Directive 2001/14/EC of the European Parliament and of the Council of 26 February 2001 on the Allocation of Railway Infrastructure Capacity and the Levying of Charges for the Use of Railway Infrastructure and Safety Certification”, *Official Journal of the European Communities*, vol. L 75, pp. 29–46, 2001.
- [61] European Commission, *White Paper—European Transport Policy for 2010: Time to Decide*, Office for Official Publications of the European Communities, Luxembourg, 2001.
- [62] Faber, J.A. (ed.), *Het spoor: 150 jaar spoorwegen in Nederland*, Meulenhoff, Amsterdam, 1989.
- [63] Fenner, W., Naumann, P., and Trinckauf, J., *Bahnsicherungstechnik*, Publicis Corporate Publishing, Erlangen, 2003.
- [64] Fiedler, J., “Die Haltezeit und ihre Einflußfaktoren”, *Eisenbahntechnische Rundschau (ETR)*, vol. 17, no. 11, pp. 474–479, 1968.
- [65] Fioole, P.J., Kroon, L.G., Maróti, G., and Schrijver, A., “A Rolling Stock Circulation Model for Combining and Splitting of Passenger Trains”, Report PNA-E0420, CWI, Amsterdam, 2004.
- [66] Floyd, R.W., “Algorithm 97: Shortest path”, *Communications of the ACM*, vol. 5, no. 6, pp. 345, 1962.
- [67] Fredman, M.L. and Tarjan, R.E., “Fibonacci Heaps and Their Uses in Improved Network Optimization Algorithms”, *Journal of the Association for Computing Machinery (ACM)*, vol. 34, no. 3, pp. 596–615, 1987.
- [68] Fries, G.A. and Van Sprakelaar, J., “Computer Aided Railway Engineering”, In: Mellitt *et al.* [132], pp. 53–59, 1998.
- [69] Garey, M.R. and Johnson, D.S., *Computers and Intractability: A Guide to Theory of NP-Completeness*, Freeman, New York, 1979.
- [70] Gaubert, S., *Théorie des Systèmes Linéaires dans les Dioïdes*, PhD thesis, L’école Nationale Supérieure des Mines de Paris, Paris, 1992.
- [71] Gaubert, S. and Mairesse, J., “Modeling and Analysis of Timed Petri Nets using Heaps of Pieces”, *IEEE Transactions on Automatic Control*, vol. 44, no. 4, pp. 683–697, 1999.
- [72] Gijzen, A. and Van den Brink, R.R.M., “Het spoor in model: energieverbruik en emissies door het railvervoer”, RIVM rapport 773002 021/2002, National Institute of Public Health and the Environment (RIVM), Bilthoven, 2002.
- [73] Golan, J.S., *Semirings and Affine Equations Over Them: Theory and Applications*, Mathematics and Its Applications, vol. 556, Kluwer, Dordrecht, 2003.
- [74] Gondran, M. and Minoux, M., “Valeurs Propres et Vecteurs Propres en Théorie des Graphes”, In: *Problèmes Combinatoires et Théorie des Graphes*, Colloques Internationaux du Centre National de la Recherche Scientifique, no. 260, pp. 181–183, CNRS, Paris, 1978.
- [75] Gondran, M. and Minoux, M., *Graphs and Algorithms*, Wiley, New York, 1984.
- [76] Goossens, J.H.M., *Models and Algorithms for Railway Line Planning Problems*, PhD thesis, Universiteit Maastricht, Maastricht, 2004.

- [77] Goossens, J.H.M., Van Hoesel, C.P.M., and Kroon, L.G., “A Branch-and-Cut Approach for Solving Railway Line-Planning Problems”, *Transportation Science*, vol. 38, no. 3, pp. 379–393, 2004.
- [78] Götz, W.W.J., “Trendanalyse 2001: Trends in veiligheid van het spoorwegsysteem in Nederland”, Rapport RnV/02/M10.008.076, Railned Spoorwegveiligheid, Utrecht, 2002.
- [79] Goverde, R.M.P., “Synchronization Control of Scheduled Train Services to Minimize Passenger Waiting Times”, In: *Proceedings of the 4th TRAIL Year Congress*, part 2, TRAIL Research School, Delft, 1998.
- [80] Goverde, R.M.P., “Analyse van treinpaden in stations m.b.v. TNV-Prepare”, In: Hansen, I.A., Olsder, G.J., and Michels, R. (eds.), *Modellen voor de beheersing van treinverkeer*, Bundeling bijdragen SMM workshop 19 mei, Utrecht, TRAIL Research School, Delft, 1999.
- [81] Goverde, R.M.P., “Improving Punctuality and Transfer Reliability by Railway Timetable Optimization”, In: *Proceedings of the 5th TRAIL Annual Congress*, TRAIL Research School, Delft, 1999.
- [82] Goverde, R.M.P., “Delay Estimation and Filtering of Train Detection Data”, In: *Proceedings TRAIL 6th Annual Congress 2000*, TRAIL Conference Proceedings Series, No. P2000/3, Part 2, TRAIL Research School, Delft, 2000.
- [83] Goverde, R.M.P., “PRRING II: Inzicht in de betrouwbaarheid van realisatiegegevens treinactiviteiten”, Rapport EXT 200307-01, versie 1.0, ProRail Strategie & Innovatie, Utrecht, 2003.
- [84] Goverde, R.M.P. and Hansen, I.A., “TNV-Prepare: Analysis of Dutch Railway Operations Based on Train Detection Data”, In: Allan *et al.* [6], pp. 779–788, 2000.
- [85] Goverde, R.M.P. and Hansen, I.A., “Delay Propagation and Process Management at Railway Stations”, In: *Proceedings CD-Rom of the World Conference on Railway Research (WCRR 2001)*, Köln, November 25–29, 2001.
- [86] Goverde, R.M.P., Hansen, I.A., Hooghiemstra, G., and Lopuhaä, H.P., “Delay Distributions in Railway Stations”, In: *Proceedings CD-Rom of the 9th World Conference on Transport Research (WCTR)*, Seoul, July 22–27, 2001.
- [87] Goverde, R.M.P., Hooghiemstra, G., and Lopuhaä, H.P., *Statistical Analysis of Train Traffic: The Eindhoven Case*, TRAIL Series in Transportation Science, no. S2001/1, Delft University Press, DUP Science, Delft, 2001. ISBN: 90-407-2201-3.
- [88] Goverde, R.M.P. and Odijk, M.A., “Performance Evaluation of Network Timetables Using PETER”, In: Allan *et al.* [7], pp. 731–740, 2002.
- [89] Goverde, R.M.P. and Soto y Koelemeijer, G., *Performance Evaluation of Periodic Railway Timetables: Theory and Algorithms*, TRAIL Studies in Transportation Science, no. S2000/2, Delft University Press, Delft, 2000.
- [90] Gröger, T.A., *Simulation der Fahrplanerstellung auf der Basis eines hierarchischen Trassenmanagements und Nachweis der Stabilität der Betriebsabwicklung*, PhD thesis, RWTH Aachen, Aachen, 2002.
- [91] Gröger, T.A., “Timetable Simulation by Sophisticated Conflict Resolution between Train Paths”, In: Allan *et al.* [5], pp. 573–582, 2004.
- [92] Hall, S., *Modern Signalling Handbook*, Ian Allan Publishing, Hersham, 3rd ed., 2001.
- [93] Hansen, I.A. and Goverde, R.M.P., “Ermittlung und Analyse von Ankunftsverspätungen in Bahnhöfen”, *Verkehr und Technik*, vol. 55, no. 10, pp. 447–453, 2002. (in German).

- [94] Hansen, I.A. and Goverde, R.M.P., “Entwicklung und Verteilung von Zugverspätungen in Bahnhöfen”, *Verkehr und Technik*, vol. 56, no. 2, pp. 69–74, 2003. (in German).
- [95] Happel, O., “Sperrzeiten als Grundlage für die Fahrplankonstruktion”, *Eisenbahntechnische Rundschau (ETR)*, vol. 8, no. 2, pp. 79–90, 1959.
- [96] Heidergott, B. and De Vries, R., “Towards a Control Theory for Transportation Networks”, *Discrete Event Dynamic Systems*, vol. 11, no. 4, pp. 371–398, 2001.
- [97] Heidergott, B. and Leahu, H., “Series Expansions of Generalised Matrix Products”, In: *Proceedings of the 44th IEEE Conference on Decision and Control and European Control Conference ECC 2005*, Sevilla, Spain, 2005 (to appear).
- [98] Hereth, K.U., “Die Übergangszeit bei Zuganschlüssen, ein wichtiges Element bei der Konstruktion des Personenzugfahrplans”, *Die Bundesbahn*, vol. 53, no. 6, pp. 407–410, 1977.
- [99] Hermann, U., *Untersuchung zur Verspätungsentwicklung von Fernreisezügen auf der Datengrundlagen der Rechnerunterstützten Zugüberwachung Frankfurt am Main*, Dissertation Nr. D17, Technische Hochschule Darmstadt, Darmstadt, 1996.
- [100] Higgins, A. and Kozan, E., “Modelling Train Delays in Urban Networks”, *Transportation Science*, vol. 32, no. 4, pp. 346–357, 1998.
- [101] Hooghiemstra, J.S., “An Automatic Timetable Generator for the Dutch Railway Network”, In: Murthy *et al.* [140], pp. 109–116, 1994.
- [102] Hooghiemstra, J.S., Kroon, L.G., Odijk, M.A., Salomon, M., and Zwaneveld, P.J., “Decision Support Systems Support the Search for Win-Win Solutions in Railway Network Design”, *Interfaces*, vol. 29, no. 2, pp. 15–32, 1999.
- [103] Howard, R.A., *Dynamic Programming and Markov Processes*, MIT Press/Wiley, New York, 1960.
- [104] Howlett, P.G. and Pudney, P.J., *Energy-Efficient Train Control*, Springer, London, 1995.
- [105] Huisman, T., Boucherie, R.J., and Van Dijk, N.M., “A Solvable Queueing Network Model for Railway Networks and its Validation and Applications for the Netherlands”, *European Journal of Operational Research*, vol. 142, no. 1, pp. 30–51, 2002.
- [106] Hürlimann, D., *Objektorientierte Modellierung von Infrastrukturelementen und Betriebsvorgängen im Eisenbahnwesen*, Dissertation ETH Nr. 14281, IVT Schriftenreihe 125, Eidgenössische Technische Hochschule (ETH), Zürich, 2002.
- [107] IVW, *Regeling Spoorverkeer*, Inspectie Verkeer en Waterstaat (IVW), Divisie Rail, Utrecht, 2005.
- [108] Jacobs, J., *Rechnerunterstützte Konfliktermittlung und Entscheidungsunterstützung bei der Disposition des Zuglaufs*, PhD thesis, RWTH Aachen, Aachen, 2003.
- [109] Jacobs, J., “Reducing Delays by Means of Computer-Aided ‘on-the-Spot’ Rescheduling”, In: Allan *et al.* [5], pp. 603–612, 2004.
- [110] Jentsch, E. and Gröpler, O., “Stochastische Zugfahrtsimulation: Zusammenhänge und Anwendungsmöglichkeiten”, In: Hertel, G. (ed.), 2. *Eisenbahnbetriebswissenschaftliches Kolloquium: Taktfahrplan und Kapazität*, Schriftenreihe des Instituts für Verkehrssystemtheorie und Bahnverkehr, vol. 2, pp. 154–171, Technische Universität Dresden, Dresden, 1996.
- [111] Johanns, R.D., *Handleiding bij de modules van de TNV-Prepare programmatuur*, Transportation and Planning Section, Delft University of Technology, Delft, 2001.
- [112] Johnson, D.B., “Efficient Algorithms for Shortest Paths in Sparse Networks”, *Journal of the Association for Computing Machinery (ACM)*, vol. 24, no. 1, pp. 1–13, 1977.

- [113] Jovanović, D. and Harker, P.T., “Tactical Scheduling of Rail Operations: The SCAN I System”, *Transportation Science*, vol. 25, no. 1, pp. 46–64, 1991.
- [114] Kaminsky, R., *Pufferzeiten in Netzen des spurgeführten Verkehrs in Abhängigkeit von Zugfolge und Infrastruktur*, Dissertation, Wissenschaftliche Arbeiten Nr. 56 des Instituts für Verkehrswesen, Eisenbahnbau und -betrieb der Universität Hannover, Hannover, 2001.
- [115] Kannengießer, F. and Wiche, B., “Einfluß der Fahrzeitzuzuschläge und Pufferzeiten auf die Pünktlichkeit”, *Die Bundesbahn*, vol. 62, no. 11, pp. 1001–1007, 1987.
- [116] Karp, R.M., “A Characterization of the Minimum Cycle Mean in a Digraph”, *Discrete Mathematics*, vol. 23, no. 3, pp. 309–311, 1978.
- [117] Karp, R.M. and Orlin, J.B., “Parametric Shortest Path Algorithms with an Application to Cyclic Staffing”, *Discrete Applied Mathematics*, vol. 3, no. 1, pp. 37–45, 1981.
- [118] Klemmt, W.-D. and Stemme, W., “Schedule Synchronization for Public Transit Networks”, In: Daduna, J.R. and Wren, A. (eds.), *Computer-Aided Transit Scheduling, Proceedings of the Fourth International Workshop on Computer-Aided Scheduling of Public Transport*, Lecture Notes in Economics and Mathematical Systems, vol. 308, pp. 327–335, Springer, Berlin, 1988.
- [119] Knuth, D.E., *The Art of Computer Programming. Volume 3: Sorting and Searching*, Addison-Wesley, Boston, 2nd ed., 1998.
- [120] Koolstra, K., “Capaciteitsmanagement in de spoorwegsector”, In: Ten Heuvelhof, E., Koolstra, K., and Stout, H. (eds.), *Capaciteitsmanagement: Beslissen over capaciteit van infrastructuur*, pp. 95–115, Lemma, Utrecht, 2001.
- [121] Kraft, K.H., *Zugverspätungen und Betriebssteuerung von Stadtschnellbahnen in systemtheoretischer Analyse*, Dissertation, Technische Universität Braunschweig, Braunschweig, 1981.
- [122] Krista, M., *Verfahren zur Fahrplanoptimierung dargestellt am Beispiel der Synchronzeiten*, Dissertation, Schriftenreihe des Instituts für Eisenbahnwesen und Verkehrssicherung, Heft 56, Technische Universität Braunschweig, Braunschweig, 1996.
- [123] Krista, M., “Fahrplanoptimierung durch Minimierung der Synchronzeiten”, *Signal + Draht*, vol. 91, no. 1–2, pp. 34–38, 1999.
- [124] Kroon, L.G., *Opsporen van sneller en beter: modelling through...*, Inaugural Addresses Research in Management Series, no. EIA-2001-03-LIS, Erasmus University Rotterdam, Rotterdam, 2001.
- [125] Kroon, L.G. and Fischetti, M., “Crew Scheduling for Netherlands Railways: “Destination: Customer””, In: Voß, S. and Daduna, J.R. (eds.), *Computer-Aided Scheduling of Public Transport*, Lecture Notes in Economics and Mathematical Systems, vol. 505, pp. 181–201, Springer, Berlin, 2001.
- [126] Laftit, S., Proth, J.-M., and Xie, X.L., “Optimization of Invariant Criteria for Event Graphs”, *IEEE Transactions on Automatic Control*, vol. 37, no. 5, pp. 547–555, 1992.
- [127] Lang, S., *Algebra*, Graduate Texts in Mathematics, vol. 211, Springer, New York, rev. 3rd ed., 2002.
- [128] Lindner, T., *Train Schedule Optimization in Public Rail Transport*, PhD thesis, Technische Universität Braunschweig, Braunschweig, 2000.
- [129] Lucchini, K., Rivier, R., and Emery, D., “CAPRES Network Capacity Assessment for Swiss North-South Rail Freight Traffic”, In: Allan *et al.* [6], pp. 221–230, 2000.

- [130] Mairesse, J., “Graphical Approach of the Spectral Theory in the $(\max, +)$ Algebra”, *IEEE Transactions on Automatic Control*, vol. 40, no. 10, pp. 1783–1789, 1995.
- [131] Mathsoft, *S-PLUS 2000 User’s Guide*, Data Analysis Products Division, Seattle, 1999.
- [132] Mellitt, B., Hill, R.J., Allan, J., Sciutto, G., and Brebbia, C.A. (eds.), *Computers in Railways VI*, Computational Mechanics Publications / WIT Press, Southampton, 1998.
- [133] Meng, Y., *Bemessung von Pufferzeiten in Anschlüssen von Reisezügen*, Dissertation, Veröffentlichen des Verkehrswissenschaftlichen Institutes der RWTH Aachen, Heft 46, Aachen, 1991.
- [134] Middelkoop, D. and Bouwman, M., “SIMONE: Large Scale Train Network Simulations”, In: Peters, B.A., Smith, J.S., Medeiros, D.J., and Rohrer, M.W. (eds.), *Proceedings of the 2001 Winter Simulation Conference*, pp. 1042–1047, IEEE, Piscataway, 2001.
- [135] Middelkoop, D. and Bouwman, M., “Testing the Stability of the Rail Network”, In: Allan *et al.* [7], pp. 995–1002, 2002.
- [136] Migom, A. and Valaert, W., “The Optimization of a Rhythmic Intercity Train Network”, *Rail International*, vol. 12, pp. 71–91, 1981.
- [137] Mühlhans, E., “Berechnung der Verspätungsentwicklung bei Zugfahrten”, *Eisenbahn-technische Rundschau (ETR)*, vol. 39, no. 7–8, pp. 465–468, 1990.
- [138] Murata, T., “Circuit Theoretic Analysis and Synthesis of Marked Graphs”, *IEEE Transactions on Circuits and Systems*, vol. CAS-24, no. 7, pp. 400–405, 1977.
- [139] Murata, T., “Petri Nets: Properties, Analysis and Applications”, *Proceedings of the IEEE*, vol. 77, no. 4, pp. 541–580, 1989.
- [140] Murthy, T.K.S., Mellitt, B., Brebbia, C.A., Sciutto, G., and Sone, S. (eds.), *Computers in Railways IV*, vol. 2, Computational Mechanics Publications, Southampton, 1994.
- [141] Nachtigall, K., “Periodic Network Optimization with Different Arc Frequencies”, *Discrete Applied Mathematics*, vol. 69, no. 1–2, pp. 1–17, 1996.
- [142] Nachtigall, K., “Cutting Planes for a Polyhedron Associated with a Periodic Network”, Internal report IB 112-96/17, Institut für Flugführung, Deutsche Forschungsanstalt für Luft- und Raumfahrt (DLR), Braunschweig, 1997.
- [143] Nachtigall, K. and Voget, S., “A Genetic Algorithm Approach to Periodic Railway Synchronization”, *Computers and Operations Research*, vol. 23, no. 5, pp. 453–463, 1996.
- [144] Nash, A. and Huerlimann, D., “Railroad Simulation Using OpenTrack”, In: Allan *et al.* [5], pp. 45–54, 2004.
- [145] Nie, L. and Hansen, I.A., “System Analysis of Train Operations and Track Occupancy at Railway Stations”, *European Journal of Transport and Infrastructure Research*, vol. 5, no. 1, pp. 31–54, 2005.
- [146] Nie, W., “Waiting: Integrating Social and Psychological Perspectives in Operations Management”, *Omega*, vol. 28, no. 6, pp. 611–629, 2000.
- [147] Nordeen, M., *Stability Analysis of Cyclic Timetables for a Highly Interconnected Rail Network*, PhD thesis nr. 1435, École Polytechnique Fédérale de Lausanne (EPFL), Lausanne, 1996.
- [148] NS, *Jaarverslag 2004*, Utrecht, 2004.
- [149] NS, ProRail, Railion, V&W, “Benutten en Bouwen: Het plan van de spoorsector”, Rapport, Nederlandse Spoorwegen, ProRail, Railion, Ministerie van Verkeer en Waterstaat, Utrecht, 2003.
- [150] NSR, *Wachttijden voor reizigerstreinen (WRT): Dienstregeling 1995/1996*, NS Reizigers Logistiek, Utrecht, 1995.

- [151] NSR, *Jaardienst Reizigerstreindienst 01 juni 1997 t/m 23 mei 1998*, NS Reizigers, Utrecht, 1997.
- [152] NSR, *Spoorboekje 97/98*, NS Reizigers, Utrecht, 1997.
- [153] Odijk, M.A., “A Constraint Generation Algorithm for the Construction of Periodic Railway Timetables”, *Transportation Research Part B*, vol. 30, no. 6, pp. 455–464, 1996.
- [154] Odijk, M.A., *Railway Timetable Generation*, PhD thesis, Delft University Press, Delft, 1997.
- [155] Olsder, G.J., Roos, K., and Van Egmond, R.J., “An Efficient Algorithm for Critical Circuits and Finite Eigenvectors in the Max-Plus Algebra”, *Linear Algebra and its Applications*, vol. 295, no. 1–3, pp. 231–240, 1999.
- [156] Olsder, G.J., Subiono, and Mc Gettrick, M., “On Timetables and Allocation of Trains”, In: *Proceedings of the Fourth Workshop on Discrete Event Systems (WODES98)*, pp. 463–468, Cagliari, 1998.
- [157] Ortúzar, J. de D. and Willumsen, L.G., *Modelling Transport*, Wiley, Chichester, 3rd ed., 2001.
- [158] Pachl, J., *Railway Operation and Control*, VTD Rail Publishing, Mountlake Terrace, 2002.
- [159] Peeters, L.W.P., *Cyclic Railway Timetable Optimization*, PhD thesis, Erasmus University Rotterdam, Rotterdam, 2003.
- [160] Peeters, M. and Kroon, L.G., “Circulation of Railway Rolling Stock: A Branch-and-Price Approach”, ERIM Report Series ERS-2003-055-LIS, Erasmus University Rotterdam, Rotterdam, 2003.
- [161] Petri, C.A., *Kommunikation mit Automaten*, Dissertation, Universität Bonn, Institut für Instrumentelle Mathematik, Schriften des IIM Nr. 2, Bonn, 1962.
- [162] Pieters, M.R. and Nieuwenhuis, P., *Gebruikershandleiding TNV Replay*, AEA Technology Rail, Utrecht, 2001.
- [163] Poort, J.P., “Grenzen aan benutting”, Rapport, NYFER, Breukelen, 2002.
- [164] Prins, M., *Het vervoersproces van planning tot uitvoering*, NS Verkeersleiding, Utrecht, 1998.
- [165] ProRail, *Network Statement 2005*, Utrecht, 2004.
- [166] ProRail, *Netwerkverklaring 2006*, Utrecht, 2005.
- [167] Proth, J.-M., Sauer, N., and Xie, X.L., “Optimization of the Number of Transportation Devices in a Flexible Manufacturing System Using Event Graphs”, *IEEE Transactions on Industrial Electronics*, vol. 44, no. 3, pp. 298–306, 1997.
- [168] Puterman, M.L., *Markov Decision Processes: Discrete Stochastic Dynamic Programming*, Wiley, New York, 1994.
- [169] Radtke, A. and Hauptmann, D., “Automated Planning of Timetables in Large Railway Networks Using a Microscopic Data Basis and Railway Simulation Techniques”, In: Allan *et al.* [5], pp. 615–625, 2004.
- [170] Ren, X. and Zhou, M., “Tactical Scheduling of Rail Operations: A Petri Net Approach”, In: *IEEE International Conference on Systems, Man and Cybernetics*, vol. 4, pp. 3087–3092, 1995.
- [171] Renkema, M. and Vas Visser, H., “TRACE Supervision System for Dispatching and Passenger Information”, In: Allan, J., Brebbia, C.A., and Hill, R.J. (eds.), *Computers in Railways V*, vol. 2, pp. 247–256, Computational Mechanics Publications, Southampton, 1996.

- [172] Rice, J.A., *Mathematical Statistics and Data Analysis*, Wadsworth and Brooks/Cole, Pacific Grove, 1988.
- [173] Rietveld, P., Bruinsma, F.R., and Van Vuuren, D.J., “Coping with Unreliability in Public Transport Chains: A Case Study for Netherlands”, *Transportation Research Part A*, vol. 35, no. 6, pp. 539–559, 2001.
- [174] Rockafellar, R.T., *Network Flows and Monotropic Optimization*, Wiley, New York, 1984.
- [175] Rothblum, U.G., “Algebraic Eigenspaces of Nonnegative Matrices”, *Linear Algebra and its Applications*, vol. 12, no. 3, pp. 281–292, 1975.
- [176] Rousseeuw, P. J. and Van Zomeren, B. C., “Unmasking Multivariate Outliers and Leverage Points”, *Journal of the American Statistical Association*, vol. 85, pp. 633–639, 1990.
- [177] Sakaguchi, T. and Tomii, N., “A Train Traffic Model Based on Coloured Petri Nets and its Application to a Train Schedule Planning System”, In: Allan, J., Brebbia, C.A., and Hill, R.J. (eds.), *Computers in Railways V*, vol. 1, pp. 457–466, Computational Mechanics Publications, Southampton, 1996.
- [178] Schaafsma, A.A.M., “Versnel het openbaar vervoer en verlies reizigers: het risico van korte reistijden in het spoorboekje”, In: Mouwen, A.M.T., Kalfs, N., and Govers, B. (eds.), *Colloquium Vervoersplanologisch Speurwerk. Beheersbare mobiliteit: een utopie?*, pp. 266–279, CVS, Delft, 1996.
- [179] Schaafsma, A.A.M., *Dynamisch Railverkeersmanagement*, PhD thesis, TRAIL Thesis Series, no. T2001/7, Delft University Press, Delft, 2001.
- [180] Schaafsma, A.A.M. and Weits, E.A.G. (eds.), *Capaciteit en Belasting van het Spoorwagennet*, Railned, Utrecht, 1996.
- [181] Schrijver, A., *Theory of Linear and Integer Programming*, Wiley, Chichester, 1986.
- [182] Schrijver, A., “Minimum Circulation of Railway Stock”, *CWI Quarterly*, vol. 6, no. 3, pp. 205–217, 1993.
- [183] Schrijver, A., “Routing and Timetabling by Topological Search”, *Documenta Mathematica Extra Volume ICM III*, pp. 687–695, 1998.
- [184] Schrijver, A. and Steenbeek, A., *Dienstregelingontwikkeling voor Railned: Rapport CADANS 1.0*, CWI, Amsterdam, 1994.
- [185] Schwanhäuß, W., *Die Bemessung der Pufferzeiten im Fahrplangefüge der Eisenbahn*, Dissertation, Veröffentlichungen des Verkehrswissenschaftlichen Institutes der RWTH Aachen, Heft 20, Aachen, 1974.
- [186] Schwanhäuß, W., “The Status of German Railway Operations Management in Research and Practice”, *Transportation Research Part A*, vol. 28, no. 6, pp. 495–500, 1994.
- [187] Seneta, E., *Non-negative Matrices and Markov Chains*, Springer, New York, 2nd ed., 1981.
- [188] Serafini, P. and Ukovich, W., “A Mathematical Model for Periodic Event Scheduling Problems”, *SIAM Journal on Discrete Mathematics*, vol. 2, no. 4, pp. 550–581, 1989.
- [189] Sontag, E.D., *Mathematical Control Theory: Deterministic Finite Dimensional Systems*, Texts in Applied Mathematics, vol. 6, Springer, New York, 1990.
- [190] Soto y Koelemeijer, G., *On the Behaviour of Classes of Min-Max-Plus Systems*, PhD thesis, Delft University of Technology, TRAIL Thesis Series, no. T2003/6, Delft, 2003.
- [191] SRA, *Capacity Utilisation Policy: Network Utilisation Strategy*, Strategic Rail Authority, London, June 2003.
- [192] SRA, “Capacity Utilisation Policy”, Consultation document, Strategic Rail Authority, London, September 2002.

- [193] Stemme, W., *Anschlußoptimierung in Netzen des öffentlichen Personennahverkehrs*, Dissertation D 83, Technische Universität Berlin, Berlin, 1988.
- [194] Stolk, A., “Automatic Conflict Detection and Advanced Decision Support for Optimal Usage of Railway Infrastructure: Purpose and Concepts”, In: Mellitt *et al.* [132], pp. 629–638, 1998.
- [195] Strang, G., *Linear Algebra and its Applications*, Harcourt Brace Jovanovich, Orlando, 3rd ed., 1988.
- [196] Subiono, *On Classes of Min-Max-Plus Systems and their Applications*, PhD thesis, TRAIL Thesis Series, no. T2000/2, Delft University Press, Delft, 2000.
- [197] Subiono and Van der Woude, J., “Power Algorithms for $(\max, +)$ - and Bipartite $(\min, \max, +)$ -Systems”, *Discrete Event Dynamic Systems*, vol. 10, no. 4, pp. 369–389, 2000.
- [198] Tarjan, R.E., “Depth First Search and Linear Graph Algorithms”, *SIAM Journal on Computing*, vol. 1, no. 2, pp. 146–160, 1972.
- [199] Tromp, J.P.M. and Hansen, I.A., “Hindrance Between Conflicting Train Movements at a Level Crossing”, In: Allan *et al.* [7], pp. 985–993, 2002.
- [200] Ullius, M., “Open Timetable: Tool for Analysis and Quality Control of Timetables”, OTT Infosheet, IVT, Eidgenössische Technische Hochschule (ETH) Zürich, Zürich, 2003.
- [201] Vakhtel, S., *Rechnerunterstützte analytische Ermittlung der Kapazität von Eisenbahnnetzen*, Dissertation, Veröffentlichungen des Verkehrswissenschaftlichen Institutes der RWTH Aachen, Heft 59, Aachen, 2002.
- [202] Van Boetzelaer, M., “Elektronische beveiliging bij de NS”, *Op de rails*, vol. 63, no. 3, pp. 94–100, 1995.
- [203] Van de Velde, D., “Dutch and Japanese Railway Reforms and Exchanges”, *Japanese Railway & Transport Review*, vol. 24, pp. 10–16, July 2000.
- [204] Van den Boom, T.J.J. and De Schutter, B., “Modelling and Control of Railway Networks”, In: *Proceedings of the American Control Conference (ACC)*, pp. 5728–5733, Boston, 2004.
- [205] Van der Aalst, W.M.P. and Odijk, M.A., “Analysis of Railway Stations by Means of Interval Timed Coloured Petri Nets”, *Real-Time Systems*, vol. 9, no. 3, pp. 241–263, 1995.
- [206] Van der Werff, M., Scholten, H., and Godziejewski, B., “Migration Strategy for Signalling Systems in the Netherlands”, *Signal + Draht*, vol. 94, no. 10, pp. 43–48, 2002.
- [207] Van Egmond, R.J., “Propagation of Delays in Public Transport”, Reports of the Faculty of Technical Mathematics and Informatics, no. 98-39, Delft University of Technology, Delft, 1998.
- [208] Van Egmond, R.J., *Railway Capacity Assessment: An Algebraic Approach*, TRAIL Studies in Transportation Science, S99/2, Delft University Press, Delft, 1999.
- [209] Van Egmond, R.J., “An Algebraic Approach for Scheduling Train Movements”, In: Voß, S. and Daduna, J.R. (eds.), *Computer-Aided Scheduling of Public Transport*, Lecture Notes in Economics and Mathematical Systems, vol. 505, Springer, Berlin, 2001.
- [210] Van Harn, P., *Rekenen of simuleren? Een onderzoek naar stabiliteit van dienstregelingen*, Master thesis, Vrije Universiteit Amsterdam, Amsterdam, 2003.
- [211] Van Hengstum, H. and Van Delft, R., “Invoering VPT-procesleiding”, *Railevant*, vol. 41, no. 3, pp. 8–11, 1995.

- [212] Van Leur, M., “NS Introduces a New Generation Automatic Train Protection”, In: Murthy *et al.* [140], pp. 319–324, 1994.
- [213] Vromans, M.J.C.M., *Reliability of Railway Systems*, PhD thesis, Erasmus University Rotterdam, Rotterdam, 2005.
- [214] Vuchic, V.R., *Urban Public Transportation: Systems and Technology*, Prentice-Hall, Englewood Cliffs, 1981.
- [215] Wagenaar, A., “Toetsing 2001/2002: Beoordeling basisurpatronen & 24-uursuitwerking”, Rapport RnT/01/123, Railned, Utrecht, 2001.
- [216] Wagneur, E., “Moduloids and Pseudomodules: 1. Dimension Theory”, *Discrete Mathematics*, vol. 98, no. 1, pp. 57–73, 1991.
- [217] Wakob, H., *Ableitung eines generellen Wartemodells zur Ermittlung der planmäßigen Wartezeiten im Eisenbahnbetrieb unter besonderer Berücksichtigung der Aspekte Leistungsfähigkeit und Anlagenbelastung*, Dissertation, Veröffentlichungen des Verkehrswissenschaftlichen Institutes der RWTH Aachen, Heft 36, Aachen, 1985.
- [218] Wang, J., *Timed Petri Nets: Theory and Applications*, Kluwer, Boston, 1998.
- [219] Warshall, S., “A Theorem on Boolean Matrices”, *Journal of the Association for Computing Machinery (ACM)*, vol. 9, no. 1, pp. 11–12, 1962.
- [220] Weigand, W., *Graphentheoretisches Verfahren zur Fahrplangestaltung in Transportnetzen unter berücksichtigung von Pufferzeiten mittels interaktiver Rechentechnik*, Dissertation, Technische Universität Braunschweig, Braunschweig, 1981.
- [221] Weigand, W., “Verspätungsübertragungen in Fernverkehrsnetzen”, *Eisenbahntechnische Rundschau (ETR)*, vol. 30, no. 12, pp. 915–920, 1981.
- [222] Weigand, W., “The Man-Machine Dialogue and Timetable Planning”, *Rail International*, vol. 14, no. 3, pp. 8–25, 1983.
- [223] Wende, D., *Fahrdynamik*, Transpress, Berlin, 1983.
- [224] Wendler, E., *Analytische Berechnung der planmäßigen Wartezeiten bei asynchroner Fahrplankonstruktion*, Dissertation, Veröffentlichungen des Verkehrswissenschaftlichen Institutes der RWTH Aachen, Heft 55, Aachen, 1999.
- [225] Wezel, M.C., Kok, J.N., Van den Berg, J., and Van Kampen, W., “Genetic Improvement of Railway Timetables”, In: Davidor, Y., Schwefel, H.P., and Manner, R. (eds.), *Proceedings of the Third Conference on Parallel Problem Solving from Nature*, Lecture Notes in Computer Science, vol. 866, pp. 566–575, Springer, Berlin, 1994.
- [226] Wiggenraad, P.B.L., “Alighting and Boarding of Passengers at Dutch Railway Stations”, In: *Papers of the TRAIL Workshop “Train Delays at Stations and Network Stability”*, TRAIL Research School, Delft, December 7, 2001.
- [227] Young, N.E., Tarjan, R.E., and Orlin, J.B., “Faster Parametric Shortest Path and Minimum Balance Algorithms”, *Networks*, vol. 21, no. 2, pp. 205–221, 1991.
- [228] Yuan, J., Goverde, R.M.P., and Hansen, I.A., “Propagation of Train Delays in Stations”, In: Allan *et al.* [7], pp. 975–984, 2002.
- [229] Zhu, P., *Betriebliche Leistung von Bahnsystemen unter Störungsbedingungen*, Dissertation, Fortschritt-Berichte VDI, Reihe 12, no. 462, VDI Verlag, Düsseldorf, 2001.
- [230] Zwaneveld, P.J., *Railway Planning: Routing of Trains and Allocation of Passenger Lines*, PhD thesis, Erasmus University Rotterdam/TRAIL Research School, Eburon Publishers, Delft, 1997.

-
- [231] Zwaneveld, P.J., Kroon, L.G., and Van Hoesel, S.P.M., “Routing Trains through a Railway Station Based on a Node Packing Model”, *European Journal of Operational Research*, vol. 128, no. 1, pp. 14–33, 2001.

Appendix A

GLOSSARY

A.1 General Abbreviations

AR	Local (Agglo/Regional) train line
ATB	<i>Automatische TreinBeïnvloeding</i> , Dutch ATP system, also ATB-EG
ATB-NG	<i>ATB-Nieuwe Generatie</i> , Dutch ATP system
ATP	Automatic Train Protection
BHP	Basic Hourly Pattern (BUP, <i>BasisUurPatroon</i>)
BPO	Basic Platform Occupation, (BSO, <i>BasisSpoorOpstelling</i>)
DONS	Designer Of Network Schedules, Dutch timetable design system
EBP	<i>Elektronische BedienPost</i> , Dutch interlocking system
EBS	<i>Elektronische Beveiliging SIMIS</i> , Dutch interlocking system
HST	High Speed Train line
IC	InterCity train line
INT	INternational train line
IR	InterRegional train line
NSR	<i>NS Reizigers</i> , passenger train division of Dutch Railways
PETER	Performance Evaluation of Timed Events in Railways
PRL	<i>PRocesLeidingssysteem</i> , Dutch dispatching system, also VPT-PRL
TNV	<i>TreinNummerVolgsysteem</i> , Dutch train describer system
VKL	<i>VerKeersLeidingssysteem</i> , Dutch traffic control system, also VPT-VKL
VGB	<i>VervoersGegevensBank</i> , Dutch railway traffic realizations database
VPI	Vital Processor Interlocking, Dutch interlocking system
VPT	<i>Vervoer Per Trein</i> , Dutch railway planning and communication system

A.2 Station Abbreviations

Dn	Deurne	Mt	Maastricht
Ehv	Eindhoven	Rtd	Rotterdam CS
Gvc	Den Haag CS	Tbwt	Tilburg West
Hlm	Haarlem	Ut	Utrecht CS
Hrl	Heerlen	VI	Venlo
Koln	Keulen (D)	Wrt	Weert

A.3 Mathematical Symbols and Variables

\oplus	Addition in a semiring; in the max-plus semiring $a \oplus b = \max(a, b)$
\otimes	Multiplication in a semiring; in the max-plus semiring $a \otimes b = a + b$
\oslash	Division in a semifield; in the max-plus semifield $a \oslash b = a - b$
A	State matrix $A = (a_{ij})$
$[A]_{\cdot i}$	i th column of matrix A
A_λ	Normalized matrix $A_\lambda = A(\lambda^{-1})$
A^\top	Transpose of matrix $A = (a_{ij})$, $A^\top = (a_{ji})$
A^+	Path matrix
A^*	Kleene star matrix
$A(X)$	Polynomial matrix
$A(\lambda^{-1})$	Evaluated polynomial matrix in λ^{-1}
$A(\gamma)$	Polynomial state matrix
\mathcal{A}	Polynomial matrix, $\mathcal{A} = A(X)$
\mathcal{A}^π	Polynomial matrix associated to policy π
B	Input matrix
C	Output matrix
χ	Cycle time vector
d	Timetable vector
d_0	Initial timetable vector
$d(k)$	Timetable vector in period k
$\text{diag}(d)$	Max-plus diagonal matrix, $[\text{diag}(d)]_{ii} = d_i$, $[\text{diag}(d)]_{ij} = \varepsilon$ if $i \neq j$
δ_{ij}	Max-plus Kronecker delta function, $\delta_{ii} = e$, $\delta_{ij} = \varepsilon$ if $i \neq j$
Δ_2	Stability margin
e	Unit element in a semiring; in the max-plus semiring $e = 0$
e_i	i th unit vector
E	Unit matrix in a matrix semiring; $[E]_{ii} = e$ and $[E]_{ij} = \varepsilon$ for all $i \neq j$
E^c	Set of critical arcs
E_{red}	Arc set of reduced graph
ε	Zero element in a semiring; in the max-plus semiring $\varepsilon = -\infty$
\mathcal{E}	Zero matrix in a matrix semiring; $[\mathcal{E}]_{ij} = \varepsilon$ for all i, j
η	Maximum cycle mean
G	Graph $G = (V, E)$
G^c	Critical graph $G = (V^c, E^c)$
G_{red}	Reduced graph $G_{\text{red}} = (V_{\text{red}}, E_{\text{red}})$
\mathcal{G}	Timed event graph $\mathcal{G} = (\mathcal{T}, \mathcal{P}, \mu, w)$
$\mathcal{G}(\mathcal{A})$	Timed event graph corresponding to polynomial matrix \mathcal{A}
γ	Shift operator
Γ	Cycle matrix
$\Gamma(i)$	Set of events accessible from i
$\text{im}(A)$	Image of A
$\text{in}(p_k)$	Input transition of place p_k
k_s	Settling period
K_λ	Set of events accessible from any principle class $\mathcal{K}(\lambda)$
$\mathcal{K}(\lambda)$	Set of principle classes with eigenvalue λ

λ	Eigenvalue
λ_0	Maximum eigenvalue
m	Number of arcs or places
M	Incidence matrix
μ	Marking vector of a timed event graph
μ_0	Initial marking vector of a timed event graph
$\mu(p_k)$	Marking of place p_k
n	Number of nodes or transitions
\mathbb{N}	Set of natural numbers, $\mathbb{N} = \{1, 2, 3, \dots\}$
\mathbb{N}_0	Set of natural numbers extended with zero, $\mathbb{N}_0 = \mathbb{Z}_+ = \{0, 1, 2, 3, \dots\}$
$\text{out}(p_k)$	Output transition of place p_k
p	Order (maximum marking)
P	Max-plus permutation matrix
\mathcal{P}	Set of places in a timed event graph
π	Policy vector
Π_i	Set of incoming places to event i
$R(\mu_0)$	Reachable set of markings in a timed event graph with initial marking μ_0
\mathbb{R}	Set of real numbers
\mathbb{R}_ε	Set of real numbers extended with $\varepsilon = -\infty$
\mathbb{R}_{\max}	Max-plus semifield $(\mathbb{R}_\varepsilon, \max, +, -\infty, 0)$
$\mathbb{R}_{\max}[X]$	Semiring of max-plus polynomials
\mathbb{R}_{\max}^n	Semimodule of n -dimensional vectors over the max-plus semifield
$\mathbb{R}_{\max}^{m \times n}$	Set of $m \times n$ matrices over the max-plus semifield
$\mathbb{R}_{\max}^{m \times n}[X]$	Set of $m \times n$ max-plus polynomial matrices
$\text{span}(A)$	Spanning set of columns of A
ρ	Throughput
$\text{spec}(A)$	Spectrum of matrix A
$\text{supp}(A)$	Support of matrix A (index set of finite entries)
S	General semiring
$S[\gamma]$	Polynomial semiring in the indeterminate γ over the semiring S
$\sigma(k)$	Firing vector of the k th firing
$\text{tr}(A)$	Trace of matrix A , $\text{tr}(A) = \bigoplus_{i=1}^n a_{ii}$
T	Timetable cycle time
\mathcal{T}	Set of transitions of a timed event graph
\mathcal{T}_i	Communication class $\mathcal{T}_i \subseteq \mathcal{T}$
u	Input vector
v	Eigenvector
V^c	Set of critical nodes or transitions
V_{red}	Node set of reduced graph, communication class
$\mathcal{V}(\lambda)$	Eigensemimodule associated to eigenvalue λ
w	Holding time (weight) vector of a timed event graph
$w(p_k)$	Holding time of place p_k
x	State vector
x_0	Initial state vector
$x(k)$	Event time vector in period k
X	An indeterminate
ξ	Circuit or path

y	Output vector
z	Delay vector
\mathbb{Z}	Set of integers, $\mathbb{Z} = \{\dots, -2, -1, 0, 1, 2, \dots\}$
\mathbb{Z}_+	Set of nonnegative integers, $\mathbb{Z}_+ = \{0, 1, 2, \dots\}$
\mathbb{Z}_-	Set of nonpositive integers, $\mathbb{Z}_- = \{0, -1, -2, \dots\}$

SUMMARY

Punctuality of Railway Operations and Timetable Stability Analysis

Rob M.P. Goverde

This thesis is concerned with the analysis of railway timetables. The considered research topics include: (1) data collection of railway operations based on train detection data; (2) statistical analysis of empirical data to find sources of structural delays; and (3) stability analysis of large-scale periodic railway timetables.

An essential element in the design of a reliable railway timetable is the feedback of empirical data from realized operations. A timetable consists of deterministic process times (running times, dwell times, transfer times, etc.), which in practice vary from hour-to-hour or day-to-day due to e.g. varying driver behaviour, fluctuating passenger volumes, and changing weather conditions. The stochastic distributions of realized process times and arrival/departure times show how well the timetable can be adhered to. In the Dutch railway practice this quality cycle is however not structurally applied. Running times are computed using advanced running time calculation models and successively increased by a given percentage — usually 7% — to compensate for larger running times. Dwell times and transfer times are based on rules-of-thumb. And also minimum headway times between pairs of trains sharing some infrastructure are based on norms, which include some (unknown) buffer time. (Chapter 3)

Empirical validation of the individual process times was not possible until recently, because of lacking accurate realization data. The traffic control systems collect and maintain a large amount of event time realizations (arrivals, departures and passages at timetable points), but these realizations are derived from passage times at entrance and exit signals (via train description steps) which causes uncertainty about the accuracy of the individual recorded event times. This data is therefore only suitable for statistics at an aggregated level, such as the percentage of trains arriving within three minutes after schedule at 32 stations over a month. (Chapter 4)

This thesis shows that accurate event time realizations are available in records (TNV-logfiles) of the train describer systems (TNV in Dutch), and describes the tool TNV-Prepare that was especially developed to recover this information from the TNV-logfiles. Train describers keep track of the progress of trains based on train numbers and infrastructure messages received from the safety and signalling systems. All received infrastructure messages and all generated train number events are recorded chronologically in TNV-logfiles. These files thus contain invaluable information. However, the infrastructure and train number messages are logged independently from a wide area. The Dutch railway network contains 13 TNV-systems, which each monitors all running trains over a large area and records all train number events, as well as all received infrastructure events related to e.g. track sections (occupation, release), signals (stop, go), and switches (left, right). Until the year 2000 — during this PhD research — the TNV-logfiles were kept for at most a week for investigation of accidents. In this PhD research the software TNV-Prepare has been developed that couples train numbers to infrastructure events based on the TNV-logfiles. This way train movements can be traced on track section occupancy level,

including the entry and exit of platform track sections, by which realised arrival, departure, and through times can be determined with an accuracy of a few seconds. (Chapter 4)

The potential of accurate empirical data is demonstrated in a case-study of the railway station Eindhoven. Eindhoven is a main Dutch transfer station at which various train lines from different directions stop, turn, or connect. The analysis is based on TNV-logfiles from 1997 that were specially collected and made available for this aim. The statistical analysis showed that Eindhoven was a source of delay growth. The mean dwell time of each train line was larger than scheduled, also when considering late trains only. The departure delays increased on the average by one minute with respect to the arrival delays. Using regression analysis, the delay expansion could be explained by a combination of dependencies between train lines, including transfer connections and conflicting routes. In particular, the double-track route between Eindhoven and Boxtel caused much hindrance, because trains with scheduled transfers in Eindhoven had to arrive or depart one after another. This bottleneck was removed in 2002 after the four-track route between Eindhoven and Boxtel became available. Other findings include a poor departure punctuality of turning trains and the resulting hindrance despite a layover time of more than thirty minutes, and conflicting routes between in- and outbound train lines with tight scheduled headway. Apart from the specific outcomes, this case-study clearly demonstrates the power of a statistical analysis of accurate train data. (Chapter 5)

Another more theoretical topic of the case-study concerned the estimation and testing of theoretical probability distributions to the various process times and delays. Stochastic mathematical models and simulation models rely on given probability distributions for process times or delays. By absence of empirical data, distributions are typically based on theoretical assumptions and often also simple exponential distributions are used which are easy to work with. The Eindhoven data has been used to fit process times and delays for each train line separately. For this data, the excess dwell times of late trains follow an exponential distribution. Also the departure delays follow an exponential distribution except for train lines heading in the same direction with close scheduled departure times. Dwell times and transfer times of cross-platform transfers follow a normal distribution, both for all trains and when considering late trains only. Arrival delays do not fit well to any simple theoretical distribution in general, mainly due to disturbances of conflicting train paths. (Chapter 5)

The second main topic of this thesis is railway timetable stability. Train traffic has to deal with a large amount of (network) dependencies. Some of these dependencies are caused by the railway timetable and logistics, such as passenger transfers, rolling stock circulations, and schedules of drivers and conductors. Other dependencies relate to the shared railway infrastructure, such as following trains on open tracks, conflicting routes at station layouts between in- and outbound trains, and meeting trains on partial single-track routes. A timetable is usually conflict-free in the sense that all conflicts between train paths have been solved in advance. However, if a train deviates from its scheduled time-distance path then it may hinder other trains, which then deviate from schedule as well, etc. Because of this domino-effect, a local primary disruption may have considerable consequences to the entire traffic network. Therefore, a stable timetable contains some buffer time between train paths which compensates for small disruptions and avoids prompt secondary delays to other trains. Testing the stability of a railway timetable requires a network model of all train interdependencies. (Chapter 3 & 6)

A railway timetable essentially describes precedence relations between events and decisions on the scheduled order of events. For instance, a train is ready-to-depart if it has arrived and the

minimum dwell time has been respected to guarantee alighting and boarding of passengers; if the train has a transfer connection with a feeder train then it also has to wait for the arrival of this feeder train plus a minimum transfer time to allow transferring passengers to board the train; and finally, the train may have to wait for trains with a conflicting inbound or outbound route before the route from the platform to the open track becomes available. Discrete-event systems where synchronization between events is the main characteristic can be formulated as ‘timed event graphs,’ a special abstract network structure (Petri net) describing time-dependent precedence relations and their process logic. A timed event graph model shows the implications of the scheduled order of events and proves whether it is (im)possible that a system becomes deadlocked. An example of this is that a train may depart to a single-track route only if all opposite trains have left the open track. These topological and behavioural properties of a timetable can be analysed by the ‘marked’ graph theory of timed event graphs. (Chapter 6)

Timetable performance and stability is effectively analysed in the event domain associated to a timed event graph. The departure times of all trains are therefore collected in a state vector and the dynamic equations describing the interactions between events are given by (max,+)-recursions in which the departure time of any train is determined by the maximum over all preceding departure times plus the subsequent minimum process times that have to be waited for. These recursive equations are linear systems in the so-called max-plus algebra. In max-plus algebra ‘addition’ of two numbers is defined as their maximum and ‘multiplication’ as conventional addition, e.g. $2 \oplus 3 = \max(2, 3) = 3$ and $2 \otimes 3 = 2 + 3 = 5$. From a systems point of view, addition of two processes implies process synchronization (a new process may start after the last preceding process has terminated) and multiplication corresponds to cascading processes (the process time of the composite process is the sum of the individual successive process times). All process times are collected in a state matrix, and the evolution of the discrete-event system is described accordingly by matrix-vector multiplications and addition of vectors, evaluated in max-plus algebra. (Chapter 7 & 8)

From an algorithmic point of view, the analysis of max-plus linear systems concentrates on solving critical-path problems and eigenproblems in max-plus algebra. This thesis therefore considers efficient algorithms to these problems given the particular application area. A timed event graph can be represented by a polynomial matrix in max-plus algebra, i.e., a polynomial with matrix coefficients, or equivalently, a matrix with polynomial entries. The polynomial matrices can also be used in a formal description of higher-order linear systems, including zero-order terms. The zero-order terms correspond to all processes that are completed within one period, the first-order terms correspond to all processes exceeding a timetable period, et cetera. The most common approach to tackle higher-order systems is to transform them into a purely first-order system to which elegant algebraic solutions exist. However, this is computationally not the most effective and also leads to practical problems, mainly because the zero-order dynamics have disappeared. This thesis shows how the existing max-plus algebra theory of matrices and first-order recursive systems can be extended to polynomial matrices and higher-order implicit systems. Special attention is given to the generalized eigenproblem of (irreducible and reducible) max-plus polynomial matrices. This theory gives the necessary background for the complete description of the eigenspace of (polynomial) matrices, and a correct interpretation of the max-plus policy-iteration algorithm in case of reducible max-plus (polynomial) matrices. The max-plus policy-iteration algorithm has been developed recently based on the well-known policy-iteration algorithm for Markov decision processes, and has proved to be very effective in solving generalized eigenproblems in max-plus algebra with a linear practical running time.

Other considered topics include efficiently computing all critical circuits and delay propagation with respect to large-scale sparse max-plus systems. (Chapter 7)

The stability test of max-plus linear systems is based on the eigenvalues of the (polynomial) state matrix. The maximum eigenvalue denotes the minimal cycle time of the railway timetable. Hence, for an hourly timetable the maximum eigenvalue must be smaller than sixty minutes to be (asymptotically) stable, in which case any initial delay will settle after a finite number of periods. The maximum eigenvalue equals the mean cycle time of a ‘critical circuit,’ which can also be computed explicitly. A critical circuit is a cyclic sequence of events and processes with the least slack over all circuits in the network. An eigenvector corresponds to a periodic timetable (departure time vector) in which the critical events are scheduled directly after each other without slack and thus allowing a cycle time equal to the maximum eigenvalue. The departure times in the eigenvector correspond to the critical paths from one of the critical events. The difference between the timetable cycle time — usually an hour — and the maximum eigenvalue gives the mean slack on the critical circuits. All processes that do not belong to a critical circuit have more slack available. Whether a stable timetable is also robust depends on the distribution of slack time over the timetable. An example of a stable timetable that is not very robust is one where the buffer time over each train line circulation is concentrated in the layover times at the terminals, by which primary delays are propagated over the entire network before they are reduced at the train line ends. The distribution of slack over a timetable is represented by the ‘recovery matrix,’ where each entry corresponds to the least total slack time over all paths between two events. The impact of any combination of initial delays can also be visualized by explicitly computing the delay propagation using the max-plus state equations. (Chapter 8)

The algorithms have been implemented in the software tool PETER (Performance Evaluation of Timed Events in Railways). Special attention has been given to the development and implementation of efficient algorithms that are capable of computing results of large-scale networks in several seconds. Furthermore, results in PETER are graphically presented by means of a projection to the railway network, thus clearly visualizing the locations of critical events and processes in the network. PETER offers a systematic and transparent stability analysis of large-scale periodic timetables and can be applied in the design process of railway timetables, for evaluating network stability in the capacity allocation process, and for developing effective dispatching policies to minimize delay propagation. (Chapter 8)

NEDERLANDSE SAMENVATTING (DUTCH SUMMARY)

Punctualiteit van railverkeer en stabiliteitsanalyse van dienstregelingen

Rob M.P. Goverde

Dit proefschrift beschrijft methoden voor de analyse van treindienstregelingen. De onderwerpen die aan bod komen zijn: (1) dataverzameling van de dienstuitvoering gebaseerd op treindetectie data; (2) statistische analyse van empirische data om oorzaken van structurele vertragingen op te sporen; en (3) stabiliteitsanalyse van periodieke dienstregelingen voor grootschalige spoor-netwerken.

Een essentieel element in het ontwerpproces van een betrouwbare dienstregeling is terugkop-peling van empirische data van de gerealiseerde dienstuitvoering. Een dienstregeling bestaat immers uit deterministische procestijden (rijtijden, halteringstijden, overstaptijden, etc.), terwijl deze in de praktijk variëren van uur-tot-uur en dag-tot-dag vanwege bijvoorbeeld verschillend rijgedrag van machinisten, fluctuerende aantallen reizigers en veranderende weersomstandighe-den. De stochastische verdelingen van gerealiseerde procestijden en aankomst- en vertrektij-den geven aan in welke mate de dienstregeling haalbaar blijkt te zijn. Deze kwaliteitscirkel is echter nauwelijks aanwezig bij de spoorpraktijk in Nederland. Rijtijden worden berekend met geavanceerde rijtijdmodellen waar vervolgens een bepaald percentage — meestal 7% — aan toe wordt gevoegd om langere rijtijden op te vangen. Halteringstijden en overstaptijden zijn gebaseerd op vuistregels. En ook de minimale volgtijden tussen twee treinen die (gedeeltelijk) gebruik maken van hetzelfde spoor zijn gebaseerd op normtijden, waarin een (onbekende) spe-ling zit verwerkt. (Hoofdstuk 3)

Empirische validatie van de afzonderlijke procestijden was tot voor kort niet mogelijk we-gens het ontbreken van nauwkeurige realisatiegegevens. Via de verkeersleidingssystemen wordt dagelijks een grote hoeveelheid aan gerealiseerde treinactiviteiten (aankomsten, vertrekken en doorkomsten op dienstregelpunten) verzameld en opgeslagen, maar deze worden afgeleid van passagetijden bij inrijseinen en vertrekseinen (via vensterverplaatsingen van het treinnummervolgsysteem) waardoor onzekerheid ontstaat over de nauwkeurigheid van de individuele geregi-streerde realisatietijden. Deze gegevens zijn daarom alleen geschikt voor statistieken op geag-gregeerd niveau, zoals het percentage treinen dat minder dan drie minuten na plan aankomt op 32 stations in een maand. (Hoofdstuk 4)

Dit proefschrift laat zien dat nauwkeurige uitvoeringstijden op individueel treinniveau wel im-pliciet aanwezig zijn in de zogenaamde TNV-logbestanden van de treinnummervolgsystemen (TNV), en beschrijft de tool TNV-Prepare die speciaal is ontwikkeld om deze gegevens boven tafel te krijgen. TNV-systemen volgen de voortgang van alle treinen op het spoornet via trein-nummers en infrastructuurmeldingen uit de beveiligings- en beheersingssystemen. Alle ele-mentmeldingen die het TNV-systeem ontvangt vanuit de beveiligings- en beheersingssystemen worden chronologisch opgeslagen in de TNV-logbestanden, evenals de gegenereerde trein-nummERMeldingen van het TNV-systeem zelf. Deze bestanden bevatten dus een schat aan

informatie. Het probleem is echter dat de inframeldingen en treinnummERMeldingen los van elkaar staan. Het Nederlandse spoornet heeft 13 TNV-systemen die ieder een gebied bedienen in grootte vergelijkbaar met een provincie. Alle treinen die in dit gebied rondrijden worden gevolgd en gelogd, evenals o.a. alle spoorsecties die bezet en onbezet raken, seinen die op rood springen en weer vrij komen, en wissels die omgelegd worden. Tot het jaar 2000 (tijdens dit promotieonderzoek) werden deze TNV-logbestanden hooguit een week bewaard voor eventuele analyse van ongelukken en vervolgens overschreven. Als onderdeel van dit promotieonderzoek is de software TNV-Prepare ontwikkeld, die op basis van TNV-logbestanden treinnummers koppelt aan inframeldingen. Hierdoor kunnen individuele treinen op spoorsectieniveau gevolgd worden, inclusief het op- en afrijden van perronsporen, waardoor gerealiseerde aankomst-, vertrek- en doorkomsttijden met een nauwkeurigheid van enkele seconden bepaald kunnen worden. (Hoofdstuk 4)

In een case-study is het potentieel van beschikbare nauwkeurige realisatietijden aangetoond. Als case is het station Eindhoven uitgekozen. Eindhoven is een belangrijk knooppunt waar diverse treinseries uit verschillende richtingen stoppen, keren en op elkaar aansluiten. De analyse is gebaseerd op TNV-logbestanden uit 1997 die destijds speciaal voor dit doel waren aangevraagd en opgeslagen. Uit de statistische analyse kwam naar voren dat Eindhoven een bron was van vertragingstoename. De gemiddelde halteringstijden van alle treinseries waren langer dan gepland, ook als alleen gekeken werd naar treinen die te laat aankwamen. De vertrekvertragingen namen gemiddeld met een minuut toe ten opzichte van de aankomstvertragingen. Met behulp van regressieanalyse kon de vertragingstoename worden verklaard uit een combinatie van afhankelijkheden tussen de treinseries, waaronder reizigersaansluitingen en conflicterende rijwegen. Met name het tweesporige baanvak tussen Eindhoven en Boxtel zorgde voor veel hinder omdat treinen die in Eindhoven op elkaar aansloten achter elkaar moesten aankomen dan wel vertrekken. Deze bottleneck is in 2002 opgeheven na het gereedkomen van de spoorverdubbeling tussen Eindhoven en Boxtel. Andere structurele vertragingsoorzaken die zijn gevonden waren kruisende rijwegen van aankomende en vertrekkende treinseries met krap geplande opvolgtijd en een slechte vertrekpunctualiteit van kerende treinen met de daardoor ontstane hinder ondanks ruim een half uur geplande keertijd. Los van de specifieke uitkomsten geeft deze case-study duidelijk de meerwaarde aan die een statistische analyse van nauwkeurige data biedt. (Hoofdstuk 5)

Een ander meer theoretisch onderdeel van de case-study was het schatten en testen van theoretische kansverdelingen voor de diverse procestijden en vertragingen. Stochastische wiskundige modellen en simulatiemodellen gaan uit van bepaalde kansverdelingen voor vertragingen en procestijden. Wegens gebrek aan empirische data worden veelal aannamen gedaan omtrent de kansverdelingen die de afzonderlijke processen goed beschrijven, en ook wordt vaak uitgegaan van eenvoudige (exponentiële) kansverdelingen waar makkelijk mee te rekenen is. Voor de Eindhovense data is gekeken naar procestijden en vertragingen per treinserie. Hier bleek dat de overschrijding van halteringstijden voor vertraagde treinen voldoet aan een exponentiële verdeling. Ook de vertrekvertraging voldoet aan een exponentiële verdeling mits de geplande vertrektijden van treinen in dezelfde richting ver genoeg uit elkaar liggen. Halteringstijden en overstaptijden van ‘cross-platform’ aansluitingen volgen een normale verdeling, zowel voor alle treinen als wanneer alleen gekeken wordt naar vertraagde treinen. Aankomsttijden zijn over het algemeen niet goed te beschrijven met enkelvoudige kansverdelingen; hindering van aankomende treinen blijkt hier een grote verstoring te zijn. (Hoofdstuk 5)

Het tweede onderwerp van dit proefschrift is de stabiliteit van dienstregelingen. Het treinverkeer over een spoorwegnetwerk heeft te maken met een groot aantal netwerkafhankelijkheden. Een aantal van deze afhankelijkheden ontstaat door de opzet van de dienstregeling en de logistieke processen, zoals reizigersaansluitingen, materieelomlopen en diensten van machinisten en conducteurs. Andere afhankelijkheden ontstaan doordat treinen over een gemeenschappelijke infrastructuur rijden. In die laatste categorie vallen achtereenvolgende treinen over baanvakken tussen stations, conflicterende rijwegen op stations tussen binnenkomende en vertrekkende treinen, en elkaar tegemoet komende treinen op gedeeltelijk enkelsporige trajecten. In de dienstregeling zijn in principe alle conflicten opgelost zodat alle treinen ongehinderd over het spoornet kunnen rijden. Zodra een trein echter van het geplande tijdwegpad afwijkt kan hinder ontstaan voor andere treinen, die daardoor ook van hun geplande pad afwijken en zo op hun beurt ook weer andere treinen kunnen hinderen. Vanwege dit domino-effect kan een lokale primaire verstoring grote gevolgen hebben voor de hele treinenloop. Een goede dienstregeling bevat daarom zogenaamde buffertijden tussen de treinpaden zodat kleine verstoringen kunnen worden opgevangen en niet direct leiden tot secundaire vertragingen voor andere treinen. Om de stabiliteit van een dienstregeling te kunnen toetsen is een modellering op netwerkniveau nodig. (Hoofdstuk 3 & 6)

Een dienstregeling beschrijft de causale verbanden tussen treinactiviteiten en de geplande volgorde van deze activiteiten. Zo mag een trein pas vertrekken nadat het is aangekomen en minstens een bepaalde minimum halteringstijd aan een perron heeft stilgestaan om reizigers de gelegenheid te geven uit en in te stappen; als de trein een aansluitrelatie heeft met een andere trein, dan moet ook worden gewacht totdat de andere trein is aangekomen en de overstappende reizigers zijn ingestapt; en tenslotte moet mogelijk worden gewacht op het vertrek of de binnenkomst van andere treinen met een conflicterende rijweg voordat de rijweg van het perronspoor naar het baanvak vrij komt. Systemen met discrete gebeurtenissen waarbij synchronisatie een belangrijke rol spelen kunnen worden beschreven met ‘timed event graphs,’ een speciaal soort abstract netwerk (Petri net) waar behalve de tijdsafhankelijke relaties tussen opeenvolgende gebeurtenissen ook de proceslogica wordt beschreven. De beschrijving als timed event graph geeft inzicht in de volgorde waarin gebeurtenissen plaatsvinden en of het mogelijk is dat het systeem vastloopt, een zogenaamde deadlock. Een voorbeeld hiervan is dat een trein niet eerder van een station met meerdere perronsporen naar een enkelsporig baanvak mag vertrekken dan nadat alle tegengestelde treinen het baanvak hebben verlaten. Dit soort topologische en gedragsafhankelijke eigenschappen van een dienstregeling kunnen worden bestudeerd met methoden uit de ‘gemarkeerde’ graaftheorie van timed event graphs. (Hoofdstuk 6)

De kwaliteit en stabiliteit van een dienstregeling kan effectief worden bestudeerd in het ‘toestandsdomein’ van de timed event graph. De vertrektijden van alle treinen worden daarvoor gezien als toestandsvector en de dynamische vergelijking die de interactie tussen de vertrektijden beschrijft is een recursieve vergelijking waarin de vertrektijd van een gegeven trein wordt gegeven als het maximum over voorgaande vertrektijden plus de daarop volgende minimum procestijden waarop gewacht moet worden. Dergelijke vergelijkingen kunnen worden opgevat als lineaire systemen in de zogenaamde ‘max-plus algebra.’ In max-plus algebra is de ‘optelling’ van twee getallen gedefinieerd als het maximum en de ‘vermenigvuldiging’ als een gewone optelling, zodat bijvoorbeeld $2 \oplus 3 = \max(2, 3) = 3$ en $2 \otimes 3 = 2 + 3 = 5$. Systeemtechnisch komt de optelling van twee processen neer op de synchronisatie van processen (een aansluitend proces kan beginnen na het voorgaande proces dat als laatste is afgerond) en vermenigvuldiging op het na elkaar uitvoeren van processen (de procestijd van het samengestelde

proces is de som van de achtereenvolgende procestijden). Alle procestijden kunnen worden samengevat in een toestandsmatrix, waarna het discrete-event systeem wordt beschreven door matrix-vector vermenigvuldigingen en optellingen van vectoren, opgevat als bewerkingen in max-plus algebra. (Hoofdstuk 7 & 8)

Algoritmisches komt de analyse van max-plus lineaire systemen neer op het oplossen van eigenwaardeproblemen in max-plus algebra en kortste-pad of kritiekste-pad problemen. In dit proefschrift is daarom aandacht besteed aan efficiënte algoritmen voor deze problemen met betrekking tot het specifieke toepassingsgebied. Een timed event graph komt direct overeen met een 'polynomiale matrix' in max-plus algebra. Dit is een polynoom waarin de coëfficiënten bestaan uit matrices, of, wat op hetzelfde neerkomt, een matrix waarvan de elementen bestaan uit polynomen. Deze polynomiale matrix kan ook worden gebruikt in de beschrijving van hogere-orde lineaire systemen, inclusief nulde-orde termen. De nulde-orde termen zijn alle processen die binnen een periode worden afgewerkt, de eerste-orde termen alle processen die over een periodegrens heenlopen, et cetera. De gebruikelijke methode bestaat uit een transformatie van het hogere-orde systeem naar een puur eerste-orde systeem, waarvoor elegante algebraïsche analysemethoden bestaan. Echter, vanuit algoritmisch oogpunt bezien is dit niet effectief en ook vanuit de toepassing geredeneerd levert deze vereenvoudiging problemen op, met name doordat de nulde-orde dynamica is verdwenen. Dit proefschrift laat zien hoe de bekende max-plus algebra theorie van matrices en eerste-orde recursieve systemen kan worden uitgebreid naar polynomiale matrices en hogere-orde impliciete systemen. Speciale aandacht is besteed aan het gegeneraliseerde eigenprobleem van max-plus polynomiale matrices, zowel voor irreducibele als reducibele polynomiale matrices. Deze theorie geeft de noodzakelijke achtergrond die nodig is voor een volledige beschrijving van de eigenruimte van (polynomiale) matrices en voor een juiste interpretatie van het max-plus 'policy'-iteratie algoritme in het geval van reducibele max-plus (polynomiale) matrices. Het max-plus policy-iteratie algoritme is recent ontwikkeld op basis van het welbekende policy-iteratie algoritme voor Markov beslissingsproblemen, en blijkt voor het oplossen van het gegeneraliseerde eigenprobleem in max-plus algebra zeer effectief te zijn met een lineaire praktische rekentijd. Andere onderwerpen die aan bod komen zijn het efficiënt berekenen van alle kritieke circuits en de vertragsvoortplanting voor grootschalige max-plus systemen. (Hoofdstuk 7)

De stabiliteitsanalyse van max-plus lineaire systemen komt neer op het berekenen van de eigenwaarden van de (polynomiale) toestandsmatrix. De maximum eigenwaarde geeft de minimale lengte van een dienstregelingsperiode aan waarmee de dienstregeling zich kan herhalen. Voor een uurdienstregeling moet de maximum eigenwaarde dus kleiner zijn dan zestig minuten. In dat geval is de dienstregeling (asymptotisch) stabiel zodat een initiële vertraging in de loop der tijd uitdempt. De maximum eigenwaarde is gelijk aan de gemiddelde procestijd over een 'kritiek circuit', wat ook expliciet kan worden berekend. Een kritiek circuit is een cyclische opeenvolging van processen en treinactiviteiten waarvoor de minste speling beschikbaar is. Een eigenvector komt overeen met een dienstregeling (vertrektijdvector) waarin de kritieke treinactiviteiten direct achter elkaar zijn gepland zodat een periodieke dienstuitvoering mogelijk is met een periode gelijk aan de maximum eigenwaarde. De vertrektijden in de eigenvector komen overeen met de kritieke paden vanaf één van de kritieke treinactiviteiten. Het verschil tussen de echte dienstregelingsperiode (meestal een uur) en de maximum eigenwaarde geeft de gemiddelde speling op de kritieke circuits aan. De treinactiviteiten die niet op een kritiek circuit liggen hebben meer speling. Of een stabiele dienstregeling ook robuust is hangt af van de verdeling van de speling over de dienstregeling. Een dienstregeling waarbij alle speling zoveel mogelijk in de

keringen zit verwerkt is bijvoorbeeld niet robuust aangezien pas bij de keringen vertraging kan worden afgebouwd. De spelingsverdeling over de dienstregeling wordt inzichtelijk gemaakt via de spelingsmatrix, de recovery matrix, waarin ieder element aangeeft hoeveel speling op het meeste kritieke pad tussen twee treinactiviteiten zit. De voortplanting van initiële vertragingen kunnen ook expliciet worden berekend via de toestandsvergelijking waardoor de impact van een combinatie van vertragingen kan worden gevisualiseerd. (Hoofdstuk 8)

De algoritmen en analysemogelijkheden zijn geïmplementeerd in de software PETER (Performance Evaluation of Timed Events in Railways). Bijzondere aandacht is besteed aan de ontwikkeling en implementatie van efficiënte algoritmen die grootschalige netwerken in enkele seconden kunnen doorrekenen. Daarnaast is in PETER aandacht besteed aan de grafische presentatie van resultaten middels een projectie op het spoor netwerk, waardoor kritieke punten duidelijk zichtbaar worden. PETER voorziet in een behoefte voor een systematische en transparante stabiliteitsanalyse van dienstregelingen voor grootschalige railverkeersnetwerken en kan worden gebruikt in het ontwerpproces van dienstregelingen, de evaluatie van netwerkstabiliteit bij de toedeling van railinfrastructuurcapaciteit en voor de ontwikkeling van effectieve afhandelingsstrategieën ter beperking van vertragingvoortplanting. (Hoofdstuk 8)

ABOUT THE AUTHOR

Rob Goverde was born in Arnhem, the Netherlands, on June 22, 1968. During 1987–1993, he studied mathematics at Utrecht University. In 1993, Rob received his MSc in Mathematics with a specialization in optimization theory. His MSc thesis dealt with a theoretical topic in impulsive optimal control theory.

During 1994–1995, Rob attended the two-year post-MSc mathematical design engineering programme WBBM at Delft University of Technology, where he received the degree of Master of Technological Design (MTD) in Mathematical Modelling and Decision Support. During 1995, in the second year design project, he worked at the Dutch National Aerospace Laboratory (NLR), where he designed a robust flight control system using H_∞ robust control theory. This project was part of the international Robust Flight Control Design Challenge formulated by the Group for Aeronautical Research and Technology in Europe (GARTEUR). In 1996, Rob also obtained the certificate of the Dutch Network on the Mathematics of Operations Research (LNMB) for attending advanced PhD courses on mathematical programming and combinatorial optimization.

Since 1996, Rob is affiliated with the Transport & Planning Department at Delft University of Technology, where he worked on his PhD research within the TRAIL Research School. During his PhD research, Rob developed mathematical models for the design and analysis of reliable railway timetables. Based on his research, Rob presented numerous papers at both national and international conferences. In 2002–2003, Rob was also detached to Railned/ProRail where he worked in the project PRRING (Planning en Realizatie van RailINfraGebruik). His research has led to two software products, TNV-Prepare and PETER, which are both presented in his PhD thesis on ‘Punctuality of Railway Operations and Timetable Stability Analysis.’ After his PhD defence in 2005, Rob will continue working at the Transport & Planning Department as post-doc.

TRAIL Thesis Series

A series of The Netherlands TRAIL Research School for theses on transport, infrastructure and logistics.

Nat, C.G.J.M., van der, *A Knowledge-based Concept Exploration Model for Submarine Design*, T99/1, March 1999, TRAIL Thesis Series, Delft University Press, The Netherlands

Westrenen, F.C., van, *The Maritime Pilot at Work: Evaluation and Use of a Time-to-boundary Model of Mental Workload in Human-machine Systems*, T99/2, May 1999, TRAIL Thesis Series, Eburon, The Netherlands

Veenstra, A.W., *Quantitative Analysis of Shipping Markets*, T99/3, April 1999, TRAIL Thesis Series, Delft University Press, The Netherlands

Minderhoud, M.M., *Supported Driving: Impacts on Motorway Traffic Flow*, T99/4, July 1999, TRAIL Thesis Series, Delft University Press, The Netherlands

Hoogendoorn, S.P., *Multiclass Continuum Modelling of Multilane Traffic Flow*, T99/5, September 1999, TRAIL Thesis Series, Delft University Press, The Netherlands

Hoedemaeker, M., *Driving with Intelligent Vehicles: Driving Behaviour with Adaptive Cruise Control and the Acceptance by Individual Drivers*, T99/6, November 1999, TRAIL Thesis Series, Delft University Press, The Netherlands

Marchau, V.A.W.J., *Technology Assessment of Automated Vehicle Guidance – Prospects for Automated Driving Implementation*, T2000/1, January 2000, TRAIL Thesis Series, Delft University Press, The Netherlands

Subiono, *On Classes of Min-max-plus Systems and their Applications*, T2000/2, June 2000, TRAIL Thesis Series, Delft University Press, The Netherlands

Meer, J.R., van, *Operational Control of Internal Transport*, T2000/5, September 2000, TRAIL Thesis Series, Delft University Press, The Netherlands

Bliemer, M.C.J., *Analytical Dynamic Traffic Assignment with Interacting User-Classes: Theoretical Advances and Applications using a Variational Inequality Approach*, T2001/1, January 2001, TRAIL Thesis Series, Delft University Press, The Netherlands

Muילerman, G.J., *Time-based logistics: An analysis of the relevance, causes and impacts*, T2001/2, April 2001, TRAIL Thesis Series, Delft University Press, The Netherlands

Roodbergen, K.J., *Layout and Routing Methods for Warehouses*, T2001/3, May 2001, TRAIL Thesis Series, The Netherlands

Willems, J.K.C.A.S., *Bundeling van infrastructuur, theoretische en praktische waarde van een ruimtelijk inrichtingsconcept*, T2001/4, June 2001, TRAIL Thesis Series, Delft University Press, The Netherlands

Binsbergen, A.J., van, J.G.S.N. Visser, *Innovation Steps towards Efficient Goods Distribution Systems for Urban Areas*, T2001/5, May 2001, TRAIL Thesis Series, Delft University Press, The Netherlands

Rosmuller, N., *Safety analysis of Transport Corridors*, T2001/6, June 2001, TRAIL Thesis Series, Delft University Press, The Netherlands

Schaafsma, A., *Dynamisch Railverkeersmanagement, besturingsconcept voor railverkeer op basis van het Lagenmodel Verkeer en Vervoer*, T2001/7, October 2001, TRAIL Thesis Series, Delft University Press, The Netherlands

Bockstael-Blok, W., *Chains and Networks in Multimodal Passenger Transport. Exploring a design approach*, T2001/8, December 2001, TRAIL Thesis Series, Delft University Press, The Netherlands

Wolters, M.J.J., *The Business of Modularity and the Modularity of Business*, T2002/1, February 2002, TRAIL Thesis Series, The Netherlands

Vis, F.A., *Planning and Control Concepts for Material Handling Systems*, T2002/2, May 2002, TRAIL Thesis Series, The Netherlands

Koppius, O.R., *Information Architecture and Electronic Market Performance*, T2002/3, May 2002, TRAIL Thesis Series, The Netherlands

Veeneman, W.W., *Mind the Gap; Bridging Theories and Practice for the Organisation of Metropolitan Public Transport*, T2002/4, June 2002, TRAIL Thesis Series, Delft University Press, The Netherlands

Nes, R. van, *Design of multimodal transport networks, a hierarchical approach*, T2002/5, September 2002, TRAIL Thesis Series, Delft University Press, The Netherlands

Pol, P.M.J., *A Renaissance of Stations, Railways and Cities, Economic Effects, Development Strategies and Organisational Issues of European High-Speed-Train Stations*, T2002/6, October 2002, TRAIL Thesis Series, Delft University Press, The Netherlands

Runhaar, H., *Freight transport: at any price? Effects of transport costs on book and newspaper supply chains in the Netherlands*, T2002/7, December 2002, TRAIL Thesis Series, Delft University Press, The Netherlands

Spek, S.C., van der, *Connectors. The Way beyond Transferring*, T2003/1, February 2003, TRAIL Thesis Series, Delft University Press, The Netherlands

Lindeijer, D.G., *Controlling Automated Traffic Agents*, T2003/2, February 2003, TRAIL Thesis Series, Eburon, The Netherlands

Riet, O.A.W.T., van de, *Policy Analysis in Multi-Actor Policy Settings. Navigating Between Negotiated Nonsense and Useless Knowledge*, T2003/3, March 2003, TRAIL Thesis Series, Eburon, The Netherlands

Reeven, P.A., van, *Competition in Scheduled Transport*, T2003/4, April 2003, TRAIL Thesis Series, Eburon, The Netherlands

Peeters, L.W.P., *Cyclic Railway Timetable Optimization*, T2003/5, June 2003, TRAIL Thesis Series, The Netherlands

Soto Y Koelemeijer, G., *On the behaviour of classes of min-max-plus systems*, T2003/6, September 2003, TRAIL Thesis Series, The Netherlands

Lindveld, Ch..D.R., *Dynamic O-D matrix estimation: a behavioural approach*, T2003/7, September 2003, TRAIL Thesis Series, Eburon, The Netherlands

Weerdt, de M.M., *Plan Merging in Multi-Agent Systems*, T2003/8, December 2003, TRAIL Thesis Series, The Netherlands

Langen, de P.W., *The Performance of Seaport Clusters*, T2004/1, January 2004, TRAIL Thesis Series, The Netherlands

Hegyi, A., *Model Predictive Control for Integrating Traffic Control Measures*, T2004/2, February 2004, TRAIL Thesis Series, The Netherlands

Lint, van, J.W.C., *Reliable Travel Time Prediction for Freeways*, T2004/3, June 2004, TRAIL Thesis Series, The Netherlands

Tabibi, M., *Design and Control of Automated Truck Traffic at Motorway Ramps*, T2004/4, July 2004, TRAIL Thesis Series, The Netherlands

Verduijn, T. M., *Dynamism in Supply Networks: Actor switching in a turbulent business environment*, T2004/5, September 2004, TRAIL Thesis Series, The Netherlands

Daamen, W., *Modelling Passenger Flows in Public Transport Facilities*, T2004/6, September 2004, TRAIL Thesis Series, The Netherlands

Zoeteman, A., *Railway Design and Maintenance from a Life-Cycle Cost Perspective: A Decision-Support Approach*, T2004/7, November 2004, TRAIL Thesis Series, The Netherlands

Bos, D.M., *Changing Seats: A Behavioural Analysis of P&R Use*, T2004/8, November 2004, TRAIL Thesis Series, The Netherlands

Versteegt, C., *Holonic Control For Large Scale Automated Logistic Systems*, T2004/9, December 2004, TRAIL Thesis Series, The Netherlands

Wees, K.A.P.C. van, *Intelligente voertuigen, veiligheidsregulering en aansprakelijkheid. Een onderzoek naar juridische aspecten van Advanced Driver Assistance Systems in het wegverkeer*, T2004/10, December 2004, TRAIL Thesis Series, The Netherlands

Tampère, C.M.J., *Human-Kinetic Multiclass Traffic Flow Theory and Modelling: With Application to Advanced Driver Assistance Systems in Congestion*, T2004/11, December 2004, TRAIL Thesis Series, The Netherlands

Rooij, R.M., *The Mobile City. The planning and design of the Network City from a mobility point of view*, T2005/1, February 2005, TRAIL Thesis Series, The Netherlands

Le-Anh, T., *Intelligent Control of Vehicle-Based Internal Transport Systems*, T2005/2, April 2005, TRAIL Thesis Series, The Netherlands

Zuidgeest, M.H.P., *Sustainable Urban Transport Development: a Dynamic Optimization Approach*, T2005/3, April 2005, TRAIL Thesis Series, The Netherlands

Hoogendoorn-Lanser, S., *Modelling Travel Behaviour in Multimodal Networks*, T2005/4, May 2005, TRAIL Thesis Series, The Netherlands

Dekker, S., *Port Investment – Towards an integrated planning of port capacity*, T2005/5, June 2005, TRAIL Thesis Series, The Netherlands

Koolstra, K., *Transport Infrastructure Slot Allocation*, T2005/6, June 2005, TRAIL Thesis Series, The Netherlands

Vromans, M., *Reliability of Railway Systems*, T2005/7, July 2005, TRAIL Thesis Series, The Netherlands

Oosten, W., *Ruimte voor een democratische rechtsstaat. Geschakelde sturing bij ruimtelijke investeringen*, T2005/8, September 2005, TRAIL Thesis Series, Sociotext, The Netherlands

Le-Duc, T., *Design and control of efficient order picking*, T2005/9, September 2005, TRAIL Thesis Series, The Netherlands

Goverde, R.M.P., *Punctuality of Railway Operations and Timetable Stability Analysis*, T2005/10, October 2005, TRAIL Thesis Series, The Netherlands